Pacific Northwest
NATIONAL LABORATORY

PNNL-35432, Rev. 0
DVZ-RPT-103, Rev. 0

200-DV-1 Laboratory Treatability Study: Proof-of-Principle Results

December 2025

Hilary P Emerson
James E Szecsody
Amanda R Lawter
Andrew E Plymale
Nancy M Escobedo
Michelle MV Snyder
Katherine A Muller
Christopher Bagwell
Danielle L Saunders
Jacqueline R Hager
Alex Kugler
Guohui Wang
C Tom Resch
Carolyn I Pearce
Nikolla P Qafoku
Sabrina Hoyle
Steven R Baum
Ian I Leavy
Rachel Anguish
Kelly Rue
Leon Hibbard
Mariah Doughman
Elsa Cordova
Jenna M Schroeder
Kaycee Bailey
Inci Demirkanli
Nicolas Huerta

U.S. DEPARTMENT of ENERGY

Prepared for the U.S. Department of Energy
under Contract DE-AC05-76RL01830

DISCLAIMER

PACIFIC NORTHWEST NATIONAL LABORATORY
operated by
BATTELLE
for the
UNITED STATES DEPARTMENT OF ENERGY
under Contract DE-AC05-76RL01830

Printed in the United States of America

Available to DOE and DOE contractors from
the Office of Scientific and Technical Information,
P.O. Box 62, Oak Ridge, TN 37831-0062
www.osti.gov
ph: (865) 576-8401
fox: (865) 576-5728
email: reports@osti.gov

Available to the public from the National Technical Information Service
5301 Shawnee Rd., Alexandria, VA 22312
ph: (800) 553-NTIS (6847)
or (703) 605-6000
email: info@ntis.gov
Online ordering: http://www.ntis.gov

PNNL-35432, Rev. 0
DVZ-RPT-103, Rev. 0

200-DV-1 Laboratory Treatability Study: Proof-of-Principle Results

December 2025

Prepared for
the U.S. Department of Energy
under Contract DE-AC05-76RL01830

Pacific Northwest National Laboratory
Richland, Washington 99354

Executive Summary

To support soil and groundwater remediation across the Hanford Site's Central Plateau, a laboratory treatability study has been initiated to evaluate site-relevant effectiveness for nine technologies that may be used to treat contaminants in specific areas of the Central Plateau grouped into the 200-DV-1 Operable Unit (OU). The 200-DV-1 OU was established in 2010 to address 43 of the Central Plateau waste sites with complex remediation challenges. Eight of the nine technologies were identified through a technology prescreening effort that evaluated remedial technologies potentially applicable to DVZ contamination in the Central Plateau, as reported in DOE/RL-2017-58, *Technology Evaluation and Treatability Studies Assessment for the Hanford Central Plateau Deep Vadose Zone*.[1] These eight technologies were selected for further study based on site-specific knowledge gaps about their effectiveness. A ninth technology was added to the treatability study based on new information from separate laboratory investigations (conducted following the prescreening effort) demonstrating the technology's potential effectiveness (see Section 2.5 for more information) and the value for inclusion in the treatability study.

Following the recommendations of the technology prescreening effort, a laboratory treatability study plan was developed for the original eight technologies: DOE/RL-2019-28, Rev. 0, *200-DV-1 Operable Unit Laboratory Treatability Study Test Plan* (hereinafter referred to as the test plan).[2] The test plan was developed to present a framework and overall guidance for detailed laboratory evaluations of each technology, focusing on the data gaps identified by the technology prescreening effort. The test plan identified potential amendments designed to immobilize or degrade the primary contaminants *in situ* within the subsurface. Therefore, contaminants would be treated *in situ* (i.e., below ground where they are located) to reduce their long-term mobility toward groundwater via delivery of different amendments targeting different processes to be evaluated for each technology. The test plan also developed a tiered approach, with initial assessment of technology effectiveness in Phase 1 and subsequent detailed evaluation in Phase 2. A process of down-selection of technologies was applied between phases to eliminate technologies that do not present significant effectiveness from further detailed evaluation.

The technologies selected for treatability evaluation rely on various biogeochemical processes, with a combination of reduction and sequestration or sequestration alone, to immobilize contaminants into solid phases, rendering them less mobile in the subsurface, or to transform them into nontoxic end products, thereby reducing continuing source contributions into the groundwater and helping to mitigate risk. The primary contaminants targeted for this treatability study were technetium-99, uranium, nitrate, and iodine-129, depending on the targeted waste sites for each technology (Table ES.1). Additional co-contaminants, including chromate, strontium, and ferrocyanide, were also included depending on the targeted waste sites.

This document presents the Phase 1 technical approach and results of laboratory-scale treatability evaluation of nine *in situ* remedial technologies (Table ES.1) for their consideration in a future feasibility study for the 200-DV-1 OU. The primary objective of this initial assessment was a proof-of-principle evaluation conducted via batch or static column experiments to determine the potential for reduction and/or sequestration of the primary contaminants of interest with and without potential co-contaminants of interest. Decisions for advancing the technologies to Phase 2 of evaluation under the treatability study plan relied on assessing the potential bulk effectiveness of the given technology and the need for or value of further evaluating the detailed mechanisms and/or processes that result in the observed effectiveness by

[1] DOE/RL-2019-28, Rev. 0, 2017. *Technology Evaluation and Treatability Studies Assessment for the Hanford Central Plateau Deep Vadose Zone*. U.S. Department of Energy, Richland Operations Office, Richland, WA
[2] DOE/RL-2019-28, Rev. 0. 2017. *200-DV-1 Operable Unit Laboratory Treatability Study Test Plan*. U.S. Department of Energy, Richland Operations Office, Richland, WA.

the project team. Therefore, the project team used the experimental results of the Phase 1 activities and an approximate effectiveness of at least 35% transformation to immobile or nontoxic end products, along with other experimental performance indicators, to determine the technologies that may benefit from further evaluation in Phase 2. The 35% transformation was determined conservatively to ensure the elimination of only those technologies that showed poor performance. For most technologies, the performance was evaluated based on a series of sequential extractions designed to evaluate the mobility of contaminants before and after treatment, with each subsequent extraction representing a relative decrease in mobility (as described in Section 3.3).

The nine technologies that were evaluated may be represented by three different groups of technologies, based on their physical characteristics: gaseous, particulate, and liquid amendments. The gas-phase technologies were selected for unsaturated vadose zone applications, while the liquid- and particulate-phase technologies were selected for saturated zone applications, potentially targeting direct treatment of contaminants in perched water or in a water table application as a permeable reactive barrier. Each of these technologies was evaluated based on its ability to transform the primary contaminants of interest under the targeted application conditions, including the potential presence of co-contaminants. The technologies target different processes for transformation of contaminants to immobile or nontoxic end products in the subsurface. Most of the primary contaminants (technetium-99, uranium, nitrate, and iodine-129) are targeted for immobilization via either reduction, sequestration, or a combination of the two processes. For example, technetium-99 may be reduced to less soluble phases (e.g., TcO_4^- to TcO_2), uranium may be transformed to less soluble phases by reaction with phosphate [e.g., $Ca_2UO_2(CO_3)_3$ to $Ca(UO_2)_2(PO_4)_2 \cdot 10\text{-}12H_2O$], or iodate may be incorporated and/or coated with calcite. However, nitrate is targeted for transformation to nontoxic end products (e.g., NO_3^- to N_2 gas). Of the nine technologies evaluated, eight passed the initial decision point criteria for Phase 1 (identified as “Go” in Table ES.1) and were recommended for Phase 2 evaluation as part of the treatability study.

The three gas-phase technologies are targeting different contaminants in the vadose zone: (1) combined bioreduction and sequestration of technetium-99 by sequential treatment with organic gas (ethane, butane, or butyl acetate) followed by carbon dioxide gas, (2) bioreduction of nitrate by organic gases (pentane, butane, ethane, or butyrate), and (3) sequestration of iodine-129 by carbon dioxide gas. The one technology that did not pass the criteria was the gas-phase combined bioreduction and chemical sequestration, which showed some sequestration of technetium-99 but was insufficient to recommend further evaluation for a potential site application. The gas-phase combined bioreduction and chemical sequestration technology is not recommended for Phase 2 evaluation as part of the treatability study. The other two gas-phase technologies, bioreduction of nitrate by organic gases and sequestration of iodine-129 by carbon dioxide, met the 35% minimum transformation threshold to temporarily immobile, immobile, or nontoxic end products and are recommended for Phase 2 evaluation as part of the treatability study. For the gas-phase bioreduction technology, butyrate and ethane gas amendments are recommended for Phase 2 evaluation, as they showed superior performance to butane and pentane. Due to the low volatility and high solubility of butyrate, the radius of treatment for butyrate gas injection in a potential field application would likely be constrained to very short distances. Therefore, ethane will be the primary gas for further evaluation.

The three particulate-phase technologies are (1) chemical sequestration by tin(II)-substituted apatite [Sn(II)-PO_4], (2) chemical sequestration by bismuth oxyhydroxide or bismuth subnitrate, and (3) combined chemical reduction and sequestration by zero valent iron or sulfur-modified iron followed by treatment with apatite-forming solutions. Each amendment was evaluated with the primary contaminants, including technetium-99 and uranium, and with and without potential co-contaminants, including strontium-90, iodine-129, hexavalent chromium, and nitrate. All of these technologies met the 35% minimum transformation threshold for both uranium and technetium-99 and are recommended to advance to Phase 2 evaluation. For the chemical sequestration by bismuth amendments and the combined

chemical reduction and sequestration technologies, a down-selection to bismuth subnitrate (as bismuth oxyhydroxide did not meet performance criteria for technetium-99) and sulfur-modified iron (as performance was decreased by delivery fluids for zero valent iron) are recommended for Phase 2 evaluation of the treatability study, respectively.

The three liquid-phase technologies are (1) chemical sequestration by polyphosphate or calcium citrate phosphate solutions, (2) combined chemical reduction and sequestration by calcium polysulfide followed by polyphosphate, and (3) combined bioreduction and sequestration by organic liquids (e.g., molasses or emulsified vegetable oil) followed by polyphosphate. Each amendment was evaluated with the primary contaminants, including Tc-99 and uranium, and with and without potential co-contaminants, including strontium-90, iodine-129, chromium, and nitrate. All of these technologies are recommended for Phase 2 evaluation of the treatability study. For the liquid-phase chemical sequestration technology, the calcium citrate phosphate amendment is recommended for Phase 2 evaluation due to its superior performance for Tc-99. However, the polyphosphate amendment will continue as the sequestration amendment for the following technologies: liquid-phase chemical reduction and sequestration, liquid-phase bioreduction and sequestration, and particulate-phase chemical reduction and sequestration, since the initial step is targeting reduction for contaminants like Tc-99. For the combined bioreduction and sequestration by organic liquids followed by polyphosphate, molasses is recommended for further testing for both water table permeable reactive barrier and direct injection to perched water based on its superior performance in these conditions, respectively, for Phase 2 of the treatability study.

The results presented here describe the down-selection of technologies based on a laboratory-scale performance comparison. The final results from this treatability study will be used to determine whether the technologies could be evaluated in a feasibility study to expand on the limited number of viable DVZ remediation technologies. After completion of the laboratory treatability study and the 200 DV-1 OU Remedial Investigation and Resource Conservation and Recovery Act Facility Investigation of the waste sites, results will be evaluated to determine whether more information is needed on effectiveness, implementability, or costs for evaluating these technologies in feasibility studies for their site-specific application.

Table ES.1. Summary of Phase 1 results and recommendations for Phase 2 of 200-DV-1 OU treatability testing.

Technology Process	Contaminants of Interest[a]	Phase 1 Amendments	Phase 1 Decision Point	Phase 2 Evaluation Recommendations
Technologies for Unsaturated Zone Applications				
Gas-phase combined bioreduction and chemical sequestration	**Tc-99**, U, I-129, Cr(VI), CN^-, nitrate	Organic gases including ethane, butane, and butyl acetate for bioreduction CO_2 for sequestration	No-Go	None
Gas-phase bioremediation	**Nitrate**, Cr	Organic gases including pentane, butyrate, ethane, and butane	Go	Ethane gas
Gas-phase chemical sequestration	**I-129**, U, Tc-99, Sr, Cr(VI)	CO_2 gas	Go	CO_2 gas
Technologies for Saturated Zone Applications at BY Cribs Groundwater or Perched Water[b]				
Particulate-phase chemical sequestration	**U**, **Tc-99**, Sr-90, Cr(VI), I-129, nitrate	Sn(II)-PO_4	Go	Sn(II)-PO_4
Particulate-phase chemical sequestration	**U, Tc-99,** Sr-90, Cr(VI), I-129, nitrate	Bismuth oxyhydroxide and bismuth subnitrate	Go	Bismuth subnitrate
Particulate-phase combined chemical reduction and sequestration	**U**, **Tc-99**, Sr-90, Cr(VI), I-129, nitrate	Zero valent iron and sulfur-modified iron for reduction Polyphosphate solutions for sequestration	Go	Sulfur-modified iron followed by polyphosphate
Liquid-phase chemical sequestration	**U**, **Tc-99**, Sr-90, Cr(VI), I-129, nitrate	Polyphosphate and citrate phosphate solutions	Go	Calcium citrate phosphate[c]
Liquid-phase combined chemical reduction and sequestration	**U**, **Tc-99**, Sr-90, Cr(VI), I-129, nitrate	Calcium polysulfide for reduction Polyphosphate solutions for sequestration	Go	Calcium polysulfide followed by polyphosphate
Liquid-phase combined bioreduction and chemical sequestration	**U**, **Tc-99**, **nitrate**, Sr-90, Cr(VI), I-129	Organic liquids including emulsified vegetable oil and blackstrap molasses for bioreduction Polyphosphate solutions for sequestration	Go	Molasses followed by polyphosphate

(a) The contaminants of interest shown in bold are primary known contaminant targets while others are potential co-contaminants to evaluate with primary contaminants.
(b) BY Cribs groundwater and perched water beneath the BC Complex represent some of the 200-DV-1 waste sites (see Section 1.2 for more information).
(c) Although calcium citrate phosphate was chosen for additional testing in the liquid-phase chemical sequestration technology, polyphosphate was chosen to move forward as the sequestration step in the following technologies: particulate-phase combined chemical, liquid-phase combined chemical reduction and sequestration, and liquid-phase combined bioreduction and sequestration.

Acknowledgments

This document was prepared by the Deep Vadose Zone – Applied Field Research Initiative at Pacific Northwest National Laboratory. Funding was provided by the U.S. Department of Energy (DOE) Richland Operations Office. Pacific Northwest National Laboratory is operated by Battelle Memorial Institute for the DOE under Contract DE-AC05-76RL01830.

The authors acknowledge Shelby M.B. Phillips, Christian D. Johnson, and Matthew Wilburn for their attention to detail in data review and technical editing and Mike Perkins for development of conceptual diagrams. The Pacific Northwest National Laboratory's Analytical Services Center and Christopher J. Thompson are appreciated for their expertise in analyzing the tremendous number of samples generated as part of this study. Brent Hicks is appreciated for their careful attention to detail and quality. James B. Duncan is acknowledged for their expert guidance on the synthesis of Sn(II)-PO_4.

Acronyms and Abbreviations

APW	artificial pore water
BET	Brunauer-Emmett-Teller method of measuring surface area
bgs	below ground surface
BOH	bismuth oxyhydroxide
BSN	bismuth subnitrate
CCug	Cold Creek unit gravel
CCu-PZsd	Cold Creek unit perching zone sand
CCuz	Cold Creek unit silt
CCV	Continuing Calibration Verification
CEC	cation exchange capacity
Ca-Cit-PO_4	calcium-citrate, sodium phosphate solution used to precipitate apatite
CN^-	cyanide
COI	contaminant of interest
CoCOI	co-contaminants of interest
CPS	calcium polysulfide
DNRA	dissimilatory NO_3 reduction to ammonium
DVZ	deep vadose zone
EOS	emulsified oil substrate
ESI	Elemental Scientific Incorporated
FIO	For Information Only
FS	feasibility study
FY	fiscal year
GG	guar gum
HCV	High Calibration Verification
HEIS	Hanford Environmental Information System
Hf	Hanford formation
KPA	kinetic phosphorescence analyzer
IC	ion chromatography
ICP-MS	inductively coupled plasma mass spectrometer
ICP-OES	inductively coupled plasma optical emission spectrometer
ICV	Initial Calibration Verification
IDL	instrument detection limit
ISTD	internal standard
LSC	liquid scintillation counting
LPG	liquefied petroleum gas
MDL	method detection limit

NDIR	non-dispersive infrared
NQAP	Nuclear Quality Assurance Program
OU	operable unit
PCOI	primary contaminant of interest
PTFE	polytetrafluoroethylene
PNNL	Pacific Northwest National Laboratory
Poly-PO_4	sodium phosphate and sodium polyphosphate solution used to precipitate apatite
PRB	permeable reactive barrier
qPCR	quantitative polymerase chain reaction
RI	remedial investigation
RFI	Resource Conservation and Recovery Act Facility Investigation
RFICS	Reagent-Free Ion Chromatography System
RW	river water
SGW	synthetic groundwater
SMI	sulfur-modified iron
Sn(II)-PO_4	tin(II)-substituted apatite
SPW	synthetic perched water
SST	single-shell tank
TC	total carbon
TIC	total inorganic carbon
TMAH	tetramethylammonium hydroxide
TOC	total organic carbon
TTER	treatability test evaluation report
UV	ultraviolet
VZ	vadose zone
WC	water content
WMA	waste management area
XG	xanthan gum
XRD	X-ray diffraction
YE	yeast extract
ZVI	zero valent iron

Contents

Figures

Tables

1.0 Introduction

The purpose of this treatability study is to assess the effectiveness of nine *in situ* remedial technologies for site-specific conditions to support future testing in the field, if needed, and to support their consideration in a feasibility study (FS). This document presents Phase 1 results (Section 4.0) of laboratory-scale treatability study of nine *in situ* remedial technologies (Table 1.1) for their consideration for the 200-DV-1 Operable Unit (OU) at the U.S. Department of Energy Hanford Site. Eight of these technologies were identified through a technology prescreening effort that evaluated remedial technologies potentially applicable to deep vadose zone (DVZ) contamination in the Hanford Site Central Plateau, as reported in DOE/RL-2017-58, *Technology Evaluation and Treatability Studies Assessment for the Hanford Central Plateau Deep Vadose Zone* (hereinafter referred to as the treatability test evaluation report [TTER]). The original eight technologies were selected for further study based on site-specific knowledge gaps about their effectiveness for the DVZ and perched water locations. The remaining technology was added to the treatability study based on new information from separate laboratory investigations (conducted following the prescreening effort) demonstrating the technology's potential effectiveness (see Section 2.5 for more information).

As shown in Table 1.1, groups of technologies that could be applicable for addressing DVZ contamination were identified in the TTER for additional laboratory studies to address site-specific data gaps. The general types of technologies cover different physical characteristics, including gas phase, particulate phase, and liquid-phase amendment injections into the subsurface, for the purpose of manipulating subsurface biogeochemistry to sequester contaminants in solid phase. While the gas-phase technologies were selected for unsaturated applications within the vadose zone (VZ) soil column, both the particulate- and liquid-phase technologies were selected for applications in saturated conditions, such as direct injection into the perched water zone (i.e., thin, saturated zone within the VZ due to geologic heterogeneities) and/or for water table applications as permeable reactive barriers (PRBs) at locations where contaminant fluxes reach groundwater. Technologies selected for the treatability testing rely on various biogeochemical processes for (1) a combination of reduction and sequestration or direct sequestration to incorporate the contaminants into solid phases and render the contaminants less mobile in the subsurface [e.g., technetium-99 (Tc-99), uranium (U), and iodine-129 (I-129)] or (2) to reduce and degrade the contaminants into gaseous, nontoxic end products (e.g., nitrate), thereby reducing continuing source contributions into the groundwater and helping to mitigate risk.

Table 1.1. Recommended laboratory studies by the TTER.

Technology Process	COI to Study	Phase 1 Amendments Selected for Testing	Examples of Potentially Applicable Waste Sites	
			Primary	Secondary Treatment Zones
Technologies for Unsaturated Zone Applications				
Gas-phase combined bioreduction and chemical sequestration	**Tc-99**, U, I-129, Cr(VI),CN^-, nitrate	Organic gases including ethane, butane, and butyl acetate for bioreduction CO_2 gas for sequestration	Tc-99 and/or CN^- BY Cribs[a] Nitrate, I-129, and Cr(VI) Unknown[a]	Tc-99 BC Cribs/Trenches[b] Cr(VI) 216-S-10[b] 216-S-8[b] 216-T-4a[b] I-129 216-S-9(b) 216-A-10[b] 216-A-5[b] 216-S-7[b] CN^- Unknown[b]
Gas-phase bioremediation	**Nitrate,** Cr(VI)	Organic gases including pentane, butyrate, ethane, and butane		
Gas-phase chemical sequestration	**I-129**, U, Tc-99, Sr, Cr(VI)	CO_2 gas		
Technologies for Saturated Zone Applications[c]				
Particulate-phase chemical sequestration	**U**, **Tc-99**, Sr-90, Cr(VI), I-129, nitrate	Sn(II)-PO_4	U and/or Tc-99 Perched water[a] Below perched water[a] Below BY Cribs[a]	U and/or Tc-99 216-U-1&2[a] S-SX Tank Farm[a] T-TX-TY Tank Farm[a] C Tank Farm[a] BC Cribs/Trenches[b] Cr(VI) 216-S-10[b] 216-S-8[b] 216-T-4a[b] I-129 216-A-10[b] 216-A-5[b] 216-S-7[b]
Particulate-phase combined chemical reduction and sequestration	**U**, **Tc-99**, Sr-90, Cr(VI), I-129, nitrate	Zero valent iron (ZVI) and sulfur-modified iron (SMI) for reduction Polyphosphate solution for sequestration		
Particulate-phase chemical sequestration (Bi)[d]	**U**, **Tc-99**, Sr-90, Cr(VI), I-129, nitrate	Bismuth oxyhydroxide and bismuth subnitrate		
Liquid-phase chemical sequestration	**U**, **Tc-99**, Sr-90, Cr(VI), I-129, nitrate	Polyphosphate and citrate phosphate solutions		
Liquid-phase combined chemical reduction and sequestration	**U**, **Tc-99**, Sr-90, Cr(VI), I-129, nitrate	Calcium polysulfide for reduction Polyphosphate solution for sequestration		
Liquid-phase combined bioreduction and chemical sequestration	**U**, **Tc-99**, **nitrate**, Sr-90, Cr(VI),I-129	Organic liquids including slow release (e.g., emulsified vegetable oil) and fast release (e.g., molasses) substrates Polyphosphate solution for sequestration		

Reference: DOE/RL-2017-58, Draft A, *Technology Evaluation and Treatability Studies Assessment for the Hanford Central Plateau Deep Vadose Zone* (referred to as the treatability test evaluation report, TTER).

Notes: Laboratory quantification of effectiveness is needed for use in combination with existing field-scale information from other sites to evaluate these technologies in an FS.

The PCOIs shown in bold are primary known contaminant targets. Other CoCOIs are potential co-contaminants to evaluate for their potential impact on PCOIs.

(a) These are likely continuing sources of contaminants to groundwater.

(b) The remedial investigation evaluation will determine the waste sites that impactgroundwater.

(c) The saturated zone applications include 200-DV-1 perched water (located beneath the B Complex) and horizontal PRB at the water table (located in groundwater beneath the BY Cribs).

(d) The technical information about the potential applicability of this technology for DVZ remediation became available through bench-scale investigations after the initiation of the treatability study. Based on this information, the technology was added to the treatability study to evaluate its site-specific effectiveness.

COI = contaminant of interest; CoCOI = co-contaminant of interest; PCOI = primary contaminant of interest

Following the recommendations of the TTER, a laboratory treatability study plan was developed for the original eight technologies: DOE/RL-2019-28, Rev. 0, *200-DV-1 Operable Unit Laboratory Treatability Study Test Plan* (hereinafter referred to as the test plan). The test plan presented a framework and overall guidance for detailed laboratory evaluations of each technology, focusing on the data gaps identified by the TTER. Based on the existing knowledge and past experiences, the test plan identified potential amendments for the reduction and sequestration processes to be evaluated for each technology, as appropriate (Table 1.1).

The evaluation approach presented in the test plan was developed to outline a tiered approach in order to provide multiple incremental decision points throughout the study for each technology to assess potential technology performance under site-specific conditions (Figure 1.1). The tiered approach was designed to apply more detailed laboratory evaluations of the technologies progressively, while eliminating those that did not show sufficient effectiveness within a given phase or tier. The approach identified an effectiveness criteria for each phase; however, the final determination of technology effectiveness and further testing needs is made collectively by a group of subject matter experts. While technology-specific testing objectives were identified for each phase (DOE/RL-2019-28) targeting specific contaminants, in general, the main components of the tiered testing approach followed a sequence of actions or phases:

- Phase 1: An initial assessment of bulk technology effectiveness in ideal conditions (as a proof-of-principle step). This determination was recommended to be based on an overall minimum success rate of 35% of contaminant transformation to immobile, temporarily immobile, or nontoxic end products.
- Phase 2: A detailed evaluation of process-specific rates and extent of reduction, degradation, and/or sequestration with an assessment of potential contaminant remobilization to determine if a minimum of 35% nonreversible sequestration/transformation is achieved.
- Phase 3: Additional characterization to evaluate the stability of immobilized contaminants as well as potential remobilization rates.

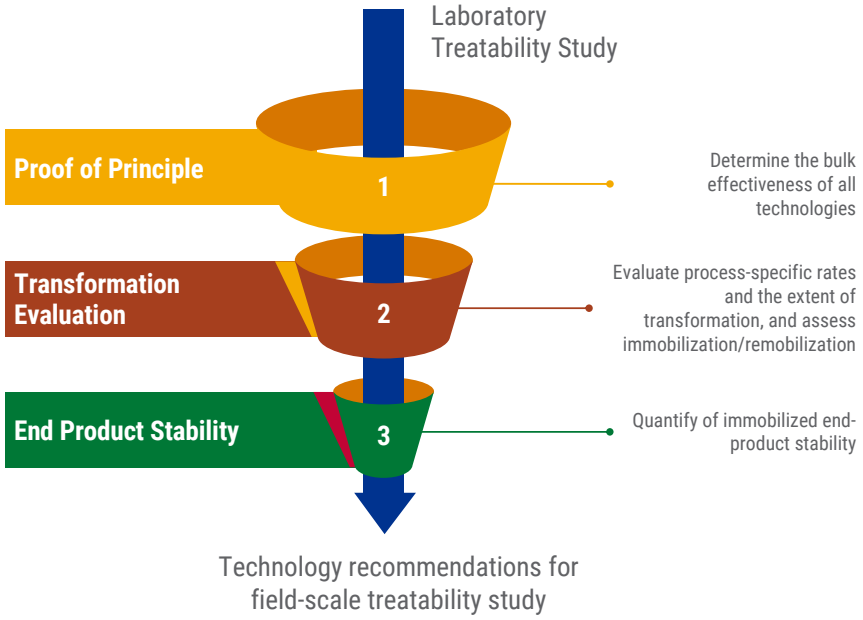

Figure 1.1. Tiered phases of the laboratory treatability testing approach for the 200-DV-1 OU.

The results presented in this report represent Phase 1 of the treatability study testing as conducted via laboratory-scale batch experiments. The final results from this treatability study, following the completion of remaining phases, will be used to determine whether the technologies evaluated can be appropriately assessed in an FS to expand on the limited number of viable DVZ remediation technologies. After the completion of the laboratory study and the 200 DV-1 OU Remedial Investigation (RI) and Resource Conservation and Recovery Act Facility Investigation (RFI) of the waste sites, results will be evaluated to determine whether field studies are needed to provide additional information on effectiveness, implementability, or costs for evaluating these technologies in the FS for their site-specific application. The effectiveness of 35% transformation to immobile, temporarily immobile [e.g., TcO_4^- to TcO_2, $Ca_2UO_2(CO_3)_3$ to $Ca(UO_2)_2(PO_4)_2 \cdot 10\text{-}12H_2O$, or IO_3^- to IO_3 incorporated into $CaCO_3$], or nontoxic end products (e.g., NO_3^- to N_2 gas), along with other experimental indicators, was used by the project team to evaluate the effectiveness of the technology and determine the need for further testing of the technologies in Phase 2. The 35% transformation threshold is based on an increase in transformation as compared with an appropriate control experiment (e.g., sediments and contaminants reacting in the absence of treatments).

More detailed information on the Hanford Site and 200-DV-1 OU are provided in Sections 1.1 and 1.2; technologies are described in Section 2.0; experimental design, materials, and methods are presented in Section 3.0, including technology-specific objectives in Section 3.5; and results are discussed in Section 4.0. Resulting conclusions and recommendations from the Phase 1 testing are summarized and discussed in Section 5.0.

1.1 Hanford Site Background

The Hanford Site consists of an area approximately 1,517 km^2 (568 mi^2) located within the Pasco Basin along the Columbia River, Washington state. The Central Plateau (Figure 1.2.) is in the central portion of the Hanford Site, including the 200 Areas, where historical chemical separation and waste management activities took place during the production era, resulting in nearly 1,100 waste sites, including ponds, cribs, ditches, trenches, tanks, and others. To support waste site remediation, more than 15 source OUs have been established in the 200 Areas of the Central Plateau (Figure 1.3). Some of the contaminants at these waste sites have migrated to the DVZ to depths where they continue to impact underlying groundwater and contribute to groundwater plumes and, therefore, require remedial action. The Central Plateau DVZ is defined as the sediment below the practical depth of typical surface-based remedies (e.g., excavation or surface engineered barrier influence), approximately 15 m (50 ft) below ground surface (bgs), and above the water table, which is located approximately 76 m (250 ft) bgs in the western portion of the Central Plateau.

The primary DVZ contaminants at the Central Plateau driving long-term risk are Tc-99 and U because of their potential adverse health effects, persistence in the environment, high inventory in the VZ, mobility, complex subsurface behavior, and long half-lives (DOE/RL-2011-102). Additional contaminants of interest in the VZ include iodine-129, hexavalent chromium [Cr(VI)], nitrate, and cyanide (CN^-) due to their mobility and historical discharges.

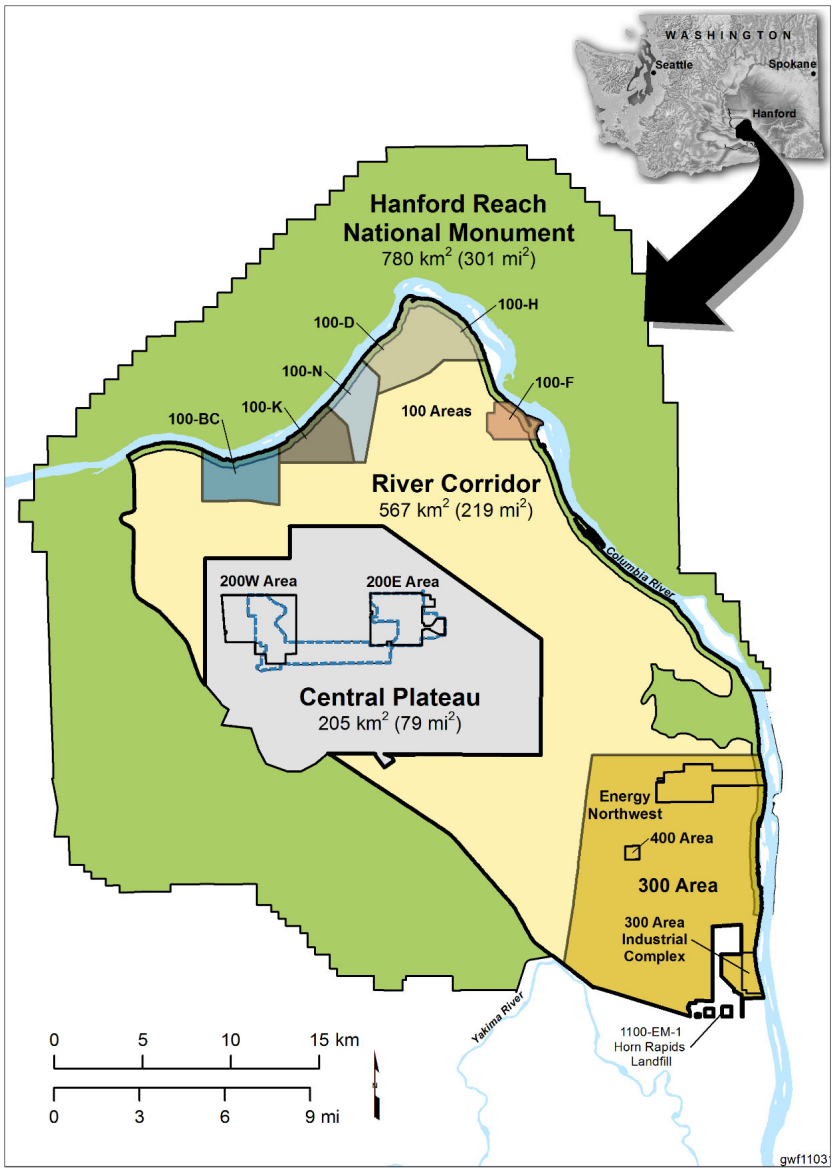

Figure 1.2. Major areas of the Hanford Site: River Corridor and Central Plateau (DOE/RL-2021-01, Rev. 0).

1.2 200-DV-1 Operable Unit Waste Sites and Geology

The 200-DV-1 OU, located in the Central Plateau of the Hanford Site, was established in 2010 to address DVZ contamination at 43 waste sites based on (1) the unique remediation challenge of mobile contamination in the DVZ, (2) the complex technical and regulatory challenges of DVZ contamination (e.g., co-mingled plumes, and determining nature and extent), and (3) the geographic proximity to waste management areas (WMAs) (DOE/RL-2011-102). These waste sites are primarily the cribs and trenches associated with the single-shell tank (SST) farms, B-BX-BY (B Complex), T-TX-TY (T Complex), and S-SX (S Complex) Tank Farm WMAs (Figure 1.4). Contaminant and hydraulic characterization of select cores from the T Complex, B Complex, and S Complex areas have been summarized previously (PNNL-27524; PNNL-27846; PNNL-26266; PNNL-26208).

The 200-DV-1 OU also includes a perched water zone below the B Complex (referred to as the 200-DV-1 OU perched water), located in the DVZ above a fine-grained unit (perching silt layer) that overlies the unconfined regional aquifer in the 200-BP-5 OU, near a depth of 225 ft bgs with a saturated thickness of about 12 ft at the highest location (PNNL-27846; PNNL-26208). The perched water zone contains elevated levels of uranium (U), Tc-99, nitrate, and other contaminants of concern as compared to interconnected groundwater. Characterization of select cores from the perched water has been summarized previously (PNNL-27524; PNNL-34300). Extraction of the contaminated water from this zone was initiated following the issuance of DOE/RL-2014-34, *Action Memorandum for 200-DV-1 Operable Unit Perched Water Pumping/Pore Water Extraction in 2014*. Extraction from this zone has been limited due to the hydraulic properties and relatively thin saturated thickness of the perched water zone. Therefore, *in situ* treatment of the contaminants in this zone is of interest to support the RI/FS process.

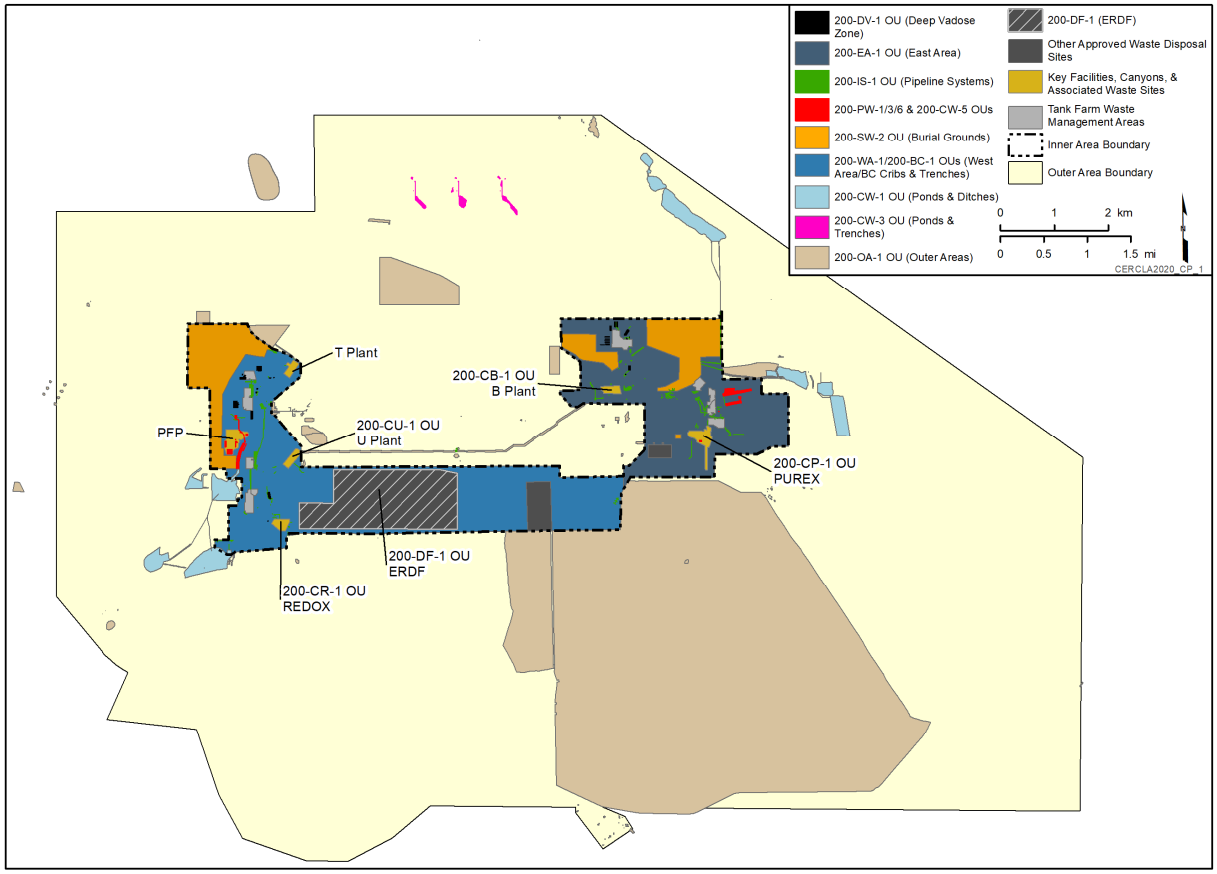

Figure 1.3. Source OUs in the Central Plateau (DOE/RL-2021-01).

200-DV-1 OU waste sites include process-based sites previously in the 200-TW-2 Tank Waste Group, the 200-TW-1 Scavenged Tank Waste Group, and the 200-PW-5 Fission Product-Rich Process Waste Group. Generally, these sites were used for disposal of waste associated with plutonium-separation operations at B and T Plants, REDOX plutonium and uranium separation at S Plant, uranium recovery and fission product scavenging at U Plant, and in-tank solidification operations at the Tank Farms (DOE/RL-2011-102). These waste sites were designed to percolate the waste into the soil column without exposure to the atmosphere via engineered systems, such as a reverse well, cribs, trenches, French drains, and a health instrument shaft. In addition to these historical waste management activities, the DVZ contamination in

these waste sites also resulted from past leaks in the SST farms or, in some cases, liquid waste sent to SSTs that overflowed to the waste sites.

The initial evaluations of the waste sites for development of the scope for RI/RFI indicated that relatively immobile contaminants such as cesium-137 and strontium-90 at these sites are most likely retained near the point of discharge. For example, in some waste sites, these contaminants were identified in the upper 4.6 m (15 ft) of the surface (DOE/RL-2011-102). Primary contaminants of interest (PCOIs), therefore, have been identified based on contaminant mobility, process knowledge of Hanford Site operations, documented contaminant waste inventories and discharge volumes for DVZ sites, Central Plateau groundwater plumes, and VZ characterization (DOE/RL-2017-58). While a definitive list of DVZ contaminants of concern has not been determined, for the technology evaluations and the purposes of the treatability study, PCOIs of moderate to high mobility have been selected (Table 1.1), with Tc-99 and U identified as the primary risk-drivers, as mentioned above.

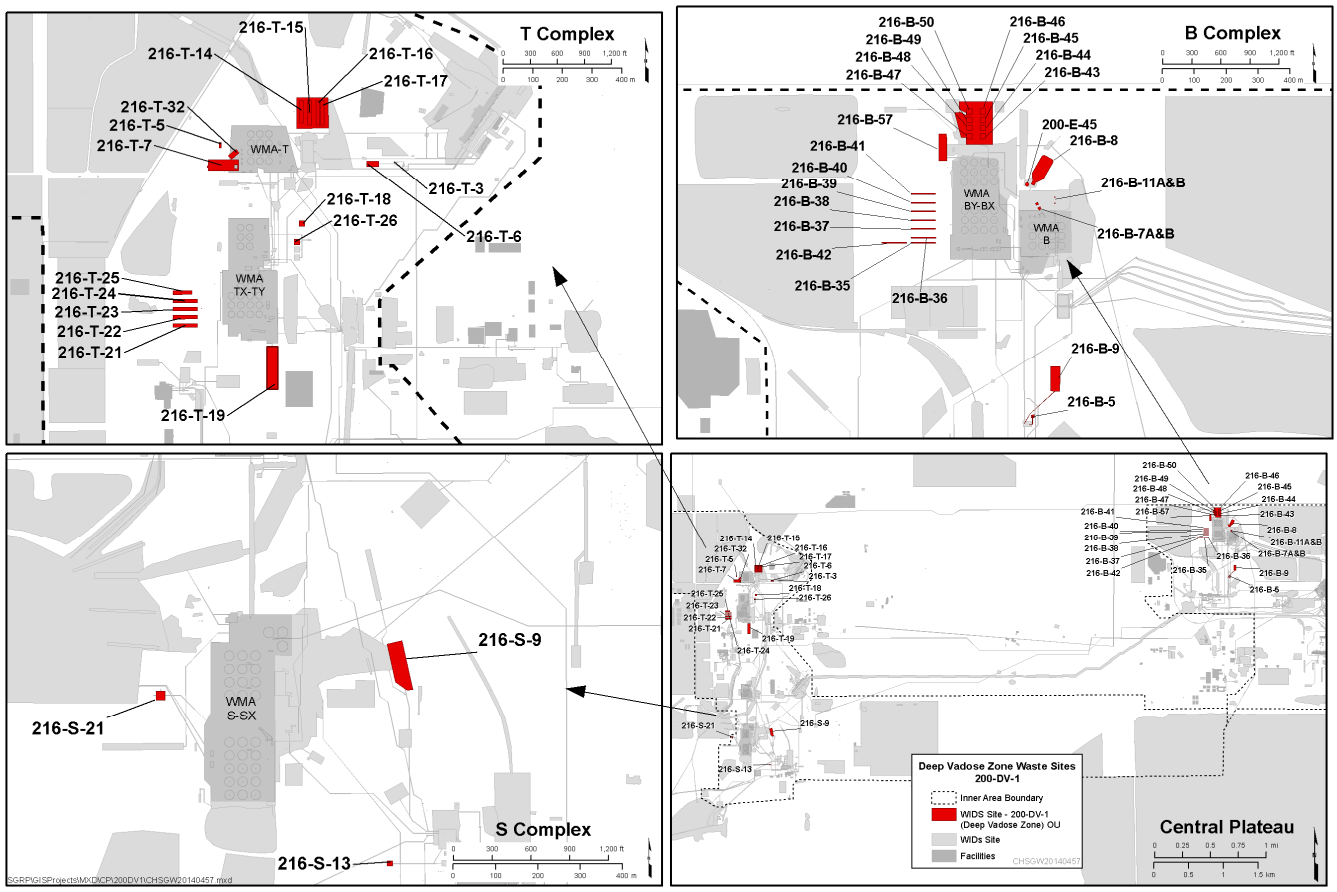

Figure 1.4. 200-DV-1 OU waste sites in the Central Plateau, adapted from DOE/RL-2011-102.

The geology of the Hanford Site has been extensively studied and characterized during previous investigations and is important for the treatability study to enable site specificity in testing approaches (e.g., PNNL-30443; PNNL-14202; DOE/RL-2011-01). Figure 1.5 presents the generalized stratigraphic column for the Hanford Site as well as the columns for the B Complex, T Complex, and S Complex areas. To provide site-specific evaluations of the selected technologies for the identified application methods (i.e., VZ, PRB, and perched water zone applications), specific sediments of geologic units targeted for application were identified for testing in various phases of the treatability study (more information is

given in Section 2.0). Sediments were identified from previous characterization efforts, which include information on geochemical, physical, and hydraulic properties of 200-DV-1 sediments (PNNL-27524; PNNL-34300; PNNL-27846; PNNL-26208).

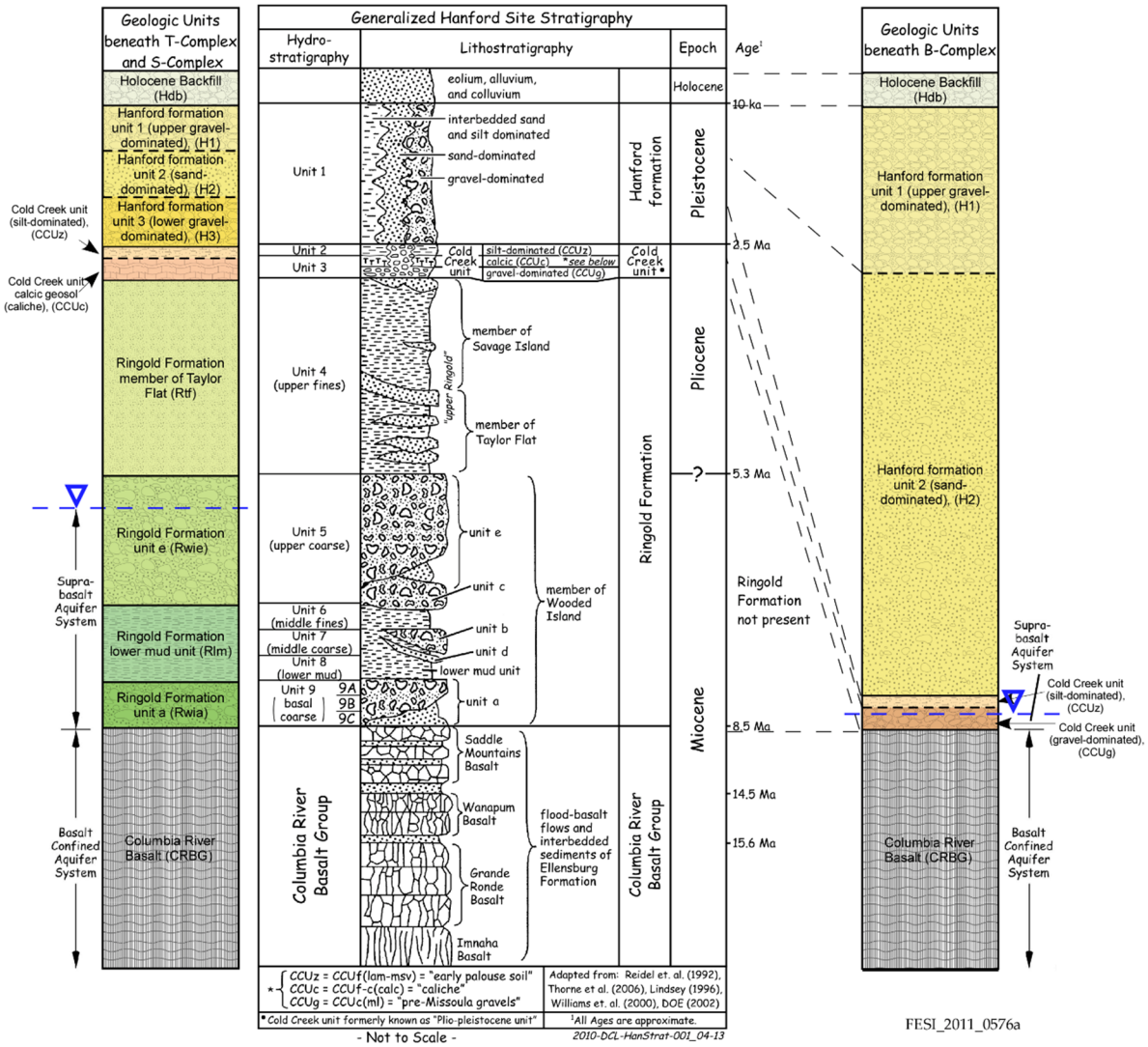

Figure 1.5. Stratigraphic and hydrostratigraphic columns for the B Complex, T Complex, and S Complex areas (DOE/RL-2011-102).

2.0 Potential 200-DV-1 OU Remediation Technologies

Each of the nine technologies selected for testing as part of the treatability study (Table 1.1) are presented in the following sections, with gas-phase technologies presented in Sections 2.1, 2.2, and 2.3; followed by particulate-phase technologies presented in Sections 2.4, 2.5, and 2.6; and ending with liquid-phase technologies in Sections 2.7, 2.8, and 2.9. For each technology, the chosen amendments are described, including the targeted mechanisms and processes for reduction and sequestration, the potential locations of application, and the PCOIs and CoCOIs.

2.1 Gas-Phase Bioreduction and Sequestration – Organic gases and carbon dioxide (CO_2)

This technology is focused on stimulating microbial activity to generate reducing conditions followed by chemical sequestration with treatment with carbon dioxide gas to form calcite and immobilize the PCOI Tc-99 with co-contaminants of interest (CoCOIs) including U, Sr-90, I-129, Cr(VI), and nitrate via injection of gas-phase amendments in two steps (Table 1.1). The concept for this two-step gas-phase amendment technology is to sequester contaminants through an initial reductive precipitation step followed by a combination of adsorption, precipitation, and coating with calcite minerals (Figure 2.1). These amendments have been identified for *in situ* remedy applications in the unsaturated VZ in the 200-DV-1 OU, including a primary treatment zone in the BY Cribs waste sites with secondary treatment zones including the BC Cribs and Trenches. Gas-phase amendments can be delivered to the VZ without injection of additional liquids that may mobilize contaminants and may have physical properties that allow for more uniform delivery (WSRC-MS-2005-00589; Muller et al. 2021a).

The first step is to introduce a nontoxic organic gas (ethane, butane, or butyl acetate) to stimulate natural microbes in sediments to generate conditions for reduction of pertechnetate ($Tc(VII)O_4^-$) in pore water, which results in Tc(IV) precipitates, e.g., TcO_2 (Figure 2.1). For this treatability study and based on the available information on the potential amendments, three different reactive gases were selected for the initial phase of testing for this technology: (1) ethane, (2) ethyl acetate, and (3) butane. Because Tc(IV) may be readily oxidized once the pore water system oxidizes, a second gas (CO_2) is introduced to precipitate calcite, which will coat some of the Tc(IV) precipitate (Figure 2.1b). This second step is needed because an effective VZ remediation technology should immobilize a significant portion of the contaminant for an extended period to decrease the mobilization potential to groundwater.

Gas-phase remediation of Tc-99 [as $Tc(VII)O_4^-$] has previously been shown to be effective in laboratory studies using a reductive gas (H_2S); however, similar to water-saturated systems, once the system becomes oxic, nearly all of the Tc-99 is re-oxidized (PNNL-20004; Szecsody et al. 2012, 2015). However, H_2S gas treatment followed by NH_3 gas treatment promotes alkaline mineral dissolution and re-precipitation where most of precipitated Tc-99 remains immobile. The TcO_2 precipitates formed by reduction with H_2S were coated with aluminosilicates as a result of secondary precipitation caused by the NH_3 gas (PNNL-20004; Szecsody et al. 2012). Because of concerns about using a toxic reductive gas (H_2S) at field scale, this study evaluated the use of nontoxic, organic gases (ethane, butane, and butyl acetate) to generate reducing conditions from biostimulation.

A recent evaluation of this combined organic gas and CO_2 technology in batch experiments showed that sediments from the Hanford Site 200-ZP-1 OU were effectively reduced following biostimulation with pentane and butyrate, which resulted in a 90% reduction of Tc-99 (Bagwell et al. 2020) in the absence of NO_3 as a CoCOI. During subsequent CO_2 injection to precipitate calcite, most of the reduced Tc-99 was sequestered, which prevented reoxidation and remobilization. In contrast, reducing conditions were generated more slowly in sediments from the Hanford BY Cribs by the addition of pentane or butyrate,

and only about 10% of the Tc-99 was reduced (Bagwell et al. 2020). After subsequent CO_2 injection, 2% to 10% of the reduced Tc-99 was sequestered and was not remobilized. Although these preliminary studies are promising, there is a need to determine the effectiveness of sequential treatment with organic gas followed by CO_2 with Tc-99 and CoCOI concentrations and mixtures that occur at specific areas of the Hanford Site (i.e., BC Cribs, BY Cribs, 216-U-8 Cribs).

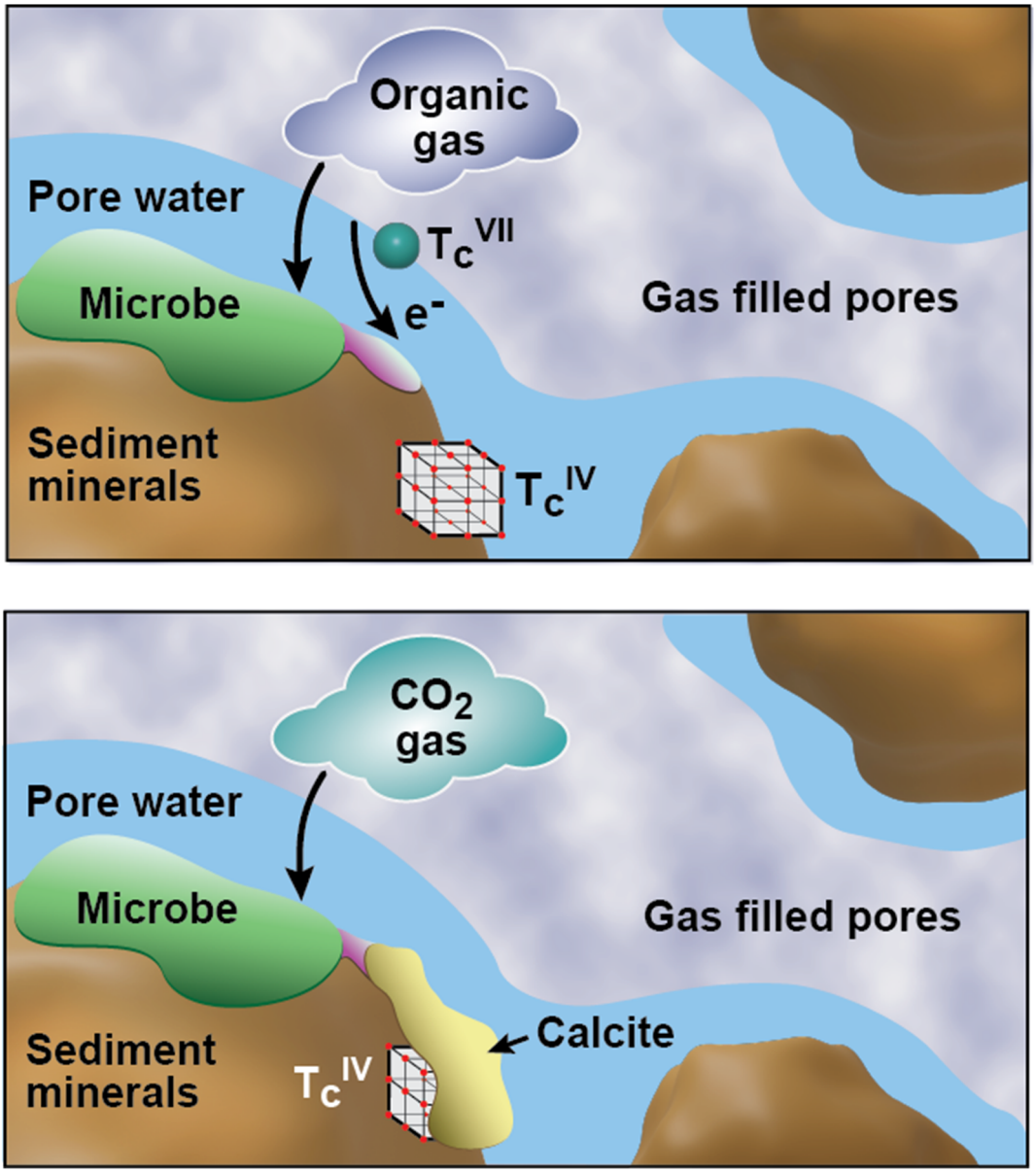

Figure 2.1. Conceptual diagram of bioreduction and sequestration of Tc-99 in VZ pore water via a two-step process: (1) injection of organic gas to partition into pore water, stimulating microbial activity and generating reducing conditions, and directly or indirectly reductively precipitating aqueous $Tc(VII)O_4$; and (2) injection of CO_2 gas, carbonate partitioning into pore water, and precipitation of calcite that coats Tc(IV) precipitates.

The objectives of this study were to quantify (1) the effectiveness of the different organic gases at decreasing mobility of Tc-99 as $Tc(VII)O_4^-$ by reduction, (2) the extent to which subsequent CO_2 gas treatment decreases TcO_2 reoxidation by coating, and (3) the effect of CoCOIs [U, Sr-90, I-129, Cr(VI), NO_3] on Tc-99 sequestration.

2.2 Gas-Phase Bioreduction – Organic gases

This technology is focused on stimulating microbial activity in VZ sediments via injection of organic gaseous amendments to act as electron donors for microbial reduction (Table 1.1). Microbial NO_3 reduction (denitrification) is an anaerobic respiratory process whereby NO_3 is sequentially reduced to gaseous products, principally dinitrogen gas (N_2). Dissimilatory NO_3 reduction to ammonium (DNRA) can be a competing pathway for NO_3 reduction, resulting in the production and accumulation of ammonium (NH_4). DNRA can be the predominant pathway for NO_3 reduction under high organic carbon loading and low NO_3 levels, which is unlikely to reflect *in situ* conditions for organic gas treatment in the unsaturated zone. The PCOI is NO_3 with CoCOIs including Cr(VI) and CN^-. For the PCOI, the objective is to convert NO_3 to nitrogenous gaseous products as shown in Figure 2.2. Although primary treatment zones have not been identified in the 200-DV-1 OU, unsaturated areas of sites with NO_3 and CoCOIs include S and T Cribs with Cr(VI) contamination and BY Cribs with CN^- contamination. Gas-phase amendments can be delivered to the VZ without injection of additional liquids that may mobilize contaminants and may have physical properties that allow for more uniform delivery (WSRC-MS-2005-00589; Muller et al. 2021a).

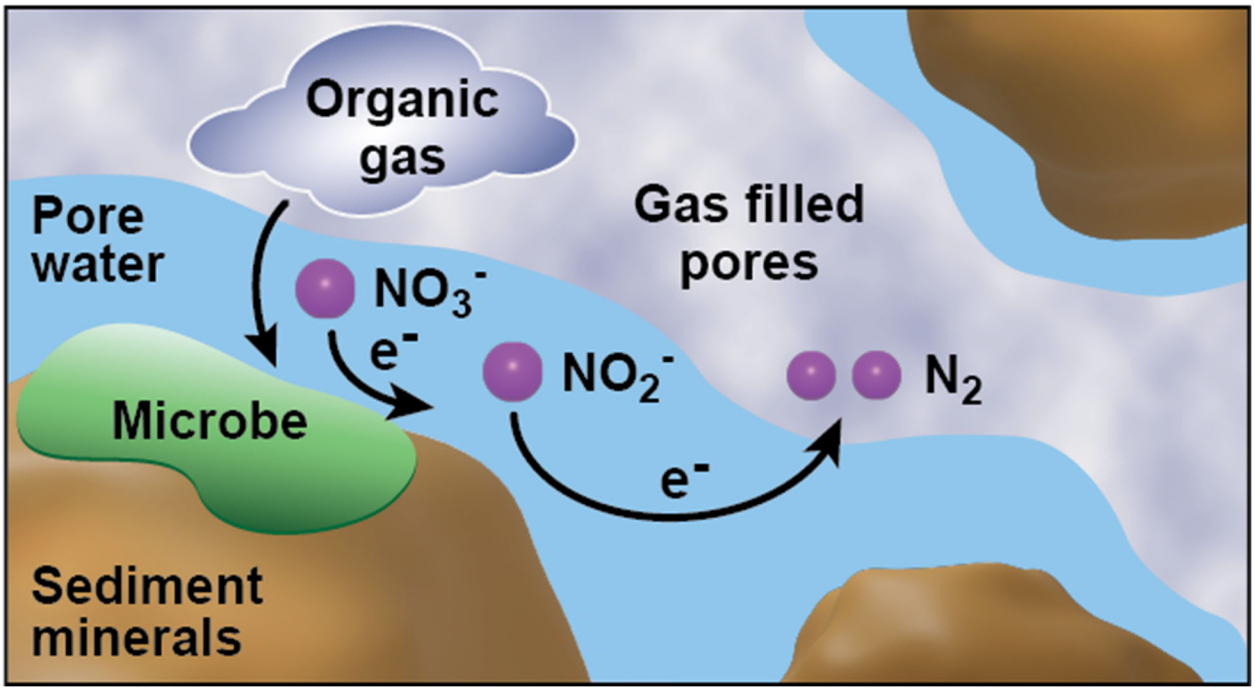

Figure 2.2. Conceptual diagram of bioreduction of aqueous NO_3^- in VZ pore water following the introduction of an organic gas to stimulate microbial activity and generate reducing conditions to turn NO_3^- into gaseous nitrogenous end products.

The application of gas-phase carbon amendments has been successfully demonstrated for stimulating subsurface microbial communities for the bioremediation of organic and inorganic contaminants in the VZ (Evans and Trute 2006; WSRC-MS-94-0323). Evans and Trute (2006) compared the effectiveness and deliverability of a variety of gaseous electron donors in sediment columns. Gaseous substrates with

favorable transport properties were shown to activate sediment microbial communities to respire perchlorate and NO_3 to nontoxic products (WSRC-MS-94-0323).

For Hanford Site-specific applications, a scoping test of gas-phase bioreduction was conducted using a series of gaseous and volatile liquid substrates (PNNL-28055). The results indicated that the Hanford Site's DVZ likely has adequate conditions (e.g., nutrients and baseline microbial communities) to support *in situ* microbial remediation. For this scoping test, microbiological reduction of Hanford Site sediments was achieved at two different volumetric water contents (WCs, 4% and 8%) for nearly all substrates evaluated. Butyrate, pentane, ethane, hydrogen, and butyl acetate generated a rapid microbial response and achieved reducing conditions within 5 days following treatment. Microbial responses were generally faster and more consistent at 8% volumetric WC compared to 4%. The results indicate the importance of substrate selection, aqueous thin films, and pore-scale water connectivity to elicit a rapid microbiological response to gaseous substrates. Nutrient amendments (with high humidity to avoid desiccation) will need to be carefully considered for sustained activity and to increase the treatment zone of influence in DVZ sediments. Based on previous results (PNNL-28055), gas-phase bioremediation may be an effective treatment to reduce the mass of NO_3 and to immobilize Cr(VI) as a targeted treatment for a continual source.

Brockman et al. conducted bench-scale studies to evaluate the feasibility of injecting gas-phase hydrocarbons and nutrients into the DVZ at the Hanford Site to stimulate microbial activity (PNNL-14535). Sediments (n = 24) from the 216-Z-9 Trench were amended with a gas mixture containing equal amounts of methane, ethane, propene, propane, and butane, along with gaseous nitrogen (i.e., N_2O). Efficient hydrocarbon consumption and microbial stimulation was reported for 19 of 24 sediments evaluated. In Evans et al. (2011), liquefied petroleum gas (LPG; injected as 79% N_2, 10% H_2, 10% LPG, 1% CO_2), which is composed primarily of propane, propene, butane, and butylene in various mixtures, was shown to stimulate nitrate/nitrite (NO_3^-/NO_2^-) bioreduction in a field test site in California (Evans et al. 2011), where nitrate and nitrite concentrations were reduced by over 90%. Both of these studies suggest that the use of gaseous hydrocarbons to increase microbial activity may be viable for an *in situ* treatment approach to Hanford DVZ sediments.

The objectives of this study were to determine the overall effectiveness of organic gases to stimulate soil microbial populations for the effective transformation of nitrate to gaseous nitrogen end products. Several organic gases having physical attributes that favor deliverability were evaluated for biostimulation of Hanford Site sediments. In addition, the effect of CoCOIs on nitrate reduction was evaluated.

2.3 Gas-Phase Sequestration – Carbon dioxide (CO_2)

This technology is focused on the gas-phase chemical sequestration of I-129 as the PCOI using CO_2 gas with U, Sr-90, Tc-99, and Cr(VI) as CoCOIs (Table 1.1). The mechanism for sequestration requires CO_2 gas partitioning into VZ sediment pore water, increasing dissolved carbonate, and eventually precipitating calcite (Figure 2.3). Calcite can incorporate some iodate (IO_3^-) into the structure. Note that although CO_2 supplies sufficient carbonate, the calcium needs to come from ion exchange sites on sediments. This treatment is targeting unsaturated zones under the 216-S-9 waste site. Gas-phase amendments can be delivered to the VZ without injection of additional liquids that may mobilize contaminants and may have physical properties that allow for more uniform delivery (WSRC-MS-2005-00589; Muller et al. 2021a). Sites that received significant acidic waste, such as 216-U-8 Crib (PNNL-29650; Szecsody et al. 2013), may be depleted in calcium and carbonate, as acids have dissolved and flushed ions to greater depth (Szecsody et al. 2013), making these sites less amenable to this technology. Potential secondary treatment zones include the 216-A-10, 216-A-5, and 216-S-7 waste sites.

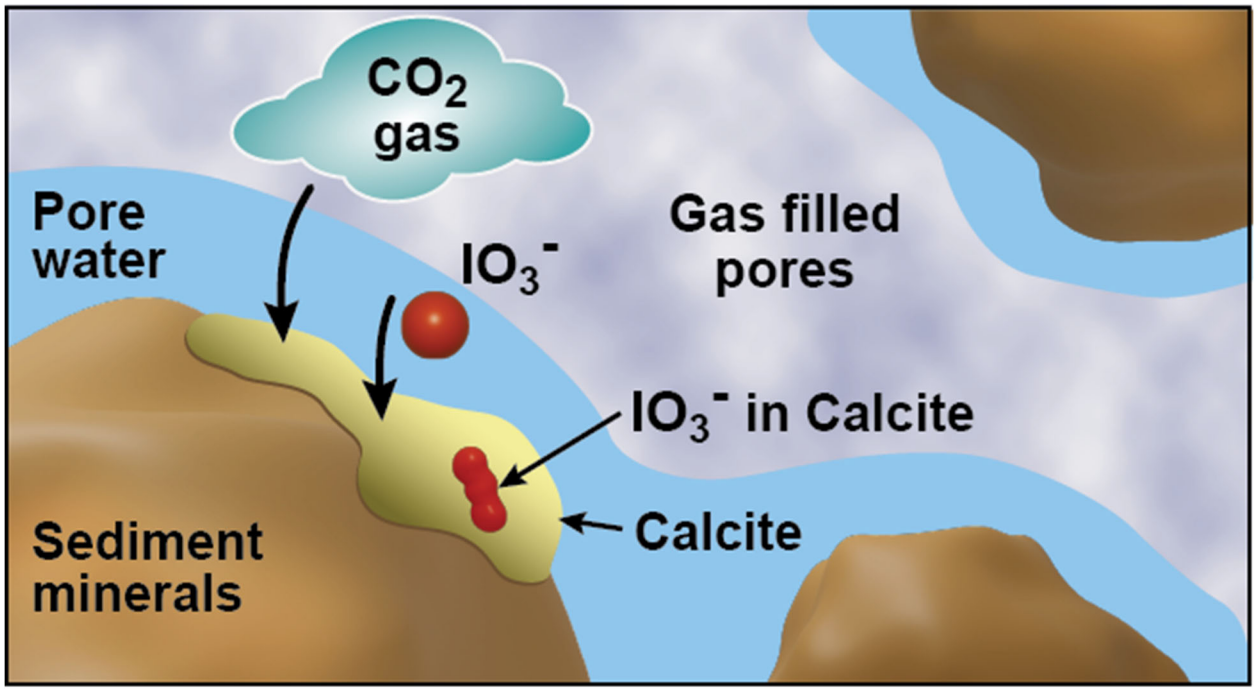

Figure 2.3. Conceptual diagram of I-129 sequestration in VZ porewater as a result of CO_2 gas injection, partitioning of carbonate into pore water, and subsequent calcite precipitation with simultaneous incorporation of aqueous IO_3^- and coating of adsorbed I species.

A recent evaluation of iodate incorporation into precipitating calcite targeted aqueous phase precipitation via concentrated $CaCl_2$ or $Ca(OH)_2$ and $NaCO_3$ solutions in metasilicate gel (Lawter et al. 2018). That study showed that a small fraction of IO_3^- (starting concentration 100 to 500 µg/L) was removed during precipitation of calcite. The fraction of IO_3^- removed from solution was small: (1) 100 µg/L IO_3^- initially, 0.28 µg/g in calcite; (2) 250 µg/L IO_3^- initially, 0.69 µg/g in calcite; and (3) 500 µg/L IO_3^- initially, 1.6 µg/g in calcite. In an older study, CO_2 gas was used to successfully decrease uranium mobility (i.e., presumed to be co-precipitation of uranium in calcite) in unsaturated sediments at 4% and 16% WC (Szecsody et al. 2012). In a more recent study, CO_2 gas was used to incorporate 25% to 60% of IO_3 into precipitating calcite (McElroy et al. 2020).

The objectives of this study were to quantify (1) the effectiveness of CO_2 gas treatment at decreasing the mobility of I-129 by co-precipitation with calcite and (2) the impact of CoCOIs [U, Tc-99, Cr(VI), Sr-90, and nitrate] on I-129 sequestration. Uncontaminated Hanford formation (Hf) sediment and contaminated vadose sediment from under the 216-S-9 Crib (primary treatment target) were used in this technology, as well as variably saturated systems.

2.4 Particulate-Phase Chemical Sequestration – Sn(II) -PO_4

This technology is focused on chemical sequestration, including U and Tc-99 as PCOIs and Sr-90, I-129, Cr(VI), and nitrate as potential CoCOIs, via injection of a solid phase particulate amendment [i.e., Sn(II)-PO_4] (Table 1.1). Conceptually, Tc-99 and U are reduced in the presence of the Sn(II) apatite, then coated by apatite or incorporated into apatite (Figure 2.4). Solid Sn(II)-PO_4 has been identified for *in situ* remedy applications in water-saturated areas, with primary treatment zones in the 200-DV-1 OU including the perched water zone at the B Complex area and/or the top of the unconfined aquifer beneath the BY Cribs (potentially applied as a PRB at the water table). Secondary treatment zones in the Central Plateau may include 216-U-1&2, S-SX Tank Farm, C Tank Farm, and BC Cribs and Trenches, where U

and/or Tc-99 are also PCOIs. A previously developed conceptual model suggests significant U and Tc-99 contamination in the VZ in the B Complex within 20 ft of the water table, which may influence ultimate remedial decisions (PNNL-19277).

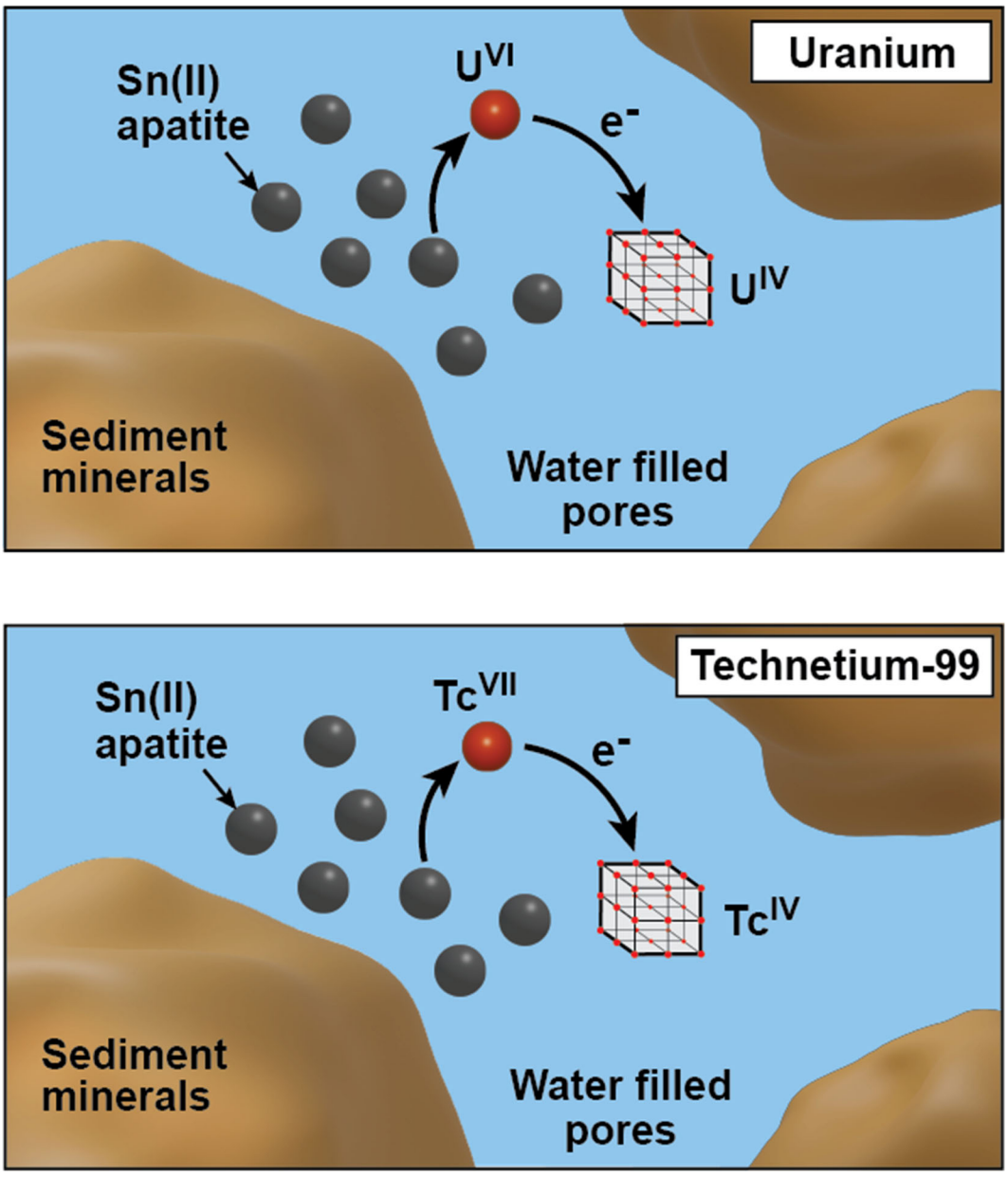

Figure 2.4. Conceptual diagram of sequestration of U (*top*) and Tc-99 (*bottom*) Sn(II)-PO_4: U(VI) or Tc(VII)O_4^- reduction and precipitation of U(IV)/Tc(IV); the reduction step is likely followed by a second, more permanent mechanism such as subsequent coating of the U(IV) or Tc(IV) by apatite or incorporation of U or Tc-99 in the apatite structure, but this mechanism is currently unknown.

Laboratory testing using solid phase Sn(II)-PO_4 has shown potential for recovery and sequestration of Tc-99 from low-activity waste simulants and for getters in cementitious waste forms (Asmussen et al. 2016, 2018; RPP-53855). Sn(II)-PO_4 potentially incorporates two mechanisms of removal via adsorption and incorporation into hydroxyapatite and reduction via Sn(II) [reduction potential of Sn(IV) to Sn(II) is 0.384 V].

Testing has not been conducted under conditions representative of the Central Plateau subsurface. Sn(II)-PO_4 has not been directly evaluated for uranium sequestration; however, apatite (with no tin substitution) has been used to sequester uranium (Wellman et al. 2005). Moreover, it is expected that the Sn(II)-PO_4 will also sequester uranium, although the stannous tin [Sn(II)] may reduce U(VI) aqueous phases and, therefore, slow precipitation of U(VI)-PO_4 precipitates. A treatability study successfully jet-injected solid phase apatite in the field at 100-NR-2 OU for sequestration of strontium-90 (SGW-47062). In this case, the pre-formed apatite was a powdered fishbone, Na-PO_4, or a mixture of both materials that was jet-injected a few feet into the subsurface using water as a delivery fluid. However, depending on the particulate size and properties, other delivery fluids (e.g., xanthan gum) may be required to improve subsurface distribution of particulate amendments. The mass of jet-injected phosphate materials decreased significantly within a few feet of the injection well (PNNL-19524).

COI uptake using solid phase Sn(II)-PO_4 has yet to be demonstrated for PCOIs in the presence of CoCOIs. It is anticipated that redox-sensitive CoCOIs will decrease Sn(II)-PO_4 reactivity for Tc(VII)O_4^- and may slightly increase the mobility of iodine-129.

The objectives of this study were to quantify (1) the effectiveness of Sn(II)-PO_4 for U and Tc-99 sequestration and (2) the impact of CoCOIs [Sr-90, I-129, Cr(VI), and nitrate] on U and Tc-99 sequestration.

2.5 Particulate Phase Chemical Sequestration – Bismuth oxyhydroxide and bismuth subnitrate

This technology is focused on chemical sequestration, including U and Tc-99 as PCOIs and Sr-90, I-129, Cr(VI), and nitrate as potential CoCOIs, via injection of bismuth (Bi)-based solid phase particulate amendments [i.e., bismuth oxyhydroxide (BOH) or bismuth subnitrate (BSN)] (Table 1.1). Solid Bi-based materials have been identified for *in situ* remedy applications in water-saturated areas, with primary treatment zones in the 200-DV-1 OU, including the perched water zone at the B Complex area and/or the water table beneath the BY Cribs (potentially applied as a PRB). Some secondary treatment zones in the Central Plateau may also include 216-U-1&2, S-SX Tank Farm, C Tank Farm, and BC Cribs and Trenches, where U and/or Tc-99 are also PCOIs. A previously developed conceptual model suggests significant U and Tc-99 contamination in the VZ below the B Complex within 20 ft of the water table, which may impact ultimate remedial decisions (PNNL-19277).

Bi-based materials can form a variety of layered and cluster structures that can accommodate a wide variety of cations and anions (Levitskaia et al. 2022; Perumal et al. 2022). Bismuth materials have been shown to remove contaminants, including uranium (U) as uranyl carbonate complexes [e.g., at pH 8, $Ca_2UO_2(CO_3)_3$ and $CaUO_2(CO_3)_3^{2-}$], technetium (Tc-99) as TcO_4^-, hexavalent chromium (Cr) as chromate (CrO_4^{2-}), and iodine (I) as iodate (IO_3^-), from a variety of geochemical environments (Lawter et al. 2021; Moore et al. 2020; Pearce et al. 2020). Sequestration of Tc-99 and U by BSN or BOH is shown in Figure 2.5, with adsorption of Tc-99 as Tc(VII)O_4^- and incorporation of U(VI) into interlayers of the Bi-materials, which are both expected to transform to bismutite ($Bi_2CO_3O_2$) under the expected geochemical conditions.

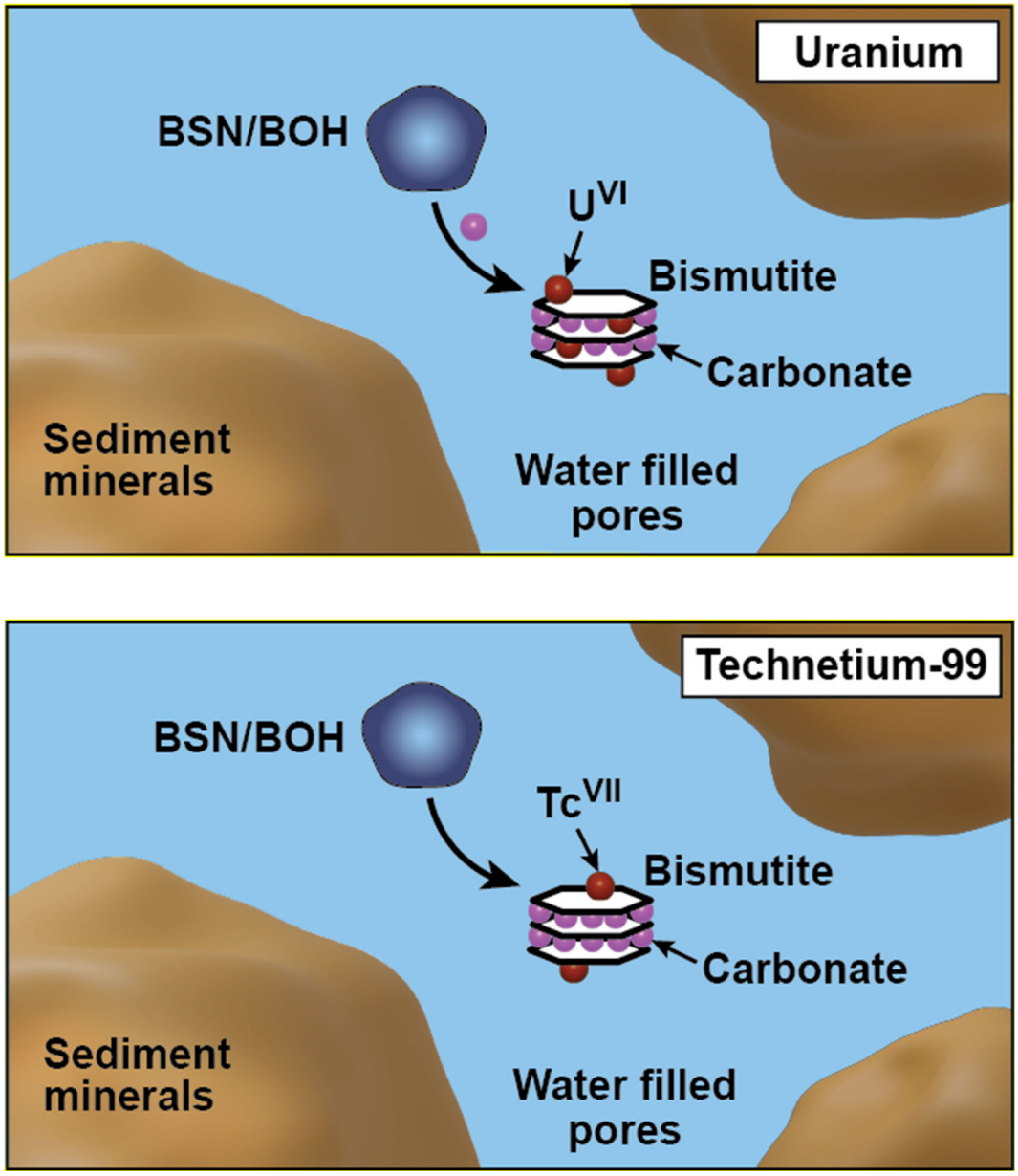

Figure 2.5. Sequestration of U (*top*) and Tc-99 (*bottom*) by Bi materials (BSN or BOH): transformation of BSN or BOH to bismutite and subsequent incorporation of U(VI) into the bismutite layers, or adsorption of U(VI) or $Tc(VII)O_4^-$ to the surface of the bismutite.

Laboratory research using solid phase BOH and BSN has shown potential for U and Tc-99 recovery and sequestration from solution in a variety of geochemical environments (Lawter et al. 2021), but these materials have not been fully evaluated for U or Tc-99 sequestration under the targeted conditions for the 200-DV-1 OU (e.g., specific sediment and contaminant mixtures). In addition, BOH has not been evaluated with delivery fluid. BSN has been evaluated for reactivity and suspendability (Muller et al. 2021b), but Cr(VI) was the only contaminant evaluated. Site-specific conditions (e.g., specific sediment and contaminant mixtures) as well as delivery fluid compatibility have yet to be evaluated for Bi-based materials.

The objectives of this study were to quantify (1) the effectiveness of BOH and BSN for U and Tc-99 sequestration and (2) the impact of CoCOIs [Sr-90, I-129, Cr(VI), and nitrate] on U and Tc-99 sequestration.

2.6 Particulate Phase Chemical Reduction – Zero valent iron/sulfur-modified iron and polyphosphate

This technology is focused on the particulate phase combined chemical reduction (with zero valent iron, ZVI, or sulfur-modified iron, SMI) followed by sequestration resulting from addition of Poly-PO_4 (i.e., sodium phosphate and sodium polyphosphate solution used to precipitate apatite), which precipitates apatite (Figure 2.6 and Figure 2.7 for Tc-99 and U, respectively) (Table 1.1). This technology is targeting two PCOIs (Tc-99 and U) and Sr-90, I-129, nitrate, and Cr(VI) as potential CoCOIs. This technology functions via injection of a solid phase amendment (1- to 5-micron particle sized ZVI or SMI) with a high-viscosity, shear-thinning delivery fluid (e.g., xanthan) to advect reactive particulates into sediments from an injection well. PRB walls of ZVI have also been created using a trenchless technique of vertically slotted wells and high-pressure injection of ZVI using guar gum as the delivery agent. These can extend 15 ft from the injection well (azimuth oriented vertical hydraulic fracturing and vertical inclusion propagation – VIP, also known as the GeoSierra PRB installation method). Once emplaced, the ZVI/SMI temporarily reduces/precipitates contaminants if reduction can occur within the residence time of contaminants in the relatively thin ZVI/SMI wall. This treatment is followed by injection of a liquid amendment (Poly-PO_4) to precipitate apatite that may either incorporate contaminants or coat precipitated contaminants. This combined treatment has been identified for *in situ* remedy applications in water-saturated areas, with primary treatment zones in the 200-DV-1 OU, including the perched water zone at the B Complex area and/or the water table beneath the BY Cribs (potentially applied as a PRB). Secondary treatment zones in the Central Plateau may also include 216-U-1&2, S-SX Tank Farm, C Tank Farm, and BC Cribs and Trenches, where U and/or Tc-99 are also PCOIs. A previously developed conceptual model suggests significant U and Tc-99 contamination in the VZ below the B Complex within 20 ft of the water table, which may impact ultimate remedial decisions (PNNL-19277).

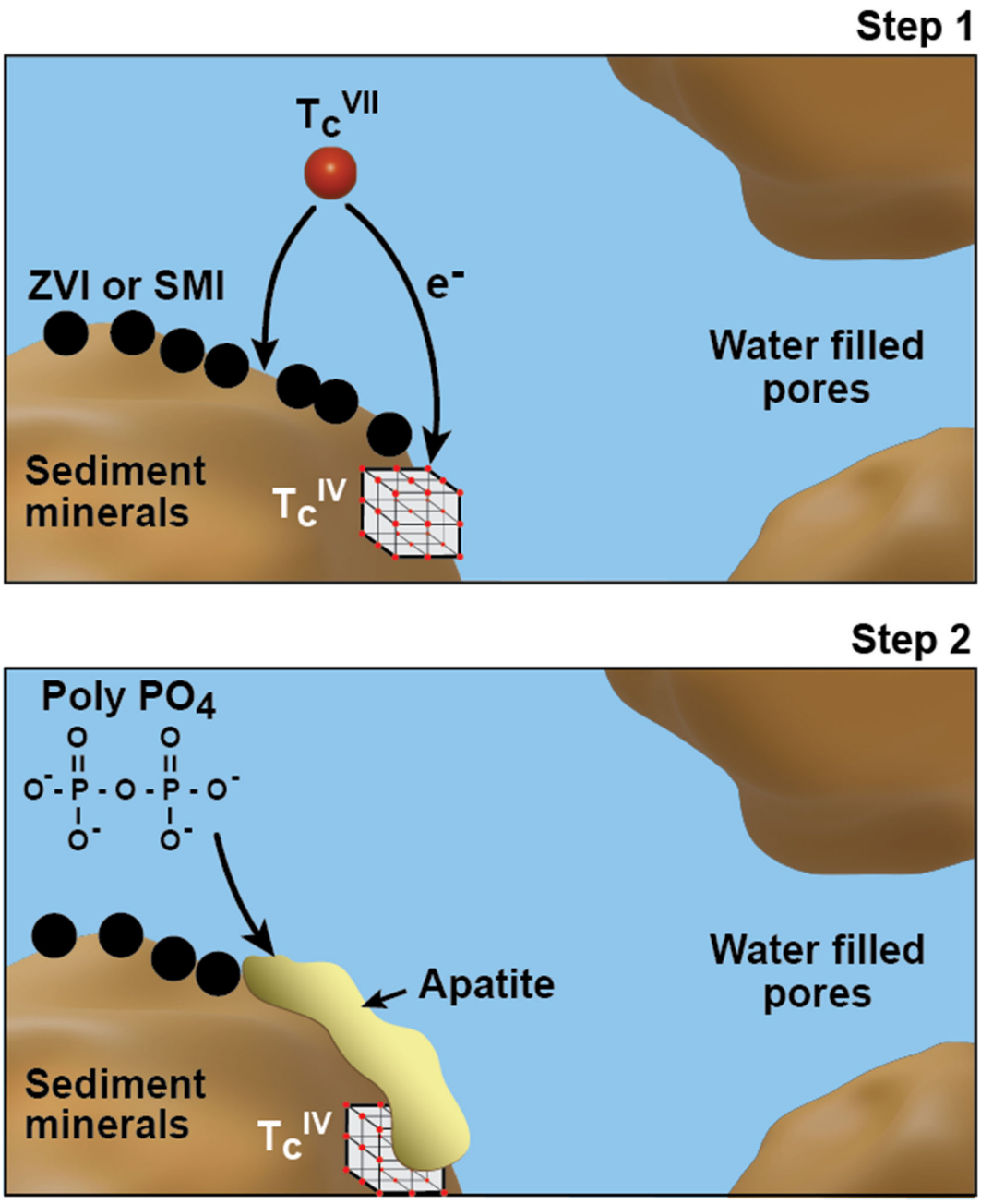

Figure 2.6. Conceptual diagram of sequestration of Tc-99 in the saturated zone by treatment with ZVI or SMI particles to stimulate reducing conditions followed by Poly-PO_4 (*top*) aqueous $Tc(VII)O_4^-$ reduction and precipitation as Tc(IV) with (*bottom*) subsequent coating of Tc(IV) by apatite following treatment with Poly-PO_4.

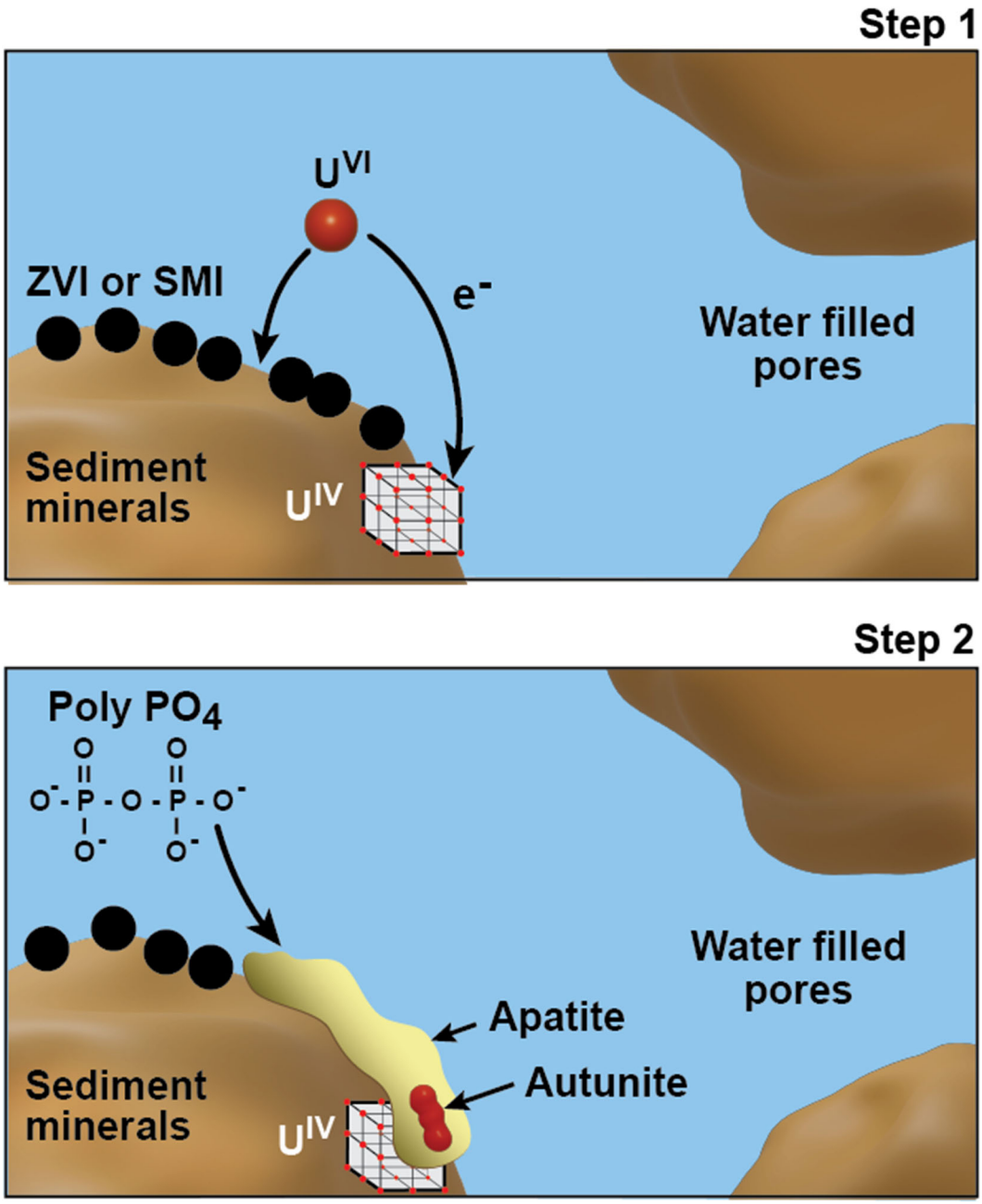

Figure 2.7. Conceptual diagram of sequestration of U in the saturated zone by treatment with ZVI or SMI particles followed by Poly-PO_4 (*top*) reduction of aqueous and adsorbed U(VI) species and precipitation of U(IV), (*bottom*) subsequent coating of U(IV) by apatite and/or incorporation of U(VI) species in apatite and autunite following treatment with Poly-PO_4.

In general, ZVI and SMI are electron donors that reduce $Tc(VII)O_4^-$ and aqueous U(VI) species, which form precipitates that are easily oxidized (and remobilized) (Szecsody et al. 2004). Following reaction of ZVI or SMI with PCOIs (with and without CoCOIs) and sediments, Poly-PO_4 is added. The subsequent addition of Poly-PO_4 results in precipitation of apatite, which can incorporate $U(VI)O_2^{2+}$ and precipitate on top of (i.e., coat) Tc^{IV} and U^{IV} species.

The oxidation steps for ZVI are generally outlined. Initial ZVI reactivity is slow due to an intrinsic passive (i.e., Fe oxide) layer, which can be eliminated by pretreatment before deployment (Guan et al. 2015). There is a loss in ZVI reactivity over time as metal hydroxide and metal carbonates precipitate on the ZVI surface. As metallic iron (Fe^0) ages (oxidizes), ferrous iron (Fe^{+2}) is created, which can adsorb to sediment minerals, form ferrous iron phases such as magnetite or green rust, or further oxidize to ferric (Fe^{3+}) minerals (Boglaienko et al. 2019, 2020; Emerson et al. 2020). While initial oxidation of Fe^0 is expected under aerobic conditions [Eq. (2.1)], anaerobic conditions [Eqs. (2.2) and (2.3)] will likely be reached within the first few days, likely allowing for oxidation by water or H^+ (de Lima Perini and Nogueira 2017). Further oxidation of ferrous iron phases results in ferric oxides and hydroxides such as hematite, depending on the pH and available ions. Moreover, the presence of trace sulfur in SMI has been shown to promote electron transfer and Fe^0 corrosion, including reduction of mineral surface Fe^{3+} by Fe^0 to Fe^{2+} [Eq. (2.4)] (Shao et al. 2018). Oxidation of sulfide also consumes significant hydroxide [Eq. (2.5)], which may be confirmed by measuring the pH over time.

$$2Fe^0 + O_2 + 2H_2O \rightarrow 2Fe^{2+} + 4OH^- \quad (2.1)$$

$$Fe^0 + 2H_2O \rightarrow Fe^{2+} + H_2 + 2OH^- \quad (2.2)$$

$$Fe^0 + 2H^+ \rightarrow Fe^{2+} + H_2 \quad (2.3)$$

$$Fe^0 + 2Fe^{3+} \rightarrow 3Fe^{2+} \quad (2.4)$$

$$H_2S + 8OH^- \rightarrow H_2SO_4 + 8e^- + 4H_2O \quad (2.5)$$

A recent evaluation of the combined ZVI/SMI treatment followed by phosphate treatment showed that the initial reduction step effectively decreased the aqueous concentration of Tc-99 and U, and the second apatite precipitation step may decrease Tc-99, U, and nitrate remobilization as the system oxidizes (PNNL-31959). Because that study was conducted in groundwater with no other contaminants, the effect of additional CoCOIs, which use ZVI/SMI reductive capacity, is not well understood. The impact of co-contaminants on reduction will likely be important based on previous research (Xin et al. 2020).

PCOIs undergo reduction with electrons from the ferrous iron generated by oxidation of from ZVI or SMI:

$$Tc^{VII}O_4^- + 3e^- + 4H^+ \rightarrow Tc^{IV}O_2(s) + 2H_2O \quad (2.6)$$

$$U^{VI}O_2^{2+} + 2e^- \rightarrow U^{IV}O_2(s) \quad (2.7)$$

where UO_2^{2+} is present as multiple uranyl carbonate complexes [i.e., at pH 8, $Ca_2UO_2(CO_3)_3$ and $CaUO_2(CO_3)_3^{2-}$]. The reduced Tc^{IV} may also be present as $Tc^{IV}S_x$ or other precipitates. The presence of multiple electron acceptors in a system has two effects on the reduction rate of PCOIs: (1) differences in the reductive potential needed to reduce different contaminants, and (2) the total reductive capacity needed to reduce contaminants. The presence of ZVI and SMI in sediment systems results in strong reducing conditions, with an Eh of -400 to -600 mV (Guan et al. 2015), respectively, which is sufficient to reduce all the PCOIs and CoCOIs in this study. These contaminants are reduced in order from contaminants that require minimal reducing conditions to promote electron transfer (IO_3^-) to contaminants that require stronger reducing conditions ($U^{VI}O_2^{2+}$)

$$IO_3^- > CrO_4^- > NO_3^- > \mathbf{TcO_4^-} > Fe^{III}(CN)_6^{3-} > UO_2^{2+} \quad (2.8)$$

Therefore, in a system that contains only the PCOIs (Tc-99 and U), all of the Tc-99 will be reduced first and more quickly, and if there is any electron donor left (i.e., reductive capacity), uranium will be reduced. If perched water is used with PCOIs, nitrate (in perched water) will be reduced first, then Tc-99, then U (i.e., the presence of nitrate slows and may prevent reduction of Tc-99 and U).

The objectives of this study were to quantify (1) the effectiveness of ZVI and SMI for U and Tc-99 sequestration and (2) the impact of CoCOIs [I-129, Cr(VI), and nitrate] on U and Tc-99 sequestration.

2.7 Liquid-Phase Chemical Sequestration – Apatite-forming solutions

This technology is focused on chemical sequestration of U and Tc-99 (as PCOIs) and I-129, Sr-90, Cr(VI), and nitrate as potential CoCOIs via injection of a liquid-phase amendment to form apatite (Table 1.1). For this treatability study and based on the available information on the potential amendments, two formulations were selected for the initial phase of testing for this technology: (1) calcium-citrate/sodium-phosphate, Ca-Cit-PO_4; and (2) sodium-phosphate/polyphosphate, Poly-PO_4. These phosphate amendments aim to sequester contaminants through a combination of adsorption, reduction, precipitation, and coating processes. These amendments have been identified for *in situ* remedy applications in water-saturated areas, with primary treatment zones in the 200-DV-1 OU including the perched water zone at the B Complex Area and/or the water table beneath the BY Cribs (potentially applied as a PRBs). Secondary treatment zones in the Central Plateau may also include 216-U-1&2, S-SX Tank Farm, C Tank Farm, and BC Cribs and Trenches, where U and/or Tc-99 are also PCOIs. A previously developed conceptual model suggests significant U and Tc-99 contamination in the VZ below the B Complex within 20 ft of the water table, which may impact ultimate remedial decisions (PNNL-19277).

While both of the selected amendments slowly precipitate apatite following injection into the subsurface, they differ slightly in the biogeochemical reactions that lead to precipitation. Ca-Cit-PO_4 slowly precipitates apatite after biodegradation of citrate. Citrate is added because it strongly complexes with Ca, keeping it soluble during delivery of the amendment to the subsurface. Once the citrate is degraded, Ca is available to precipitate with PO_4 and form apatite. The citrate biodegradation also results in mild reducing conditions, which may reduce Tc-99 (as TcO_4^-) and U(VI) aqueous species, leading to formation of low-solubility solid phases (e.g., TcO_2 and UO_2). During subsequent apatite precipitation, reduced Tc-99 and U phases may be adsorbed or coated by apatite, with remaining U(VI) also potentially being incorporated into apatite and/or forming autunite as depicted for Ca-Cit-PO_4 in Figure 2.8. Poly-PO_4 reacts differently than Ca-Cit-PO_4 and slowly precipitates apatite after PO_4 chains break apart and precipitate with Ca, as depicted in Figure 2.9. The PO_4 chains allow for delivery of the amendment to the subsurface before precipitation. The major difference between the two amendments is the mildly reducing conditions that form with Ca-Cit-PO_4 but not Poly-PO_4, which potentially enhances removal from the aqueous phase and sequestration of oxidized species of the PCOIs [e.g., $Tc(VII)O_4^-$ and U(VI) carbonate species].

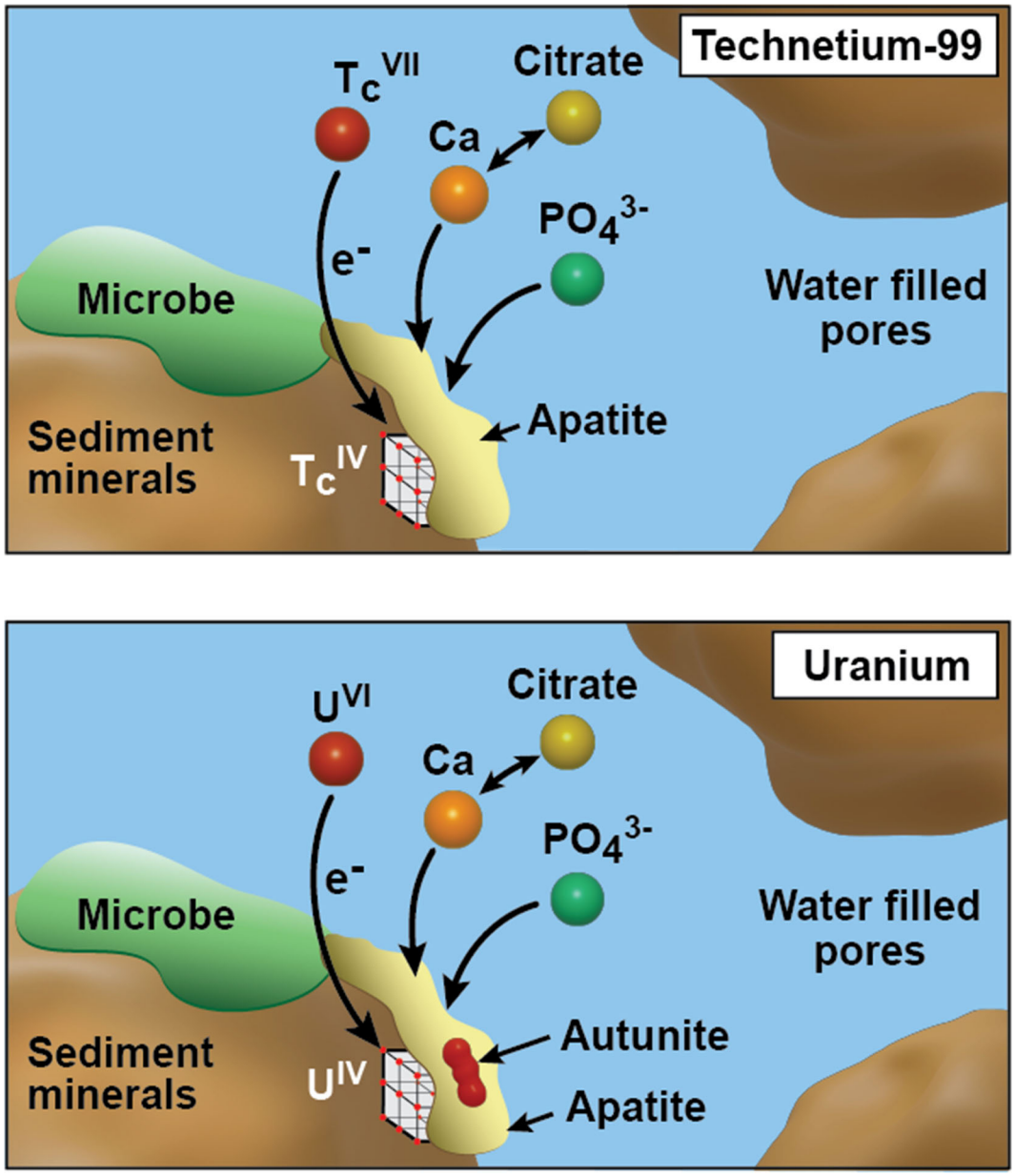

Figure 2.8. Sequestration of Tc-99 (*top*) and U (*bottom*) in the saturated zone by treatment with a solution of Ca-Cit-PO_4 occurs simultaneously via the following processes: citrate biodegradation to generate conditions for aqueous $Tc(VII)O_4^-$ and U(VI) reduction and precipitation as Tc(IV) and U(IV), citrate degradation leaving Ca available to precipitate with PO_4 and form apatite leading to coating of Tc(IV) and U(IV) by apatite as well as incorporation of U(VI) into autunite and apatite phases.

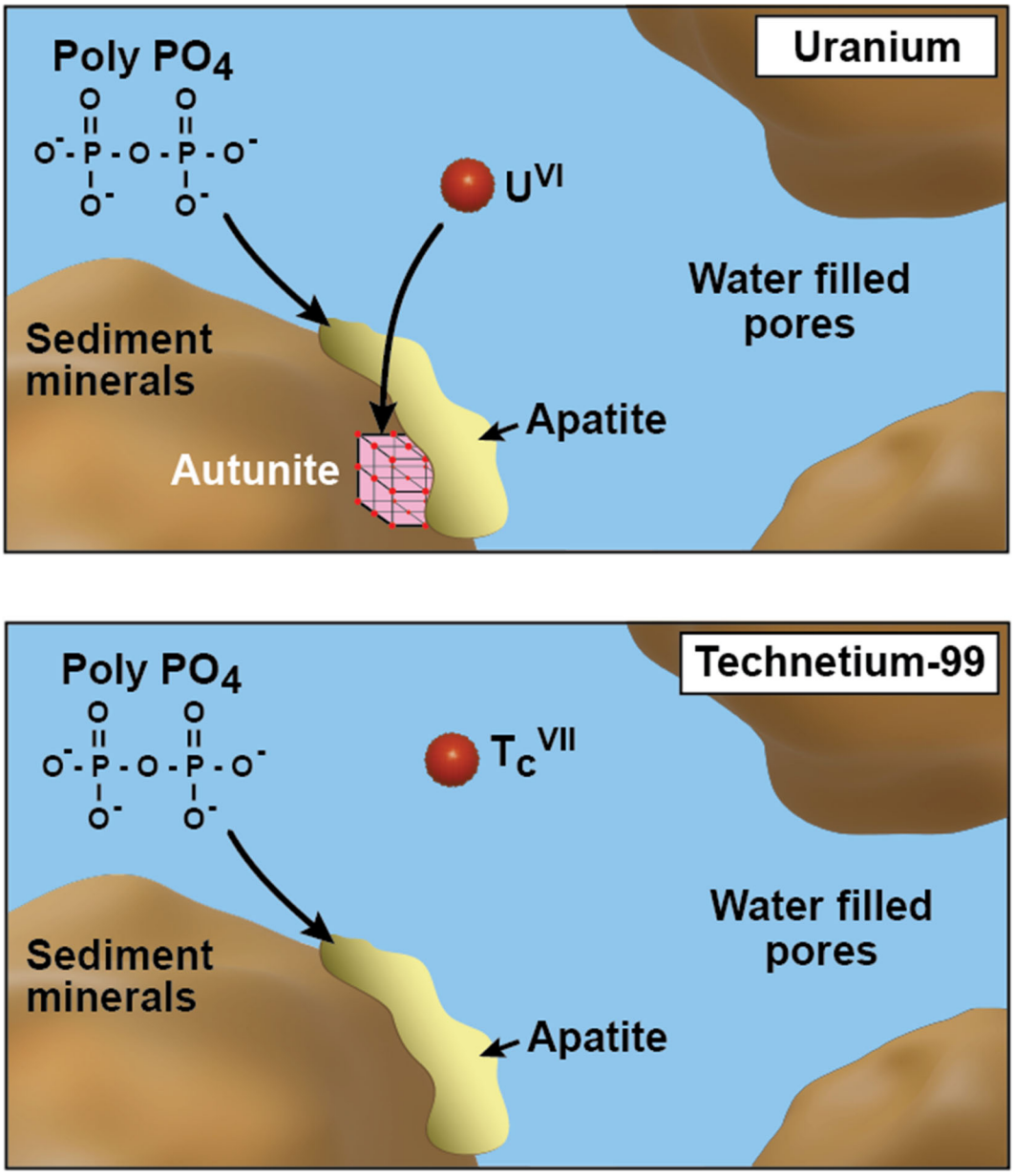

Figure 2.9. Sequestration of U (*top*) and Tc-99 (*bottom*) in the saturated zone by treatment with a Poly-PO_4 solution via the following processes: aqueous U(VI) incorporation into apatite and formation of autunite precipitates along with coating of adsorbed and precipitated U(VI) by apatite and limited adsorption of aqueous TcO_4^- to sediments with coating by apatite.

Chemical sequestration using these liquid-phase amendments has been demonstrated previously in the field along the river corridor at the Hanford Site for both U and Sr-90 via Ca-Cit-PO_4 and for U via Poly-PO_4 (SGW-47062; SGW-59614; SGW-63113; PNNL-29650; PNNL-18529; Vermeul et al. 2014). Other sites have also implemented these technologies for U sequestration (Fuller et al. 2003; Lammers et al. 2017; PNNL-25303). In addition, treatment via Poly-PO_4 and dihydrogen phosphate (NaH_2PO_4) has been shown to be effective in water-saturated Hf sediments for U at the laboratory scale (Pan et al. 2016; PNNL-SA-65124). Ca-Cit-PO_4 was also shown to be effective at the laboratory scale for Sr-90 (Robinson et al. 2023). However, these technologies have not been implemented at the field scale in the presence of the other PCOI (Tc-99) or CoCOIs (except Sr-90). Moreover, there is only limited data showing (1) Tc-99

is not removed from solution during apatite formation without a reductant and (2) there is potential for substitution of C-14 into the apatite structure via carbonation at the laboratory scale (Heslop et al. 2005; PNNL-28054).

The objectives of this study were to quantify (1) the effectiveness of Ca-Cit-PO_4 and Poly-PO_4 for U and Tc-99 sequestration and (2) the impact of CoCOIs [Sr-90, I-129, Cr(VI), and nitrate] on U and Tc-99 sequestration.

2.8 Liquid-Phase Chemical Reduction and Chemical Sequestration – Calcium polysulfide and sodium polyphosphate

This technology is focused on a two-step chemical reduction and sequestration of PCOIs including U and Tc-99 alongside I-129, Sr-90, Cr(VI), and nitrate as potential CoCOIs via sequential injection of two liquid-phase amendments, including calcium polysulfide (CPS) to initiate reducing conditions followed by sodium-phosphate/polyphosphate (Poly-PO_4) to form apatite (Figure 2.10 and Figure 2.11 for Tc-99 and U, respectively) (Table 1.1). The CPS amendment is added to initially reduce PCOIs to lower solubility oxidation states. Next, the Poly-PO_4 is added to sequester contaminants in the long term via a combination of processes, including adsorption, precipitation, and coating. This technology differs from the Ca-Cit-PO_4 technology in that sequential injections of CPS and then Poly-PO_4 are performed for this technology, while the Ca-Cit-PO_4 is added altogether and initiates mildly reducing conditions during apatite precipitation due to the natural microbes consuming available oxygen. The concentration of the CPS can be changed based on primary and CoCOI concentrations, whereas with the Ca-Cit-PO_4 technology, the citrate concentration is based on the concentration of available Ca to form Ca-citrate complexes.

These amendments have been identified for *in situ* remedy applications in water-saturated areas, with primary treatment zones in the 200-DV-1 OU including the perched water zone at the B Complex area and/or the water table beneath the BY Cribs (potentially applied as a PRBs). Secondary treatment zones in the Central Plateau may also include 216-U-1&2, S-SX Tank Farm, C Tank Farm, and BC Cribs and Trenches, where U and/or Tc-99 are also PCOIs. A previously developed conceptual model suggests significant U and Tc-99 contamination in the VZ below the B Complex within 20 ft of the water table, which may influence ultimate remedial decisions (PNNL-19277).

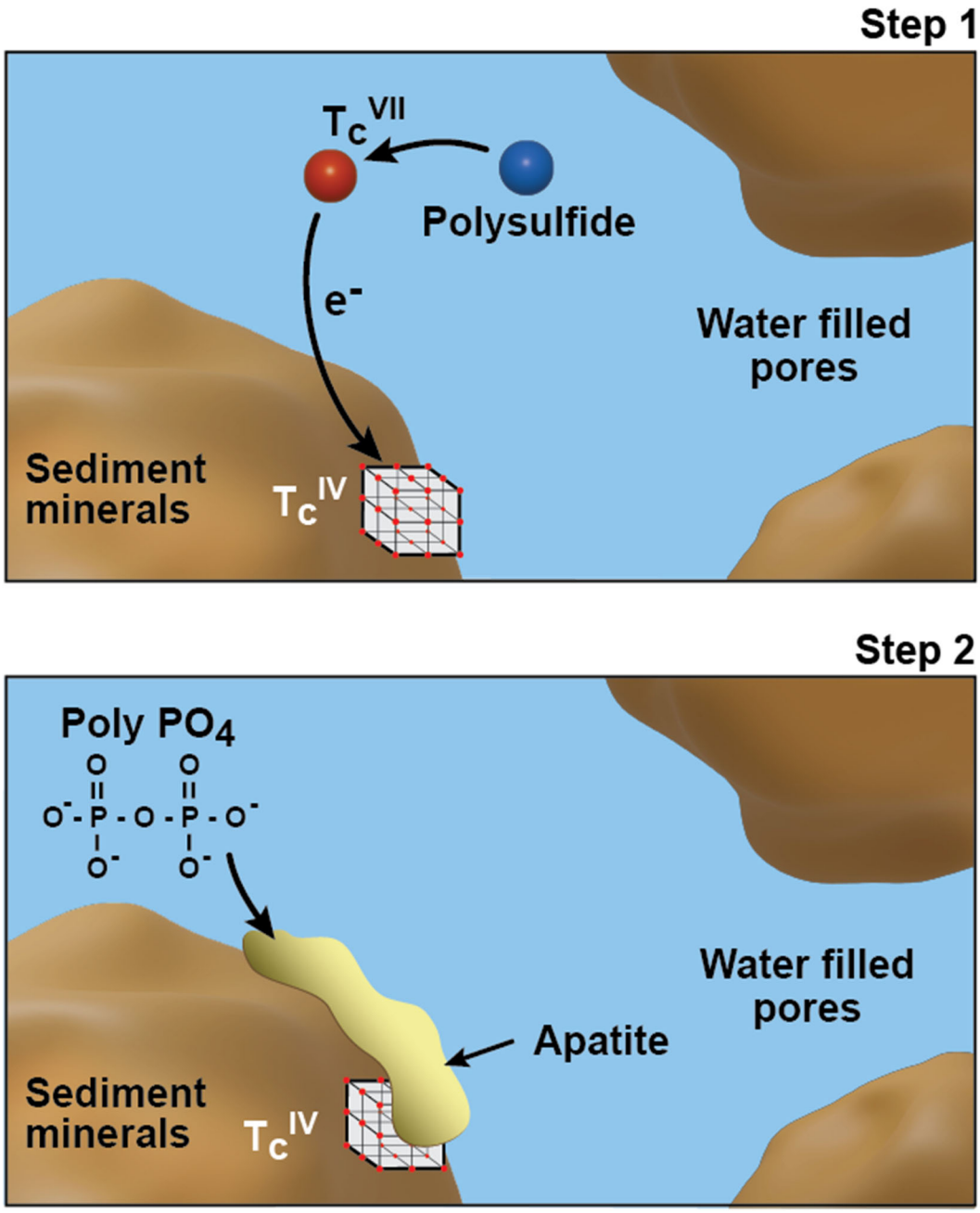

Figure 2.10. Sequestration of Tc-99 in the saturated zone via treatment with sequential solutions of calcium polysulfide followed by sodium polyphosphate via the following processes: (Step 1, *top*) aqueous $Tc(VII)O_4^-$ reduction by sulfide followed by reductive precipitation as Tc(IV) with (Step 2, *bottom*) subsequent injection of Poly-PO_4 for coating of Tc(IV) by apatite.

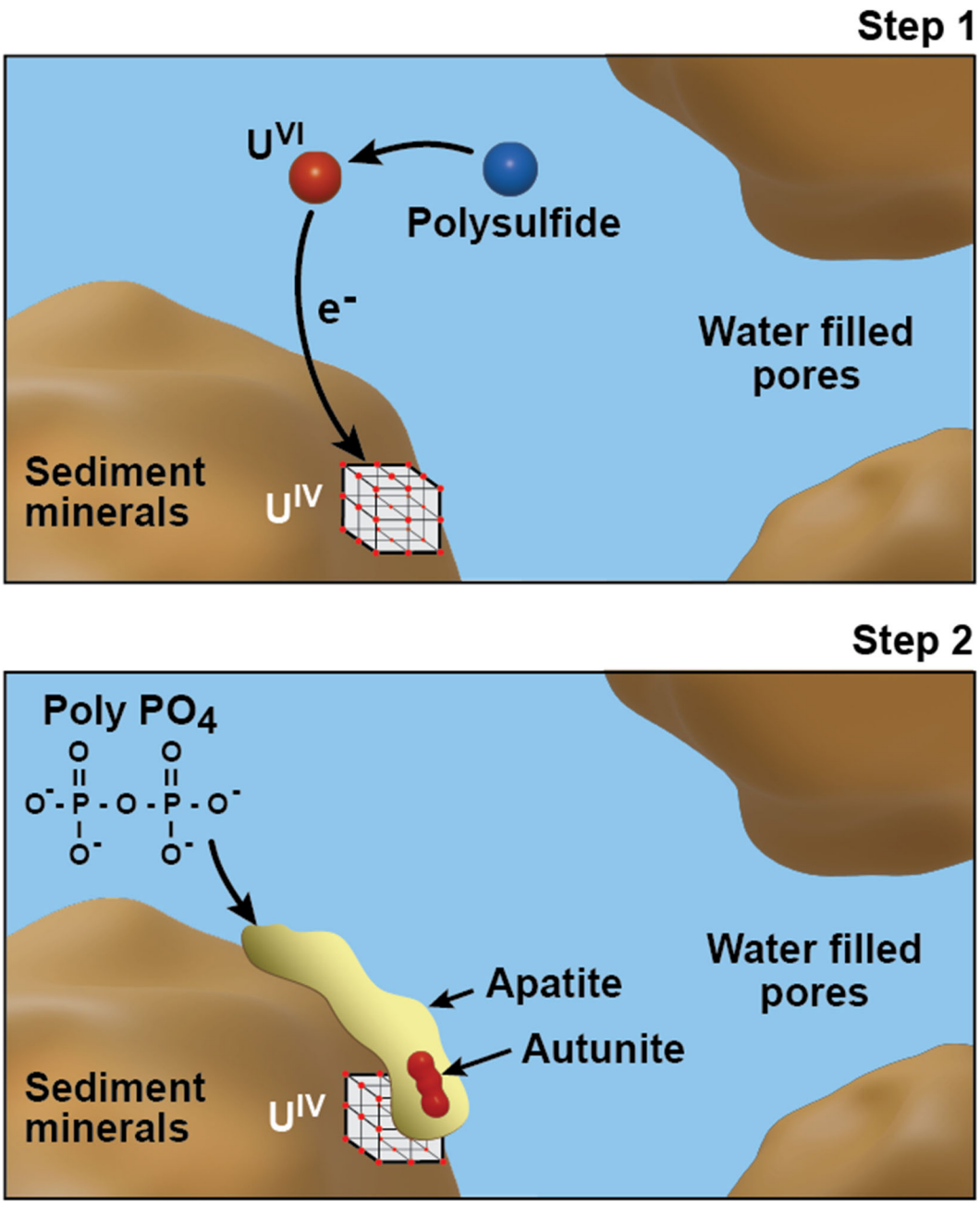

Figure 2.11. Sequestration of U in the saturated zone via treatment with sequential solutions of CPS followed by sodium polyphosphate via the following processes (Step 1, *top*) injection of CPS for reduction of aqueous and adsorbed U(VI) species by sulfide and precipitation of U(IV) followed by (Step 2, *bottom*) subsequent coating of precipitated U(IV) and adsorbed U(VI) by apatite and/or incorporation of U(VI) species in apatite and autunite.

Chemical reduction using CPS has been demonstrated previously for Cr(VI) (Chrysochoou et al. 2010; Zhang et al. 2020), with some testing for Tc-99 and U with CPS followed by a second apatite chemical sequestration step at the laboratory scale, including preliminary testing with Hanford Site sediments (PNNL-17674; PNNL-31959). However, these technologies have yet to be used at the field scale. Chemical sequestration using liquid-phase Poly-PO_4 has been demonstrated previously by itself in the field along the river corridor at the Hanford Site for both U and Sr-90 (SGW-59614; SGW-63113; PNNL-

19524; PNNL-29650), and other sites have implemented it for U sequestration (Fuller et al. 2003; Lammers et al. 2017; PNNL-25303). In addition, treatment has been shown to be effective in water-saturated Hf sediments for U at the laboratory scale (Pan et al. 2016; PNNL-SA-65124). However, the sequestration technology has not been implemented at the field scale in the presence of the other PCOI (Tc-99) or CoCOIs (except Sr-90). Moreover, there is only limited data showing (1) Tc-99 is not removed from solution during apatite formation without a reductant and (2) there is potential for substitution of carbonate into the apatite structure via carbonation at the laboratory scale (Heslop et al. 2005; PNNL-28054).

The objectives of this study were to quantify (1) the effectiveness of CPS at reductively precipitating Tc-99 and U, (2) the extent to which subsequent Poly-PO_4 treatment decreases re-mobilization of Tc-99 and U, and (3) the impact of CoCOIs [Sr-90, I-129, Cr(VI), and nitrate] on Tc-99 and U sequestration.

2.9 Liquid-Phase Bioreduction and Chemical Sequestration – Organic liquids and polyphosphate

This technology is focused on a two-step bioreduction and chemical sequestration of PCOIs U, Tc-99, and nitrate, alongside I-129, Sr-90, and Cr(VI) as potential CoCOIs via injection of two liquid-phase amendments (Table 1.1). This two-step technology is initiated with the introduction of an organic substrate (either a relatively long- or short-lasting carbon source) into the treatment zone to sustain anaerobic microbial activity and dissimilatory reductive processes, which catalyze the reduction of soluble, oxidized contaminant species to less soluble and/or mobile forms (e.g., conceptual diagram shown in Figure 2.12 and Figure 2.13 for Tc-99 and U, respectively) or gaseous, non-toxic forms (e.g., formation of N_2 or NH_3 from NO_3^-). This treatment phase is followed by the application of a Poly-PO_4 solution to improve sequestration as described in Section 2.7.

These amendments have been identified for *in situ* remedy applications in water-saturated areas, with primary treatment zones in the 200-DV-1 OU, including the perched water zone at the B Complex Area and/or the groundwater beneath the BY Cribs (potentially applied as a PRB at the water table). Secondary treatment zones in the Central Plateau may also include 216-U-1&2, S-SX Tank Farm, C Tank Farm, and BC Cribs and Trenches, where U and/or Tc-99 are also PCOIs. A previously developed conceptual model suggests significant U and Tc-99 contamination located in the VZ below the B Complex within 20 ft of the water table, which may impact ultimate remedial decisions (PNNL-19277).

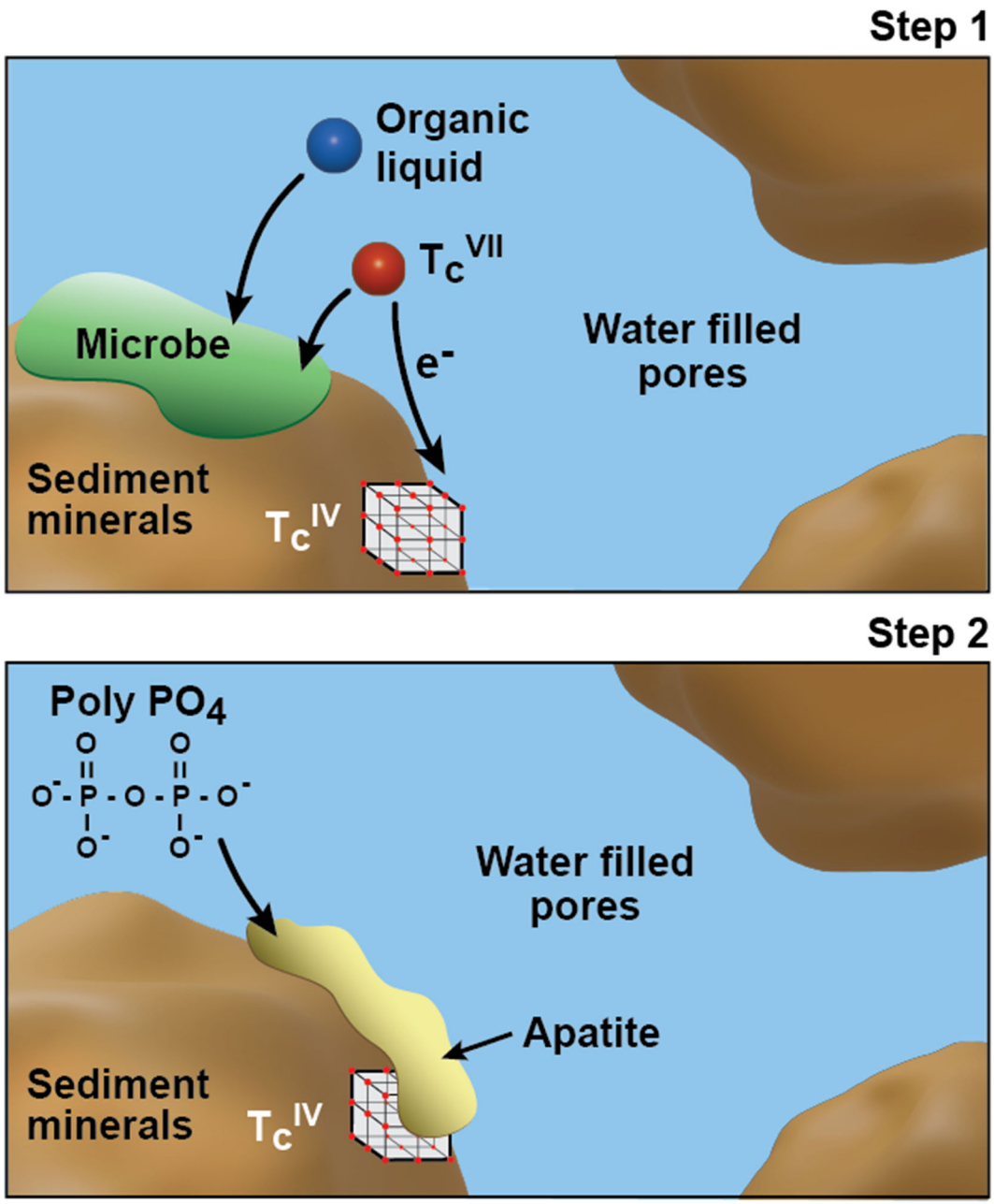

Figure 2.12. Sequestration of Tc-99 in the saturated zone via sequential solutions of an organic substrate followed by sodium polyphosphate where (Step 1, *top*) an organic substrate is injected and stimulates microbial activity to generate reducing conditions to reductively precipitate aqueous $Tc(VII)O_4^-$ as Tc(IV) followed by (Step 2, *bottom*) injection of Poly-PO_4 solutions for subsequent coating of Tc(IV) by apatite.

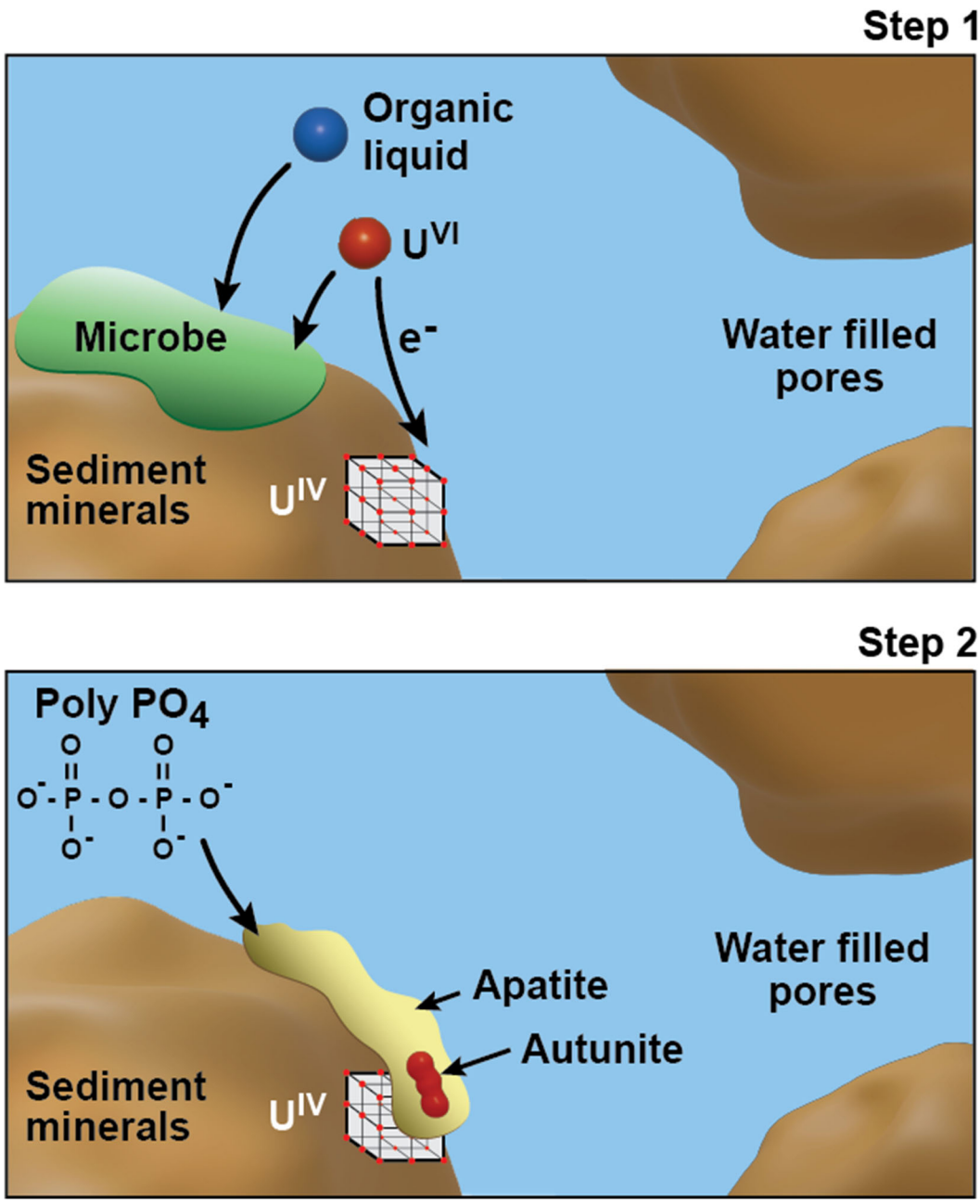

Figure 2.13. Sequestration of U in the saturated zone via sequential solutions of an organic substrate followed by sodium polyphosphate where (Step 1, *top*) an organic substrate is injected and stimulates microbial activity to generate reducing conditions to reductively precipitate aqueous U(VI) as U(IV) followed by (Step 2, *bottom*) injection of Poly-PO_4 solutions for subsequent coating of precipitated U(IV) and adsorbed U(VI) by apatite and/or incorporation of U(VI) species in apatite and autunite.

In situ bioremediation by injecting a readily available carbon/energy source (i.e., organic electron donor) is an effective means of decreasing aqueous concentrations of inorganic contaminants in the subsurface. Organic carbon supplies in the subsurface are generally present at low concentrations (< 4 mg/L;) (Konopka et al. 2013; Regan et al. 2017); therefore, alleviating this limitation rapidly stimulates indigenous microbial metabolism and growth. Numerous studies have validated this remedial approach by

coupling substrate oxidation with respiratory reduction of inorganic contaminants to less soluble species (Newsome et al. 2014). Successful demonstrations have been performed for U at the Old Rifle Processing Site (CO, USA) (Williams et al. 2011), and for U, Tc-99, and nitrate at the Oak Ridge Reservation (TN, USA) (Istok et al. 2004). Unlike Cr(VI), which reduces to highly stable, insoluble Cr(III) (Rahman and Thomas 2021), U and Tc-99 are challenging because reduced species can rapidly reoxidize, and mobilize if the system returns to oxic conditions [e.g., Komlos et al. (2008); Newsome et al. (2014)]. Therefore, stabilization of Tc-99 and U may require an additional treatment step post-reduction to coat or incorporate these reduced species into a stable mineral form (e.g., phosphate).

Chemical sequestration using liquid-phase Poly-PO_4 has been demonstrated previously by itself in the field along the river corridor at the Hanford Site for both U and Sr-90 (SGW-59614; SGW-63113; PNNL-19524; PNNL-29650), and other sites have implemented it for U sequestration (Fuller et al. 2003; Lammers et al. 2017; PNNL-25303). Phosphate treatment has been shown to be effective in water-saturated Hf sediments for U at the laboratory scale (Pan et al. 2016; PNNL-SA-65124). However, the sequestration technology has not been implemented at the field scale in the presence of the other PCOI (Tc-99) or CoCOIs (except Sr-90). Moreover, there is only limited data showing (1) Tc-99 is not removed from solution during apatite formation without a reductant and (2) there is potential for substitution of carbonate into the apatite structure via carbonation at the laboratory scale (Heslop et al. 2005; PNNL-28054). Notably, these two remediation methods have not been previously evaluated in combination.

The objectives of this study were to quantify (1) the effectiveness of biostimulation with organic liquids at reducing nitrate and reductively precipitating Tc-99 and U, (2) the extent to which subsequent Poly-PO_4 treatment decreases re-mobilization of Tc-99 and U, and (3) the impact of CoCOIs [Sr-90, I-129, Cr(VI)] on Tc-99 and U sequestration.

3.0 Experimental Approach

3.1 Sediments

Three composite sediments were used across experiments to represent the major focus areas discussed in Section 2.0 and to allow for cross-comparison between technologies. Each of these sediments was procured from areas without significant impacts from historical waste disposal operations or radiological contamination. Therefore, these sediments represent the formations targeted for remediation but may not capture historical anthropological impacts. Contaminants were added either directly to the sediments or via reaction with synthetic solutions, and all sediments were sieved to remove particles > 2 mm, unless noted elsewhere. Table 3.1 shows the particle size distribution of each sediment as received with additional laser particle size distributions in Appendix A, Section A.2. All sediments were stored in the refrigerator at approximately 4 °C prior to use.

An uncontaminated Hf sediment was procured from the Central Pre-Mix Concrete Company's gravel pit located in Pasco, WA. This sediment was used for most experiments, as it is representative of the Hf, which covers a significant portion of the VZ in the Central Plateau subsurface and represents similar mineralogy across the different formations within the saturated zones. As collected, the sediment had a moisture content of approximately 6.2% and particle density of 2.83 ± 0.04 g/cm^3. These sediments were also analyzed by X-ray diffraction (XRD) and the Brunauer-Emmett-Teller (BET) method of surface area measurement, as shown in Table 3.2 and Table 3.3, respectively. This distribution is consistent with previous characterization of Central Plateau sediments (PNNL-30443; PNNL-14202). Previous characterization noted that the formation ranges from 20 ft to several hundred feet in thickness and comprises poorly sorted, unconsolidated glaciofluvial material. These sediments are believed to originate from the Pleistocene epoch, which is characterized by localized cataclysmic flooding (Baker et al. 1991). The Hf sediments are coarse-textured silty-sandy-gravels consisting of approximately 50% gravel, 40% sand, and 10% silt (DOE/RL-88-09) and are composed primarily of quartz, feldspars, and ferromagnesian minerals (DOE/RL-92-24). These characterizations are consistent with the characterization of sediments conducted for this testing.

In some cases, additional sediments were used for testing to account for specific conditions of interest (e.g., natural microbial populations, liquid waste impacts, or CoCOIs). Two additional composite sediments were used for some testing as described within each technology description. These two composite sediments were generated to represent the two formations targeted for saturated areas of the subsurface, including formations within the BY Cribs groundwater and the B Complex perched water zones. A Cold Creek Unit gravel (CCug) and perching zone sand (PZsd) composite sediment was homogenized from cores within those formations from previous DV-1 characterization campaigns for the D0112 borehole (SGW-67996; PNNL-34300). Additional details on the specific cores chosen are included in Appendix A.

Additional site-specific conditions were used for select technologies to include some site-specific and/or waste-impacted conditions as described in the approach for each technology (Section 3.5). For most sediments collected from the Hanford Site, background contaminant concentrations were measured and are summarized in Appendix A, Section A.7, including for BY and 216-S-9, in addition to PZsd and CCug sediments. Some previous characterization was conducted on these sediments, focusing on measuring contaminant concentrations, and is summarized here. Tc-99-contaminated vadose zone sediments were available from under BY Cribs: boreholes C9552, 106' and C9487, 130′ depth (PNNL-19524; PNNL-26266; PNNL-26208), 216-S-9 (borehole C9512, 120′ depth, (PNNL-26266; PNNL-26208) and BC cribs [borehole C7540 52' depth (PNNL-18879)]. In addition, a vadose zone sediment from under 216-U-8 was used for select experiments and had Tc-99, U, and HNO_3 contamination (PNNL-

26902). There is additional contaminant characterization in these previous studies that includes batch sequential extractions and leaches.

Briefly, the BY field-contaminated sediment contained 115 pCi/g Tc-99 (and near natural 0.42 µg/g U), and the BC field-contaminated sediment contained 46 pCi/g of Tc-99 (and near natural 0.18 µg/g U). The field-contaminated 216-S-9 sediment contained 235 µg/g nitrate, 0.27 µg/g U, 0.66 µg/g Cr, and 0.025 µg/g I-127. The 216-U-8 sediment contained 526 pCi/g Tc-99, 26.9 µg/g U, and had acidic co-contaminants, which appears to have removed a significant amount of the calcite and ion exchangeable Ca out of the sediment (PNNL-26902). The maximum groundwater Tc-99 concentration found in BY Cribs area (96.7 pCi/g) was near the BY Cribs VZ sediment concentration (115 pCi/g), and above the BC Crib VZ sediment (46 pCi/g), but well below the 216-U-8 sediment Tc-99 concentration of 526 pCi/g.

For technologies involving microbial activity, select samples were heat-treated to inactivate cellular processes and functions in sediments (100 °C for 60 minutes). However, some changes in mineralogy are likely occurring with this heat treatment, as XRD results suggested a small increase in quartz content and decrease in feldspar content (Appendix A, Section A.1). In a previous study on uranium mobility, heat > 35 °C resulted in crystallization of amorphous iron oxides, which significantly impacted uranium sorption and incorporation into iron oxides (Payne et al. 1994). Although some differences in XRD results may be due to heterogeneity in the distribution of minerals and their orientation during measurement, the impact of heat treatment on the sediment mineralogy is unclear.

The XRD data for the sediments show very little to no amorphous material. This can happen because the uncertainties in these measurements can add up and will accumulate in the amorphous estimate. The uncertainties come from some preferred orientation, but primarily from how accurately the model crystal structures represent the actual minerals. And because this is all weight percent, different compositions in the minerals can affect the weight fraction without changing the XRD pattern significantly (e.g., Ca/Na substitution in feldspar). Therefore, minerals are reported more generally by groups (e.g., feldspar), although the specific mineral used for fitting is included in Appendix A, Section A.1.

Table 3.1. Wentworth particle size distribution based on dry sieve analysis.

Classification	Hf	CCug	PZsd
Gravel (> 2 mm)	13%	54%	10%
Sand (2 mm to 63 µm)	85%	42%	51%
Silt/Clay (< 63 µm)	1%	3%	39%

Table 3.2. X-ray diffraction of the < 2 mm size fraction of sediments. Note: Amorphous fraction subtracted from total to estimate crystalline mineral fractions. These data are For Information Only.

Mineral Name	Hf	PZsd	CCug	216-S-9 (B)[a]	216-S-9 (C)[a]	BY
Quartz	32.7%	39.5%	31.8%	40.8%	35.5%	34.7%
Feldspar	49.5%	40.1%	48.4%	40.9%	47.4%	48.8%
Mica	5.0%	7.8%	6.7%	6.9%	8.3%	6.3%
Amphibole	4.0%	4.9%	2.5%	5.3%	2.2%	3.8%
Pyroxene	5.9%	1.7%	6.4%	1.9%	2.6%	1.3%
Chlorite	2.9%	6.0%	4.2%	4.1%	3.9%	4.9%

(a) Two cores were opened from 216-S-9; Batch “B” was used for batch experiments.

Table 3.3. BET surface area measurements on the < 2 mm size fraction of sediments.

Sediment	Surface Area (m^2/g)
Hf	11.4 ± 2.0
CCug	7.2 ± 1.6
PZsd	8.0 ± 0.2
216-S-9 (B)[(a)]	6.0 ± 0.1
216-S-9 (C)[(a)]	7.5 ± 0.5
BY	2.6 ± 0.7

(a) Two cores were opened from 216-S-9; Batch "B" was used for batch experiments

3.2 Background Solutions

Synthetic groundwater (SGW), synthetic perched water (SPW), and artificial pore water (APW) were developed based on relevant historical monitoring data from the Central Plateau of the Hanford Site. Targeted contaminant concentrations were also based on historical data. These site-specific simulants were used for testing each technology based on the targeted treatment locations (i.e., groundwater, perched water, or VZ for pore water). All contaminants may have been included and/or adjusted based on specific testing needs, with any deviations noted in the methods for the individual technology. For example, specific contaminant solid phase concentrations were targeted (i.e., µg/g Tc-99), so higher aqueous Tc-99 was needed in unsaturated (i.e., at 4% WC or 0.04 mL/g) compared to water-saturated experiments, which had 2 mL/g of sediment.

The representative SGW is based on cation and anion averages of 54 well samples from the 200-UP-1 and 200-ZP-1 OUs from 2010 to 2018 (Lawter et al. 2021) (Table 3.4), and the SPW is based on cation and anion data from monitoring wells (299-E33-18, 299-E33-205, and 299-E33-341 to 345) in the 200-BP-5 OU for the period from 2010 to 2015 (PNNL-28054) (Table 3.5). APW for unsaturated experiments approximates the composition of Hanford 200 Area pore water, based on cation and anion averages of pore water extractions from sediments (Table 3.6) (PNNL-24297).

The PCOIs and the potential CoCOIs were added to solutions in batch systems to approximate field groundwater and perched water (Table 3.7) or pore water (Table 3.8) contaminant concentrations, although some constituents were added based on natural isotope concentrations in the subsurface (i.e., Sr and I), and Tc-99 concentrations were elevated with respect to contamination levels to improve the minimum fraction detectable in the aqueous phase (i.e., targeted detection of < 1% remaining in the aqueous phase). VZ contaminant concentrations used in unsaturated experiments were based on reported field-scale values and were generally similar to the saturated zone, except for much higher nitrate concentration.

COI concentrations for groundwater table and VZ conditions were based on previously measured concentrations from the Hanford Environmental Information System (HEIS) database, including data up to December 2021, for the BY Tank Farm, located in the 200 West Area of the Central Plateau. Because data was limited, core concentrations from both saturated and unsaturated depths were combined. PCOI and CoCOI concentrations for the BY Cribs are based on 35 to 70 measurements for each in sediments for groundwater table conditions. U, CN^-, and Cr(VI) were added based on the maximum solid phase concentrations measured in BY Tank Area cores as reported in HEIS. Nitrate was added based on average solid phase concentrations (instead of maximum) measured in BY Tank Area cores as reported in HEIS, because higher nitrate concentrations were considered for the perched water condition. Iodine was added as I-127 based on previous literature measuring background, natural iodine in Hanford groundwater (Kimmig et al. 2021; Zhang et al. 2013), as these treatments are not isotope specific and

natural/anthropogenic I-127 is significantly greater than I-129. Maximum I-129 concentrations reported in HEIS for the BY Tank Area are 0.03 µg/g and the maximum I-127 concentration measured at a 104-ft depth under BY Cribs was 2.0 µg/g. Sr was also added based on total maximum Sr concentrations in the BY Cribs and BY Tank Areas instead of Sr-90, as there is a significant natural Sr-87 background. The maximum Sr-90 measured in the BY Tank Area was 5.7×10^{-9} µg/g as compared to 125 µg/g of total Sr. The maximum Tc-99 measured in the BY Tank Area was 0.006 µg/g, though added concentrations are greater to improve the minimum fraction detectable in the aqueous phase.

For perched water conditions, U and nitrate concentrations are based on perched water extraction well data from the pump and treat facility (i.e., wells 299-E33-344, 299-E33-350, 299-E33-351) from 2019 through 2021, which includes 43 to 88 measurements. Nitrate data from the perched water extraction wells are also similar to previous extractions for B Complex cores (PNNL-31959; PNNL-26266). Tc-99 concentrations for perched water conditions were the same as for BY Cribs water table conditions to improve the minimum fraction detectable in the aqueous phase detection. The maximum concentration measured in the perched water extraction wells was for well 299-E33-350 (82,400 pCi/L or 4.8 µg/L).

Table 3.4. Synthetic groundwater with pH adjustment to approximately 7.8.

Constituent	Concentration (mmol/L)
$MgSO_4$	0.37
$MgCl_2$	0.25
$CaCl_2$	1.07
$KHCO_3$	0.12
$NaHCO_3$	1.59

Table 3.5. Synthetic perched water with pH adjustment to approximately 8.2.

Constituent	Concentration (mmol/L)
$CaSO_4$	0.56
$MgSO_4$	2.7
Na_2SO_4	1.74
NaCl	3.30
$NaHCO_3$	10.71
$KHCO_3$	0.31

Table 3.6. Artificial pore water with pH adjustment to pH 7.0 to 7.2.

Constituent	Concentration (mmol/L)
$CaSO_4$	12
NaCl	1.7
$NaHCO_3$	0.4
$NaNO_3$	3.4
$MgSO_4$	2.6
$MgCl_2$	2.4
KCl	0.7

Table 3.7. Contaminants of interest in µg/g based on targeted field sediment concentration to mimic actual contamination for technologies targeting saturated zones and µg/L based on a 1:2 sediment-to-solution ratio.

	BY Cribs Groundwater		Perched Water		
Contaminant	(µg/L)	(µg/g)	(µg/L)	(µg/g)	Added as
Tc-99	100	0.2	100	0.2	NH_4TcO_4
U	1000	2	50,000	100	UO_2Cl_2 or $UO_2(NO_3)_2$
I-127	150	0.3	-	-	$NaIO_3$
Cr	17,500	35	-	-	Na_2CrO_4 or $K_2Cr_2O_7$
Sr[(a)]	25,000	50	-	-	$Sr(NO_3)_2$
NO_3^-	50,000	100	800,000	1600	$NaNO_3$

(a) Sr added as natural abundance (^{84}Sr 0.56%, ^{86}Sr 9.86%, ^{87}Sr 7.0%, and ^{88}Sr 82.58%).

Table 3.8. Contaminants of interest in µg/g based on targeted field sediment concentration to mimic actual contamination for technologies targeting unsaturated zones.

Contaminant	(µg/g)
Tc-99	0.2
U	2
I-127	0.3
Cr	35
Sr-87	50
NO_3^-	100
CN^-	2.7

3.3 Sequential Extractions

Sequential liquid extractions have been used to characterize a wide variety of metals present in sediments in multiple surface phases (Beckett 1989; Chao and Zhou 1983; Gleyzes et al. 2002; Hall et al. 1996; Larner et al. 2006; Mossop and Davidson 2003). A series of extractions are used to evaluate the different forms of PCOIs and CoCOIs in the sediment, including *Extraction 1:* aqueous, *Extraction 2:* adsorbed, *Extraction 3:* reduced and readily oxidized, *Extraction 4:* precipitated in calcite, and *Extraction 5:* precipitated into hard-to-extract phases (i.e., oxides, silicates, aluminosilicates). Note that although targeted fractions are identified for each extraction step, each of these phases is operationally defined and may not be representative of the actual phases released. However, each step of the extractions represents a relative decrease in mobilization potential of the phases with which the PCOIs and CoCOIs are associated, providing a qualitative understanding of the potential for re-mobilization.

Technologies that involve a reduction process use all five sequential extractions at selected time intervals. Technologies that do not involve a reduction process generally use four sequential extractions, omitting the third (i.e., reducible, oxidizable) extraction. Further, the assumption for Extraction 3 is that the mass of dissolved oxygen in the liquid (and O_2 diffusing into liquid from the air headspace) is greater than the mass of reduced contaminants (and other phases such as ferrous iron precipitates) on the sediment surface. In addition, the first extraction step could be omitted in saturated batch experiments if the supernatant was analyzed prior to extractions, although in some cases the first extraction was still conducted.

Extractions were conducted in polytetrafluoroethylene (PTFE) or polycarbonate centrifuge tubes or other compatible container at a 1:3 or 1:2 sediment-to-solution ratio. Volumes indicated for each extraction assume 5 g of sediment with a liquid volume of 15 mL (for a 1:3 ratio), but this is adjusted depending on the actual sediment mass and ratio as stated for each technology. For these extractions, the first step is to remove an aliquot of the sediment from the batch or column experiment and weigh the sediment that was placed in the centrifuge tube in an anaerobic chamber, as some PCOI and CoCOI phases may be reduced (and could be readily oxidized). The exact weight of sediment added is recorded (to at least 10 mg accuracy). Upon sampling, the tube is centrifuged at 3,000 rpm for 10 minutes, then liquid is drawn off the top of the sediment and filtered with a syringe filter prior to analysis. For technologies not involving microbes, 0.22- or 0.45-µm polyvinylidene fluoride or polyethersulfone or PTFE filters were used, while equivalent 0.22-µm pore size syringe filters were used for any technologies involving microbes. Nylon filters were used for Extractions 1 through 4 (PTFE filters for Extraction 5) for the gas-phase bioreduction and sequestration technology (Section 3.5.1). Extractions 1 through 4 are conducted at room temperature (20 to 25 °C), and Extractions 1 and 2 are conducted in the glovebox under anaerobic conditions. A preparation blank and blank spike were also prepared to check background contaminant concentrations (blanks) and confirm that contaminants were soluble in extractions and results were reproducible and without interferences (blank spikes) for each extraction. The blanks consisted of the extraction solutions (i.e., reagents 1 through 5) without contaminants added to solution.

Each extraction is described in greater detail below based on a 1:3 sediment-to-solution ratio.

Extraction 1. “Aqueous”: 15 mL of *anaerobic* SGW or SPW prepared in degassed ultrapure water, ≥ 18 MΩ·cm) is mixed with 5 (± 0.5) g of sediment (or smaller mass at the same sediment-to-solution ratio) in an anaerobic chamber. The tube is placed in a compatible container for 50 minutes and mixed by placing the tube on a slow (< 30-rpm) mixer.

Extraction 2. “Adsorbed/Exchangeable”: 15 mL of the *anaerobic* ion exchange solution (0.5 M magnesium nitrate ($Mg[NO_3]_2$) prepared in degassed ultrapure water, ≥ 18 MΩ·cm; dissolved oxygen is removed from solution by vigorous N_2 bubbling for 15 minutes followed by vacuum, and the solution is kept in an anaerobic chamber) is added to the tube containing sediment after the previous extraction solution is removed in an anaerobic chamber, and mixed for 50 minutes.

Extraction 3. “Reduced, Readily Oxidized”: 15 mL of ion exchange solution (0.5 M $Mg[NO_3]_2$ prepared in ultrapure water, ≥ 18 MΩ·cm) is added to the tube containing sediment after the previous extraction solution is removed *outside* the anaerobic chamber with air headspace and mixed for 50 minutes.

Extraction 4. “Carbonates”: 15 mL of the pH 2.3 acetic acid solution [0.66 mL glacial acetic acid (CH_3COOH,17.4 mol/L) plus 47.2 g $Ca(NO_3)_2{\cdot}4H_2O$, pH 2.3, balance deionized H_2O to 2.0 liters] is added to the tube containing sediment after the previous extraction solution is removed and mixed for 5 days (±3 hours).

Extraction 5. “Residual/Other”: 15 mL of 8 mol/L nitric acid is added to the tube containing sediment after the previous extraction solution is removed and mixed intermittently for 2 to 3 hours at 95 °C or heated in a mod block without mixing (2 hours at 95 °C).

Sequential extraction results presented in this report are shown as a fraction of PCOI or CoCOI in each extraction. These results were normalized based on the total mass initially added to the system. Depending on the PCOI or CoCOI and its behavior and natural abundance in the sediments, recoveries may fluctuate. For example, the total recovery as summed across all extractions is frequently < 100% because the final extraction does not completely dissolve all solids. In addition, PCOIs or CoCOIs may not be distributed homogenously in sediments (i.e., a sediment aliquot may not be representative), and

some solids may be lost during the extraction process. If PCOIs or CoCOIs remain in the solid phase after the fifth extraction, the resulting immobilized fraction estimated will be conservatively low. However, for naturally occurring PCOIs or CoCOIs, the recovery is often > 100% due to background concentrations found in the sediments used in these tests, though it can also be due to their distribution in sediments. For U, recoveries may be greater than 1.0 due to the presence of naturally occurring U (1.20 ± 0.03 µg/g naturally occurring in Hf sediments as compared to targeted addition of 3 and 100 µg/g of U for BY Cribs groundwater and perched water conditions, respectively).

In addition, the sequential extraction results are discussed based on the summation of Extractions 4 and 5 for immobile and Extraction 3 for temporarily immobile when referring to the 35% minimum transformation threshold for all PCOIs except nitrate, which is quantified based on the transformation of aqueous NO_3^- to gaseous nitrogen species.

3.4 Aqueous Phase Contaminant Analysis

3.4.1 Inductively Coupled Plasma Mass Spectrometry

3.4.1.1 ICP-MS of metals

Select samples were analyzed quantitatively for U, Tc-99, Ag, As, Ba, Cd, Cr, Cs, Cu, Hg, Mo, Pb, Re, Ru, Sb, and Se using a Thermo Scientific X-Series II quadrupole inductively coupled plasma-mass spectrometer (ICP-MS) with an Elemental Scientific Incorporated (ESI) SC4 DX FAST auto-sampler interface. All samples and standards were diluted with 2% Fisher Scientific Optima trace metal grade nitric acid and twice deionized water with a resistivity no less than 18.0 MΩ-cm. A 20-µg/L internal standard (ISTD) solution was added in-line to all samples, standards, and blanks during the analysis to demonstrate the stability of the instrument and sample introduction system. Method detection limits (MDLs) were established by running a low-level calibration standard seven consecutive times and multiplying the standard deviation of those seven replicates by 3.143 (student t-test value) to establish an instrument detection limit (IDL) and then multiplying that number by 5 to get the MDL. This process was repeated three times on non-consecutive days and averaged to establish a working MDL in µg/L.

The instrument was calibrated using standards made by the High-Purity Standards Corporation to generate calibration curves. The calibration standards ranged from 0.05 to 5 µg/L, with a High Calibration Verification (HCV) standard of 10 µg/L, used to verify the upper linear calibration range. The calibration was verified with an Initial Calibration Verification (ICV) and during sample analysis with a Continuing Calibration Verification (CCV) run every 10 samples, at a minimum. Calibration blanks were analyzed following each calibration verification solution to remove background signals and to confirm that potential carryover effects were not a factor. The calibration was independently verified using standards made by Inorganic Ventures.

3.4.1.2 ICP-MS of I-127

Samples were analyzed quantitatively at mass 127 using either a Thermo Scientific X-Series II quadrupole ICP-MS with an ESI SC4 DX FAST auto-sampler interface or a Thermo Scientific iCAP-RQ quadrupole ICP-MS with a Teledyne CETAC Technologies ASX-560 auto-sampler interface. All samples and standards were diluted with a solution of 0.5% triethylene tetramine and twice deionized water with a resistivity no lower than 18.0 MΩ-cm. The triethylene tetramine solution is made by Inorganic Ventures (product # UNS-2B). MDLs were established as described in Section 3.4.1.1.

X-Series II ICP-MS Calibration

The instrument was calibrated using standards made by the High-Purity Standards Corporation to generate calibration curves. The calibration standards ranged from 0.05 to 5 µg/L, with an HCV standard of 10 µg/L, used to verify the upper linear calibration range. The calibration was verified with an ICV and during sample analysis with a CCV run every 10 samples, at a minimum. Calibration blanks were analyzed following each calibration verification solution to remove background signals and to confirm that potential carryover effects were not a factor. The calibration was independently verified using standards made by Inorganic Ventures. A 20-µg/L ISTD solution was added in-line to all samples, standards, and blanks during the analysis to demonstrate the stability of the instrument and sample introduction system.

iCAP-RQ ICP-MS Calibration

The instrument was calibrated using standards made by the High-Purity Standards Corporation to generate calibration curves. The calibration standards ranged from 0.02 to 3 µg/L, with an HCV standard of 5 µg/L, used to verify the upper linear calibration range. The calibration was verified with an ICV and during sample analysis with a CCV run every 10 samples, at a minimum. Calibration blanks were analyzed following each calibration verification solution to remove background signals and to confirm that potential carryover effects were not a factor. The calibration was independently verified using standards made by Inorganic Ventures. A 200-ng/L ISTD solution was added in-line to all samples, standards, and blanks during the analysis to demonstrate the stability of the instrument and sample introduction system.

3.4.2 Inductively Coupled Plasma Optical Emission Spectrometry

Select samples were analyzed quantitatively for Ag, Al, As, B, Ba, Be, Bi, Ca, Cd, Co, Cr(VI),Cs, Cu, Fe, Gd, K, Li, Mg, Mn, Mo, Na, Ni, P, Pb, Re, S, Sb, Se, Si, Sn, Sr, Ti, Tl, V, Zn, and Zr using a PerkinElmer Optima 8300 dual view inductively coupled plasma optical emission spectrometer (ICP-OES) with a PerkinElmer S-10 auto-sampler interface or for Al, Ba, Ca, Cr(VI), Fe, Mg, Mn, Na, P, Si, and Sr using a PerkinElmer model Optima 2100DV with PerkinElmer S3-plus auto-sampler. All samples and standards were diluted with 2% Fisher Scientific Optima trace metal grade nitric acid and twice deionized water with resistivity no less than 18.0 MΩ-cm. Samples were run at several dilutions to bring their various elemental concentrations within the optimal analytical ranges of the instrument and to provide another level of result confirmation. An ISTD solution was added in-line to all samples, standards, and blanks to demonstrate the stability of the instrument and sample introduction system.

MDLs were established by running the lowest calibration standard seven consecutive times and multiplying the standard deviation of those seven replicates by 3.143 (student t-test value) to establish an IDL and then multiplying that number by 5 to get the MDL. This process was repeated three times on non-consecutive days and averaged to establish a working MDL in µg/L.

The instrument was calibrated using standards made by the High-Purity Standards Corporation or Inorganic Ventures, Inc. to generate calibration curves. The range of the calibration curves for the PerkinElmer Optima 8300 dual view was 50 ng/L to 50 µg/L. The range of the calibration curves for the PerkinElmer Optima 2100DV was 0.5 to 3000 µg/L. This calibration was verified with an ICV and during sample analysis with a CCV run every 10 samples, at a minimum. Calibration blanks were analyzed following each calibration verification solution to remove background signals and to confirm that potential carryover effects were not a factor. The calibration was independently verified using standards made by Inorganic Ventures or High-Purity Standards, depending on which was used for the calibration as different sets of standards are used for calibration and verification.

3.4.3 Anion Chromatography

3.4.3.1 Major anions

Samples were analyzed quantitatively using a Dionex Reagent-Free Ion Chromatography System (RFICS) 2000 with an AS-1 auto-sampler interface or a Dionex RFICS 5000 with an AS-AP auto-sampler interface or Dionex ICS-2000 anion chromatograph with AS40 auto-sampler. The anions analyzed were bromide (Br^-), chloride (Cl^-), fluoride (F^-), nitrite (NO_2^-), nitrate (NO_3^-), phosphate (PO_4^{-3}), and sulfate (SO_4^{-2}). All samples and standards were diluted with twice deionized water with a resistivity no less than 18.0 MΩ-cm. MDLs were established by running a low-level calibration standard seven consecutive times and multiplying the standard deviation of those seven replicates by 3.143 (student t-test value) to establish an IDL and then multiplying that number by 5 to get the MDL. This process was repeated three times on non-consecutive days and averaged to establish a working MDL in mg/L.

The instruments were calibrated using a multi-element anion standard purchased from Inorganic Ventures to generate calibration curves. The calibration standards ranged from 0.03 to 7.5 mg/L or 25 to 120 mg/L, with an HCV standard of 30 mg/L, used to verify the upper linear calibration range. The calibration was verified with an ICV and during sample analysis with a CCV run every 10 samples, at a minimum. Calibration blanks were analyzed following each calibration verification solution to remove background signals and to confirm that potential carryover effects were not a factor. The calibration was independently verified using anion standards purchased from SPEX CertiPrep.

3.4.4 Liquid Scintillation Counting of Tc-99

Tc-99 was measured for select samples using a PerkinElmer 3100TR liquid scintillation counter for select experiments. A series of quench standards were used for Tc-99 to accurately convert the energy-specific light emission spectra into Tc-99 concentrations. The detection limit was approximately 0.12 µg/L (2 pCi/mL) by liquid scintillation counting (LSC) for a 1.0-mL sample, although limits varied based on the total volume of samples for LSC. For sequential extraction samples, Extractions 1 and 4 used 1.0 mL of sample with 5.0 mL of Optifluor cocktail (PerkinElmer). Extractions 2 and 3 used 1.0 mL of sample with 5.0 mL of Hionic-Fluor cocktail (PerkinElmer). Extraction 5 used 0.25 mL of sample with 5.0 mL of Ultima Gold AB cocktail (PerkinElmer). In all cases, 6.5-mL plastic LSC vials were used. Duplicate samples were prepared randomly from 10% of samples. Five extraction blanks were run for each set of samples along with three ISTDs. A 7-point set of quench standards for Tc-99 was also used.

3.4.5 Kinetic Phosphorescence Analysis of Uranium

U was analyzed with a kinetic phosphorescence analyzer (KPA) for U^{VI} for select samples by reaction with Uraplex using light from a pulsed nitrogen laser with an excitation wavelength of 425 nm and measurement of the ultraviolet (UV) emission at 515 nm (Brina and Miller 1992). The detection limit for U was 0.5 µg/L for KPA and 0.08 µg/L for ICP-MS. U detection limits for KPA were higher in specific matrices, though all samples were acidified with 2% HNO_3 prior to analysis. For example, some pH 2.3 acetic acid extractions of ZVI/SMI were orange colored and had U detection limits of 50 to 200 µg/L. Daily 7-point calibration standards were used (0.25 to 30 µg/L, SPEX CertiPrep) and 30 µg/L verification standards (High-Purity Standards) in water and extraction solutions.

Uraplex from Chemchek, Inc. (Richland, WA) was used for all samples prior to July 15, 2023, after which Chemchek no longer supplied Uraplex. Based on a 1978 patent (4198568, J. Robbins and J. Kinrade), Uraplex was synthesized at Pacific Northwest National Laboratory (PNNL) (formula in Table 3.9) and used for all samples after July 15, 2023. This PNNL Uraplex was 150 mM total phosphate that was 90% orthophosphate and 10% straight chain (pyro- and tripoly-) and cyclic (trimeta- and hexameta-)

polyphosphates. In terms of performance, fresh Chemchek Uraplex with a new laser cartridge in the KPA showed the greatest sensitivity at all uranium concentrations (Figure 3.1, 5/11/11 calibration). This performance is consistent with independent analysis of others (NBL-345; Zook et al. 1981). The Chemchek fresh and old Uraplex calibrations in 2022 and 2023 showed slightly lower sensitivity, likely due to the decreased performance of the laser after 10 years. The PNNL Uraplex (Figure 3.1, black dots) showed the same to slightly better sensitivity at all uranium concentrations compared to the 2022 and 2023 Chemchek Uraplex. The PNNL Uraplex was mixed and used within 7 days because over time polyphosphates depolymerize, which would decrease the U concentration sensitivity.

Table 3.9. Composition of Uraplex synthesized at PNNL.

Compound	Formula	CAS Number	Solubility (g/100 mL)	Formula Wt (g/mol)	Mass Added (g/L)
Na_2HPO_4	Na_2HPO_4	7558-79-4	7.7	142	12.71
NaH_2PO_4	NaH_2PO_4	7558-80-7	50.9	120	1.895
Na pyro-PO_4	$Na_4(PO_4)_2 \cdot 10H_2O$	7722-88-5	6.7	466	1.514
Na tripoly-PO_4	$Na_4P_3O_{10}$	7758-29-4	14.5	368	1.196
Na trimeta-PO_4	$Na_3P_3O_9$	7785-84-4	22	305.9	0.994
Na hexameta-PO_4	$(NaPO_4)_6$	68915-31-1	0.2	611.8	0.7158

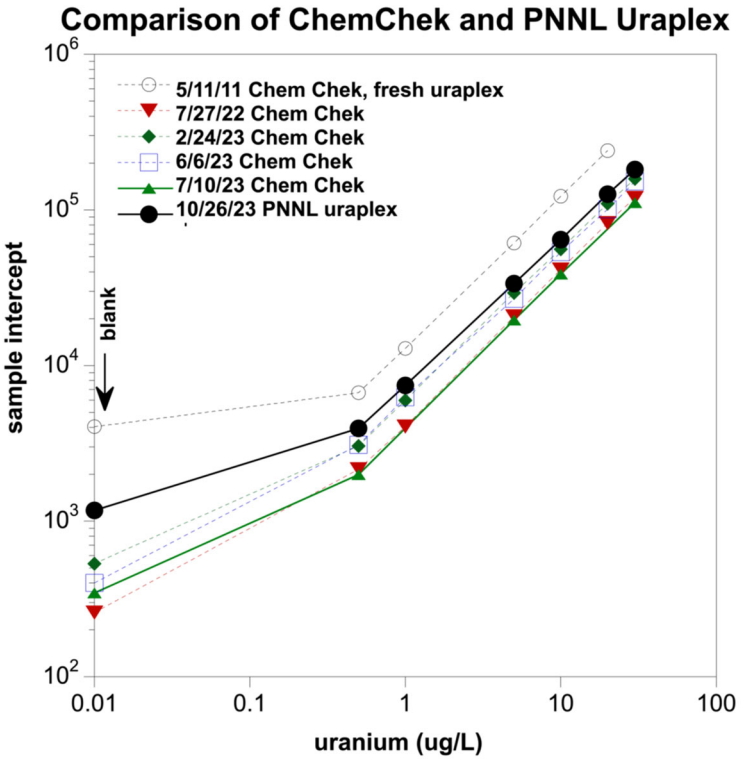

Figure 3.1. Comparison of Chemchek to PNNL Uraplex.

3.4.6 Ultraviolet Spectroscopy of Cyanide

Iron cyanide complexes were quantified by UV absorption at 320 nm (ferrous cyanide) and 420 nm (ferric cyanide) (SW-846 Update V). Five-point calibration curves were used for quantification of the ferrous cyanide concentration from the UV absorption. The detection limit was 280 µg/L (5 µmol/L). Because

ferrous cyanide was the added contaminant and the system did not contain strong oxidants, no ferric cyanide was detected in samples.

3.5 Experimental Approach by Technology

In general, each of the technologies were evaluated in batch-type or static column experiments (no flow, for VZ, gaseous amendments) to address the following objectives:

Objective 1: Quantify the removal of Tc-99 and U, and the order of magnitude rate of removal, using a single or two-step treatment, in the presence and absence of CoCOIs.

Objective 2: Quantify the amount of Tc-99 and U sequestered by the treatment, in the presence and absence of CoCOIs.

Experimental details for each technology are presented based on the objectives outlined in the test plan (DOE/RL-2019-28) with deviations from the original plan and the reasons supporting those changes in each respective section. The effectiveness of 35% transformation to immobile, temporarily immobile [e.g., TcO_4^- to TcO_2, $Ca_2UO_2(CO_3)_3$ to $Ca(UO_2)_2(PO_4)_2 \cdot 10\text{-}12H_2O$, or IO_3^- to IO_3 incorporated into $CaCO_3$], or nontoxic end products (e.g., NO_3^- to N_2 gas), along with other indicators, was used by the project team to evaluate the effectiveness of the technology and determine the need for further testing of the technologies in Phase 2. The 35% transformation threshold is based on an increase in transformation as compared to an appropriate control (e.g., sediments and contaminants reacting in the absence of treatments).

3.5.1 Gas-Phase Bioreduction and Chemical Sequestration – Organic gases and CO_2 gas

The focus was quantifying (1) the effectiveness of different organic gases at decreasing mobility of the PCOI, Tc-99 as $Tc(VII)O_4^-$, by reduction; (2) the extent to which CO_2 gas treatment decreases Tc-99 reoxidation by forming a coating of carbonate mineral; and (3) the effect of CoCOIs [U, Sr-90, I-129, Cr(VI), nitrate] on Tc-99 remediation. These amendments have been identified for *in situ* remedy applications in the unsaturated VZ in the 200-DV-1 OU, including a primary treatment zone in the BY Cribs waste sites with secondary treatment zones including the BC Cribs and Trenches (Table 1.1).

Although most experiments were conducted with Tc-99-spiked Hf sediment (as with other technologies), a select few were conducted with contaminated sediments. These site-specific sediments were used to evaluate whether Tc-99 in contact with sediment for decades could be remediated with this sequential gas technology. Tc-99-contaminated vadose zone sediments were available from under BY Cribs [C9552, 106' (PNNL-26266)] and BC cribs (C7540 52' (PNNL-18879)], so were used in this technology. In addition, a vadose zone sediment from under 216-U-8, Tc-99 with U and acid contamination was used (PNNL-26208) The BY field-contaminated sediment contained 115 pCi/g Tc-99 (and near natural 0.42 µg/g U) and the BC field contaminated sediment contained 46 pCi/g (and near natural 0.18 µg/g U). The 216-U-8 sediment contained 526 pCi/g Tc-99, 26.9 µg/g U, and had acidic co-contaminants, which appears to have removed a significant amount of the calcite and ion exchangeable Ca out of the sediment (PNNL-26902). There is additional contaminant characterization in these previous studies that includes sequential extractions and leaches. This 216-U-8 sediment was specifically used to evaluate whether CO_2 gas introduction would result in calcite precipitation in a site with acidic co-contaminants where there was little available ion-exchangeable Ca. The maximum groundwater Tc-99 concentration found in the BY Cribs area (96.7 pCi/g) was near the BY Cribs VZ sediment concentration (115 pCi/g), and above the BC Crib VZ sediment (46 pCi/g), but well below the 216-U-8 sediment Tc-99 concentration of 526 pCi/g.

For most of the experiments, the uncontaminated Hf sediment had 135 pCi/g of added Tc-99 to be close to the maximum groundwater Tc-99 concentration.

Experiments consisted of 127 columns filled with Hf sediments at low (4%) WC and spiked with $Tc(VII)O_4^-$ or $Tc(VII)O_4^-$ and CoCOIs that were injected with one of three different organic gases and allowed to react for 14 to 105 days, then injected with CO_2 and allowed to react for 14 to 70 days. Three organic gases (ethane, butane, and butyl acetate) were selected based on their ability to create a bioreduced environment and to be injected and partition into pore water, as described in Appendix B, Table B.1. Experiments were conducted in 4% WC columns rather than water-saturated batch systems as described in the TTER to accurately assess contaminant mobility changes in field-relevant systems. Water saturation is an important factor in assessing contaminant mobility under field-relevant conditions.

The WC used for this and other vadose zone technologies (4% for most) was based on the average field WC of B, S, and T-Complex vadose sediments (4.28 ± 1.68%, 17 sediments) previously evaluated (PNNL-27524; PNNL-26266; PNNL-26208). Finer grained zones are at higher field WC (measured vadose zone sediments as high as 15%, water saturation varied 18-21%), so for some technologies, 8% WC was additionally used. Similarly, units with significant gravel content have lower WCs (as low as 2.1% WC), so for some technologies, 2% WC was used for selected experiments.

The change in Tc-99 and CoCOI mobility was evaluated at multiple time points during the initial bioreduction step resulting from organic gas introduction, and during a secondary step of CO_2 gas treatment, with the targeted processes for sequestration depicted in Figure 2.1. Changes in $Tc(VII)O_4^-$ and CoCOI mobility were quantified by sequential liquid extractions to measure aqueous, adsorbed, reduced, and precipitated phases as described in Section 3.3 with analysis of the aqueous phase as described in Section 3.4. Table 3.10 shows the matrix as broken down by objective, with Objectives 1a and 1b representing the first step of treatment with an organic gas and both sequential steps (organic gas + CO_2 gas), respectively, without CoCOIs. Objectives 2a and 2b similarly represent the first step and both steps of treatment but with both CoCOIs.

Table 3.10. Experimental conditions for organic gas/CO_2 treatment columns.

Objective	Gas	Sediments	# of Columns (%WC)	Bio Control Columns	CoCOIs Added
1a	Ethane	Hf	6 (4%)	1	None
1a	Butyl acetate	Hf	6 (4%)	1	None
1a	Butane	Hf	6 (4%)	1	None
1a	None	Hf	2 (4%)	-	None
1a	Ethane	BY Cribs	2 (4%)	1	None
1a	Ethane	BC Cribs	2 (4%)	1	None
1a	Ethane	216-U-8 Crib	2 (4%)	1	None
1b	Ethane, CO_2	Hf	4 (4%)	1	None
1b	Butyl acetate, CO_2	Hf	4 (4%)	1	None
1b	Butane, CO_2	Hf	4 (4%)	1	None
1b	None	Hf	2 (4%)	-	None
1b	Ethane, CO_2	BY Cribs	2 (4%)	1	None
1b	Ethane, CO_2	BC Cribs	2 (4%)	1	None
1b	Ethane, CO_2	216-U-8 Crib	2 (4%)	1	None
2a	Ethane	Hf	6 (4%)	1	U, I-127, nitrate, Cr(VI), CN^-
2a	Butyl acetate	Hf	6 (4%)	1	U, I-127, nitrate, Cr(VI), CN^-
2a	Butane	Hf	6 (4%)	1	U, I-127, nitrate, Cr(VI), CN^-
2a	None	Hf	2 (4%)	-	U, I-127, nitrate, Cr(VI), CN^-
2b	Ethane, CO_2	Hf	4 (4%)	1	U, I-127, nitrate, Cr(VI), CN^-
2b	Butyl acetate, CO_2	Hf	4 (4%)	1	U, I-127, nitrate, Cr(VI), CN^-
2b	Butane, CO_2	Hf	4 (4%)	1	U, I-127, nitrate, Cr(VI), CN^-
2b	None	Hf	2 (4%)	-	U, I-127, nitrate, Cr(VI), CN^-

3.5.1.1 Objective 1: Quantify Tc-99 order of magnitude and rate of removal via treatment with organic gases and CO_2 without CoCOIs

The first objective was to quantify the extent of removal from the aqueous phase or sequestration of the PCOI, Tc-99, with only the first treatment step, i.e., stimulation of reducing conditions via organic gas treatment. These reduction experiments were conducted without co-contaminants (Objective 1a, Table 3.10) or with co-contaminants (Objective 1b). Each set consisted of a set of columns that were packed with sediment at 4% WC and treated (if applicable) at time zero. Experiments were conducted at 4% WC based on previous characterization of Hanford Site VZ sediments (Hanford, Ringold, and CCug sediments averaging 4.01 ± 1.67% WC) (PNNL-27524; PNNL-26266; PNNL-26208). Most were conducted with the uncontaminated Hf sediment, but select experiments were conducted with a BY Cribs sediment (C9552 106-07' bgs), BC Cribs sediment (C9540 at 52' bgs), or 216-U-8 Crib sediment (C9515 49.2-49.7' bgs), each of which had multiple contaminants based on previous characterization (PNNL-26266). Then, each column was sacrificed after 7, 21, 42, 70, or 105 days for sequential extractions (Table 3.11). Therefore, there were 31 total columns reacted with only the PCOI with a second set of 25 columns receiving both the PCOI, Tc-99, and the CoCOIs [U, Sr, I-127, Cr(VI),nitrate, CN^-]. For untreated sediments, K_d (distribution coefficient) values were calculated from the aqueous and sorbed fraction using:

K_d = solute sorbed concentration (μg/g) / solute aqueous concentration (μg/mL)

Each column was treated with one of three organic gases with a specified number of pore volumes for each (ethane, butane, and ethyl acetate; see Appendix B, Section B.1 for details on how these gases were selected and treated). Ethane, butane, and ethyl acetate were chosen due to good biodegradation performance (Bagwell et al. 2020) similar to pentane and butyrate, but better gas transport characteristics. Butyrate has very low volatility ($K_h = 8.71 \times 10^{-6}$), so it would be challenging to inject sufficient mass as a gas (and might require heating at field scale to inject sufficient mass), whereas pentane has high volatility but also a high gas density, so it would be difficult to contain in a portion of the VZ. Two control columns were also conducted, one with no organic gas added, labeled as a control, and one that used sterilized sediment (as described in Section 3.1) but was treated with organic gas, labeled as a biocontrol.

This study used small stainless-steel columns in the absence of flow of solution or gas (static) to both control the humidity of the sediments and allow for injection-specific volumes of organic gases and CO_2. Columns were 0.78 cm diameter by 11 cm long, which was equivalent to a total column volume of 5.14 cm^3. When filled with approximately 7.5 g of sediment at 4% WC, the total gas pore volume was 1.7 cm^3. In most cases, the organic gas was injected over the course of approximately 5 minutes (Table 3.11), but for 20% of experiments, a gas bag filled with the organic gas of interest was connected to the columns for the entire treatment time after injecting the appropriate gas into the column to evaluate whether the 5-minute treatment time was sufficient to achieve gas/pore water equilibrium. The PCOI or CoCOI behaviors with these two organic gas contact methods were compared to evaluate whether organic gas transfer to pore water was rapid and achieved equilibrium within the 5-minute injection period. To reach the 4% WC (g/g), the sediments were dried to 1% WC, then PCOIs (with or without CoCOIs) were added in the specified concentration (Table 3.8) in a volume equivalent to 3% WC of APW so that the final WC was 4%. Once sediments were mixed with Tc-99 and CoCOI additions, columns were packed and weighed with the sediment added.

Sequential extractions were conducted with a 1:2 sediment-to-solution ratio as described in Section 3.3 at selected time points to quantify the rate and extent of sequestration with treatment by organic gases. Aqueous aliquots were analyzed for PCOIs and CoCOIs as described in Section 3.4.

Selected sediment samples before and after organic gas treatment were used to quantify the change in microbial biomass by measurement using a molecular method (quantitative polymerase chain reaction, qPCR, as described in Appendix A, Section A.6).

3.5.1.2 Objective 2: Quantify Tc-99 order of magnitude and rate of removal by treatment with organic gases and CO_2 with CoCOIs

The second objective was to quantify the rate and extent of sequestration of the PCOI, Tc-99, with both treatment steps, stimulation of reducing conditions via organic gas treatment followed by carbon dioxide (Table 3.11). After reduction with an organic gas, which may only temporarily reduce Tc-99, more permanent immobilization could occur if reduced Tc-99 was coated by or incorporated into a precipitate such as calcite. Reduction and sequestration experiments were conducted without co-contaminants (Objective 2a, Table 3.10) or with co-contaminants (Objective 2b). CO_2 or organic gas was injected over the course of 5 minutes (Table 3.11); but for 20% of experiments, CO_2 in gas bags was connected to columns to passively exchange for the entire duration. Then, columns were sacrificed at specified times (14, 42, or 70 days) for sequential extractions as described for Objective 1. Therefore, there are 22 total columns (one duplicate for each organic treatment) receiving only the PCOI, Tc-99, and an additional set of 16 receiving both Tc-99 and the CoCOIs [U, Sr, I-127, Cr(VI), nitrate, CN^-].

Table 3.11. Gas injection approach.

Objective	Gas	Gas Conc. (%)	Gas Vol. (mL)[a]	Gas[b]	Gas Conc (%)	Gas Vol. (mL)[a]
1a and 2a	Butane	47%	17 (10 pore vol.)	NA[c]	NA	NA
1a and 2a	Ethane	4.6%	17 (10 pore vol.)	NA	NA	NA
1a and 2a	Butyl acetate	0.0075%	42 (25 pore vol.)	NA	NA	NA
1b and 2b	Butane	47%	17 (10 pore vol.)	CO_2	100%	17 (10 pore vol.)
1b and 2b	Ethane	4.6%	17 (10 pore vol.)	CO_2	100%	17 (10 pore vol.)
1b and 2b	Butyl acetate	0.0075%	42 (25 pore vol.)	CO_2	100%	17 (10 pore vol.)

(a) At atmospheric pressure and temperature
(b) After a 63-day reaction period for organic gas
(c) NA = not applicable

3.5.2 Gas-Phase Bioreduction – Organic gases

The focus was quantifying microbiological stimulation and subsequent reduction of a PCOI, nitrate, and the potential influence of another CoCOI, Cr(VI), by treatment with four different organic gases. The matrix for this technology is given in Table 3.12 and Table 3.13. Because the goal of this technology is to reductively transform NO_3^- to gaseous nitrogen end products and few mechanisms for sequestration into the solid phase exist, the focus was on quantifying the magnitude of removal or transformation and measuring potential intermediate species (e.g., NH_4^+).

To fulfill this objective, batch experiments were conducted to determine the overall effectiveness of organic gases to stimulate soil microbe activity for the effective transformation of NO_3^- to gaseous nitrogen end products (e.g., N_2O, N_2, NH_3 in increasing reduction order). A detailed experimental design for this technology is summarized in Table 3.12 and Table 3.13. Batch experiments were conducted in triplicate using sediments from representative waste sites or formations and at two different sediment-to-APW ratios (1:2 and 1:1). The APW is described in Table 3.6. Samples were prepared in tubes or bottles that were aluminum crimp-sealed with butyl rubber stoppers following purging with N_2 gas (1:1 ratio) or equilibration for 15 minutes in a Coy anaerobic glovebag (approximately 2% H_2, 98% N_2, O_2 < 20 mg/L) (1:2 ratio). Nitrate, Cr(VI), and yeast extract (YE, 0.01%) were added from oxic 100× stocks to the samples before anoxic equilibration in the glovebag. For the Hf sediment samples, NO_3^- was added at 50 mg/L and Cr(VI) was excluded.

Gases were added with needle and syringe immediately after tubes or bottles were purged with N_2. For butane or ethane additions, an air-tight gas sampling bag (Supelco) was filled with the organic gas from a lecture bottle of 100% butane or ethane (Sigma-Aldrich), and aliquots were pulled from the septum of the bag using an N_2-degassed syringe with a 22-gauge needle. For pentane additions, an N_2-degassed syringe with a 22-gauge needle was used to pull gas from a manufacturer's (Sigma-Aldrich) bottle of 100% pentane sealed with a cloth septum. For butyrate additions, aliquots of butyric acid were pulled from a manufacturer's (Aldrich) glass bottle using a syringe and metal canula, and then the canula was replaced with a 22-gauge needle to inject the liquid-phase butyric acid into an N_2-purged glass serum bottle aluminum-crimp-sealed with a butyl rubber stopper. Butyric acid gas was then pulled from the serum bottle using a syringe and needle. All gases (1 mL) were immediately added to sealed serum bottles using the needle and syringe. Additional gas spikes (2 mL) were added at 1 month for all gas treatments and again at ~2 months [BY + Cr(VI) treatments] or 4 months [216-S-9 +/- Cr(VI) treatments, BY – Cr(VI) treatment].

VZ sediments from the BY Cribs (C9487, 130′ depth) and 216-S-9 Crib (C9512, 120′ depth) as well as uncontaminated Hf sediments (characterization described in Section 3.1) were used. BY Cribs and 216-S-9 Crib sediments were characterized previously (PNNL-26266; PNNL-24709) though these specific cores are also characterized herein (Section 3.1). The field-contaminated 216-S-9 sediment contained 235 µg/g nitrate, 0.27 µg/g U, 0.66 µg/g Cr, and 0.025 µg/g I-127. The BY Cribs sediment contained 0.42 µg/g U and 115 pCi/g Tc-99. For the BY and 216-S-9 sediment microcosms, sediments were subsampled directly from bulk core material without sieving to maintain representative native mineralogical and microbiological complexity. For the Hf sediment, material was sieved to remove particles > 2 mm.

VZ sediments from the BY Cribs (C9487, 130′ depth) and S Cribs (C9512, 120′ depth) as well as uncontaminated Hf sediments (characterization described in Section 3.1) were used. BY Cribs and 216-S-9 Crib sediments were characterized previously (PNNL-26266; PNNL-26208), though these specific cores are also characterized herein (Section 3.1). For the BY and 216-S-9 sediment microcosms, sediments were subsampled directly from bulk core material without sieving to maintain representative native mineralogical and microbiological complexity. For the Hf sediment, material was sieved to remove particles > 2 mm.

Samples were incubated at room temperature on their sides with gentle shaking (~30 rpm). For sampling, ~0.75 mL of the aqueous phase was removed using an N_2-purged syringe and 22-gauge hypodermic needle, and the subsample was then filtered with a 13-mm PTFE 0.2-µm syringe filter (Pall Acrodisc) into a glass sample vial. Changes in pH were also monitored over time as an indication of H^+ consumption during nitrate reduction. The sample pH was immediately measured during sampling using a LAQUAtwin pH-11 pH meter and electrode with the remaining filtrate stored in the dark at 4 °C until analysis for NO_3^- and NO_2^- via ion chromatography (IC) and Cr(VI) via ICP-OES, additional analytes of interest including Fe and Mn were also monitored via ICP-OES as described in Section 3.4. Sequential extractions were not conducted for this technology as the goal is to transform nitrate to other species (N_2, N_2O, NH_4^+). Aqueous NO_3^- and NO_2^- were measured by IC and NH_4^+ accumulation was monitored indirectly by pH.

Selected sediment samples before and after organic gas treatment were used to quantify the change in microbial biomass by measurement using a molecular method (qPCR, as described in Appendix A, Section A.6).

3.5.2.1 Objective 1: Quantify nitrate order of magnitude and rate of removal via treatment with organic gases without CoCOIs

Experiments at a 1:1 sediment-to-liquid ratio were conducted (10 g of sediment and 10 mL of APW) in ~22-mL glass Balch tubes. NO_3^- was added at 75 mg/L. Native nitrate in the 216-S-9 sediment increased nitrate in the solutions by approximately 6.8 mg/L, based on a water extract conducted on untreated sediment. Native nitrate was below detection (1 mg/L) in the BY sediment. Native nitrite was below detection (1 mg/L) in both sediments. For the Balch tubes at a 1:1 liquid:solid ratio, NO_3^- was added at ~75 mg/L. Native nitrate in 2:1 extracts of the 216-S-9 sediment was ~7 mg/L and was below detection in the BY sediment 2:1 extract. Nitrite was below detection in both sediments. Gases were added with needle and syringe, as indicated above, immediately after the Balch tubes were purged with N_2. Bottles were sampled after 4 months of reaction. Batch experiments at a 1:2 sediment-to-liquid ratio (10 g of sediment + 20 mL of APW) were in 60-mL glass serum bottles. For the 216-S-9 and BY sediments, NO_3^- was added at an initial 20 mg/L, with a repeat addition at 84 days to increase by 30 mg/L. Bottles were sampled monthly for 5 months.

3.5.2.2 Objective 2: Quantify nitrate order of magnitude and rate of removal via treatment with organic gases with CoCOIs

Batch experiments at a 1:2 sediment-to-liquid ratio (10 g of sediment + 20 mL of APW) were in 60-mL glass serum bottles. For the 216-S-9 and BY sediments, NO_3^- was added at an initial 20 mg/L, with a repeat addition at 84 days to increase by 30 mg/L. Cr(VI) was at 18 mg/L Cr as Na_2CrO_4. Bottles were samples monthly for 5 months.

Table 3.12. Experimental overview for organic gas treatment in Balch tubes at a 1:1 sediment-to-solution (APW) ratio.

Organic Gas Treatment	Nitrate	CoCOI	Sediment	Nutrients	Sediment
Pentane	Y	-	Y	0.01% YE	Hf
Butyrate	Y	-	Y	0.01% YE	Hf
Ethane	Y	-	Y	0.01% YE	Hf
Butane	Y	-	Y	0.01% YE	Hf
None	Y	-	Y	0.01% YE	Hf
None	Y	-	Y	0.01% YE	Hf (Heat Inactivated)
None	Y	-	N	0.01% YE	NA
Organic Gas Treatment	Nitrate	CoCOI	Sediment	Nutrients	Sediment
Pentane	Y	-	Y	0.01% YE	BY Cribs (C9487), Hf
Butyrate	Y	-	Y	0.01% YE	BY Cribs (C9487), Hf
Ethane	Y	-	Y	0.01% YE	BY Cribs (C9487), Hf
Butane	Y	-	Y	0.01% YE	BY Cribs (C9487), Hf
None	Y	-	Y	0.01% YE	BY Cribs (C9487), Hf
None	Y	-	Y	0.01% YE	BY Cribs (C9487), Hf (heat inactivated)
No-Sediment Controls	Y	-	N	0.01% YE	NA
Organic Gas Treatment	Nitrate	CoCOI	Sediment	Nutrients	Sediment Origin
Pentane	Y	-	Y	0.01% YE	216-S-9 (C9512), Hf
Butyrate	Y	-	Y	0.01% YE	216-S-9 (C9512), Hf
Ethane	Y	-	Y	0.01% YE	216-S-9 (C9512), Hf
Butane	Y	-	Y	0.01% YE	216-S-9 (C9512), Hf
None	Y	-	Y	0.01% YE	216-S-9 (C9512), Hf
None	Y	-	Y	0.01% YE	216-S-9 (C9512), Hf (heat inactivated)
None	Y	-	N	0.01% YE	NA

NA = not applicable
CoCOI = Cr(VI) is the only co-contaminant

Table 3.13. Experimental overview for organic gas treatment in serum bottles at a 1:2 sediment-to-solution (APW) ratio.

Organic Gas Treatment	Nitrate	CoCOI (Cr)	Sediment	Nutrients	Sediment
Pentane	Y	-	Y	0.01% YE	Hf
Butyrate	Y	-	Y	0.01% YE	Hf
Ethane	Y	-	Y	0.01% YE	Hf
Butane	Y	-	Y	0.01% YE	Hf
None	Y	-	Y	0.01% YE	Hf
None	Y	-	Y	N	Hf (Heat Inactivated)
None	N	-	Y	N	Hf (no PCOI or CoCOI added)
None	Y	-	N	N	NA
Organic Gas Treatment	Nitrate	CoCOI	Sediment	Nutrients	Sediment
Pentane	Y	+/-	Y	0.01% YE	BY Cribs (C9487), Hf
Butyrate	Y	+/-	Y	0.01% YE	BY Cribs (C9487), Hf
Ethane	Y	+/-	Y	0.01% YE	BY Cribs (C9487), Hf
Butane	Y	+/-	Y	0.01% YE	BY Cribs (C9487), Hf
None	Y	+/-	Y	0.01% YE	BY Cribs (C9487), Hf
None	Y	+/-	Y	N	BY Cribs (C9487), Hf (heat inactivated)
None	N	-	Y	N	BY Cribs (C9487), Hf (no PCOI or CoCOI added)
None	Y	+/-	N	N	NA
Organic Gas Treatment	Nitrate	CoCOI	Sediment	Nutrients	Sediment Origin
Pentane	Y	+/-	Y	0.01% YE	216-S-9 (C9512), Hf
Butyrate	Y	+/-	Y	0.01% YE	216-S-9 (C9512), Hf
Ethane	Y	+/-	Y	0.01% YE	216-S-9 (C9512), Hf
Butane	Y	+/-	Y	0.01% YE	216-S-9 (C9512), Hf
None	Y	+/-	Y	0.01% YE	216-S-9 (C9512), Hf
None	Y	+/-	Y	N	216-S-9 (C9512), Hf (heat inactivated)
None	N	-	Y	N	216-S-9 (C9512), Hf (no PCOI or CoCOI added)
None	Y	+/-	N	N	NA

NA = not applicable

3.5.3 Gas-Phase Chemical Sequestration – CO_2 gas

The focus was on sequestration of I-129 under VZ conditions via injection of CO_2 gas into unsaturated sediments. However, a subset (Objective 2) included CoCOIs [U, Tc-99, Cr(VI), and Sr]. The goal of CO_2 gas injection is to partition carbonate into pore water, leading to calcite precipitation as calcite can incorporate iodate (IO_3^-) into the structure and decrease its mobility. Because of the focus of this technology on the VZ, an additional subset (Objective 3) was included to measure sequestration at variable WC.

3.5.3.1 Objective 1: Quantify I sequestration without CoCOIs with CO_2 gas treatment

Water-saturated experiments were conducted for Objectives 1 (IO_3 only) and 2 (IO_3 and CoCOI), where batch vials (in triplicate) are attached to a 22-liter metallized gas bag filled with CO_2 (60 days), then flushed with air (90 days; Table 3.14). The air treatment is to measure IO_3 remobilization (part of Objectives 1 and 2) that would occur over the long term as the CO_2 gas reacted and/or diffused and air-filled pore space returned to natural conditions (including natural pH conditions).

These experiments were conducted with aqueous samples collected at four time periods during the first 60 days and three time periods during the subsequent 90 days. Sequential extractions were conducted on sediments at 60 days and 150 days. All Objective 1 and 2 experiments were conducted in water-saturated batch systems at a sediment:water ratio of 1:7 (i.e., 20 g/140 mL). Aqueous iodine was measured (as described in Section 3.4.1.2) at 1, 10, 30, 60, 90, 120, and 150 days, and separate, sacrificial batch vials were used for sequential extractions at 60 days (end of CO_2 gas treatment) and 150 days (end of air treatment; Table 3.14). Batch experiments were mixed on a shaker table between sampling events. Each condition was conducted in triplicate, including no-treatment controls.

The changes in IO_3 and CoCOIs as aqueous, adsorbed, and precipitated species were quantified with four sequential liquid extractions on sediments following aqueous phase analysis. I-127 was initially present as IO_3^-, and U as uranyl carbonate aqueous species [U(VI)], nitrate, Cr(VI) as $Cr(VI)O_4^-$, Tc-99 as $Tc(VII)O_4^-$, and Sr as Sr^{2+} (Table 3.8). Extractions were conducted with a 1:2 sediment-to-solution ratio as described in Section 3.3, although the third extract was skipped because reducing conditions were not generated. Analysis of PCOIs and CoCOIs from the recovered liquids is described in Section 3.4.

Table 3.14. Treatments for Objectives 1, 2, and 3.

Objective	PCOI	CoCOIs	Water (S-saturated; U-unsaturated), Sediment	# Samples	Aqueous Sample Times (days)	Sequential Extraction Times (days)
1	I-127	None	S, Hf	6	1, 10, 30, 60, 90, 120, 150	60, 150
2	I-127	U, Tc-99, Cr, Sr-90, nitrate	S, Hf	6	1, 10, 30, 60, 90, 120, 150	60, 150
1	I-127	None	S, Hf	3	None (no gas control)	150
2	I-127	U, Tc-99, Cr, Sr-90, nitrate	S, Hf	3	None (no gas control)	150
3	I-127	None	U 4%, Hf	9	1, 10, 30, 60, 90, 120, 150	60, 150
3	I-127	None	U 8%, Hf	9	1, 10, 30, 60, 90, 120, 150	60, 150
3	I-127	None	U 4%, Hf	2	None (no gas control)	150
3	I-127	U, Tc-99, Cr, Sr-90, nitrate	U 4% Hf	9	1, 10, 30, 60, 90, 120, 150	60, 150
3	I-127	U, Tc-99, Cr,Sr-90, nitrate	U 4%, 216-S-9 sed.	9	1, 10, 30, 60, 90, 120, 150	60, 150
3	I-127	U, Tc-99, Cr, Sr-90, nitrate	U 4%, 216-S-9 sed.	3	None (no gas control)	150

3.5.3.2 Objective 2: Quantify I sequestration with CoCOIs with CO_2 treatment

Objective 2 experiments are water-saturated similar to Objective 1 but are conducted with both IO_3 and CoCOIs rather than only IO_3. These experiments were also conducted with 60 days of CO_2 treatment followed by 90 days of air treatment (Table 3.14), with aqueous iodine measured at 1, 10, 30, 60, 90, 120, and 150 days and sequential extractions at 60 and 150 days.

3.5.3.3 Objective 3: Quantify I sequestration with CoCOIs in unsaturated conditions with CO_2 treatment

Unsaturated batch experiments for Objective 3 were conducted to evaluate sequestration (i.e., incorporation and/or coating) of IO_3 by inducing precipitation of calcite under more field-realistic WCs in VZ sediments, which includes (1) 4% WC with IO_3 only and (2) 8% WC with IO_3 only, 4% WC with IO_3 and CoCOIs. Objective 3 experiments were conducted with the Hf sediments. Some experiments for Objective 3 were additionally conducted with an iodine-contaminated 216-S-9 sediment (C9512 8C, 100′ depth, containing 0.025 µg/g total iodine and 235 µg/g nitrate), which is the primary proposed

application waste site. This 216-S-9 sediment also had other co-contaminants, including U (268 µg/g) and Cr(VI) (657 µg/g) (PNNL-26208).

Unsaturated sediment columns conducted for Objective 3 consisted of ~7 g of sediment packed into a small stainless-steel column at either 4% or 8% WC containing IO_3 only or IO_3 with CoCOIs. These WCs were chosen to be representative of DVZ sediments in the 200-DV-1 OU based on previous research. For example, sandy gravel and gravely sand-sized Hanford, CCug, and Ringold formation sediments averaged 4.01 ± 1.67% WC (PNNL-27524; PNNL-26266; PNNL-26208), whereas finer grained low-permeability zones are typically at higher WC up to water-saturated conditions (~16% g/g). Carbon dioxide treatment consisted of injecting 10 pore volumes of CO_2 gas through the column to saturate the air-filled pores with CO_2, then capping both column ends. At 60 days, 10 pore volumes of air were then injected through the column. For sample times of 1, 10, 30, 90 and 120 days, only the aqueous extraction was conducted. For sample times of 60 and 150 days, the four sequential extractions were conducted with sediments. One column in each set was sacrificed for each of the seven sample times except for 60 and 150 days, when three columns (triplicates) were sacrificed.

3.5.4 Particulate Phase Chemical Sequestration – Sn(II)-PO_4

The focus was on chemical sequestration including U and Tc-99 as PCOIs and Sr-90, I-129, Cr(VI), and nitrate as potential CoCOIs via treatment with particulate Sn(II)-PO_4. Sn(II)-PO_4 has been identified for primary treatment zones, including the 200-DV-1 OU perched water aquifer and/or groundwater beneath the BY Cribs, and secondary treatment zones, including 216-U-1&2, S-SX Tank Farm, C Tank Farm, and BC Cribs and Trenches (Table 1.1).

3.5.4.1 Objective 1: Quantify Tc-99 and U removal and order of magnitude rate by treatment with Sn(II)-PO_4

The first objective was to quantify the rate of removal from the aqueous phase or sequestration of the PCOIs. Batch-type experiments were used to determine the overall effectiveness of Sn(II)-PO_4 at successfully transforming contaminants to less-mobile phases. The matrix (Table 3.15) was evaluated in batch conducted in triplicate with a 1:2 sediment-to-solution ratio (10 g of sediment + 20 mL of solution), with samples collected over 28 days. The duration was based on scoping work (Appendix E, Section E.2). Batch experiments were mixed on a shaker table between sampling events. At five time points, an aliquot (0.75 mL) of the aqueous phase was removed following centrifugation (10 minutes at 5000 rpm), filtered (0.2-µm PTFE syringe filter), and analyzed for select contaminants and elements of interest using methods described in Section 3.4. PCOIs were analyzed at each time point, while CoCOIs and other relevant analytes were analyzed only for the final time point. The total volume change during sampling was < 20% to minimize change to the sediment-to-solution ratio.

For batch experiments containing the Sn(II)-PO_4 treatment, 0.3 g of Sn(II)-PO_4 (3 wt%), synthesized in house (Appendix E, Section E.1) was added; the amount of Sn(II)-PO_4 added was based on results of scoping experiments (Section E.2). Both Hf sediment and Sn(II)-PO_4 were added to the batch tube first, followed by SGW or SPW solutions. Experiments conducted under BY Cribs groundwater conditions used SGW, while SPW was used for perched water conditions. PCOIs (with or without CoCOIs) were added directly to the SGW or SPW solutions so that concentrations were consistent across all batch tubes. Non-radioactive isotopes of Sr and I were used, as discussed in Table 3.7. For batch experiments containing delivery fluid, xanthan gum was added (800 mg/L) to the background solution (SGW or SPW). Xanthan gum was chosen as a common delivery fluid used in remedial applications and based on previous delivery fluid testing with other particulate amendments (e.g., ZVI, SMI, and bismuth) (Muller et al. 2021b).

Table 3.15. Matrix for Sn(II)-PO_4 particulate phase treatment.

Description	Sn(II)-PO_4	Sediment	Background Solution	Delivery Fluid	PCOIs	CoCOIs
BY Cribs – PCOIs						
Sn(II)-PO_4 treatment	Y	Y	SGW	N	Y	N
Sn(II)-PO_4 treatment with delivery fluid	Y	Y	SGW	Y	Y	N
Sediment only – no treatment	N	Y	SGW	N	Y	N
BY Cribs – PCOIs & CoCOIs						
Sn(II)-PO_4 treatment (CoCOIs)	Y	Y	SGW	N	Y	Y
Sn(II)-PO_4 treatment with delivery fluid (CoCOIs)	Y	Y	SGW	Y	Y	Y
Sediment only – no treatment (CoCOIs)	N	Y	SGW	N	Y	Y
BY Cribs – No Sediment Controls						
Sn(II)-PO_4 treatment – no sediment	Y	N	SGW	N	Y	N
Sn(II)-PO_4 treatment with delivery fluid – no sediment	Y	N	SGW	Y	Y	N
Sn(II)-PO_4 treatment – no sediment (CoCOIs)	Y	N	SGW	N	Y	Y
Sn(II)-PO_4 treatment with delivery fluid – no sediment (CoCOIs)	Y	N	SGW	Y	Y	Y
Perched Water – PCOIs & CoCOIs						
Sn(II)-PO_4 treatment	Y	Y	SPW	N	Y	Y
Sn(II)-PO_4 treatment with delivery fluid	Y	Y	SPW	Y	Y	Y
Sediment only – no treatment	N	Y	SPW	N	Y	Y
Perched Water – No Sediment Controls						
Sn(II)-PO_4 treatment – no sediment	Y	N	SPW	N	Y	Y
Sn(II)-PO_4 treatment with delivery fluid – no sediment	Y	N	SPW	Y	Y	Y

Y = yes, included; N = No, not included,
PCOIs included Tc-99 and U; CoCOIs included Cr(VI),I, Sr, and nitrate; concentrations are defined in Table 3.7.

3.5.4.2 Objective 2: Quantify Tc-99 and U sequestration by treatment with Sn(II)-PO_4

The second objective was to quantify the sequestration of the PCOIs (U and Tc-99) based on sequential extractions on the sediments in batch reactors with a 1:3 sediment-to-solution ratio after the final sampling time point of the Objective 1 batch experiments. The sequential extraction methods are described in Section 3.3.

3.5.5 Particulate Phase Chemical Sequestration – Bismuth oxyhydroxide and bismuth subnitrate

This testing was focused on chemical sequestration including U and Tc-99 as PCOIs and Sr-90, I-129, Cr(VI), and nitrate as potential CoCOIs via injection of particulate Bi-based materials (BOH or BSN). Bi-based materials have been identified for primary treatment zones, including the 200-DV-1 OU perched water aquifer and/or groundwater beneath the BY Cribs, and secondary treatment zones, including 216-U-1&2, S-SX Tank Farm, C Tank Farm, and BC Cribs and Trenches (Table 1.1).

3.5.5.1 Objective 1: Quantify Tc-99 and U removal and order of magnitude rate by treatment with BOH or BSN

The first objective was to quantify the removal rate of the PCOIs. Batch-type experiments were used to determine the overall effectiveness of BOH or BSN at successfully transforming contaminants to immobile end products. PCOIs and CoCOIs in solutions were analyzed following five sampling events. Experiments conducted under BY Cribs groundwater conditions used SGW while SPW was used for

perched water conditions, both with Hf sediments. The matrix (Table 3.16) was evaluated in triplicate with a 1:2 sediment-to-liquid ratio (10 g of sediment + 20 mL of solution) with samples collected over 28 days. At five time points, an aliquot (0.75 mL) of the aqueous phase was removed following centrifugation (10 minutes at 5,000 rpm), filtered (0.2-µm PTFE syringe filter), and analyzed for select contaminants and elements of interest (Section 3.4). Samples were mixed on a shaker table between sampling events. PCOIs were analyzed at each time point, while CoCOIs and other relevant analytes were analyzed only for the final time point. The total volume change during sampling was < 20% to minimize change to the sediment-to-solution ratio with time.

For batch experiments containing the BOH or BSN treatment, 0.3 g (or 3 wt%) of BOH (synthesized in house, Appendix F, Section F.1) or BSN (Sigma-Aldrich) was added; the amount of Bi-based material added was based on the Sn(II)-PO_4 amendment to allow for comparison of particulate amendments (Section 3.5.4). Both Hf sediment and BOH or BSN were added to the batch tube first, followed by SGW or SPW solutions. PCOIs (with or without CoCOIs) were added directly to the SGW or SPW solutions. Non-radioactive isotopes of Sr and I were used, as discussed in Table 3.7. For batch experiments containing delivery fluid, guar gum was added (800 mg/L) to the background solution (SGW or SPW). Guar gum was chosen as a common delivery fluid used in remedial applications (Muller et al. 2021a) and based on performance of various delivery fluids in scoping tests (Section F.2).

Table 3.16. Matrix for Bi-based materials

Number	Description	BOH/BSN	Sediment	Aqueous Solution	Delivery Fluid	PCOIs	CoCOIs
			BY Cribs – PCOIs				
1	BOH/BSN treatment	Y	Y	SGW	N	Tc-99, U	N
2	BOH/BSN treatment with delivery fluid	Y	Y	SGW	Y	Tc-99, U	N
3	No treatment	N	Y	SGW	N	Tc-99, U	N
4	No treatment with delivery fluid	N	Y	SGW	Y	Tc-99, U	N
			BY Cribs – PCOIs & CoCOIs				
5	BOH/BSN treatment (CoCOIs)	Y	Y	SGW	N	Tc-99, U	Cr(VI), I-127, nitrate, Sr
6	No treatment (CoCOIs)	N	Y	SGW	N	Tc-99, U	Cr(VI), I-127, nitrate, Sr
			BY Cribs – No-Sediment Controls				
7	BOH/BSN treatment – no-sediment control	Y	N	SGW	N	Tc-99, U	N
8	BOH/BSN treatment with delivery fluid – No-sediment control	Y	N	SGW	Y	Tc-99, U	N
9	BOH/BSN treatment – no-sediment control (CoCOIs)	Y	N	SGW	N	Tc-99, U	Cr(VI), I-127, nitrate, Sr
			Perched Water – PCOIs & CoCOIs				
10	BOH/BSN treatment	Y	Y	SPW	N	Tc-99, U	Nitrate
11	BOH/BSN treatment with delivery fluid	Y	Y	SPW	Y	Tc-99, U	Nitrate
12	No treatment	N	Y	SPW	N	Tc-99, U	Nitrate
13	No treatment with delivery fluid	N	Y	SPW	Y	Tc-99, U	Nitrate
			Perched Water – No-Sediment Controls				
14	BOH/BSN treatment – no-sediment control	Y	N	SPW	N	Tc-99, U	Nitrate
15	BOH/BSN treatment with delivery fluid – no-sediment control	Y	N	SPW	Y	Tc-99, U	Nitrate

Y = yes, included; A "yes" in the BOH/BSN column indicates tests will be conducted, in triplicate, for BOH as well as BSN. N = No, not included
PCOIs included Tc-99 and U; CoCOIs included Cr(VI), I, Sr, and nitrate; concentrations are defined in Table 3.7.

3.5.5.2 Objective 2: Quantify Tc-99 and U sequestration by treatment with BOH or BSN

The second objective was to quantify the sequestration of the PCOIs (U and Tc-99) based on sequential extractions on the sediments in batch reactors with a 1:3 sediment-to-solution ratio after the final sampling time point of Objective 1. This occurred at 28 days for most experiments, but some were repeated with sequential extractions conducted after 1 day of reaction time. These "1-day" experiments were included to determine if the mobility of sequestered contaminants changed over time. The sequential extraction methods are described in Section 3.3.

3.5.6 Particulate-Phase Combined Chemical Reduction and Sequestration – Zero valent iron/sulfur-modified iron (ZVI/SMI) and polyphosphate

This technology was evaluated with a sequential remediation approach with initial reduction of PCOIs using solid phase ZVI or SMI followed by precipitation of apatite from a Poly-PO_4 solution with and without CoCOIs [Sr-90, I-129, Cr(VI), and NO_3]. ZVI and SMI have been identified for primary treatment zones (Table 1.1) including the 200-DV-1 OU perched water and/or groundwater beneath the BY Cribs and secondary treatment zones including 216-U-1&2, S-SX Tank Farm, C Tank Farm, and BC Cribs and Trenches. The ZVI used was Hepure Ferox Flow 100 mesh, and XRD showed 100% Fe metal. The SMI used was North American Hoganas R-12S, and XRD showed 60% Fe metal, 33% magnetite (Fe_3O_4), 7% wustite (FeO), and a trace of S. Additional ZVI and SMI characterization is discussed in Appendix G, Section G.1.

The primary objectives were to quantify the decrease in PCOI (Tc-99 and U) mass, which corresponds to contaminant sequestration, and order of magnitude sequestration rate, by treatment combinations as described in Section 2.6. This was broken down into two sub-objectives based on the presence or absence of CoCOIs as considered in Objective 1 and 2, respectively. Objective 2 also considered the effect of the delivery fluid on Tc-99 and U mobility.

To address Objective 1, experiments were conducted with Tc-99 and U (no CoCOIs), SMI, ZVI, and Poly-PO_4 with Hf sediments (untreated Hf and BY Cribs sediment). To address Objective 2a, experiments were conducted with Tc-99 and U and different combinations of CoCOIs and water, SMI, ZVI, and Poly-PO_4, with and without sediments (as described in DOE/RL-2018-28, Table 7-2). To address Objective 2b, experiments were conducted with Tc-99 and U and different combinations of CoCOIs, SMI or ZVI, Poly-PO_4, sediments, and a delivery fluid (xanthan gum). Contaminant sequestration and rates are quantified by sequential extractions, which quantify contaminant mass that is aqueous, adsorbed, and reduced but readily oxidized (all considered mobile mass, Extractions 1, 2, and 3) and the amount of mass that is sequestered in precipitates (Extractions 4 and 5, described in Section 3.3).

3.5.6.1 Objective 1: Quantify Tc-99 and U removal and order of magnitude rate by treatment with ZVI or SMI and Poly-PO_4 without CoCOIs

Water-saturated batch experiments (1:2 sediment-to-solution ratio) were conducted to evaluate PCOI (Tc-99, U) change in mobility and sequestration rate with (1) ZVI or SMI reductant and (2) Hf or CCug sediments. Each condition (Table 3.17) was conducted with vials that were sacrificed at specified times (below) and subjected to sequential extractions. Concentrations of PCOIs used were 10 μg/L Tc-99 (20 ng/g or 300 pCi/g) and 1000 μg/L U (2 μg/g) for groundwater or 10 μg/L Tc-99 and 50,000 μg/L for perched water application. The mass of SMI and ZVI per gram of sediment was based on a previous study (PNNL-31959), but additional experiments over a wider mass loading range were also conducted. The concentrated phosphate solution was made from phosphoric acid, sodium hydroxide, potassium hydroxide, and Na-pyroPO_4, as described elsewhere (PNNL-29650). Briefly, the Poly-PO_4 solution composition was based on the 300 Area field-scale Poly-PO_4 injections (i.e., 88 mmol/L total PO_4 with

90% orthophosphate and 10% pyrophosphate), and a total of 35 mM PO_4 was added from 0.66 mL of 874-mM orthophosphate solution [adjusted to pH 7.6, and containing 42.85 mL of H_2O, 2.52 mL H_3PO_4, 2.53 mL NaOH, 2.1 mL KOH, and 2.16 g Na-pyroPO_4, $Na_4(PO_4)_2 \bullet 10H_2O$]. Sediments contained sufficient calcium to precipitate apatite (based on the cation exchange capacity and ions present, Appendix A, Section A.4), but for experiments that contained no sediments, calcium was added using 0.58 mL of 2 mol/L $CaCl_2$ solution. Sequential extractions were corrected for the additional phosphate and calcium volume added.

Different sediments were used to represent the different formations present in the targeted perched and groundwater application areas. Sediments included field-contaminated BY Cribs sediment (HF, C9552 106-107' bgs, stored at 4 °C), which was characterized previously (PNNL-26266), and the Hanford Cold Creek Unit silt [CCuz, Pasco, WA, (Placencia-Gómez et al. 2023)]. The CCuz has a higher calcite ($CaCO_3$) fraction, which will result in some pH buffering due to the buffering capacity of carbonates with the pK_a of 10.3 for HCO_3^- to CO_3^{-2}. This could influence PCOI treatment with ZVI and SMI, as these amendments alter the pH. The buffering capacity in high calcite sediments, e.g., CCuz, will limit the pH increase caused by the ZVI and SMI. This difference in pH will alter aqueous U speciation and will potentially influence subsequent reduction and sequestration by ZVI and SMI.

Objective 1 experiments consisted of loading 45-mL tubes with 10 g of sediment, 20 mL of SGW or SPW (containing U and Tc-99) with 0.07 g SMI or 0.08 g ZVI in an anaerobic chamber, mixing for 14 days, then adding 35 mmol/L Poly-PO_4 and mixing for an additional 36 days. These SMI and ZVI loadings are the same as other technologies in terms of equivalents of reductant per equivalents of uranium (Tc-99 is significantly lower concentration). Sacrificial batch experiments were conducted with sampling of the aqueous before Poly-PO_4 was added at 1 day, 7 days, 14 days, and after Poly-PO_4 was added at 21 days and 50 days, with triplicate tubes for the last time point to give a total of 42 sample tubes. Batch experiments were mixed on a shaker table between sampling events. For each sample, destructive sampling with five sequential extractions was conducted on sediments remaining after solutions were removed at the aforementioned time point (details in Section 3.3).

ZVI/SMI loadings were similar except the ZVI or SMI loading varied at 0.10, 0.3, 1, 3, 7.8, and 20 mg SMI/g sediment or ZVI/g sediment. The ZVI or SMI in sediment reacted for 14 days, then 35 mmol/L Poly-PO_4 was added, and the sediment was reacted for an additional 14 days. Loadings were used to evaluate the rate of PCOI (electron acceptors) reduction in a system ranging from excess reductive capacity (with more ZVI or SMI added than was required to reduce the PCOIs) to excess electron acceptor (i.e., insufficient ZVI or SMI to reduce contaminants). Field systems with a reduced zone will start with excess electron donor, and thus generally rapidly reduce contaminants, but over time, as the reductive capacity is consumed by PCOIs or CoCOIs, the rate of contaminant reduction will slow considerably. Note that contaminants require different ratios of electron donor [e.g., Eqs. (2.3) and (2.4) in Section 2.6], so three moles of Fe^{2+} are needed to reduce one mole of $Tc(VII)O_4^-$ to Tc(IV), but only two moles of Fe^{2+} are needed to reduce one mole of $U^{VI}O_2^{2+}$ to U(IV).

3.5.6.2 Objective 2a: Quantify the Tc-99 and U sequestration rate impacted by CoCOIs by treatment with ZVI or SMI and Poly-PO_4

Objective 2a experiments are similar to Objective 1 except for the presence of CoCOIs, which consume ZVI or SMI reductive capacity. Some experiments were also conducted without sediment and in groundwater or perched water. Water-saturated batch experiments were conducted to evaluate the influence of CoCOIs on the rate and extent of PCOI (Tc-99 and U) reduction and sequestration. ZVI or SMI were added initially, and the Poly-PO_4 solution was added at 14 days. Experiments were sampled before Poly-PO_4 addition at 1 day, 7 days, 14 days, and after Poly-PO_4 addition at 21 days and 50 days,

with triplicate tubes for the last time point. This is a total of 42 tubes (5 sample times for each × 6 conditions). For each vial, the series of five sequential extractions was conducted (Section 3.3).

3.5.6.3 Objective 2b: Quantify the Tc-99 and U sequestration rate impacted by a delivery fluid by treatment with ZVI or SMI and Poly-PO_4

Water-saturated batch experiments were conducted to evaluate the impact of a delivery fluid (xanthan) on the rate of PCOI (Tc-99, U) reduction and sequestration using (1) ZVI or SMI as the reductant, and (2) without and with NO_3 (Table 3.17). All experiments included 800 mg/L xanthan, a common high-viscosity, shear thinning delivery fluid that has been used for other solid technologies [i.e., Sn(II)-PO_4, BOH, BSN]. Using SGW with PCOIs (U, Tc-99) without and with CoCOIs (NO_3, CrO_4, and IO_3) or SPW (with PCOIs and without or with NO_3), the ZVI or SMI were added initially and the Poly-PO_4 solution at 14 days. Experiments were sampled before Poly-PO_4 addition at 1 day, 7 days, 14 days, and after Poly-PO_4 addition at 21 days and 50 days, with triplicate tubes for the last time point. This is a total of 20 tubes (5 sample times for each × 4 conditions). For each experimental vial, the series of five sequential extractions was conducted (Section 3.3).

Table 3.17. Conditions for ZVI/SMI/ Poly-PO_4 experiments.

Objective	Primary COIs	CoCOIs	Water	Reductant	PO_4	Sediment	Delivery Fluid
1	Tc-99, U	None	SGW	SMI	Poly-PO_4	Hf	None
1	Tc-99, U	None	SGW	ZVI	Poly-PO_4	Hf	None
1	Tc-99, U	None	SGW	ZVI	Poly-PO_4	CCuz (silt)	None
1	Tc-99, U	None	SGW	SMI	Poly-PO_4	CCuz (silt)	None
1	Tc-99, U	None	SGW	ZVI	Poly-PO_4	BY Cribs	None
1	Tc-99, U	None	SGW	SMI	Poly-PO_4	BY Cribs	None
1	Tc-99, U	None	SGW	None	None	Hf	Control – no treat
1	Tc-99, U	None	SGW	None	None	CCuz (silt)	Control – no treat
1	Tc-99, U	None	SGW	None	None	BY Cribs	Control – no treat
2a	Tc-99, U	None	SGW	SMI	Poly-PO_4	None	None
2a	Tc-99, U	None	SGW	ZVI	Poly-PO_4	None	None
2a	Tc-99, U	NO_3, Cr(VI), I-127	SGW	SMI	Poly-PO_4	None	None
2a	Tc-99, U	NO_3	SPW	SMI	Poly-PO_4	None	None
2a	Tc-99, U	NO_3, Cr(VI), I-127	SGW	ZVI	Poly-PO_4	None	None
2a	Tc-99, U	NO_3	SPW	ZVI	Poly-PO_4	None	None
2a	Tc-99, U	NO_3, Cr(VI), I-127	SGW	None	None	Hf	Control – no treat
2a	Tc-99, U	NO_3	SPW	None	None	Hf	Control – no treat
2b	Tc-99, U	None	SGW	SMI	Poly-PO_4	Hf	Xanthan
2b	Tc-99, U	NO_3	SPW	SMI	Poly-PO_4	Hf	Xanthan
2b	Tc-99, U	None	SGW	ZVI	Poly-PO_4	Hf	Xanthan
2b	Tc-99, U	NO_3	SPW	ZVI	Poly-PO_4	Hf	Xanthan

3.5.7 Liquid-Phase Chemical Sequestration – Apatite-forming solutions

The focus was chemical sequestration of U and Tc-99 as PCOIs and Cr(VI), I-129, Sr, and NO_3 as potential CoCOIs via injection of liquid, apatite-forming amendments. The matrix for batch experiments is described in Table 3.18. This two-step technology has been identified for high-water-content areas (Table 1.1). The primary treatment zones include the 200-DV-1 OU perched water zones and/or

groundwater beneath the BY Cribs, and the secondary treatment zones include 216-U-1&2, S-SX Tank Farm, C Tank Farm, and BC Cribs and Trenches.

3.5.7.1 Objective 1: Quantify Tc-99 and U order of magnitude rate of removal by treatment with liquid apatite-forming solutions

The first objective was to quantify the removal or sequestration rate of the PCOIs (Tc-99 and U). Batch experiments were conducted in triplicate with a 1:2 sediment-to-solution ratio (10 g of sediment + 20 mL of solution) with at least four samples collected over a 21-day period after treatment. The 21-day treatment was based on previous development testing of the liquid apatite technologies to allow for precipitation of apatite from the liquid phosphate amendments (Wellman et al. 2008, 2011; PNNL-SA-65124).

Batch experiments were used to determine the overall effectiveness of addition of either Ca-Cit-PO_4 or Poly-PO_4 as apatite-forming solutions to successfully transform contaminants to immobile or temporarily immobile end products. Table 3.18 presents the matrix for a series of batch experiments conducted under BY Cribs groundwater or perched water conditions. The batch experiment constituents were added in the following order: (1) sediments, (2) SGW or SPW, (3) PCOIs (with or without CoCOIs), (4) liquid apatite-forming solutions. Experiments conducted under BY Cribs groundwater conditions used SGW and under perched water conditions used SPW. At least four samples were taken over the 21-day batch and the concentrations of PCOIs (Tc-99 and U) in solution were analyzed; the concentrations of CoCOIs [i.e., Cr(VI), I-127, NO_3^-] in solution were only analyzed for the final time point. At each sampling point, solution was passed through 0.22-µm PTFE filters. The total volume change during sampling was limited to < 20% to change in the sediment-to-solution ratio. Batch experiments were mixed on a shaker table between sampling events.

The addition of Poly-PO_4 or Ca-Cit-PO_4 solutions is described in Table 3.18. The sodium polyphosphate (Poly-PO_4) amendment was added as two solutions with a 1:1 ratio by volume: (1) 48 mM total PO_4 with the following ratio of species – 75.8% Na_2HPO_4, 14.2% NaH_2PO_4, and 1% $Na_5P_3O_{10}$; and (2) 72.3 mM $CaCl_2$. These solutions resulted in final P and Ca concentrations of 24 and 36.15 mM, respectively. The method requires approximately 1.67 times more Ca than PO_4 based on their ratio in apatite [$Ca_5(PO_4)_3$]. However, less Ca is added based on the amount of Ca released from the Hf sediments. Details for how the sediment Ca was estimated are included in Appendix A, Section A.4. Ca was not added during previous Poly-PO_4 field injections, as it is assumed to be exchanged from sediments for Na in the PO_4 solution (PNNL-29650). Depending on the targeted conditions, the solutions for the liquid amendments were prepared in either SGW for BY Cribs groundwater conditions or SPW for perched water conditions.

The calcium citrate/sodium phosphate (Ca-Cit-PO_4) amendment was added as two solutions with a 1:1 ratio by volume: (1) 48 mM total PO_4 with the following ratio of species – 81% Na_2HPO_4, 14% NaH_2PO_4, and 5% $(NH_4)_2HPO_4$; and (2) 72.3 mM $CaCl_2$ (same overall concentrations as for Poly-PO_4). However, 90.4 mM sodium citrate ($NaC_6H_5O_7$) was added to both solutions to reduce the likelihood that solutions would immediately precipitate. Citrate ($C_6H_5O_7^-$) is degraded by naturally occurring bacteria, leading to a slower precipitation process and potentially stimulating bacteria that can generate reducing conditions. River water (RW) was used to prepare the Ca-Cit-PO_4 amendment, as it provides a source of bacteria in the solutions that will be injected into the subsurface, based on previous use for injection of PO_4 amendments in the Hanford Site's river corridor (PNNL-18303).

Table 3.18. Experimental matrix for liquid apatite-forming amendments.

Description	PCOI	CoCOI[(a)]	Sediment	Sediment Microbes[(b)]	Solution Microbes[(c)]	Simulant Water	Amendment
BY Cribs Groundwater + Calcium citrate phosphate							
Calcium citrate phosphate + river H_2O	Y	N	Y	Y	Y	RW	Ca-Cit-PO_4
Calcium citrate phosphate + sterile river H_2O	Y	N	Y	Y	N	RW	Ca-Cit-PO_4
Calcium citrate phosphate + sterile sediment + sterile river H_2O	Y	N	Y	N	N	RW	Ca-Cit-PO_4
Calcium citrate phosphate + sterile sediment + river H_2O	Y	N	Y	N	Y	RW	Ca-Cit-PO_4
Calcium citrate phosphate + river H_2O + CoCOIs	Y	Y	Y	Y	Y	RW	Ca-Cit-PO_4
BY Cribs Groundwater + Polyphosphate							
Polyphosphate	Y	N	Y	Y	N	SGW	Poly-PO_4 + Ca
Polyphosphate + CoCOIs	Y	Y	Y	Y	N	SGW	Poly-PO_4 + Ca
BY Cribs Groundwater Controls							
SGW	Y	N	Y	Y	N	SGW	-
River H_2O	Y	N	Y	Y	Y	RW	-
River H_2O + CoCOIs	Y	Y	Y	Y	Y	RW	-
River H_2O + sterile sediment	Y	N	Y	N	Y	RW	-
Sterile River H_2O + sterile sediment	Y	N	Y	N	N	RW	-
SGW + CoCOIs	Y	Y	Y	Y	N	SGW	-
Perched Water + Calcium citrate phosphate							
Calcium citrate phosphate + river H_2O	Y	Y	Y	Y	Y	RW	Ca-Cit-PO_4
Calcium citrate phosphate + sterile river H_2O	Y	Y	Y	Y	N	RW	Ca-Cit-PO_4
Calcium citrate phosphate + sterile sediment + sterile river H_2O	Y	Y	Y	N	N	RW	Ca-Cit-PO_4
Calcium citrate phosphate + sterile sediment + river H_2O	Y	Y	Y	N	Y	RW	Ca-Cit-PO_4
Perched Water + Polyphosphate							
Polyphosphate	Y	Y	Y	Y	N	SPW	Poly-PO_4 + Ca
Perched Water Controls							
Perched H_2O	Y	Y	Y	Y	N	SPW	-
River H_2O	Y	Y	Y	Y	Y	RW	-

Y = yes, included; N = No, not included.
(a) CoCOIs included Cr(VI), I, Sr, and NO_3 at concentrations defined in Table 3.7.
(b) Samples that excluded sediment microbes were heat inactivated prior (60 minutes at 100 °C).
(c) Samples that excluded solution microbes were filter sterilized prior.

3.5.7.2 Objective 2: Quantify Tc-99 and U sequestration by treatment with liquid apatite-forming solutions

The second objective was to quantify the amount of PCOIs (U and Tc-99) sequestered based on sequential extractions (Section 3.3) of the sediments in batch reactors after the final sampling time point, which occurred at 21 days.

3.5.8 Liquid-Phase Combined Chemical Reduction and Sequestration – Calcium polysulfide and polyphosphate solutions

This technology was focused on chemical reduction and sequestration of PCOIs (U and Tc-99), with and without CoCOIs [Cr(VI), I-129, Sr, and NO_3], via injection of liquid CPS followed by liquid, apatite-forming amendments (sodium polyphosphate, Poly-PO_4). CPS is added to reductively precipitate

reducible PCOIs. However, because the reduction is likely temporary, a second sequestration step involves addition of Poly-PO_4. This two-step technology has been identified for high-water-content areas (Table 1.1). The primary treatment zones include the 200-DV-1 OU perched water zones and/or groundwater beneath the BY Cribs, and the secondary treatment zones include 216-U-1&2, S-SX Tank Farm, C Tank Farm, and BC Cribs and Trenches.

3.5.8.1 Objective 1: Quantify Tc-99 and U order of magnitude rate of removal by treatment with CPS and Poly-PO_4 treatment

The first objective was to quantify the removal or sequestration rate of the PCOIs (Tc-99 and U). Batch experiments were conducted in triplicate with a 1:2 sediment-to-solution ratio (10 g of sediment + 20 mL of solution). CPS was added at the start, followed by Poly-PO_4 after 14 days, with at least four samples collected over the 42-day treatment period.

Batch experiments were used to determine the overall effectiveness of addition of an inorganic reductant (CPS) followed by apatite-forming solutions (Poly-PO_4) to successfully transform contaminants into immobile or temporarily immobile end products. The batch matrix conducted under either BY Cribs groundwater or perched water conditions is described in Table 3.19. The batch constituents were added in the following order: (1) sediments, (2) SGW or SPW, (3) PCOIs (with or without CoCOIs), (4) CPS solutions (first four steps all at time zero), and (5) Poly-PO_4 solutions (after 14 days).

CPS was added at a concentration of approximately 2.5 wt% to reductively precipitate reducible PCOIs. Poly-PO_4 amendment was added at day 14 as two solutions with a 1:1 ratio by volume: (1) 240 mM total PO_4 with the following ratio of species – 75.8% Na_2HPO_4, 14.2% NaH_2PO_4, and 1% $Na_5P_3O_{10}$; and (2) 361.5 mM $CaCl_2$ added as approximately 3 mL to a total volume of 30 mL. These solutions resulted in final P and Ca concentrations of 24 and 36.15 mM, respectively. The method requires approximately 1.67 times more Ca than PO_4 based on their ratio in apatite [$Ca_5(PO_4)_3$]. Depending on the targeted conditions, the solutions for the liquid amendments were prepared in either SGW for BY Cribs groundwater conditions or SPW for perched water conditions.

CPS was added at the start, then Poly-PO_4 was added after a 14-day reaction time, followed by reaction for another 28 days. At least four samples were collected over the 42-day treatment time. Concentrations of PCOIs (Tc-99 and U) and CoCOIs [i.e., Cr(VI), I-127, NO_3^-] were measured in the solution samples from the batch experiments, and in the solutions obtained from the sequential extractions. The matrix that was evaluated in batch experiments for liquid-phase chemical reduction and sequestration was conducted in triplicate with a 1:2 sediment-to-solution ratio (15 g of sediment + 30 mL of solution) as described in Table 3.19. The total volume change during sampling was kept to < 20% to minimize change in the sediment-to-solution ratio. Batch experiments were mixed on a shaker table between sampling events.

Table 3.19. Experimental matrix for liquid calcium polysulfide and apatite-forming amendments.

Description	PCOI	CoCOI	NO_3	Sediment	Amendment 1	Amendment 2	Simulant Water
BY Cribs Groundwater - Treated							
CPS + PCOIs – no sediment	Y	N	N	N	CPS	N	SGW
CPS + PCOIs	Y	N	N	Y	CPS	N	SGW
CPS + PCOIs + CoCOIs	Y	Y	N	Y	CPS	N	SGW
CPS + Poly-PO_4 + PCOIs – No sediment	Y	N	N	N	CPS	Poly-PO_4	SGW
CPS + Poly-PO_4 + PCOIs	Y	N	N	Y	CPS	Poly-PO_4	SGW
CPS + Poly-PO_4 + PCOIs + CoCOIs	Y	Y	N	Y	CPS	Poly-PO_4	SGW
BY Cribs Groundwater - Controls							
SGW + PCOIs – no sediment	Y	N	N	N	N	N	SGW
SGW + PCOIs	Y	N	N	Y	N	N	SGW
SGW + PCOIs + CoCOIs – No sediment	Y	Y	N	N	N	N	SGW
SGW + PCOIs + CoCOIs	Y	Y	N	Y	N	N	SGW
SGW + PCOIs – no sediment	Y	N	N	N	N	N	SGW
Perched Water (including Control)							
CPS + PCOIs + NO_3	Y	Y	Y	Y	CPS	N	SPW
CPS + Poly-PO_4 + PCOIs + NO_3	Y	Y	Y	Y	CPS	Poly-PO_4	SPW
SPW + PCOIs + NO_3	Y	Y	Y	Y	N	N	SPW

3.5.8.2 Objective 2: Quantify Tc-99 and U sequestration by treatment with CPS and Poly-PO_4 treatment

The second objective was to quantify the amount of the PCOIs (U and Tc-99) sequestered in the sediments, based on sequential extractions (Section 3.3) of the final sample taken from the batch experiments. For most samples, this occurred at 42 days; however, select samples were also prepared at shorter time points to monitor how sequestration changed with time.

3.5.9 Liquid-Phase Combined Bioreduction and Chemical Sequestration – Organic and polyphosphate solutions

This technology was focused on combined microbiological reduction and chemical sequestration, including U, Tc-99 and NO_3 as PCOIs and Cr(VI), I-129 and Sr^{+2} as potential CoCOIs. Poly-PO_4 formed apatite has been identified for high-water-content areas. This could include primary treatment zones, such as the 200-DV-1 OU perched water zones and/or water table PRBs beneath the BY/BC Cribs and Trenches, or the secondary treatment zones, including 216-U-1&2, S-SX Tank Farm, C Tank Farm, and BC Cribs and Trenches. However, there may be a need for an additional reduction step for contaminants that may not be carried with apatite (e.g., Tc-99). This may be accomplished by addition of an organic substrate as described in Section 2.9. The matrix for batch experiments is summarized in Table 3.20. Molasses and emulsified oil substrate (EOS) were chosen as fast-release and slow-release liquid organic amendments, respectively, based on scoping experiments (Appendix J) and on previous remedial application of these amendments at the Hanford Site (PNNL-28055; Bagwell et al. 2020; Gartman et al. 2019; PNNL-31959). The molasses used was food-grade backstrap molasses (Plantation, unsulphured molasses). The EOS (EOSPro, Redox Tech, Cary, NC) was an emulsified vegetable (approximately 59.8% soybean) oil containing proprietary surfactants, including B12 at a neutral pH with 74% total fermentable carbon. Each were added at approximately 0.39 g/L of total organic carbon (TOC).

3.5.9.1 Objective 1: Quantify NO_3, Tc-99, and U removal and order of magnitude rate with two-step treatment by organic liquids followed by Poly-PO_4

Batch-type experiments (1:2 sediment-to-solution ratio) were performed to determine the overall effectiveness of slow and fast release organic amendments to stimulate soil microbial activity followed by Poly-PO_4 addition to sequester long-lived contaminants. Experiments conducted under BY Cribs groundwater conditions used SGW (Table 3.4), and SPW (Table 3.5) was used for perched water conditions. Non-sieved, composite CCug and PZsd sediments were used in this technology evaluation for the BY Cribs groundwater and perched water conditions, respectively (described in Section 3.1 and Appendix A). PCOIs [NO_3, Tc-99, U(VI)] and CoCOIs [Cr(VI), I-127, Sr] in the aqueous phase were analyzed throughout the microbiological reduction phase and after the Poly-PO_4 treatment. The matrix for the batch experiments is summarized in Table 3.20.

Table 3.20. Experimental matrix for microbial reduction and apatite-forming amendments.

Amendment Description	PCOI	CoCOI	NO_3	Sediment	Amendment 1	Amendment 2	Simulant Water
BY Cribs Groundwater + PCOIs							
Emulsified oil substrate (EOS)	Y	N	Y	Y	Y	Poly-PO_4	SGW
Blackstrap molasses	Y	N	Y	Y	Y	Poly-PO_4	SGW
No-donor controls	Y	N	Y	Y	N	Poly-PO_4	SGW
No-sediment with EOS	Y	N	Y	N	Y	N	SGW
No-sediment with molasses	Y	N	Y	N	Y	N	SGW
No-sediment or donor	Y	N	Y	N	N	N	SGW
BY Cribs Groundwater + PCOIs + CoCOIs							
EOS	Y	Y	Y	Y	Y	Poly-PO_4	SGW
Blackstrap molasses	Y	Y	Y	Y	Y	Poly-PO_4	SGW
No-donor controls	Y	Y	Y	Y	N	Poly-PO_4	SGW
No-sediment with EOS	Y	Y	Y	N	Y	N	SGW
No-sediment with molasses	Y	Y	Y	N	Y	N	SGW
No-sediment or donor	Y	Y	Y	N	N	N	SGW
Perched Water							
EOS	Y	N	Y	Y	Y	Poly-PO_4	SPW
Blackstrap molasses	Y	N	Y	Y	Y	Poly-PO_4	SPW
No-donor controls	Y	N	Y	Y	N	Poly-PO_4	SPW
No-sediment with EOS	Y	N	Y	N	Y	N	SPW
No-sediment with molasses	Y	N	Y	N	Y	N	SPW
No-sediment or donor	Y	N	Y	N	N	N	SPW

The matrix presented in Table 3.20 were arranged to allow for destructive sampling at time points 0, 7, and 14 days (after the addition of Amendment 1), once between 45 and 47 days (right before the addition of Amendment 2), and once between 90 and 132 days (after the addition of Amendment 2). For no-sediment tests, non-destructive sampling was performed at time points 0, 12, 98, and 113 days.

To prepare 1:2 sediment:liquid microcosms, 3.5 g of sediment (as is) was weighed on the benchtop (room air) into an autoclaved 20-mL glass headspace vial. Vials were then sealed with an autoclaved butyl-rubber stopper and the sediment aliquots were stored in the dark at 4 °C until contaminant addition and treatment. Sediment aliquots were transferred and sealed into an inert gas chamber (MBraun, 100% N_2, O_2 < 0.1 ppm, ~21 °C). Then, anoxic aqueous matrix (SPW + PCOIs, SGW + PCOIs, or SGW + PCOIs +

CoCOIs, as identified in Table 3.20) was added to each vial after unsealing. To initiate testing, a sterile, anoxic aliquot of amendment was added, as molasses or EOS, or, for the no-donor controls, ultrapure water. After electron donor or water additions, the vials were re-sealed with butyl rubber stopper, crimp-sealed with aluminum, and then placed on their sides, in the dark, on a 100-rpm rotary shaker in the chamber. Periodically, during the incubation, gas production in the microcosms was assessed by using a needle and syringe to gauge overpressure, to give a relative indication of gas production/consumption over time in the various treatments.

Only experiments intended to run between 90 and 132 days were treated with Amendment 2 between 45 and 47 days (Table 3.20). Tests were amended with calcium and phosphate, apatite-forming solutions, targeting 35 mM Ca from $CaCl_2$ and 24 mM PO_4 as diluted from a stock Poly-PO_4 solution (874 mM PO_4, adjusted to pH 7.6, and containing 42.85 mL of H_2O, 2.52 mL H_3PO_4, 2.53 mL NaOH, 2.1 mL KOH, and 2.16 g sodium Pyro-PO_4) as described previously (PNNL-29650). Microcosms were returned to the 100-rpm shaker after calcium and phosphate additions.

Destructive sampling at time points specified above was performed by centrifuging the entire contents in the glass vials inside the MBraun for 15 minutes at 3000 × *g* at ~21 °C. After centrifugation, the supernatant solution was syringe-filtered through a 0.2-µm syringe filter (polyethersulfone, Acrodisc, Cytiva formerly Pall Life Science). For time points 0, between 45 and 47, and between 90 and132 days only, the remaining sediment after centrifugation was subjected to sequential sediment extractions (see Section 3.5). Following destructive sampling, pH was measured on supernatant solutions collected from SGW + PCOI and SPW + PCOI tests at 45 and 113 days, and 47 and 91 days for SPW, respectively, using a HORIBA LAQUAtwin pH-22 hand-held pH electrode. Filtrates from destructive sampling and sequential extractions were analyzed for NO_3^-, NO_2^-, and SO_4^{-2} by IC; Cr(VI) and Sr by ICP-OES; and Tc-99, U, and I-127 by ICP-MS, as described in Section 3.4.

Sediment samples were sampled at the end of combined treatment for microbial analysis. Genomic DNA was extracted for phylogenic analysis, as described in Appendix A, Section A.6.

3.5.9.2 Objective 2: Quantify Tc-99 and U sequestration with two-step treatment with organic liquids followed by Poly-PO_4

The second objective was to quantify the sequestration of PCOIs (U and Tc-99) based on sequential extractions (Section 3.3) on the sediments. At the 0-, ~45-, and ~90-day time points, sequential extractions were carried out on the sediment remaining after the aqueous-phase sampling, using a 1:3 sediment-to-solution ratio as described in Section 3.5.

4.0 Results

4.1 Gas-Phase Bioreduction and Chemical Sequestration – Organic gas and CO_2 gas

This technology was focused on biogeochemical sequestration of Tc-99 as the PCOI and U, I-127, Sr, Cr(VI), and nitrate as CoCOIs via stepwise injection of two gas-phase amendments: (1) an organic gas to stimulate microbial activity and generate a reduced environment, and (2) carbon dioxide gas to form calcite. Table 4.1 describes the targeting testing conditions and amendments. The selection of organic gases used in this study (ethane, butane, butyl acetate) is described in Appendix B, Section B.1.

Section 4.1.1 describes the quantification of the mass of Tc-99 (PCOI) immobilized and the rate of sequestration with treatment only with different organic gases, with and without CoCOIs, to meet Objective 1. Section 4.1.2 describes the quantification of the mass of immobilized Tc-99 and the rate of sequestration with organic gas treatment followed by injection of carbon dioxide gas with and without CoCOIs to meet Objective 2. Finally, Section 4.1.2.2 describes the bioreduction and sequestration of Tc-99 in field-contaminated sediments from under BY Cribs, BC Cribs, and 216-U-8 Cribs. Any discussion of CoCOIs in the following sections is focused on their impact on the PCOI Tc-99, and not their fate upon treatment with organic gases and carbon dioxide. The bioreduction and sequestration of CoCOIs for both objectives are summarized in Appendix B, Sections B.3 through B.9.

Overall, these results show that none of the organic gases evaluated (ethane, butane, butyl acetate) were sufficiently effective for Tc-99 to meet the minimum threshold of 35% transformation to immobile or temporarily immobile end products under VZ conditions (i.e., 4% WC in unsaturated sediments) over 107 days of treatment. There were differences in Tc-99 reduction and sequestration between the three organic gases. After only organic gas treatment, ethane immobilized 13 ± 2% Tc-99, butane immobilized 17 ± 5% Tc-99, and butyl acetate immobilized 31 ± 10% Tc-99 compared to 12 ± 5% Tc-99 for untreated sediment. Although the mild reducing conditions created were insufficient to reduce Tc-99, 65% to 99% of an easily reduced co-contaminant (Cr) was sequestered. The subsequent CO_2 treatment generally resulted in an increase in Tc-99 mobility. Therefore, this technology will not be considered in future Phase 2 evaluation. Recommendations for additional testing conducted in the future include assessment of (1) the impact of moisture content and (2) the addition of nutrients for the microbial community on PCOI removal.

Table 4.1. Summary of remediation conditions and amendments for gas-phase bioreduction and chemical sequestration technologies. Note: No amendments met minimum threshold testing and thus these amendments will not move forward with Phase 2 evaluation.

Primary Conditions and Amendments	
PCOI	Tc-99
Primary treatment zone/ applicable 200-DV-1 waste sites	BY Cribs
Secondary treatment zone/ applicable 200-DV-1 waste sites	BC Cribs/Trenches
Potential co-contaminants	U, NO_3^-, Sr-90, I-129, Cr(VI)
Bioreduction treatments	Ethane; ethyl acetate, butane
Chemical sequestration treatments	CO_2
Phase 1 decision point	No-Go

Note: The treatment and conditions moving forward to Phase 2 evaluation are **bolded**. If no amendment passed the minimum threshold, none are bolded and no additional testing will be conducted.
CN (BY Cribs): Potential co-contaminant but primarily present as ferrocyanide; additional testing ongoing.

4.1.1 Objective 1: Quantify Tc-99 order of magnitude and rate of removal via treatment with organic gases

For the Hf sediment at 4% WC, organic gas treatment for 2570 hours (107 days) resulted in some reduction and immobilization of Tc-99. For control sediments that received no treatment, 19 ± 6% of Tc-99 was temporarily removed from solution (Extractions 3, 4, 5) and 12 ± 5% of the Tc-99 was permanently immobilized (Table 4.2 and Figure 4.1a, left-most bars, Extractions 4 and 5, light and dark green fractions, respectively). Although ethane treatment alone did not change the Tc-99 mobility (13 ± 2% immobilized), butyl acetate treatment decreased Tc-99 mobility slightly (17 ± 5% immobilized), though within error of the no-treatment control. Butyl acetate showed that 41 ± 10% of Tc-99 was temporarily sequestered and 27 ± 9% was permanently sequestered, which was statistically greater than the control. However, because the control (i.e., no gas treatment) showed some Tc-99 sequestration, butane temporarily sequestered only 22% (i.e., 41% minus 19%) and permanently sequestered only 14% (i.e., 27% minus 13%), which is significantly below the minimum of 35% transformation to immobile or temporarily immobile end products for the technology to move forward.

There were additional indicators that mildly reducing conditions were established by the organic gas addition. Experiments with CoCOIs showed most (66% to 99%) CrO_4 (Appendix B, Table B.3, Section B.4) and some (34% to 57%) IO_3 were sequestered (Section B.6), both of which are more easily reduced than pertechnetate. However, no nitrate reduction was observed (Section B.5), although nitrate is more easily reduced than pertechnetate. Measurement of microbial biomass changes generally shows an increase for ethane, butane, and butyl acetate (Figure B.2).

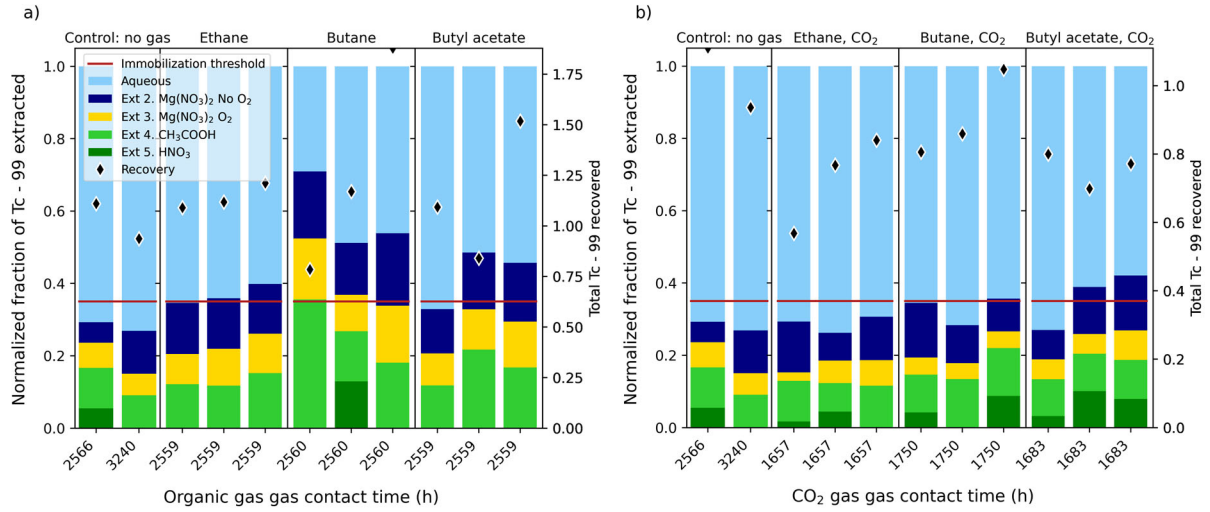

Figure 4.1. Change in Tc-99 mobility from gas-phase treatment of contaminant-spiked Hf sediment at 4% WC for controls (no gas) to treatments with (a) ethane, butane, or butyl acetate for 2500 hours; and (b) organic gases (ethane, butane, or butyl acetate) for 1500 hours; then CO_2 gas for 1700 hours, presented as triplicate tests with controls (no gas treatment) aligned on the left. Note: The 35% minimum transformation threshold is shown by the solid red line.

Table 4.2. Tc-99 sequestration fraction and approximate rates for organic gas and CO_2 treatments. Note: Treatment marked in **bold** met the 35% transformation target.

Contaminant	Treatment	Tc-99 Temp + Seq. Fraction	Tc-99 Sequestered Fraction	Sequestration Half-Life (weeks)
Tc-99	Control (no gas)	0.193 ± 0.061	0.129 ± 0.054	NM
Tc-99 + CoCOI	Control (no gas)	0.237 ± 0.060	0.135 ± 0.031	NM
Tc-99	Ethane	0.229 ± 0.029	0.130 ± 0.019	3
Tc-99	Ethane + CO_2	0.175 ± 0.019	0.123 ± 0.007	4[(a)]
Tc-99 + CoCOI	Ethane	0.279 ± 0.057	0.181 ± 0.052	3
Tc-99 + CoCOI	Ethane + CO_2	0.190 ± 0.055	0.131 ± 0.050	5[(a)]
Tc-99	Butane	**0.410 ± 0.100**	0.268 ± 0.087	5
Tc-99	Butane + CO_2	0.213 ± 0.047	0.167 ± 0.046	2
Tc-99 + CoCOI	Butane	0.323 ± 0.033	0.242 ± 0.030	4
Tc-99 + CoCOI	Butane + CO_2	0.208 ± 0.049	0.164 ± 0.047	2[(a)]
Tc-99	Butyl acetate	0.277 ± 0.063	0.168 ± 0.050	3
Tc-99	Butyl acetate + CO_2	0.239 ± 0.044	0.175 ± 0.037	None
Tc-99 + CoCOI	Butyl acetate	0.257 ± 0.047	0.147 ± 0.020	3
Tc-99 + CoCOI	Butyl acetate + CO_2	0.216 ± 0.053	0.136 ± 0.022	4[(a)]

(a) Contaminant mobility increased after step 2 (CO_2 gas) treatment.

Time series data for ethane, butane, and butyl acetate (Figure 4.2, Figure 4.3, and Figure 4.4, respectively) show Tc-99 mobility changes with time for each organic gas treatment, with changes that occurred because of the subsequent CO_2 treatment. The influence of the CO_2 treatment is described in Section 4.1.2. The presence of redox-reactive CoCOIs may slow the bioreduction rate of $Tc(VII)O_4^-$ as some CoCOIs are more easily reduced and will consume reductive capacity first:

$$IO_3^- > CrO_4^- > NO_3^- > \mathbf{TcO_4^-} > Fe^{III}(CN)_6^{3-} > UO_2^{2+}$$

For ethane treatments, time series data show that Tc-99 reduction leveled off by 1030 hours (Figure 4.2a) without and with the presence of CoCOIs and showed nearly the same rate of change (Figure 4.2c). The extent and rate of CoCOI sequestration (part of Objective 2) is additionally useful for quantifying the redox conditions created by bioreduction of the different organic gases (described in detail in Appendix B, Sections B.2 through B.8).

Heat-treated controls (final bar graph on the right side of subplots in Figure 4.2) showed variable results. The 100 °C treatment likely killed most microbes and crystallized amorphous Fe oxides and other phases, as observed previously (Payne et al. 1994), so it may have resulted in geochemical changes that influenced Tc-99 sequestration. Experiments were also conducted with 1500 hours of ethane treatment followed by CO_2 treatment times varying from 170 to 1700 hours. All CO_2 treatments showed less Tc-99 sequestration (Figure 4.2b and d) compared to ethane treatment alone (Figure 4.2a and c). It is hypothesized that the 100% CO_2 resulted in slight acidification of the pore water [pH 5.5 to 6.0, based on the previous study (PNNL-18303)], which may have dissolved some calcite and Fe oxides that may have coated or co-precipitated with TcO_2. With insufficient time for pH neutralization to occur (likely 3 to 6 months), it is unlikely that any calcite precipitated. The pH neutralization was accelerated in the previous study by 30 days of CO_2 treatment followed by 30 days to 1 year of treatment with air. In that previous study, there was a significant decrease in U mobility, likely the result of calcite precipitation coating U surface phases and/or incorporation of some U in calcite.

The injection of 10 pore volumes of ethane or CO_2 gas over 5 minutes should achieve gas-pore water equilibrium given the high surface area of a thin water film on sediment surfaces in the column and if the gas-to-liquid transfer rate is relatively fast. Some sediment columns were in contact with a large volume of ethane or CO_2 gas over the entire period to test this hypothesis of fast gas-to-liquid transfer rate (times marked with a * in Figure 4.2). For ethane treatment alone at 2500 hours, there was no difference between 5-minute contact time and 2500-hour contact time with ethane (Figure 4.2a).

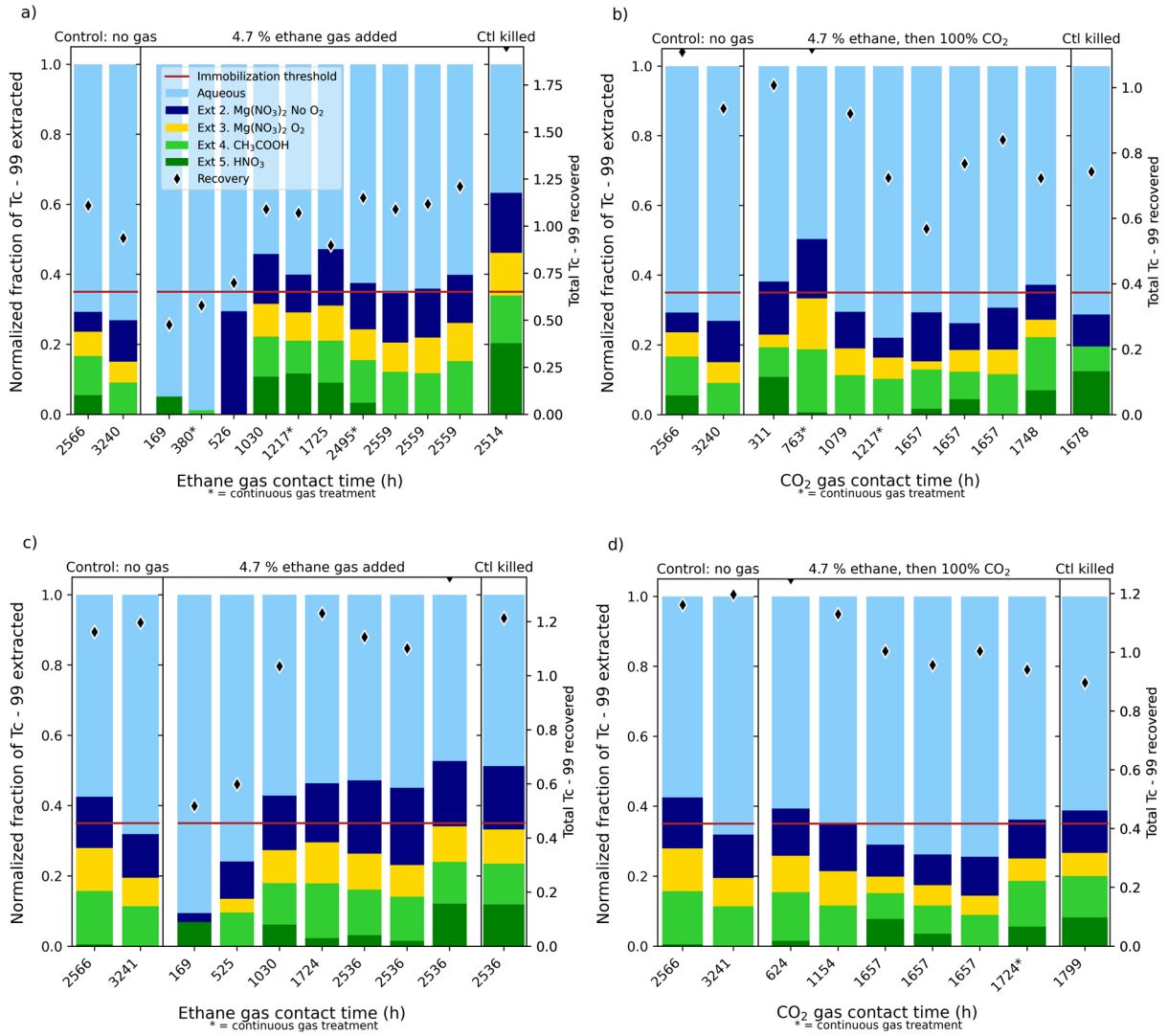

Figure 4.2. Change in Tc-99 mobility from gas-phase treatment of contaminant-spiked Hf sediment at 4% WC with time for the following gas treatments: (a) ethane without CoCOIs, (b) ethane then CO_2 without CoCOIs, (c) ethane in the presence of CoCOIs, and (d) ethane then CO_2 in the presence of CoCOIs. Note: Controls with no gas treatment are aligned on the left and "ctl killed" defined as heat-treated sediments with no gas treatment are aligned on the right. X-axis times with an asterisk received continuous gas treatment while all others received gas treatment over approximately 5 minutes. The 35% minimum transformation threshold is shown by the solid red line.

For butane treatments, sequestration was slower, as reduction leveled off by 1725 hours (Figure 4.3a). Tc-99 reduction in the presence of CoCOIs was more rapid, as reduction leveled off by 1030 hours (Figure 4.3c). The presence of CoCOIs also resulted in slightly less Tc-99 sequestration, which was within error between triplicate samples. A comparison of 10 pore volumes of butane injection over 5 minutes (most experiments) to continuous butane exposure over the time (experiments marked with a *) showed no differences, indicating butane gas injection achieved rapid gas-to-pore-water equilibrium within the 5-minute gas injection period.

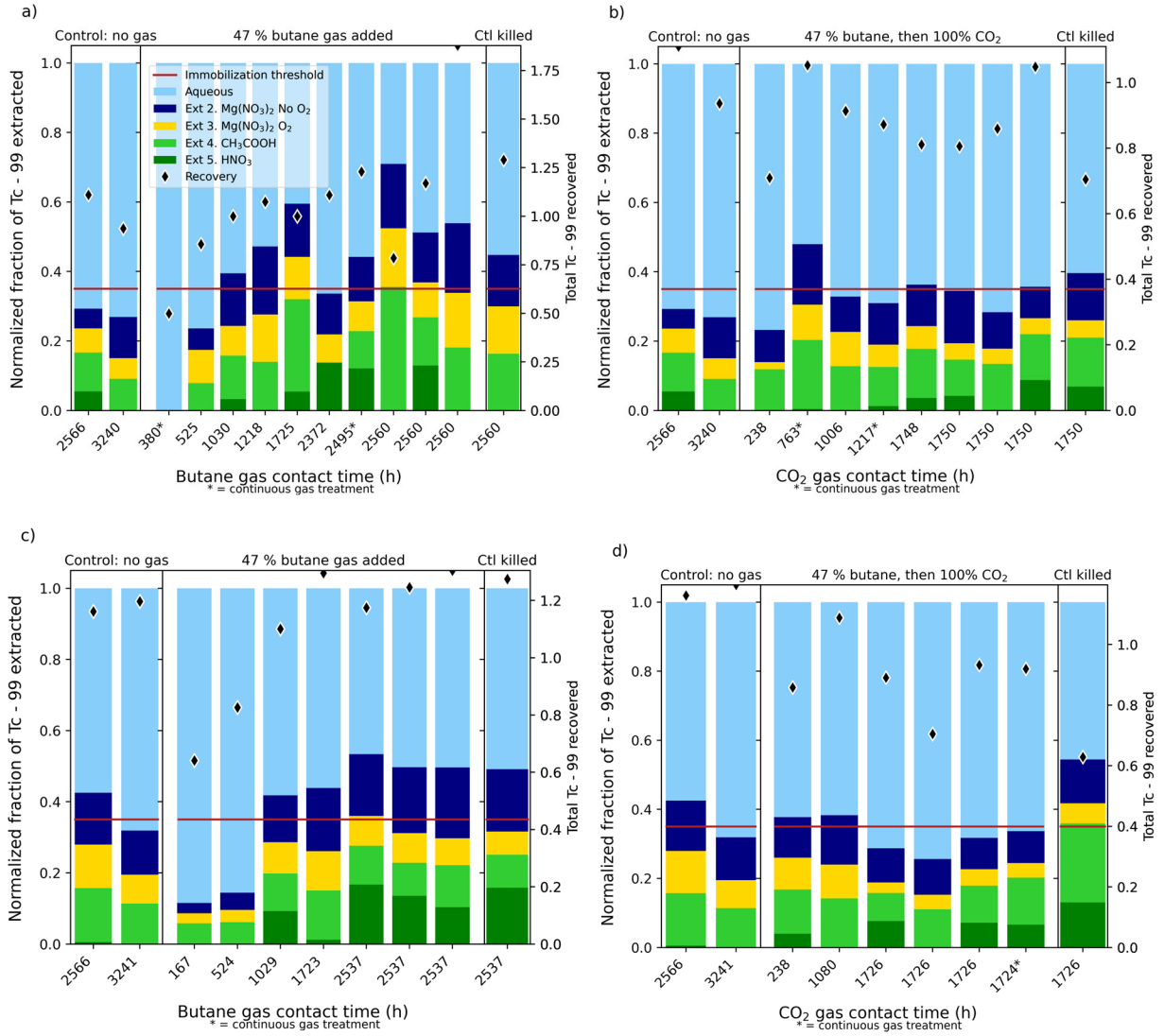

Figure 4.3. Change in Tc-99 mobility with time for gas-phase treatment of contaminant-spiked Hf sediment at 4% WC: (a) butane with Tc-99 only, (b) butane then CO_2 with Tc-99 only, (c) butane in the presence of CoCOIs, and (d) butane then CO_2 in the presence of CoCOIs. Note: Controls with no gas treatment are aligned on the left and "ctl killed" defined as heat-treated sediments with no gas treatment are aligned on the right. X-axis times with an asterisk received continuous gas treatment while all others received one treatment over approximately 5 minutes. The 35% minimum transformation threshold is shown by the solid red line.

For butyl acetate treatments, the Tc-99 sequestration without or with CoCOIs leveled off by 1030 hours (Figure 4.4a and c). Similar to ethane and butane treatments, the presence of CoCOIs results in slightly less Tc-99 sequestration for butyl acetate treatment, which was within error between triplicate samples. A comparison of 20 pore volumes of butyl acetate injection over 5 minutes (most experiments) to continuous butyl acetate exposure over time (experiments marked with a *) showed no differences, indicating butyl acetate gas injection achieved rapid pore water equilibrium.

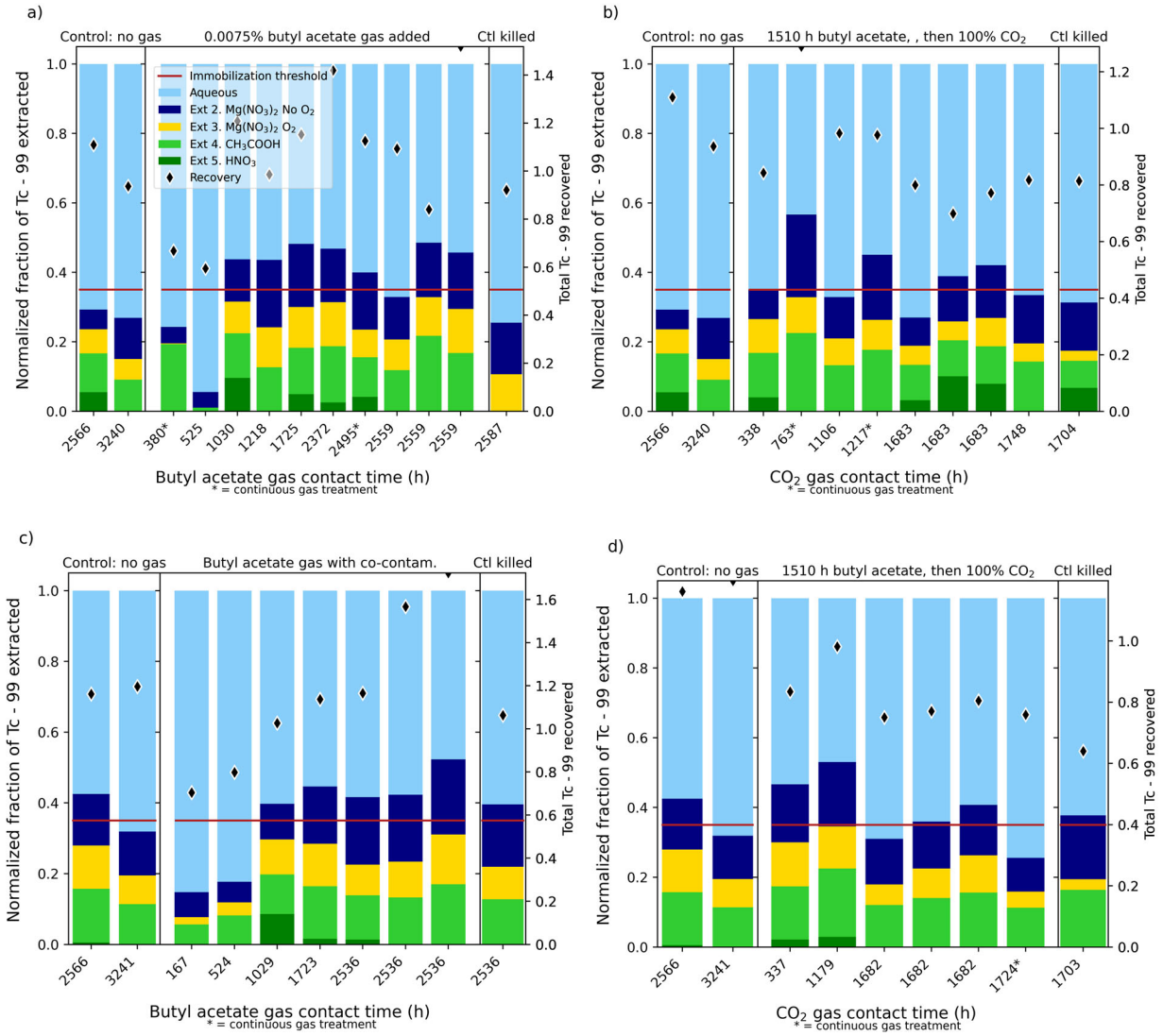

Figure 4.4. Change in Tc-99 mobility with time for gas-phase treatment of contaminant-spiked Hf sediment at 4% WC for the following gas treatments: (a) butyl acetate, (b) butyl acetate then CO_2, (c) butyl acetate in the presence of CoCOIs, and (d) butyl acetate then CO_2 in the presence of CoCOIs. Note: Controls with no gas treatment are aligned on the left and "ctl killed" defined as heat-treated sediments with no gas treatment are aligned on the right. X-axis times with an asterisk received continuous gas treatment while all others received one treatment over approximately 5 minutes. The 35% minimum transformation threshold is shown by the solid red line.

4.1.2 Objective 2: Quantify Tc-99 order of magnitude and rate of removal via treatment with organic gases and CO_2

4.1.2.1 Tc-99 order of magnitude and rate of removal via treatment with organic gases and CO_2 in contaminant-spiked sediments

For the Hf sediment at 4% WC, ethane then CO_2 treatment did not change the Tc-99 sequestration (13.0 ± 1.9%) greater than the control (12.9 ± 5.4%), butyl acetate treatment sequestered some Tc-99 within error (16.8 ± 5.0%), and butane sequestered some Tc-99 (26.8 ± 8.7%) that was statistically greater than the control. However, because the control (i.e., no gas) showed some Tc-99 sequestration, butane temporarily sequestered only 14% (i.e., 27% minus 13%), which is significantly below the minimum of 35% transformation to temporarily immobile or immobile end products to move forward. Measurement of microbial biomass changes generally showed an increase for ethane, butane, and butyl acetate (Appendix B, Figure B.2).

Experiments conducted with 1500 hours of ethane treatment followed by CO_2 treatment times varying from 170 to 1700 hours all showed less Tc-99 sequestration (Figure 4.2b and d) compared to ethane treatment alone (Figure 4.2a and c). Experiments conducted with 1500 hours of butane treatment followed by CO_2 treatment all showed 5% to 10% less Tc-99 sequestration (Figure 4.3b and d) compared to butane treatment alone (Figure 4.3a and c). Finally, experiments conducted with 1500 hours of butyl acetate treatment followed by CO_2 treatment all showed 5% to 15% less Tc-99 sequestration (Figure 4.4b and d) compared to butyl acetate treatment alone (Figure 4.4a and c). As described earlier, the acidification of the pore water (pH 5.5 to 6.0) because of the 100% CO_2 treatment needed months for pH neutralization to occur, which did not occur in these 1700-hour (70-day) experiments. While ethane/CO_2 and butyl acetate/CO_2 treatment showed nearly no change in Tc-99 mobility (12.3 ± 0.7% and 17.5 ± 3.7% sequestered, respectively), butane/CO_2 treatment showed a 10% increase in Tc-99 mobility (16.7 ± 4.6% sequestered; Figure 4.4b). It is likely that additional CO_2-sediment reaction time was needed to precipitate calcite. For most ethane/CO_2, butane/CO_2, and butyl acetate/CO_2 treatments, CO_2 treatment was conducted by 100% CO_2 gas injection for 20 pore volumes over a 5-minute time interval. Some parallel sediment columns were hooked up to a gas bag containing 100% CO_2 for the entire treatment period (Figure 4.2, Figure 4.3, Figure 4.4, shown with an • next to the time). There was no difference between 5-minute and hundreds to 1700 hours of CO_2 treatment, indicating CO_2 gas-to-pore-water equilibrium was likely achieved within the 5-minute injections.

It is hypothesized that the 100% CO_2 treatment resulted in slight acidification of the pore water [pH 5.5 to 6.0, based on the previous study (PNNL-18879)], which may have dissolved some calcite and Fe oxides that may have coated or co-precipitated with TcO_2. With insufficient time for pH neutralization to occur (likely 3 to 6 months), it is unlikely that any calcite precipitated. The pH neutralization was accelerated in the previous study by 30 days of CO_2 treatment followed by 30 days to 1 year of treatment with air. In that previous study, there was a significant decrease in U mobility, likely the result of calcite precipitation coating U surface phases and/or incorporation of some U in calcite.

Measurement of microbial biomass after organic gas and subsequent CO_2 gas treatment showed a large decrease for ethane/CO_2, but no change for butane/CO_2 and butyl acetate/CO_2 treatments (Appendix B, Figure B.2; note that the x-axis scale shows times for organic gas and CO_2 treatments).

4.1.2.2 Tc-99 order of magnitude and rate of removal via treatment with organic gases and CO_2 in field-contaminated sediments

A limited number of experiments were conducted using field-contaminated VZ sediments to evaluate organic gas and CO_2 treatment on targeted VZ areas under the BY Cribs and BC Cribs. In addition, a sediment from under the 216-U-8 Crib was used because acidic waste should have decreased microbial activity, potentially decreasing bioreduction with the addition of organic gas. For these field sediments, Tc-99 and CoCOIs that have been in contact with sediments for decades likely result in contaminants present in more secondary precipitate phases compared to when Tc-99 was added in weeks prior to an experiment. Therefore, organic gas and CO_2 treatments may be less effective.

One organic gas (ethane) was used to treat sediments for 2500 hours, which resulted in a small decrease in Tc-99 mobility for BY Cribs and BC Cribs sediments but a significant (15-20%) increase in Tc-99 mobility for the 216-U-8 sediment (Table 4.3, Figure 4.5a in fraction Tc-99 in phase and Figure 4.5c in μg/g). For the BY Cribs sediment, the temporary increase in sequestration was 20%, whereas the final sequestered change (relative to the no gas control) was 12% (Table 4.3). For the BC Cribs sediment, the temporary increase in sequestration was 3% and the final sequestered change was -6% (i.e., more mobile). For the 216-U-8 Crib sediment, the temporary increase in sequestration was -20% and the final sequestered change was -29% (i.e., more mobile)

With the subsequent CO_2 gas treatment for 1700 hours, Tc-99 mobility significantly increased by 15% to 20% compared to untreated BY Cribs and BC Cribs sediments (Figure 4.5b and d). The CO_2 gas treatment for 216-U-8 sediments had little effect on Tc-99 mobility, possibly because the CO_2 treatment resulted in slight acidification, i.e., pore water was likely pH 5.5 to 6.0 based on a previous study (PNNL-20004; Triplett et al. 2010), and 216-U-8 sediments had already been subjected to acidic wastes. Microbial biomass characterization of untreated, ethane-treated, and ethane/CO_2-treated sediments did not indicate consistent trends. For the BY Cribs sediments, ethane treatment did result in elevated microbial biomass (Appendix B, Figure B.3), but no change was observed for BC Cribs and 216-U-8 Crib sediments.

Table 4.3. Change in Tc-99 sequestration in BY Cribs, BC Cribs, and 216-U-8 Crib sediments from ethane and CO_2 gas treatments based on sequential extractions with Extraction 3 defined as temporarily sequestered and Extractions 4 and 5 defined as sequestered.

Gas Treatment	BY Cribs Temporary	BY Cribs Sequestered	BC Cribs Temporary	BC Cribs Sequestered	216-U-8 Crib Temporary	216-U-8 Crib Sequestered
Control (no gas)	0.21	0.21	0.19	0.19	0.50	0.50
Ethane	0.41 ± 0.07	0.329 ± 0.073	0.22 ± 0.02	0.13 ± 0.02	0.30 ± 0.01	0.21± 0.01
Ethane + CO_2	0.12 ± 0.04	0.101 ± 0.044	0.15 ± 0.12	0.12 ± 0.08	0.38 ± 0.04	0.33 ± 0.05

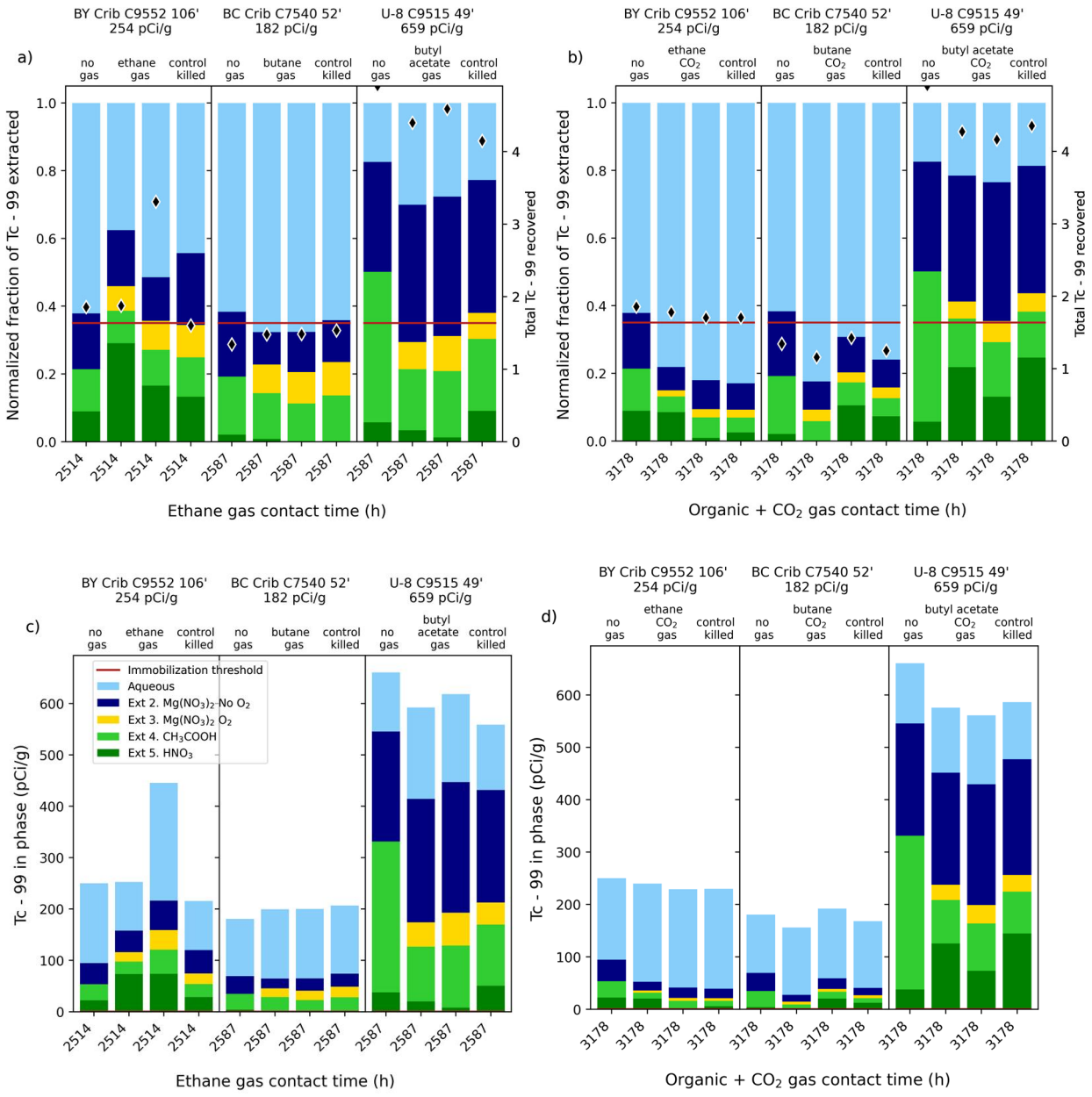

Figure 4.5. Change in Tc-99 mobility for field-contaminated VZ sediments at 4% WC from Hanford Site under BY Cribs, BC Cribs, and 216-U-8 Crib with (a) 2500 hours of ethane gas treatment (normalized fraction of Tc-99), (b) 1500 hours of ethane gas treatment followed by 1700 hours of CO_2 gas treatment (normalized fraction of Tc-99), (c) 2500 hours of ethane gas treatment (pCi/g Tc-99 with total in sediments in description), and (d) 1500 hours of ethane gas treatment followed by 1700 hours of CO_2 gas treatment (pCi/gTc-99 with total in sediments in description). Note: The 35% minimum transformation threshold is shown by the solid red line.

4.2 Gas-Phase Bioreduction – Organic gas

This technology was focused on the bioreduction of nitrate following treatment with four different organic gases (pentane, ethane, butane, and butyrate). Table 4.6 presents the targeted testing conditions and amendments and shows which are moving forward to Phase 2 of testing. Sections 4.2.1 and 4.2.2 present the transformation of nitrate in the aqueous phase with time in batch experiments with and without Cr(VI) as a CoCOI, respectively. After 154 days of reaction of sediments and PCOIs (with or without CoCOI) with organic gases, aqueous NO_3^- and NO_2^- were measured to quantify the transformation of aqueous nitrate species toward gaseous nitrogenous end products.

Overall, these results show that organic gases were effective for nitrate and met the minimum threshold of 35% transformation to nontoxic end products for select VZ conditions, and this technology will move forward with additional site-specific testing. For nitrate, the transformation to nontoxic end products was determined based on measurement of aqueous NO_3^- and NO_2^- assuming that the remaining N was transformed to gaseous, nontoxic end products. For the VZ application (evaluated with BY Cribs, 216-S-9 sediments, and Hf sediments as described in Section 3.1), the 35% minimum transformation threshold was met for all four organic gases depending on the conditions. The minimum threshold was met when Cr(VI) was not present with nitrate for most conditions, although some variability was observed between the three sediments and two sediment-to-solution ratios. Pentane was the worst performing gas and butyrate and ethane were the best performing gases, although transformation of nitrate when Cr(VI) was present was variable (Section 4.2.2). Nitrate transformation in 216-S-9 sediments met the minimum threshold with added Cr(VI), but the BY Cribs sediment did not meet the minimum transformation threshold of 35% and will not be considered in future testing.

Table 4.4. Summary of remediation conditions and amendments for gas-phase bioreduction technologies.

Primary Conditions and Amendments	
PCOI	NO_3^-
Primary treatment zone/ applicable 200-DV-1 waste sites	Unknown (testing conducted for BY and **S Cribs**)
Secondary treatment zone/ applicable 200-DV-1 waste sites	Unknown
Potential co-contaminants	Cr(VI)
Bioremediation treatments	**Ethane**; pentane; butyrate; butane
Phase 1 decision point	Go

Note: The treatment and conditions moving forward to Phase 2 evaluation are **bolded**. If no amendment passed the minimum threshold, none are bolded and no additional testing will be conducted.
CN (BY Cribs): Potential co-contaminant but primarily present as ferrocyanide; testing ongoing.

4.2.1 Objective 1: Transformation of nitrate with organic gas treatment without Cr(VI)

Two different types of experiments were conducted with different sediment-to-solution ratios with field-contaminated 216-S-9 Crib or BY Cribs sediments or contaminant-spiked Hf sediments as described in Section 3.5.2. Results are presented based on the aqueous concentrations of NO_3^- and NO_2^- as well as the total aqueous fraction (as NO_3^- and NO_2^-) over time.

In 1:2 sediment-to-APW (serum bottle) microcosms with Hf sediment, nitrate was reduced from an initial 55 mg/L to below detection (1 mg/L), with no detectable NO_2 by 56 days in all treatments (Table 4.5, treatments in this context include the addition of organic gases and nutrients; heat treatment is conducted to reduce microbe populations and is not considered a treatment for nitrate). In the 2:1 APW:sediment

batches with the 216-S-9 and BY sediment without Cr(VI), NO_3^- and NO_2^- levels were below detection at 56 days (from an initial 26 mg/L NO_3^- added), so at 84 days, an additional nitrate spike was added to bring the total nitrate values to the levels received by the Hf sediment microcosms. Different organic gases resulted in different rates of denitrification from the most rapid to the slowest (butyrate, then ethane, then butane, then pentane) (Figure 4.6). The approximate degradation half-life of nitrate was 21 days for butyrate and 91 days for pentane. In the microcosms without Cr(VI), NO_2^- transiently increased after the 84-day supplemental nitrate spike, reaching lower end-point levels in the 216-S-9 sediment microcosms than in the BY sediment microcosms (Figure 4.7). At the end point (~84 days), the fractions of total aqueous N products remaining as compared to the initial concentration (NO_2^- + NO_3^-) were all below the minimum transformation threshold (Figure 4.9). At the end point in the 216-S-9 and BY sediment microcosms, pH values, as an indication of H^+ consumption during nitrate reduction, were higher in the treatments not receiving Cr(VI) as compared to those receiving Cr(VI), as expected based on the decrease in nitrate reduction with Cr(VI) present (Appendix D, Figure D.4 and Figure D.5).

Table 4.5. Aqueous NO_2^- and NO_3^- for 1:2 Hf sediment-to-APW (serum bottle) samples for Hf sediment microcosms with comparison to no-sediment controls. Note: Values are averages of triplicates with the standard deviations in parentheses. Approximately 55 mg/L NO_3^- was added to all samples except the no-COI samples.

		Time Point			
		56 days		112 days	
Sample	Treatment	NO_2^- (mg/L)	NO_3^- (mg/L)	NO_2^- (mg/L)	NO_3^- (mg/L)
Hf sediment	Pentane + YE	< 1	< 1	NS	NS
Hf sediment	Butyrate + YE	< 1	< 1	NS	NS
Hf sediment	Butane + YE	< 1	< 1	NS	NS
Hf sediment	Ethane + YE	< 1	< 1	NS	NS
Hf sediment	+ YE	< 0.5	< 0.5	NS	NS
Heat-treated Hf sediment	- YE	18.5 (15.8)	18.3 (30.9)	17.8 (11.4)	17.6 (27.1)
Hf sediment	No PCOI or CoCOI – YE	< 0.5	< 0.5	NS	NS
No sediment	- YE	< 0.5	54.7 (1.8)	< 1	56.2 (0.9)

NS = not sampled

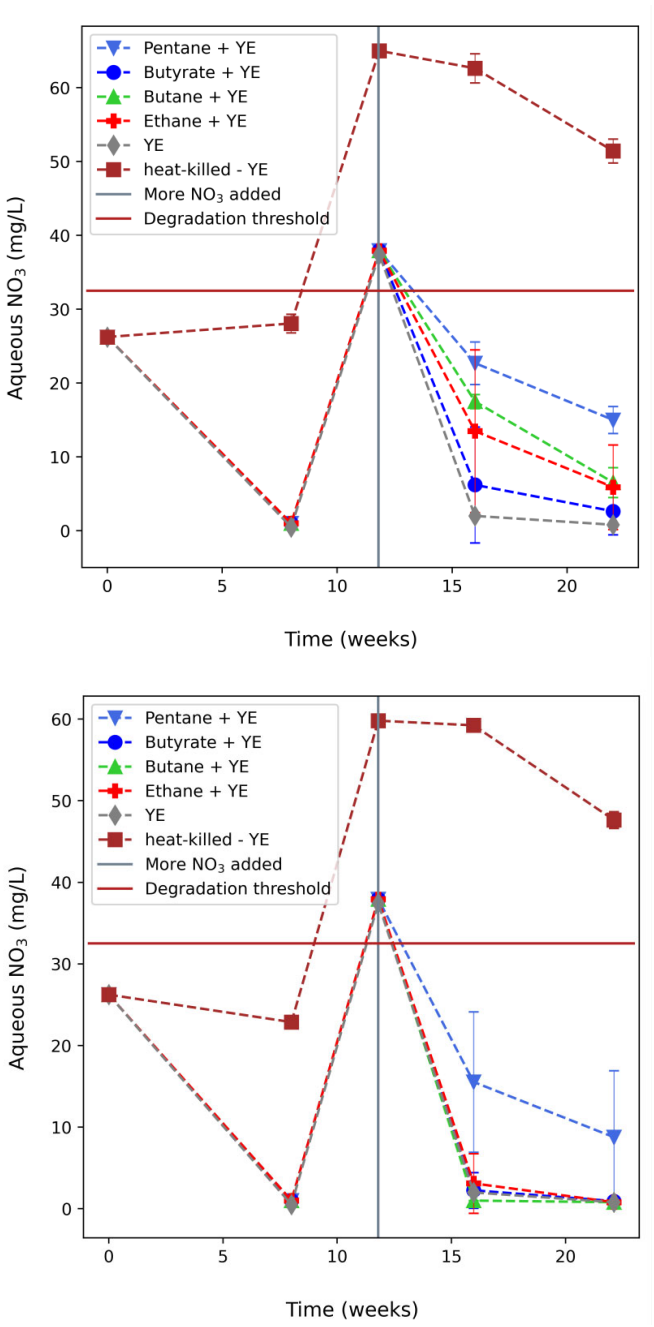

Figure 4.6. Aqueous NO_3^- (in mg/L) over time in the 1:2 sediment-to-APW batch (serum bottles) without added Cr(VI) with treatment with pentane, butane, or butyrate. (*top*) 216-S-9 sediment microcosms and (*bottom*) BY sediment microcosms. Native NO_3^- in the 216-S-9 sediment contributed 7 mg/L NO_3^- in addition to the added NO_3^- and BY sediment was below detection. Note: Additional NO_3^- was added at approximately 102 days (*gray vertical line*). The 35% minimum transformation threshold is shown by the solid red line. Error bars are based on analysis of triplicate batch reactors. Lines are used to guide the eye and do not represent a model. Three different types of controls are included: YE – yeast extract with NO_3^- and sediment, heat-treated YE – yeast extract with NO_3^- in heat-treated sediments to reduce native microbial population, and no PCOI or CoCOI YE – yeast extract with sediments but no added NO_3^-.

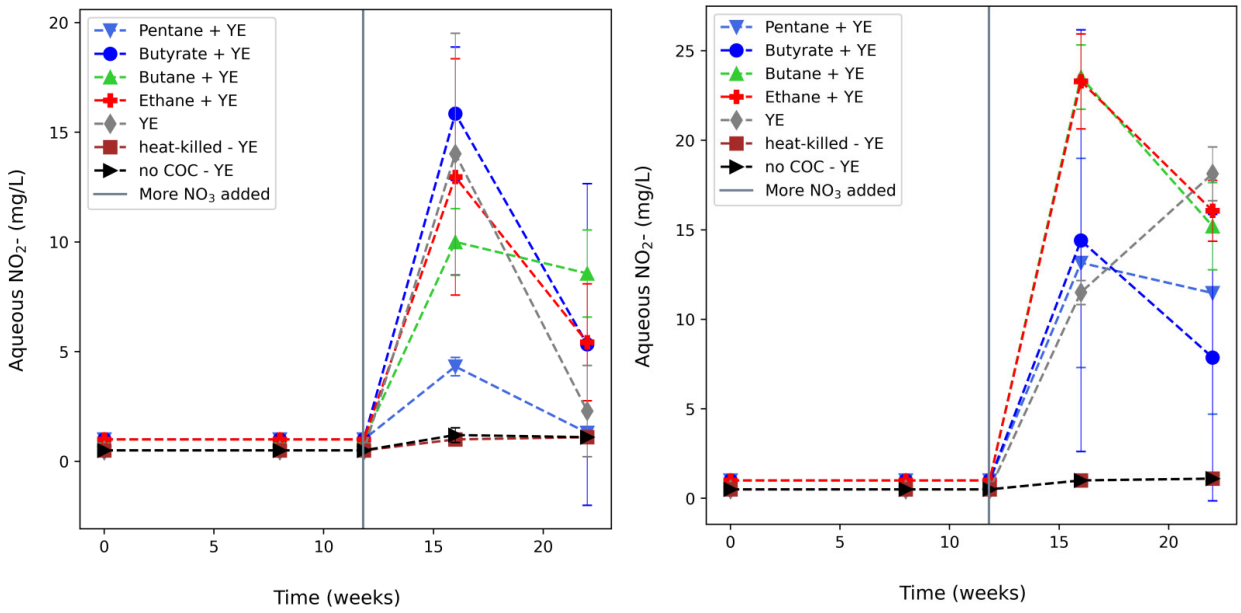

Figure 4.7. Aqueous NO_2^- over time in the 1:2 sediment-to-APW batch (serum bottles) without Cr(VI) with (*top*) 216-S-9 sediment microcosms and (*bottom*) BY sediment microcosms with treatment with pentane, butane, or butyrate. Note: Additional NO_3^- was added at approximately 102 days (*gray vertical line*). Error bars are based on analysis of triplicate batch reactors. Lines are used to guide the eye and do not represent a model. Three different types of controls are included: YE – yeast extract with NO_3^- and sediment, heat-treated YE – yeast extract with NO_3 in heat-treated sediments to reduce native microbial population, and no PCOI or CoCOI YE – yeast extract with sediments but no added NO_3^-.

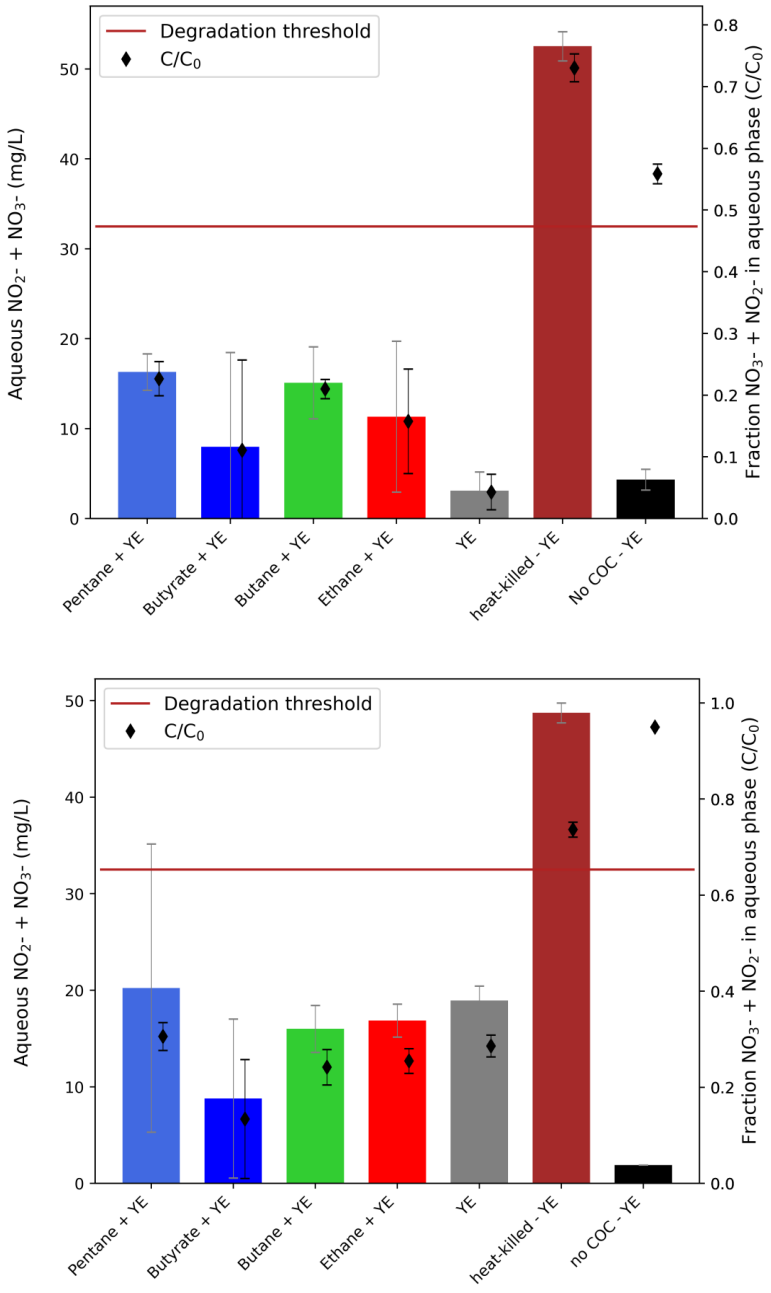

Figure 4.8. Aqueous NO_2^- and NO_3^- (primary y-axis indicates concentration in mg/L and secondary y-axis indicates fraction of total added) at the end point (~154 days) in the 1:2 sediment-to-APW batch (serum bottles) without added Cr(VI) with treatment with pentane, butane, or butyrate) for (*top*) 216-S-9 sediment and (*bottom*) BY Cribs sediment. Note: The 35% minimum transformation threshold is shown by the solid red line. Error bars are based on analysis of triplicate batch reactors. Three different types of controls are included: YE – yeast extract with NO_3^- and sediment, heat-treated YE – yeast extract with NO_3^- in heat-treated sediments to reduce native microbial population, and no PCOI or CoCOI YE – yeast extract with sediments but no added NO_3^-.

In the 1:1 sediment-to-APW batch (Balch tubes), all gas treatments in the BY microcosms were below the 35% minimum transformation (shown as 65% aqueous fraction remaining as NO_3^- and NO_2^-) threshold at the 119-day end point (Figure 4.9). However, in the 216-S-9 sediment microcosms, only the pentane, butyrate, and butane treatments were below the 35% transformation threshold (65% remaining in the aqueous phase) (Figure 4.9) (The fraction of total aqueous N products remaining as compared to the initial concentration for the ethane treatment was 0.67.) (Individual NO_2^- and NO_3^- values are plotted in Appendix D, Figure D.3.) In the 1:1 Hf sediment-to-APW sediment microcosms, NO_3^- was reduced from an initial 74 mg/L to below detection (0.8 mg/L) over 56 days for the treatments receiving (in addition to 0.01% YE) pentane, butane, or ethane (Figure 4.10). NO_2^- was below detection (1.1 mg/L) in all treatments except the heat-treated YE treatment (Figure 4.10). In the 1:1 sediment-to-APW microcosms, pH values at the 119-day end point ranged from 7.2 to 7.5 for all sediment treatments (Hf, 216-S-9, and BY Cribs sediments) (*data not shown*). (The end point pH value for the no-sediment controls was 7.1.)

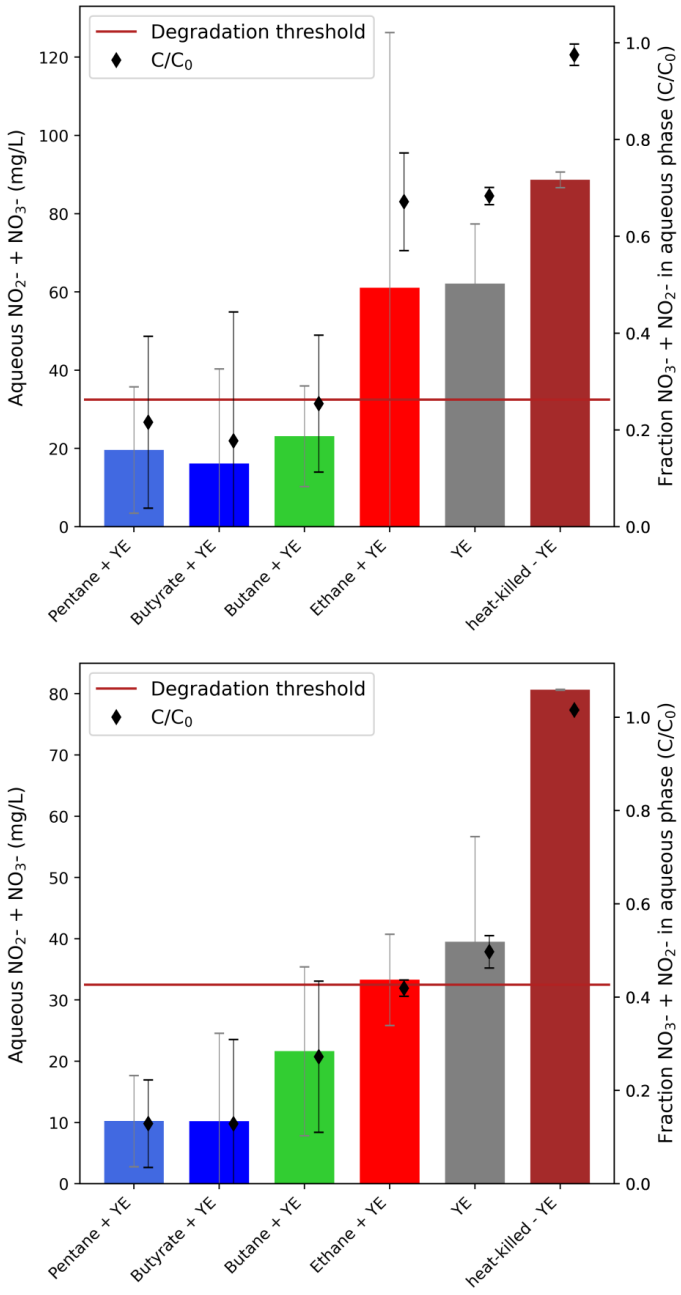

Figure 4.9. Aqueous NO_2^- and NO_3^- (primary y-axis indicates concentration in mg/L and secondary y-axis indicates fraction of total added) at the end point (~119 days) in the 1:1 sediment-to-APW batch (Balch tubes) without added Cr(VI). (*top*) 216-S-9 sediment microcosms and (*bottom*) BY Cribs sediment microcosms. Note: The 35% minimum transformation threshold is shown by the solid red line. Error bars are based on analysis of triplicate batch reactors. Lines are used to guide the eye and do not represent a model. Three different types of controls are included: YE – yeast extract with NO_3^- and sediment, heat-treated YE – yeast extract with NO_3^- in heat-treated sediments to reduce native microbial population, and no PCOI or CoCOI YE – yeast extract with sediments but no added NO_3^-.

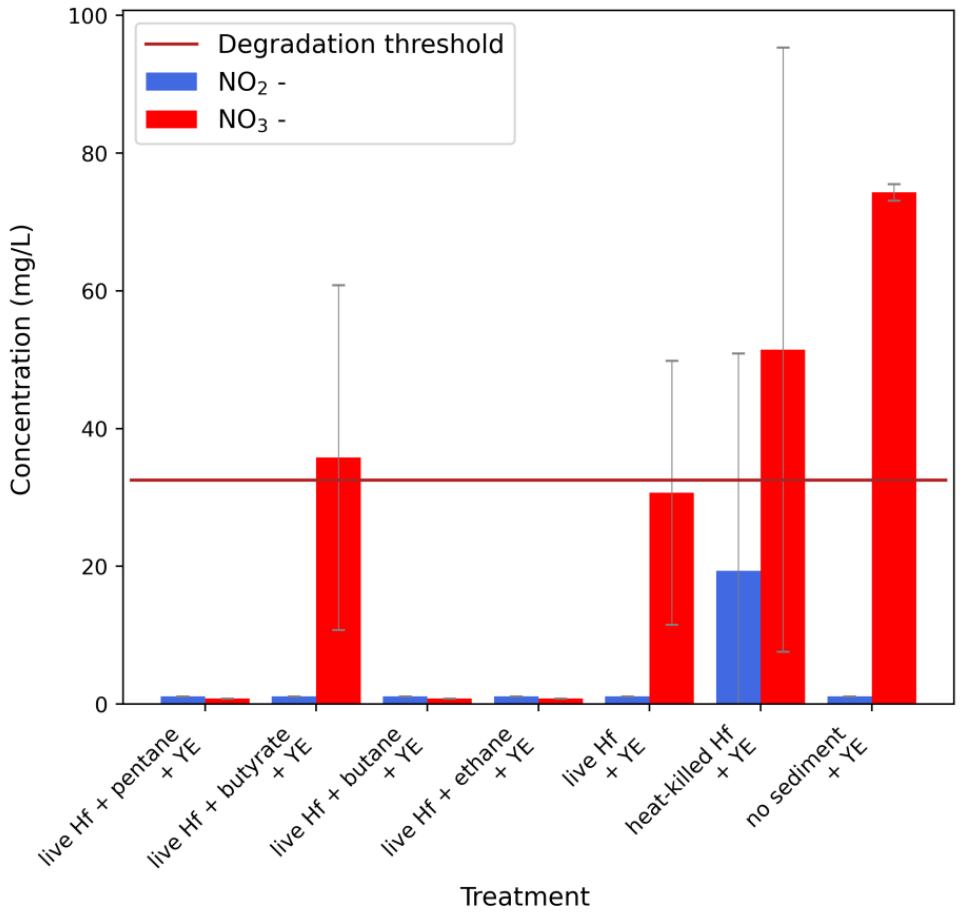

Figure 4.10. Aqueous NO_2^- and NO_3^- concentrations (mg/L) at the end point (~119 days) in the 1:1 sediment-to-APW batch (Balch tubes) with Hf sediment without added Cr(VI)with treatment with pentane, butane, or butyrate. Note: The 35% minimum transformation threshold is shown by the solid red line. Error bars are based on analysis of triplicate batch reactors. Lines are used to guide the eye and do not represent a model. Three different types of controls are included: YE – yeast extract with NO_3^- and sediment, heat-treated YE – yeast extract with NO_3^- in heat-treated sediments to reduce native microbial population, and no PCOI or CoCOI YE – yeast extract with sediments but no added NO_3^-.

Table 4.6. Qualitative transformation half-life for nitrate by *in situ* biostimulation with organic gases.

	Hf Sediment		BY Cribs Sediment		216-S-9 Crib Sediment	
	Treatment Duration	Top-Performing Gases	Treatment Duration	Top-Performing Gases	Treatment Duration	Top-Performing Gases
PCOI only	Weeks	All 4 gases	Weeks	Butyrate, ethane, butane	Weeks	Butyrate, ethane, butane
With CoCOI	NM	NM	Months	All 4 gases	Weeks, Months	Butyrate, ethane, butane

NM = not measured

4.2.2 Objective 2: Transformation of NO_3 with organic gas treatment with Cr(VI)

In the 1:2 sediment-to-APW batch, with the addition of Cr(VI) (as CrO_4^-) in the 216-S-9 sediment, denitrification decreased for pentane, butane, and ethane, but not for butyrate (Figure 4.11). In contrast, denitrification without Cr(VI) present in the BY Cribs sediments showed a ~3-week half-life for butyrate, ethane, and butane, but a slower (~5-week) half-life for pentane (Figure 4.11), indicating the local microbial consortium differs between the waste sites. Denitrification in the BY Cribs sediment in the presence of Cr(VI) as a CoCOI decreased nitrate degradation to a > 9-month half-life for all organic gases. After the ~84-day supplemental NO_3^- spike, NO_2^- transiently increased in the 216-S-9 microcosms to levels similar to those in the treatments without Cr(VI) (Figure 4.12). However, in the BY microcosms, NO_2 accumulation was much lower (Figure 4.12), consistent with the lower levels of nitrate reduction observed (Figure 4.11).

At the end point (~154 days), the fractions of total aqueous N products remaining were compared to the initial concentration (NO_3^- + NO_2^-) values and were greater in the BY Cribs sediment microcosms than in the 216-S-9 sediment microcosms (Figure 4.13). However, all values in the gas treatments were below the minimum transformation threshold (Figure 4.13). At the end point in the 216-S-9 and BY microcosms, pH values, as an indication of H^+ consumption during nitrate reduction, were higher in the live 216-S-9 microcosms than in the BY microcosms (Appendix D, Figure D.4 and Figure D.5), consistent with the greater nitrate reduction in the 216-S-9 sediment with Cr(VI) compared with the BY Cribs sediment with Cr. No experiments with Cr(VI) were conducted with Hf sediment.

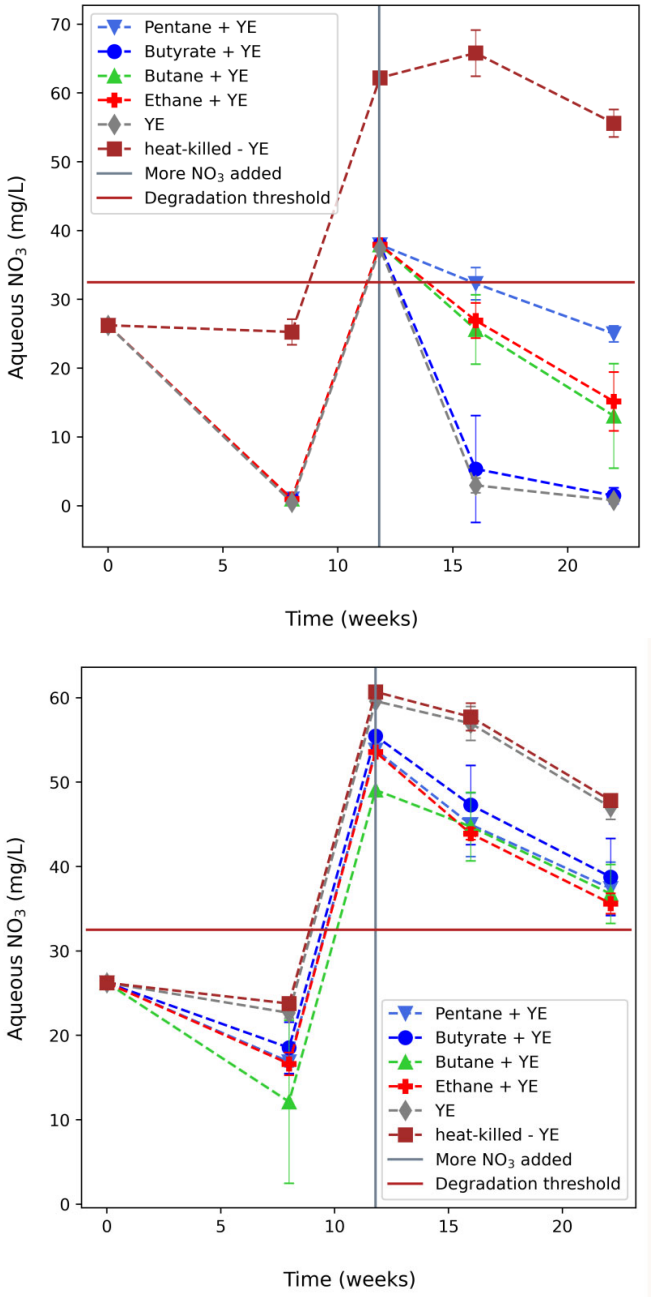

Figure 4.11. Aqueous NO_3^- (mg/L) over time in the 1:2 sediment-to-APW batch with 216-S-9 (A) and BY (B) sediment with added Cr(VI). Note: Additional NO_3^- was added at ~ 84 days (*gray vertical line*). Native NO_3^- in the 216-S-9 sediment contributed 14 mg/L NO_3^- in addition to the added NO_3^-, and BY sediment was below detection. The 35% minimum transformation threshold is shown by the solid red line. Error bars are based on analysis of triplicate batch reactors. Lines are used to guide the eye and do not represent a model. Three different types of controls are included: YE – yeast extract with NO_3^- and sediment, heat-treated YE – yeast extract with NO_3^- in heat-treated sediments to reduce native microbial population, and no PCOI or CoCOI YE – yeast extract with sediments but no added NO_3^-.

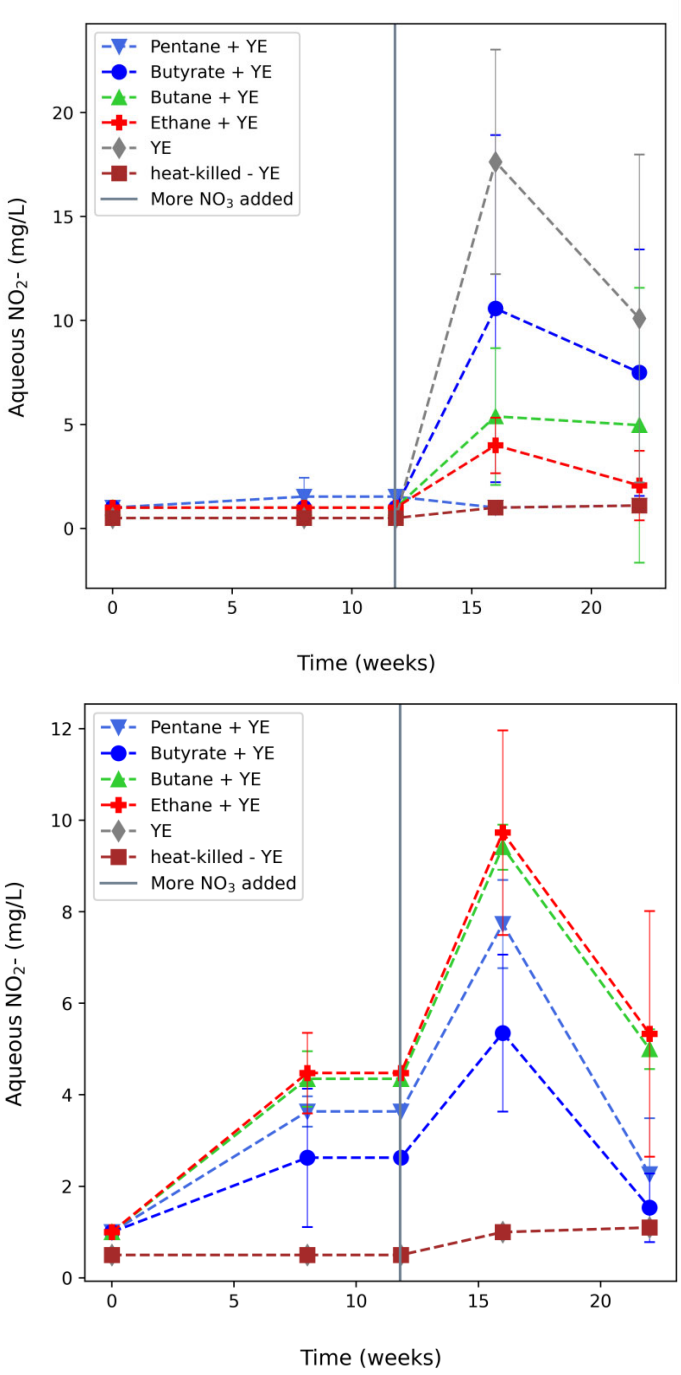

Figure 4.12. Aqueous NO_2^- over time in the 1:2 sediment-to-APW batch (serum bottles) with Cr(VI). (A) 216-S-9 sediment microcosms and B) BY sediment microcosms. Note: Additional NO_3^- was added at ~84 days (*gray vertical line*). Error bars are based on analysis of triplicate batch reactors. Lines are used to guide the eye and do not represent a model. Three different types of controls are included: YE – yeast extract with NO_3^- and sediment, heat-treated YE – yeast extract with NO_3^- in heat-treated sediments to reduce native microbial population, and no PCOI or CoCOI YE – yeast extract with sediments but no added NO_3^-.

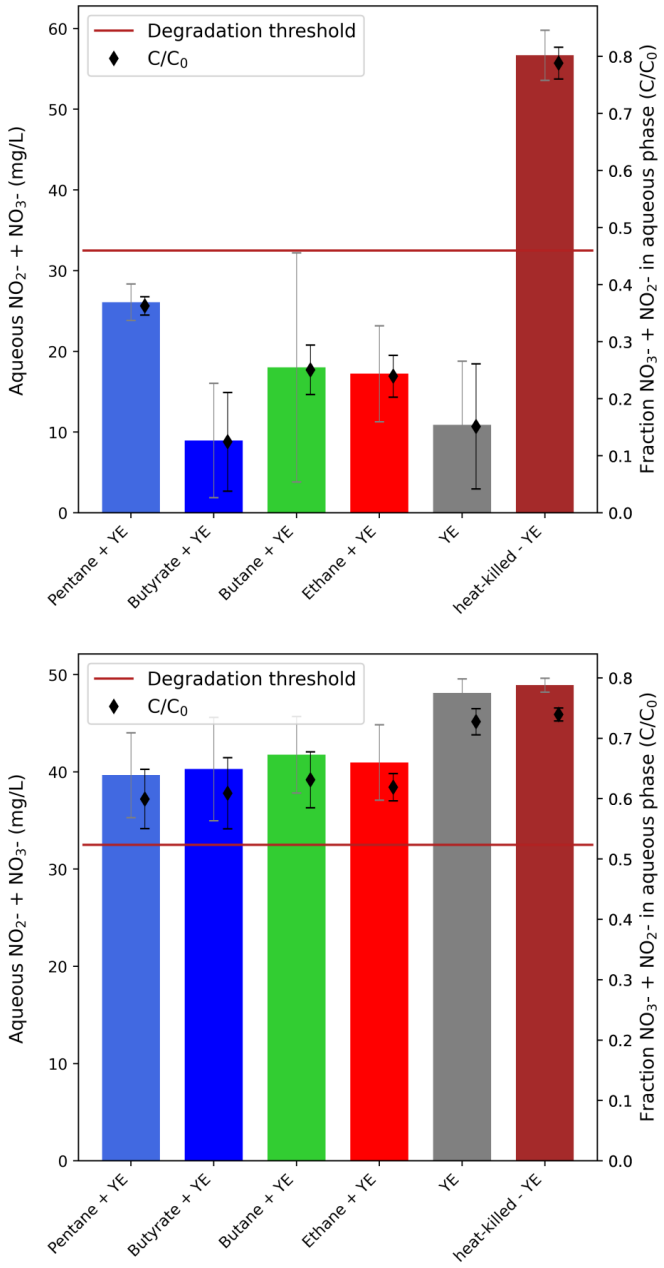

Figure 4.13. Aqueous NO_2^- and NO_3^- (primary y-axis indicates concentration in mg/L and secondary y-axis indicates fraction of total added) at the end point (~154 days) in the 1:2 sediment-to-APW batch with 216-S-9 (A) and BY (B) sediment with added Cr(VI). Note: The 35% minimum transformation threshold is shown by the solid red line. Error bars are based on analysis of triplicate batch reactors. Three different types of controls are included: YE – yeast extract with NO_3^- and sediment, heat-treated YE – yeast extract with NO_3 in heat-treated sediments to reduce native microbial population, and no PCOI or CoCOI YE – yeast extract with sediments but no added NO_3^-.

4.3 Gas-Phase Chemical Sequestration – CO_2 gas

This technology was focused on the chemical sequestration of IO_3 following treatment with CO_2 gas. Table 4.7 presents the targeted testing conditions and amendments and shows which are forward to Phase 2 of testing. The removal of IO_3 from the aqueous phase is quantified, as well as the relative change in mobility, via sequential extractions on sediments at variable time points up to 150 days (60 days of reaction with CO_2 followed by flushing with air and an additional 90 days of reaction). Water-saturated experiments without CoCOIs are described in Section 4.3.1 (Objective 1), water-saturated experiments with CoCOIs are described in Section 4.3.2 (Objective 2), and unsaturated experiments without and with CoCOIs are described in Section 4.3.3 (Objective 3).

Overall, these results show that CO_2 gas treatment for sequestration of IO_3 was less effective under saturated conditions but potentially effective under unsaturated conditions. This technology met the minimum threshold of 35% for transformation to temporarily immobile or immobile end products for VZ conditions and will move forward with additional site-specific laboratory-scale testing. However, it is notable that sequestration of IO_3 was more effective in uncontaminated Hf sediments with CoCOIs added as compared to contaminated sediments from 216-S-9. The potential impact of site-specific conditions and other CoCOIs will need to be considered in Phase 2 evaluation.

Table 4.7. Summary of remediation conditions and amendments for gas-phase chemical sequestration technologies.

Primary Conditions and Amendments	
PCOI	I-129
Primary treatment zone/ applicable 200-DV-1 waste sites	**216-S-9 Cribs**
Secondary treatment zone/ applicable 200-DV-1 waste sites	S-7, A-5, and A-10
Potential co-contaminants	U, Tc-99, Sr-90, Cr(VI)
Chemical sequestration treatments	**CO_2**
Phase 1 decision point	Go

Note: The treatment and conditions moving forward to Phase 2 evaluation are **bolded**. If no amendment passed the minimum threshold, none are bolded and no additional testing will be conducted.
CN (BY Cribs): Potential co-contaminant but primarily present as ferrocyanide; additional testing ongoing.

4.3.1 Objective 1: Sequestration of I with CO_2 gas treatment without CoCOIs

The concentration of natural I-127 in Hf sediments was approximately 0.092 µg/g, which was distributed between aqueous, adsorbed, and multiple precipitate phases (Figure 4.14). The I-127 added as IO_3 was roughly 20 times this natural amount (~2 µg/g), most of which was aqueous. The K_d values were 0.07 mL/g (no CoCOIs) or 0.12 mL/g (with CoCOIs) under water-saturated conditions.

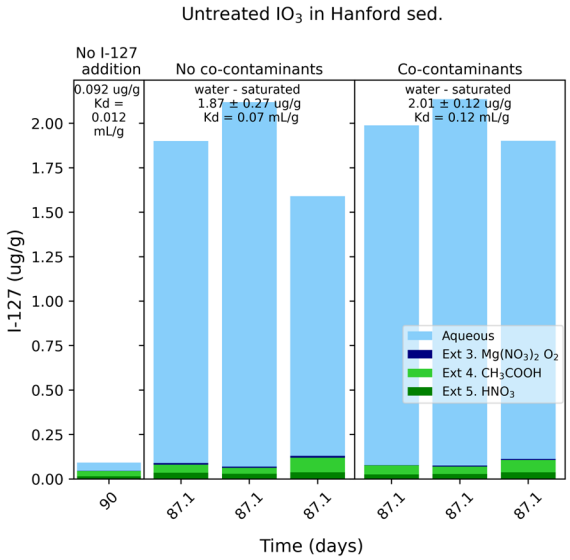

Figure 4.14. Results for amount of I-127 (added as IO_3) present in water-saturated Hf sediment in different phases naturally (*left*) and after IO_3 addition without and with CoCOIs (*center* and *right*, respectively).

Triplicate batch experiments (sediment:solution ratio = 1:7) showed a 5% to 6% decrease in aqueous IO_3 without CoCOIs both with and without treatment (Figure 4.15a). This may be due to a small amount of sequestration, as sequential extractions at selected time points showed a small increase (Figure 4.15b). However, this amount of sequestration was nearly the same as untreated sediments (Figure 4.15). This minimal amount of iodate sequestration indicates that the system may not have been at equilibrium with respect to carbonate partitioning between the gaseous, aqueous, and solid phases. For example, the pH of solutions in untreated sediments was 8.13 ± 0.08, whereas with CO_2 treatment, the pH decreased slightly (7.6 to 7.9, Appendix C, Figure C.2), indicating that there was likely only a small amount of CO_2 gas partitioning into the aqueous solution (and subsequently only a small amount of calcite precipitation). In a previous study of CO_2 gas injection into unsaturated columns, the pore water pH decreased to 6.0 over months (PNNL-18879). Moreover, diffusion simulations indicated that approximately 42 days were needed to reach even 50% CO_2 saturation at the sediment-water interface (Appendix C, Section C.1), so the CO_2 treatments conducted over 60 days were likely still time-limited by the rate of CO_2 diffusion through water. Sequential extractions of untreated sediments and CO_2-treated sediments (conducted at 60 and 150 days) confirmed that > 95% of the iodine remained aqueous (Figure 4.15b). Results show nearly no IO_3 uptake, likely because the low sediment:solution ratio had little CO_2 gas partitioning into water. Moreover, these types of experiments are not a realistic representation of VZ conditions; therefore, additional experiments were conducted as presented in Section 4.3.3.

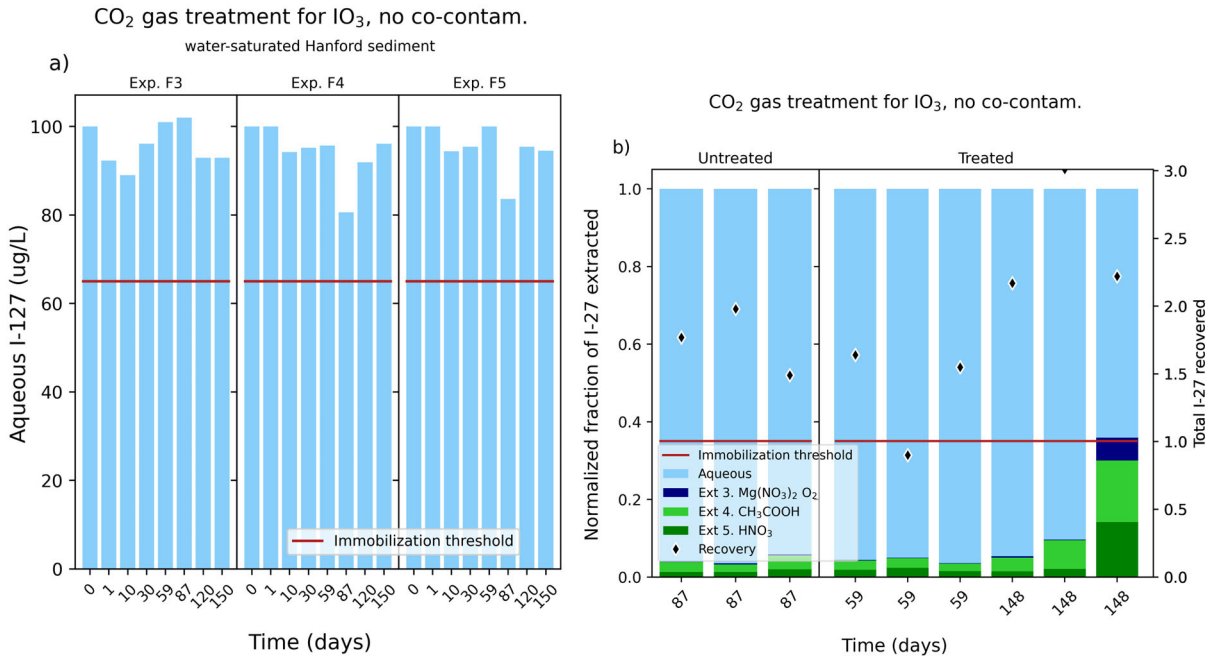

Figure 4.15. Results for I-127 (added as IO_3) changes in triplicate water-saturated batch experiments (F3, F4, and F5 at 1:7 sediment-to-solution ratio) with Hf sediments with CO_2 gas treatment over 60 days followed by flushing with air for another 90 days: (a) aqueous I-127 (in µg/L) with no CoCOIs over time, and (b) sequential I-127 extractions at 59 days with no CoCOIs. Triplicate no-treatment controls shown in (b) apply to (a). Note: The transformation threshold at 65% remaining in the aqueous phase (35% transformed) is shown by the solid red line. Black diamonds represent the overall contaminant recovery across all extractions.

4.3.2 Objective 2: Sequestration of I with CO_2 gas treatment with CoCOIs

Triplicate water-saturated experiments with IO_3 treated with CO_2 gas in the presence of CoCOIs showed an 8% decrease in aqueous IO_3 (Figure 4.16a) compared to 5.6% without CoCOIs (untreated results in Figure 4.16b). Sequential extractions at 150 days (i.e., 90 days of CO_2 treatment followed by 60 days of air treatment for pH neutralization) showed no increase in calcite-bound IO_3 compared to untreated sediments (Figure 4.16b). The IO_3 sorption in untreated sediment was small (K_d = 0.12 mL/g, Figure 4.15), so only a small fraction of IO_3 was sorbed to sediment. CoCOIs added included U, Tc-99, Cr(VI), Sr, and nitrate. Oxyanion CrO_4 may decrease IO_3 uptake as it will compete with IO_3 for substitution into the calcite structure (Tang et al. 2007). U (as uranyl cation) and Sr^{2+} substitute for Ca^{2+} in calcite (Carlson 1980; Kelly et al. 2003) and do not directly impact potential IO_3 substitution. NO_3^- and $Tc(VII)O_4^-$ do not substitute in calcite, but high nitrate concentrations may distort the outermost surface of calcite (Hofmann et al. 2016), which may decrease cation substitution in calcite and increase anionic substitution (Hofmann et al. 2014).

The pH of the solution in untreated sediments was 8.13 ± 0.08, whereas with CO_2 treatment, the pH decreased slightly (7.6 to 7.9, Appendix C, Figure C.2b), so there was likely only a small amount of CO_2 gas partitioning into the aqueous solution (and subsequently only a small amount of calcite precipitation). As described earlier, diffusion simulations indicated 42 days were needed to reach even 50% CO_2 saturation at the sediment-water interface in these water-saturated experiments (Section C.1), so the CO_2 treatment conducted over 90 days was still time-limited by the rate of CO_2 diffusion through water. These experiments showed essentially no IO_3 uptake. However, the lower sediment:solution ratio with little CO_2

gas partitioning into water was not a realistic representation of VZ conditions. Therefore, additional experiments were conducted in unsaturated water conditions that were more representative of field conditions (Section 4.3.3).

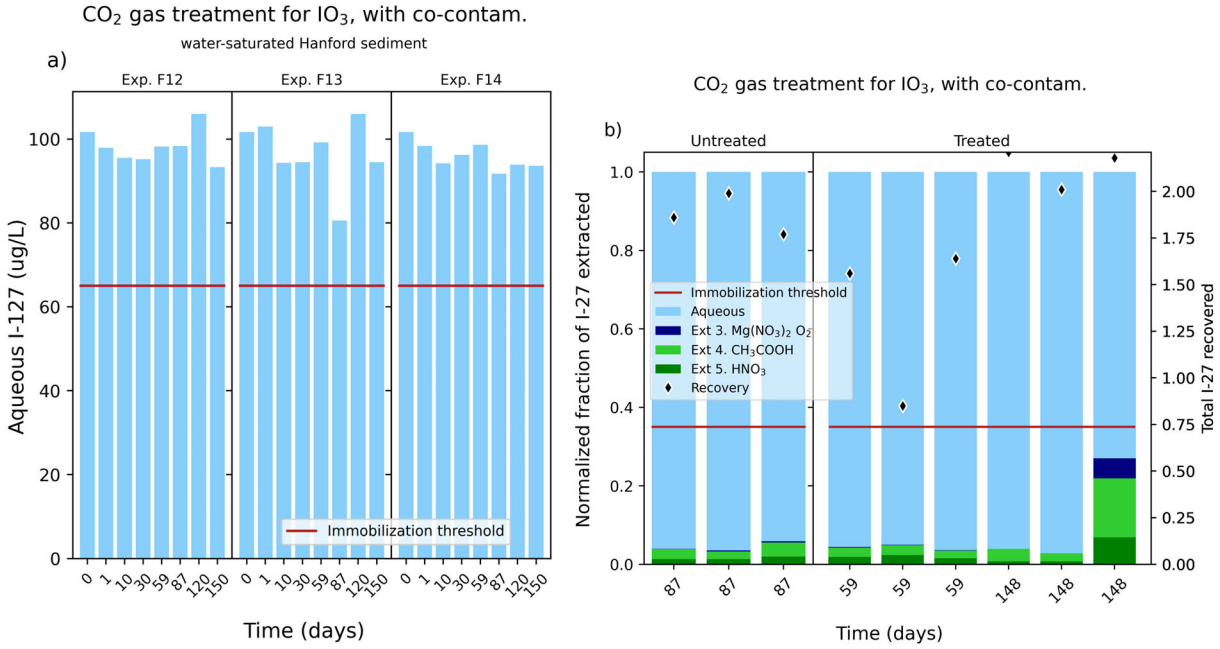

Figure 4.16. Results for I-127 (added as IO_3) changes in water-saturated Hf sediment with CoCOIs (F12, F13, F14 at a 1:7 sediment:solution ratio) with CO_2 gas treatment for 60 days followed by flushing with air and reaction for another 90 days: (a) aqueous I-127 over time with triplicate samples with CoCOIs, and (b) sequential I-127 extractions at 59 days with CoCOIs. Triplicate no-treatment controls shown in (b) apply to (a). Note: The transformation threshold at 65% remaining in the aqueous phase (35% transformed) is shown by the solid red line. Black diamonds represent the overall contaminant recovery across all extractions and remaining aqueous.

4.3.3 Objective 3: Sequestration of IO_3 in unsaturated sediments

4.3.3.1 Sequestration of I by CO_2 gas treatment in unsaturated sediments without CoCOIs

Unsaturated experiments for Objective 3 were conducted to better approximate field conditions in the VZ, where diffusion into pore water is significantly more rapid (theoretical diffusion estimates in Appendix C, Section C.1). Hf sediments at 4% or 8% WC into were packed small 1-D columns and subjected to CO_2 gas treatment for 60 days, followed by air treatment for an additional 90 days. Air treatment approximated long-term pH neutralization that would occur at field scale over years to decades and was used to evaluate any change in IO_3 mobility.

The pH measurements of the aqueous extraction water showed that the pH decreased from 8.15 in untreated sediments to 7.75 to 7.9 by 60 days, then did not appear to change for the next 90 days of air treatment (Appendix C, Figure C.3). Note that there is a 50x dilution from pore water to extraction water, so pH measurements in the extraction water do not accurately reflect the pore water pH. Diffusion simulations of CO_2 gas through the thin film of pore water at 4% WC indicated 7 seconds were needed to reach 50% CO_2 saturation at the sediment:water interface (Appendix C, Section C.1), so the CO_2

treatment conducted over 60 days was most likely at equilibrium, and oversaturated aqueous Ca and carbonate should have resulted in calcite precipitation.

The untreated Hf sediment had 0.092 µg/g natural I-127 and 0.26 µg/g total I-127 after I-127 was added, with approximately 45% and 21% of I-127 in the aqueous fraction for untreated Hf sediments without and with addition of I-127. The 216-S-9 sediment had 0.021 µg/g natural I-127 and 0.15 µg/g total I-127 after I-127 as IO_3 was added (Figure 4.17).

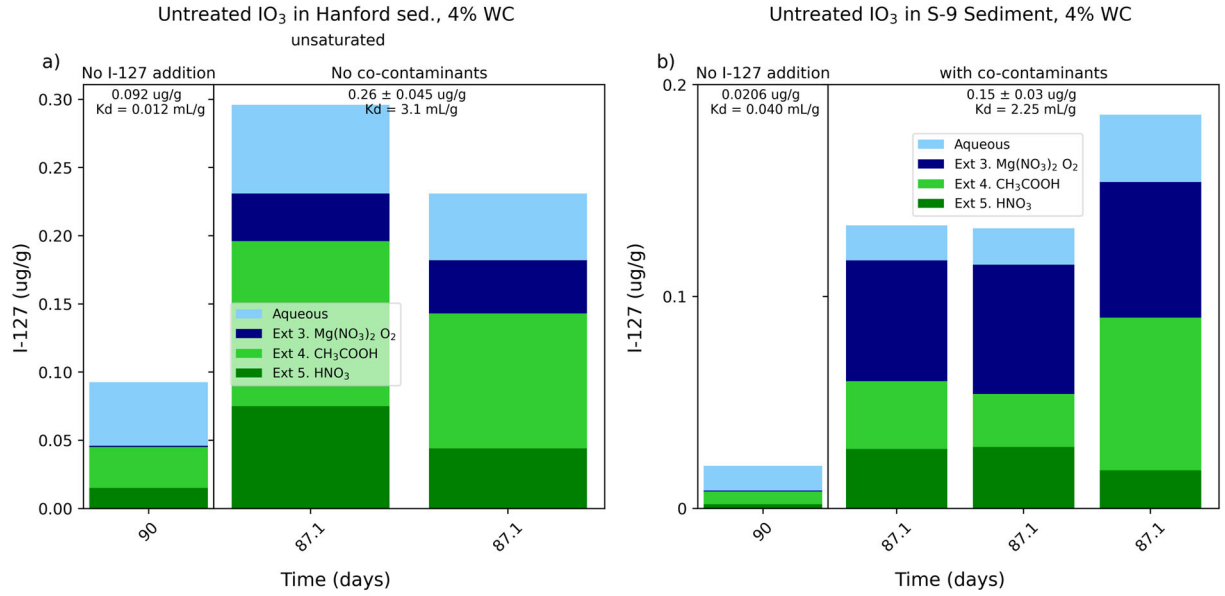

Figure 4.17. Results for I-127 (added as IO_3) following sequential extractions of sediments reacted for ~87 days without treatment at 4% WC for (a) uncontaminated Hf sediment without I-127 addition and with I-127 addition (in duplicate), and (b) contaminated 216-S-9 sediment without I-127 addition and with I-127 addition (in triplicate).

The CO_2 gas treatments at 4% WC showed 87.3 ± 3.6% and the 8% WC showed 88.0 ± 5.4% IO_3 removal from aqueous solution (Figure 4.18a and b), but IO_3 removal from the aqueous phase was more rapid at 4% WC (i.e., approximately 70% by 10 days compared to 50% at 10 days at 8% WC). IO_3 removal from the aqueous phase was consistent over 150 days, indicating a slow approach to equilibrium. This is in contrast to a previous study of water-saturated systems that showed greater IO_3 removal from the aqueous phase during initial calcite precipitation (within hours) followed by repartitioning of IO_3 back into solution at longer times. This was attributed to the initial precipitation of vaterite (µ-$CaCO_3$), which may incorporate less IO_3 in its structure, followed by recrystallization to calcite (McElroy et al. 2020).

Sequential extractions after 60 and 150 days of CO_2 gas treatment of the 4% WC Hf sediment columns showed that carbonate-associated I-127 (light green) increased from 36% for untreated sediment to 54% for 150 days of CO_2 treatment (Figure 4.18c). Sequential extractions after 60, 120, and 150 days of CO_2 treatment of the 8% WC Hf sediment columns showed decreasing aqueous I-127 and increasing carbonate-associated I-127 (Extraction 4, light green) over time. CoCOI behavior in these systems was consistent with calcite formation (described in Appendix C, Section C.3), where increases in CoCOI uptake were large for Sr (30% to 60%) and U (20% to 70%), which both have previously been observed to incorporate into calcite (Carlson 1980; Kelly et al. 2003).

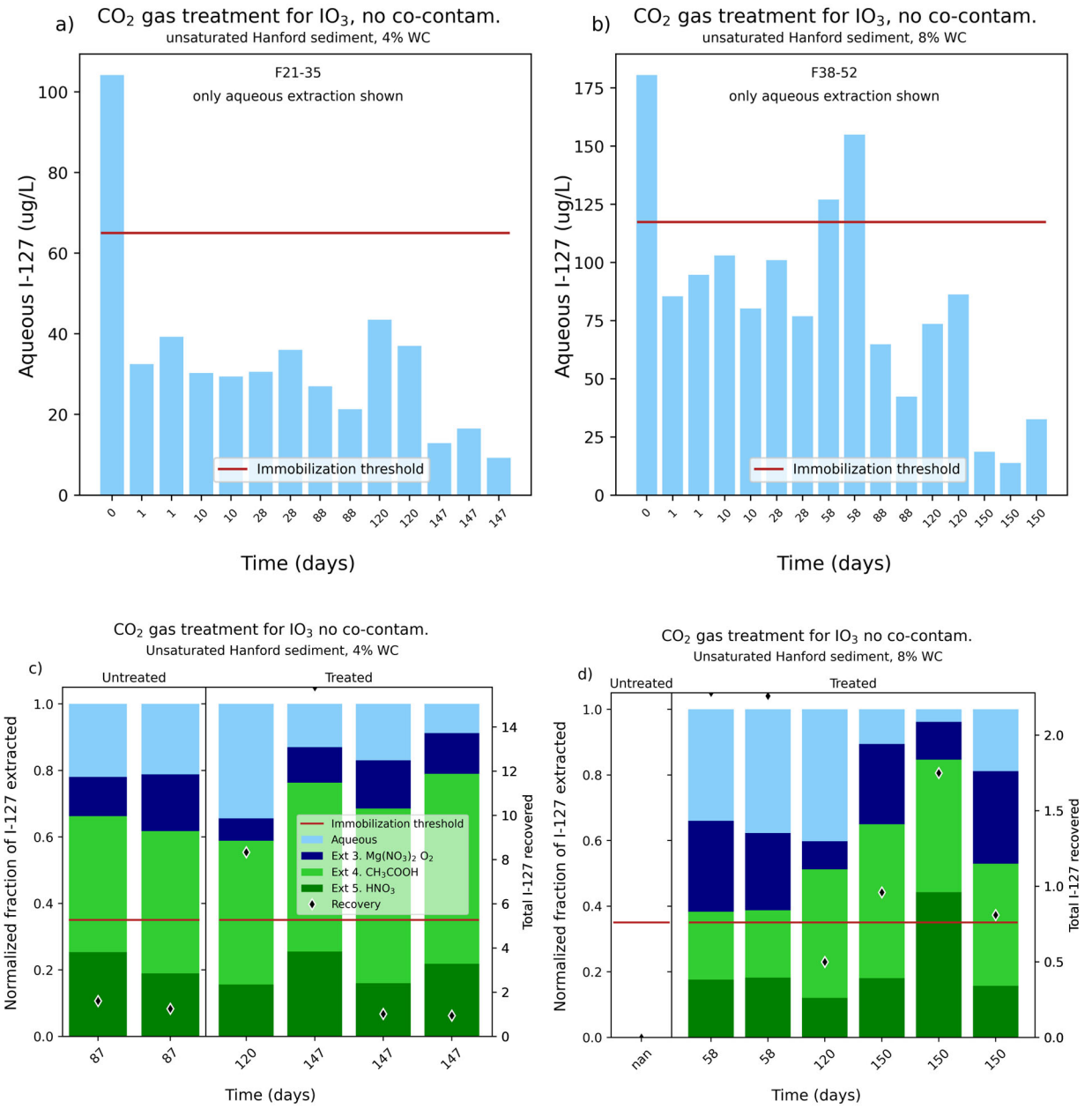

Figure 4.18. Results for I-127 (added as IO_3) without CoCOIs in Hf sediment columns at 4% (a, c) or 8% WC (b, d) treated with 100% CO_2 gas and reacted for 60 days then flushed with air and reacted for another 90 days (150 days in total). Time series change of aqueous I-127 is shown in (a) and (b), whereas sequential I-127 extractions for specific times are shown in (c) and (d). Controls for (a) are untreated data shown in (c) and controls for (b) are untreated data in (d). Note: The 35% minimum transformation threshold is shown by the solid red line. Black diamonds represent the overall contaminant recovery across all extractions and remaining aqueous.

4.3.3.2 IO_3 sequestration by CO_2 gas treatment in unsaturated sediment with CoCOIs

Unsaturated sediment column experiments were conducted at 4% WC with IO_3 in the presence of CoCOIs [U, Tc-99, Cr(VI), Sr] in Hf sediments (i.e., uncontaminated sediment from Pasco, WA) and an Hf sediment under the 216-S-9 Crib [C9512 65' depth, contained 2.21 µg/Kg I-127 (PNNL-26208)]. CoCOIs added included 2 µg/g U, 6 ng/g (100 pCi/g) Tc-99, 35 µg/g Cr(VI), 50 µg/g Sr, and 3300 mg/L NO_3^-. The pH levels of the diluted extraction water for both sediments were 8.05 to 8.2 before treatment and slowly decreased to 7.7 over the 60 days of CO_2 treatment, then slowly returned to 7.9 to 8.2 by 150 days after air injection (Appendix C, Figure C.4), which suggests CO_2 was partitioning into the pore water, resulting in some acidification. Diffusion simulations of CO_2 gas through the thin film of pore water at 4% WC indicated 7 seconds were needed to reach 50% CO_2 saturation at the sediment:water interface (Section C.1), so the CO_2 treatments conducted over 90 days were at equilibrium and oversaturated aqueous Ca and carbonate should result in calcite precipitation. Solid phase measurements of the total inorganic carbon (i.e., calcite) in sediments with no treatment and 150 days of CO_2 treatment did not show a consistent change (Table 4.8), with a small calcite increase observed for the Hf sediment and a decrease for the 216-S-9 sediment. These results were expected, as the amount of calcite that precipitates because the CO_2 treatment may be small. However, changes in co-contaminant concentrations from aqueous into the pH 2.3 acetate extraction (targeting calcite) did show large increases for contaminants that are known to substitute into calcite (i.e., U, Sr; see Appendix C, Section C.3).

Table 4.8. Change in solid phase inorganic carbon (calcite) for untreated and CO_2-treated sediment columns.

	% Inorganic Carbon	
Sediment	No Treatment	150 Days CO_2
Hanford fm, 4% WC	0.0	0.057 ± 0.039
216-S-9, 4% WC	0.283 ± 0.037	0.0

The CO_2 treatment with the Hf sediment with CoCOIs showed 84% IO_3 removal from the aqueous phase by 150 days (Figure 4.19a and c), which was slightly less than the 88% without CoCOIs (Figure 4.19a, c). Sequential extractions showed a decrease in aqueous IO_3 from 52% to 16% and a corresponding increase in the acetic acid extraction (i.e., calcite-associated, light green) from 32.6% to 65.3 ± 8.6% for CO_2-treated (Figure 4.19c). In contrast, the CO_2 treatment of the contaminated 216-S-9 sediment showed little change (Figure 4.19b and d). The untreated 216-S-9 sediment averaged 14.1 ± 2.6% aqueous (55% aqueous + adsorbed) I-127 and 27.3 ± 10.2% carbonate-associated I-127, whereas the CO_2-treated sediment at 150 days averaged 27.6 ± 5.2% aqueous (54% aqueous + adsorbed) I-127 and 34.0 ± 8.6% carbonate-associated I-127. Therefore, the fraction of mobile I-127 was unchanged (i.e., aqueous + adsorbed) at 54%, likely due to the high ionic strength of the pore water, but there was a small (6.4%) increase in the carbonate-associated I-127.

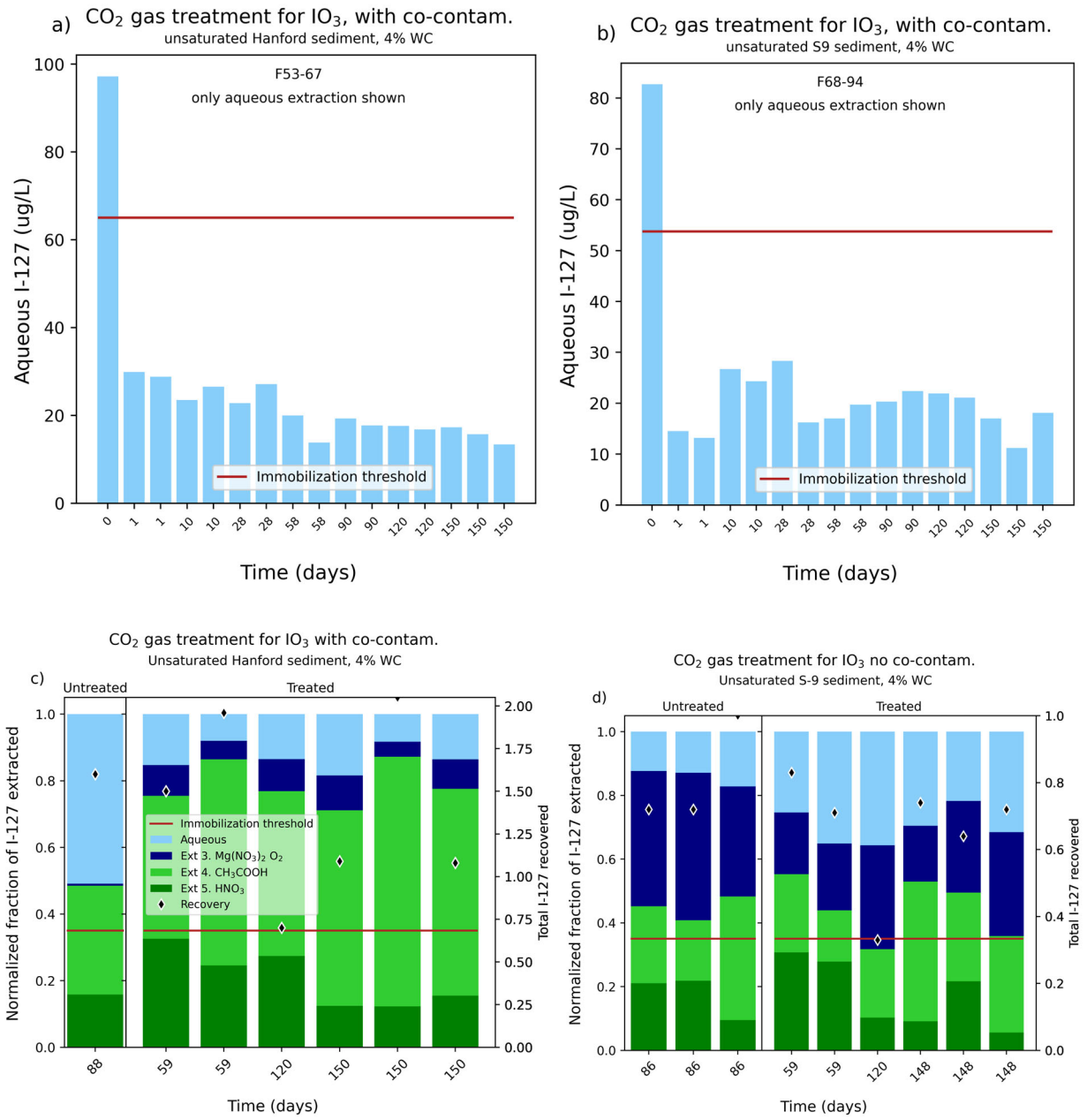

Figure 4.19. I-127 (as IO_3) in unsaturated columns at 4% WC in the presence of CoCOIs with CO_2 gas treatment: (a) aqueous I-127 changes over time in Hf sediment, (b) aqueous I-127 changes over time in 216-S-9 sediment, (c) sequential I-127 extractions with Hf sediment, and (d) sequential I-127 extractions with 216-S-9 sediment. Control for (a) is the untreated extraction in (c) and controls for (b) are the three untreated extractions in (d). Note: The 35% minimum transformation threshold is shown by the solid red line. Black diamonds represent the overall contaminant recovery across all extractions and remaining aqueous.

The evaluation of the change in mobility of co-contaminants due to the CO_2 gas treatment of sediments provided additional evidence that calcite precipitated, and some contaminants were partitioning into calcite (or other) precipitate. Sr and U are known to incorporate/substitute into calcite, whereas CrO_4^{2-} may form a $CaCrO_4$ co-precipitate, and pertechnetate may sparingly incorporate into calcite. Unsaturated

and water-saturated sediment experiments showed that Sr in the pH 2.3 acetate extraction (i.e., targeting calcite) increased from 30% to 60% (Appendix C, Figure C.5c) for both unsaturated Hf and 216-S-9 sediments and from 30% to 45% for water-saturated Hf sediments. U present as uranyl carbonate aqueous species in unsaturated conditions showed a large increase in U in pH 2.3 precipitates from 23% to 80-92% (Hf sediment) or from 10% to 30% (216-S-9 sediment, Figure C.5b). Water-saturated Hf sediments also showed an increase in U in pH 2.3 precipitate extraction. In contrast, CrO_4^{2-} showed a smaller increase in pH 2.3 acetate extraction in unsaturated experiments from 3.5% to 22-45% for both the Hanford and 216-S-9 sediments (Figure C.5d), and no increase for the water-saturated Hf sediment. Finally, pertechnetate also showed a small increase in the pH 2.3 acetate extraction in unsaturated conditions from 0% (untreated) to 3-12% for the Hanford and 216-S-9 sediments (Figure C.5a). There was also some (4% to 6%) Tc-99 incorporation into calcite in water-saturated experiments.

4.3.3.3 IO_3 sequestration in unsaturated sediments with other co-contaminants

Greater incorporation of IO_3 into calcite can occur by slowing the rate of calcite precipitation. Specific aqueous species known to slow calcite precipitation include (1) silica, (2) organic matter, (3) magnesium, (4) sulfate, and (5) nitrate. A limited number of experiments were conducted to evaluate the effect that these aqueous species have on the IO_3 incorporation rate and extent, as different waste sites can have significantly different concentrations of these species, so the CO_2 sequestration technology effectiveness may significantly change at different waste sites. For example, waste sites that were primarily acidic have elevated silica concentrations (BC Cribs, 216-U-8 Crib, 300 Area), waste sites with sulfuric acid disposal (less common) have elevated aqueous sulfate, and waste sites with nitric acid disposal (most common) have elevated aqueous nitrate.

The addition of nitrate to unsaturated sediments at 4% WC was already addressed by comparing 88% IO_3 removal from the aqueous phase with no nitrate (Figure 4.18a, c) to 84% IO_3 removal from the aqueous phase with nitrate and other CoCOIs that included 3300 mg/L NO_3^- (Figure 4.19a and c). Additional experiments were conducted with the 216-S-9 sediment at 4% WC in the presence of elevated aqueous silica, Mg-sulfate, and citrate (known to form aqueous complexes with calcium, thus slowing calcite precipitation). A comparison of IO_3 removal from the aqueous phase with CO_2 only to systems with additional silica, Mg-sulfate, or citrate in pore water showed slightly less IO_3 removal from the aqueous phase with additional aqueous ions (Figure 4.20a). Sequential extractions in untreated and treated samples showed no consistent change in the I-127 fractions in different phases with silica, Mg-sulfate, or citrate additions compared to just CO_2 treatment (Figure 4.20b). However, the total amount of I-127 extracted for silica, Mg-sulfate, or citrate addition was poor, at about 50% of the I-127 recovered for other experiments.

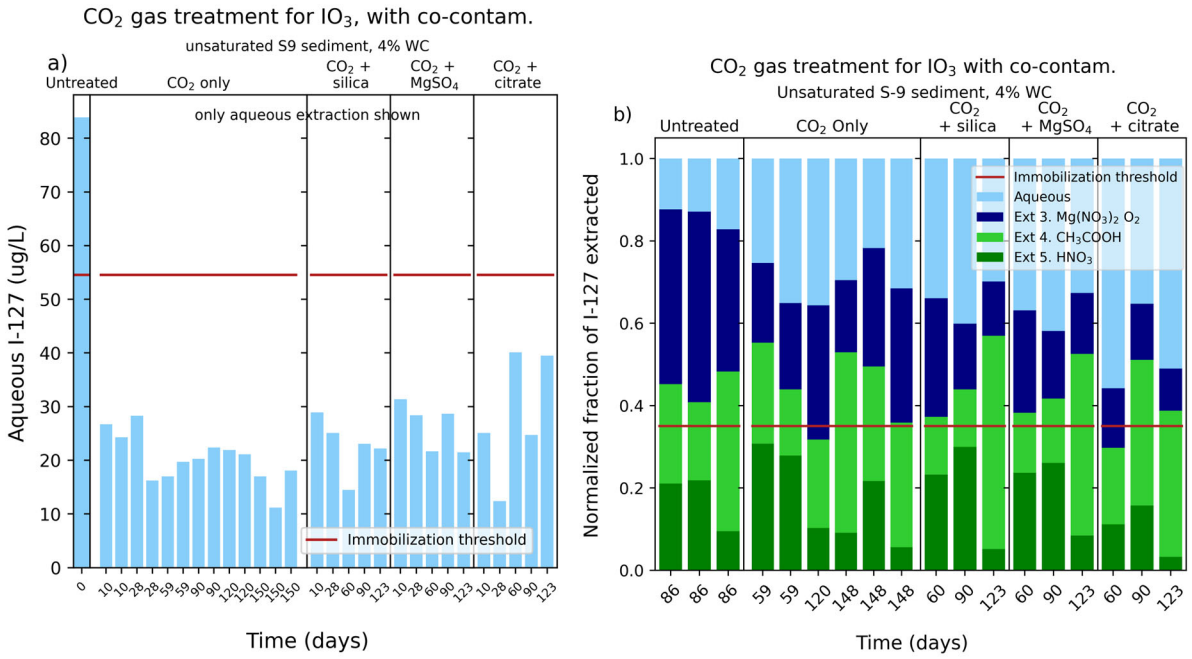

Figure 4.20. I-127 (added as IO_3) removal from porewater in the presence of 216-S-9 sediment (at 4% WC) with CO_2 gas treatment with additional silica, Mg-sulfate, or citrate in pore water as shown by (a) change in aqueous I-127 over time, and (b) sequential extractions at selected times. No-treatment controls in (a) are the triplicate no treatments shown in (b). Note: The 35% minimum transformation threshold is shown by the solid red line.

4.4 Particulate-Phase Chemical Sequestration – Sn(II)-PO_4

This technology was focused on the chemical sequestration of two PCOIs (U and Tc-99) following treatment with particulate Sn(II)-PO_4, though Sn(II)-PO_4 may remove contaminants from the aqueous phase through reduction. Table 4.9 presents the targeted testing conditions and amendments and shows which are moving forward to Phase 2 of testing. The removal rate for aqueous U and Tc-99 using Sn(II)-PO_4 was determined from batch tests described in Section 3.5.4.1, followed by sequential extractions described in Section 3.3 to determine the extent of sequestration. Sections 4.4.1 and 4.4.3 describe the removal of U and Tc-99, respectively, from the aqueous phase with time in batch experiments, while Sections 4.4.2 and 4.4.4 describe the extent of removal based on sequential extraction results U and Tc-99, respectively.

Batch results are shown as a fraction of Tc-99 or U removed over time from 2 hours to 28 days. The sequential extraction results are shown as fractions of Tc-99 or U measured in each extraction, representing increasingly immobile phases.

Any CoCOIs listed in Table 3.15 are discussed here regarding the impact on aqueous removal of PCOIs. The fate of CoCOIs (including CrO_4^-, Sr^{2+}, and IO_3^-) is not discussed here but is included in Appendix E, Section E.4.

Overall, these results show that under BY Cribs groundwater and perched water conditions, the Sn(II)-PO_4 was effective for Tc-99 and U and met the minimum removal threshold of 35% for transformation to temporarily immobile or immobile end products, with > 80% of Tc-99 and U found in

immobilized phases at the conclusions. Therefore, Sn(II)-PO_4 will move forward with the next phase of testing for this technology.

Table 4.9. Summary of remediation conditions and amendments for gas-phase chemical sequestration technologies.

Primary Conditions and Amendments	
PCOI	U, Tc-99
Primary treatment zone/ applicable 200-DV-1 waste sites	**BY Cribs, perched water**
Secondary treatment zone/ applicable 200-DV-1 waste sites	U-1, U-2, S-SX Tank Farm, T-TX-TY Tank Farm, C Tank Farm, BC Cribs and Trenches
Potential co-contaminants	I-129, Sr-90, NO_3^-, Cr(VI)
Chemical sequestration treatments	Sn(II)-PO_4
Phase 1 decision point	Go

Note: The treatment and conditions moving forward to Phase 2 evaluation are **bolded**. If no amendment passed the minimum threshold, none are bolded and no additional testing will be conducted.
CN (BY Cribs): Potential co-contaminant but primarily present as ferrocyanide; additional testing ongoing.

4.4.1 Objective 1: Rate of sequestration of U with Sn(II)-PO_4

Particulate Sn(II)-PO_4 was effective at removing U from aqueous solution in both BY Cribs groundwater and perched water conditions.

In the BY Cribs groundwater condition, aqueous U removal occurred quickly, with nearly all of the U removed from the aqueous phase within the first hours. The sediment alone [see Figure 4.21, Sediment only (No TA)] removed up to 35% of the aqueous fraction of U in the BY Cribs groundwater condition. The presence of CoCOIs did not affect the removal of aqueous U in the BY Cribs condition with treatment [i.e., with Sn(II)-PO_4 present] (Appendix E, Section E.4). However, with CoCOIs present, the aqueous U decreased by ~90% in the control [sediment without Sn(II)-PO_4], indicating something in the CoCOI led to some precipitation of U.

In the perched water conditions, the aqueous removal of U occurred more slowly compared to the BY Cribs conditions, with the maximum removal observed at the final 28-day time point. In perched water conditions, removal of U from the aqueous phase was greater with sediment present than without sediment present until the final 28-day time point. While not observable in the “Sediment only (No TA)” control within the perched water conditions due to the high initial concentration of U, some removal of U by the sediment may explain the higher removal at earlier time points in the batch tests conducted with sediment present compared to the Sn(II)-PO_4 without sediment.

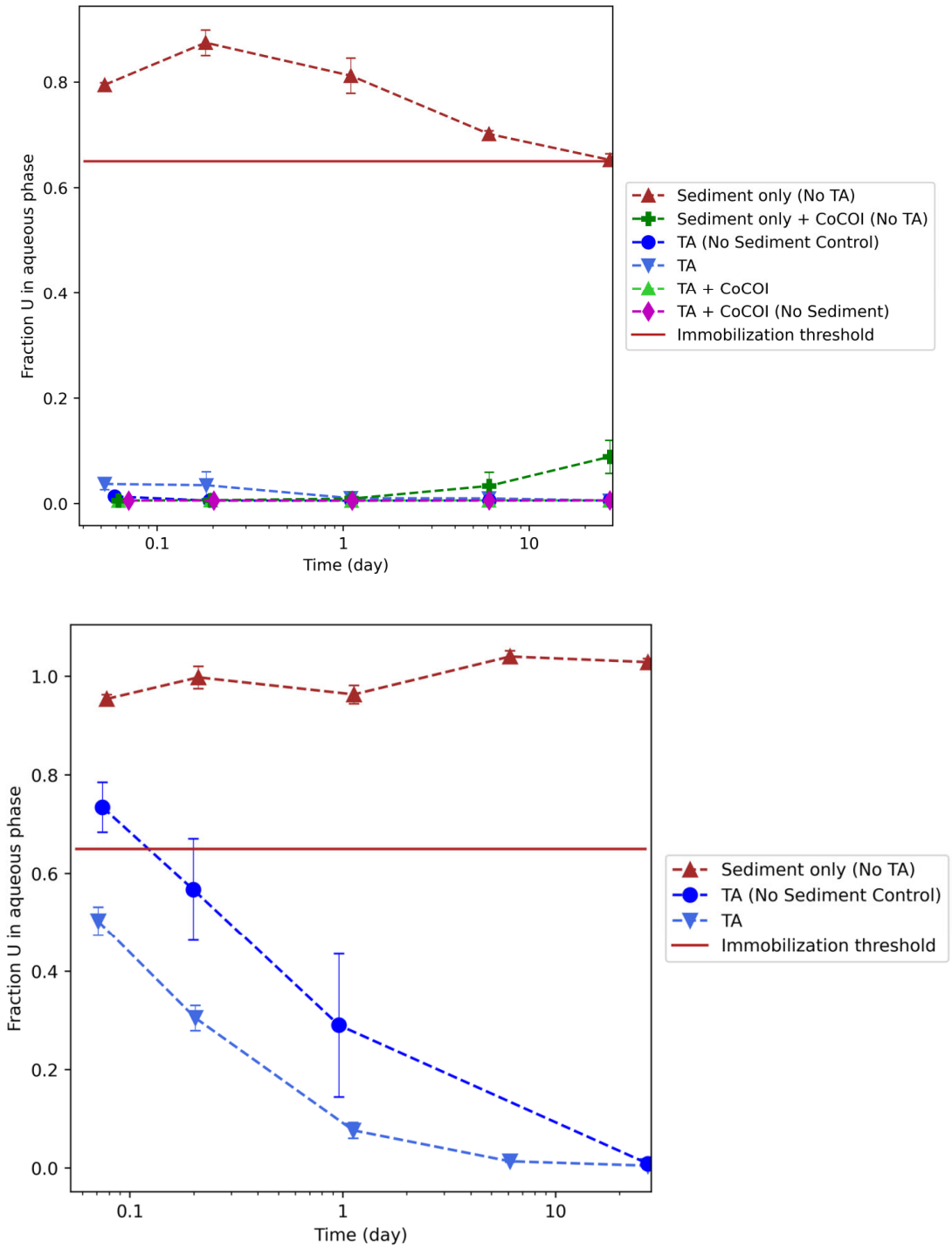

Figure 4.21. Fraction of U in the aqueous phase over time in BY Cribs groundwater conditions (*top*) and perched water conditions (*bottom*) in batch experiments with Hf sediments conducted over 28 days. "TA" had Sn(II)-PO_4 present while "No TA" did not have Sn(II)-PO_4. Note: The transformation threshold at 65% remaining in the aqueous phase is shown by the solid red line. Error bars are based on analysis of triplicate batch reactors. Lines connecting data points are used to guide the eye and do not represent a model. Table 4.10. Qualitative removal half-life for U by Sn(II)-PO_4.

	BY Cribs Groundwater	Perched Water
PCOIs only	Hours	NM
With CoCOIs	Hours	Days
NM = not measured		

4.4.2 Objective 2: Extent of sequestration of U with Sn(II)-PO_4

With or without sediment present, U removed from the aqueous phase by Sn(II)-PO_4 was found to be nearly all immobilized in both the BY Cribs groundwater and perched water conditions.

Nearly all of the U was immobilized (e.g., found in Extraction 4 or 5) in the BY Cribs groundwater conditions, with or without sediment present (Figure 4.22). Without Sn(II)-PO_4 present (in the presence of sediment only), approximately 35% of the U in the BY Cribs groundwater conditions was immobilized (e.g., found in Extraction 4 or 5), indicating the sediment had some adsorption capacity for U (Figure 4.22). Including CoCOIs in the BY Cribs groundwater condition did not significantly change the amount of U immobilized compared to the BY Cribs groundwater condition without CoCOIs. However, the presence of CoCOIs had a significant impact on the immobilization of U without Sn(II)-PO_4 present, increasing the U immobilization to approximately 90% compared to approximately 35% immobilized in the sediment only [no Sn(II)-PO_4 present] batch without CoCOIs present.

In the perched water condition sediment control [without Sn(II)-PO_4 present], approximately 3% of the U was immobilized (e.g., found in Extraction 4 or 5). With Sn(II)-PO_4 present, nearly all of the U was immobilized (e.g., found in Extraction 4 or 5).

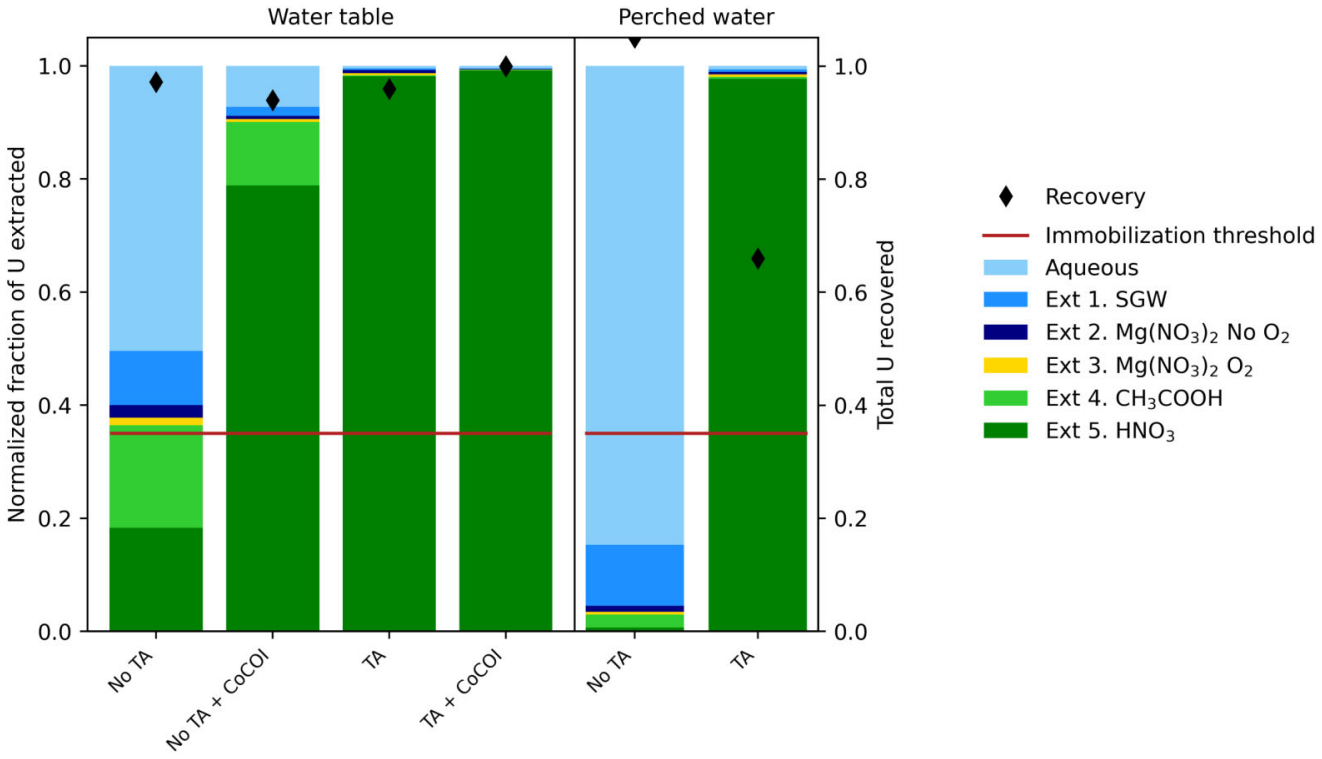

Figure 4.22. Change in U mobility from particulate phase treatment of contaminant-spiked Hf sediment after reaction for 28 days following sequestration by Sn(II)-PO_4 in BY Cribs groundwater (without and with CoCOIs) and perched water conditions. "TA" had Sn(II)-PO_4 present while "No TA" did not have Sn(II)-PO_4. Note: The 35% minimum transformation threshold is shown by the solid red line and black diamonds represent the overall contaminant recovery across all extractions and remaining aqueous.

4.4.3 Objective 1: Rate of sequestration of Tc-99 with Sn(II)-PO_4

Sn(II)-PO_4 removed nearly all Tc-99 from the aqueous phase within the first 1 to 2 hours (Figure 4.23). The Tc-99 remained out of solution for the duration of the 28-day experiments. Unlike results for U (Section 4.4.1), the sediment did not impact removal of aqueous Tc-99. The presence of CoCOIs had little to no effect on the removal of Tc-99 from solution (Figure 4.23) under these conditions.

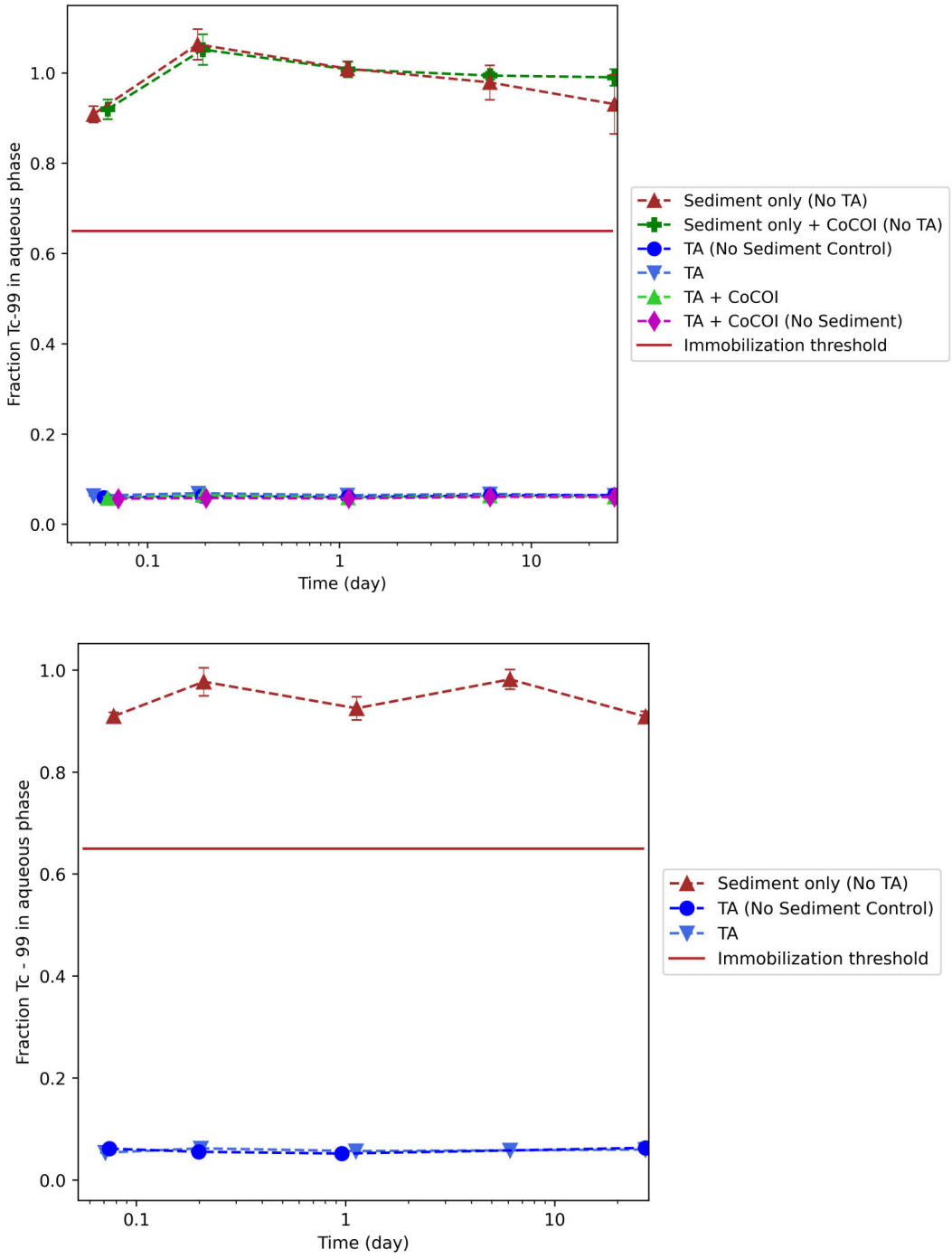

Figure 4.23. Fraction of Tc-99 in the aqueous phase over time in BY Cribs groundwater conditions (*top*) and perched water conditions (*bottom*) in batch experiments with Hf sediments conducted over 28 days. "TA" had Sn(II)-PO_4 present while "No TA" did not have Sn(II)-PO_4. Note: The transformation threshold at 65% remaining in the aqueous phase is shown by the solid red line. Error bars are based on analysis of triplicate batch reactors. Lines connecting points are used to guide the eye and do not represent a model. Table 4.11. Qualitative removal half-life for Tc-99 by Sn(II)-PO_4.

	BY Cribs Groundwater	Perched Water
PCOIs only	Hours	NM
With CoCOIs	Hours	Hours
NM = not measured		

4.4.4 Objective 2: Extent of sequestration of Tc-99 with Sn(II)-PO_4

In the BY Cribs groundwater conditions, 86% to 87% of the aqueous Tc-99 was found in the immobile phase (i.e., Extractions 4 and 5), with or without CoCOIs (Figure 4.24). In controls without Sn(II)-PO_4, only 2% of the Tc-99 was immobilized, with most of the Tc-99 remaining in the aqueous phase.

Similar results were observed in the perched water conditions, with 98% of the Tc-99 immobilized with Sn(II)-PO_4 present and 3% immobilized in the absence of Sn(II)-PO_4 (Figure 4.24).

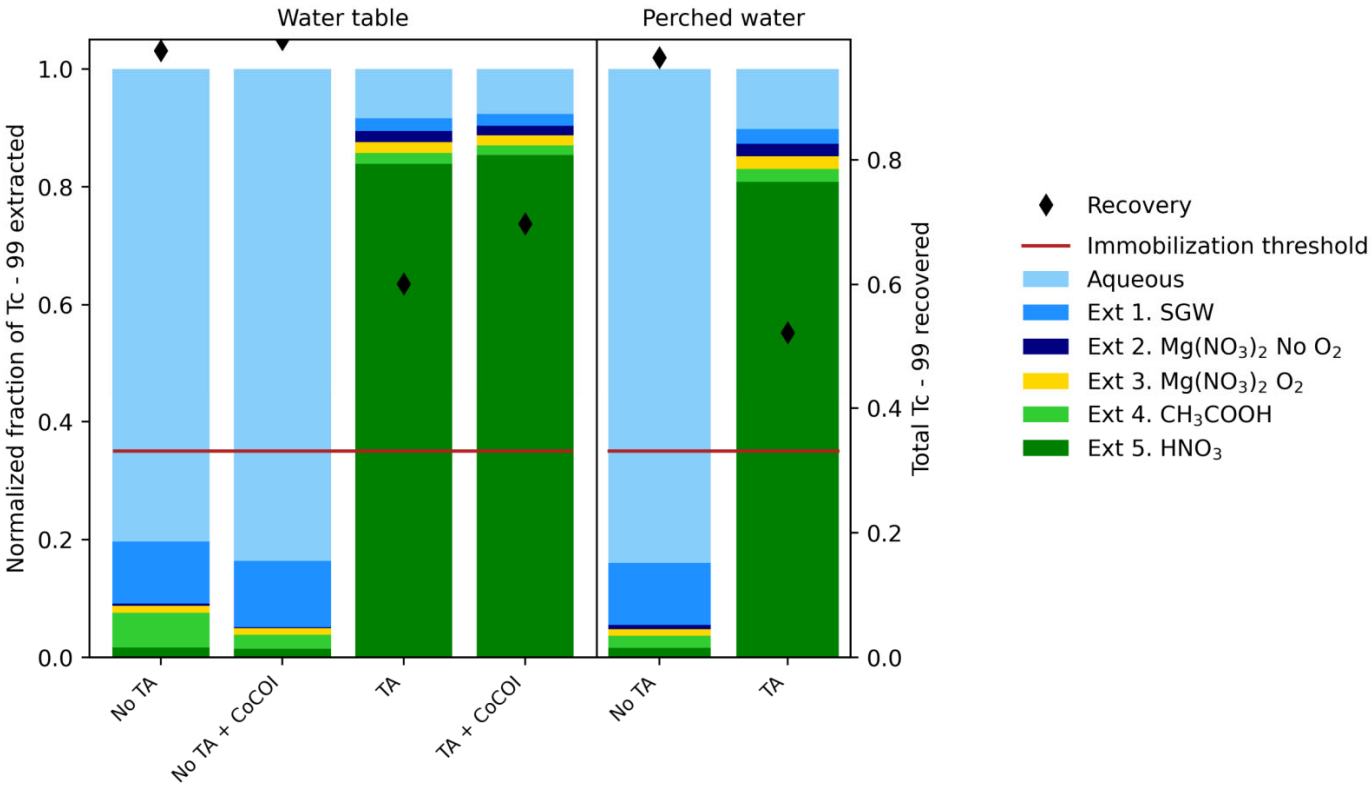

Figure 4.24. Change in Tc-99 mobility from particulate phase treatment of contaminant-spiked Hf sediment after reaction for 28 days following sequestration by Sn(II)-PO_4 in BY Cribs groundwater (without and with CoCOIs) and perched water conditions. "TA" had Sn(II)-PO_4 present while "No TA" did not have Sn(II)-PO_4. Note: The 35% minimum transformation threshold is shown by the solid red line and black diamonds represent the overall contaminant recovery across all extractions and remaining aqueous.

4.5 Particulate-Phase Chemical Sequestration – Bismuth oxyhydroxide and bismuth subnitrate

The bismuth materials sequester the two PCOIs (U and Tc-99) through different mechanisms. Tc-99 is sequestered through outer-sphere complexation or ion exchange, while U can form inner-sphere complexation. Table 4.12 presents the targeted testing conditions and amendments and shows which are moving forward to Phase 2 of testing. The rate of aqueous removal of U and Tc-99 using BOH or BSN was determined using batch experiments as described in Section 3.5.5.1, followed by sequential extractions as described in Section 3.3 to determine the extent of the contaminant removal.

The batch results are shown as a fraction of Tc-99 or U removed over time (from 2 hours to 28 days).

CoCOIs as listed in Table 3.16 are discussed here regarding the impact on aqueous removal of PCOIs. Aqueous removal of CoCOIs is included in Appendix E, Section E.4.

Overall, these results show that under BY Cribs groundwater conditions and perched water conditions, the BSN and BOH were effective for Tc-99 and U and met the minimum removal threshold of 35% for transformation to temporarily immobile or immobile end products. For the perched water conditions, BSN performed better than the BOH for Tc-99, with a higher fraction of the aqueous Tc-99 removed, and a higher fraction of the removed Tc-99 was found in immobile phases following the batch experiments. Therefore, BSN will advance to the next phase of testing for this technology.

Table 4.12. Summary of remediation conditions and amendments for gas-phase chemical sequestration technologies.

Primary Conditions and Amendments	
PCOI	U, Tc-99
Primary treatment zone/ applicable 200-DV-1 waste sites	**BY Cribs, perched water**
Secondary treatment zone/ applicable 200-DV-1 waste sites	U-1, U-2, S-SX Tank Farm, T-TX-TY Tank Farm, C Tank Farm, BC Cribs and Trenches
Potential co-contaminants	I-129, Sr-90, NO_3^-, Cr(VI)
Chemical sequestration treatments	**BSN** and BOH
Phase 1 decision point	Go

Note: The treatment and conditions moving forward to Phase 2 evaluation are **bolded**. If no amendment passed the minimum threshold, none are bolded and no additional testing will be conducted.
CN (BY Cribs): Potential co-contaminant but primarily present as ferrocyanide; additional testing ongoing.

4.5.1 Objective 1: Rate of sequestration of U with bismuth materials

In the BY Cribs groundwater and perched water conditions, BOH and BSN removed U to near or below IDLs within 1 day when sediment was present in the system. Without sediment, BSN did not perform well in the BY Cribs groundwater conditions because hydrolysis of BSN causes a decrease in pH. When sediment is present, the pH is buffered despite the ongoing hydrolysis and, therefore, the pH does not decrease significantly (Appendix F, Table F.1). This did not affect BOH because hydrolysis was completed during the formation of the BOH material. In the perched water experiments without sediment present, BSN still performed well because the pH did not decrease below ~5 (compared to pH ~2 in the BY Cribs) and may be due to the U spike used. In the BY Cribs groundwater conditions, U was added as uranyl nitrate, while U was added as uranyl chloride in perched water because the uranyl chloride was

available in a higher stock concentration, which was necessary to reach the starting concentration required for the perched water. Without bismuth present, the sediment removed ~40% of the aqueous U.

Additional experiments were conducted under BY Cribs groundwater conditions in the presence of CoCOIs [Sr, Cr(VI), I, and nitrate]. The presence of CoCOIs did not affect removal of aqueous U in BOH or BSN under these conditions (Figure 4.25), although CoCOIs may have a greater impact in Phase 2 evaluation with column experiments due to the different sediment-to-solution ratios and the use of site-specific sediments.

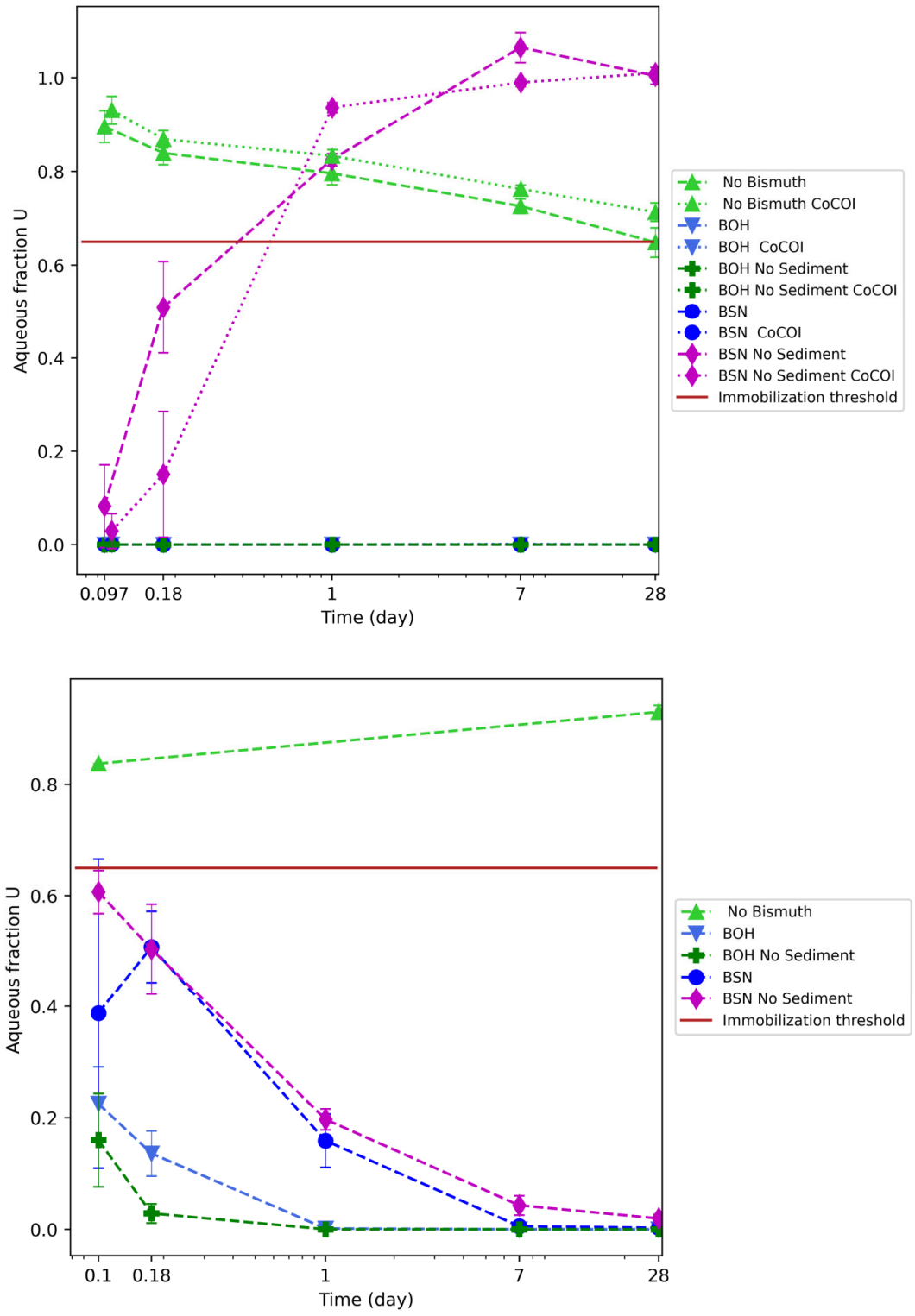

Figure 4.25. Fraction of U in the aqueous phase over time in BY Cribs groundwater conditions (*top*) and perched water conditions (*bottom*) in batch experiments with Hf sediments conducted over 28 days. Note: The transformation threshold at 65% remaining in the aqueous phase is shown by the solid red line. Error bars are based on analysis of triplicate batch reactors. Lines are used to guide the eye and do not represent a model.

Table 4.13. Qualitative removal half-life for U by bismuth materials.

	BY Cribs Groundwater		Perched Water	
	BSN	BOH	BSN	BOH
PCOIs only	Hours	Hours	NM	NM
With CoCOIs	Hours	Hours	Hours	Hours
NM = not measured				

4.5.2 Objective 2: Extent of sequestration of U with bismuth materials

After 28 days of reaction time, sequential extractions were used to determine the extent of the U removal. In BY Cribs groundwater conditions, ~70% of the aqueous U removed by the BOH or BSN was immobilized, represented by the final two extractions. Additional experiments were conducted with the sequential extractions after 1 day of reaction time to evaluate changes in mobility of the sequestered PCOIs or CoCOIs over time. These results showed less permanent immobilization of U and had similar percentages of U found in the immobile phases (Extractions 4 and 5) as the control without bismuth present, indicating most of the immobilization was likely due to the sediment in this short amount of time. The 1-day results had no U in the oxidizable phase compared to ~10% at 28 days, indicating a small amount of the U may have been removed from the aqueous phase through reduction during the longer reaction time.

In perched water conditions, the relatively higher concentration of U made a difference in the percent of U removed by the sediment alone (represented by the no Bi test). With BSN or BOH present, > 90% of the U was found to be the immobile phases represented by Extractions 4 and 5 at the end of 28 days. After 1 day, BOH had already reached > 90% U immobilized while BSN was at ~55%, indicating that BSN required more time to immobilize the larger quantity of U (150 mg/L) compared to BOH.

Despite the higher concentration of U in the perched water compared to the BY Cribs groundwater (150 mg/L and 1 mg/L, respectively), the perched water had much higher concentrations of U in immobile phases after 28 days (~95% and ~68% immobilized, respectively). U speciation is highly dependent on pH and ionic strength of the background solution, and the differences in the SPW and 200W SGW are a likely source of the differences in the sequential extraction results.

A majority of the U was found in the carbonate phase, represented by Extraction 4, especially under the perched water condition tests. This is expected because when exposed to water containing carbonate, BSN transforms into bismutite, a carbonate mineral [layered $Bi_2O_2(CO_3)$]. Without carbonate present, the BSN transforms to bismuth hydroxy-nitrate. BOH already contains carbonate in the starting material and is able to transform to bismutite with or without additional carbonate present. During the transformation to bismutite, U present as uranyl carbonate is incorporated into the bismutite structure as the nitrate in the starting material is exchanged for carbonate.

When CoCOIs were added to BY Cribs groundwater condition, the total amount of U in immobile phases (from Extractions 4 and 5) was unchanged. However, when looking at the two final extractions separately, more of the U was found in Extraction 4 than in Extraction 5 (~30% in Extraction 5 for tests with CoCOIs compared to ~40% in tests with PCOIs only; the fractions are reversed for Extraction 4; Appendix F, Section F.3, and Figure 4.26).

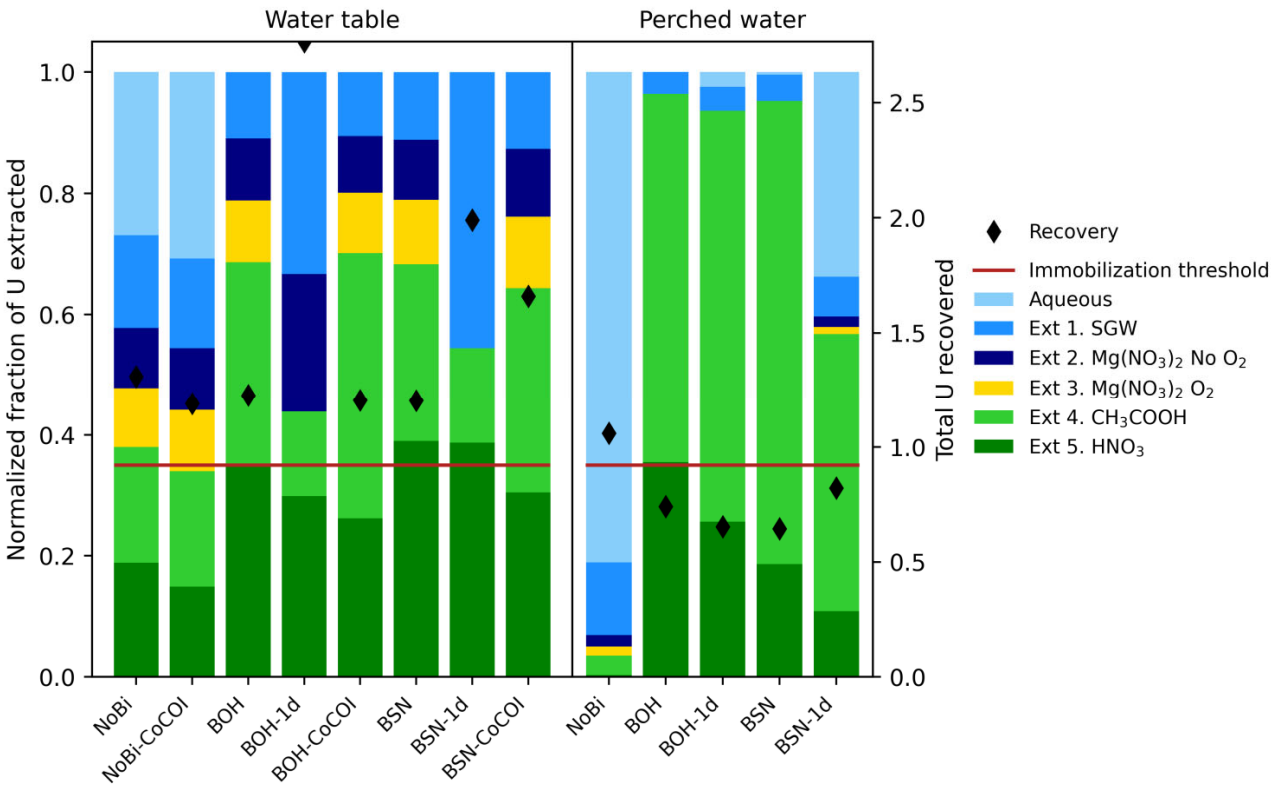

Figure 4.26. Change in U mobility from particulate phase treatment of contaminant-spiked Hf sediment after reaction for 1 and 28 days following sequestration by BOH or BSN in BY Cribs groundwater (without and with CoCOIs) and perched water conditions. Note: The 35% minimum transformation threshold is shown by the solid red line and black diamonds represent the overall contaminant recovery across all extractions and remaining aqueous.

4.5.3 Objective 1: Rate of sequestration of Tc-99 with bismuth materials

In the BY Cribs groundwater conditions, removal of Tc-99 was similar to the removal of U, with > 90% Tc-99 removed with BOH (with or without sediment) and BSN (with sediment only). Similar to U removal, BSN initially removed Tc-99 from solution, but it was then released within the first week. Unlike the U removal, however, the BOH and BSN tests with sediments released some Tc-99 (~20%) back into solution before the 28-day conclusion while the BOH with sediment remained near or below the IDLs.

In the perched water, aqueous Tc-99 was removed from solution to below the 35% minimum transformation threshold but did not reach the same level of removal as in the BY Cribs groundwater. While the Tc-99 concentration was the same between the two experiments (0.1 mg/L), the significantly higher concentration of U in the perched water may have overwhelmed adsorption sites. While Tc-99 plateaued for all other conditions after 7 days, BSN without sediment continued to decrease the Tc-99, and removal from the aqueous phase reached > 80% by the 28-day conclusion.

Additional experiments were conducted under BY Cribs groundwater conditions in the presence of CoCOIs [Sr, Cr(VI), I, and nitrate]. With BOH, the presence of CoCOIs did not affect removal of aqueous Tc-99 (Figure 4.27). For BSN, when sediment was not present, the Tc-99 removal increased and nearly matched the Tc-99 removal with sediment (Figure 4.27).

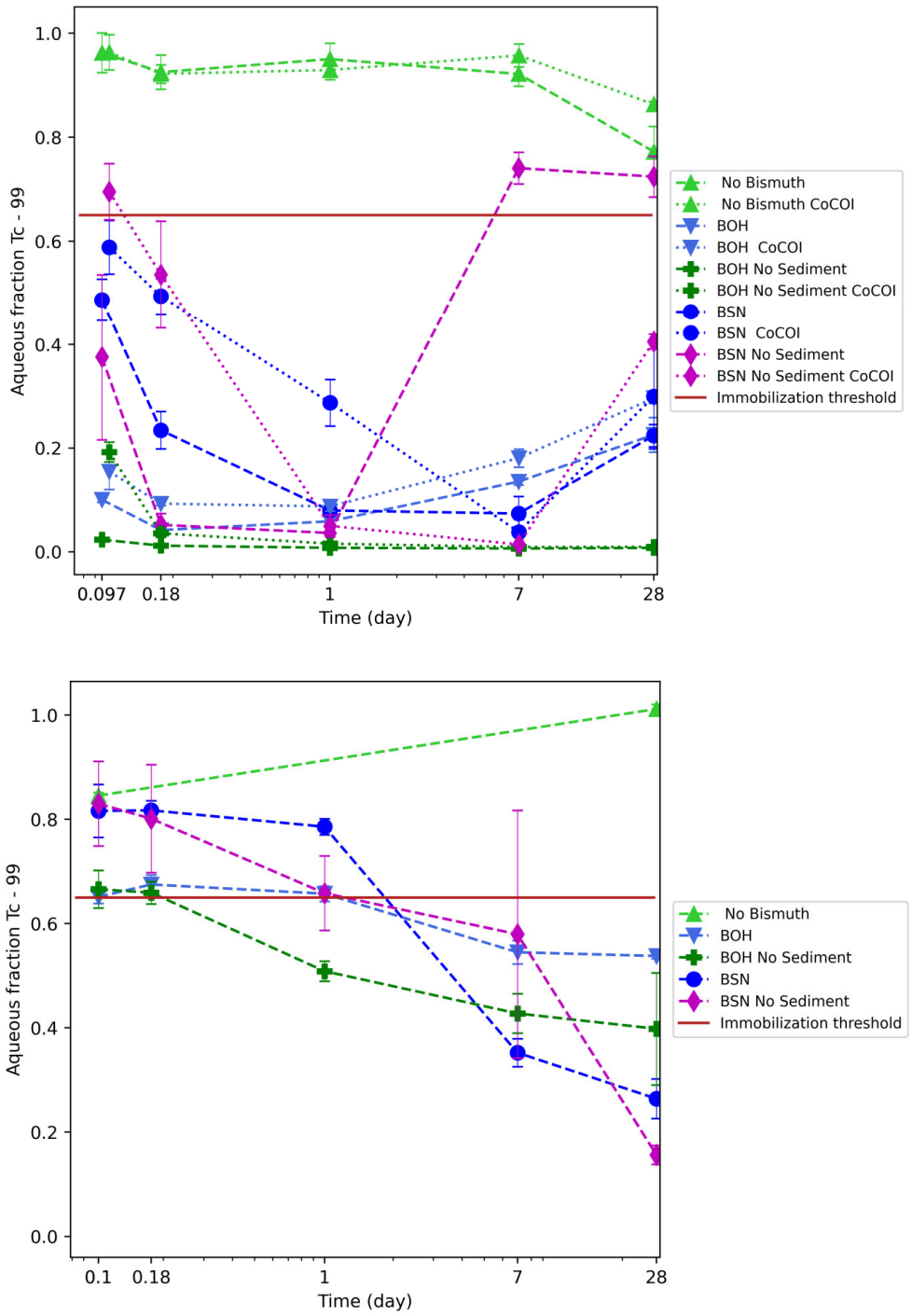

Figure 4.27. Fraction of Tc-99 in the aqueous phase over time in BY Cribs groundwater conditions (*top*) and perched water conditions (*bottom*) in batch experiments with Hf sediments conducted over 28 days. Note: The transformation threshold at 65% remaining in the aqueous phase is shown by the solid red line. Error bars are based on analysis of triplicate batch reactors. Lines are used to guide the eye and do not represent a model.

Table 4.14. Qualitative removal half-life for Tc-99 by bismuth materials.

	BY Cribs Groundwater		Perched Water	
	BSN	BOH	BSN	BOH
PCOIs only	Hours to days	Hours	NM	NM
With CoCOIs	Hours to days	Hours	Days to weeks	Days to weeks
NM = not measured				

4.5.4 Objective 2: Extent of sequestration of Tc-99 with bismuth materials

After 28 days of reaction time, sequential extractions were used to determine the extent of the Tc-99 removal. Additional experiments were conducted with the sequential extractions after 1 day of reaction time to evaluate changes in mobility of the sequestered PCOIs or CoCOIs over time.

More than 40% of the Tc-99 and 50% in the BOH BY Cribs groundwater conditions were found in an immobile phase after 28 days, represented by Extractions 4 and 5. When the extraction was conducted after 1 day of reaction time, less Tc-99 was immobilized (~30% for BSN and ~35% for BOH), indicating a time-dependent reaction to transfer additional Tc-99 from temporarily immobilized phases to immobilized phases.

In the perched water, BSN was able to immobilize more aqueous Tc-99 than BOH, with ~50% and 30% found in Extractions 4 and 5, respectively, after 28 days. In the extractions after 1 day, significantly less Tc-99 was immobilized, with ~15% found in Extractions 4 and 5 for both BSN and BOH.

For BY Cribs groundwater conditions with CoCOIs, Tc-99 was found in roughly the same phases in the sequential extraction results as without CoCOIs (Figure 4.28).

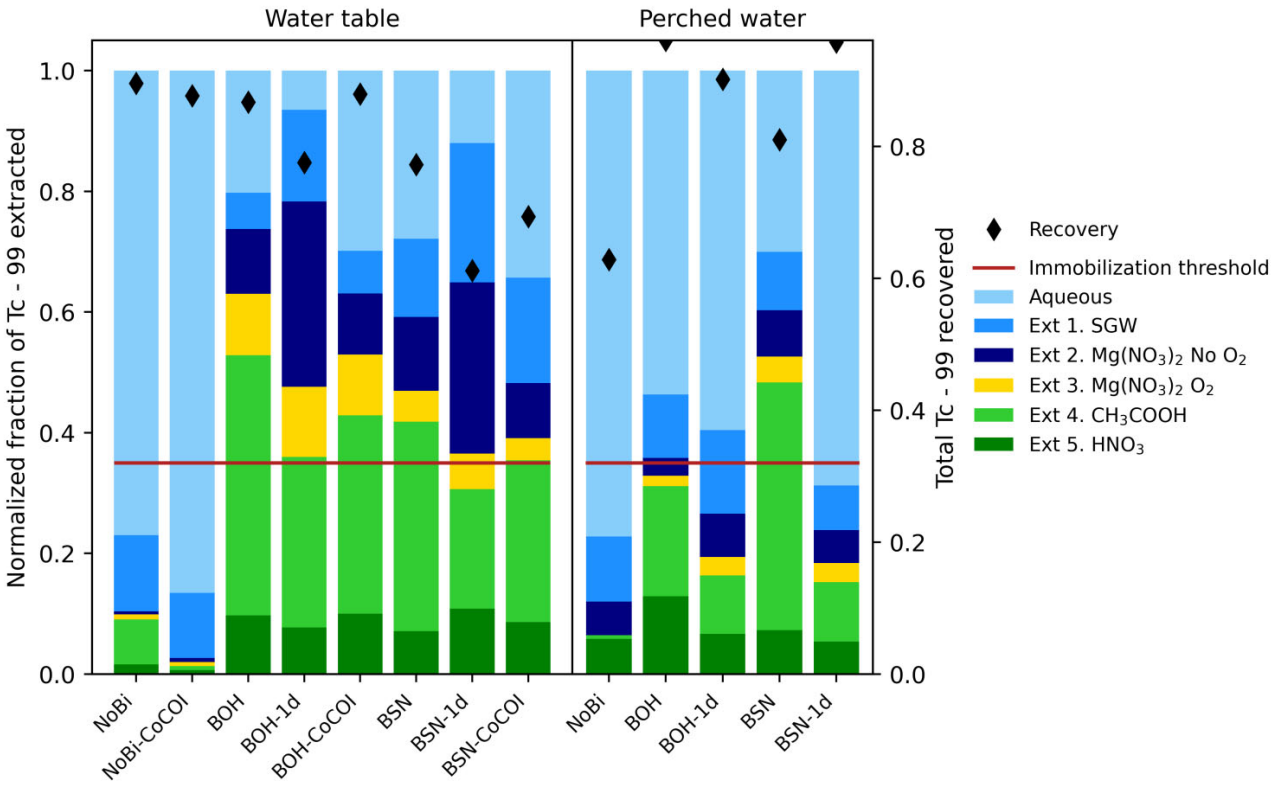

Figure 4.28. Change in mobility of Tc-99 from particulate phase treatment of contaminant-spiked Hf sediment after reaction for 28 days following sequestration by BOH or BSN in BY Cribs groundwater (without and with CoCOIs) and perched water conditions. Note: The 35% minimum transformation threshold is shown by the solid red line and black diamonds represent the overall contaminant recovery across all extractions and remaining aqueous.

4.6 Particulate-Phase Combined Chemical Reduction and Sequestration – ZVI/SMI and polyphosphate

This technology was focused on the reductive precipitation of two PCOIs [Tc-99 as TcO_4^- and U as multiple U(VI) species], followed by incorporation and/or coating by apatite, which is precipitated from a Poly-PO_4 solution. Results show specific combinations of amendments, sediments, and delivery fluid for this technology that were outlined in DOE/RL-2018-28 (Table 7-2) and are separated into the following sections based on sub-objectives for sequestration of Tc-99 and U without CoCOIs (Objective 1) and with CoCOIs (Objective 2). Table 4.15 presents the targeted testing conditions and amendments and shows which are moving forward to Phase 2 of testing. Experiments evaluated different combinations of sediments (Hf, CCuz, BY Crib, no sediment), groundwater or perched water, without or with CoCOIs, and reductant (ZVI or SMI), as described in detail in the Section 3.5.6.

Overall, these results show that both technologies (ZVI or SMI, with subsequent Poly-PO_4 treatment) were effective for U removal and met the minimum threshold of 35% transformation to temporarily immobile or immobile end products for both BY Cribs groundwater and perched water conditions. The fraction of Tc-99 and U transformed to immobile or temporarily immobile phases was slightly greater for SMI compared to ZVI. Therefore, SMI will move forward with additional site-specific, laboratory-scale column testing.

Table 4.15. Summary of remediation conditions and amendments for gas-phase chemical sequestration technologies.

Primary Conditions and Amendments	
PCOI	U, Tc-99
Primary treatment zone/ applicable 200-DV-1 waste sites	**BY Cribs, perched water**
Secondary treatment zone/ applicable 200-DV-1 waste sites	U-1, U-2, S-SX Tank Farm, T-TX-TY Tank Farm, C Tank Farm, BC Cribs and Trenches
Potential co-contaminants	I-129, Sr-90, NO_3^-, Cr(VI)
Chemical reduction treatments	ZVI and **SMI**
Chemical sequestration treatments	**Poly-PO_4**
Phase 1 decision point	Go

Note: The treatment and conditions moving forward to Phase 2 evaluation are **bolded**. If no amendment passed the minimum threshold, none are bolded and no additional testing will be conducted.
CN (BY Cribs): Potential co-contaminant but primarily present as ferrocyanide; additional testing ongoing.

4.6.1 Objective 1: Sequestration of Tc-99 and U by ZVI or SMI and Poly-PO_4 without CoCOIs

4.6.1.1 Tc-99 sequestration by ZVI or SMI without sediments

Comparison of the immobilization results for the ZVI and SMI treatment with subsequent Poly-PO_4 treatment without sediments (this section) with results in the presence of sediment (Section 4.6.1.2) shows the complex reactions that occur with sediments. Immobilization is quantified based on sequential extraction results; however, it is expected that ZVI and SMI immobilize Tc-99 and U via reduction processes while Poly-PO_4 immobilizes Tc-99 and U via adsorption, co-precipitation, and coating processes (sequestration) as described previously in Section 2.6. In the no-sediment systems, Tc-99 immobilization in groundwater by SMI was considerably faster (< 1 day, Appendix G, Figure G.5c) than for ZVI (14 days, Figure G.5a). This is consistent with a previous evaluation of the limitations of ZVI compared to ferrous and mixed ferrous/ferric oxides, such as SMI (Guan et al. 2015). The electron donor (ZVI or SMI) to acceptor (i.e., Tc-99 and U) ratio in these systems was about 11,000, so orders of magnitude more reductant were present. The ratio of electron donor to acceptor decreased to 59 when CoCOIs (NO_3^-, CrO_4^{-2}, IO_3^-) were present in groundwater. Experiments in perched water had the same Tc-99 concentration (260 pCi/g or 15 ng/g), but higher U (50 mg/L) and nitrate (800 mg/L), so the electron donor/acceptor ratio was 3.7. The Tc-99 immobilization rate in perched water with nitrate was slower (Figure G.5c and d) than in groundwater for both ZVI and SMI, as nitrate should be reduced before $Tc(VII)O_4^-$ [Eq. (2.5].

4.6.1.2 Tc-99 sequestration by ZVI or SMI with sediments

Untreated Hf sediment exhibited virtually no sorption capacity for Tc-99 as $Tc(VII)O_4^-$ over 50 days without CoCOIs (K_d < 0.006 mL/g; Figure 4.29a). In the presence of CoCOIs (i.e., perched water), untreated Hf sediment also exhibited virtually no sorption capacity for $Tc(VII)O_4^-$ (K_d < 0.006 mL/g), but after 50 days, some Tc-99 was present in precipitates (Figure 4.29a).

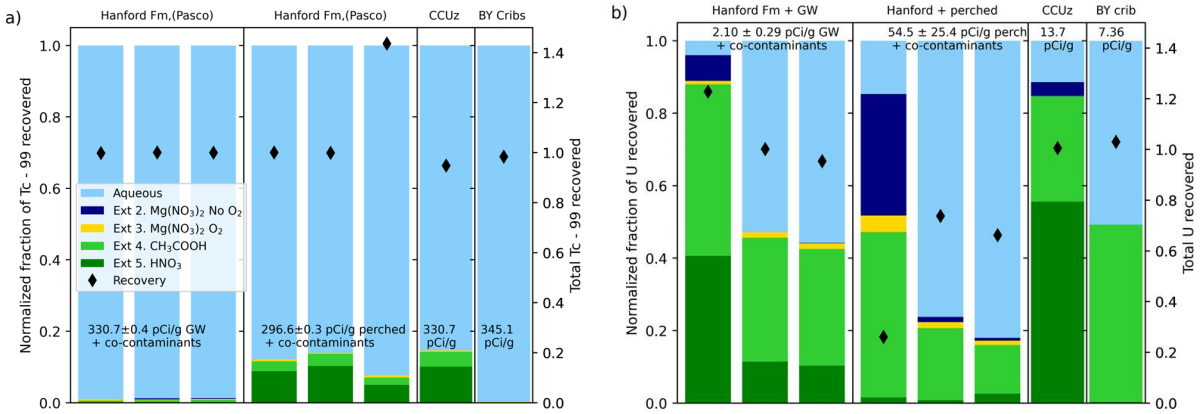

Figure 4.29. Tc-99 (a) and U (b) sequential extraction after 50 days in untreated Hf sediment in groundwater (Tc-99 and U) and perched water (Tc-99, U, and nitrate), Cold Creek Unit silt (CCuz, Tc-99 and U), and BY Cribs sediment (Tc-99, U, and nitrate) in groundwater. Note: Black diamonds represent the overall contaminant recovery in extractions.

ZVI or SMI were added at time zero and PCOI immobilization was evaluated over 14 days, then Poly-PO_4 solution was added at 14 days and an additional 36 days were used to evaluate apatite precipitation effect on contaminant immobilization (total of 50 days). Both SMI and ZVI addition (0.008 g/g) to groundwater resulted in the redox potential decreasing from +130 to +160 mV for untreated sediments to -400 to -600 mV after 14 days (Appendix G, Figure G.3a) and the pH increasing from 7.5 to 8.1-9.0 (Figure G.3b). At 14 days, the Poly-PO_4 solution was added. By 50 days, the redox potential was largely the same, but the pH increased in most cases to 8.8 to 9.7.

The extent of immobilization of Tc-99 by ZVI was > 99% in Hf sediment (Figure 4.30a) and CCuz sediment (Figure 4.30b) and incomplete (91%) in the BY Cribs sediment that contains high nitrate (Figure 4.30c), highlighting the potential for commingled contaminants to consume reduction capacity. The Tc-99 immobilization in Hf sediment by ZVI was slower compared to when no sediment was present (Figure G.5a). The possible ZVI reactions with sediment include (1) contaminant adsorption to sediment, (2) sediment adsorption of ferrous iron from the ZVI, and (3) ZVI reduction of some ferric oxides in sediment. For the CCuz sediment (Figure 4.30b), Tc-99 immobilization was more rapid than without sediment (Figure G.5a). Although this uncontaminated CCuz sediment had no other CoCOIs, the higher calcite in the sediment may have affected Tc-99 reduction due to pH buffering of the pH change that occurs from the ZVI or SMI. The field-contaminated BY Cribs sediment exhibited incomplete Tc-99 immobilization, likely from the high nitrate concentration. (No nitrate was added, but 1817 mg/L NO_3^- was present in the sediment.) This high nitrate concentration resulted in an electron donor/acceptor ratio of 1.6, meaning 99.96% of the ZVI reductive capacity was being used to reduce nitrate.

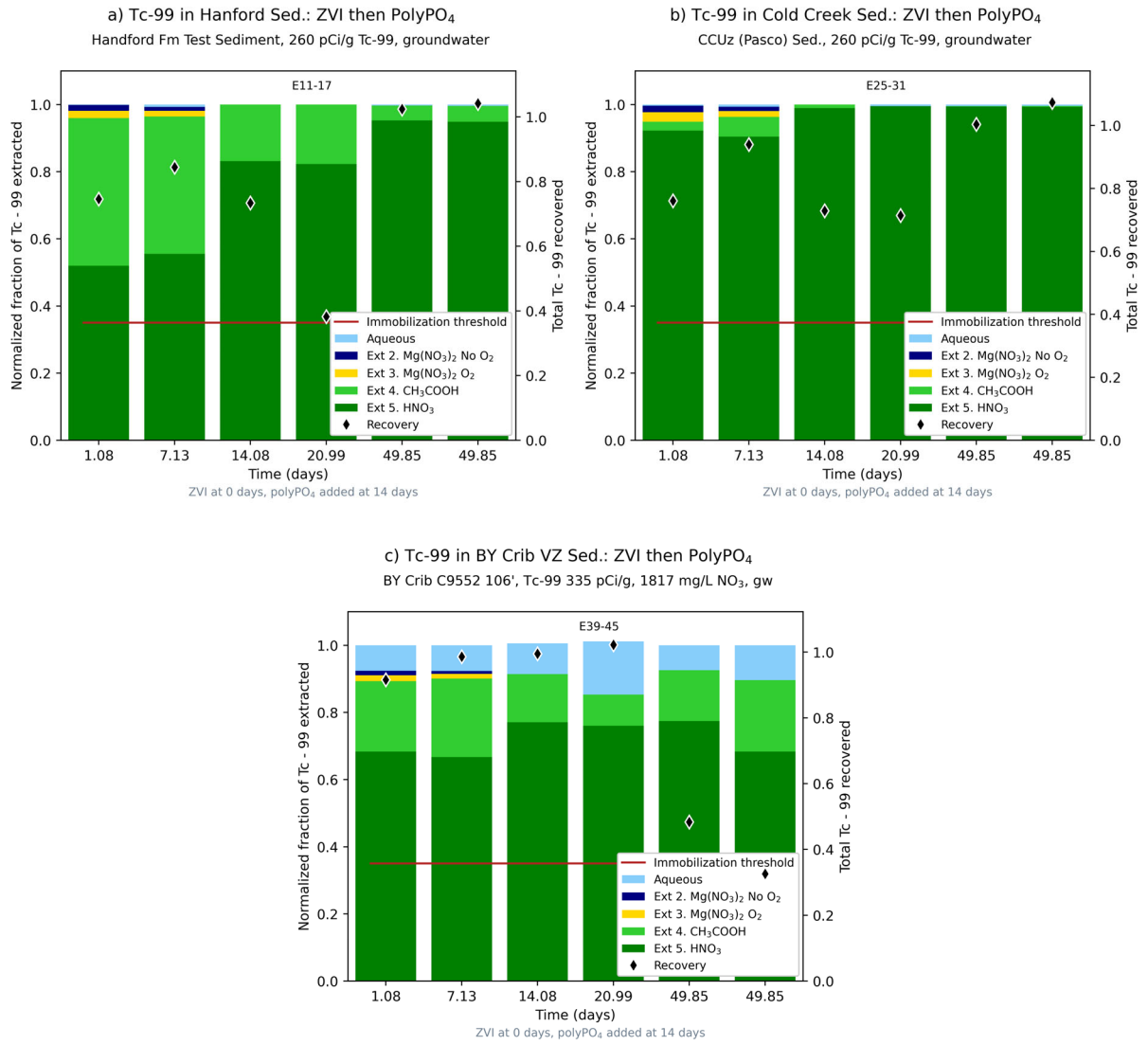

Figure 4.30. Change in Tc-99 mobility from ZVI particulate phase treatment of (a) Hf sediment, (b) CCuz sediment, and (c) BY Cribs sediment in batch experiments with SGW and no added CoCOIs at a 1:2 sediment-to-solution ratio. Note: The 35% minimum transformation threshold is shown by the solid red line and black diamonds represent the overall contaminant recovery across all extractions and remaining aqueous. ZVI treatment started at 0 days; Poly-PO_4 treatment started at 14 days. No-treatment controls are shown in Figure 4.29a.

The extent of immobilization of Tc-99 by SMI in different sediments was nearly the same as ZVI (i.e., > 99% for Hf and CCuz sediments), but the rate was more rapid. For the Hf sediment, Tc-99 immobilization was slightly slower (Figure 4.31a) than without sediment (Appendix G, Figure G.5c). Tc-99 immobilization by SMI in the CCuz sediment was fast and complete by 1 day (Figure 4.31b). Tc-99 immobilization by SMI in the field-contaminated BY Cribs sediment showed mixed behavior with variable removal from the aqueous phase over time, with 12% aqueous Tc-99 after 50 days (Figure 4.31c), which was about the same as ZVI in the nitrate-contaminated BY Cribs sediment (Figure 4.31c).

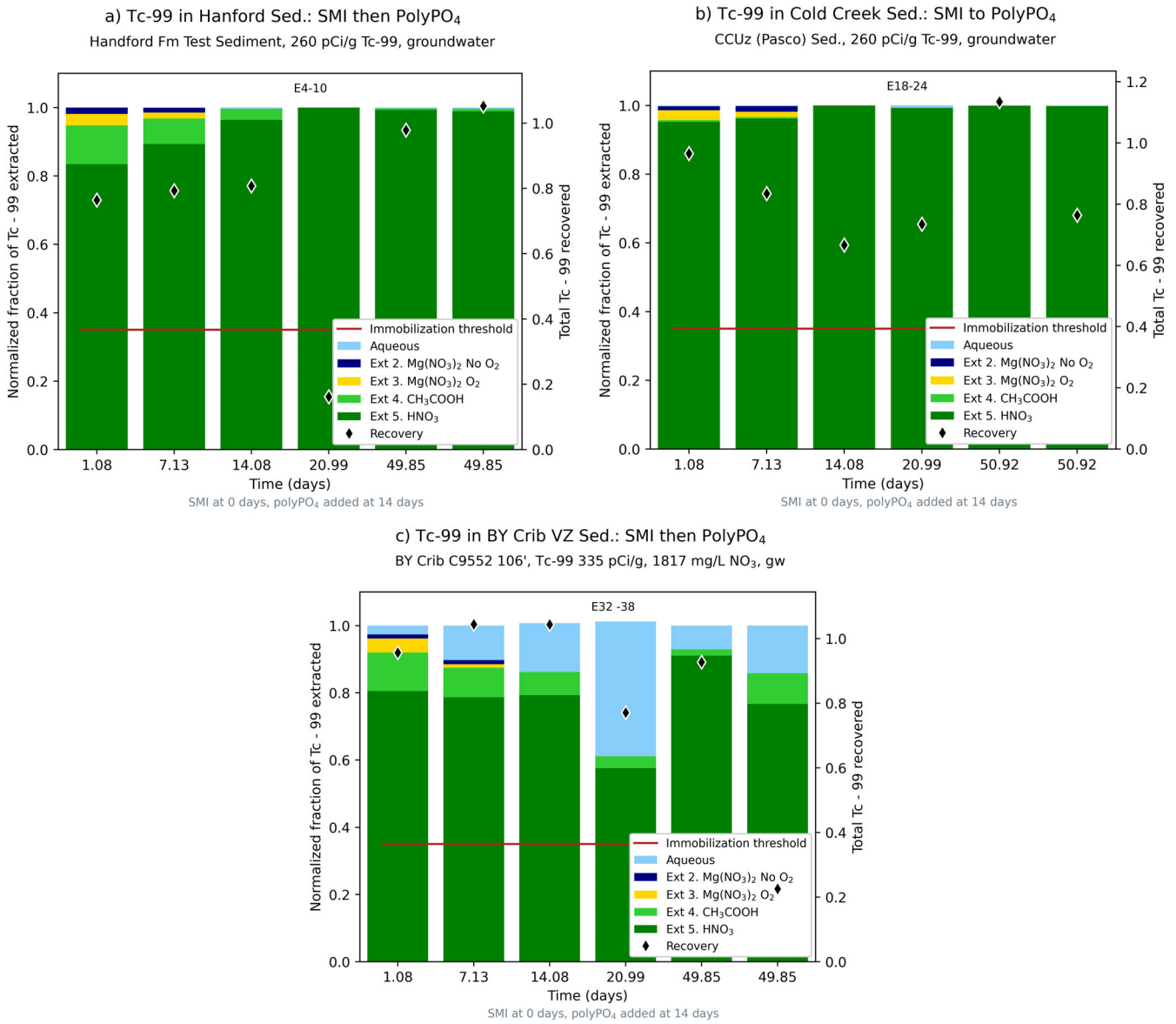

Figure 4.31. Change in Tc-99 mobility from SMI particulate phase treatment of (a) Hf sediment, (b) CCuz sediment, and (c) BY Cribs sediment in batch experiments with SGW and no added CoCOIs at a 1:2 sediment-to-solution ratio in different sediments. Note: The 35% minimum transformation threshold is shown by the solid red line and black diamonds represent the overall contaminant recovery across all extractions and remaining aqueous. SMI treatment started at 0 days; Poly-PO_4 treatment started at 14 days. No-treatment controls are shown in Figure 4.29a.

4.6.1.3 U sequestration by ZVI or SMI without sediments

Uranium immobilization by ZVI or SMI with subsequent Poly-PO_4 treatment without sediments was evaluated in groundwater or perched water with differing CoCOI concentrations (i.e., differing electron donor-to-acceptor ratios). U immobilization by ZVI or SMI in groundwater with no CoCOIs was complete (> 99%) within 7 days (Appendix G, Figure G.6), while in the presence of CoCOIs, U immobilization was complete (> 99%) for SMI whereas only 91% of U was immobilized by ZVI (Figure G.6b). In perched water, both ZVI and SMI treatments resulted in nearly complete U immobilization (> 99%) by 14 days (Figure G.7).

4.6.1.4 U sequestration by ZVI or SMI with sediments

The extent of immobilization of U by ZVI was complete (98%) in Hf sediment (Figure 4.32a) and CCuz sediment (Figure 4.32b) but incomplete (93%) in the field-contaminated BY Cribs sediment, which contains high nitrate (Figure 4.32c). The rate and extent of U immobilization by ZVI was less in the presence of Hf sediment than when no sediment was present (Appendix G, Figure G.7a), similar to the results for Tc-99 (Figure 4.31c). The BY Cribs sediment exhibited incomplete U immobilization by 50 days (averaging 93%), likely from the high nitrate present in this field-contaminated sediment. This high nitrate concentration resulted in an electron donor/acceptor ratio of 1.6, meaning 99.96% of the ZVI reductive capacity was being used to reduce nitrate.

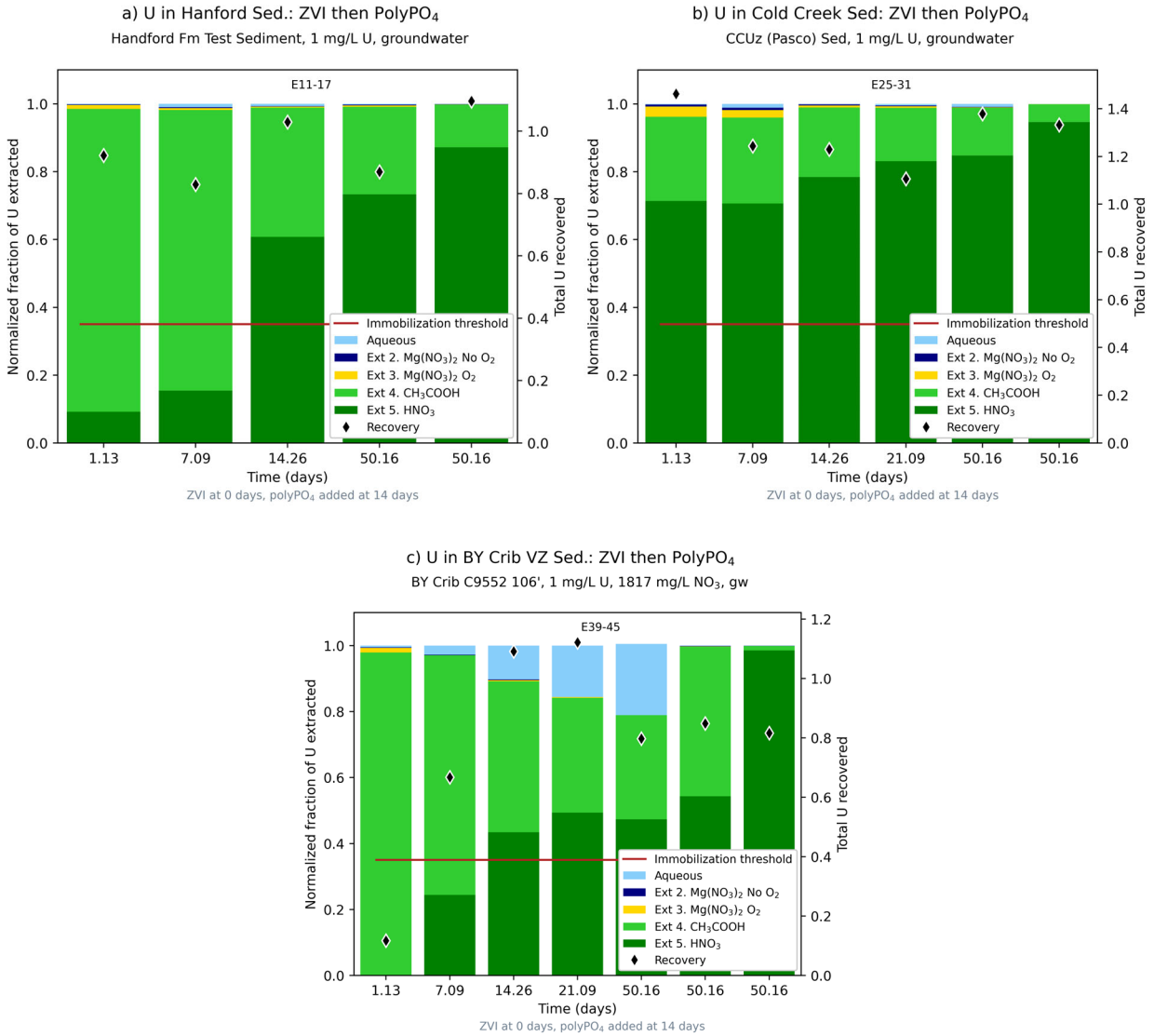

Figure 4.32. Change in U(VI) mobility from ZVI particulate phase treatment of (a) Hanford test sediment, (b) Cold Creek sediment, and (c) BY Cribs sediment in batch experiments with SGW and no added CoCOIs. Note: The 35% minimum transformation threshold is shown by the solid red line and black diamonds represent the overall contaminant recovery across all extractions and remaining aqueous. ZVI treatment started at 0 days; Poly-PO_4 treatment started at 14 days. No-treatment controls are shown in Figure 4.29b.

The extent of immobilization of U by SMI was nearly complete for the Hf sediment (98% by 50 days, Figure 4.33) but slightly less for the CCuz sediment (averaging 97% by 50 days, Figure 4.33b). U immobilization by SMI in the nitrate-contaminated BY Cribs sediment showed inconsistent behavior, with 96% reduction after 1 day, 70% reduction by 21 days, then nearly complete reduction by 50 days (Figure 4.33c).

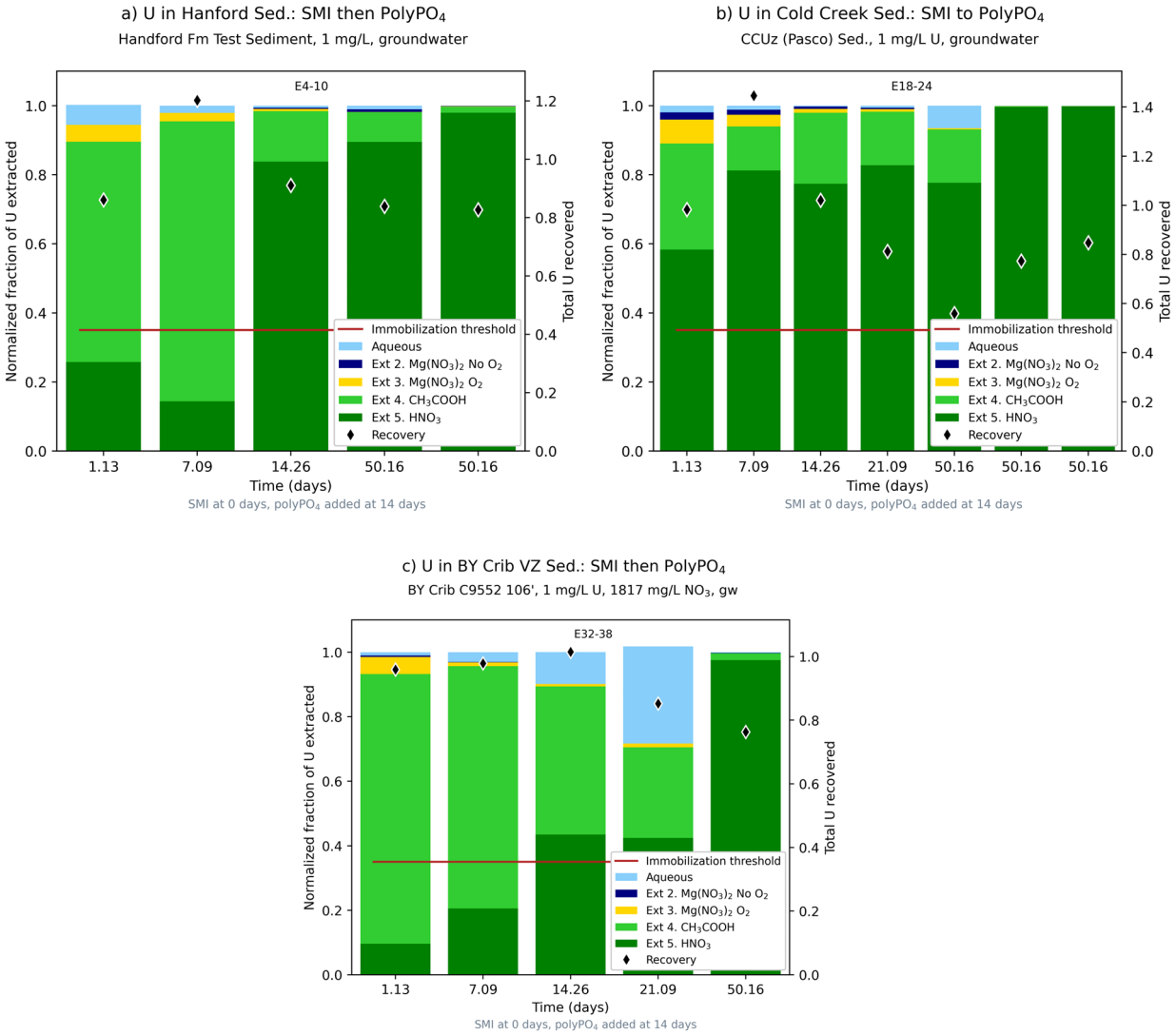

Figure 4.33. Change in U(VI) mobility from SMI particulate phase treatment of (a) Hanford test sediment, (b) Cold Creek sediment, and (c) BY Cribs sediment in batch experiments with SGW and no added CoCOIs. Note: The 35% minimum transformation threshold is shown by the solid red line and black diamonds represent the overall contaminant recovery across all extractions and remaining aqueous. ZVI treatment started at 0 days; Poly-PO_4 treatment started at 14 days. No-treatment controls are shown in Figure 4.29b.

4.6.2 Objective 2a: Sequestration of Tc-99 and U by ZVI or SMI and Poly-PO_4 with addition of CoCOIs

4.6.2.1 Tc-99 sequestration by ZVI or SMI with sediments

The presence of CoCOIs has two effects on PCOI (Tc-99 and U) reduction: (1) electrons from the ZVI or SMI are consumed by CoCOIs, and (2) CoCOIs may be reduced prior to or after Tc-99, depending on the relative reductive potentials needed for the reactions. As shown in Appendix G, Figure G.2, while Tc-99 may be immobilized quickly and to a greater extent in systems with excess electron donor (i.e., ZVI or SMI), as the electron acceptor concentration increases, Tc-99 immobilization rate may decrease and/or the extent may be more limited. For Tc-99 reduction by ZVI, there was an inconsistent change in the

Tc-99 rate and extent as the ratio of electron donor/acceptor changed from 11,000 (> 99% Tc-99 immobilized, Figure 4.34a) to 59 (78% immobilized, Figure 4.34b) to 3.7 (95% immobilized, Figure 4.34c), and finally to 1.6 (88% immobilized, Figure 4.34d) with different concentrations of CoCOIs (Appendix G, Table G.2). As shown in Figure 4.34d, the field-contaminated BY Cribs sediment contained 3510 μg/g NO_3^-, so the calculated nitrate in these batch conditions was 1817 mg/L. In all cases, nitrate was present as the highest electron acceptor concentration, and, because nitrate is more easily reduced compared to $Tc(VII)O_4^-$ [Eq. (2.5)], it caused the change in the Tc-99 immobilization rate. Batch experiments were also conducted under varying conditions from excess electron donor to excess electron acceptor to evaluate Tc-99 and U reduction in cases where a more easily reduced co-contaminant (nitrate) was present (Figure G.1). Data describing changes in CoCOI concentrations due to the ZVI/SMI and Poly-PO_4 treatment are in presented Appendix G, Sections G.5 to G.7.

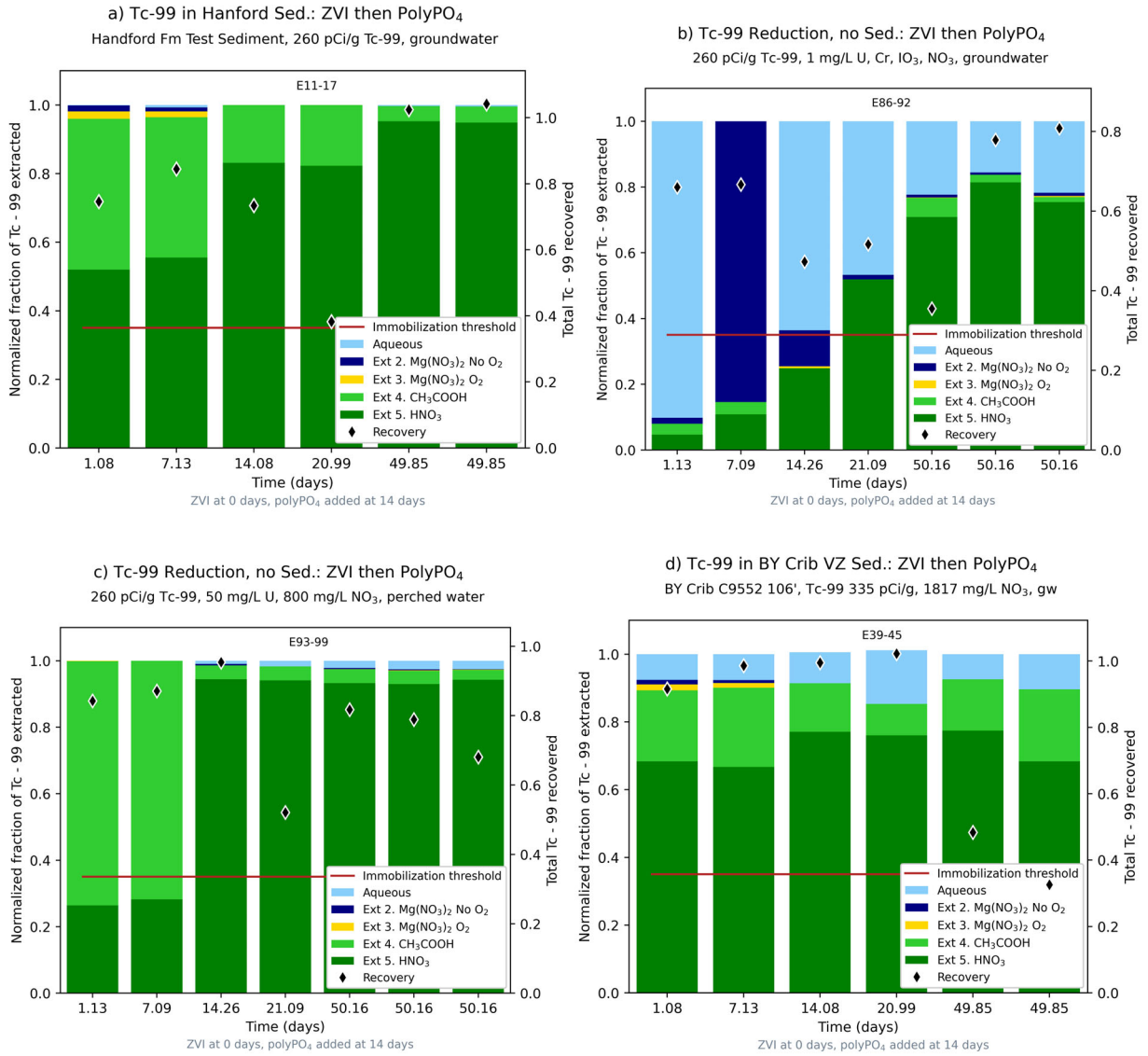

Figure 4.34. Change in Tc-99 mobility from ZVI particulate phase treatment in systems with differing CoCOIs: (a) Tc-99 in SGW (Hf sediment); (b) Tc-99, U, Cr(VI), IO_3, and nitrate in SGW (no sediment); (c) Tc-99, U, and 800 mg/L NO_3^- in SPW (no sediment); and (d) Tc-99, U, and 1817 mg/L NO_3^- in SGW (BY Cribs sediment). Note: The 35% minimum transformation threshold is shown by the solid red line and black diamonds represent the overall contaminant recovery across all extractions and remaining aqueous. ZVI treatment started at 0 days; Poly-PO_4 treatment started at 14 days. No-treatment controls for (a) and (d) are shown in Figure 4.29a.

In contrast to ZVI, the immobilization of Tc-99 by SMI in systems with increasing CoCOI concentrations showed expected behavior with slower Tc-99 immobilization and less extent with high nitrate (electron acceptor) present (Figure 4.35). In cases of excess electron donor/acceptor (11,000 in Figure 4.35a and 59 in Figure 4.35b), Tc-99 immobilization was complete (> 99%) and rapid (< 1 day). Tc-99 immobilization extent was 97% and was slower when the electron donor/acceptor ratio was 3.7 (Figure 4.35c). Finally, Tc-99 immobilization was only 85% by 50 days when the electron donor/acceptor ratio was 1.6, leaving 15% aqueous Tc-99 (Figure 4.35d).

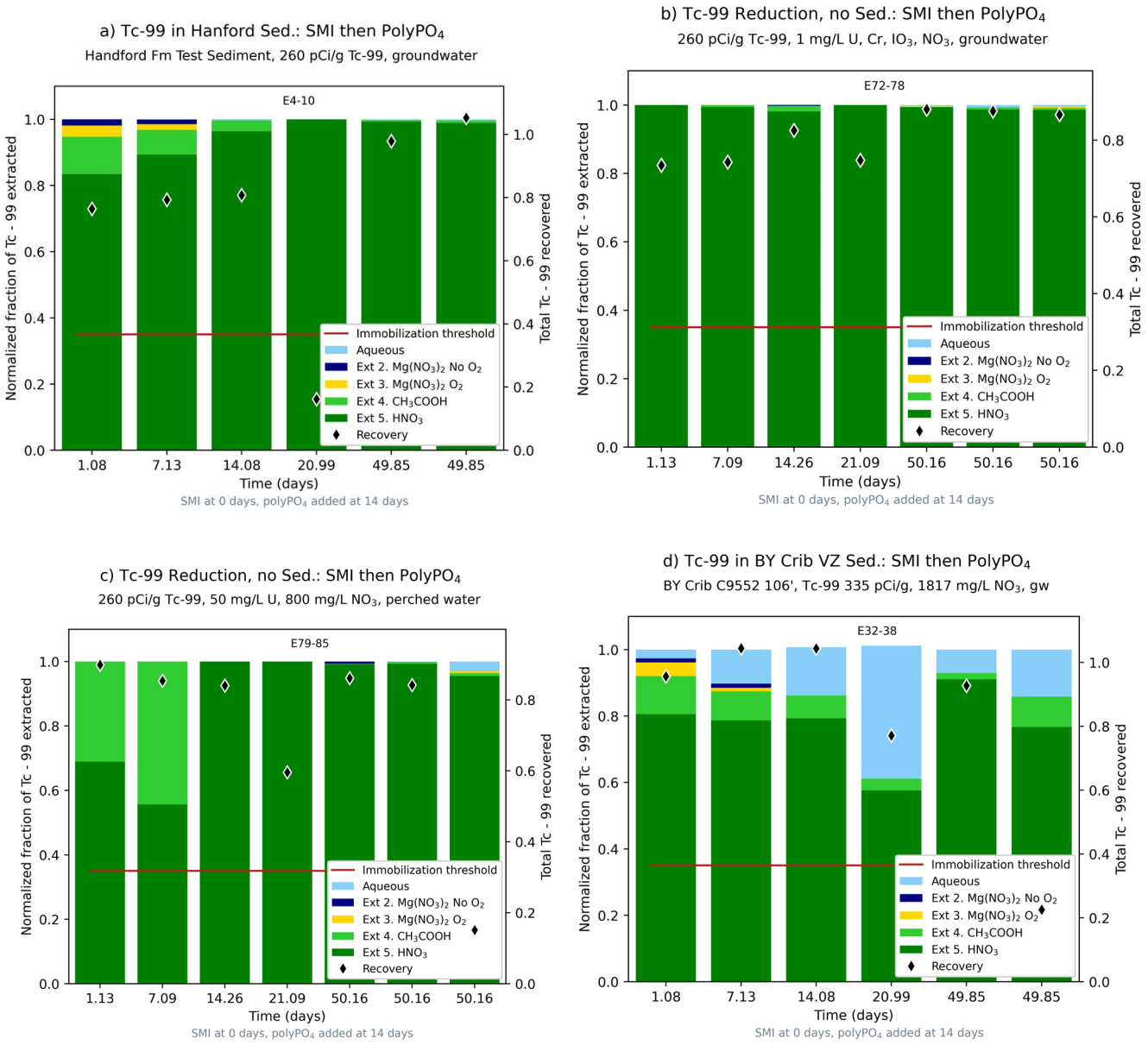

Figure 4.35. Change in Tc-99 mobility from SMI particulate phase treatment in systems with differing CoCOIs: (a) Tc-99 in SGW (Hf sediment); (b) Tc-99, U, Cr(VI), IO_3, and nitrate in SGW (no sediment); (c) Tc-99, U, and 800 mg/L NO_3^- in SPW (no sediment); and (d) Tc-99, U, and 1817 mg/L NO_3^- in SGW (BY Cribs sediment). Note: The 35% minimum transformation threshold is shown by the solid red line and black diamonds represent the overall contaminant recovery across all extractions. ZVI treatment started at 0 days; Poly-PO_4 treatment started at 14 days. No-treatment controls for (a) and (d) are shown in Figure 4.29a.

4.6.2.2 U sequestration by ZVI or SMI with sediments

For U immobilization by ZVI, there was also an inconsistent change in the extent as the ratio of electron donor/acceptor changed from 11,000 (> 99% U immobilized, Figure 4.36a) to 59 (94% U immobilized, Figure 4.36b) to 3.7 (99% U immobilized, Figure 4.36c), and finally to 1.6 (averaging 92% U immobilized, Figure 4.36d) with different concentrations of CoCOIs (Table G.2). In all cases, nitrate was present as the highest electron acceptor concentration, and because nitrate is more easily reduced compared to U(VI) [Eq. (2.5)], it exerts significant thermodynamic control on the change in the U immobilization extent and rate. Similar to Tc-99 results, the slowest U immobilization was in the system with a significant number of different CoCOIs (Figure 4.36b), rather than the system with the lowest electron donor/acceptor ratio (Figure 4.36d).

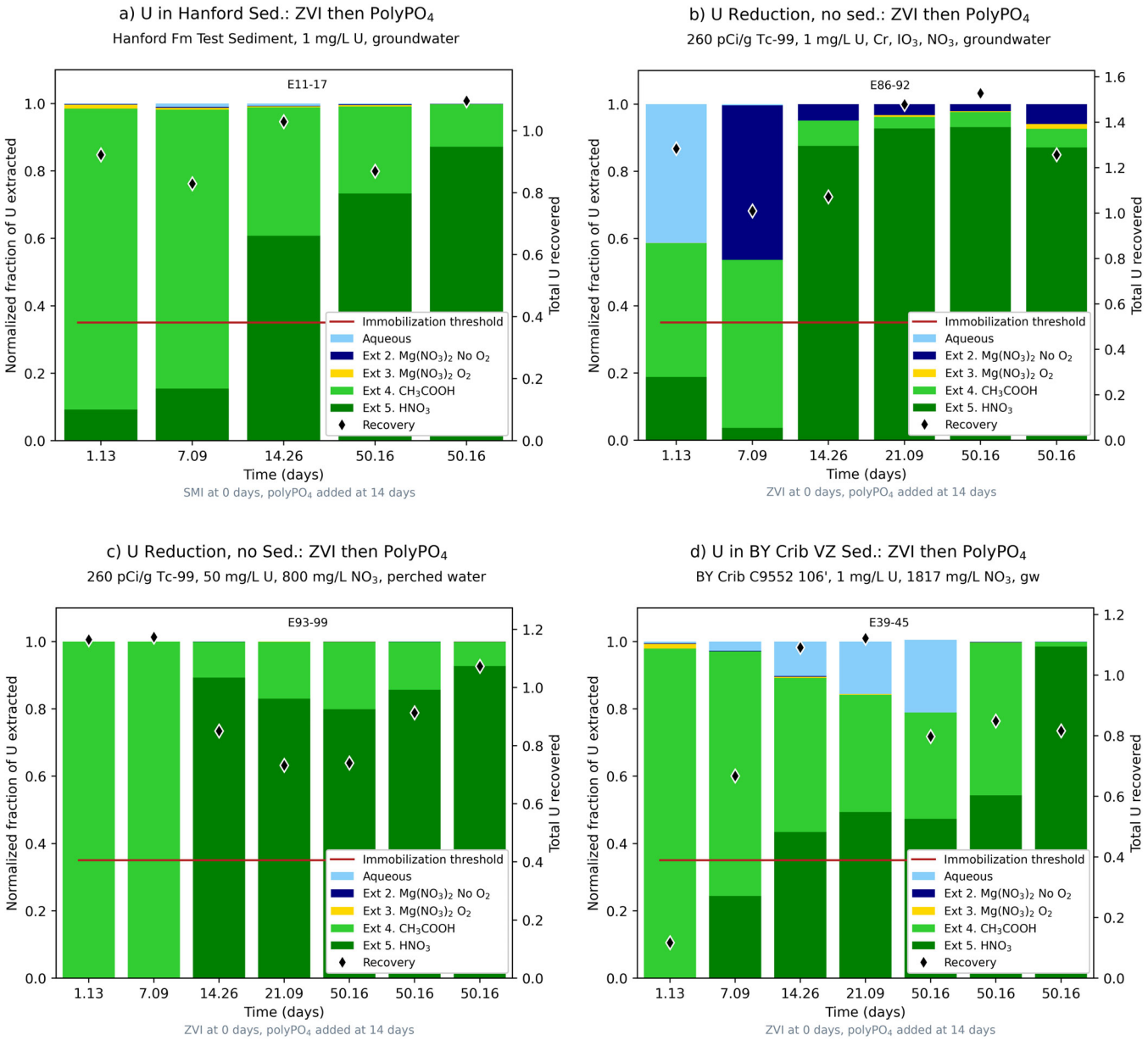

Figure 4.36. Change in U(VI) mobility from ZVI particulate phase treatment in sediment/water systems with differing CoCOI concentrations: (a) Tc-99 and U in groundwater (Hf sediment); (b) Tc-99, U, Cr(VI), IO_3, and nitrate in groundwater (no sediment); (c) Tc-99, U, and 800 mg/L NO_3^- in perched water (no sediment); and (d) Tc-99, U, and 1817 mg/L NO_3^- in groundwater (BY Cribs sediment). Note: The 35% minimum transformation threshold is shown by the solid red line and black diamonds represent the overall contaminant recovery across all extractions and remaining aqueous. ZVI treatment started at 0 days; Poly-PO_4 treatment started at 14 days. No-treatment controls for (a) and (d) are shown in Figure 4.29b.

In contrast to ZVI, SMI the extent of immobilization of U in systems with increasing CoCOI concentrations was slower and to a lesser extent with high nitrate present (Figure 4.37). In cases of excess electron donor/acceptor (11,000) in Figure 4.37a, U(VI) a ratio of 59 (Figure 4.37b) and 3.7 (Figure 4.37c), U immobilization was complete within 1 day (> 99%). However, when the electron

donor/acceptor ratio was 1.6, U immobilization extent was 71% at 21 days, then was more complete (99%) by 50 days (Figure 4.37d).

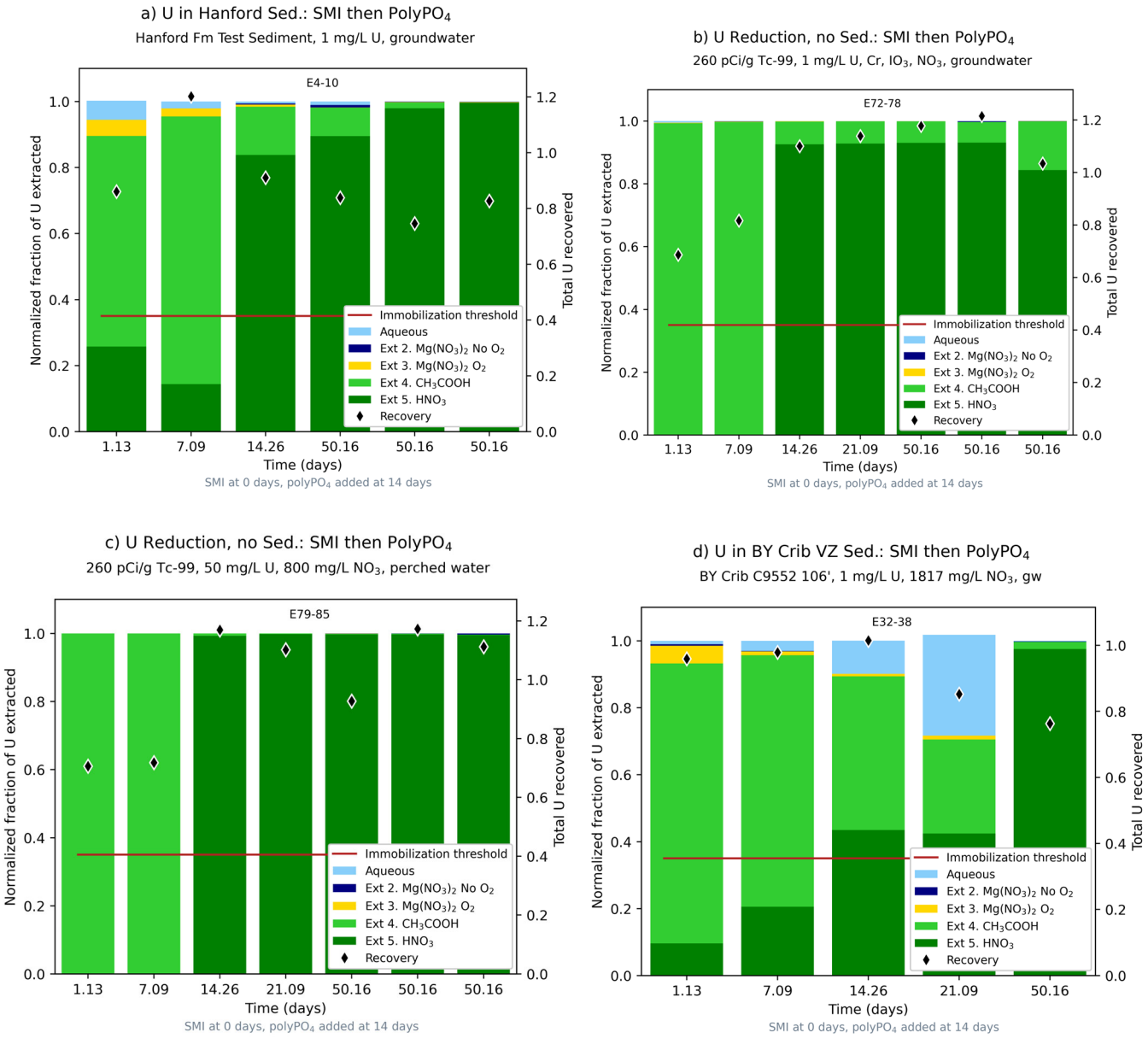

Figure 4.37. Change in U(VI) mobility from SMI particulate phase treatment in sediment/water systems with differing CoCOI concentrations: (a) Tc-99 and U in groundwater (Hf sediment); (b) Tc-99, U, Cr(VI), IO_3, and nitrate in groundwater (no sediment); (c) Tc-99, U, and 800 mg/L NO_3^- in perched water (no sediment); and (d) Tc-99, U, and 1817 mg/L NO_3^- in groundwater (BY Cribs sediment). Note: The 35% minimum transformation threshold is shown by the solid red line and black diamonds represent the overall contaminant recovery across all extractions and remaining aqueous. ZVI treatment started at 0 days; Poly-PO_4 treatment started at 14 days. No-treatment controls for (a) and (d) are shown in Figure 4.29b.

4.6.3 Objective 2b: Quantify the Tc-99 and U sequestration rate by treatment with ZVI or SMI and Poly-PO_4 with a delivery fluid

Delivery of dense (i.e., ~8 g/cm^3) ZVI or SMI particles requires a high-viscosity fluid such as xanthan, as a high-viscosity fluid will hold the dense ZVI/SMI particles in solution and enable injection to a greater horizontal extent with less vertical gravity slumping of the particles downward. Batch experiments were conducted in similar sediment/water systems without and with xanthan to evaluate the effect of xanthan on Tc-99 and U immobilization rate (described in Appendix G, Section G.4). Note that xanthan (and other high-viscosity fluids) is commonly used to inject ZVI. Portions of the xanthan polymer are redox reactive to hydrolyze and result in an Eh and pH shift (Kool et al. 2014).

Tc-99 immobilization by ZVI and Poly-PO_4 in groundwater without CoCOIs (i.e., electron donor/acceptor ratio = 11,000) showed no influence of the xanthan, with the same Tc-99 reduction extent (> 99%) without or with xanthan (Appendix G, Figure G.8a and b). In contrast, Tc-99 reduction by ZVI in perched water with 800 mg/L NO_3^- (i.e., electron donor/acceptor ratio = 3.7) showed that the addition of xanthan greatly decreased the ability of ZVI to reduce Tc-99, with 65% Tc-99 remaining aqueous (i.e., 35% Tc-99 immobilized) after 50 days in the presence of xanthan compared to 4% without xanthan (Figure G.8c and d). In contrast, the Tc-99 immobilization extent by SMI in groundwater without CoCOIs (i.e., electron donor/acceptor ratio = 11,000) also showed no influence of the xanthan, with the same Tc-99 reduction extent without and with xanthan (Figure G.9a and b). In addition, Tc-99 immobilization extent by SMI in perched water with 800 mg/L NO_3^- (i.e., electron donor/acceptor ratio = 3.7) also showed no effect of the presence of xanthan (Figure G.9c and d), but ZVI-induced immobilization of Tc-99 was significantly affected in perched water in the presence of xanthan (Figure G.8c and d). Because ZVI performance was significantly affected by the presence of xanthan, yet SMI reduction performance was not, it suggests that the Fe^0 itself (100% in ZVI, 60% in SMI) may be reacting with xanthan (consuming electrons).

Similar to Tc-99, U immobilization extent by ZVI in groundwater without CoCOIs (i.e., electron donor/acceptor ratio = 11,000) showed no influence of the xanthan (Figure G.10a and b), with 98% of the U immobilized by 50 days. In contrast, U immobilization by ZVI in perched water with 800 mg/L NO_3^- (i.e., electron donor/acceptor ratio = 3.7) showed that the addition of xanthan decreased U immobilization extent to 86%, leaving 14% U remaining aqueous after 14 days (and 10% by 50 days) in the presence of xanthan compared to < 1% without xanthan (Figure G.10c and d). The U immobilization extent by SMI in groundwater without CoCOIs (i.e., electron donor/acceptor ratio = 11,000) showed no influence of xanthan (Figure G.11a and b). U immobilization extent by SMI in perched water with 800 mg/L NO_3^- (i.e., electron donor/acceptor ratio = 3.7) also showed no influence from the presence of xanthan (Figure G.11c and d). Similar to observations for Tc-99, because ZVI reduction performance was significantly affected by the presence of xanthan, yet SMI reduction performance was not, it suggests that the Fe^0 itself (100% in ZVI, 60% in SMI) may be reacting with xanthan (consuming electrons).

4.7 Liquid-Phase Chemical Sequestration – Apatite-forming solutions

This technology was focused on the chemical sequestration of two PCOIs (U and Tc-99) following treatment with two different apatite-forming solutions, either Poly-PO_4 or Ca-Cit-PO_4. Table 4.16 presents the targeted testing conditions and amendments and shows which are moving forward to Phase 2 of testing. The removal of U and Tc-99 from the aqueous phase with time in batch experiments is described in Sections 4.7.1 and 4.7.3, respectively, while the extent of removal-based sequential extraction results is described in Sections 4.7.2 and 4.7.4, respectively. After 21 days of reaction of sediments and PCOIs (with and without CoCOIs) with apatite-forming solutions with monitoring of the

aqueous phase concentrations over time, sequential extractions were conducted to determine the relative likelihood of re-mobilization based on the recalcitrance of the solid phases. Results are also shown as µg/g in sediments for each extraction step in Appendix H, Section H.1, for comparison.

Overall, these results show that both technologies (Poly-PO_4 and Ca-Cit-PO_4) were effective for U and met the minimum transformation threshold of 35% for testing for both BY Cribs groundwater and perched water conditions as U is transformed to immobile end products based on the fraction of U in Extractions 4 and 5. Tc-99 removal met the minimum threshold when treated with Ca-Cit-PO_4 but was not effectively removed from the aqueous phase by the Poly-PO_4 treatment method. The Ca-Cit-PO_4 amendment will move forward with additional site-specific, laboratory-scale column testing. However, the Poly-PO_4 amendment will advance as the sequestration amendment for the following two-step technologies as they have an initial reduction step: (1) particulate-phase reduction and sequestration (described in Section 2.6), (2) liquid-phase reduction and sequestration (described in Section 2.8), and (3) liquid-phase bioreduction and sequestration (described in Section 2.9).

Any discussion of CoCOIs listed in Table 3.18 in the following sections is focused on their impact on the PCOIs and not their fate upon treatment with apatite-forming solutions. The fate of CoCOIs (including CrO_4^-, Sr^{2+}, and IO_3^-) is not discussed here, but is included in Appendix H, Section H.2. Additional discussion is also included in the appendix on the impact of carbonate on the Poly-PO_4 technology (Section H.6) and the impact of microbe source on the Ca-Cit-PO_4 technology (Section H.5).

Table 4.16. Summary of remediation technology testing conditions and amendments for gas-phase chemical sequestration technologies.

Primary Conditions and Amendments	
PCOI	U, Tc-99
Primary treatment zone/ applicable 200-DV-1 waste sites	**BY Cribs, perched water**
Secondary treatment zone/ applicable 200-DV-1 waste sites	U-1, U-2, S-SX Tank Farm, T-TX-TY Tank Farm, C Tank Farm, BC Cribs and Trenches
Potential co-contaminants	I-129, Sr-90, NO_3^-, Cr(VI)
Chemical sequestration treatments	**Ca-Cit-PO_4** and Poly-PO_4
Phase 1 decision point	Go

Note: The treatment and conditions moving forward to Phase 2 evaluation are **bolded**. If no amendment passed the minimum threshold, none are bolded and no additional testing will be conducted.
CN (BY Cribs): Potential co-contaminant but primarily present as ferrocyanide; additional testing ongoing.

4.7.1 Objective 1: Rate of sequestration of U with apatite-forming solutions

Liquid Poly-PO_4 was an effective treatment method for U, with > 99% removed from the aqueous phase under BY Cribs groundwater (Figure 4.38) and perched water conditions (Figure 4.39) within 21 days. These two figures show the removal of U from the aqueous phase over time for BY Cribs groundwater and perched water conditions, respectively.

For the BY Cribs groundwater condition, U was removed from the aqueous phase within hours with Poly-PO_4 treatment. It is notable that, based on aqueous phase analysis, treatment was not significantly impacted by the presence of CoCOIs under BY Cribs groundwater conditions evaluated in these batch experiments. The controls without CoCOIs are shown in Figure 4.38 while controls with CoCOIs are shown in Appendix H, Section H.1, for the final time point for comparison. The reaction of U with sediments without treatment (SGW and RW series) is relatively slow compared with the Poly-PO_4

treatment. Moreover, U was also removed from solution within hours with Poly-PO_4 treatment for the perched water condition (Table 3.5 or Table 3.6), even though the perched water condition had approximately 50 times more U present (Table 3.7).

Calcium (Ca) was added to the solution because the low solid-to-liquid ratio meant there was insufficient Ca in the sediment to precipitate apatite (estimates included in Appendix A, Section A.4). In the field, however, it is likely that Poly-PO_4 treatment will occur more slowly as Ca must be exchanged from sediments for apatite precipitation to occur and may depend on how the solutions are delivered to the subsurface (PNNL-29650; Wellman et al. 2011). These results are consistent with previous testing on other Hf sediments (PNNL-29650; Wellman et al. 2011). For example, in the 300 Area of the Hanford Site, Poly-PO_4 injections resulted in a decrease in U mobility of > 50% depending on the metric (PNNL-29650).

Ca-Cit-PO_4 was also an effective treatment method for U, with > 94% removed under BY Cribs groundwater (Figure 4.38) and perched water conditions (Figure 4.39) within 21 days. Similar to what was observed for Poly-PO_4, Ca-Cit-PO_4 treatment was not impacted by CoCOIs under BY Cribs groundwater conditions (Table 3.5). However, the speed of removal of U from the aqueous phase was much slower with the Ca-Cit-PO_4 treatment, occurring over weeks.

The rates of removal are different for perched water as compared to BY Cribs groundwater conditions (Table 3.6). Initial removal of U was faster in perched water conditions, while removal in BY Cribs groundwater conditions was slower. This could indicate that secondary precipitation reactions occurred in the perched water condition prior to citrate degradation and apatite precipitation. The higher ionic strength and U concentration may have led to precipitation, especially if the pH fluctuated below 6.5, where precipitation of rutherfordine (UO_2CO_3) may occur based on speciation modeling with Geochemist's Workbench (Appendix H, Section H.4). U removal occurred on the order of weeks (Figure 4.38 and Figure 4.39). Although removal was slow in comparison to the Poly-PO_4 method under these conditions, U was transformed to the extent necessary to exceed the minimum threshold (35%).

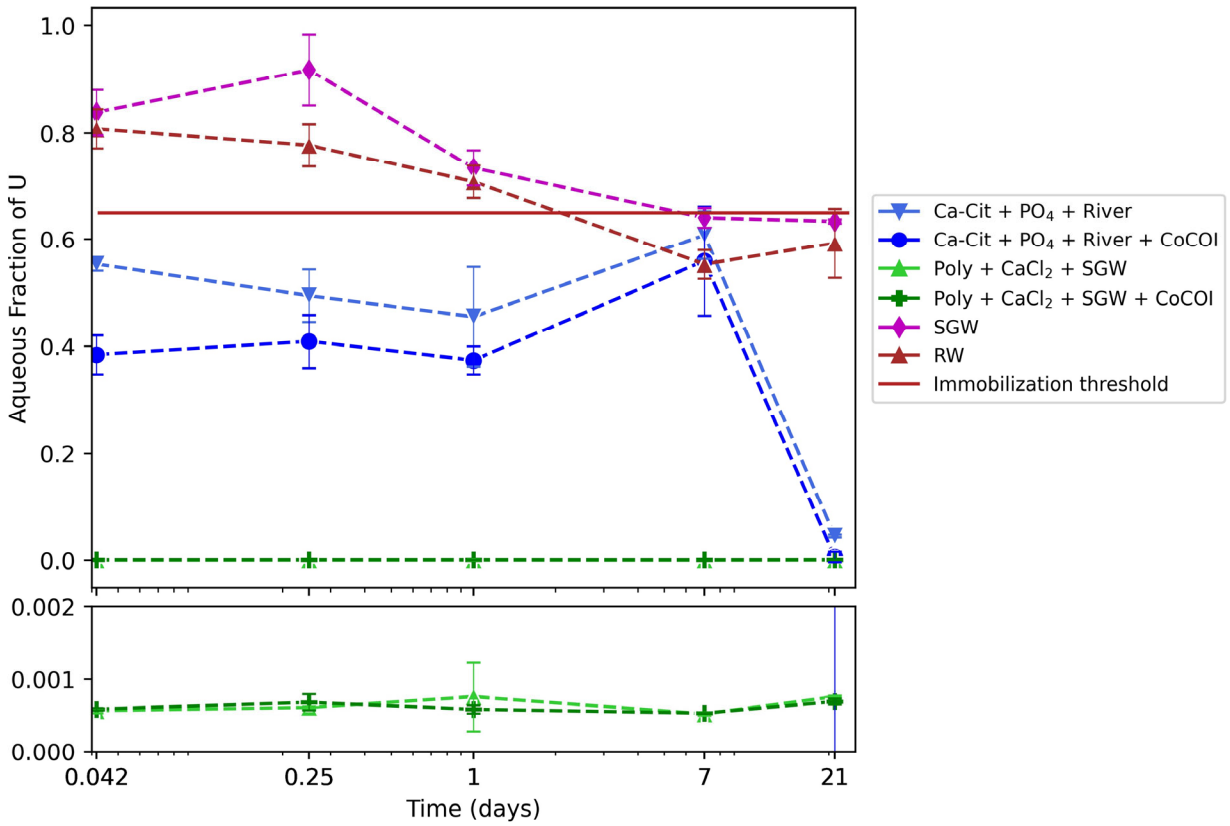

Figure 4.38. Results for U remaining in the aqueous phase in batch experiments with contaminant-spiked Hf sediments conducted over 21 days with following treatment with dashed lines for Ca-Cit-PO_4 (*blue*) or Poly-PO_4 (*green*) under BY Cribs groundwater conditions with RW or SGW as compared to controls without treatment (*red/pink*) with and without CoCOIs as specified by the symbols with the transformation threshold at 65% remaining in the aqueous phase (35% transformed, *solid red line*). Error bars are based on analysis of triplicate batch reactors. Lines are used to guide the eye and do not represent a model.

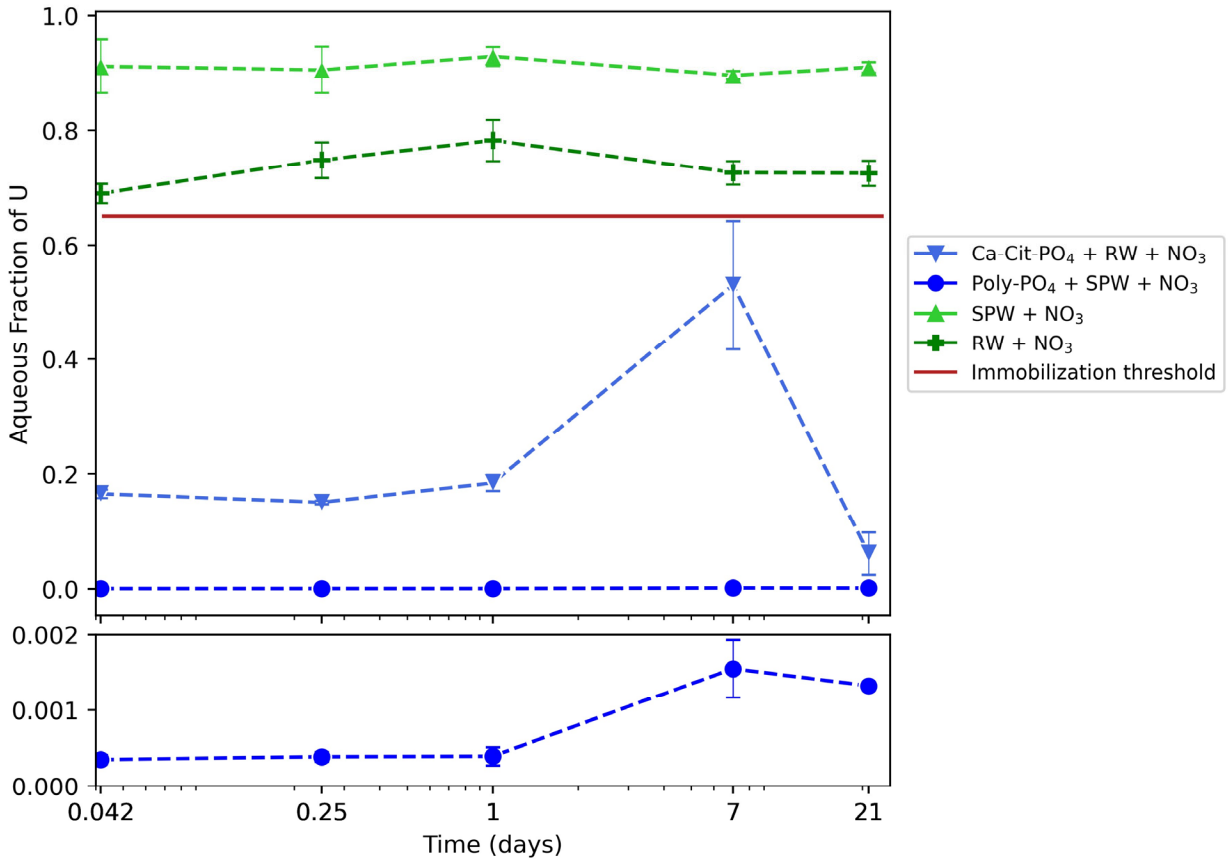

Figure 4.39. Results for U remaining in the aqueous phase in batch experiments with contaminant-spiked Hf sediments conducted over 21 days following treatment, with dashed lines for Ca-Cit-PO_4 (*blue triangles*) or Poly-PO_4 (*blue circles*) under perched water conditions with RW or SPW as compared to controls without treatment (*green*) with nitrate as a CoCOI in all conditions and the minimum transformation threshold at 65% remaining in the aqueous phase (35% transformed, *solid red line*). Error bars are based on analysis of triplicate batch reactors. Lines are used to guide the eye and do not represent a model.

Table 4.17. Qualitative removal half-life for U by apatite-forming solutions.

	BY Cribs Groundwater		Perched Water	
	Ca-Cit-PO_4	Poly-PO_4	Ca-Cit-PO_4	Poly-PO_4
PCOIs only	Weeks	Hours	NM	NM
With CoCOIs	Weeks	Hours	Days to weeks	Hours
NM = not measured				

4.7.2 Objective 2: Extent of sequestration of U with apatite-forming solutions

After 21 days of reaction of sediments and PCOIs (with and without CoCOIs) with apatite-forming solutions, sequential extractions demonstrated a significant increase in the fraction of U in the most immobile or recalcitrant extraction (5 – HNO_3) in addition to the increase in removal from the aqueous phase demonstrated by batch experiments. This result highlights that U is not only removed from solution but is also less likely to re-enter the aqueous phase following treatment with apatite-forming solutions.

Following treatment with Poly-PO_4, greater than 70% of U is relatively immobile and present in the last two extractions (4 – CH_3COOH, "Carbonates," and 5 – HNO_3, "Residual/Other") as shown in Figure 4.40. Moreover, this result is consistent across both the BY Cribs groundwater and perched water conditions, highlighting that the higher total U, presence of CoCOIs, and elevated ionic strength did not significantly impact removal under the conditions of these batch experiments.

For the Ca-Cit-PO_4 treatment, immobilization was even better, with greater than 90% of U being relatively immobile under BY Cribs groundwater conditions. Under perched water conditions, however, U immobilization was slightly decreased, though it was still > 70%, likely due to the impact of higher ionic strength on microbial growth and release of Ca via degradation of citrate leading to a decrease in apatite formation.

For both Poly-PO_4 and Ca-Cit-PO_4 treatment, U was likely associated with phosphorus precipitates either via adsorption, (co)precipitation, or coating processes. The distribution of phosphorus in sequential extractions following treatment was similar, with greater than 60% in the immobile fractions for both amendments under both conditions (Appendix H, Section H.3). Previous research has demonstrated the removal mechanisms of apatite-forming solutions including Poly-PO_4 and Ca-Cit-PO_4 (Dresel et al. 2011; Lammers et al. 2017; PNNL-29650; Wellman et al. 2008, 2011).

These results represent a significant increase in the immobile fraction of U with apatite-forming solutions as compared to controls without treatment (Figure 4.40). For controls under perched water conditions, U was highly mobile, with less than 20% of U present in the most recalcitrant fractions (Extractions 4 and 5). The increased mobility of U under these conditions without treatment was likely due to the higher ionic strength decreasing the potential for adsorption in the absence of apatite-forming solutions. For the controls for BY Cribs groundwater conditions, U was somewhat less mobile, with 35% to 40% of U present in the most recalcitrant fractions, when CoCOIs were not present. When CoCOIs were present, U was even less mobile in the BY Cribs groundwater conditions without treatment.

The lesser mobility of U when CoCOIs were present in the BY Cribs groundwater conditions without treatment may have been due to the CoCOIs themselves or the secondary ions that were added with them leading to precipitation, although U precipitates were not predicted in speciation modeling (Appendix H, Section H.4). However, the addition of the CoCOIs also impacted pH and may have changed the likelihood of adsorption and precipitation of U. U speciation is very complex, and there are a multitude of precipitates that could form with small changes in pH in the neutral range. In the BY Cribs groundwater conditions, the pH was approximately 0.5 pH units lower when CoCOIs were added (pH of 8.48 ± 0.07 versus 7.98 ± 0.16 without and with CoCOIs, respectively, over the course of the experiment). In this pH window, the dominance of negatively versus neutrally charged Ca-U-CO_3 species in the aqueous phase may be changing, with each having a different likelihood of adsorption and precipitation. However, it should be noted that these impacts were not observed in the presence of apatite-forming solutions under BY Cribs groundwater conditions.

Even with the decreased mobility of U when CoCOIs were present without treatment in the BY Cribs groundwater conditions, Ca-Cit-PO_4 still met the minimum threshold (35% greater than the untreated control). However, Poly-PO_4 did not meet the minimum threshold when CoCOIs were present in the BY Cribs groundwater conditions.

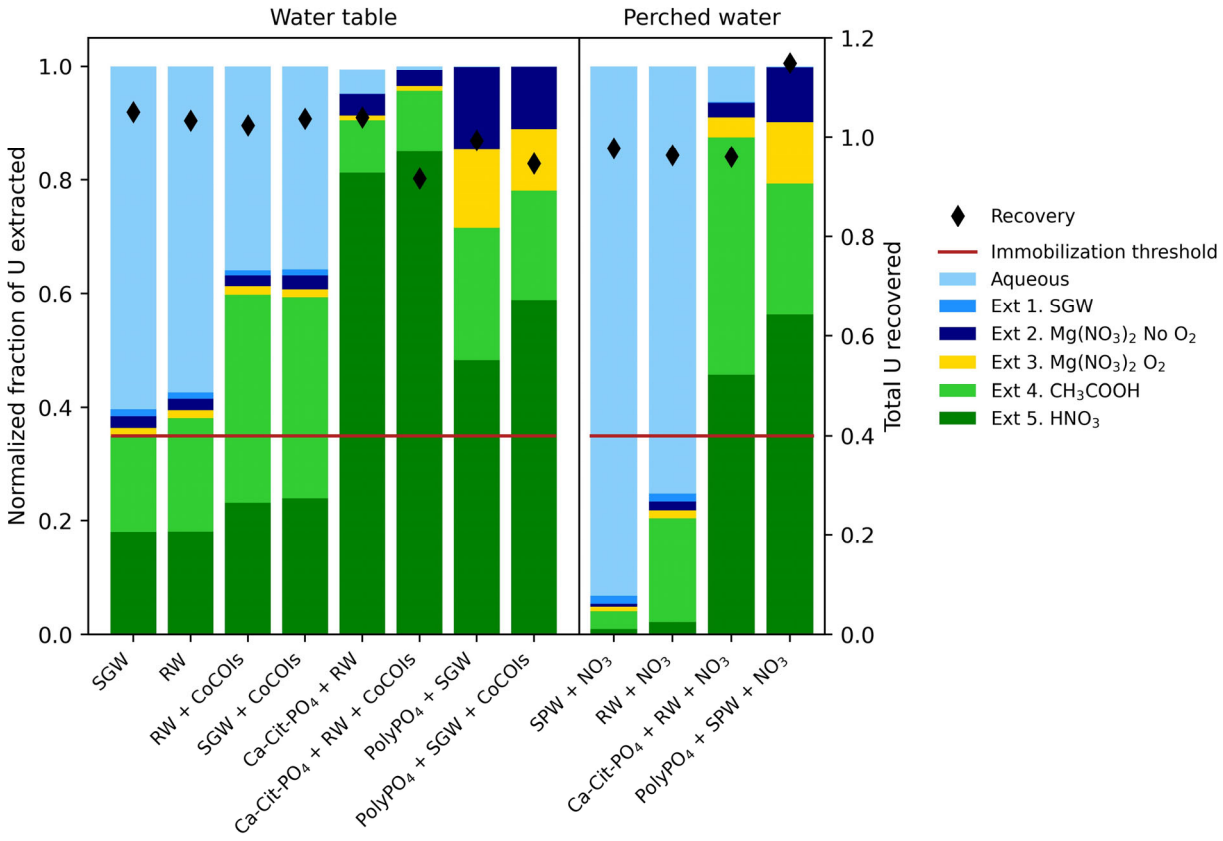

Figure 4.40. Change in U mobility from liquid-phase treatment following batch experiments with Hf sediments reacted with apatite-forming solutions for 21 days as compared to controls without treatment aligned to the left for each group with (*left*) BY Cribs groundwater conditions (SGW or RW with and without CoCOIs) and (*right*) perched water conditions (SPW or RW + nitrate). Note: The 35% minimum transformation threshold is shown by the solid red line and black diamonds represent the overall contaminant recovery across all extractions and remaining aqueous.

4.7.3 Objective 1: Rate of Tc-99 sequestration with apatite-forming solutions

Poly-PO_4 was not an effective treatment method for Tc-99 within 21 days under either of the conditions included in this study (Figure 4.41 and Figure 4.42). Significant removal of Tc-99 from the aqueous phase was not observed over 21 days. Moreover, results were not significantly different from controls without treatment containing only background solutions (i.e., SGW or SPW). This result is consistent with the conceptual model for reaction of Tc-99 with apatite (Figure 2.7), as significant sequestration was not expected without an initial reduction mechanism for Tc-99, and aligns with previous research (Gartman et al. 2019; PNNL-31959).

Ca-Cit-PO_4 was an effective treatment method for Tc-99, with > 90% removed under BY Cribs groundwater conditions (Figure 4.41) and > 55% removed under perched water conditions (Figure 4.42) within 21 days. Removal of Tc-99 from the aqueous phase with treatment by Ca-Cit-PO_4 solutions was relatively slow, occurring over weeks, with approximately 70% removed after 7 days of treatment with or without CoCOIs present. Similar to results for U, there was no significant difference between the presence or absence of CoCOIs in the BY Cribs groundwater conditions.

Further, Ca-Cit-PO_4 treatment was impacted by CoCOIs under perched water conditions but not under BY Cribs groundwater conditions. It is likely that Tc-99 removal was impacted by CoCOIs (nitrate) and elevated ionic strength conditions in perched water. The Ca-Cit-PO_4 requires the growth of natural microbes in sediments and solutions to degrade citrate and release Ca for precipitation with PO_4. However, in addition to degrading the citrate, the microbes also consume dissolved oxygen and generate reducing conditions as shown by Eh measurements over time in these batch experiments (Appendix H, Section H.4). Therefore, it is likely that Tc-99 removal was impacted in perched water conditions due to the presence of significantly greater concentrations of competing, reducible compounds in the system (e.g., nitrate).

Tc-99 removal occurred on the order of days to weeks with Ca-Cit-PO_4 (Table 4.18), with slightly faster and greater removal of Tc-99 in the BY Cribs groundwater conditions as compared to perched water. Although removal was relatively slow, Tc-99 was easily treated to the minimum transformation threshold (35%) for both the BY Cribs groundwater and perched water conditions by 21 days.

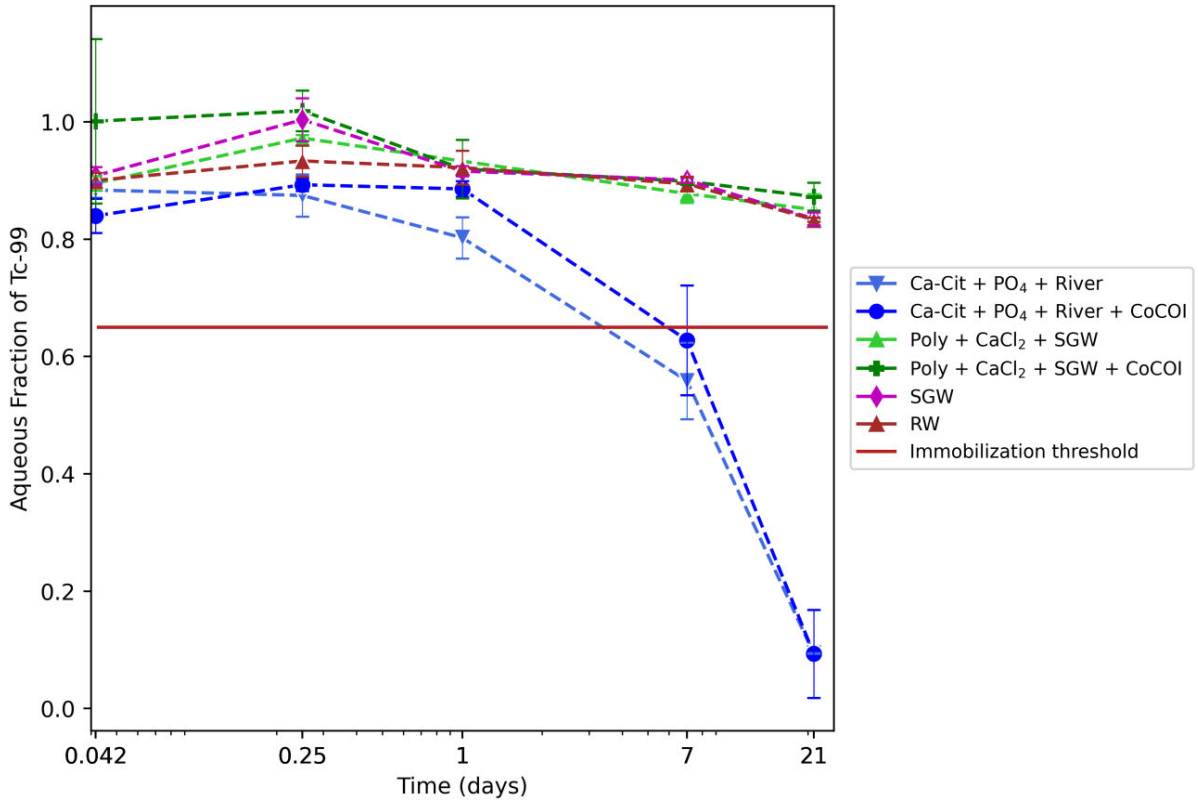

Figure 4.41. Results for Tc-99 remaining in the aqueous phase in batch experiments with contaminant-spiked Hf sediments conducted over 21 days following treatment with dashed lines for Ca-Cit-PO_4 (*blue*) or Poly-PO_4 (*green*) under BY Cribs groundwater condition as compared to controls without treatment (*pink/red*) with and without CoCOIs based on symbols. Note: The 35% minimum transformation threshold is shown by the solid red line. Error bars are based on analysis of triplicate batch reactors. Lines are used to guide the eye and do not represent a model.

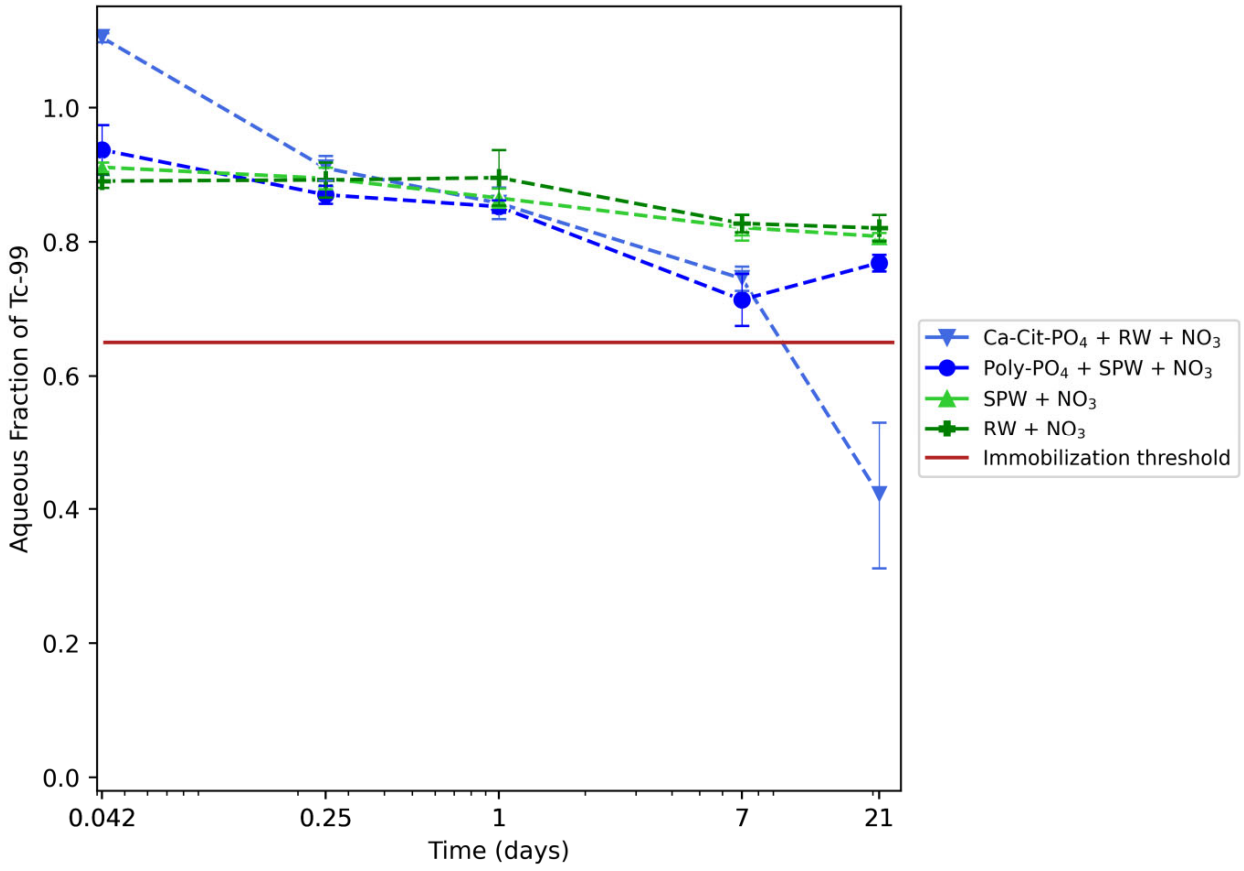

Figure 4.42. Results for Tc-99 remaining in the aqueous phase in batch experiments with contaminant-spiked Hf sediments conducted over 21 days following treatment with dashed lines for Ca-Cit-PO_4 (*blue triangles*) or Poly-PO_4 (*blue circles*) under perched water conditions as compared to controls without treatment (*green*) with nitrate in all systems as a CoCOI. Note: The 35% minimum transformation threshold is shown by the solid red line. Error bars are based on analysis of triplicate batch reactors. Lines are used to guide the eye and do not represent a model.

Table 4.18. Qualitative removal half-life for Tc-99 by apatite-forming solutions.

	BY Cribs Groundwater		Perched Water	
	Ca-Cit-PO_4	Poly-PO_4	Ca-Cit-PO_4	Poly-PO_4
PCOIs only	Weeks	None	NM	NM
With CoCOIs	Weeks	None	Days to Weeks	None
NM = Not measured				

4.7.4 Objective 2: Extent of sequestration of Tc-99 with apatite-forming solutions

After 21 days of reaction of sediments and CoCOIs with apatite-forming solutions, sequential extractions demonstrated a significant increase in the fraction of Tc-99 in the most immobile or recalcitrant extractions (4 – CH_3COOH and 5 – HNO_3) for the Ca-Cit-PO_4 treatment in addition to the increase in removal from the aqueous phase demonstrated by batch experiments. However, consistent with the Tc-99 aqueous phase measurements over time, no change in Tc-99 mobility was observed for the Poly-PO_4 treatment.

Following treatment with Poly-PO_4, there was no change in Tc-99 mobility as compared to the controls without treatment (Figure 4.43). More than 90% of the Tc-99 remained in the aqueous phase after treatment with Poly-PO_4, which was only slightly better than the untreated controls (SGW, RW, and SPW). Moreover, this result was consistent across both the BY Cribs groundwater and perched water conditions, demonstrating that the presence of CoCOIs and elevated ionic strength did not significantly impact removal.

For the Ca-Cit-PO_4 treatment, > 80% of Tc-99 was relatively immobile under BY Cribs groundwater conditions. Under perched water conditions, however, Tc-99 immobilization was slightly decreased, though still ~50%, likely due to the consumption of reducing capacity by elevated nitrate and the impact of higher ionic strength on microbial growth and release of Ca via degradation of citrate leading to a decrease in apatite formation. Tc-99 was likely reduced and then associated with phosphorus precipitates either via adsorption, (co)precipitation, or coating processes. However, Tc-99 immobilization mechanisms have not been previously investigated, though there is some evidence that Tc-99 cannot be immobilized by apatite without a reductant (PNNL-31959; PNNL-28054).

These results represent a significant increase in the immobile fraction of Tc-99 with Ca-Cit-PO_4 as compared to controls without treatment with apatite-forming solutions (Figure 4.43). The increased immobilization of Tc-99 for Ca-Cit-PO_4 as compared to Poly-PO_4 is likely due to the reducing conditions generated by stimulation of natural microbes in the sediments as they degrade the citrate and consume available oxygen. Appendix H, Section H.4, includes a comparison of Eh measurements of the aqueous solutions over time for the BY Cribs groundwater condition and shows that the Eh dropped significantly by 21 days with the Ca-Cit-PO_4 treatment. In the controls without treatment, under both BY Cribs groundwater and perched water conditions, Tc-99 remained highly mobile, and less than 10% of Tc-99 was present in the most recalcitrant fractions (Extractions 4 – CH_3COOH and 5 – HNO_3).

This result highlights that Tc-99 was not only removed from solution with the Ca-Cit-PO_4 treatment but was also less likely to re-enter the aqueous phase following treatment with apatite-forming solutions. Moreover, the minimum transformation threshold was easily exceeded for Tc-99 with Ca-Cit-PO_4 treatment when compared to the untreated controls.

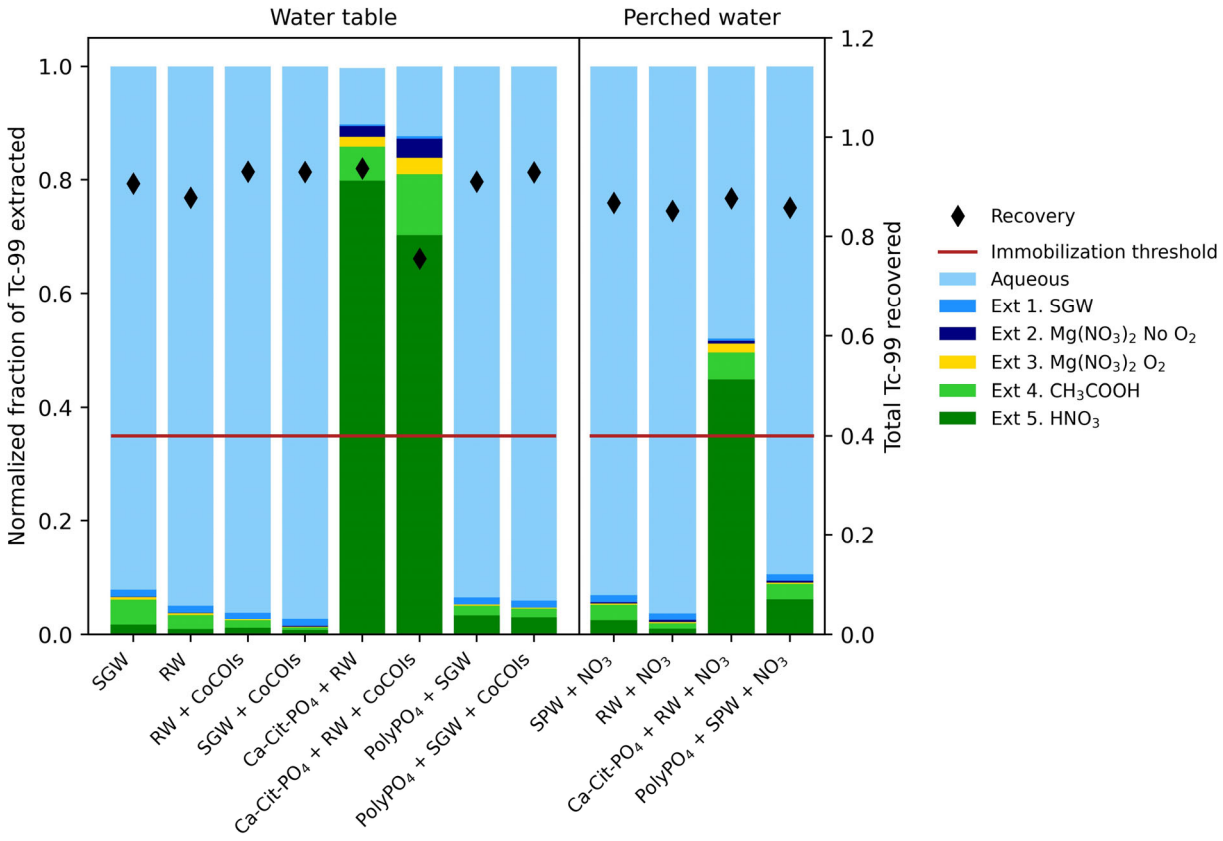

Figure 4.43. Change in Tc-99 mobility from liquid-phase treatment following batch experiments with Hf sediments reacted with apatite-forming solutions for 21 days as compared to controls without treatment aligned to the left for each group with (*left*) BY Cribs groundwater conditions and (*right*) perched water conditions. Note: The 35% minimum transformation threshold is shown by the solid red line and black diamonds represent the overall contaminant recovery across all extractions and remaining aqueous.

4.8 Liquid-Phase Combined Chemical Reduction and Sequestration – Polysulfide and apatite-forming solutions

This technology was focused on the chemical reduction and sequestration of two PCOIs (U and Tc-99) following treatment with two different solutions in series, CPS and then Poly-PO_4. The removal of U and Tc-99 from the aqueous phase with time in batch experiments is described in Sections 4.8.1 and 4.8.2, respectively, while the extent of removal-based sequential extraction results is described in Sections 4.8.3 and 4.8.4, respectively.

After 42 days of reaction of sediments and PCOIs (with and without CoCOIs) with liquid amendments (14 days with CPS followed by an additional 28 days after Poly-PO_4 was added), sequential extractions were conducted to determine the relative likelihood of re-mobilization based on the recalcitrance of the solid phases. Results are also shown as µg/g in sediments for each extraction step in Appendix I, Section I.1, for comparison. Additional supporting data for scoping experiments with variable CPS concentrations are included in Section I.2.1. Under the conditions in SGW and without CoCOIs, a minimum of 0.5% of CPS in solution was required for complete reduction and precipitation of both U and Tc-99. However, a greater concentration (2.5%) was added to be comparable with other chemical reduction amendments

evaluated with the particulate-phase technologies including Sn(II)-PO_4, ZVI, and SMI as described in Sections 2.4, 2.6, and 2.8.

Any discussion of CoCOIs in the following sections is focused on their impact on the PCOIs and not their fate upon treatment with CPS or Poly-PO_4 solutions. The fate of CoCOIs (including CrO_4^-, Sr^{2+}, and IO_3^-) is not discussed here but is included in an Appendix I, Section I.4. Additional discussion is also included in the appendix by treatment with only CPS (without the second step, Poly-PO_4, Sections I.2.1 and I.2.2), redox and pH fluctuations (Section I.5), and the impact of the presence of sediments on amendment efficacy (Sections I.3 and I.3.2).

Overall, these results show that this two-step technology (CPS + Poly-PO_4) was effective for U and Tc-99 and met the minimum transformation threshold of 35% for testing for both BY Cribs groundwater and perched water conditions. This technology will move forward with additional site-specific, laboratory-scale column testing.

Table 4.19. Summary of remediation technology testing conditions and amendments for gas-phase chemical sequestration technologies.

Primary Conditions and Amendments	
PCOI	U, Tc-99
Primary treatment zone/ applicable 200-DV-1 waste sites	**BY Cribs, perched water**
Secondary treatment zone/ applicable 200-DV-1 waste sites	U-1, U-2, S-SX Tank Farm, T-TX-TY Tank Farm, C Tank Farm, BC Cribs and Trenches
Potential co-contaminants	I-129, Sr-90, NO_3^-, Cr(VI)
Chemical reduction treatments	**CPS**
Chemical sequestration treatments	**Poly-PO_4**
Phase 1 decision point	Go

Note: The treatment and conditions moving forward to Phase 2 evaluation are **bolded**. If no amendment passed the minimum threshold, none are bolded and no additional testing will be conducted.
CN (BY Cribs): Potential co-contaminant but primarily present as ferrocyanide; additional testing ongoing.

4.8.1 Objective 1: Rate of sequestration of U with CPS and Poly-PO_4 treatment

Treatment with CPS with subsequent Poly-PO_4 treatment was effective for U, with > 99% removed from the aqueous phase under BY Cribs groundwater conditions and perched water conditions after 42 days. U was removed from solution within hours in the batch experiments, regardless of solution conditions (BY Cribs groundwater or perched water) (Table 3.5 or Table 3.6). However, field conditions including oxygen availability and CoCOIs will likely significantly impact the performance of the reductant, CPS. These experiments were conducted under anaerobic conditions to consider reduction of PCOIs without the potential for oxygen to deplete reduction capacity, although this will need to be factored into implementation for specific sites or areas of interest.

Nearly all U was removed from the aqueous phase within hours of treatment for the BY Cribs groundwater conditions. For comparison, 30-35% of U was removed from solution without treatment under the BY Cribs groundwater conditions with Hf sediments. Under the conditions of these batch experiments, CoCOIs did not significantly impact amendment performance for BY Cribs groundwater conditions (Figure 4.44).

Similar results were observed for the perched water conditions with treatment, with > 99% of U removed from solution within hours (Figure 4.44 and Figure 4.45). For comparison, controls without treatment and with Hf sediments for perched water conditions had approximately 93% of U remaining in solution. In addition, the perched water condition had approximately 50 times more U present (Table 3.7) and still resulted in a similar removal efficiency. Similar results were also observed with amendments added in the absence of sediments (Appendix I, Section I.3), even though the pH fluctuated significantly between the samples with and without sediments (Section I.5).

Previous research has evaluated CPS for reductive immobilization of U in seawater (Ma et al. 2015). Moreover, sulfides have been shown to effectively reduce many contaminants, including U, Tc-99, Cr(VI), and nitrate. In testing with only CPS treatment, > 99% of U was removed from solution under all conditions with Hf sediments present (Section I.2.2), without Hf sediment present (Section I.3), and in variable CPS loading as long as > 0.5% CPS was present (2.5% CPS was added in all testing with the exception of variable loading testing, Section I.2.1). However, testing of sequential treatment with CPS followed by Poly-PO_4 has only been conducted under limited conditions for U and Tc-99 previously (PNNL-31959). Previous tests showed that the addition of CPS increased removal of U from 74% to 96% when comparing treatment with Poly-PO_4 versus CPS + Poly-PO_4. These results are consistent with results presented here, though removal of U was relatively similar for both Poly-PO_4 and CPS + Poly-PO_4 as shown in Figure 4.44 and Figure 4.45 for CPS + Poly-PO_4 and for only Poly-PO_4 in Figure 4.38 and Figure 4.39.

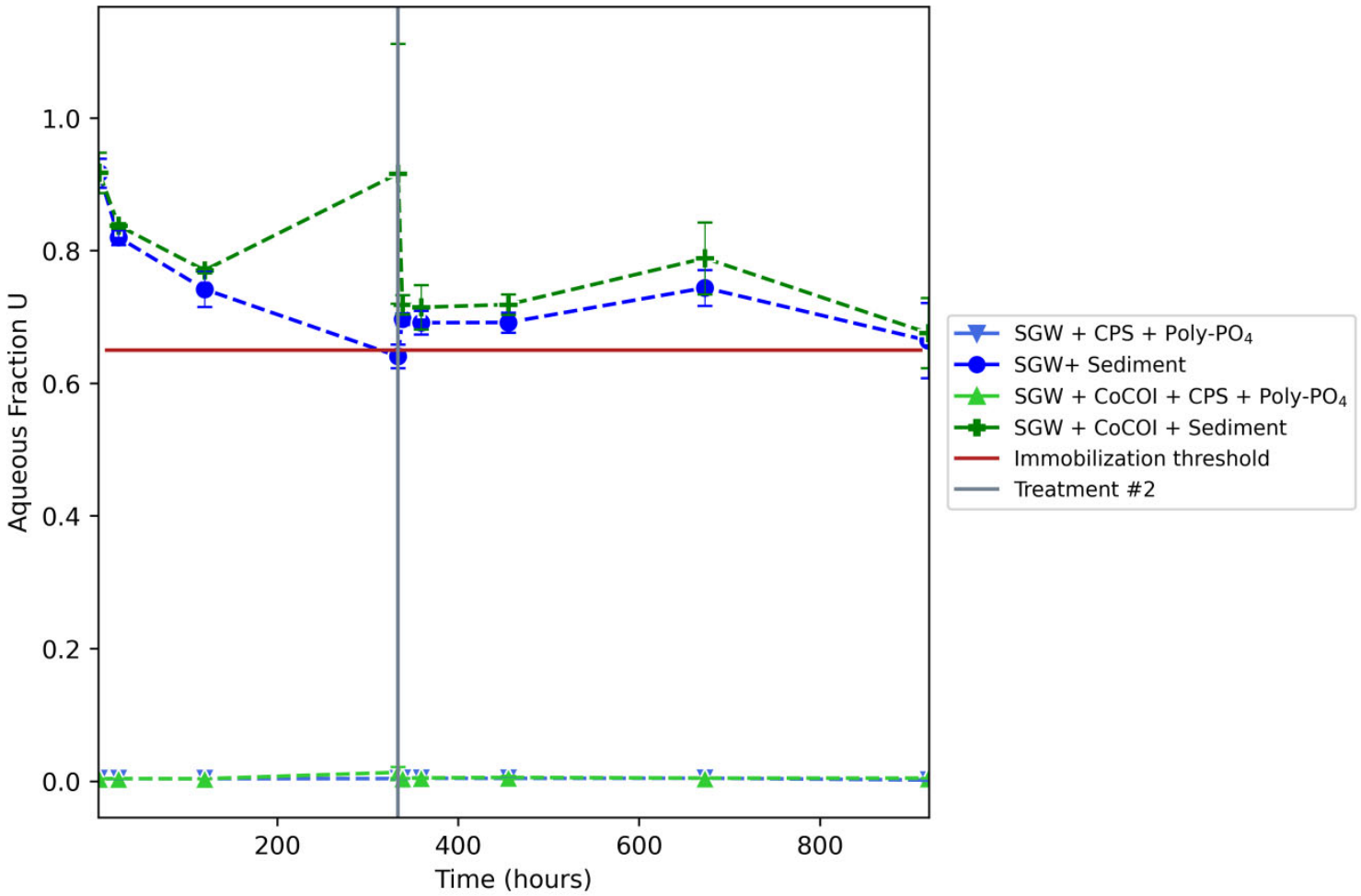

Figure 4.44. Results for U remaining in the aqueous phase in batch experiments with contaminant-spiked Hf sediment conducted over 42 days following treatment with dashed lines for CPS treatment at day 0 and Poly-PO_4 treatment at day 14 (*triangles*) under BY Cribs groundwater conditions with and without CoCOIs as compared to controls (*other*) without treatment. Note: The 35% minimum transformation threshold is shown by the solid red line. Error bars are based on analysis of triplicate batch reactors. Lines are used to guide the eye and do not represent a model.

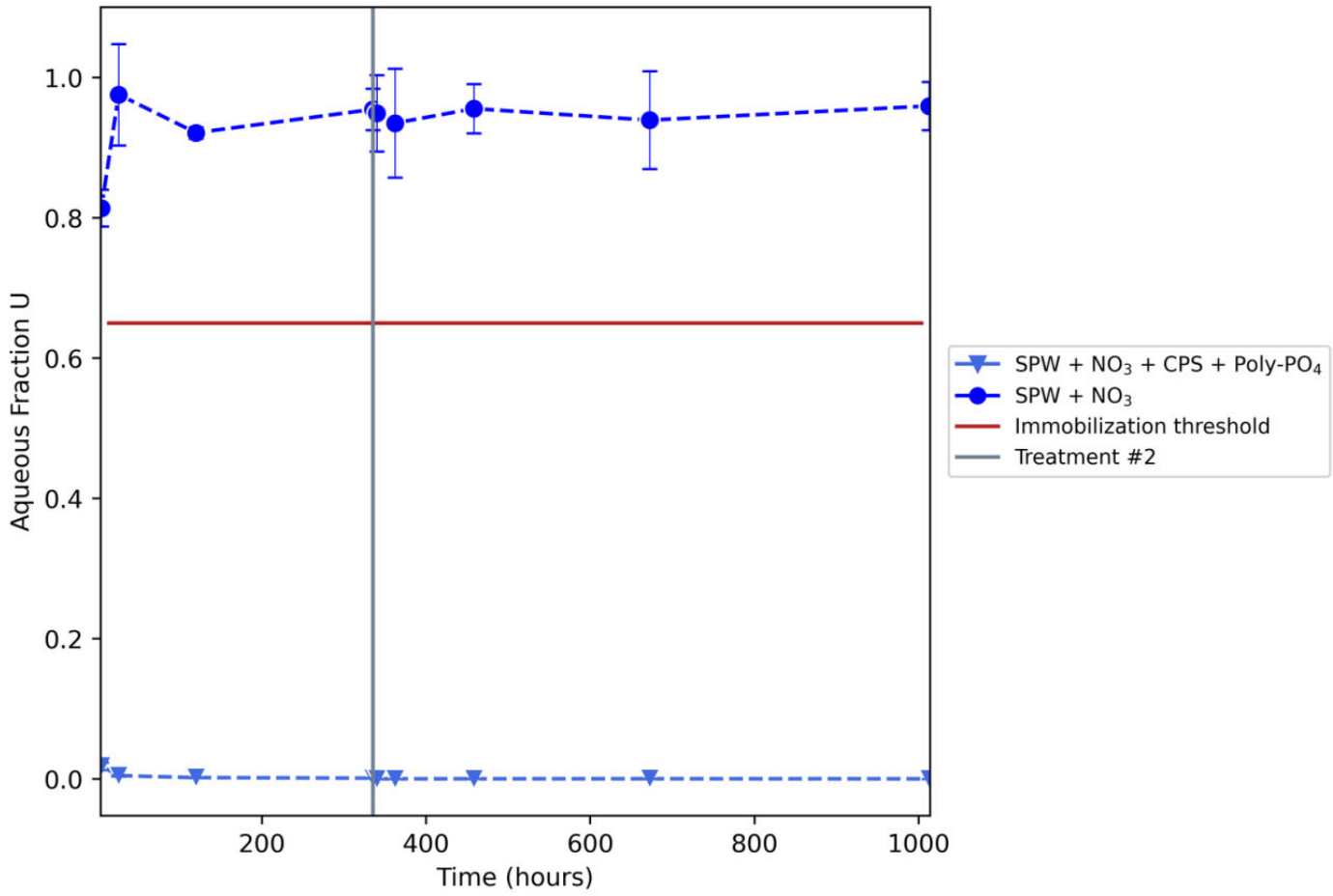

Figure 4.45. Results for U remaining in the aqueous phase in batch experiments with contaminant-spiked Hf sediment conducted over 42 days following treatment with dashed lines for CPS treatment at day 0 and Poly-PO_4 treatment at day 14 (*triangles*) under perched water conditions with nitrate in all samples as the CoCOI as compared to controls (*circles)* without treatment. Note: The 35% minimum transformation threshold is shown by the solid red line. Error bars are based on analysis of triplicate batch reactors. Lines are used to guide the eye and do not represent a model.

Table 4.20. Qualitative removal half-life for U by apatite-forming solutions.

	BY Cribs Groundwater	Perched Water
	CPS + Poly-PO_4	CPS + Poly-PO_4
PCOIs only	Hours	NM
With CoCOIs	Hours	Hours
NM = not measured		

4.8.2 Objective 2: Extent of sequestration of U with CPS and Poly-PO_4 treatment

After 42 days of reaction of sediments and PCOIs (with and without CoCOIs) with CPS and Poly-PO_4 (14-day reaction with CPS with subsequent Poly-PO_4 treatment and monitoring for another 28 days), sequential extractions demonstrated a significant increase in the fraction of U in the most immobile or recalcitrant extraction (5 – HNO_3) in addition to the increase in removal from the aqueous phase demonstrated by batch experiments. This result highlights that U was not only removed from solution but was also less likely to re-enter the aqueous phase following the two-step treatment with CPS and Poly-PO_4.

Following treatment with either CPS or CPS and Poly-PO_4, greater than 90% of U was relatively immobile and present in the last two extractions (4 – CH_3COOH, "Carbonates," and 5 – HNO_3, "Residual/Other") for the BY Cribs groundwater as shown in Figure 4.46 with no significant impact of CoCOIs on immobilization. With treatment with both CPS and Poly-PO_4, U mobility decreased more as shown by the change in the fraction present in Extractions 4 and 5 with both sets of treatments.

For the perched water condition, greater than 90% of U was relatively immobile (in the last two extractions) when treated with both CPS and Poly-PO_4, but only 70% was immobile with only CPS treatment. The trend of increasing immobilization of U with the subsequent Poly-PO_4 treatment is consistent with the results for the BY Cribs groundwater conditions. The decrease in immobilization with CPS treatment alone in the perched water condition is likely due to a decrease in reduction of U due to consumption of reduction capacity by excess nitrate. Extractions were conducted at three additional intermediate time points; however, the distribution of U did not change significantly over time as shown in Appendix I, Section I.1.3.

Treatment with both CPS and Poly-PO_4 resulted in stronger immobilization than CPS alone. This result was observed in both the BY Cribs groundwater and perched water conditions. The change in fractions with which the U was associated with and without Poly-PO_4 treatment showed that Poly-PO_4 transformed U into more recalcitrant phases. Following the two-step treatment, greater than 90% of U was present in the final extraction, representing the most refractory phases (i.e., nearly everything in Extraction 4 was moved to Extraction 5). The significant difference in the relatively immobile fractions for CPS versus CPS and Poly-PO_4 treatment in the perched water condition confirmed this conclusion.

Additional comparison with the Poly-PO_4 treatment alone (Figure 4.40) further highlights the value in the two-step treatment as the fraction in the relatively immobile extractions (4 – CH_3COOH, "Carbonates," and 5 – HNO_3, "Residual/Other") was greater when both treatments were added (70 to 80% with Poly-PO_4 versus > 90% with CPS and Poly-PO_4 for BY Cribs groundwater conditions).

These results demonstrate that treatment with CPS and Poly-PO_4 was more effective for U immobilization than treatment with CPS alone. Moreover, both CPS and CPS with subsequent Poly-PO_4 treatment easily met the minimum threshold for transformation of U to immobile phases. However, because these batch experiments were conducted under anaerobic conditions, conditions were optimized for continued reduction. In a field setting, it would be less likely for the U to remain reduced with CPS treatment alone.

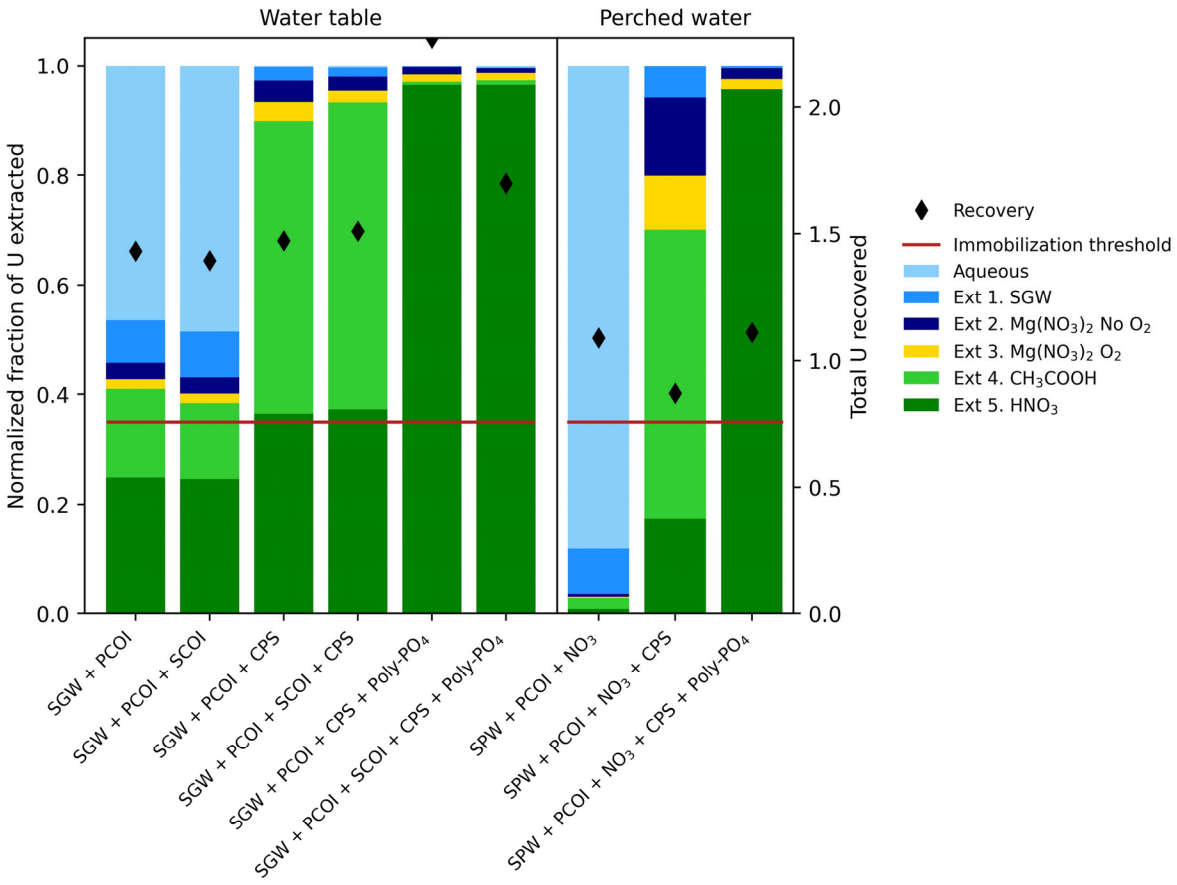

Figure 4.46. Change in U mobility from liquid-phase treatment following batch experiments with Hf sediments reacted with CPS at day 0 followed by Poly-PO_4 treatment at day 14 with a total reaction period of 42 days as compared to controls without treatment aligned to the left with each group with (*left*) BY Cribs groundwater conditions (SGW with and without CoCOIs) and (*right*) perched water conditions (SPW with and without nitrate as the only CoCOI). Note: The 35% minimum transformation threshold is shown by the solid red line and black diamonds represent the overall contaminant recovery across all extractions and remaining aqueous.

4.8.3 Objective 1: Rate of sequestration of Tc-99 with CPS and Poly-PO_4 treatment

The two-step treatment with CPS followed by Poly-PO_4 was effective for Tc-99, with > 99% removed from the aqueous phase after 42 days under the BY Cribs groundwater and perched water conditions (Figure 4.47 and Figure 4.48, respectively). Similar results were observed without sediments and with only CPS treatment as shown in Appendix I, Sections I.3.2 and I.2.2, respectively, even though the pH increased significantly in the presence of sediments, likely due to redox reactions with iron in sediments (Section I.5).

For the BY Cribs groundwater condition, Tc-99 was removed from the aqueous phase within hours. The treatment was not significantly impacted by CoCOIs for the BY Cribs groundwater condition, although the error on triplicate samples was greater in the absence of CoCOIs. These results are similar to the rates of removal from the aqueous phase observed for U with treatment by CPS followed by Poly-PO_4.

Treatment with CPS followed by Poly-PO_4 was still effective for the perched water condition (> 99% removed after 42 days), with removal from the aqueous phase occurring over days. Even though the rate was decreased as compared to the BY Cribs groundwater conditions, likely due to the high ionic strength of the SPW and the presence of elevated nitrate which consumes reduction capacity, the impact was minimal under these conditions.

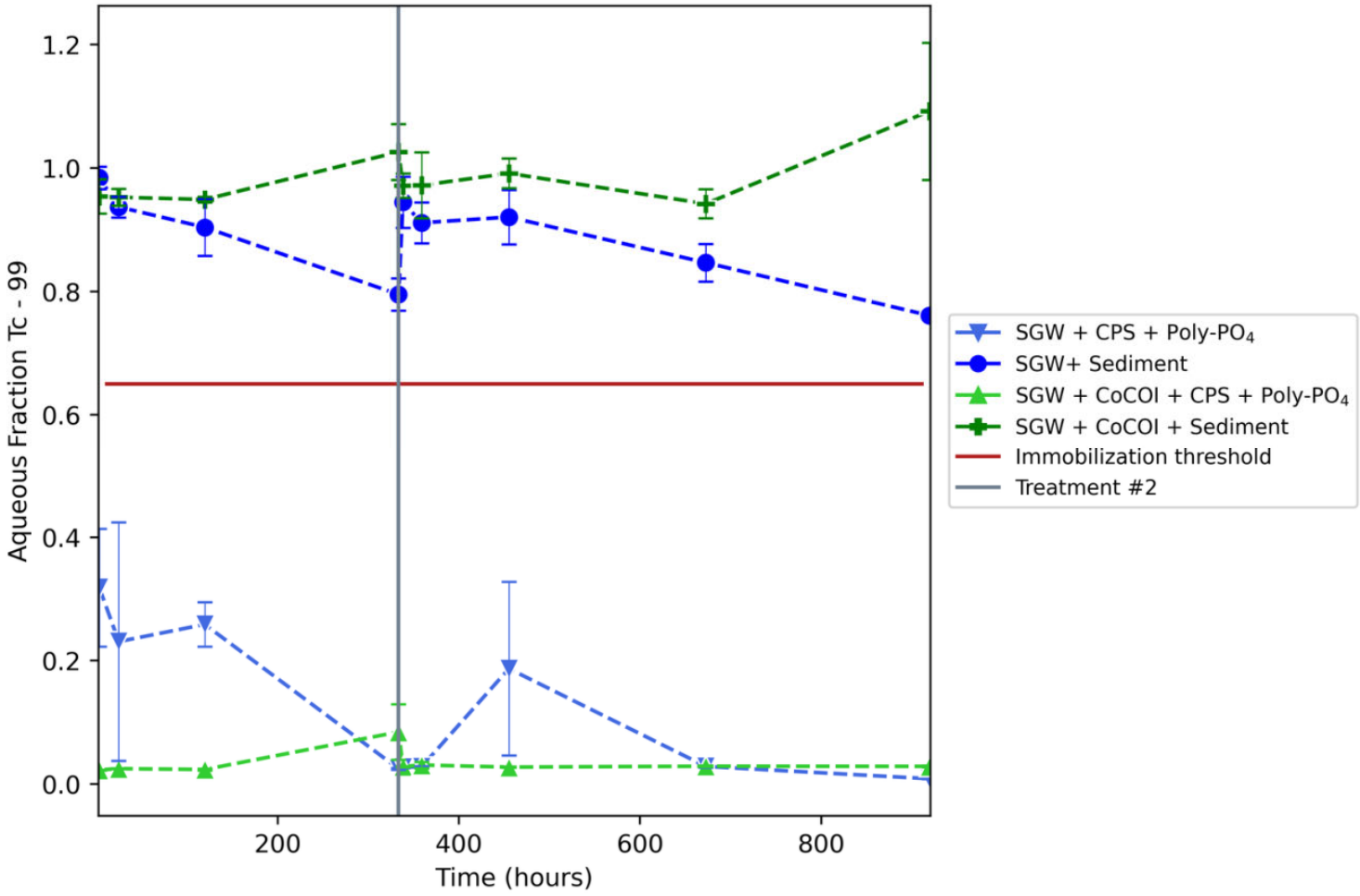

Figure 4.47. Results for Tc-99 remaining in the aqueous phase in batch experiments with contaminant-spiked Hf sediment conducted over 42 days following treatment with dashed lines for CPS treatment at day 0 and Poly-PO_4 treatment at day 14 (*triangles*) under BY Cribs groundwater conditions as compared to controls without treatment (*blue*) with (*triangles*) and without CoCOIs (*circles*). Note: The 35% minimum transformation threshold is shown by the solid red line. Error bars are based on analysis of triplicate batch reactors. Lines are used to guide the eye and do not represent a model.

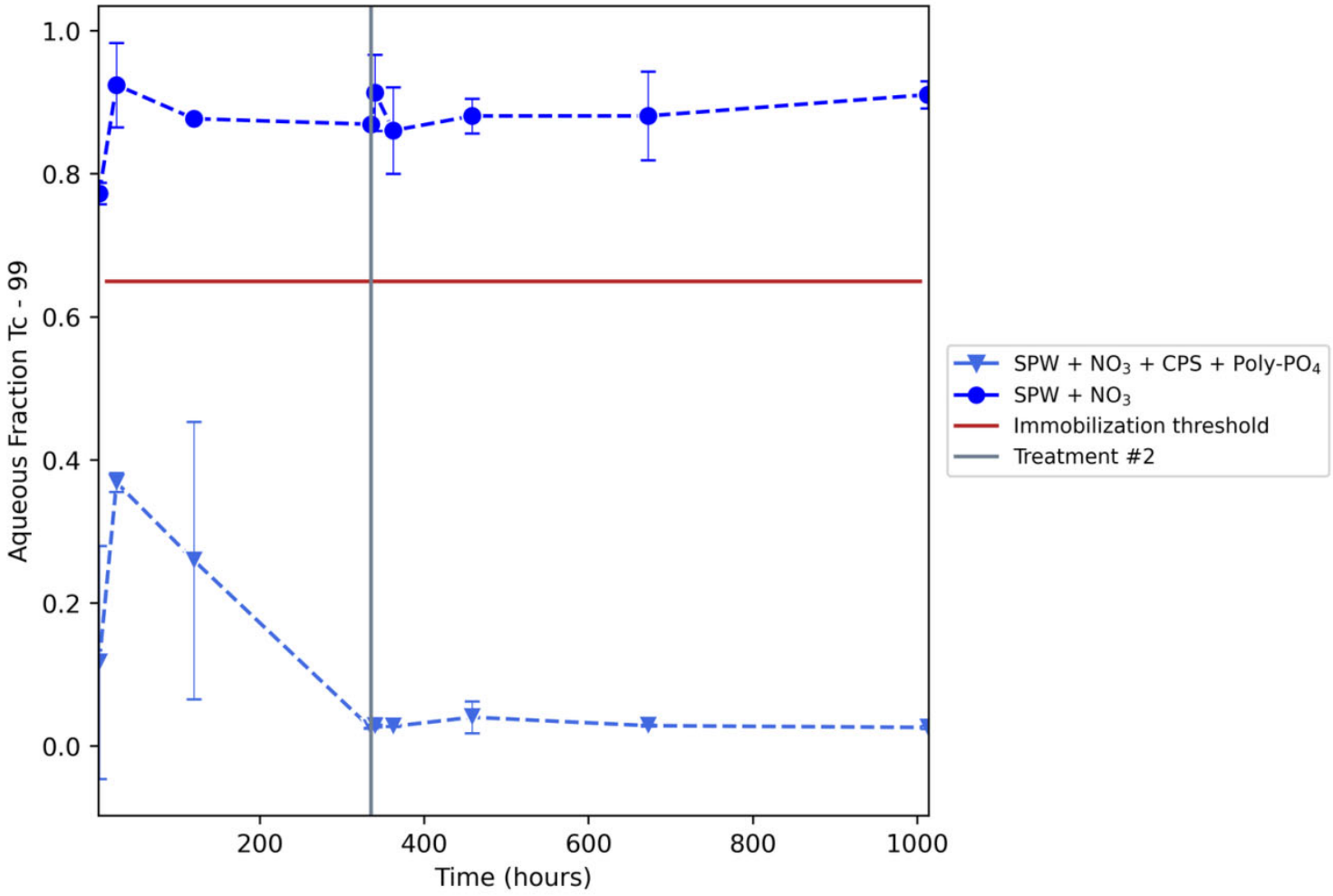

Figure 4.48. Results for Tc-99 remaining in the aqueous phase in batch experiments with contaminant-spiked Hf sediments conducted over 42 days following treatment with dashed lines for CPS treatment at day 0 and Poly-PO_4 treatment at day 14 (*triangles*) under perched water conditions with nitrate in all samples as a CoCOI as compared to controls without treatment (*circles*). Note: The 35% minimum transformation threshold is shown by the solid red line. Error bars are based on analysis of triplicate batch reactors. Lines are used to guide the eye and do not represent a model.

Table 4.21. Qualitative removal half-life for Tc-99 by apatite-forming solutions.

	BY Cribs	Perched Water
	CPS + Poly-PO_4	CPS + Poly-PO_4
PCOIs only	Hours	NM
With CoCOIs	Hours	Days
NM = not measured		

4.8.4 Objective 2: Extent of sequestration of Tc-99 with CPS and Poly-PO_4 treatment

After 42 days of reaction of sediments and PCOIs (with and without CoCOIs) with CPS and Poly-PO_4 (14-day reaction with CPS with subsequent Poly-PO_4 treatment and monitoring for another 28 days), sequential extractions demonstrated a significant increase in the fraction of Tc-99 in the most immobile or recalcitrant extraction (5 – HNO_3), in addition to the increase in removal from the aqueous phase demonstrated by batch experiments. This result highlights that Tc-99 is not only removed from solution but is also less likely to re-enter the aqueous phase following the two-step treatment with CPS and Poly-PO_4.

Following treatment with either CPS or CPS and Poly-PO_4, greater than 60% of Tc-99 was relatively immobile and present in the last two extractions (4 – CH_3COOH, "Carbonates" and 5 – HNO_3, "Residual/Other") for both the BY Cribs groundwater and perched water condition as shown in Figure 4.46. Overall, CPS with subsequent Poly-PO_4 treatment performed better for the BY Cribs groundwater condition, with > 70% of Tc-99 in the relatively immobile fractions. Moreover, some impact of CoCOIs on Tc-99 immobilization was observed under the BY Cribs groundwater conditions. Notably, the presence of CoCOIs slightly increased immobilization for both CPS only and CPS with subsequent Poly-PO_4 treatment. Extractions were conducted at three additional intermediate time points; however, the distribution of Tc-99 did not change significantly over time as shown in Appendix I, Section I.1.3.

For the perched water conditions, greater than 60% of Tc-99 was relatively immobile (in the last two extractions) when treated with both CPS and Poly-PO_4, with similar fractions observed with only CPS treatment. The elevated nitrate and ionic strength in the perched water condition had a much greater impact on Tc-99 than U treatment in terms of the extent of immobilization. This result could suggest that there were localized reduction zones with different species reacting in different zones depending on their mobility. However, it may also be that reduction of U was decreased but still immobilized by Poly-PO_4 since it immobilized U(VI) species but not Tc(VII) species as shown in Section 4.7.4. This may be supported by the rates of reaction observed between Tc-99 and U, as the rate of removal of Tc-99 from the aqueous phase was decreased significantly more than U (Figure 4.48 and Figure 4.45, respectively).

Both CPS and CPS with subsequent Poly-PO_4 treatment easily met the minimum threshold for transformation of U to immobile phases. Treatment with both CPS and Poly-PO_4 resulted in more immobile Tc-99 than treatment with CPS alone for the BY Cribs groundwater conditions. The results for the perched water condition showed similar amounts of relatively immobile Tc-99 with CPS treatment alone and with CPS followed by Poly-PO_4 treatment. Thus, the additional Poly-PO_4 treatment had less effect on Tc-99 immobilization than on U immobilization. However, these batch experiments were conducted under anaerobic conditions, and it is likely that these differences would be greater for Tc-99 if more oxygen was present. Therefore, oxygen content will need to be considered in future testing under site-specific conditions.

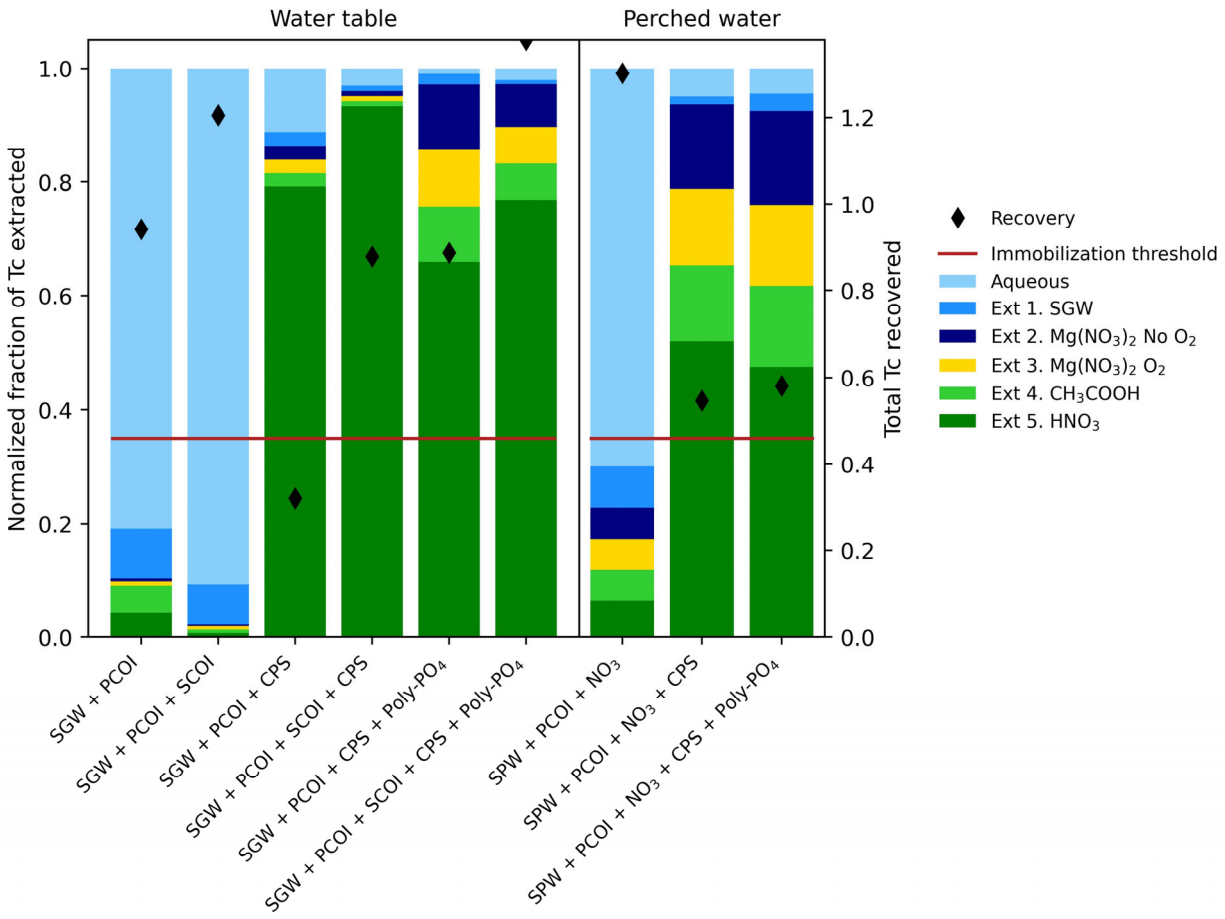

Figure 4.49. Change in Tc-99 mobility from liquid-phase treatment following batch experiments reacted with CPS at day 0 followed by Poly-PO_4 treatment at day 14 with a total reaction period of 42 days as compared to controls without treatment aligned to the left for each group with (*left*) BY Cribs groundwater conditions (SGW with and without CoCOIs) and (*right*) perched water conditions (SPW with and without nitrate as the only CoCOI). Note: The 35% minimum transformation threshold is shown by the solid red line and black diamonds represent the overall contaminant recovery across all extractions and remaining aqueous.

4.9 Liquid-Phase Combined Bioreduction and Chemical Sequestration – Organic liquids and Poly-PO_4

The results for the combined liquid-phase bioreduction and chemical sequestration are given in Section 4.9.1 (BY Cribs groundwater conditions without or without CoCOIs) and Section 4.9.2 (perched water conditions). Within each of these sections, removal of nitrate, U, and Tc-99 from the aqueous phase over time (up to final time points of 91 to 132 days) is described first, followed by the extent of removal as described by sequential extractions (for treatments without CoCOIs) at approximately 0 days (initial conditions), a mid-point of 45 to 47 days (during sustained anaerobic microbial activity), and a final time point of 91 to 113 days (following Poly-PO_4 treatment).

Appendix J summarizes results of scoping experiments using additional organic carbon sources, results for CoCOIs, ancillary aqueous geochemical results (e.g., pH), and additional results for controls without sediments. Any discussion of CoCOIs in the following sections is focused on their impact on the PCOIs

and not their fate upon treatment with organic liquids or Poly-PO_4 solutions. The fate of CoCOIs (including CrO_4^-, Sr^{2+}, and IO_3^-) is detailed in Appendix J.

In all scenarios evaluated, both molasses and EOS were effective in promoting bioreduction of nitrate, with nitrate and nitrite both being reduced to below detection (0.012 and 0.014 mg/L for NO_3^- and NO_2^-, respectively) by 7 days. Notably, bioreduction to below detection by 7 days occurred even in the perched zone treatments with an initial 800 mg/L initial nitrate, or ~10x the initial nitrate in the water table scenario (~80 mg/L). Results are shown for BY Cribs groundwater conditions in Figure 4.50 and Figure 4.55 without and with CoCOIs, respectively, and for the perched water conditions in Figure 4.58. The molasses treatment was particularly effective for Tc-99, with > 95% of aqueous Tc-99 removed from solution by 14, 46, and 91 days for the CCug without CoCOIs, CCug with CoCOIs, and PZsd scenarios, respectively (as shown for the BY Cribs groundwater conditions in Figure 4.51 and Figure 4.56 without and with CoCOIs, respectively, and for perched water conditions in Figure 4.59). Removal of Tc-99 was slower for the EOS treatment as compared to molasses in the BY Cribs groundwater conditions, with removal of > 95% observed at 46 as opposed to 14 days, respectively, without CoCOIs and a similar trend for CoCOIs (Figure 4.51). Sequential extractions were consistent with the trends observed in the aqueous phase (Figure 4.53). Similar trends were observed for the perched water conditions (as shown in Figure 4.59 and Figure 4.61). With respect to U, results with molasses and EOS were comparable in terms of aqueous phase concentrations and sequential extraction results for all conditions (for BY Cribs groundwater conditions without CoCOIs, Figure 4.52 and Figure 4.54; with CoCOIs in Figure 4.57; and for perched water conditions in Figure 4.60 and Figure 4.62).

Overall, these results showed that this two-step technology (organic liquids + Poly-PO_4) was effective for nitrate, U, and Tc-99 and met the minimum transformation threshold of 35% for testing for both BY Cribs groundwater and perched water conditions for both EOS and molasses. This technology will move forward with additional site-specific, laboratory-scale column testing for molasses, because sequestration was faster and more complete with molasses as compared to EOS.

Table 4.22. Summary of remediation technology testing conditions and amendments for gas-phase chemical sequestration technologies.

Primary Conditions and Amendments	
PCOI	U, Tc-99, NO_3^-
Primary treatment zone/ applicable 200-DV-1 waste sites	**BY Cribs, perched water**
Secondary treatment zone/ applicable 200-DV-1 waste sites	U-1, U-2, S-SX Tank Farm, T-TX-TY Tank Farm, C Tank Farm, BC Cribs and Trenches
Potential co-contaminants	Sr-90, I-129, Cr(VI)
Bioreduction treatments	**Molasses** and EOS
Chemical sequestration treatments	**Poly-PO_4**
Phase 1 decision point	Go

Note: The treatment and conditions moving forward to Phase 2 evaluation are **bolded**. If no amendment passed the minimum threshold, none are bolded and no additional testing will be conducted.
CN (BY Cribs): Potential co-contaminant but primarily present as ferrocyanide; additional testing ongoing.

4.9.1 BY Cribs groundwater Conditions

The two-step bioreduction and chemical sequestration technology was evaluated as a water table application under representative BY Cribs conditions and typical contaminant concentrations. Water table applications rely on a steady supply of organic carbon to sustain reduced conditions over a treatment area to achieve remedial objectives.

As a water table application, one set of batch experiments was conducted with PCOIs (nitrate, Tc-99, U) as described in Sections 4.9.1.1 and 4.9.1.2 for aqueous phase analysis and sequential extractions, respectively, and a parallel set was conducted with PCOIs and CoCOIs [IO_3^-, Sr^{+2}, and Cr(VI)] as described in Section 4.9.1.3. The bioreduction incubation phase was conducted for ~45 days, followed by Poly-PO_4 treatment, after which samples were incubated for an additional > 45 days to allow for apatite formation. Thermodynamically, reduction of inorganic contaminants at molar equivalence should proceed in the order of $NO_3^- > CrO_4^{2-} > IO_3^- > TcO_4^- > UO_2^{+2}$, though this ranking can be influenced by a variety of environmental conditions including, but not limited to, the relative concentrations of contaminants, the presence of other redox sensitive elements such as iron or manganese in the sediments or sulfate in the synthetic waters, and radioactivity (which initiate electron loss or gain changing equilibria) (Konhauser 2009; Plymale et al. 2011).

4.9.1.1 Objective 1: Rate of sequestration PCOIs in the absence of CoCOIs with organic liquids and Poly-PO_4

Figure 4.50 shows the results for bioreduction of nitrate for batch experiments with CCug sediments without CoCOIs for a potential water table application. The starting nitrate concentration in SGW was 47 mg/L. However, in the no-donor controls, there was indication that the CCug sediment was contributing more nitrate, given that the nitrate concentration in batch tests ranged from 74 to 79 mg/L between 7 to 45 days. Results from 1-hour water extractions performed on CCug sediments indicated that CCug had a background nitrate concentration of approximately 10 mg/L; however, results from the no-donor controls indicate that the sediments contributed up to 32 mg/L nitrate. In the EOS and molasses treatments, NO_3^- and NO_2^- were below detection by 7 days. In the no-donor treatment, minimal nitrate reduction was observed through 45 days, though there was ~20% reduction between approximately 45 and 90 days, after the addition of Poly-PO_4. Likewise, in no-sediment controls with 50 mg/L NO_3^- added initially, NO_3^- and NO_2^- both were below detection by an initial 12-day sampling point with EOS and molasses treatments, whereas NO_3^- remained at ≥ 95% of the initial value through 98 days in the no-donor treatment, and no NO_2^- was detected (Appendix J, Figure J.9).

Similarly, biological growth, as indicated by turbidity, was evident in the molasses no-sediment control by 12 days. (The EOS treatment was initially turbid, due to the EOS, so no comparison could be made.) Biological contamination of the no-sediment controls with EOS and molasses was likely from aerosolized microbial populations in the airspace of the anaerobic chamber. (In addition, neither the molasses nor EOS stocks were sterilized, due to the impracticality of sterilizing viscous, organic liquids via either heat or filtration.) After 46 days (i.e., the final sampling point before Poly-PO_4 amendment addition), aqueous chromium in the EOS and molasses treatments remained at 27% and 17%, respectively, indicating that native denitrifying populations may preferentially reduce nitrate over chromate, consistent with relative redox couple considerations (Grundl et al. 2011).

Figure 4.51 shows the results for bioreduction of TcO_4^- with CCug sediments without CoCOIs. In early time points (up to 14 days), molasses likely led to faster generation of reducing conditions and faster Tc-99 reductive precipitation. However, by 45 days, the initial 100 µg/L Tc-99 was reduced to below the detection limit (3.7 µg/L, dilution-corrected from analysis) in both molasses and EOS treatments and remained below detection through 113 days, including after addition of Poly-PO_4. Likewise, sulfate was

below detection in both the EOS and the molasses treatments at 45 days (Appendix J, Figure J.6), suggesting that the microcosms had proceeded past Mn(IV) and Fe(III) reduction to sulfate reducing conditions (Lee et al. 2014; Tang et al. 2013). For U, both amendments gave similar results, with 79±2% (EOS) and 86±1% (molasses) removed from the aqueous phase by 45 days (before Poly-PO_4 addition) and > 98% after Poly-PO_4 addition (Figure 4.52).

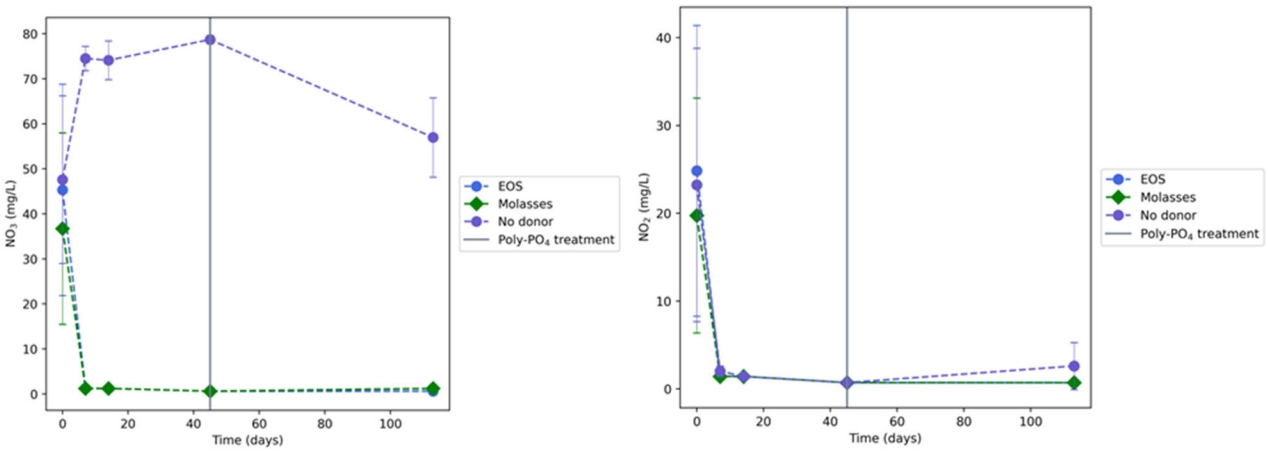

Figure 4.50. Aqueous nitrate and nitrite concentrations over time for contaminant-spiked CCug sediments and SGW for BY Cribs groundwater conditions in batch experiments with PCOIs and without CoCOIs by treatment. Organic liquids at approximately 0.39 g/L of TOC from EOS or molasses were provided to batch systems at time zero followed by Poly-PO_4 treatment at 45 days to all treatments (including the no-donor controls). . Note: Error bars are based on analysis of triplicate batch reactors. In the no-donor controls, NO_3^- values are higher than the 50 mg/L NO_3^- added initially, due to aqueous NO_3^- contributions from native NO_3^- in the CCug sediment.

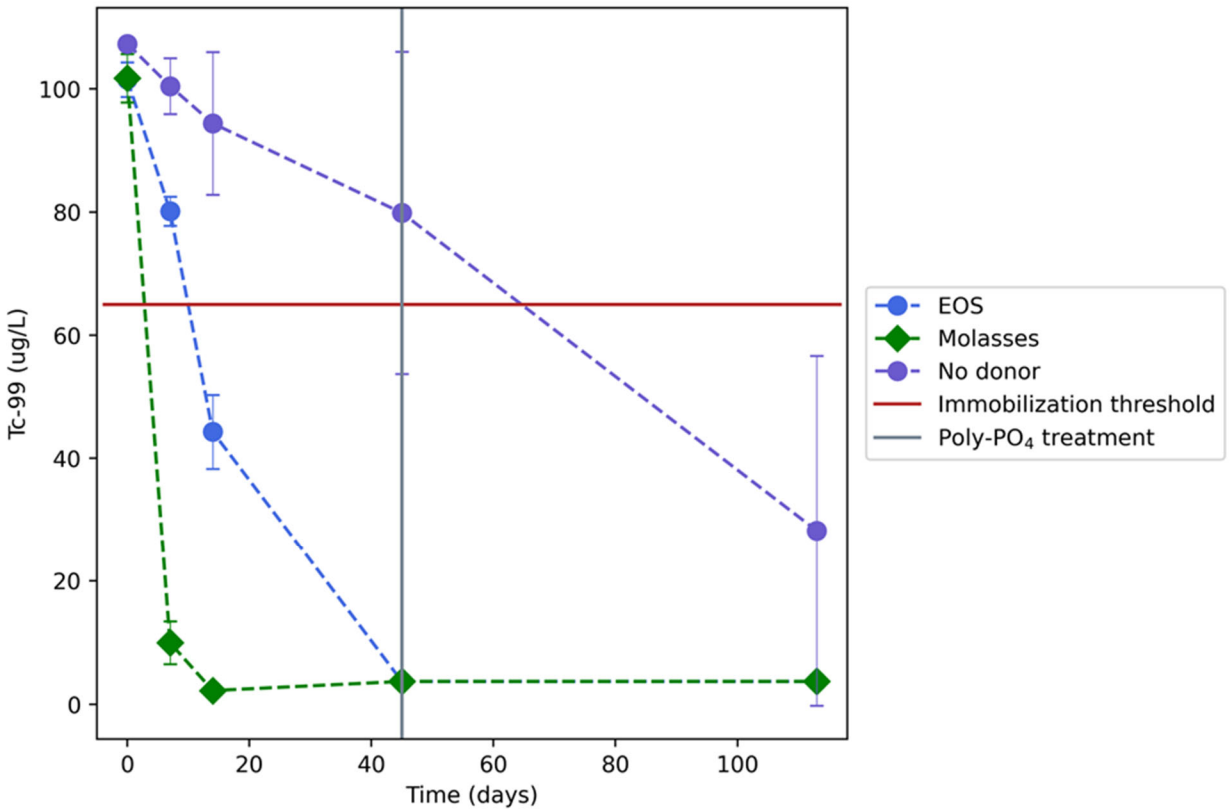

Figure 4.51. Aqueous Tc-99 concentrations over time for contaminant-spiked CCug sediments and SGW for BY Cribs groundwater conditions in batch experiments with PCOIs and without CoCOIs by treatment. Organic liquids at approximately 0.39 g/L of TOC from EOS or molasses were provided to batch systems at time zero followed by Poly-PO_4 treatment at 45 days compared to no-donor controls. Note: Error bars are based on analysis of triplicate batch reactors. Lines are used to guide the eye and do not represent a model.

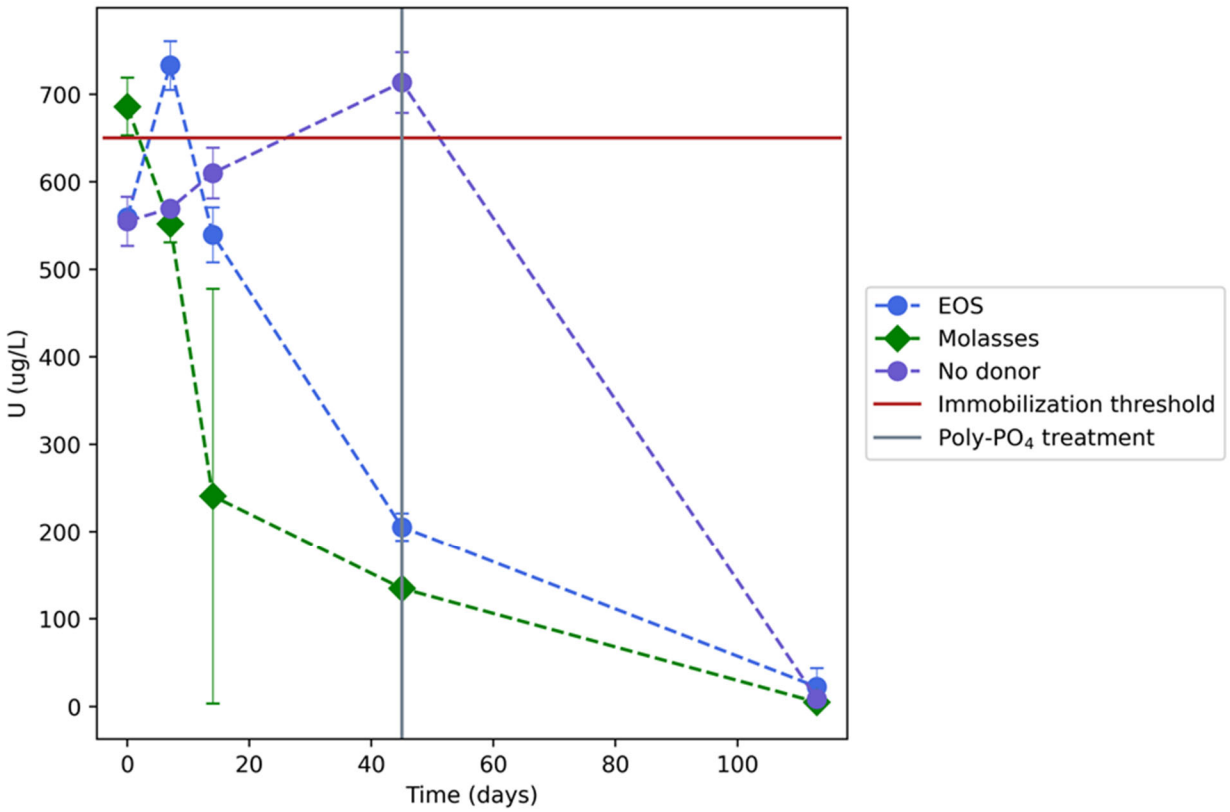

Figure 4.52. Aqueous U concentrations over time for contaminant-spiked CCug sediments and SGW for BY Cribs groundwater conditions in batch experiments with PCOIs and without CoCOIs by treatment. Organic liquids at approximately 0.39 g/L of TOC from EOS or molasses were provided to batch systems at time zero followed by Poly-PO_4 treatment at 45 days compared to no-donor controls. Note: Error bars are based on analysis of triplicate batch reactors. Lines are used to guide the eye and do not represent a model.

4.9.1.2 Objective 2: Extent of sequestration of PCOIs in the absence of CoCOIs with organic liquids and Poly-PO_4

Solid-phase sequestration results are presented for Tc-99 and U immobilization following two-step treatment with organic liquids and Poly-PO_4 as evaluated at the final time point (113 days) via sequential extractions. Tc-99, by 45 days, was ≥ 80% sequestered in both EOS and molasses treatments, compared with 21% in the no-donor control (Figure 4.53). The addition of Poly-PO_4 to all treatments at 45 days followed by incubation to 113 days only marginally increased Tc-99 sequestration in the EOS and molasses treatments but increased the sequestered Tc-99 to ~55% in the no-donor treatment. As indicated above, the EOS and molasses microcosms achieved sulfate reducing conditions by 45 days, such that the sequestered Tc-99 in the EOS and molasses treatments was likely Tc(IV)-Fe and Tc(IV)-S phases (Fredrickson et al. 2009; Lee et al. 2014). U, by 45 days, was ~74% and ~85% sequestered in immobile phases in the EOS and molasses treatments, respectively, in comparison with ~48% in the no-donor treatment (Figure 4.54). After the addition of Poly-PO_4 to all treatments and incubating to 113 days, U sequestration was > 90% in EOS and molasses treatments and 88% in the no-donor treatment.

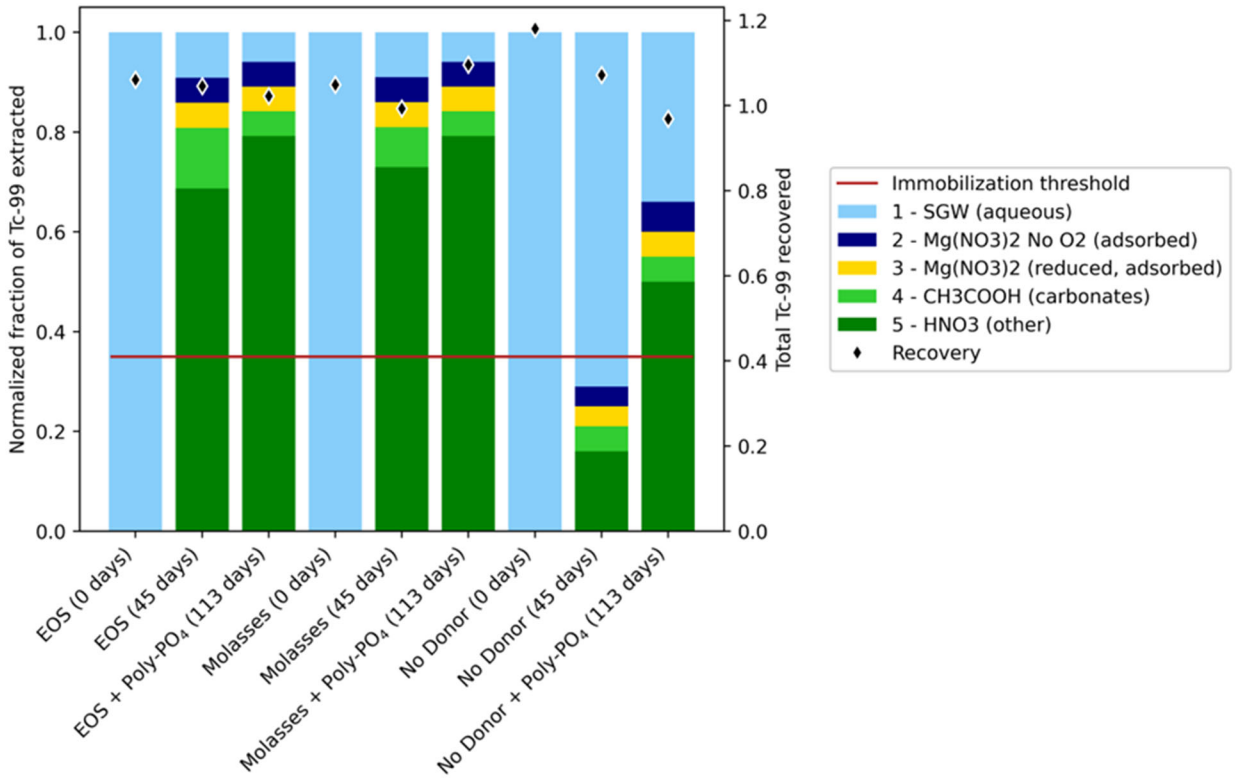

Figure 4.53. Change in Tc-99 mobility from liquid-phase treatment of contaminant-spiked CCug sediment in SGW without CoCOIs reacted with a liquid organic substrate (0.34 g/L of TOC, from EOS or molasses) at time zero followed by Poly-PO_4 at 45 days via sequential extractions at 0, 45, and 113 days compared to no-donor controls. Note: The 35% minimum transformation threshold is shown by the solid red line and black diamonds represent the overall contaminant recovery across all extractions and remaining aqueous.

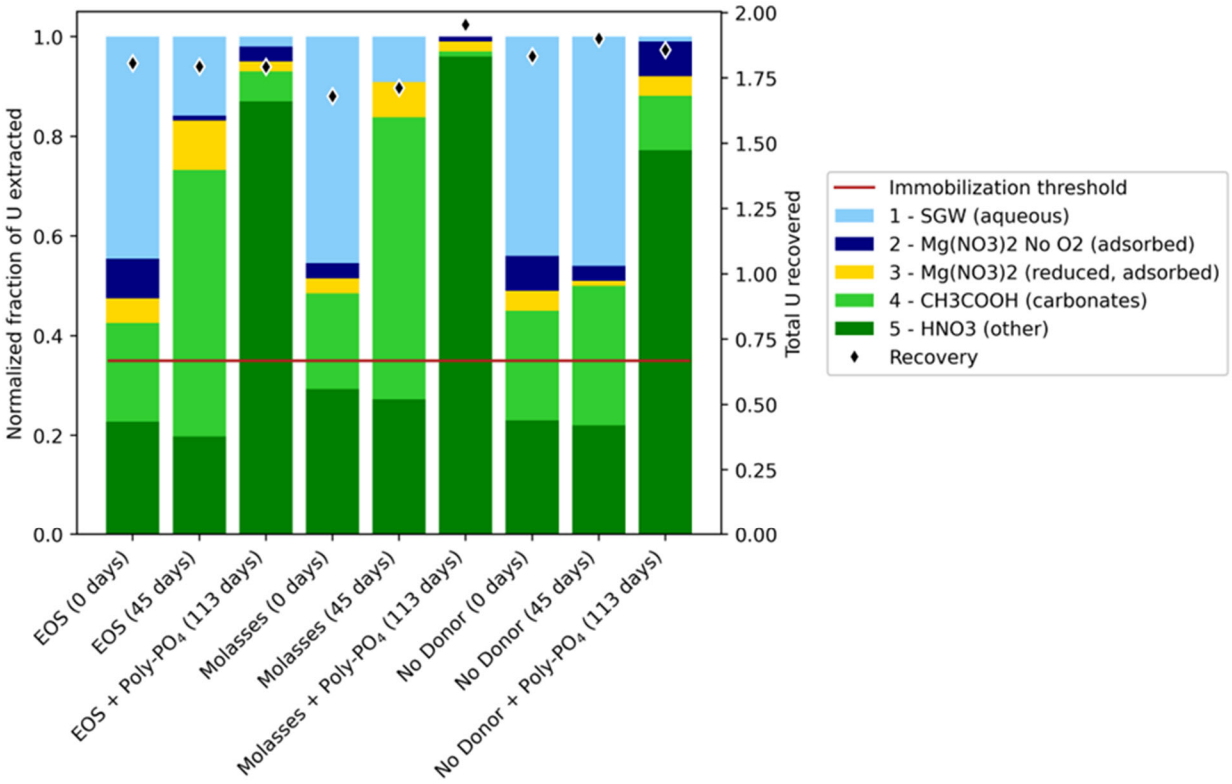

Figure 4.54. Change in U mobility from liquid-phase treatment of contaminant-spiked CCug sediment in SGW without CoCOIs reacted with a liquid organic substrate (0.34 g/L of TOC, from EOS or molasses) at time zero followed by Poly-PO_4 at 45 days via sequential extractions at 0, 45, and 113 days compared to no-donor controls. Note: The 35% minimum transformation threshold is shown by the solid red line and black diamonds represent the overall contaminant recovery across all extractions and remaining aqueous.

4.9.1.3 Objective 1: Rate of sequestration of PCOIs in the presence of CoCOIs with organic liquids and Poly-PO_4

Figure 4.55 shows the results for bioreduction of nitrate in batch experiments with CCug sediments with CoCOIs for a potential water table application. The starting nitrate concentration in SGW was 56 mg/L. However, there was indication that the CCug sediment contributed more nitrate given that the nitrate concentration in batch tests ranged from 76 to 89 mg/L for treatment by EOS and molasses at 1 day, and for no-donor controls at all time points (up to 32 mg/L, as stated in Section 4.9.1.1). In the EOS and molasses treatments, NO_3^- and NO_2^- were below detection by 7 days. In the no-donor treatment, minimal NO_3^- reduction was observed through 45 days, though there was a ~10% reduction between ~45 and ~90 days, after the addition of Poly-PO_4 at ~45 days. In no-sediment controls, NO_3^- remained at ≥ 85% of initial values in all treatments after 129 days, in contrast to the EOS and molasses no-sediment controls in the absence of CoCOIs, where NO_3^- and NO_2^- were below detection by 12 days (Appendix J, Figure J.9).

Figure 4.56 shows the results for bioreduction of Tc-99 with CCug sediments and CoCOIs. In contrast to microcosms without CoCOIs, where aqueous Tc-99 was below detection at 14 and 45 days for molasses and EOS treatments, respectively, in microcosms with CoCOIs, aqueous Tc-99 was not below detection until 46 (final time point before Poly-PO_4 addition) and 132 days (end point, after Poly-PO_4 addition) in molasses and EOS treatments, respectively, consistent with aqueous chromate, as a competitive electron acceptor, remaining in the system throughout the incubation (Appendix J, Figure J.4). Aqueous sulfate

concentrations, as an indication of relative sulfate bioreduction in the two organic carbon treatments, were 19.8 and 65.4 mg/L in molasses and EOS treatments, respectively, at 46 days, and below detection (molasses) and 53.7 mg/L (EOS) at 132 days (Appendix J, Figure J.7). U removal was significantly decreased in the presence of CoCOIs as compared to without (Figure 4.52 without CoCOIs versus Figure 4.57 with CoCOIs), presumably due to chromate acting as a competitive electron acceptor or microbial inhibitor, or both. However, similar removal was observed after Poly-PO_4 addition with or without CoCOIs present.

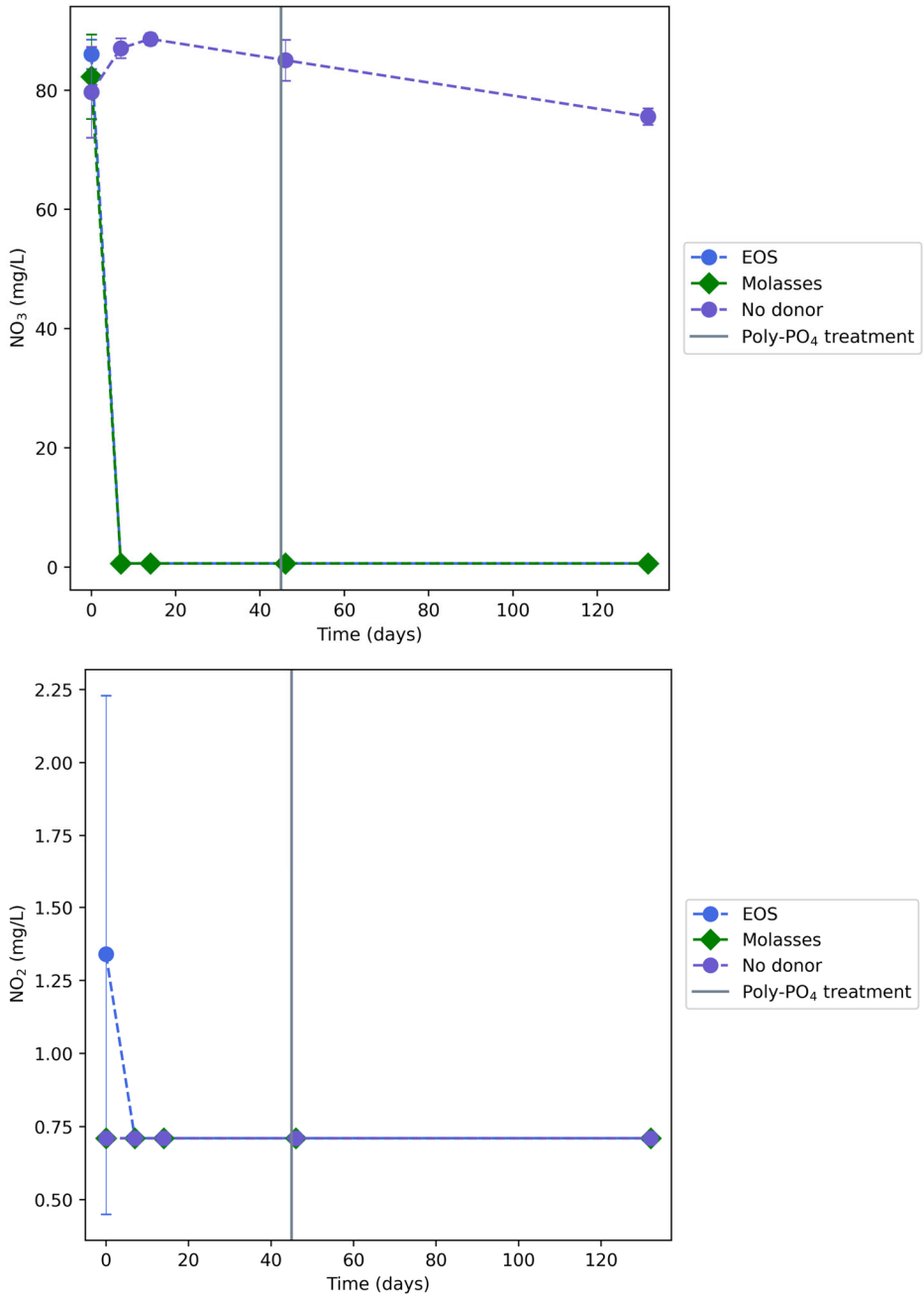

Figure 4.55. Aqueous nitrate (*top*) and nitrite (*bottom*) concentrations over time for contaminant-spiked CCug sediments and SGW for BY Cribs groundwater conditions in batch experiments with PCOIs with CoCOIs with treatment with organic substrates (0.39 g/L of TOC from EOS or molasses) at day 0 followed by Poly-PO_4 treatment at day 45 compared to no-donor controls. Note: Error bars are based on analysis of triplicate batch reactors.

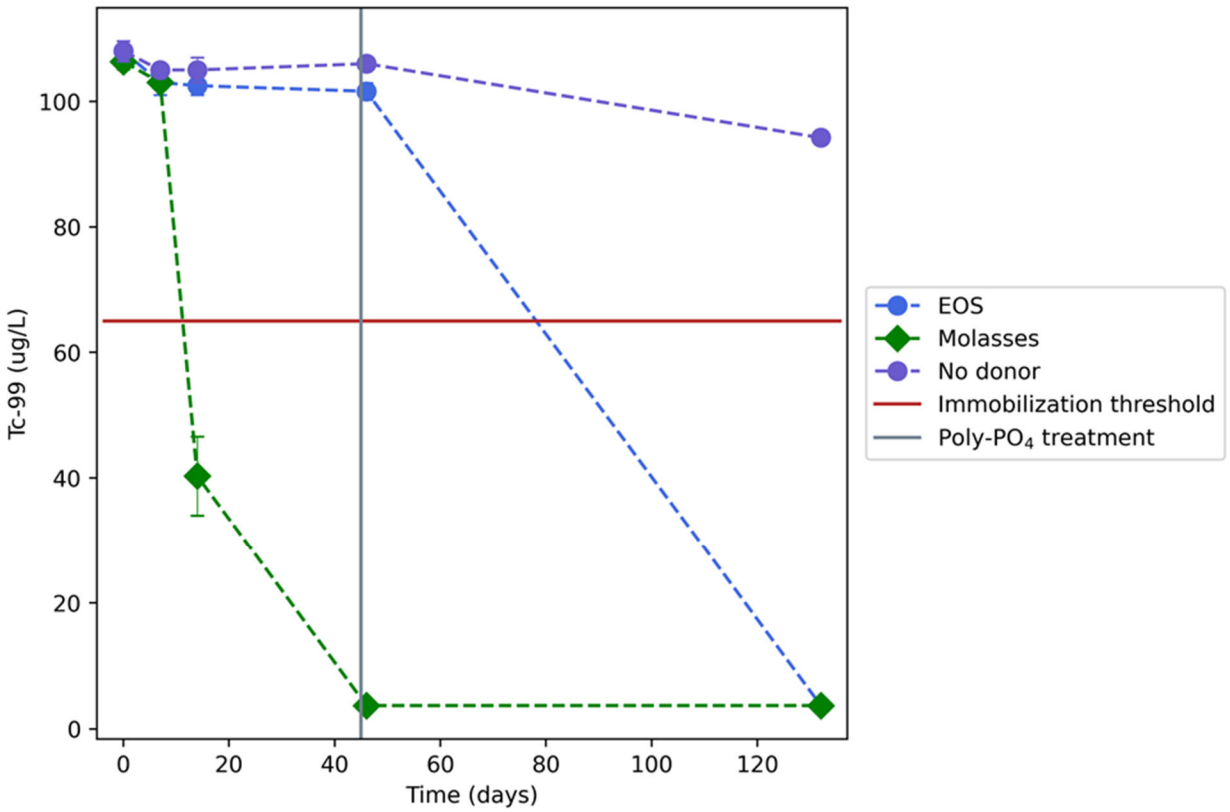

Figure 4.56. Aqueous Tc-99 concentrations over time for contaminant-spiked CCug sediments and SGW for BY Cribs groundwater conditions in batch experiments with PCOIs with CoCOIs with treatment with organic substrates (0.39 g/L of TOC from EOS or molasses) at day 0 followed by Poly-PO_4 treatment at day 45 compared to no-donor controls. Note: Error bars are based on analysis of triplicate batch reactors.

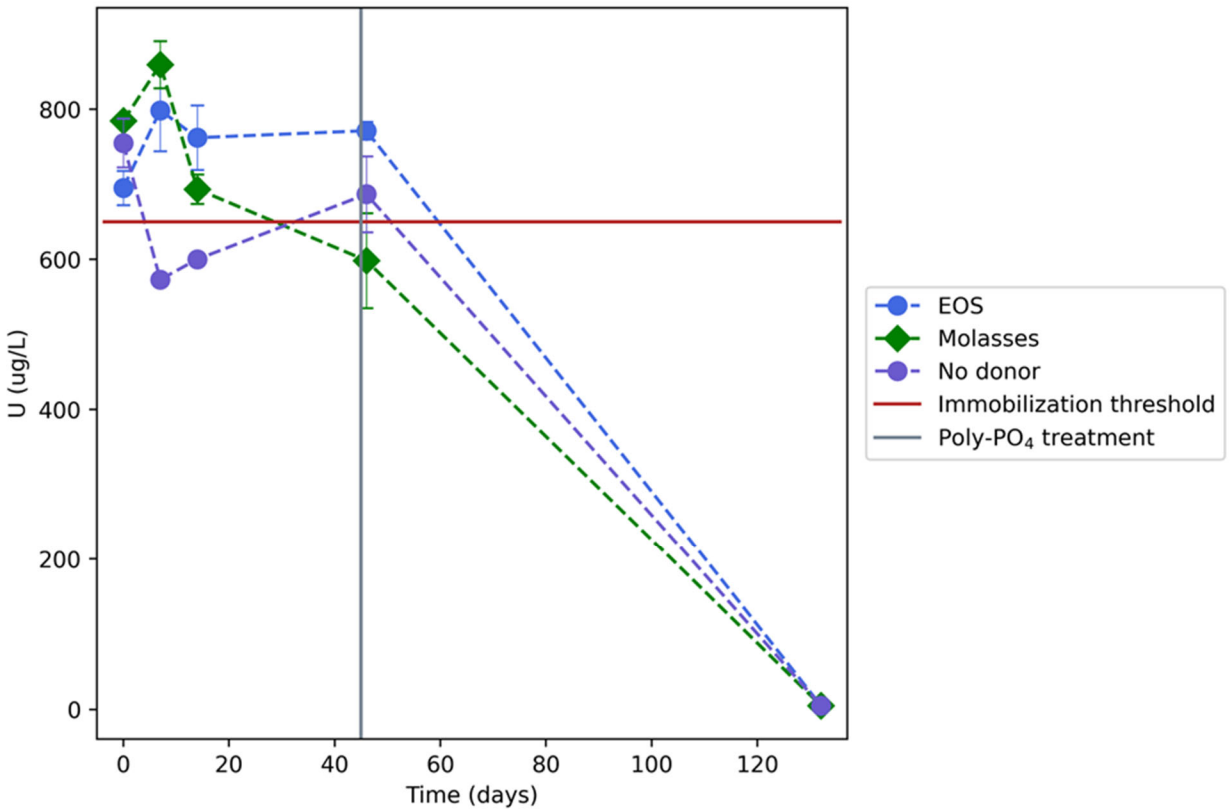

Figure 4.57. Aqueous U concentrations over time for contaminant-spiked CCug sediments and SGW for BY Cribs groundwater conditions in batch experiments with PCOIs with CoCOIs with treatment with organic substrates (0.39 g/L of TOC from EOS or molasses) at day 0 followed by Poly-PO_4 treatment at day 45 compared to no-donor controls. Note: Error bars are based on analysis of triplicate batch reactors. Lines are used to guide the eye and do not represent a model.

4.9.2 Perched Water Conditions

The two-step bioreduction and chemical sequestration technology was also evaluated under perched water conditions in the presence of PCOIs only. However, for the perched water conditions, the concentrations of added nitrate and U were 14× and 24× the added concentrations in the water table conditions described above, while the concentration of added Tc-99 was the same concentration as for the water table. Moreover, the PZsd sediment was contributing additional U (~68 µg/g). The starting concentration of U in SPW used for the batch experiments was 21,800 µg/L, and the concentration ranged between 34,566 to 48,200 µg/L after the start of testing.

4.9.2.1 Objective 1: Rate of sequestration of PCOIs with organic liquids and Poly-PO_4

Figure 4.58, Figure 4.59, and Figure 4.60 show the results for bioreduction of nitrate, Tc-99, and U, respectively, for the PZsd sediments treated under high ionic strength perching conditions.

Despite initial measured nitrate concentrations of 733 mg/L, aqueous NO_3^- and NO_2^- values were both below detection limits by the 7-day time point in the EOS and molasses treatments, while in the no-donor treatment, NO_3^- remained > 86% of initial aqueous concentrations by 91 days (Figure 4.58). Interestingly, in the no-donor treatment, NO_2^- values initially increased from below detection (0.71 mg/L) at time zero

to 35.7 mg/L at the 7 days, dropping again to below detection at 14 days, and increasing again to 3.69 and 6.74 mg/L, respectively, after 46 and 91 days. Fluctuations in NO_2^- could be due to samples sitting for 7 to 21 days between destructive sampling and analytical measurements of the filtrates. In the no-sediment control samples (shown in Appendix J, Figure J.8), NO_3^- reduction in the presence of EOS or molasses was less than in the CCug system without CoCOIs but greater than in the CCug system with CoCOIs (see Appendix J, Figure J.9).

Figure 4.59 shows the results for bioreduction of Tc-99 with PZsd sediment (added at the same aqueous concentration as for the CCug treatments above). The Tc-99 was more quickly and more thoroughly removed from solution by the molasses treatment compared with the EOS treatment, suggesting that molasses, the "fast-release" electron donor, more readily promoted Fe(III) reduction, to produce biogenic Fe(II) capable of reducing Tc(VII) (Fredrickson et al. 2004; Plymale et al. 2011), compared with the "slow-release" EOS electron donor. This is consistent with results observed for the CCug sediments under the BY Cribs groundwater conditions (Figure 4.51 and Figure 4.56).

As shown in Figure 4.60, neither organic liquid was effective at generating conditions for removing aqueous U from solution at the higher U and nitrate concentrations (as compared with CCug), without the addition of Poly-PO_4. It is also possible that the higher bicarbonate concentrations in the PZsd (11.0 mM added HCO_3^-) in comparison with the CCug (1.71 mM added HCO_3^-) hindered reduction of U(VI) due to the formation of stable calcium uranyl carbonate complexes that are resistant to bioreduction (Brooks et al. 2003). However, sulfate reduction was minimal and comparable with both EOS and molasses treatments at 47 days (Appendix J, Figure J.8), suggesting that the lack of U reduction was due to electron donor limitations. However, as shown in Figure 4.60, with the addition of Poly-PO_4, U was effectively removed from solution in all three treatments.

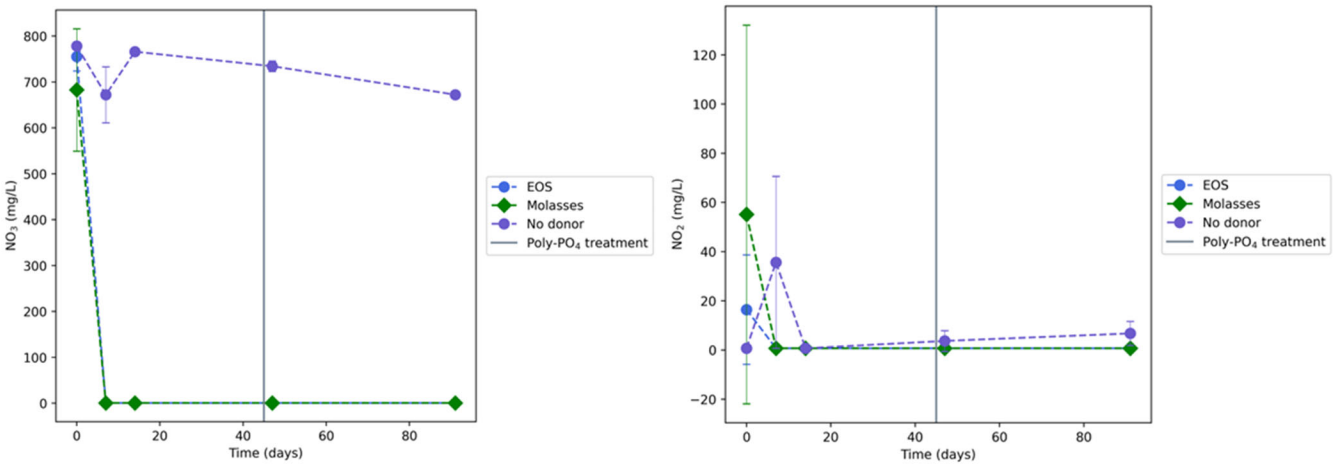

Figure 4.58. Aqueous nitrate and nitrite concentrations over time for contaminant-spiked PZsd sediments and SPW for perched water conditions in batch experiments. Organic liquids at approximately 0.39 g/L of TOC from EOS or molasses were added to batch systems at time zero followed by Poly-PO_4 treatment at 45 days compared to no-donor controls. Note: Error bars are based on analysis of triplicate batch reactors. Lines are used to guide the eye and do not represent a model.

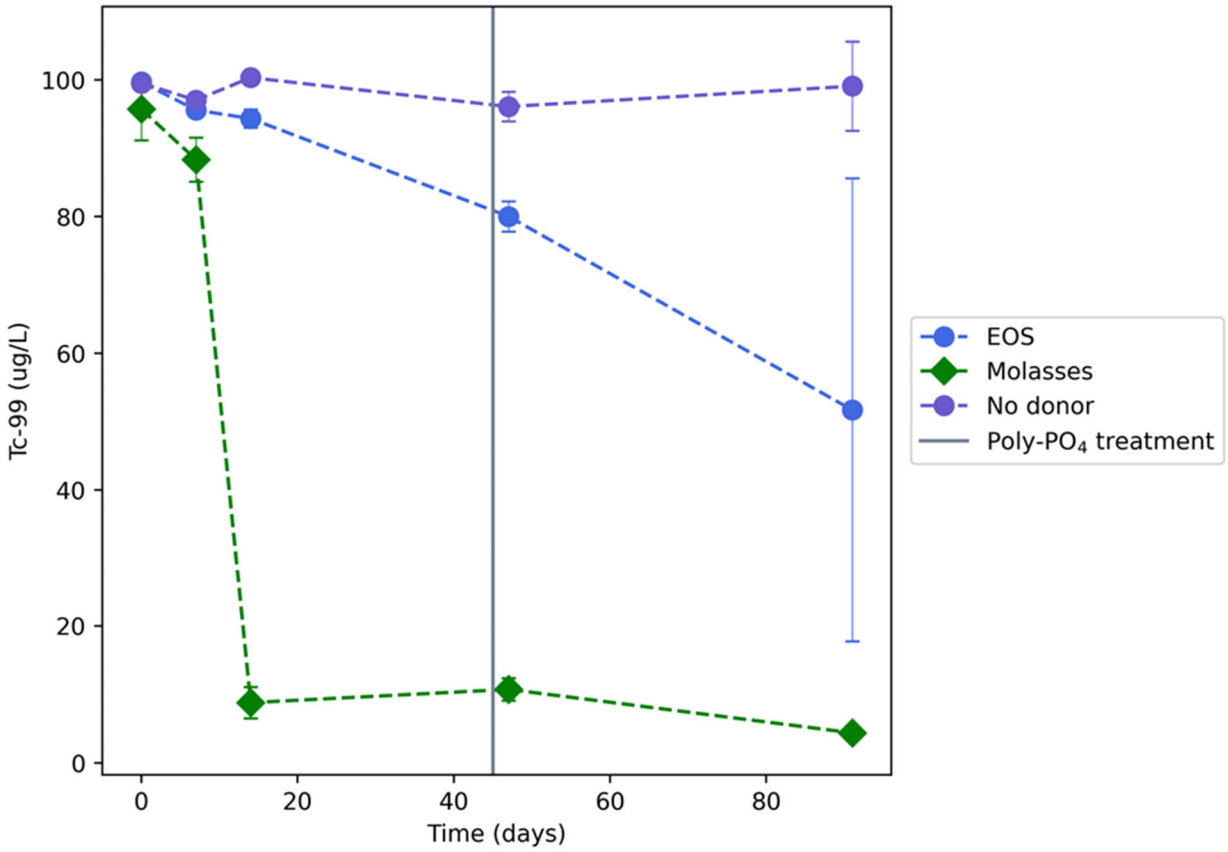

Figure 4.59. Aqueous Tc-99 concentrations over time for contaminant-spiked PZsd sediments and SPW for perched water conditions in batch experiments. Organic liquids at approximately 0.39 g/L of TOC from EOS or molasses were added to batch systems at time zero followed by Poly-PO_4 treatment at 45 days compared to no-donor controls. Note: Error bars are based on analysis of triplicate batch reactors. Lines are used to guide the eye and do not represent a model.

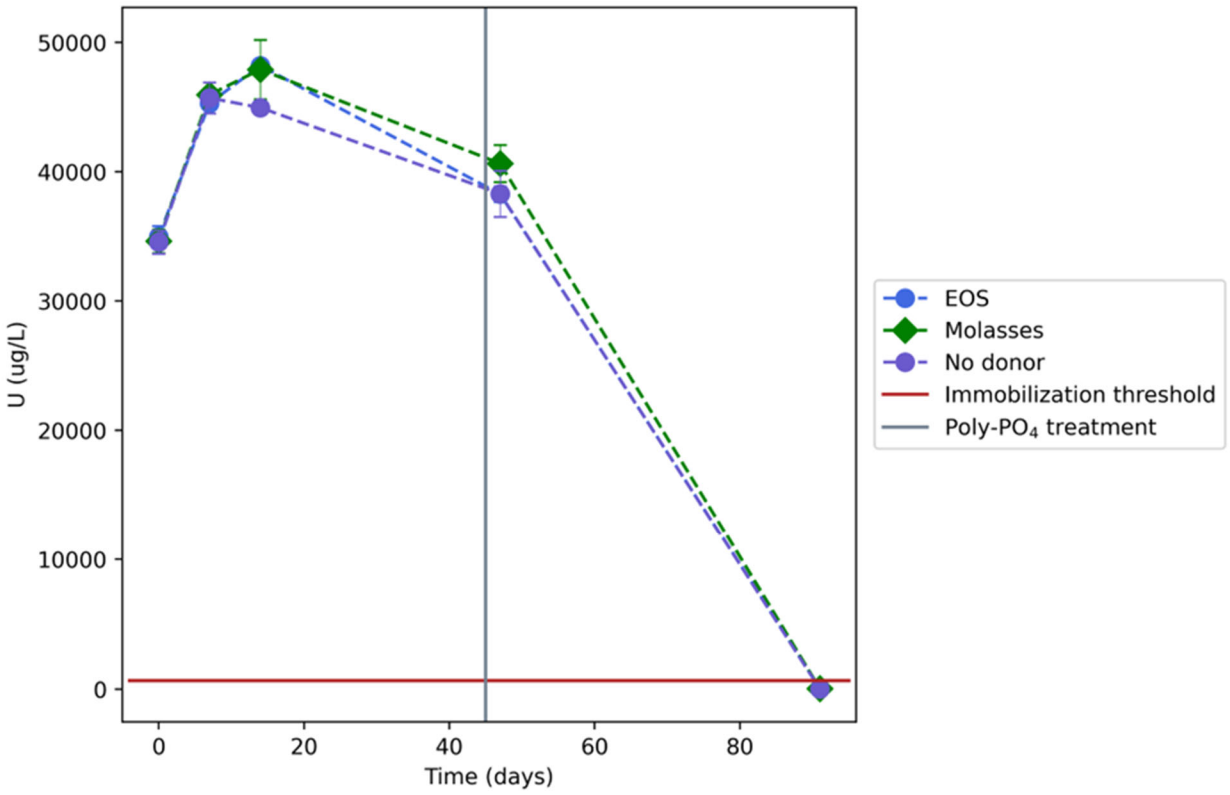

Figure 4.60. Aqueous U concentrations over time for contaminant-spiked PZsd sediments and SPW for perched water conditions in batch experiments. Organic liquids at approximately 0.39 g/L of TOC from EOS or molasses were added to batch systems at time zero followed by Poly-PO_4 treatment at 45 days compared to no-donor controls. Note: Error bars are based on analysis of triplicate batch reactors. Lines are used to guide the eye and do not represent a model.

4.9.2.2 Objective 2: Extent of sequestration of U and Tc-99 with two-step treatment with organic liquids and Poly-PO_4

As shown in Figure 4.61, the molasses treatment sequestered 73% of added Tc-99 by the 45-day time point, compared with 15% for EOS and 8% for the no-donor treatment. After addition of Poly-PO_4 and additional incubation to 91 days, sequestered Tc-99 increased to 39% and 81% in EOS and molasses treatments, respectively, compared with 7% in the no-donor treatment. In the case of U, in spite of sequestration of less than 11% of U at 46 days for all conditions evaluated, the addition of Poly-PO_4 and further incubation to 91 days led to the sequestration of 95%, 84%, and 78% of U in the molasses, EOS, and no-donor treatments, respectively (Figure 4.62).

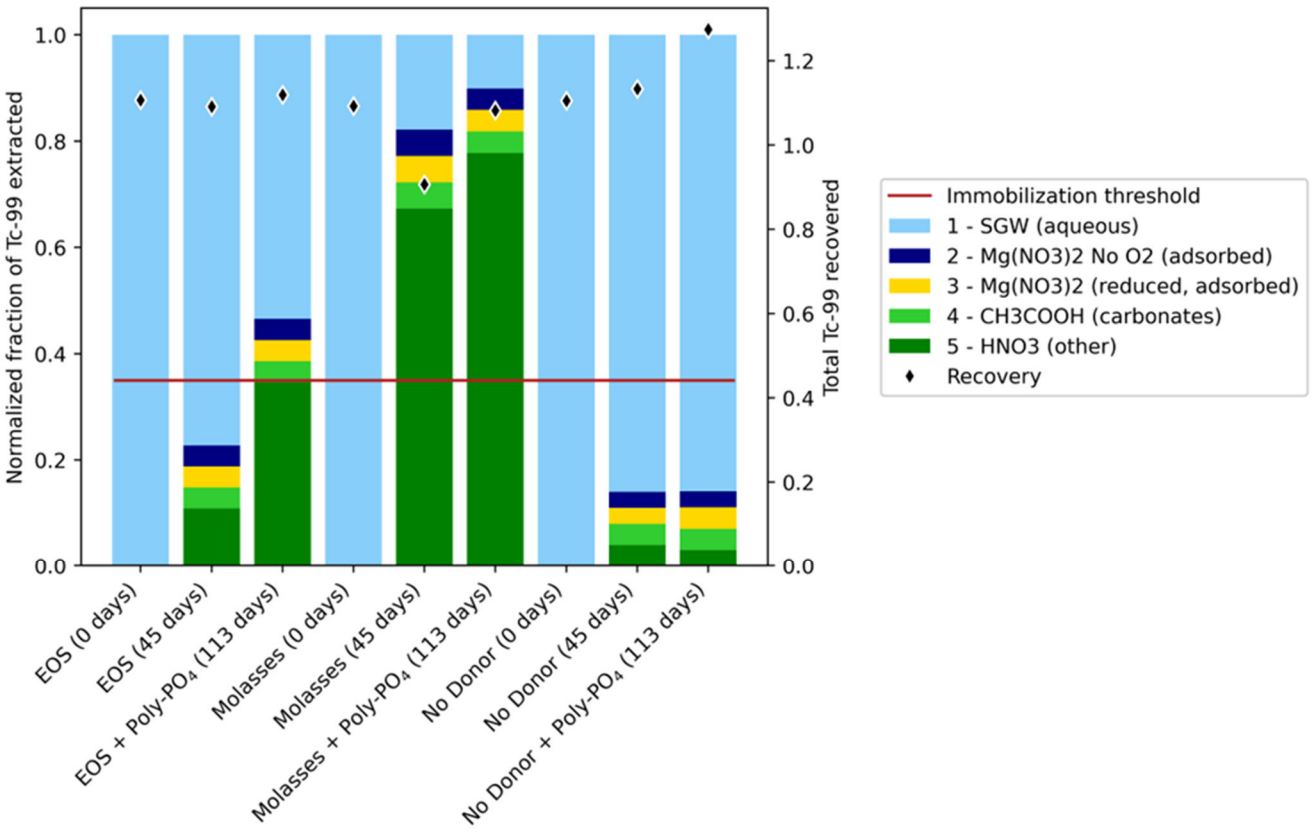

Figure 4.61. Change in Tc-99 mobility from liquid-phase treatment of contaminant-spiked PZsd sediment in SPW for perched water conditions reacted with a liquid organic substrate (0.34 g/L of TOC, from EOS or molasses) at time zero followed by Poly-PO_4 at 45 days via sequential extractions at 0, 45, and 113 days compared to no-donor controls. Note: The 35% minimum transformation threshold is shown by the solid red line and black diamonds represent the overall contaminant recovery across all extractions and remaining aqueous.

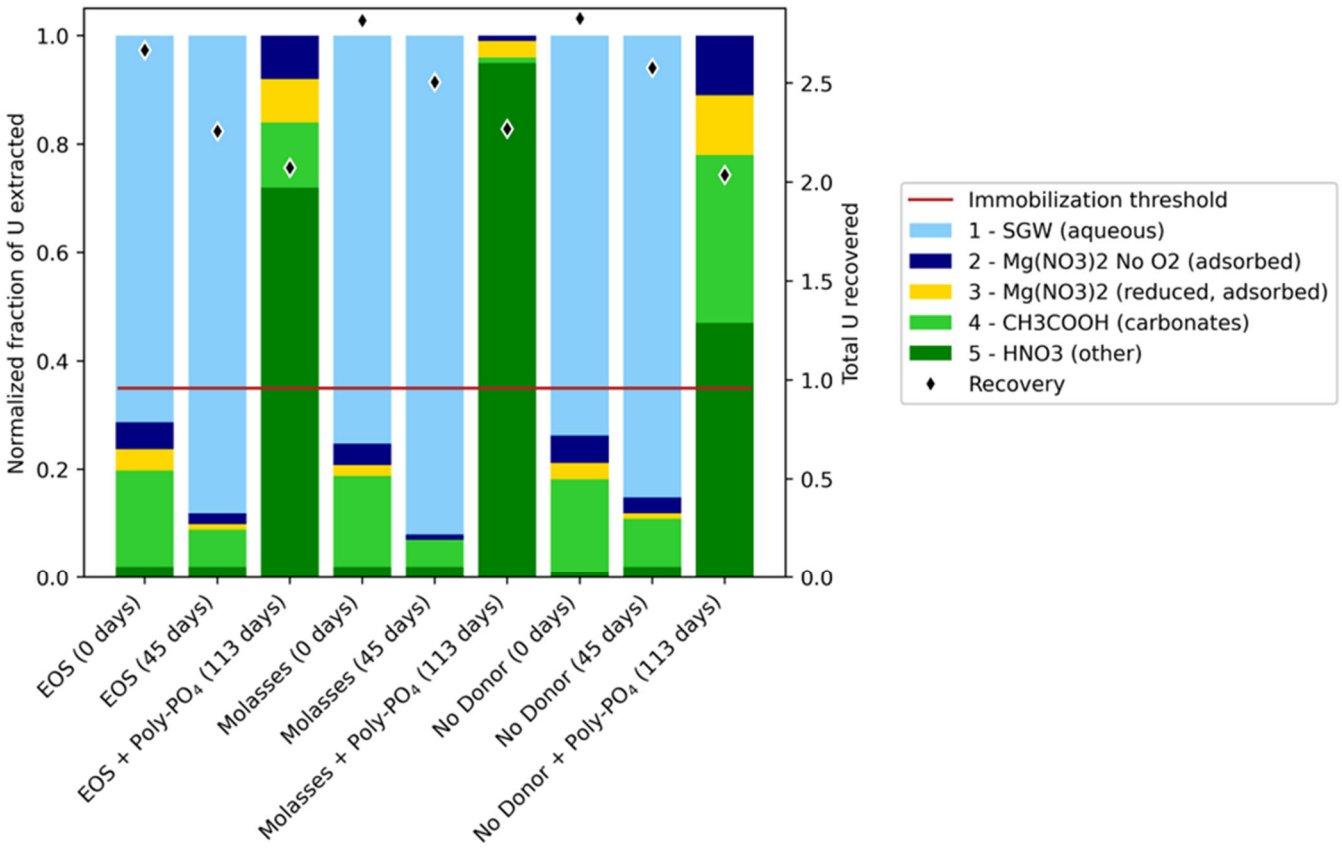

Figure 4.62. Change in U mobility from liquid-phase treatment of contaminant-spiked PZsd sediment in SPW for perched water conditions reacted with a liquid organic substrate (0.34 g/L of TOC, from EOS or molasses) at time zero followed by Poly-PO_4 at 45 days via sequential extractions at 0, 45, and 113 days compared to no-donor controls. Note: The 35% minimum transformation threshold is shown by the solid red line and black diamonds represent the overall contaminant recovery across all extractions and remaining aqueous.

5.0 Conclusions and Recommendations

The results of Phase 1 testing (as described in Section 4.0) were evaluated by the project team to assess the nine different technologies. The transformation to immobile, temporarily immobile, or nontoxic end products was considered based on the minimum 35% threshold alongside other experimental indicators for the targeted, site-specific conditions for each technology to determine whether they were recommended for Phase 2 evaluation of the treatability studies. The following subsections summarize the conclusions and recommendations for each technology, as outlined in Table 5.1. Appendix K also includes considerations for scale-up and delivery.

Table 5.1. Summary of Phase 1 results and recommendations for Phase 2 of 200-DV-1 OU treatability testing.

Technology Process	Contaminants of Interest[a]	Phase 1 Amendments	Phase 1 Decision Point	Phase 2 Evaluation Recommendations
Technologies for Unsaturated Zone Applications				
Gas-phase combined bioreduction and chemical sequestration	**Tc-99**, U, I-129, Cr(VI), CN^-, nitrate	Organic gases including ethane, butane, and butyl acetate for bioreduction CO_2 for sequestration	No-Go	None
Gas-phase bioremediation	**Nitrate**, Cr	Organic gases including pentane, butyrate, ethane, and butane	Go	Ethane gas
Gas-phase chemical sequestration	**I-129**, U, Tc-99, Sr, Cr(VI)	CO_2 gas	Go	CO_2 gas
Technologies for Saturated Zone Applications at BY Cribs groundwater or Perched Water[b]				
Particulate-phase chemical sequestration	**U**, **Tc-99**, Sr-90, Cr(VI), I-129, nitrate	Sn(II)-PO_4	Go	Sn(II)-PO_4
Particulate-phase chemical sequestration	**U, Tc-99,** Sr-90, Cr(VI),I-129, nitrate	Bismuth oxyhydroxide and bismuth subnitrate	Go	Bismuth subnitrate
Particulate-phase combined chemical reduction and sequestration	**U**, **Tc-99**, Sr-90, Cr(VI), I-129, nitrate	Zero valent iron and sulfur-modified iron for reduction Polyphosphate solutions for sequestration	Go	Sulfur-modified iron followed by polyphosphate
Liquid-phase chemical sequestration	**U**, **Tc-99**, Sr-90, Cr(VI), I-129, nitrate	Polyphosphate and citrate phosphate solutions	Go	Calcium citrate phosphate[b]
Liquid-phase combined chemical reduction and sequestration	**U**, **Tc-99**, Sr-90, Cr(VI) ,I-129, nitrate	Calcium polysulfide for reduction Polyphosphate solutions for sequestration	Go	Calcium polysulfide followed by polyphosphate
Liquid-phase combined bioreduction and chemical sequestration	**U**, **Tc-99**, **nitrate**, Sr-90, Cr(VI), I-129	Organic liquids including emulsified vegetable oil and blackstrap molasses for bioreduction Polyphosphate solutions for sequestration	Go	Molasses followed by polyphosphate

(a) The contaminants of interest shown in bold are primary known contaminant targets while others are potential co-contaminants to evaluate with primary contaminants.
(b) BY Cribs and perched water applications represent some of the 200-DV-1 waste sites (see Section 1.2 for more information).
(c) Although calcium citrate phosphate was chosen for additional testing in the liquid-phase chemical sequestration technology, polyphosphate was chosen to move forward as the sequestration step in the following technologies: particulate-phase combined chemical, liquid-phase combined chemical reduction and sequestration, and liquid-phase combined bioreduction and sequestration.

5.1 Gas-Phase Bioreduction and Sequestration – Organic gases and carbon dioxide (CO_2)

The gas-phase bioreduction and sequestration technology evaluated two sequential treatment steps with organic gases (ethane, butane, or butyl acetate) for *in situ* bioreduction followed by CO_2 gas treatment for further sequestration targeting VZ conditions. This two-step gas technology did not show sufficient immobilization of Tc-99 to meet the minimum transformation threshold of 35% for the selected conditions. Therefore, this technology is not recommended for further testing in Phase 2 of the treatability studies. However, this technology may still prove to be promising in other site-relevant conditions (e.g., other source OUs); and, if additional testing is conducted in the future, the impact of moisture content and addition of nutrients for the microbial community should be considered.

5.2 Gas-Phase Bioreduction – Organic gases

The gas-phase bioreduction technology evaluated four different organic gases (pentane, butyrate, ethane, and butane) for *in situ* bioreduction targeting VZ conditions. The results indicated sufficient transformation of nitrate surpassing the minimum transformation threshold of 35%, for select conditions. Therefore, this technology is recommended for further testing in Phase 2 of the treatability studies. The transformation to nontoxic end products was determined based on measurement of aqueous NO_3^- and NO_2^- assuming that the remaining N is transformed to gaseous, nontoxic end products. The minimum threshold was met when Cr(VI) was not present with nitrate for most conditions, although some variability was observed between the three site-specific sediments and two sediment-to-solution ratios. Pentane was the worst performing gas and butyrate and ethane were the best performing gases, although transformation of nitrate when Cr(VI) was present was variable. This technology is recommended for Phase 2 evaluation with a focus on the top-performing organic gas amendments, butyrate and ethane. Due to the low volatility and high solubility of butyrate, the radius of treatment for butyrate gas injection in a potential field application would likely be constrained to very short distances. Therefore, ethane will be the primary gas for further testing. The observed impacts from co-contaminants and sediments highlight the importance of understanding the site-specific conditions for effective bioreduction, including differing microbial populations or activities as well as more variable nitrate concentrations between waste sites and sediments.

5.3 Gas-Phase Sequestration – Carbon dioxide (CO_2) gas

The gas-phase sequestration technology evaluated CO_2 gas for *in situ* immobilization of I-129 targeting VZ conditions. CO_2 gas treatment was sufficient for sequestration of iodine, surpassing the 35% minimum transformation threshold for select conditions. The threshold was not met in water-saturated batch experiments for iodine with or without co-contaminants, likely due to limitations in equilibration of carbon dioxide gas between the solid, liquid, and gas phases. However, in unsaturated columns conducted in the absence of flow, the minimum transformation threshold was met for iodine with and without co-contaminants, although success was dependent on WC. This technology is recommended for Phase 2 evaluation in the treatability studies.

5.4 Particulate-Phase Chemical Sequestration – Sn(II)-PO_4

The particulate-phase sequestration technology evaluated Sn(II)-PO_4 amendments for *in situ* immobilization of Tc-99 and U under saturated conditions targeting the BY Cribs groundwater and perched water areas. Sn(II)-PO_4 treatment met the 35% minimum transformation threshold for both BY Cribs groundwater and perched water conditions, with > 80% of Tc-99 and uranium removed from the aqueous phase after 28 days of reaction, including with co-contaminants (Cr, NO_3, Sr, and IO_3) present.

Although Tc-99 reduction and sequestration rates were not decreased in perched water conditions (relatively higher ionic strength and NO_3), reduction and sequestration of U was slower in perched water conditions as compared to the BY Cribs groundwater conditions (hours versus days). This result highlights that the presence of redox active co-contaminants may significantly impact treatability in different sites, especially for U, which is more difficult to reduce than Tc-99. This technology is recommended for Phase 2 evaluation of the treatability studies.

5.5 Particulate Phase Chemical Sequestration – Bismuth oxyhydroxide and bismuth subnitrate

The particulate phase sequestration technology evaluated two different bismuth amendments, BSN and BOH, for *in situ* immobilization of Tc-99 and U under saturated conditions targeting the BY Cribs groundwater and perched water conditions. Both bismuth materials met the 35% minimum transformation threshold for BY Cribs groundwater for U and Tc-99, including with co-contaminants (Cr, NO_3, Sr, and IO_3) present, while only BSN met the minimum transformation threshold for Tc-99 for perched water conditions in batch experiments. Both bismuth materials sequestered U and Tc-99 more slowly in perched water conditions, but the sequestration for both contaminants differed. Sequestration was greater for U in perched water conditions as compared to BY Cribs groundwater conditions, although the opposite was observed for Tc-99. Because BOH did not meet the minimum transformation threshold for Tc-99 under perched water conditions, BSN is recommended for Phase 2 evaluation of the treatability studies.

5.6 Particulate Phase Chemical Reduction – Zero valent iron / sulfur-modified iron (ZVI/SMI) and polyphosphate

The particulate-phase combined chemical reduction and sequestration technology evaluated two different iron materials, ZVI and SMI, followed by Poly-PO_4 treatment for *in situ* immobilization of Tc-99 and U under saturated conditions targeting the BY Cribs groundwater and perched water conditions. Both iron materials with subsequent treatment with Poly-PO_4 met the 35% minimum transformation threshold for both BY Cribs groundwater and perched water conditions for U and Tc-99. Greater than 99% of U was sequestered for all three sediments for BY Cribs groundwater conditions in the absence of co-contaminants (Cr, NO_3, Sr, and IO_3). However, the SMI reduced uranium and Tc-99 more quickly than ZVI. Greater than 99% of Tc-99 was sequestered for the BY Cribs groundwater condition for Hf and CCuz sediments and > 90% in BY Cribs VZ sediments. U sequestration decreased to > 85% when NO_3 was added for both amendments, and with BY Cribs sediments containing high concentrations of NO_3. SMI performance was not affected by the presence of a delivery fluid (xanthan), whereas ZVI performance decreased in the presence of xanthan.

5.7 Liquid-Phase Chemical Sequestration – Apatite-forming solutions

The liquid-phase chemical sequestration technology evaluated two different apatite-forming solutions, Poly-PO_4 and Ca-Cit-PO_4, for *in situ* immobilization of Tc-99 and U under saturated conditions targeting the BY Cribs groundwater and perched water conditions. Both apatite-forming solutions met the 35% minimum transformation threshold for both BY Cribs groundwater and perched water conditions for U (> 70% immobilized for all conditions). For Tc-99, however, the minimum threshold was only met for Ca-Cit-PO_4 (> 50%). Ca-Cit-PO_4 likely performed better due to the formation of mildly reducing conditions from biostimulation of natural sediment microbes due to the presence of citrate. However, the rate of removal and total sequestration of Tc-99 with Ca-Cit-PO_4 was reduced in perched water conditions, likely due to the presence of other reducible co-contaminants. Based on these results, the

Ca-Cit-PO_4 amendment is recommended for Phase 2 evaluation of the treatability studies. However, Poly-PO_4 was chosen as the sequestration step for the following two-step technologies: particulate-phase combined chemical reduction and sequestration, liquid-phase combined chemical reduction and sequestration, and liquid-phase combined bioreduction and sequestration.

5.8 Liquid-Phase Chemical Reduction and Chemical Sequestration – Calcium polysulfide and polyphosphate

The liquid-phase chemical reduction and sequestration technology evaluated a two-step treatment with liquid CPS followed by Poly-PO_4 for *in situ* immobilization of Tc-99 and U under saturated conditions targeting BY Cribs groundwater and perched water conditions. These amendments met the 35% minimum transformation threshold for both BY Cribs groundwater and perched water conditions for U and Tc-99. Greater than 90% and 60% were sequestered for uranium and Tc-99, respectively, including with co-contaminants present (Cr, NO_3, Sr, and IO_3). The removal rate was slightly faster for U than Tc-99, although both were removed within days. Under perched water conditions, the relatively high ionic strength and concentration of NO_3, a competing redox-active contaminant, limited total Tc-99 sequestered (> 60% versus > 80% with BY Cribs groundwater conditions) but did not affect the amount of U sequestered. This technology is recommended for Phase 2 evaluation of the treatability studies.

5.9 Liquid-Phase Bioreduction and Chemical Sequestration – Organic liquids and polyphosphate

The liquid-phase bioreduction and chemical sequestration technology evaluated two different organic liquids (EOS as a slow-release donor and molasses as a fast-release donor) following scoping experiments with additional amendments for *in situ* immobilization and transformation targeting BY Cribs groundwater and perched water conditions. The results indicated sufficient transformation of NO_3 and sequestration of Tc-99 and U, surpassing the minimum threshold of 35% for all treatment conditions for both EOS and molasses. Notably, U required the second step of treatment with Poly-PO_4 to meet the minimum threshold for all conditions except the BY Cribs groundwater condition without CoCOIs. For Tc-99, the minimum transformation threshold was met for all conditions for both EOS and molasses; however, reductive sequestration was significantly impacted by the high ionic strength and high nitrate in the perched water conditions, where > 50% remained in solution with EOS treatment as compared to < 5% for all BY Cribs groundwater conditions with EOS. In addition, treatment occurred at a faster rate for molasses as compared to EOS. Therefore, this technology is recommended for further testing in Phase 2 of the treatability studies, with a focus on the top-performing organic liquid amendment, molasses, followed by Poly-PO_4. The observed impacts from co-contaminants, groundwater, and sediments highlight the importance of understanding the site-specific conditions for effective bioreduction, including differing microbial populations or activities as well as more variable nitrate concentrations between waste sites and sediments.

5.10 Summary Conclusions and Recommendations

The three gas-phase technologies targeted different contaminants in the VZ, including (1) combined bioreduction and sequestration of Tc-99 by sequential treatment with organic gas followed by carbon dioxide gas, (2) bioreduction of NO_3 by organic gases, and (3) sequestration of I-129 by carbon dioxide gas. The one technology that did not pass the criteria was the gas-phase combined bioreduction and chemical sequestration, which showed some sequestration of Tc-99 but was insufficient to recommend further testing for a potential site application. The other two gas-phase technologies, bioreduction of NO_3 by organic gases and sequestration of I-129 by carbon dioxide, met the 35% minimum transformation to temporarily immobile, immobile, or nontoxic end products threshold and will advance to Phase 2

evaluation. The gas-phase bioreduction technology butyrate and ethane gas amendments (further down-selecting to ethane for practical reasons) are recommended for Phase 2 evaluation, as they showed superior performance to butane and pentane.

All the three particulate-phase technologies are recommended for Phase 2 evaluation, including (1) chemical sequestration by Sn(II)-PO_4, (2) chemical sequestration by BOH or BSN, and (3) combined chemical reduction and sequestration by ZVI or SMI followed by treatment with apatite-forming solutions. Each amendment was evaluated with the primary contaminants, including Tc-99 and U, and with and without potential co-contaminants, including Sr, I-129, Cr, and NO_3. All of these technologies met the 35% minimum transformation threshold for both U and Tc-99. For the chemical sequestration by bismuth amendments and the combined chemical reduction and sequestration technologies, a down-selection to BSN and SMI is recommended for Phase 2 evaluation, respectively.

The three liquid-phase technologies are (1) chemical sequestration by Poly-PO_4 or Ca-Cit-PO_4 solutions, (2) combined chemical reduction and sequestration by CPS followed by Poly-PO_4, and (3) combined bioreduction and sequestration by organic liquids followed by Poly-PO_4. Each amendment was evaluated with the primary contaminants, including Tc-99 and U, and with and without potential co-contaminants, including Sr, I-129, Cr, and NO_3. All of these technologies are recommended to advance to Phase 2 evaluation. For the liquid-phase chemical sequestration technology, the Ca-Cit-PO_4 amendment is recommended for Phase 2 evaluation due to its superior performance for Tc-99. However, the Poly-PO_4 amendment will continue as the sequestration amendment for the following technologies: liquid-phase chemical reduction and sequestration, liquid-phase bioreduction and sequestration, and particulate-phase chemical reduction and sequestration. For the combined bioreduction and sequestration by organic liquids followed by Poly-PO_4, molasses is recommended for PRB at the water table and direct treatment of perched water based on its superior performance in these conditions.

The results presented here will be used to inform testing for Phase 2 of this treatability study for further evaluation of selected technologies. The final results from the treatability study, following the completion of remaining phases, will be used to determine whether the technologies can be appropriately evaluated in an FS to expand on the limited number of viable DVZ remediation technologies. After completion of the laboratory treatability study and the 200 DV-1 OU RI and RFI of the waste sites, results will be evaluated to determine whether additional information is needed on effectiveness, implementability, or costs for evaluating these technologies in the FS for their site-specific application.

6.0 Quality Assurance

This work was performed in accordance with the PNNL Nuclear Quality Assurance Program (NQAP). The NQAP complies with DOE Order 414.1D, *Quality Assurance*. The NQAP uses NQA-1-2012, *Quality Assurance Requirements for Nuclear Facility Application*, as its consensus standard and NQA-1-2012 Subpart 4.2.1 as the basis for its graded approach to quality.

7.0 References

Angus, M. J., and F. P. Glasser. 1985. "The Chemical Environment in Cement Matrices." *MRS Online Proceedings Library* 50: 547-586. https://doi.org/10.1557/PROC-50-547.

Asmussen, R. M., C. I. Pearce, B. W. Miller, A. R. Lawter, J. J. Neeway, W. W. Lukens, M. E. Bowden, M. A. Miller, E. C. Buck, R. J. Serne, and N. P. Qafoku. 2018. "Getters for Improved Technetium Containment in Cementitious Waste Forms." *Journal of Hazardous Materials* 341: 238-247. https://doi.org/10.1016/j.jhazmat.2017.07.055.

Asmussen, R. M., J. J. Neeway, A. R. Lawter, T. G. Levitskaia, W. W. Lukens, and N. P. Qafoku. 2016. "The Function of Sn(II)-Apatite as a Tc Immobilizing Agent." *Journal of Nuclear Materials* 480: 393-402. https://doi.org/10.1016/j.jnucmat.2016.09.002.

ASTM B822-20. 2020. *Standard Test Method for Particle Size Distribution of Metal Powders and Related Compounds by Light Scattering*. West Conshohocken, PA: ASTM International.

ASTM D4464-15. 2020. *Standard Test Method for Particle Size Distribution of Catalytic Materials by Laser Light Scattering*. West Conshohocken, PA: ASTM International.

Bagwell, C. E., E. C. Gillispie, A. R. Lawter, and N. P. Qafoku. 2020. "Evaluation of Gaseous Substrates for Microbial Immobilization of Contaminant Mixtures in Unsaturated Subsurface Sediments." *Journal of Environmental Radioactivity* 214-215: 106183. https://doi.org/10.1016/j.jenvrad.2020.106183.

Baker, V. R., B. N. Bjornstad, A. J. Busacca, K. R. Fecht, E. P. Kiver, U. L. Moody, J. G. Rigby, D. F. Stradling, and A. M. Tallman. 1991. "Quaternary Geology of the Columbia Plateau." In *Quaternary Nonglacial Geology; Conterminous U.S.: Boulder, Colorado*. Boulder, CO: Geological Society of America.

Beckett, P. H. T. 1989. "The Use of Extractants in Studies on Trace Metals in Soils, Sewage Sludges, and Sludge-Treated Soils." In *Advances in Soil Science*, edited by B. A. Stewart, 144-176. New York: Springer. https://doi.org/10.1007/978-1-4612-3532-3_3.

Bethke, C., and S. Yeakel. 2010. *The Geochemist's Workbench: Reaction Modelling Guide*. University of Illinois Urbana-Champaign.

Boglaienko, D., H. P. Emerson, Y. P. Katsenovich, and T. G. Levitskaia. 2019. "Comparative Analysis of ZVI Materials for Reductive Separation of ^{99}Tc(VII) from Aqueous Waste Streams." *Journal of Hazardous Materials* 380: 120836. https://doi.org/10.1016/j.jhazmat.2019.120836.

Boglaienko, D., J. A. Soltis, R. K. Kukkadapu, Y. Du, L. E. Sweet, V. E. Holfeltz, G. B. Hall, E. C. Buck, C. U. Segre, H. P. Emerson, Y. Katsenovich, and T. Levitskaia. 2020. "Spontaneous Redox Continuum Reveals Sequestered Technetium Clusters and Retarded Mineral Transformation of Iron." *Communications Chemistry* 3 (1): 87. https://doi.org/10.1038/s42004-020-0334-x.

Borden, R. C. 2006. *Protocol for Enhanced In Situ Bioremediation Using Emulsified Edible Oil.* Environmental Security Technology Certification Program. Washington, D.C. https://serdp-estcp.mil/resources/details/2e7fd405-6c86-44a9-ad57-a97b869caf6b .

Brina, R., and A. G. Miller. 1992. "Direct Detection of Trace Levels of Uranium by Laser-Induced Kinetic Phosphorimetry." *Analytical Chemistry* 64 (13): 1413-1418. https://doi.org/10.1021/ac00037a020.

Brockman, F. J., J. S. Selker, and M. L. Rockhold. 2004. *Integrated Field, Laboratory, and Modeling Studies to Determine the Effects of Linked Microbial and Physical Spatial Heterogeneity on Engineered Vadose Zone Bioremediation.* Pacific Northwest National Laboratory PNNL-14535. Richland, WA. https://www.osti.gov/biblio/951879.

Brooks, S. C., J. K. Fredrickson, S. L. Carroll, D. W. Kennedy, J. M. Zachara, A. E. Plymale, S. D. Kelly, K. M. Kemner, and S. Fendorf. 2003. "Inhihition of Bacterial U(VI) Reduction by Calcium." *Environmental Science & Technology* 37 (9): 1850-1858. https://doi.org/10.1021/es0210042.

Carlson, W. 1980. "The Calcite–Aragonite Equilibrium: Effects of Sr Substitution and Anion Orientional Disorder." *American Mineralogist* 65 (11-12): 1252-1262.

Chao, T. T., and L. Zhou. 1983. "Extraction Techniques for Selective Dissolution of Amorphous Iron Oxides from Soils and Sediments." *Soil Science Society of America Journal* 47 (2): 225-232. https://doi.org/10.2136/sssaj1983.03615995004700020010x.

Chrysochoou, M., D. R. Ferreira, and C. P. Johnston. 2010. "Calcium Polysulfide Treatment of Cr(VI)-Contaminated Soil." *Journal of Hazardous Materials* 179 (1-3): 650-657. https://doi.org/10.1016/j.jhazmat.2010.03.052.

Crank, J. 1975. *The Mathematics of Diffusion*. 2nd ed. Oxford, UK: Clarendon Press.

de Lima Perini, J. A., and R. F. P. Nogueira. 2017. "Effect of Particle Size, Iron Ligands and Anions on Ciprofloxacin Degradation in Zero-Valent Iron Process: Application to Sewage Treatment Plant Effluent." *Journal of Chemical Technology and Biotechnology* 92 (9): 2300-2308. https://doi.org/10.1002/jctb.5227.

DOE/RL-2011-01. 2011. *Overview of Hanford Hydrogeology and Geochemistry.* U.S. Department of Energy, Richland, WA.

DOE/RL-2011-102, Rev. 0. 2011. *Remedial Investigation/Feasibility Study and Rcra Facility Investigative/Corrective Measures Study Work Plan for the 200-DV-1 Operable Unit*. U.S. Department of Energy, Richland Operations Office, Richland, WA.

DOE/RL-2014-34. 2014. *Action Memorandum for 200-DV-1 Operable Unit Perched Water Pumping/Pore Water Extraction in 2014*. U.S. Department of Energy, Richland Operations Office, Richland, WA.

DOE/RL-2017-58, Rev. 0.0. 2017. *Technology Evaluation and Treatability Studies Assessment for the Hanford Central Plateau Deep Vadose Zone.* U.S. Department of Energy Richland Office, Richland, WA.

DOE/RL-2018-28. 20XX. *Title*. U.S. Department of Energy Richland Office, Richland, WA

DOE/RL-2019-28, Rev. 0. 2014. *200-DV-1 Operable Unit Laboratory Treatability Study Test Plan.* U.S. Department of Energy, Richland Operations Office, Richland, WA.

DOE/RL-2021-01. 2021. *Hanford Site Fifth CERCLA Five-Year Review Report, Draft A.* U.S. Department of Energy, Richland Office, Richland, WA. https://www.hanford.gov/files.cfm/DOE-RL-2021-01-00.pdf.

DOE/RL-88-09. 1988. *183-H Solar Evaporation Basins Closure/Post-Closure Plan.* U.S. Department of Energy, Richland Operations Office, Richland, WA.

DOE/RL-92-24, Rev. 1. 1993. *Hanford Site Background: Part 1, Soil Background for Nonradioactive Analytes.* U.S. Department of Energy, Richland Operations Office, Richland, WA.

Dresel, P. E., D. M. Wellman, K. J. Cantrell, and M. J. Truex. 2011. "Review: Technical and Policy Challenges in Deep Vadose Zone Remediation of Metals and Radionuclides." *Environmental Science & Technology* 45 (10): 4207-4216. https://doi.org/10.1021/es101211t.

Emerson, H. P., A. Gebru, D. Boglaienko, Y. P. Katsenovich, S. Kandel, and T. G. Levitskaia. 2020. "Impact of Zero Valent Iron Aging on Reductive Removal of Technetium-99." *Journal of Environmental Chemical Engineering* 8 (3): 103767. https://doi.org/10.1016/j.jece.2020.103767.

Evans, P. J., and M. M. Trute. 2006. "In Situ Bioremediation of Nitrate and Perchlorate in Vadose Zone Soil for Groundwater Protection Using Gaseous Electron Donor Injection Technology." *Water Environment Research* 78 (13): 2436-2446. https://doi.org/10.2175/106143006X123076.

Evans, P. J., R. A. Fricke, K. Hopfensperger, and T. Titus. 2011. "In Situ Destruction of Perchlorate and Nitrate Using Gaseous Electron Donor Injection Technology." *Groundwater Monitoring & Remediation* 31 (4): 103-112. https://doi.org/10.1111/j.1745-6592.2011.01355.x.

Fredrickson, J. K., J. M. Zachara, A. E. Plymale, S. M. Heald, J. P. McKinley, D. W. Kennedy, C. Liu, and P. Nachimuthu. 2009. "Oxidative Dissolution Potential of Biogenic and Abiogenic TcO_2 in Subsurface Sediments." *Geochimica et Cosmochimica Acta* 73 (8): 2299-2313. https://doi.org/10.1016/j.gca.2009.01.027.

Fredrickson, J. K., J. M. Zachara, D. W. Kennedy, R. K. Kukkadapu, J. P. McKinley, S. M. Heald, C. Liu, and A. E. Plymale. 2004. "Reduction of TcO_4^- by Sediment-Associated Biogenic Fe(II)." *Geochimica et Cosmochimica Acta* 68 (15): 3171-3187. https://doi.org/10.1016/j.gca.2003.10.024.

Fuller, C. C., J. R. Bargar, and J. A. Davis. 2003. "Molecular-Scale Characterization of Uranium Sorption by Bone Apatite Materials for a Permeable Reactive Barrier Demonstration." *Environmental Science & Technology* 37 (20): 4642-4649. https://doi.org/10.1021/es0343959.

Gartman, B., E. Arnold, J. Szecsody, N. Qafoku, C. Bagwell, C. Brown, and V. Freedman. 2019. "Evaluation of a Two-Step Remediation Strategy for the Highly Concentrated Perched Water Zone at Hanford, WA." American Geophysical Union Annual Fall Meeting 2019, San Francisco, CA, December 9–13, 2019.

Gleyzes, C., S. Tellier, and M. Astruc. 2002. "Fractionation Studies of Trace Elements in Contaminated Soils and Sediments: A Review of Sequential Extraction Procedures." *TrAC Trends in Analytical Chemistry* 21 (6-7): 451-467. https://doi.org/10.1016/S0165-9936(02)00603-9.

Grenthe, I., X. Gaona, A. V. Plyasunov, L. Rao, W. H. Runde, B. Grambow, R. J. M. Konings, A. L. Smith, and E. E. Moore. 2020. *Second Update on the Chemical Thermodynamics of Uranium, Neptunium,*

Plutonium, Americium, and Technetium. OECD Nuclear Energy Agency. Paris. https://www.oecd-nea.org/jcms/pl_46643/second-update-on-the-chemical-thermodynamics-of-u-np-pu-am-and-tc.

Grundl, T. J., S. Haderlein, J. T. Nurmi, and P. G. Tratnyek. 2011. "Introduction to Aquatic Redox Chemistry." In *Aquatic Redox Chemistry*, 1-14. ACS Publications.

Guan, X., Y. Sun, H. Qin, J. Li, I. M. Lo, D. He, and H. Dong. 2015. "The Limitations of Applying Zero-Valent Iron Technology in Contaminants Sequestration and the Corresponding Countermeasures: The Development in Zero-Valent Iron Technology in the Last Two Decades (1994–2014)." *Water Research* 75: 224-248. https://doi.org/10.1016/j.watres.2015.02.034.

Guillaumont, R., T. Fanghänel, J. Fuger, I. Grenthe, V. Neck, D. A. Palmer, and M. H. Rand. 2003. *Update on the Chemical Thermodynamics of Uranium, Neptunium, Plutonium, Americium and Technetium*. OECD Nuclear Energy Agency.

Hall, G. E. M., J. E. Vaive, R. Beer, and M. Hoashi. 1996. "Selective Leaches Revisited, with Emphasis on the Amorphous Fe Oxyhydroxide Phase Extraction." *Journal of Geochemical Exploration* 56 (1): 59-78. https://doi.org/10.1016/0375-6742(95)00050-X.

Heslop, D. D., Y. Bi, A. A. Baig, M. Otsuka, and W. I. Higuchi. 2005. "A Comparative Study of the Metastable Equilibrium Solubility Behavior of High-Crystallinity and Low-Crystallinity Carbonated Apatites Using Ph and Solution Strontium as Independent Variables." *Journal of Colloid and Interface Science* 289 (1): 14-25. https://doi.org/10.1016/j.jcis.2004.12.050.

Hess, N. J., O. Qafoku, Y. Xia, D. A. Moore, and A. R. Felmy. 2008. "Thermodynamic Model for the Solubility of $TcO_2{\cdot}xH_2O$ in Aqueous Oxalate Systems." *Journal of Solution Chemistry* 37 (11): 1471-1487. https://doi.org/10.1007/s10953-008-9328-5.

Hofmann, S., K. Voïtchovsky, M. Schmidt, and T. Stumpf. 2014. "Trace Concentration – Huge Impact: Nitrate in the Calcite/Eu(III) System." *Geochimica et Cosmochimica Acta* 125: 528-538. https://doi.org/10.1016/j.gca.2013.10.008.

Hofmann, S., K. Voïtchovsky, P. Spijker, M. Schmidt, and T. Stumpf. 2016. "Visualizing the Molecular Alteration of the Calcite (104)–Water Interface by Sodium Nitrate." *Scientific Reports* 6: 21576. https://doi.org/10.1038/srep21576.

Icenhower, J. P., N. P. Qafoku, J. M. Zachara, and W. J. Martin. 2010. "The Biogeochemistry of Technetium: A Review of the Behavior of an Artificial Element in the Natural Environment." *American Journal of Science* 310 (8): 721-752. https://doi.org/10.2475/08.2010.02.

Istok, J. D., J. M. Senko, L. R. Krumholz, D. Watson, M. A. Bogle, A. Peacock, Y.-J. Chang, and D. C. White. 2004. "In Situ Bioreduction of Technetium and Uranium in a Nitrate-Contaminated Aquifer." *Environmental Science & Technology* 38 (2): 468-475. https://doi.org/10.1021/es034639p.

Kelly, S. D., M. G. Newville, L. Cheng, K. M. Kemner, S. R. Sutton, P. Fenter, N. C. Sturchio, and C. Spötl. 2003. "Uranyl Incorporation in Natural Calcite." *Environmental Science & Technology* 37 (7): 1284-1287. https://doi.org/10.1021/es025962f.

Kimmig, S. R., C. Thompson, S. R. Baum, and C. F. Brown. 2021. "Evaluation of Iodine Speciation and $^{129}I/^{127}I$ Ratios at Low Concentrations in Environmental Samples Using IC-ICP-MS." *Journal of Radioanalytical and Nuclear Chemistry* 327: 929-937. https://doi.org/10.1007/s10967-020-07537-3.

Komlos, J., A. Peacock, R. K. Kukkadapu, and P. R. Jaffé. 2008. "Long-Term Dynamics of Uranium Reduction/Reoxidation under Low Sulfate Conditions." *Geochimica et Cosmochimica Acta* 72 (15): 3603-3615. https://doi.org/10.1016/j.gca.2008.05.040.

Konhauser, K. O. 2009. *Introduction to Geomicrobiology*. John Wiley & Sons.

Konopka, A., A. E. Plymale, D. A. Carvajal, X. Lin, and J. P. McKinley. 2013. "Environmental Controls on the Activity of Aquifer Microbial Communities in the 300 Area of the Hanford Site." *Microbial Ecology* 66 (4): 889-896. https://doi.org/10.1007/s00248-013-0283-3.

Kool, M. M., H. Gruppen, G. Sworn, and H. A. Schols. 2014. "The Influence of the Six Constituent Xanthan Repeating Units on the Order–Disorder Transition of Xanthan." *Carbohydrate Polymers* 104: 94-100. https://doi.org/10.1016/j.carbpol.2013.12.073.

LAB-RPT-12-00001. 2012. *Laboratory Report on the Reduction and Stabilization (Immobilization) of Pertechnetate to Technetium Dioxide Using Tin(II) Apatite.* Washington River Protection Solutions, Richland, WA. https://www.osti.gov/biblio/1045370.

LAB-RPT-12-00002, Rev. 0. 2012. *Laboratory Report on the Removal of Pertechnetate from Tank 241-AN-105 Simulant Using Purolite A530E.* Washington River Protection Solutions, Richland, WA. https://www.osti.gov/biblio/1040714.

Lammers, L. N., H. Rasmussen, D. Adilman, J. L. deLemos, P. Zeeb, D. G. Larson, and A. N. Quicksall. 2017. "Groundwater Uranium Stabilization by a Metastable Hydroxyapatite." *Applied Geochemistry* 84: 105-113. https://doi.org/10.1016/j.apgeochem.2017.06.001.

Larner, B. L., A. J. Seen, and A. T. Townsend. 2006. "Comparative Study of Optimised BCR Sequential Extraction Scheme and Acid Leaching of Elements in the Certified Reference Material NIST 2711." *Analytica Chimica Acta* 556 (2): 444-449. https://doi.org/10.1016/j.aca.2005.09.058.

Lawter, A. R., T. G. Levitskaia, O. Qafoku, M. E. Bowden, F. C. Colon, and N. P. Qafoku. 2021. "Simultaneous Immobilization of Aqueous Co-Contaminants Using a Bismuth Layered Material." *Journal of Environmental Radioactivity* 237: 106711. https://doi.org/10.1016/j.jenvrad.2021.106711.

Lawter, A. R., W. L. Garcia, R. K. Kukkadapu, O. Qafoku, M. E. Bowden, S. A. Saslow, and N. P. Qafoku. 2018. "Technetium and Iodine Aqueous Species Immobilization and Transformations in the Presence of Strong Reductants and Calcite-Forming Solutions: Remedial Action Implications." *Science of the Total Environment* 636: 588-595. https://doi.org/10.1016/j.scitotenv.2018.04.240.

Lee, J. H., J. K. Fredrickson, A. E. Plymale, A. C. Dohnalkova, C. T. Resch, J. P. McKinley, and L. Shi. 2015. "An Autotrophic H_2-Oxidizing, Nitrate-Respiring, Tc(VII)-Reducing *Acidovorax* Sp. Isolated from a Subsurface Oxic-Anoxic Transition Zone." *Environmental Microbiology Reports* 7 (3): 395-403. https://doi.org/10.1111/1758-2229.12263.

Lee, J.-H., J. K. Fredrickson, R. K. Kukkadapu, M. I. Boyanov, K. M. Kemner, X. Lin, D. W. Kennedy, B. N. Bjornstad, A. E. Konopka, D. A. Moore, C. T. Resch, and J. L. Phillips. 2012. "Microbial Reductive Transformation of Phyllosilicate Fe(III) and U(VI) in Fluvial Subsurface Sediments." *Environmental Science & Technology* 46 (7): 3721-3730. https://doi.org/10.1021/es204528m.

Lee, J.-H., J. M. Zachara, J. K. Fredrickson, S. M. Heald, J. P. McKinley, A. E. Plymale, C. T. Resch, and D. A. Moore. 2014. "Fe(II)- and Sulfide-Facilitated Reduction of $^{99}Tc(VII)O_4^-$ in Microbially Reduced

Hyporheic Zone Sediments." *Geochimica et Cosmochimica Acta* 136: 247-264. https://doi.org/10.1016/j.gca.2013.08.017.

Levitskaia, T. G., N. P. Qafoku, M. E. Bowden, R. M. Asmussen, E. C. Buck, V. L. Freedman, and C. I. Pearce. 2022. "A Review of Bismuth(III)-Based Materials for Remediation of Contaminated Sites." *ACS Earth and Space Chemistry* 6 (4): 883-908. https://doi.org/10.1021/acsearthspacechem.1c00114.

Ma, S., L. Huang, L. Ma, Y. Shim, S. M. Islam, P. Wang, L.-D. Zhao, S. Wang, G. Sun, X. Yang, and M. G. Kanatzidis. 2015. "Efficient Uranium Capture by Polysulfide/Layered Double Hydroxide Composites." *Journal of the American Chemical Society* 137 (10): 3670-3677. https://doi.org/10.1021/jacs.5b00762.

McElroy, E., A. R. Lawter, D. Appriou, F. Smith, M. Bowden, O. Qafoku, L. Kovarik, J. E. Szecsody, M. J. Truex, and N. P. Qafoku. 2020. "Iodate Interactions with Calcite: Implications for Natural Attenuation." *Environmental Earth Sciences* 79: 306. https://doi.org/10.1007/s12665-020-09023-1.

McKinley, J. P., J. M. Zachara, J. Wan, D. E. McCready, and S. M. Heald. 2007. "Geochemical Controls on Contaminant Uranium in Vadose Hanford Formation Sediments at the 200 Area and 300 Area, Hanford Site, Washington." *Vadose Zone Journal* 6 (4): 1004-1017. https://doi.org/10.2136/vzj2006.0184.

Moore, R. C., C. I. Pearce, J. Morad, S. Chatterjee, T. Levitskaia, R. M. Asmussen, A. R. Lawter, J. J. Neeway, N. P. Qafoku, M. J. Rigali, S. A. Saslow, J. E. Szecsody, P. D. Thallapally, G. Wang, and V. L. Freedman. 2020. "Iodine Immobilization by Materials through Sorption and Redox-Driven Processes: A Literature Review." *Science of the Total Environment* 716: 132820. https://doi.org/10.1016/j.scitotenv.2019.06.166.

Mossop, K. F., and C. M. Davidson. 2003. "Comparison of Original and Modified BCR Sequential Extraction Procedures for the Fractionation of Copper, Iron, Lead, Manganese and Zinc in Soils and Sediments." *Analytica Chimica Acta* 478 (1): 111-118. https://doi.org/10.1016/S0003-2670(02)01485-X.

Muller, K. A., C. D. Johnson, C. E. Bagwell, and M. J. Truex. 2021a. "Methods for Delivery and Distribution of Amendments for Subsurface Remediation: A Critical Review." *Groundwater Monitoring & Remediation* 41 (1): 46-75. https://doi.org/10.1111/gwmr.12418.

Muller, K. A., L. Zhong, and C. E. Bagwell. 2021b. "Characterizing the Influence of Organic Polymers on the Specific Reactivity of Particulate Remedial Amendments." *Frontiers in Environmental Science* 9: 703851. https://doi.org/10.3389/fenvs.2021.703851.

NBL-345. 1997. *Evaluation of Kinetic Phosphorescence Analysis for the Determination of Uranium.* New Brunswick Laboratory, Argonne, IL. https://www.osti.gov/biblio/335168.

Newsome, L., K. Morris, and J. R. Lloyd. 2014. "The Biogeochemistry and Bioremediation of Uranium and Other Priority Radionuclides." *Chemical Geology* 363: 164-184. https://doi.org/10.1016/j.chemgeo.2013.10.034.

Pan, Z., D. E. Giammar, V. Mehta, L. D. Troyer, J. G. Catalano, and Z. Wang. 2016. "Phosphate-Induced Immobilization of Uranium in Hanford Sediments." *Environmental Science & Technology* 50 (24): 13486-13494. https://doi.org/10.1021/acs.est.6b02928.

Payne, T. E., J. A. Davis, and T. D. Waite. 1994. “Uranium Retention by Weathered Schists - the Role of Iron Minerals.” *Radiochimica Acta* 66-67 (s1): 297-304. https://doi.org/10.1524/ract.1994.6667.special-issue.297.

Pearce, C. I., R. C. Moore, J. W. Morad, R. M. Asmussen, S. Chatterjee, A. R. Lawter, T. G. Levitskaia, J. J. Neeway, N. P. Qafoku, M. J. Rigali, S. A. Saslow, J. E. Szecsody, P. K. Thallapally, G. Wang, and V. L. Freedman. 2020. “Technetium Immobilization by Materials through Sorption and Redox-Driven Processes: A Literature Review.” *Science of the Total Environment* 716: 132849. https://doi.org/10.1016/j.scitotenv.2019.06.195.

Perumal, S., W. Lee, and R. Atchudan. 2022. “A Review on Bismuth-Based Materials for the Removal of Organic and Inorganic Pollutants.” *Chemosphere* 306: 135521. https://doi.org/10.1016/j.chemosphere.2022.135521.

Piscopo, A. N., R. M. Neupauer, and D. C. Mays. 2013. “Engineered Injection and Extraction to Enhance Reaction for Improved In Situ Remediation.” *Water Resources Research* 49 (6): 3618-3625. https://doi.org/10.1002/wrcr.20209.

Placencia-Gómez, E., J. Robinson, L. Slater, and N. P. Qafoku. 2023. “Spectral Induced Polarization Monitoring of Induced Calcite Precipitation in Subsurface Sediments.” *Geophysical Journal International* 232 (1): 57-69. https://doi.org/10.1093/gji/ggac318.

Plymale, A. E., J. K. Fredrickson, J. M. Zachara, A. C. Dohnalkova, S. M. Heald, D. A. Moore, D. W. Kennedy, M. J. Marshall, C. Wang, C. T. Resch, and P. Nachimuthu. 2011. “Competitive Reduction of Pertechnetate ($^{99}TcO_4^-$) by Dissimilatory Metal Reducing Bacteria and Biogenic Fe(II).” *Environmental Science & Technology* 45 (3): 951-957. https://doi.org/10.1021/es1027647.

PNL-10899. 1996. *Strontium-90 Adsorption-Desorption Properties and Sediment Characterization at the 100 N-Area.* Pacific Northwest National Laboratory, Richland, WA. https://www.osti.gov/biblio/186728.

PNNL-14202. 2003. *Mineralogical and Bulk-Rock Geochemical Signatures of Ringold and Hanford Formation Sediments.* Pacific Northwest National Laboratory, Richland, WA. https://www.osti.gov/biblio/15010111.

PNNL-17674. 2008. *Geochemical Characterization of Chromate Contamination in the 100 Area Vadose Zone at the Hanford Site.* Pacific Northwest National Laboratory, Richland, WA. https://www.osti.gov/biblio/936761.

PNNL-17821. 2009. *Electrical Resistivity Correlation to Vadose Zone Sediment and Pore-Water Composition for the BC Cribs and Trenches Area.* Pacific Northwest National Laboratory, Richland, WA. https://www.osti.gov/biblio/962849.

PNNL-18303. 2009. *Sequestration of Sr-90 Subsurface Contamination in the Hanford 100-N Area by Surface Infiltration of a Ca-Citrate-Phosphate Solution.* Pacific Northwest National Laboratory, Richland, WA. https://www.osti.gov/biblio/985589.

PNNL-18529. 2009. *300 Area Uranium Stabilization through Polyphosphate Injection: Final Report.* Pacific Northwest National Laboratory, Richland, WA. https://www.osti.gov/biblio/967237.

PNNL-18879. 2010. *Remediation of Uranium in the Hanford Vadose Zone Using Gas-Transported Reactants: Laboratory-Scale Experiments.* Pacific Northwest National Laboratory, Richland, WA. https://www.osti.gov/biblio/973415.

PNNL-19277. 2010. *Conceptual Models for Migration of Key Groundwater Contaminants through the Vadose Zone and into the Upper Unconfined Aquifer Below the B-Complex.* Pacific Northwest National Laboratory, Richland, WA. https://www.osti.gov/biblio/991093.

PNNL-19524. 2010. *Hanford 100-N Area In Situ Apatite and Phosphate Emplacement by Groundwater and Jet Injection: Geochemical and Physical Core Analysis.* Pacific Northwest National Laboratory, Richland, WA. https://www.osti.gov/biblio/985586.

PNNL-20004. 2010. *Remediation of Uranium in the Hanford Vadose Zone Using Ammonia Gas: FY 2010 Laboratory-Scale Experiments.* Pacific Northwest National Laboratory, Richland, WA. https://www.osti.gov/biblio/1006311.

PNNL-24297, Rev. 1. 2016. *Extended Leach Testing of Simulated LAW Cast Stone Monoliths.* Pacific Northwest National Laboratory. Richland, WA. https://www.osti.gov/biblio/1365453.

PNNL-24709, Rev. 1. 2017. *Conceptual Model of Iodine Behavior in the Subsurface at the Hanford Site.* Pacific Northwest National Laboratory, Richland, WA.

PNNL-25303. 2016. *Use of a Ca-Citrate-Phosphate Solution to Form Hydroxyapatite for Uranium Stabilization of Old Rifle Sediments: Laboratory Proof of Principle Studies.* Pacific Northwest National Laboratory, Richland, WA. https://www.osti.gov/biblio/1561202.

PNNL-26208. 2017. *Contaminant Attenuation and Transport Characterization of 200-DV-1 Operable Unit Sediment Samples.* Pacific Northwest National Laboratory, Richland, WA. https://www.osti.gov/biblio/1368134.

PNNL-26266, Rev. 1. 2018. *Geochemical, Microbial, and Physical Characterization of 200-DV-1 Operable Unit B-Complex Cores from Boreholes C9552, C9487, and C9488 on the Hanford Site Central Plateau.* Pacific Northwest National Laboratory, Richland, WA. https://www.osti.gov/biblio/1488861.

PNNL-26730. 2017. *The Evaluation of Novel Tin Materials for the Removal of Technetium from Groundwater.* Pacific Northwest National Laboratory, Richland, WA. https://www.osti.gov/biblio/1419155.

PNNL-26902. 2018. *Deep Vadose Zone Treatability Test of Soil Desiccation for the Hanford Central Plateau: Final Report.* Pacific Northwest National Laboratory, Richland, WA. https://www.osti.gov/biblio/1423418.

PNNL-27524. 2018. *Contaminant Attenuation and Transport Characterization of 200-DV-1 Operable Unit Sediment Samples from Boreholes C9497, C9498, C9603, C9488, and C9513.* Pacific Northwest National Laboratory, Richland, WA. https://www.osti.gov/biblio/1468977.

PNNL-27846, Rev 0. 2018. *Physical and Hydraulic Properties of Sediments from the 200-DV-1 Operable Unit.* Pacific Northwest National Laboratory, Richland, WA.

PNNL-28054. 2018. *Evaluation of Perched Water Post-Extraction Remedy Technologies: Interim Status Report.* Pacific Northwest National Laboratory, Richland, WA. https://www.osti.gov/biblio/1485489.

PNNL-28055. 2018. *Evaluation of Central Plateau Remediation Alternatives: Interim Status Report.* Pacific Northwest National Laboratory, Richland, WA.

PNNL-29650. 2020. *Evaluation of the Change in Uranium Mobility in Sediments from the Hanford 300-FF-5 Stage B Polyphosphate Field Injection.* Pacific Northwest National Laboratory, Richland, WA. https://www.osti.gov/biblio/1614680.

PNNL-30440, Rev. 1. 2021. *Spectral Induced Polarization-Biogeochemical Relationships for Remediation Amendment Monitoring.* Pacific Northwest National Laboratory, Richland, WA. https://www.osti.gov/biblio/1835069.

PNNL-30443. 2020. *Sediment Mineralogy Data Review for the Hanford Central Plateau.* Pacific Northwest National Laboratory, Richland, WA. https://www.osti.gov/biblio/1735746.

PNNL-31959. 2021. *Combined Technologies for In Situ Remediation of Tc-99 and U in Subsurface Sediments.* Pacific Northwest National Laboratory, Richland, WA. https://www.osti.gov/biblio/1832171.

PNNL-34300. 2023. *200-DV-1 Operable Unit Perched Water Zone Characterization: Borehole D0112.* Pacific Northwest National Laboratory, Richland, WA.

Rahman, Z., and L. Thomas. 2021. "Chemical-Assisted Microbially Mediated Chromium (Cr) (VI) Reduction under the Influence of Various Electron Donors, Redox Mediators, and Other Additives: An Outlook on Enhanced Cr(VI) Removal." *Frontiers in Microbiology* 11: 619766. https://doi.org/10.3389/fmicb.2020.619766.

Regan, S., P. Hynds, and R. Flynn. 2017. "An Overview of Dissolved Organic Carbon in Groundwater and Implications for Drinking Water Safety." *Hydrogeology Journal* 25: 959-967. https://doi.org/10.1007/s10040-017-1583-3.

Robinson, C., S. Shaw, J. R. Lloyd, J. Graham, and K. Morris. 2023. "Phosphate (Bio)Mineralization Remediation of ^{90}Sr-Contaminated Groundwaters." *ACS ES&T Water* 3 (10): 3223-3234. https://doi.org/10.1021/acsestwater.3c00159.

RPP-53855. 2012. *Reduction and Stabilization (Immobilization) of Pertechnetate to an Immobile Reduced Technetium Species Using Tin(II)Apatite.* Washington River Protection Solutions, Richland, WA. https://www.osti.gov/biblio/1055730.

SGW-47062. 2010. *Treatability Test Report for Field-Scale Apatite Jet Injection Demonstration for the 100-NR-2 Operable Unit.* CH2M Hill Plateau Remediation Company, Richland, WA.

SGW-59614, Rev. 0.0. 2016. *300-FF5 Operable Unit Enhanced Attenuation Stage A Delivery Performance Report.* CH2M Hill Plateau Remediation Company, Richland, WA.

SGW-63113, Rev. 0.0. 2020. *300-FF-5 Operable Unit Enhanced Attenuation Uranium Sequestration Completion Report.* CH2M Hill Plateau Remediation Company, Richland, WA.

SGW-67996, Rev. 0. 2022. *Field Summary Report for the 200-DV-1 Operable Unit Extractions Wells, FY2020-2022.* Central Plateau Cleanup Company, Richland, WA.

Shanahan, P. 2004. “Bioremediation” (Lecture Materials). In “Waste Containment and Remediation Technology.” Massachusetts Institute of Technology, MIT OpenCourseWare. https://ocw.mit.edu/courses/1-34-waste-containment-and-remediation-technology-spring-2004/.

Shao, Q., C. Xu, Y. Wang, S. Huang, B. Zhang, L. Huang, D. Fan, and P. G. Tratnyek. 2018. “Dynamic Interactions between Sulfidated Zerovalent Iron and Dissolved Oxygen: Mechanistic Insights for Enhanced Chromate Removal.” *Water Research* 135: 322-330. https://doi.org/10.1016/j.watres.2018.02.030.

SRNL-STI-2009-00637. 2009. *Reduction Capacity of Saltstone and Saltstone Components.* Savannah River National Laboratory, Aiken, SC. https://www.osti.gov/biblio/969345.

SW-846 Update V. 2014. *Metal Cyanide Complexes in Waters and Waste Extracts Using Anion Exchange Chromatography and UV Detection, Method 9015 Rev. 1.0.* U.S. Environmental Protection Agency, Washington, D.C.

Szecsody, J. E., J. S. Fruchter, M. D. Williams, V. R. Vermeul, and D. Sklarew. 2004. “In Situ Chemical Reduction of Aquifer Sediments: Enhancement of Reactive Iron Phases and TCE Dechlorination.” *Environmental Science & Technology* 38 (17): 4656-4663. https://doi.org/10.1021/es034756k.

Szecsody, J. E., M. J. Truex, L. Zhong, J. P. McKinley, N. P. Qafoku, B. D. Lee, and S. D. Saurey. 2015. “Remediation of Technetium in Vadose Zone Sediments Using Ammonia and Hydrogen Sulfide Gases.” *Vadose Zone Journal* 14 (7): 1-12. https://doi.org/1.2136/vzj2014.09.0134.

Szecsody, J. E., M. J. Truex, L. Zhong, T. C. Johnson, N. P. Qafoku, M. D. Williams, W. J. Greenwood, E. L. Wallin, J. D. Bargar, and D. K. Faurie. 2012. “Geochemical and Geophysical Changes during Ammonia Gas Treatment of Vadose Zone Sediments for Uranium Remediation.” *Vadose Zone Journal* 11 (4): 1-13. https://doi.org/10.2136/vzj2011.0158.

Szecsody, J. E., M. J. Truex, N. P. Qafoku, D. M. Wellman, T. Resch, and L. R. Zhong. 2013. “Influence of Acidic and Alkaline Waste Solution Properties on Uranium Migration in Subsurface Sediments.” *Journal of Contaminant Hydrology* 151: 155-175. https://doi.org/10.1016/j.jconhyd.2013.05.009.

Tang, G., W.-M. Wu, D. B. Watson, J. C. Parker, C. W. Schadt, X. Shi, and S. C. Brooks. 2013. “U(VI) Bioreduction with Emulsified Vegetable Oil as the Electron Donor – Microcosm Tests and Model Development.” *Environmental Science & Technology* 47 (7): 3209-3217. https://doi.org/10.1021/es304641b.

Tang, Y., E. J. Ezinga, Y. J. Lee, and R. J. Reeder. 2007. “Coprecipitation of Chromate with Calcite: Batch Experiments and X-Ray Absorption Spectroscopy.” *Geochimica et Cosmochimica Acta* 71 (6): 1480-1493. https://doi.org/10.1016/j.gca.2006.12.010.

Trevors, J. T. 1996. “Sterilization and Inhibition of Microbial Activity in Soil.” *Journal of Microbiological Methods* 26 (1-2): 53-59. https://doi.org/10.1016/0167-7012(96)00843-3.

Triplett, M. B., M. D. Freshley, M. J. Truex, D. M. Wellman, K. D. Gerdes, B. L. Charboneau, J. G. Morse, R. W. Lober, and G. B. Chronister. 2010. “Integrated Strategy to Address Hanford's Deep Vadose Zone Remediation Challenges.” ASME 13th International Conference on Environmental Remediation and Radioactive Waste Management, Tsukuba, Japan, October 3–7, 2010. https://doi.org/10.1115/ICEM2010-40262.

Um, W., J.-S. Yang, R. J. Serne, and J. H. Westsik. 2015. "Reductive Capacity Measurement of Waste Forms for Secondary Radioactive Wastes." *Journal of Nuclear Materials* 467, no. 1: 251-259. https://doi.org/10.1016/j.jnucmat.2015.09.045.

Vermeul, V. R., J. E. Szecsody, B. G. Fritz, M. D. Williams, R. C. Moore, and J. S. Fruchter. 2014. "An Injectable Apatite Permeable Reactive Barrier for In Situ ^{90}Sr Immobilization." *Groundwater Monitoring & Remediation* 34 (2): 28-41. https://doi.org/10.1111/gwmr.12055.

Wellman, D. M., E. M. Pierce, C. C. Bovaird, K. M. Griswold, K. M. Gunderson, S. M. Webb, and J. R. Bargar. 2009. *Laboratory Development of Polyphosphate Remediation Technology for In Situ Treatment of Uranium Contamination in the Vadose Zone and Capillary Fringe.* Pacific Northwest National Laboratory PNNL-SA-65124. Richland, WA. https://www.osti.gov/biblio/1040996.

Wellman, D. M., J. G. Catalano, J. P. Icenhower, and A. P. Gamerdinger. 2005. "Synthesis and Characterization of Sodium Meta-Autunite, $Na[UO_2PO_4]\cdot 3H_2O$." *Radiochimica Acta* 93 (7): 393-399. https://doi.org/10.1524/ract.2005.93.7.393.

Wellman, D. M., J. N. Glovack, K. Parker, E. L. Richards, and E. M. Pierce. 2008. "Sequestration and Retention of Uranium(VI) in the Presence of Hydroxylapatite under Dynamic Geochemical Conditions." *Environmental Chemistry* 5 (1): 40-50. https://doi.org/10.1071/en07060.

Wellman, D. M., J. S. Fruchter, V. R. Vermeul, E. Richards, D. P. Jansik, and E. Edge. 2011. "Evaluation of the Efficacy of Polyphosphate Remediation Technology: Direct and Indirect Remediation of Uranium under Alkaline Conditions." *Technology & Innovation* 13 (2): 151-164. https://doi.org/10.3727/194982411X13085939956544.

Wildung, R. E., Y. A. Gorby, K. M. Krupka, N. J. Hess, S. W. Li, A. E. Plymale, J. P. McKinley, and J. K. Fredrickson. 2000. "Effect of Electron Donor and Solution Chemistry on Products of Dissimilatory Reduction of Technetium by *Shewanella Putrefaciens*." *Applied and Environmental Microbiology* 66 (6): 2451-2460. https://doi.org/10.1128/AEM.66.6.2451-2460.2000. PMCID: PMC110556.

Williams, K. H., P. E. Long, J. A. Davis, M. J. Wilkins, A. L. N'Guessan, C. I. Steefel, L. Yang, D. Newcomer, F. A. Spane, and L. J. Kerkhof. 2011. "Acetate Availability and Its Influence on Sustainable Bioremediation of Uranium-Contaminated Groundwater." *Geomicrobiology Journal* 28 (5-6): 519-539. https://doi.org/10.1080/01490451.2010.520074.

WSRC-MS-2005-00589. 2005. *Gas: A Neglected Phase in Remediation of Metals and Radionuclides.* Savannah River National Laboratory, Aiken, SC.

WSRC-MS-94-0323. 1994. *Technology Summary of the In Situ Bioremediation Demonstration (Methane Biostimulation) via Horizontal Wells at the Savannah River Site Integrated Demonstration Project.* Savannah River Site, Aiken, SC.

Xin, J., F. Tang, X. Zheng, H. Shao, and O. Kolditz. 2016. "Transport and Retention of Xanthan Gum-Stabilized Microscale Zero-Valent Iron Particles in Saturated Porous Media." *Water Research* 88: 199-206. https://doi.org/10.1016/j.watres.2015.10.005.

Xin, J., S. Fan, M. Yuan, X. Wang, X. Zhang, and X. Zheng. 2020. "Effects of Co-Existing Nitrate on TCE Removal by mZVI under Different Pollution Load Scenarios: Kinetics, Electron Efficiency and Mechanisms." *Science of the Total Environment* 716: 137111. https://doi.org/10.1016/j.scitotenv.2020.137111.

Zhang, S., C. Xu, D. Creeley, Y.-F. Ho, H.-P. Li, R. Grandbois, K. A. Schwehr, D. I. Kaplan, C. M. Yeager, D. Wellman, and P. H. Santschi. 2013. "Iodine-129 and Iodine-127 Speciation in Groundwater at the Hanford Site, US: Iodate Incorporation into Calcite." *Environmental Science & Technology* 47 (17): 9635-9642. https://doi.org/10.1021/es401816e.

Zhang, T., T. Wang, W. Wang, B. Liu, W. Li, and Y. Liu. 2020. "Reduction and Stabilization of Cr(VI) in Soil by Using Calcium Polysulfide: Catalysis of Natural Iron Oxides." *Environmental Research* 190: 109992. https://doi.org/10.1016/j.envres.2020.109992.

Zook, A. C., L. H. Collins, and C. E. Pietri. 1981. "Determination of Nanogram Quantities of Uranium by Pulsed-Laser Fluorometry." *Microchimica Acta* 76: 457-468. https://doi.org/10.1007/BF01196964.

Appendix A – Sediment Characterization

A.1 X-ray Diffraction

The < 2-mm size fractions for the Cold Creek Unit gravel (CCug), Hanford formation (Hf), and perching zone sand (PZsd) sediments were dried at ambient conditions and then powdered using a mortar and pestle. Zinc oxide powder (standard reference material 1979, NIST) was added at 10 wt% to the pulverized sediments, and then homogenized a second time using a mortar and pestle again. X-ray diffraction (XRD) patterns were collected with Cu Kα radiation (λ=1.5418 Å) using a Rigaku Miniflex II unit. The Miniflex was operated at 30 kV and 15 mA and patterns were collected between 3 and 90 °2θ, using a scan width of 0.04° and a 5-second count time. Identification of material phases was carried out using JADE XRD pattern processing software and reference patterns from the International Centre for Diffraction Data powder diffraction database. Quantitation of material phases was done using TOPAS software.

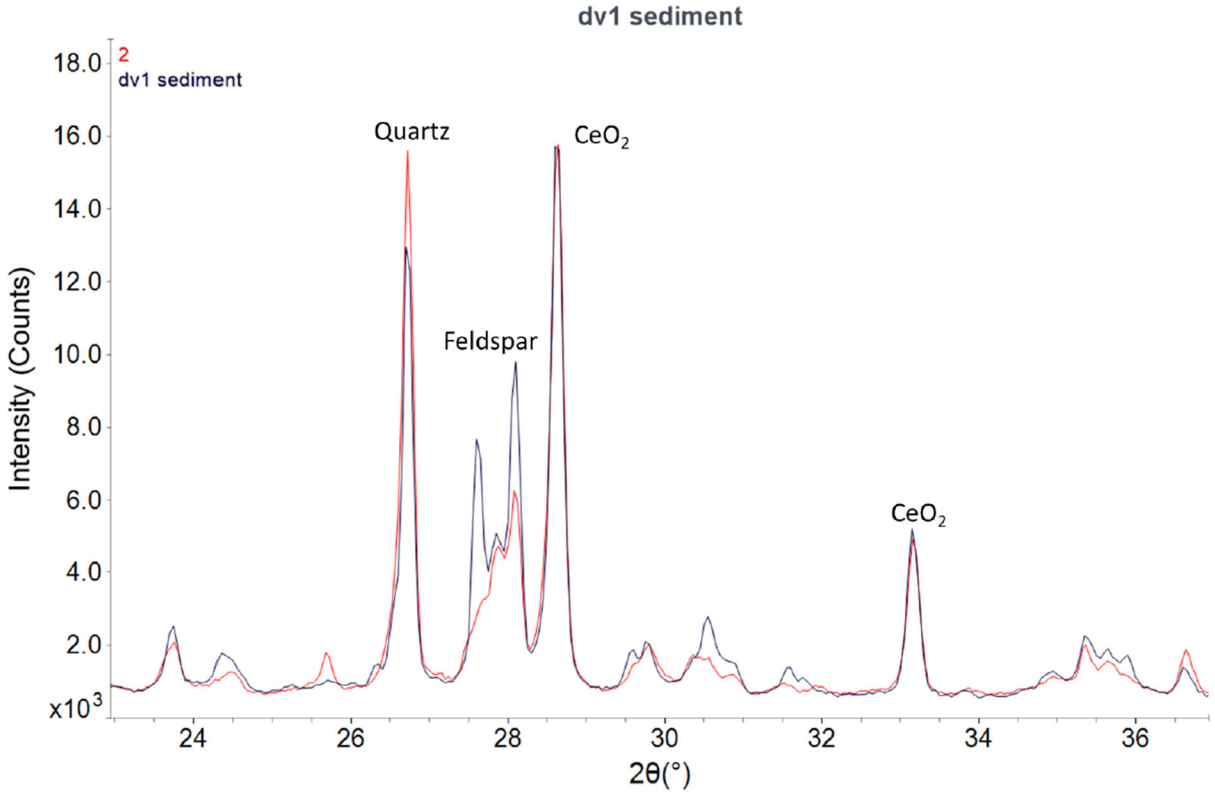

Figure A.1. Comparison of XRD patterns for uncontaminated Hf sediment before (blue) and after (red) heat treatment.

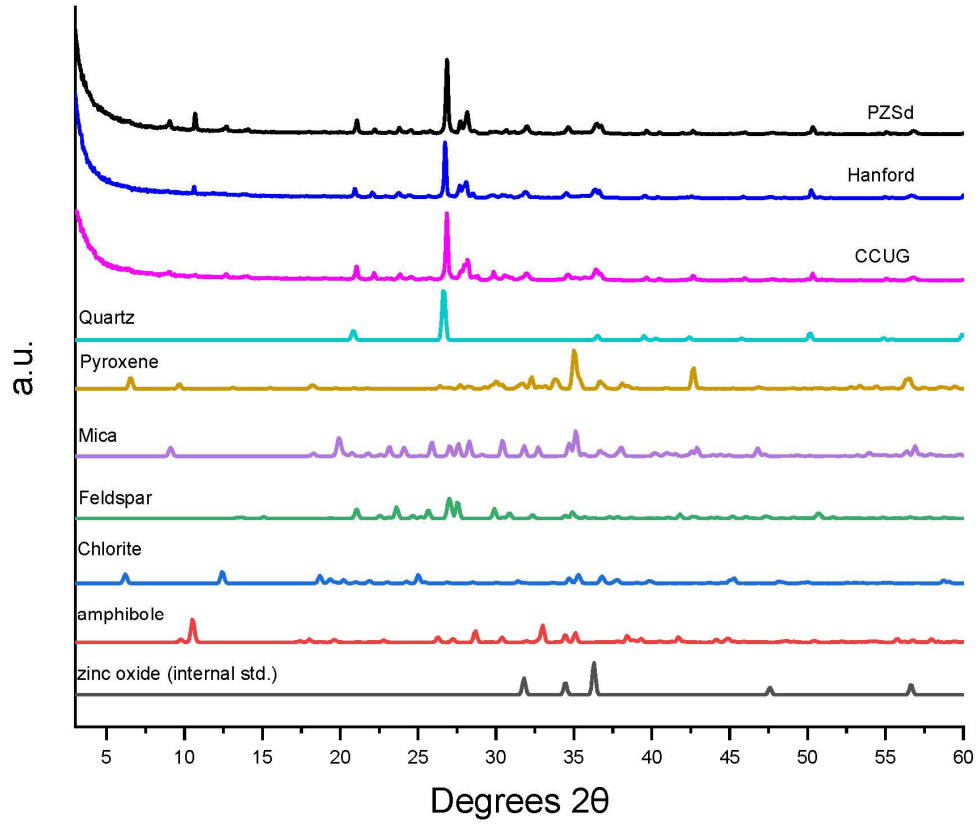

Figure A.2. Comparison of XRD pattern for PZsd, CCug, and Hf sediments alongside major minerals. Note: a.u.is arbitrary units.

A.2 Particle Size

Sediment particle size analysis was conducted by sieve analysis and laser particle size analysis on air-dried sediments. Sieve particle size analysis was conducted on all composite sediments. Laser particle size analysis (ASTM B822-20) was conducted on the sediments on the < 2-mm size fraction in addition to sieve analysis as shown in Figure A.3. The two methods are not directly comparable but do indicate that there is a significant fraction of clay-sized particles coating larger sand particles within the Hf sediment that are likely broken up during sonication with the laser particle size analysis method.

Particle size analysis of the DV-1 sediments was conducted using a Horiba LA-950V2 Laser Scatter Particle Size Analyzer in accordance with the ASTM D4464-15 standard. A subsample of the < 2 mm fraction was dried and introduced into the instrument reservoir containing deionized water until the sample's transmittance fell below 90%. The analyzer was set to operate with a circulation speed of 7 and an agitation speed of 5. To ensure uniform dispersion and break apart material clumps, the samples were subjected to ultrasonication for 20 seconds immediately prior to measurement.

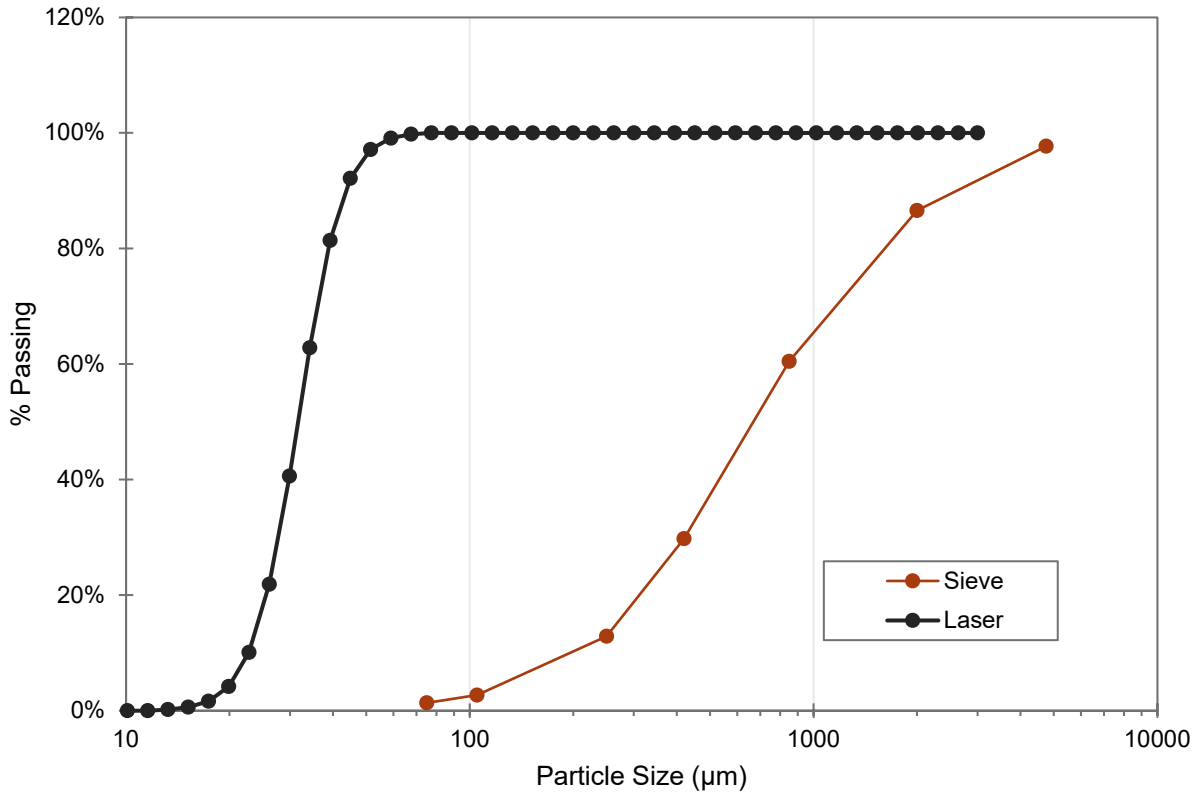

Figure A.3. Comparison of laser (*black*) and sieve (*orange*) particle size analysis for uncontaminated Hf sediment with the cumulative percent passing through the indicated particle size.

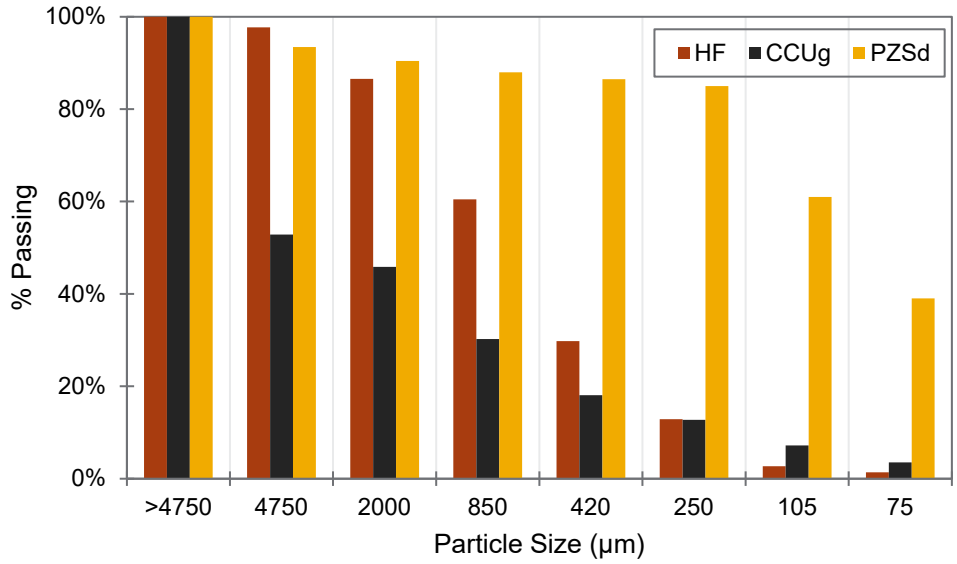

Figure A.4. Sieve particle size analysis for composite sediments with Hf sediments (*black*), CCug sediments (*red*), and PZsd (*yellow*).

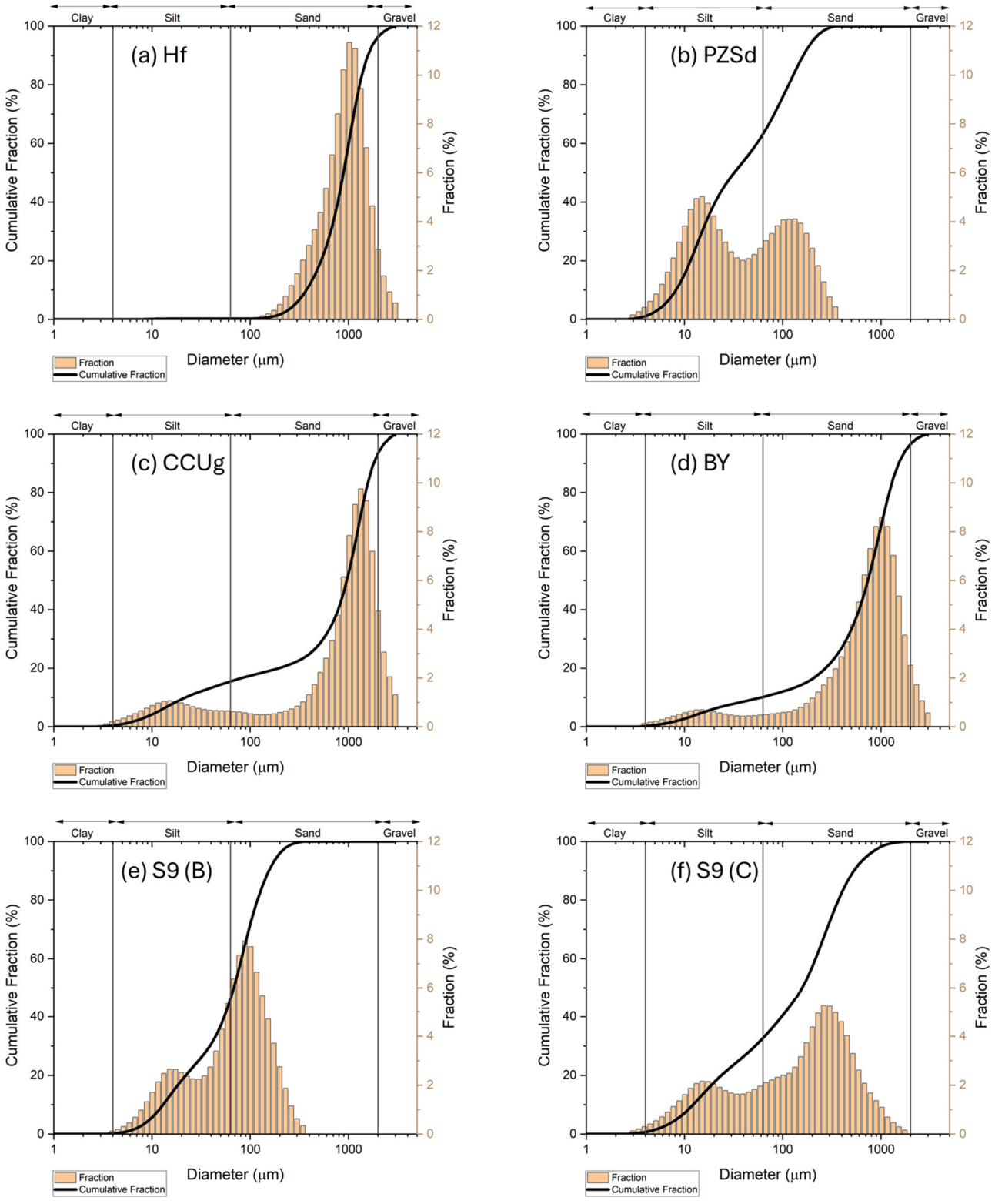

Figure A.5. Laser particle size analysis for the < 2 mm size fraction of the composite sediments (a) Hf, (b) PZsd, (c) CCug, (d) BY, (e) 216-S-9 (B – batch), and (f) 216-S-9 (C – column).

A.3 BET Surface Area

The samples, Hf, CCug, 216-S-9, BY, and PZsd, were analyzed in triplicate by the Brunauer-Emmett-Teller (BET) method for specific surface area using an accelerated surface area and porosity system from Micromeritics. Nitrogen gas adsorption and desorption isotherms were recorded at 77K by volumetric adsorption in a relative pressure range, P/Po, of 0.01-0.22, 0.06-0.19, and 0.07-0.20, respectively. Specific surface area was calculated from these pressure ranges using the BET equation. Samples were prepared prior to analysis by degassing 0.5 g of material in vacuum (133.3 kPa) at 25 °C for 9 hours to remove humidity and possible contaminants. Degas parameters were chosen based on previous experience with similar materials and to avoid material decomposition. Two aluminosilicate standards (Micromeritics) with known surface areas of 215 ± 6 m^2/g and 216 ± 6 m^2/g, respectively, were analyzed before and after analysis of samples. The average measured surface area of the initial standard was 207.7 m^2/g (three replicates), and 211.9 m^2/g for the final standard analysis (single replicate). An additional alumina standard (Micromeritics) with a known surface area of 26.6 ± 2.0 m^2/g was analyzed before and after analysis of samples. The average measured surface area of all standard measurements was 25.02 m^2/g (three replicates). These values were within 10% of the certified value or within the acceptable range specified for each specific standard.

Three particulate amendment samples, sulfur-modified iron, SnAp-A, and SnAp-B were analyzed in triplicate by the BET method for specific surface area using a TriStar II Plus Surface Area and Porosity Analyzer from Micromeritics. Nitrogen gas adsorption and desorption isotherms were recorded at 77K by volumetric adsorption in a relative pressure range, P/P_o, of 0.05- 0.30. Specific surface area was calculated from these pressure ranges using the BET equation. Samples were prepared prior to analysis by degassing 1.0 g of material in vacuum (100 μmHg) at 25 °C overnight to remove humidity and possible contaminants. Degas parameters were chosen based on previous experience with similar materials and to avoid material decomposition. An alumina standard (Micromeritics) with a known surface area of 26.6 ± 2.0 m^2/g was analyzed before and after analysis of samples. The average measured surface area of all standard measurements was 26.22 m^2/g (five replicates). These values are within 2% of the certified value.

A.4 Cation Exchange Capacity Assumptions

The cation exchange capacity (CEC) is important for estimating the amount of Ca to be added for both Poly-PO_4 and Ca-Cit-PO_4 technologies to form apatite. Therefore, an estimated CEC value was used for the following technologies to estimate the needed Ca to form apatite based on a required molar ratio of 1.67:1 for Ca:P: particulate phase chemical reduction and sequestration (Section 3.5.6), liquid-phase chemical sequestration (Section 3.5.7), liquid-phase chemical reduction and sequestration (Section 3.5.8), and liquid-phase bioreduction and sequestration (Section 3.5.9). The CEC of each sediment was not measured; however, an estimate was used based on previous characterization of similar sediments. For the Hf, previous estimates of CEC ranged from 1 to 5 meq per 100 g of sediment (PNNL-30443), 5.3 meq/100g for B-Complex sediments (McKinley et al. 2007), and 3 to 9 meq/100 g (averaging 6.5) for BC Cribs boreholes (PNNL-17821) with approximately 77% of the exchange sites being Ca (Szecsody et al. 2012). A conservative assumption of 2 meq per 100 g total CEC with 77% as Ca was used, resulting in an estimated 0.0077 mmol Ca/g of sediment, although there may be additional Ca available from dissolution of other minerals (e.g., calcite). Therefore, for typical batch experiments (1:2 sediment-to-liquid ratio), some additional aqueous Ca^{2+} is needed for both liquid apatite amendments (Poly-PO_4 and Ca-Cit-PO_4) to be added based on the calculated Ca/PO_4 ratio for apatite (Ca:PO_4 is 1.67) as approximately 3.85 mmol Ca/L would be available in the 1:2 sediment-to-solution ratio, allowing for a maximum of 2.31 mmol PO_4/L (as compared to treatment of 24 to 36 mmol PO_4/L here).

A.5 Total and Inorganic Carbon

Total carbon (TC) and total inorganic carbon (TIC) of sediments were measured using a carbon analyzer (Shimadzu model TOC-L CSH/CSN E100V). For TC analysis of solid samples, the combustion temperature in the SSM-5000A solid sample module is set to 900 °C. The CO_2 gas passes through a non-dispersive infrared (NDIR) gas analyzer, where the CO_2 is detected. The analog signal of the NDIR detector forms a peak and the area is measured by the data processor. For TIC analysis of solid samples using the SSM-5000A solid sample module, 25% phosphoric acid is added to the ceramic sample boat containing the sample at 200 °C. This produces CO_2, which is measured by the NDIR detector, as described above. Then, total organic carbon is calculated from TC minus TIC.

A.6 Microbial Characterization

A.6.1 DNA Extraction

Sediment samples (0.25 g) were extracted using the DNeasy PowerSoil Pro Kit (Qiagen) following the manufacturer's instructions, along with blanks for quality control. DNA quality and quantity were quantified using a NanoDrop 8000 UV-Vis Spectrophotometer (Thermo Scientific, Wilmington, DE).

A.6.2 Quantitative Polymerase Chain Reaction

Microbial biomass estimations were determined using quantitative polymerase chain reaction (qPCR) and universal 16S rRNA gene primers. qPCR assays were performed using a Bio-Rad CFX96 Real-Time PCR Detection System (Bio-Rad Laboratories, Hercules, CA). An Advanced SYBR Green supermix kit (Bio-Rad Laboratories, Hercules, CA) was used for amplification and real-time fluorescence measurement. Each PCR reaction was 20 µL final volume and contained 1X of hot-start Sso7d-fusion polymerase, SYBR Green dye, dNTPs, $MgCl_2$, and stabilizers. Amplification conditions included an extended denaturation step of 2 minutes at 98 °C, followed by 40 cycles of denaturation at 98 °C (30 seconds), 48 °C annealing for 30 seconds, and a 30-second extension. Fluorescence was read at the end of each extension step. DNA from *E.coli* K-12 was used as a positive control and calibration standard to calculate gene copy number from samples.

A.7 Baseline Contaminant Concentrations

Extractions were conducted on sediments collected from the Hanford Site to measure background contaminant concentrations present from either natural abundance or potential waste components in contaminated regions of the Hanford Site subsurface. For comparison, the Hf sediment from Pasco, WA, measured approximately 1.2 µg/g U. Results for the primary contaminants of interest and co-contaminants of interest are presented in Table A.1 based on an average of 2-4 samples digested using the following methods.

Water and tetramethylammonium hydroxide (TMAH) extractions were conducted by spiking 1 g of sediment with 20 mL of water or 5% TMAH. Water samples were placed on a shaker and allowed to shake for 1 hour at 200 rpm. TMAH samples were placed in an oven at 70 °C for 3 hours and were shaken approximately every 15 minutes. Full acid and 8 M HNO_3 extractions were conducted by spiking 0.1 g of sediment with 7 mL of a HNO_3, HCl, and HF mixture and HNO_3 respectively. Samples were placed in a heating block at 90 °C for 2 hours. All samples were then subjected to centrifugation at 3000 rpm for 10 minutes. Thereafter, supernatant was removed, filtered with a 0.45-µm pore size syringe filter, and submitted for analysis as described in Section 3.4.

Table A.1. Contaminant concentrations in composite sediments prior to contaminant additions.

Sediment	Cr (µg/g)[a]	Sr (µg/g)[a]	I (µg/g)[b]	Tc-99 (µg/g)[c]	U (µg/g)[c]
216-S-9	24.4	181	0.21	0.02	0.75
BY Cribs	22.8	191	0.08	0.02	0.65
CCug	18.1	205	0.07	0.02	2.88
PZsd	39.1	201	0.27	0.03	70.30

(a) Full acid (HNO_3, HCl, and HF) extraction
(b) TMAH extraction
(c) 8 M HNO_3 extraction

Appendix B – Supporting Data for Gas-Phase Bioreduction and Chemical Sequestration Technology

B.1 Selection of Organic Gases for Bioreduction

Of the nine organic compounds investigated in previous studies (Bagwell et al. 2020), five created a reducing environment resulting in reduction of Tc-99 [as $Tc(VII)O_4^-$] and uranium at both 4% and 8% water content (WC) (pentane, butane, ethane, butyl acetate, butyrate, Table B.1). Two gases were effective only at 8% WC (propane, ethanol), while the two remaining gases did not reduce contaminants under any conditions (ethyl acetate, dimethyl sulfoxide). Additional physicochemical properties of the gases (i.e., gas/liquid partitioning, density, adsorption to sediments) were evaluated in this study before three organic gases were selected (ethane, butane, butyl acetate). For compounds with a low Henry's law partition coefficient (green, Table B.1), a high fraction of the organic mass will partition into the liquid phase, but there is still sufficient mass in the gas phase to inject. For these two gases (ethyl acetate and ethanol), at 4% WC in vadose zone (VZ) sediment (average for the Hanford formation), 40 pore volumes are needed for ethyl acetate, or 1071 pore volumes of injection are needed for ethanol to reach gas-liquid equilibrium, which is easily achieved at field scale. Finally, for compounds with a very low Henry's law partition coefficient (gray, Table B.1), because the gas phase mass is so small, a very large (26,000+) number of pore volumes are needed to inject enough mass in gas phase to achieve gas-liquid equilibrium. These low-volatility organic compounds are not suitable for gas-phase VZ injection.

Selected gas-phase injection concentrations of 4.6% ethane, 47% butane, and 0.0075% butyl acetate were calculated to achieve 30 mg/L of each organic in pore water (Table B.1). For butane and ethane, if higher gas-phase concentrations are used, the aqueous solubility would limit partitioning to ~60 mg/L. A higher gas-phase concentration for butyl acetate should not be used, as the aqueous solubility of 6800 mg/L would be toxic to the microbial population. These three gases also exhibit low sorption to sediment, which results in a small retardation (sediment/water retardation estimated at 3.8 to 5.3, Table B.1), which will increase the mass at the sediment/pore water interface where microbes are.

Although previous bioreduction experiments used pentane and butyrate, the physico-chemical characteristics of the different gases (i.e., Henry's law partitioning, gas density) create additional constraints on which gases are most useful at field scale. More importantly, at field scale, maintaining gases in an injection zone (both laterally and vertically) will be difficult due to high gas-phase diffusion (of all gases) diluting the concentration and density sinking for those gases denser than air. For the group of highly volatile gases (in white, Table B.1), ethane has a density nearly the same as air (1.225 kg/m^3), but nearly all of the other highly volatile gases have much greater densities relative to air, so would sink. This results in these gases being difficult to maintain at the same location vertically in the VZ (i.e., injection zone), if most of the mass remained as a gas. This could be controlled by gas recirculation. In this study, three organic gases (ethane, butane, and ethyl acetate) were selected, based on the ability to create a reducing environment, reduce contaminants, and physico-chemical characteristics that enable gas-phase injection but reactivity in pore water. Although ethane, butane, and ethyl acetate are currently selected, different gases may be selected after additional consideration of bioreduction and characteristics.

Table B.1. Bioreduction and physico-chemical properties of organic gases.

compound	K_H dimensionless	aq. solubility (mg/L)	liquid/gas Rf (4% H_2O)	liquid/gas Rf (8% H_2O)	sed./H_2O Rf (sorption)	gas density (kg/m3)	biodeg.** (4%, 8% WC)	organic gas (%)* at 4% WC	organic gas (%)* at 8% WC
pentane	51.32	40	1.006	1.016	6.33	2.964	yes	0.23	0.60
ethane	1.980	56.8	1.150	1.427	3.85	1.26	yes	0.49	1.03
propane	27.71	47	1.011	1.030	4.43	1.865	8% not 4%	0.38	0.97
butane	37.79	61	1.008	1.022	5.27	2.496	yes	0.29	0.74
butyl acetate	1.19E-02	6800	26.0	72.15	3.96	0.0631	yes	5.59E-03	5.25E-03
ethyl acetate	6.40E-03	83000	47.44	133.13	3.12	0.3858	no	4.04E-03	3.75E-03
ethanol	2.1879E-05	miscible	13577	38623.6	2.58	1.59	8% only	2.70E-05	2.47E-05
butyrate	8.84E-06	miscible	33583	95541	0.00	0.5959	yes	5.71E-06	5.22E-06
dimethyl sulfoxide	2.03E-06	miscible	146315	416266	2.27	3.013	no	1.48E-06	1.35E-06
air						1.205			
carbon dioxide						1.839			

* to inject in gas phase to achieve 30 mg/L organic in pore water

The lateral diffusion of organic gases in the VZ results in dilution of the gas-phase concentration. Diffusion calculations show that at a 15-ft lateral distance, after about 60 to 80 days, the gas-phase concentration decreases by 50% (Figure B.1a). These 1-D diffusion simulations used an analytical solution (see Appendix C, Section C.1). Gas-phase diffusion is slower at higher WC due to greater tortuosity (Figure B.1b).

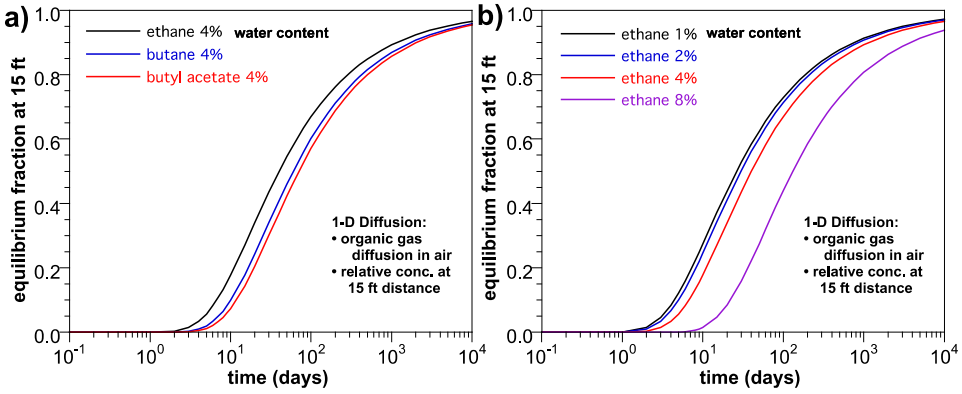

Figure B.1. Calculated 1-D gas diffusion through VZ sediment of (a) different gases at 4% WC, and (b) ethane at different WC. These data are For Information Only (FIO).

B.2 Bioreduction and Sequestration of Tc-99 in Field-Contaminated Sediments – Microbial characterization

For the Hanford test sediment, measurement of microbial biomass (data are FIO) after organic gas and subsequent CO_2 gas treatment showed a large decrease for ethane/CO_2 but no change for butane/CO_2 and butyl acetate/CO_2 treatments (Figure B.2; note that the x-axis scale shows times for organic gas and CO_2 treatments).

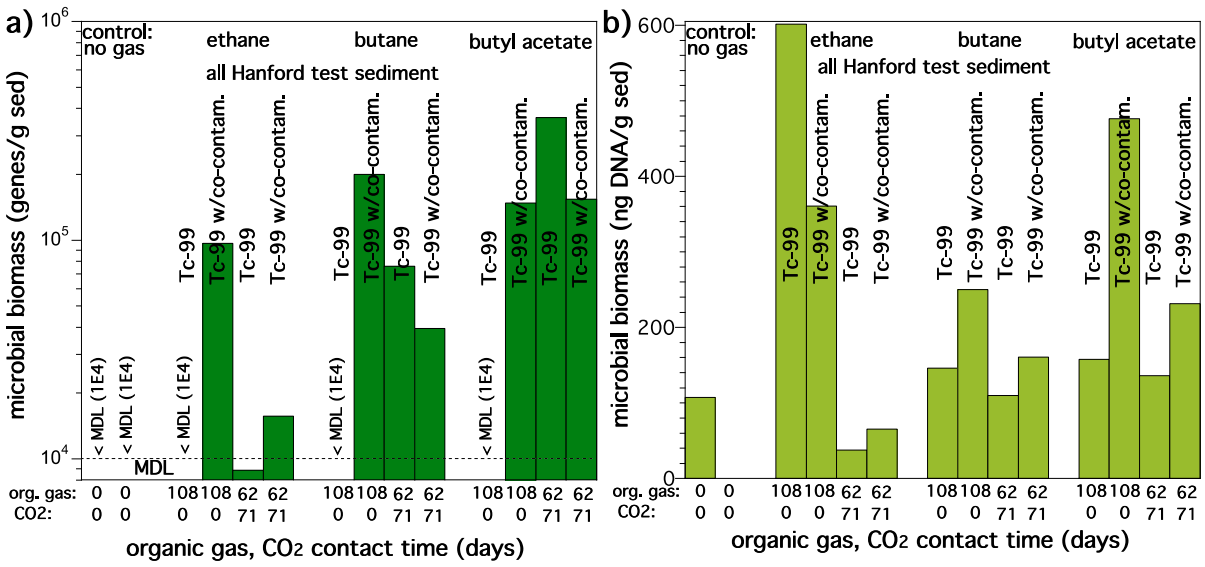

Figure B.2. Change in microbial biomass for Hanford formation sediment subjected to organic gas then CO_2 gas treatments. Data shown as (a) genes/g sediment, and (b) ng DNA/g sediment. These data are FIO.

For the field-contaminated sediments, microbial biomass characterization of untreated, ethane treated, and ethane/CO_2 treated sediments did not indicate consistent trends. For the BY Cribs sediments, ethane treatment did result in elevated microbial biomass (Figure B.3), but no change was observed for BC Cribs and 216-U-8 Crib sediments. This information is FIO.

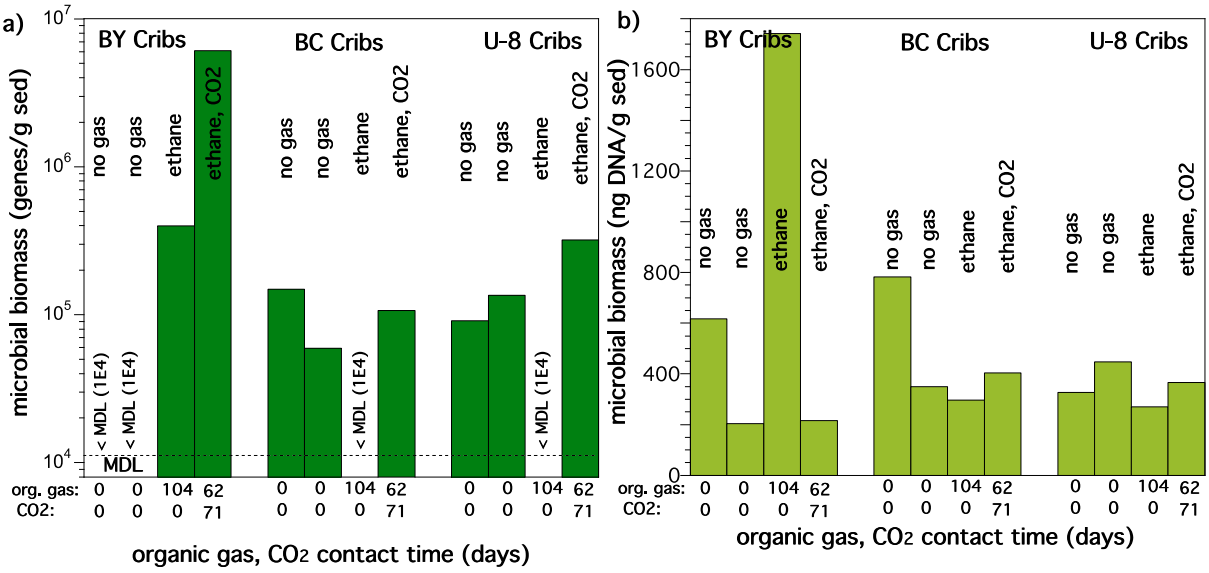

Figure B.3. Changes in microbial biomass for BY Cribs, BC Cribs, and 216-U-8 Crib sediments from ethane and CO_2 gas treatments. Data shown as (a) genes/g sediment, and (b) ng DNA/g sediment. These data are FIO.

B.3 Rate and Extent of Bioreduction and Sequestration of CoCOIs

Most of the co-contaminants of interest (CoCOIs) present are redox reactive species (initially as $I^{V}O_3$, $Cr^{VI}O_4$, $N^{V}O_3$, U^{VI}, and CN), but Sr is not and will be present as a divalent cation (Sr^{2+}). Creation of the bioreducing environment by addition of one of the organic gases can result in no, partial, or complete reduction of redox-reactive contaminants, depending on the redox potential and capacity. Based on the redox potential needed to reduce contaminants, it is expected that IO_3^-, CrO_4^{-2}, and NO_3^- will be reduced before $Tc(VII)O_4^-$:

$$IO_3^- > CrO_4^- > NO_3^- > \mathbf{TcO_4^-} > Fe^{III}(CN)_6^{3-} > UO_2^{2+}$$

Reduction of these CoCOIs can decrease the reduction of $Tc(VII)O_4^-$ as reductive capacity is consumed by CoCOI reduction.

For the subsequent CO_2 treatment that should result in calcite precipitation, co-precipitation and coating has been previously shown to decrease contaminant mobility (Table B.2). Some CoCOIs are readily incorporated into calcite [Sr^{2+} substitution for Ca^{2+} in calcite, co-precipitation of $CaCrO_4$, $U(VI)O_2^+$ substitution into calcite] and some contaminants have a more limited substitution into calcite (IO_3^- and TcO_4^-). In addition, any contaminants that precipitated in the reducing environment [i.e., $U(IV)O_2$, $Tc(IV)O_2$] might be coated by the calcite precipitate, thus decreasing its mobility. Nitrate is not expected to incorporate into calcite or be coated by calcite. Cyanide was added as the reduced species commonly found [$Fe^{II}(CN)_6^{4-}$], so no reduction is expected.

Table B.2. Predicted effect of organic gas bioreduction and calcite precipitation on CoCOI mobility.

Gas	Process	IO_3^-	CrO_4^-	NO_3^-	TcO_4^-	$Fe^{III}(CN)_6^{3-}$	$Ca_2UO_2(CO_3)_3$ (aq)	Sr^{2+}
Organic	Bioreduction	Reduced, mobile	Reduced, perm. ng/L	Reduced, mobile	Reduced, temp. ng/L	Reduced, mobile	Reduced, temp. ng/L	No change
CO_2	Calcite precipitation	Some incorp.	High incorp.	No change	Some incorp., coating	Some coating	Some incorp., coating	High incorp.

Changes in concentrations of IO_3^-, CrO_4^-, U, CN^-, and nitrate during bioreduction with the three organic gases indicated that mild reducing conditions were created by the addition of ethane, butane, or butyl acetate to sediments that stimulated microbial biodegradation (Table B.3, detailed plots in Sections B.4 to B.9). While most chromate (66% to 88%) was reduced to immobile precipitates that are not easily oxidized, about half of the IO_3 was sequestered (44% to 56%). Although NO_3^- is more easily reduced compared to $Tc(VII)O_4^-$, no NO_3^- reduction was observed. This may be due to the very high nitrate concentration present in pore water (5400 ± 680 mg/L, Figure B.6). For contaminants that required stronger reducing conditions, 10% to 30% of the Tc-99 was reduced and only a small fraction of uranium was sequestered (7% to 16%) that was greater than the no-gas control (69.6%) and was also only slightly greater than the standard deviation of the control (12.1%).

These data indicate that the organic gas additions created mild reducing conditions, as easily reduced species were mainly reduced (i.e., chromate) and species requiring a greater reduction potential had no reduction or only a small fraction was reduced [i.e., $Tc(VII)O_4^-$ and U(VI) species]. Strontium (stable isotopes Sr-84, Sr-86, Sr-87, Sr-88) initially present as a cation (Sr^{2+}) is not redox reactive and mainly adsorbs strongly to sediment ion exchange sites with a similar affinity to that of Ca^{2+}. Therefore, the mild

reducing conditions resulting from the organic gas treatment of the sediment should not influence Sr-87 mobility. Extractions showed a slight increase in Sr sequestration, from 52% (no-gas control) to 57%, for ethane and butane that was greater than the standard deviation (1.5%). This may have resulted from precipitation of Sr-carbonate.

Table B.3. Summary of change in CoCOI mobility because of the organic gas and CO_2 treatments. Color indicates performance increase of 1 (light green), 2 (medium green), or 3+ (dark green) standard deviations or worse performance (pink)

Treatment	IO_3^- seq.	CrO_4^- seq.	NO_3^- seq.	TcO_4^- seq.	$Fe^{III}(CN)_6^{3-}$ seq.	$Ca_2UO_2(CO_3)_3$ seq.	Sr^{+2} seq.
control (no gas)	0.00	0.00	0.00	0.129	0.00	0.70	0.52
ethane	0.49	0.79 ± 0.04	0.00	0.18 ± 0.02	0.20 ± 0.16	0.77 ± 0.03	0.57 ± 0.02
ethane + CO_2	0.069	0.99 ± 0.01	0.00	0.13 ± 0.05	0.20 ± 0.23	0.66 ± 0.04	0.00
butane	0.45	0.88 ± 0.05	0.00	0.24 ± 0.04	0.12 ± 0.27	0.76 ± 0.03	0.57 ± 0.01
butane + CO_2	-0.03	0.99 ± 0.01	0.00	0.16 ± 0.05	0.12 ± 0.18	0.62 ± 0.18	0.47
butyl acetate	0.57	0.66 ± 0.52	0.00	0.15 ± 0.02	0.22 ± 0.24	0.86 ± 0.08	0.51 ± 0.01
butyl acetate + CO_2	0.34	0.99 ± 0.01	0.09 ± 0.08	0.14 ± 0.02	0.37 ± 0.22	0.78 ± 0.08	0.00

For the subsequent CO_2 gas treatment, the influence on contaminants was mixed. Once chromate is reduced to $Cr(III)(OH)_3$ by the initial organic gas reduction, it is difficult to oxidize even in an aerobic environment. Treatment with CO_2 resulted in additional removal of chromate from aqueous solution (Section B.4), so all three organic gases with subsequent CO_2 treatment had > 99% of the aqueous chromate sequestered in precipitates. Sr^{2+}, which should incorporate into precipitating calcite, showed a large decrease in sequestration (i.e., increase in mobility), greater than the no-gas control. This was likely because the Sr^{2+} cation was more mobile in the mildly acidic (i.e., pH 5.5) pore water.

For most of the redox-reactive contaminants (IO_3, TcO_4, and U), the subsequent CO_2 gas treatment resulted in greater contaminant mobilization compared to the organic-gas-only treatment. For pertechnetate, while organic gas treatment decreased mobility to a small extent (5% to 20%), the subsequent CO_2 treatment returned pertechnetate mobility to no-treatment levels (Table B.4). For uranium, organic gas treatment resulted in 7% to 16% mobility decrease, and subsequent CO_2 treatment for ethane and butane resulted in greater uranium mobility than untreated sediments. IO_3 mobility also increased substantially with CO_2 gas treatment. Because it is hypothesized that the CO_2 gas treatment for 1700 hours was an insufficient time to result in calcite precipitation, these changes in TcO_4, U, and IO_3 mobility likely resulted from the slight acidification of the pore water (to pH 5.5), which would dissolve some existing calcite (which may incorporate IO_3, TcO_4, and U). In addition, uranium sorption would decrease at pH 5.5 compared to pretreatment pH 8. The Sr^{2+} data, which should also highly incorporate into precipitating calcite, were consistent with U and pertechnetate data in that Sr^{2+} sequestration decreased (i.e., mobility increased) with the addition of CO_2 because little or no calcite precipitated during the 2 months of CO_2 treatment time. The rate of change of Sr^{2+} sequestration due to the organic gas treatment had a half-life of ~1200 hours for ethane and butane. Nitrate mobility was unchanged by the organic gas and subsequent CO_2 treatment, indicating nitrate was neither reduced nor precipitated.

Table B.4. Rate of CoCOI reduction and sequestration.

	IO_3^-	CrO_4^-	NO_3^-	TcO_4^-	$Fe^{III}(CN)_6^{3-}$	$Ca_2UO_2(CO_3)_3$	Sr^{+2}
Treatment	Half-Life (h)	Half-Life (weeks)	Half-Life (weeks)	Half-Life (weeks)	Half-Life (weeks)	Half-Life (weeks)	Half-Life (weeks)
Ethane	*	7	No change	3	5	No change	7
Ethane + CO_2	*	No change	No change	No change	5	5	< 2
Butane	*	7	5	7	5	No change	7
Butane + CO_2	*	No change	No change	5	5	5	5
Butyl acetate	*	7	No change	500	No change	7	No change
Butyl acetate + CO_2	*	No change	5	5	5	5	3

*Rate experiments not conducted for IO_3^-

B.4 Bioreduction and Sequestration of a CoCOI (Chromate) in Hanford Sediment

Change in chromate concentration as a result of organic gas treatment and organic gas then CO_2 treatment is reported in fraction of chromate in each surface phase (Figure B.4) and in μg/g in each surface phase (Figure B.5). For ethane, butane, and butyl acetate treatments, there was a significant (66% to 88%) decrease in mobile chromate (i.e., aqueous and adsorbed), which is difficult to observe on plots of fraction chromate due to the large amount of natural chromium present in the sediment (i.e., light and dark green, Figure B.4), but is more easily observed in plots without the 8 M HNO_3 extraction (Figure B.5). Subsequent CO_2 treatment increased chromium mobility compared to just organic treatment, likely due to some dissolution of calcite in the acidic pore water, which may contain co-precipitated Ca-chromate (Figure B.5b, d, and f).

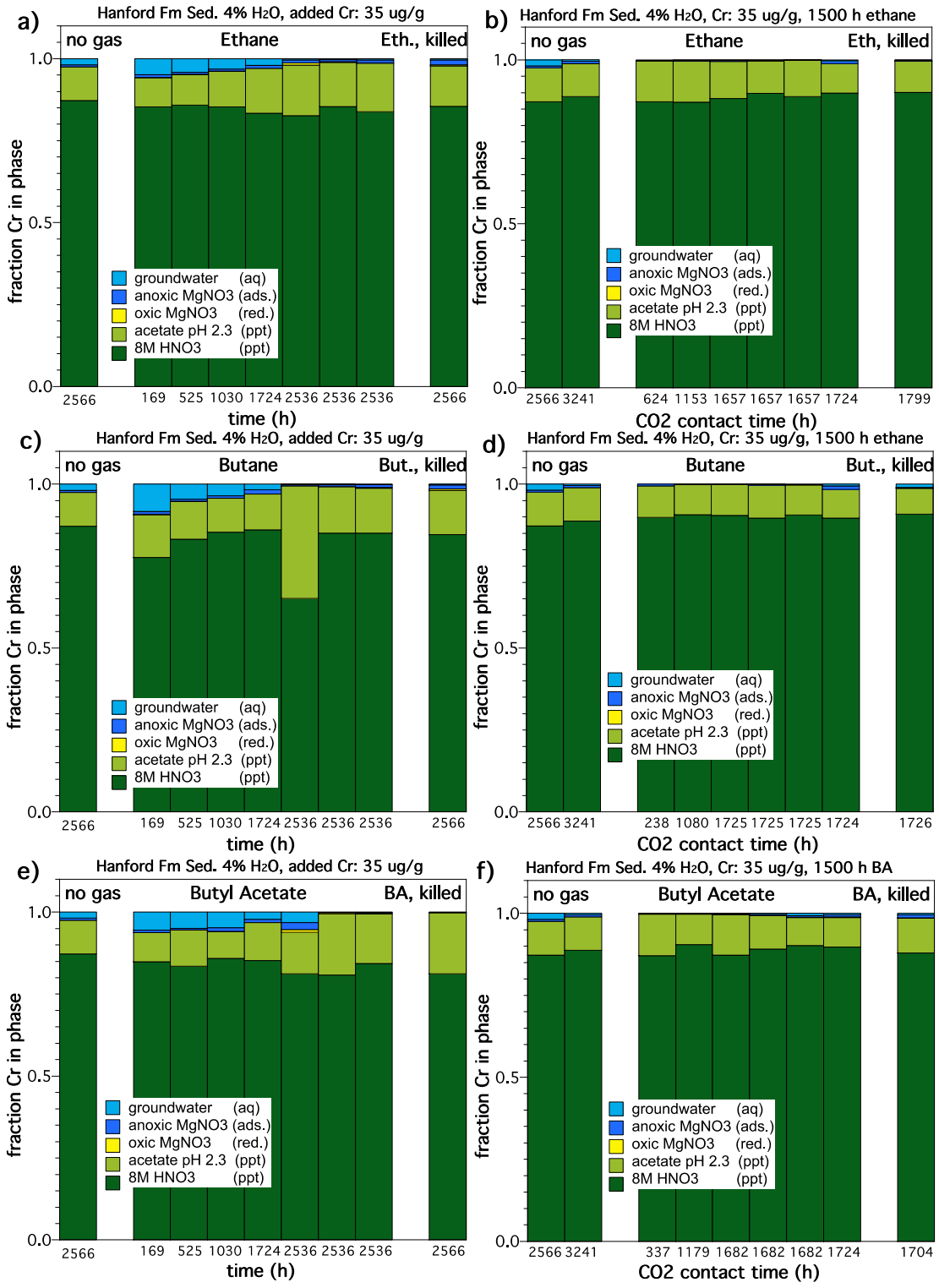

Figure B.4. Change in chromate mobility (reported as a fraction in each surface phase) as a result of (a) ethane gas, (b) ethane then CO_2, (c) butane gas, (d) butane then CO_2, (e) butyl acetate gas, and (f) butyl acetate then CO_2.

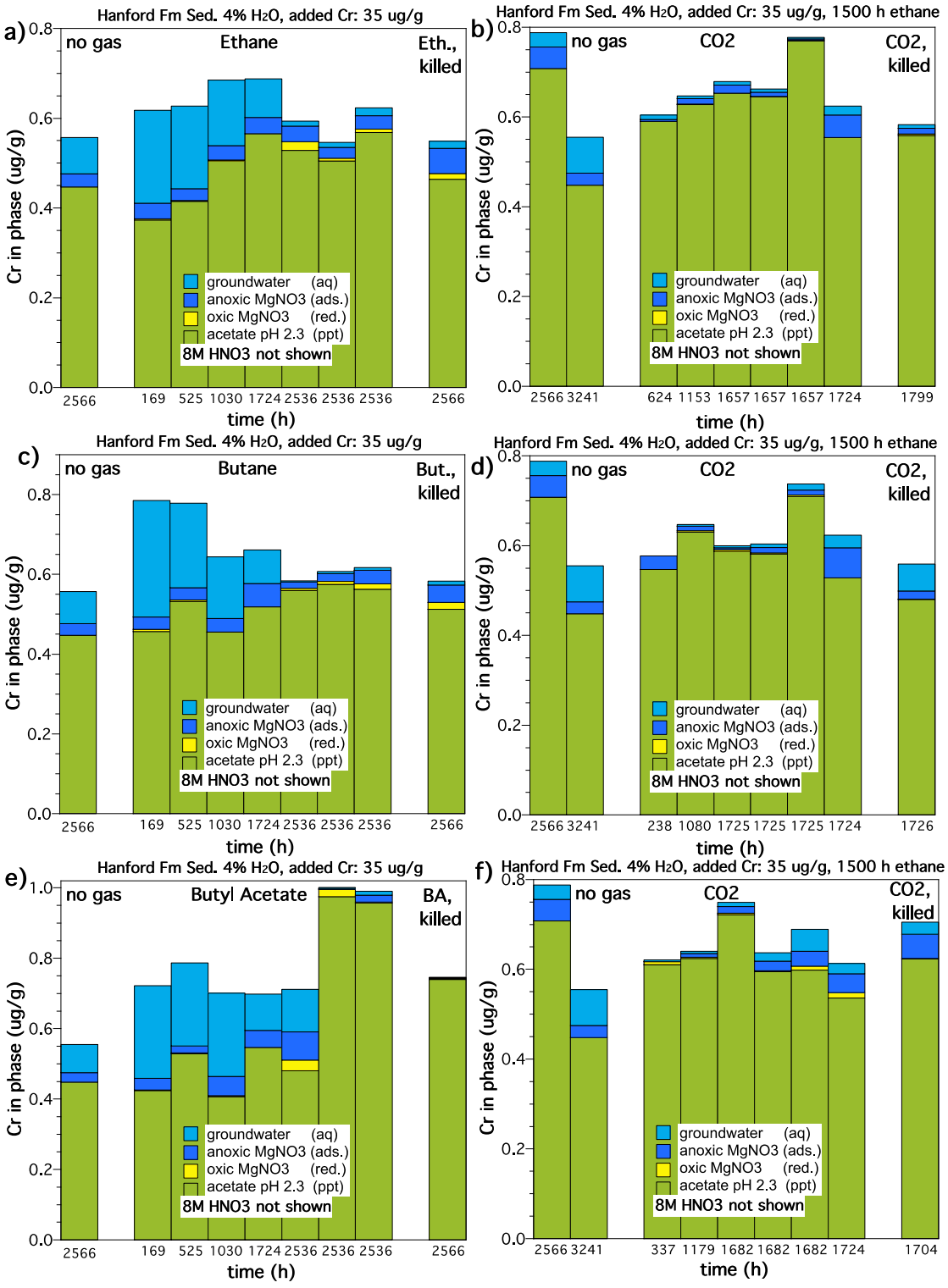

Figure B.5. Change in chromate mobility (reported µg/g for each surface phase) as a result of (a) ethane gas, (b) ethane then CO_2, (c) butane gas, (d) butane then CO_2, (e) butyl acetate gas, and (f) butyl acetate then CO_2.

B.5 Bioreduction and Sequestration of a CoCOI (Nitrate) in Hanford Sediment

Nitrate was measured only in the first extraction (aqueous) in untreated, organic gas treated, and organic gas then CO_2 treated sediments (Figure B.6). For ethane, butane, and butyl acetate treatments, there was no change in the nitrate concentration. Although nitrate bioreduction is expected at low concentrations to nitrite (aqueous), ammonia (adsorbs as a cation), and N_2 gas, the very high nitrate concentration may have limited the degradation. Nitrate was not possible to measure in other extractions as the remaining extractions contained NO_3^-. NO_3^- is not expected to adsorb (Extractions 2 and 3) or precipitate.

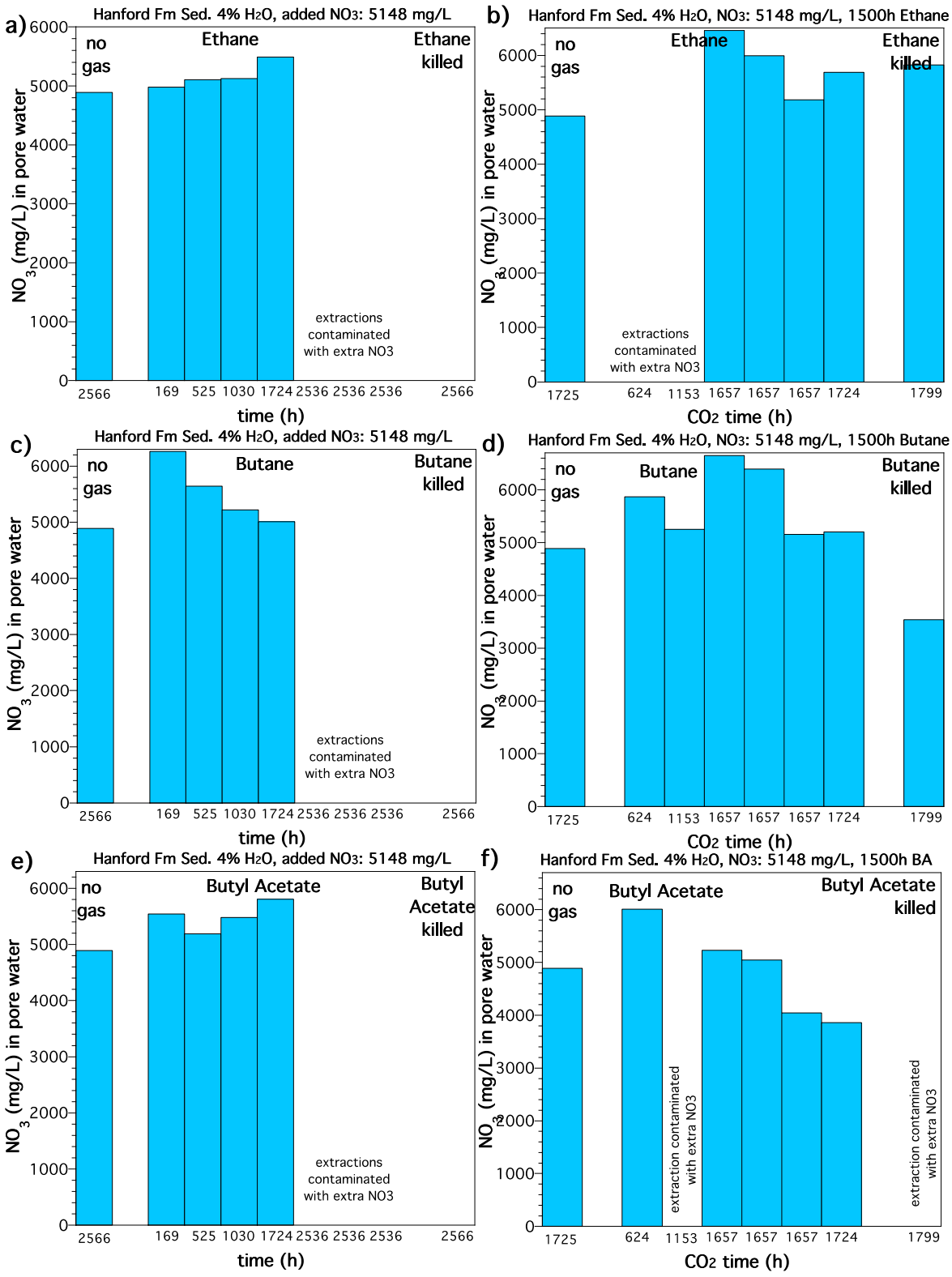

Figure B.6. Change in pore water NO_3^- concentration (mg/L) as a result of (a) ethane gas, (b) ethane then CO_2, (c) butane gas, (d) butane then CO_2, (e) butyl acetate gas, and (f) butyl acetate then CO_2.

B.6 Bioreduction and Sequestration of a CoCOI (IO_3) in Hanford Sediment

The CoCOI I-129 was added as I-127 (IO_3) as most of the iodine in the subsurface is natural I-127, so any remediation technology will involve both I-127 and I-129. IO_3 is easily reduced to iodide in mild reducing conditions, but both IO_3^- and I^- have high mobility due to small sorption. IO_3 has slightly greater sorption than iodide, so reduction of IO_3^- and I^- increases iodine mobility. All IO_3 (I-127) subjected to ethane, butane, or butyl acetate for 2500 hours showed a decrease in aqueous iodine, but an increase in adsorbed iodine, and an overall decrease in aqueous + adsorbed iodine (and corresponding increase in the acetate-extractable iodine, Figure B.7a). The 8M nitric acid extraction was not analyzed for iodine, as I_2 gas formed under highly acidic conditions. The same data plotted in μg/g show organic gas extractions were ~20% less than for the untreated sample (Figure B.7c). Finally, the aqueous sample only analyzed for iodine species showed an increase in aqueous iodide of as much as 70% compared to the untreated sample with 90% IO_3 and 10% I (Figure B.7e).

With the subsequent CO_2 treatment following organic gas treatment, the I-127 mobility increased back to no-treatment mobility (for butane) or nearly no-treatment mobility (for ethane and butyl acetate, Figure B.7b). The concentration of total aqueous I-127 was unchanged for the organic gas and CO_2 treatments (Figure B.7d). However, there was mass loss for iodine species measurements (Figure B.7e). While organic gas (i.e., reduction) treatment resulted in decreased IO_3 and increased I, as expected, the subsequent CO_2 treatment resulted in mainly IO_3 (Figure B.7f).

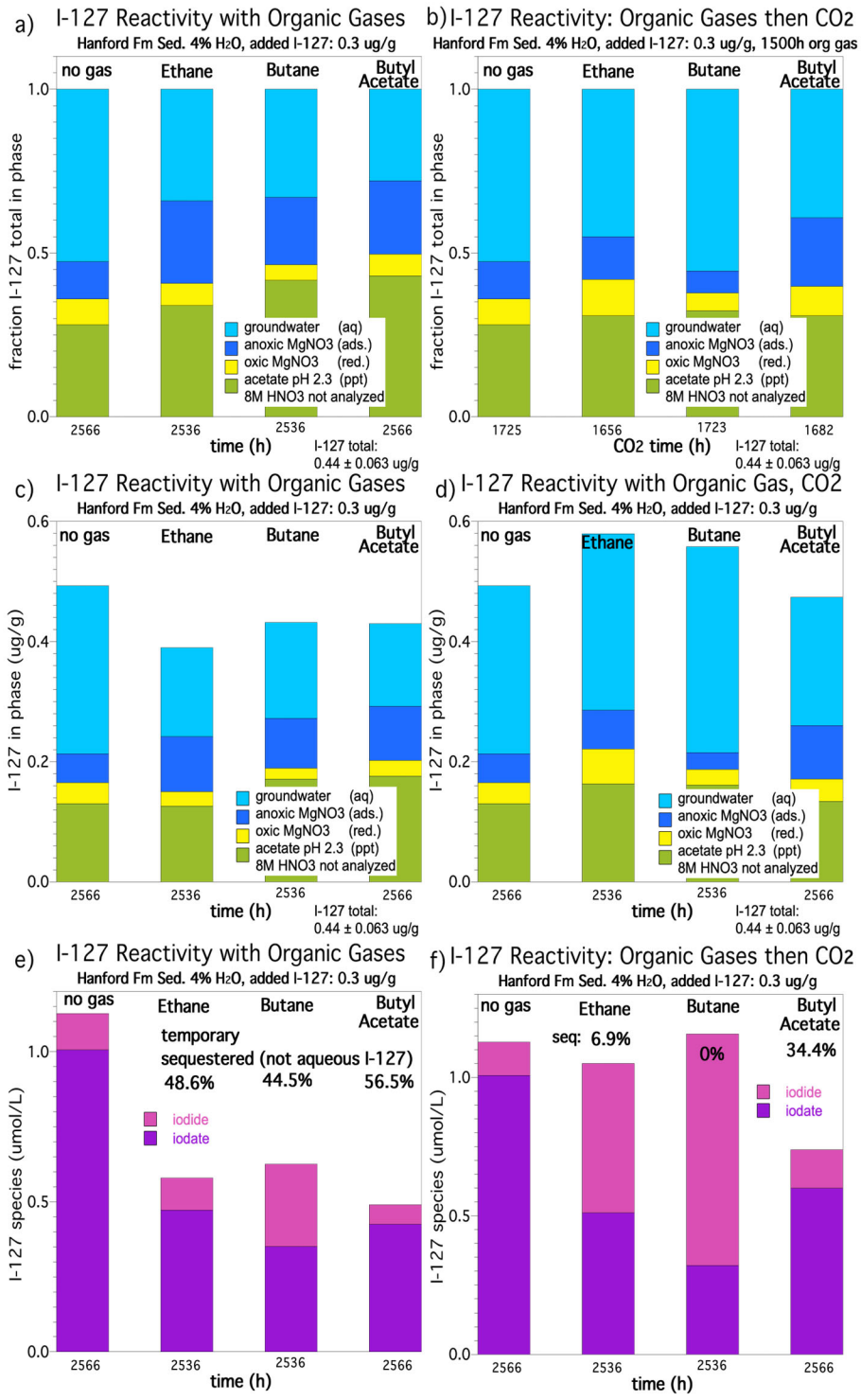

Figure B.7. Change in I-127 as a result of (a) organic gases (total I-127 fraction in each phase shown), (b) organic gases then CO_2 (total I-127 fraction in each phase shown), (c) organic gases (total I-127 in µg/g in each phase shown), (d) organic gases then CO_2 (total I-127 in µg/g in each phase shown, (e) organic gases (I-127 species in just the aqueous extraction in µmol/L), and (f) organic gases then CO_2 (I-127 species in just the aqueous extraction in µmol/L).

B.7 Bioreduction and Sequestration of a CoCOI (Uranium) in Hanford Sediment

Changes in uranium surface phases and mobility as a result of organic gas treatment and organic gas then CO_2 treatment is reported in fraction of uranium in each surface phase (Figure B.8) and in μg/g in each surface phase (Figure B.9). For ethane and butane for 2600 hours, there was no change in uranium mobility except for a slight decrease in aqueous and a slight increase in the adsorbed fraction (Figure B.8a and c). For butyl acetate, there was a slight decrease in the aqueous plus adsorbed fraction over 2600 hours (Figure B.8e). The same time series data plotted with uranium concentrations (μg/g) in each surface phase showed generally little variability between triplicate samples (at 2536 hours) but an occasional extraction with significantly different total extractable uranium (Figure B.9a, c, and e).

The subsequent CO_2 treatment after organic gas treatment significantly increased the mobile uranium (i.e., aqueous plus adsorbed fraction; Figure B.8b, d, and f), probably due to the pH 5.5 acidic pore water causing less adsorption. However, by 1700 hours, the aqueous fraction was decreasing to near untreated values, which may reflect the pH being buffered to some extent to near neutral, where greater uranium sorption would occur. The same time series data plotted with uranium concentrations (μg/g) in each surface phase showed little variability between triplicate samples, with an occasional extraction with significantly different total extractable uranium concentrations (Figure B.9b, d, and f).

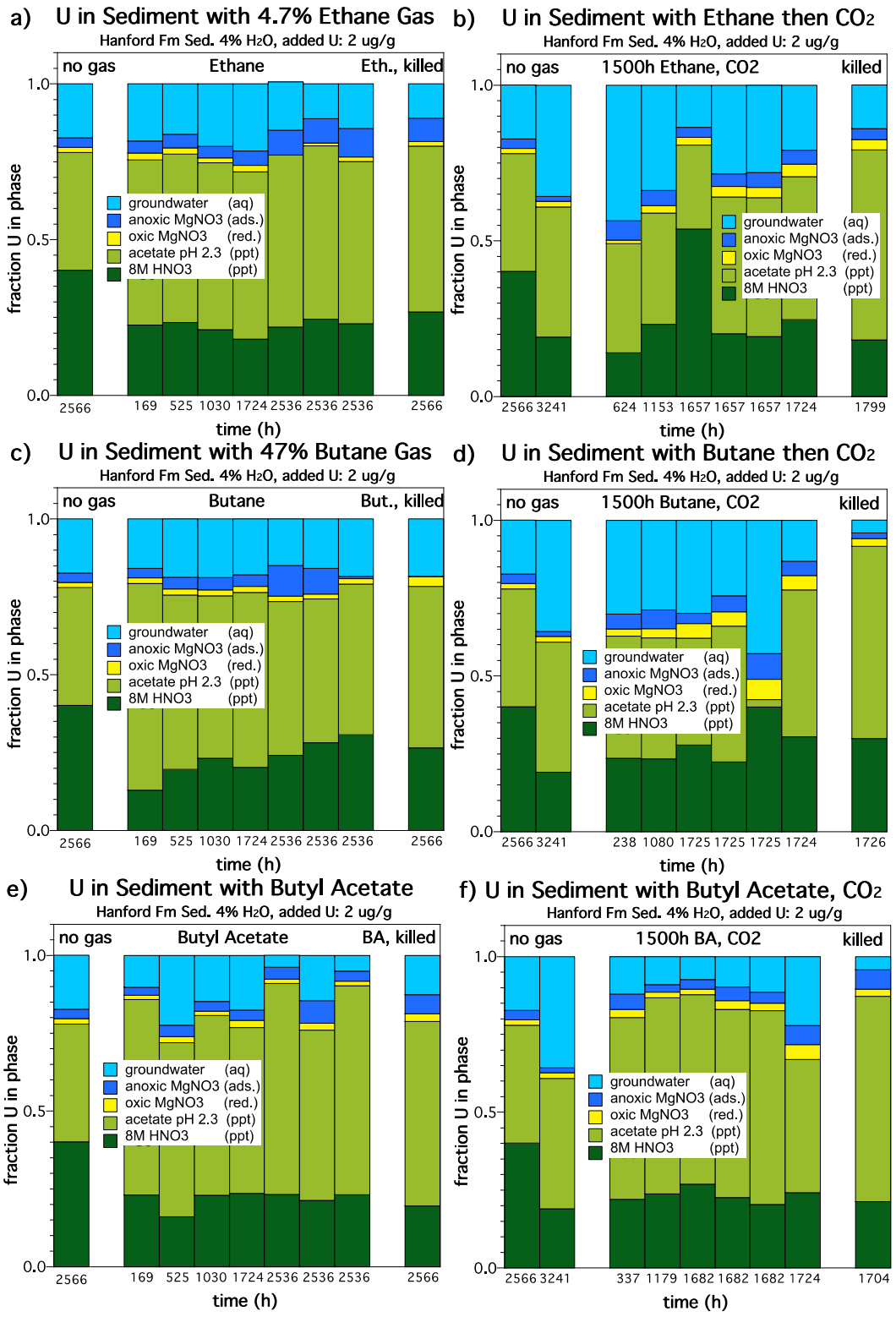

Figure B.8. Change in uranium mobility (reported as a fraction in each surface phase) as a result of (a) ethane gas, (b) ethane then CO_2, (c) butane gas, (d) butane then CO_2, (e) butyl acetate gas, and (f) butyl acetate then CO_2.

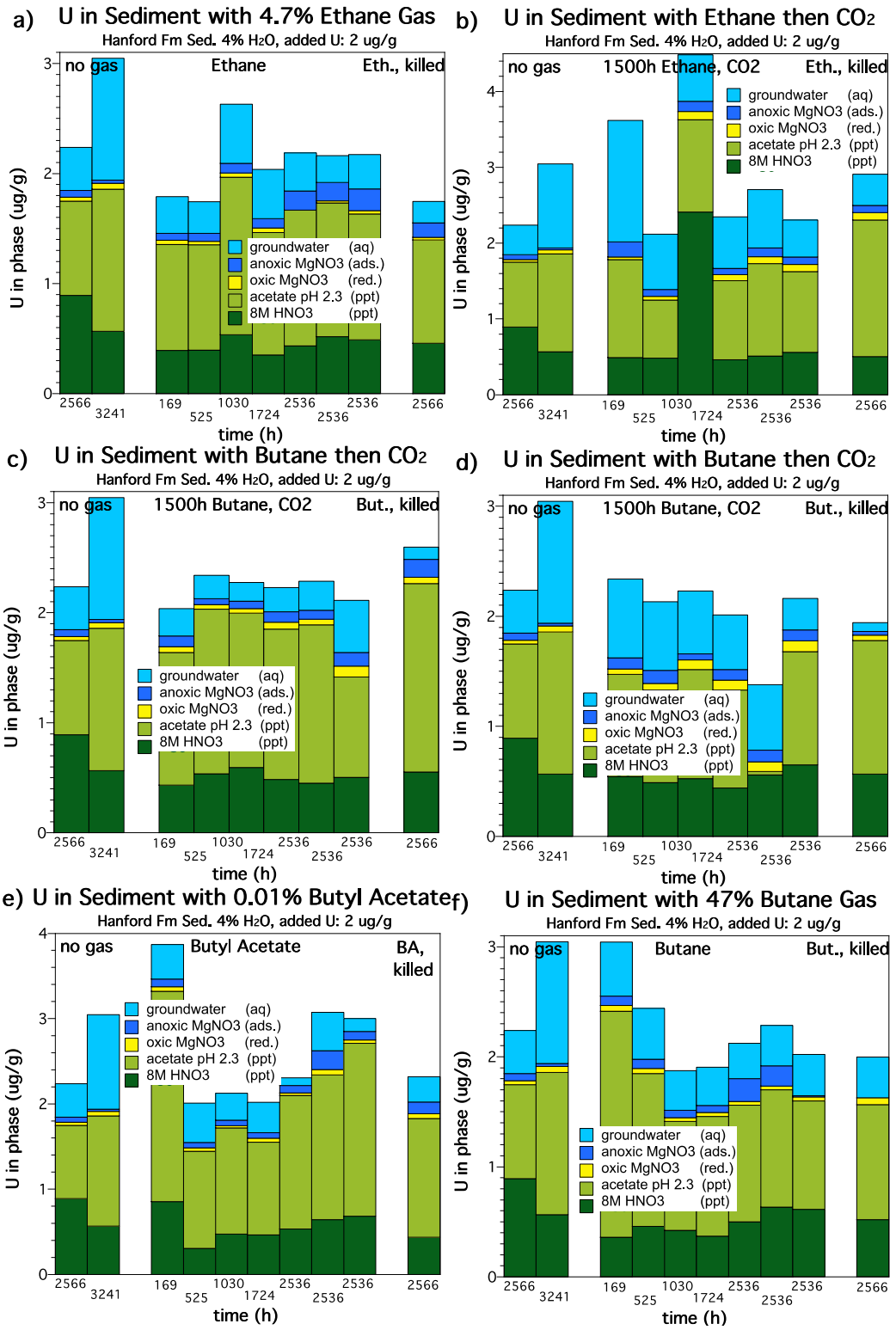

Figure B.9. Change in uranium mobility (reported µg/g for each surface phase) as a result of (a) ethane gas, (b) ethane then CO_2, (c) butane gas, (d) butane then CO_2, (e) butyl acetate gas, and (f) butyl acetate then CO_2.

B.8 Bioreduction and Sequestration of a CoCOI (Cyanide) in Hanford Sediment

The most common cyanide species found in the Hanford subsurface is $Fe^{II}(CN)_6^{4-}$, which was the species added as a CoCOI. In oxic water, $Fe^{III}(CN)_6^{3-}$ is present (Figure B.10) and in mild to strong reducing conditions, $Fe^{II}(CN)_6^{4-}$ is present.

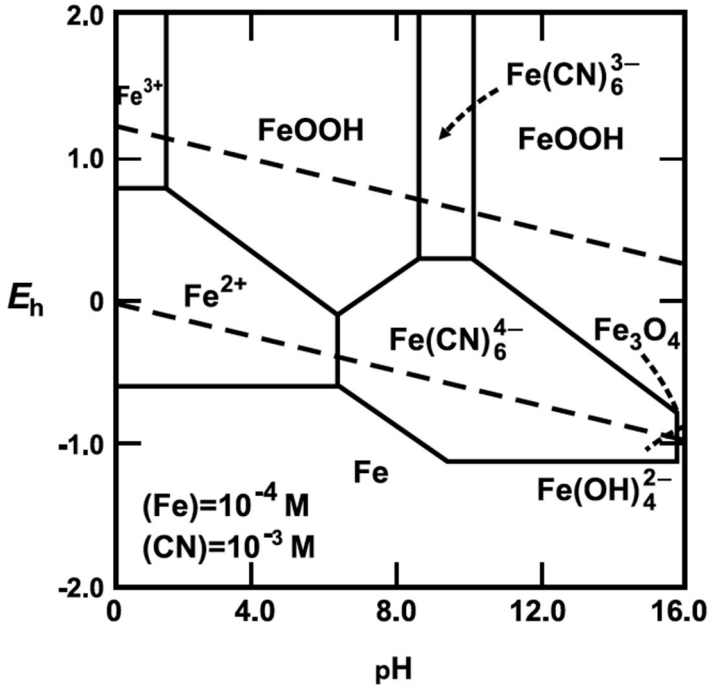

Figure B.10. Iron-cyanide aqueous speciation as a function of pH and redox conditions (FIO).

Cyanide species showed little change after organic gas treatments and organic gas/CO_2 treatments (Figure B.11). Measurements of $Fe^{II}(CN)_6^{4-}$ and $Fe^{III}(CN)_6^{3-}$ were made on a spectrophotometer at different wavelengths. All $Fe^{III}(CN)_6^{3-}$ measurements were zero (i.e., at the detection limit), so no oxidation of $Fe^{II}(CN)_6^{4-}$ occurred. These cyanide measurements were made only on aqueous samples, and results are reported in µmol/L concentration in pore water (Figure B.11). Adsorption of cyanide would show up as decreased concentrations compared to untreated samples. There were no consistent changes in organic gas or organic gas/CO_2 treatments. There were difficulties accurately measuring $Fe^{II}(CN)_6^{4-}$ in the heat-killed samples.

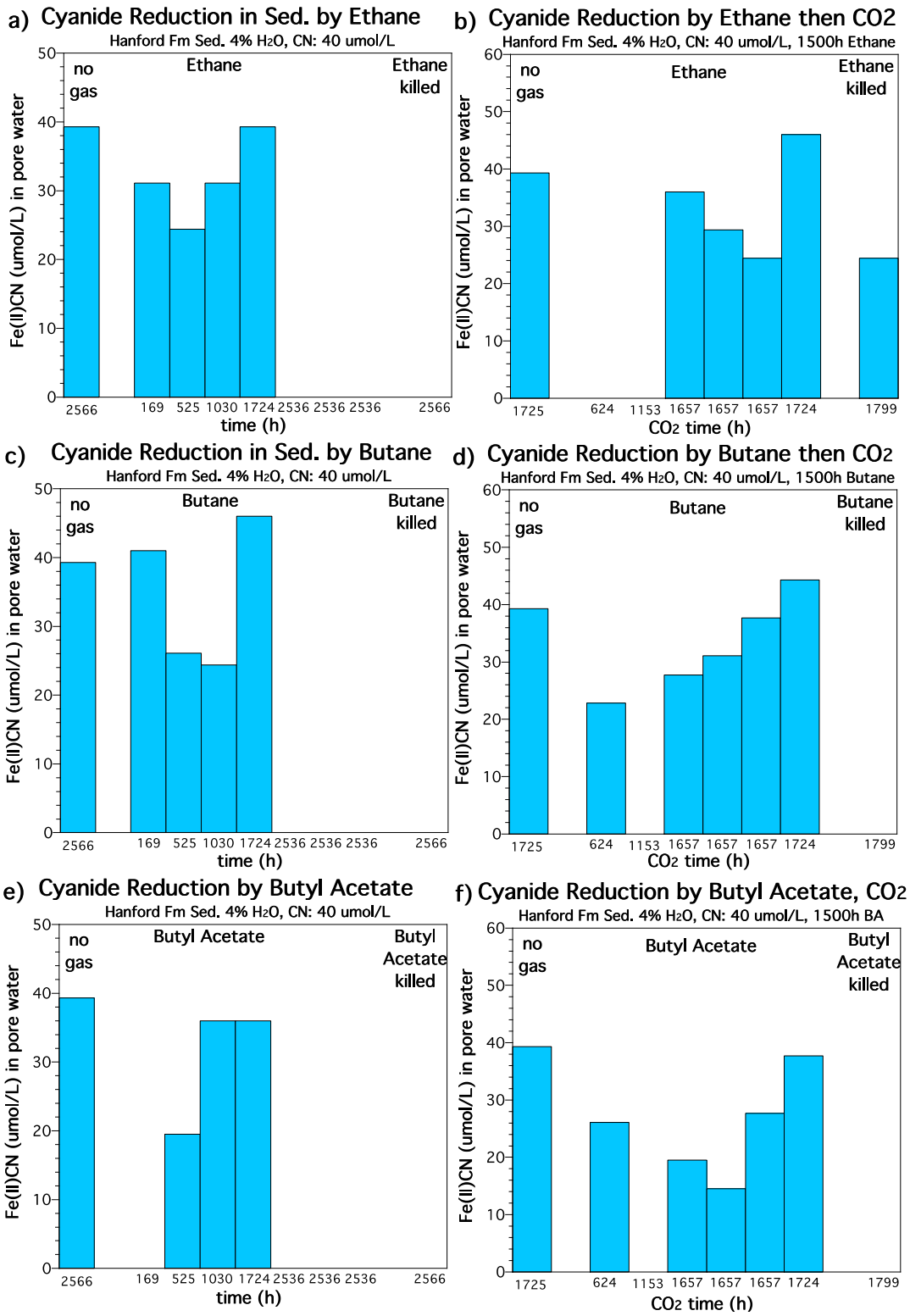

Figure B.11. Change in $Fe^{II}(CN)_6^{4-}$ mobility (reported as a fraction in each surface phase) as a result of (a) ethane gas, (b) ethane then CO_2, (c) butane gas, (d) butane then CO_2, (e) butyl acetate gas, and (f) butyl acetate then CO_2.

B.9 Bioreduction and Sequestration of a CoCOI (Strontium) in Hanford Sediment

Because the Hanford subsurface has natural strontium at 0.05 to 0.1 mg/L in groundwater and 20 µg/g in solid phase (PNNL-18303) and Sr-90 is typically present at 3 to 5 orders of magnitude lower concentration than Sr-87, experiments were conducted spiked with 50 µg/g Sr-87. A remediation technology would have to sequester all Sr, regardless of the isotope. There are no redox reactions expected for Sr^{2+}, but calcite precipitation will incorporate Sr^{2+} (PNL-10899). Note that a high (162 mg/L) aqueous Sr^{2+} concentration was added to achieve 50 µg/g Sr-90 in sediments, and this may be above solubility limits of Sr-carbonates, so there may be an initial decrease in aqueous and adsorbed Sr^{2+} concentrations due to precipitation.

Changes in strontium surface phases and mobility as a result of organic gas treatment and organic gas then CO_2 treatment are reported in fraction of strontium in each surface phase (Figure B.12) and in µg/g in each surface phase (Figure B.13). For ethane and butane for 2600 hours, there was a slight decrease in the mobile Sr fraction (i.e., aqueous + adsorbed + reduced, first three extractions), which resulted in an increase in the sequestered (precipitated) Sr from 52% (untreated) to 57%. There was no change for butyl acetate (i.e., 51% sequestered). The subsequent CO_2 treatment after organic gas treatment significantly increased strontium mobility, much more than the untreated sediment (and Figure B.12b, d, and f). The slight acidity of the CO_2-saturated pore water likely dissolved some calcite that contained natural Sr-87. Calcite dissolution should decrease the pH 2.3 acetate extracted fraction, and results do not show a change in that extraction (light green on Figure B.13b, d, and f).

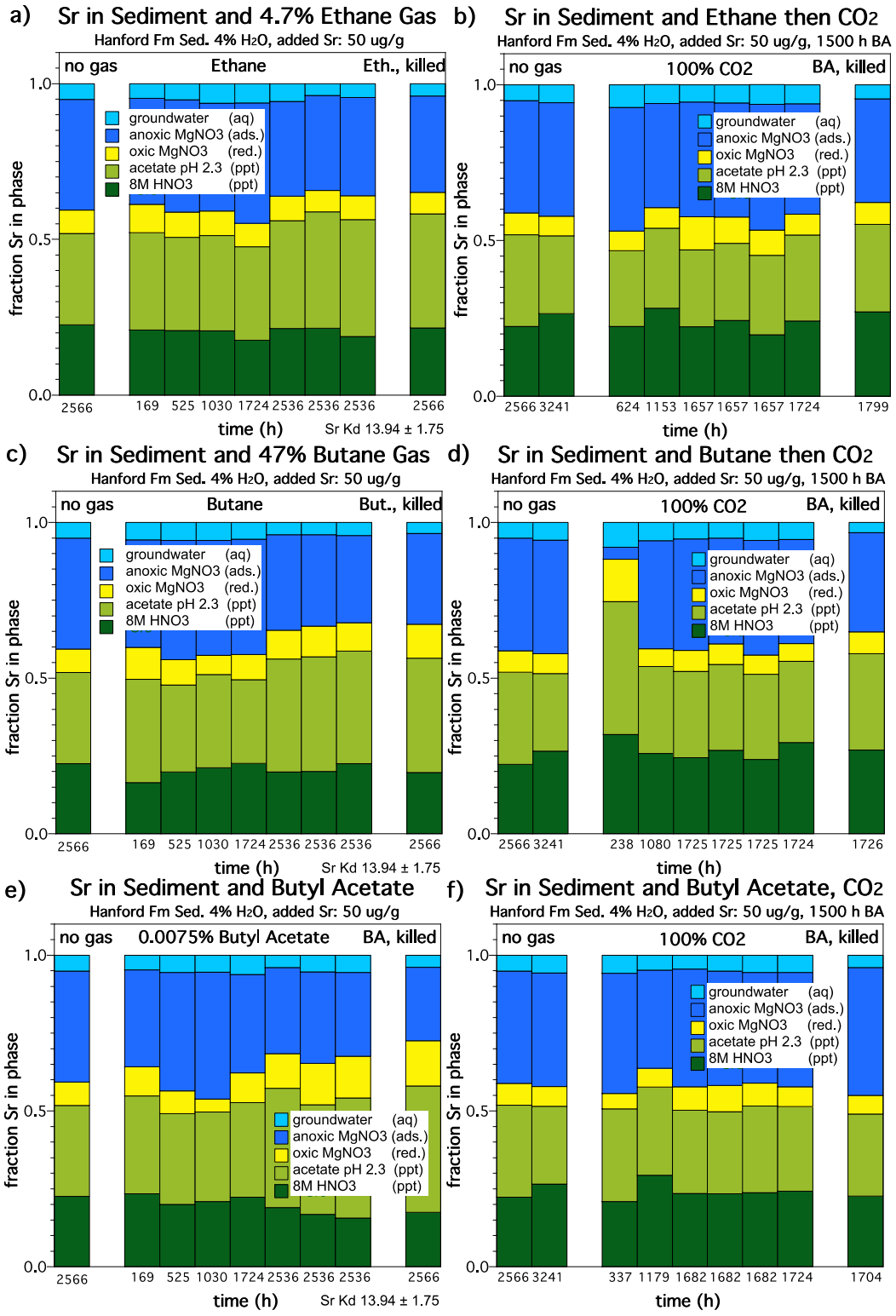

Figure B.12. Change in strontium mobility (reported as a fraction in each surface phase) as a result of (a) ethane gas, (b) ethane then CO_2, (c) butane gas, (d) butane then CO_2, (e) butyl acetate gas, and (f) butyl acetate then CO_2.

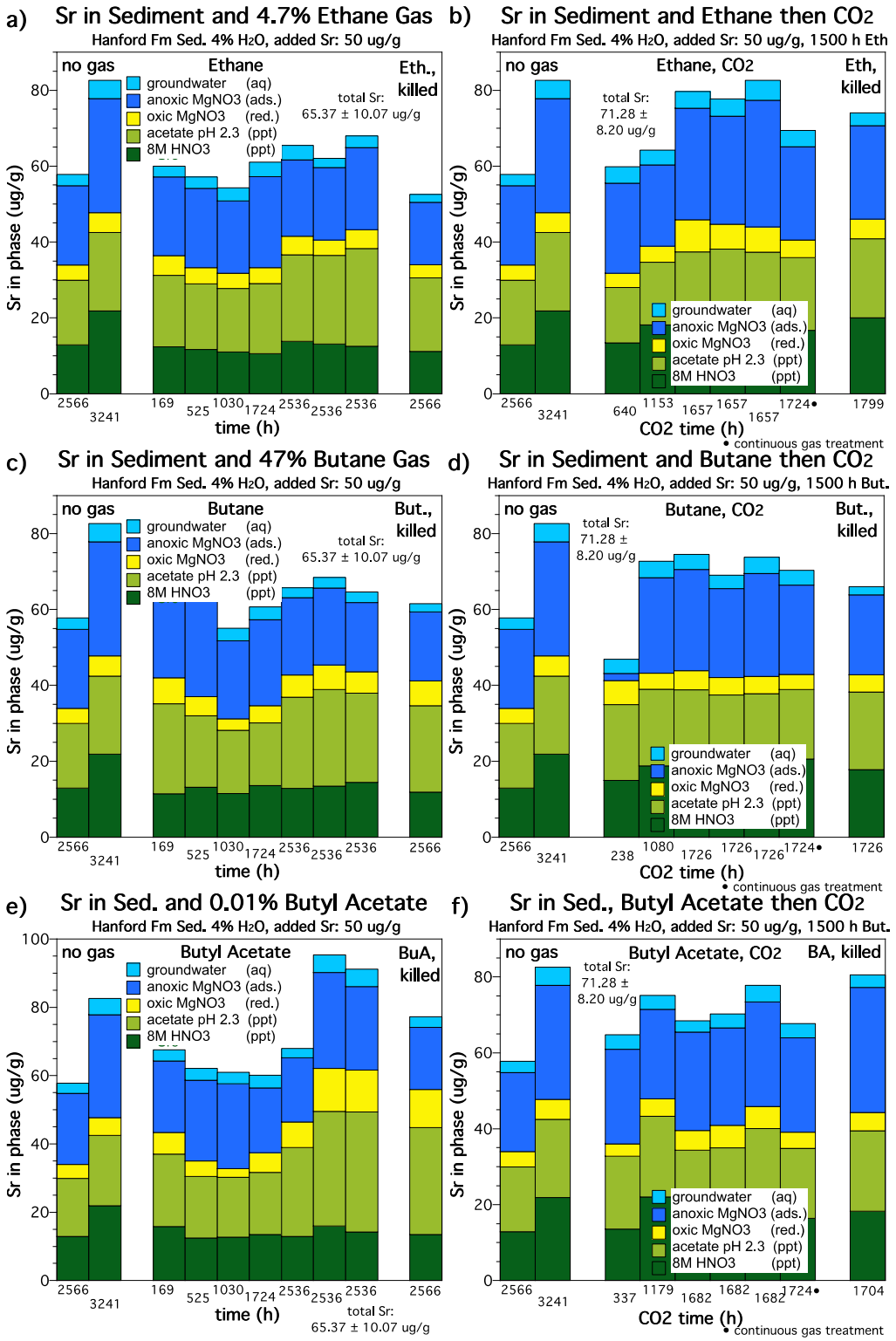

Figure B.13. Change in strontium mobility (reported in µg/g in each surface phase) as a result of (a) ethane gas, (b) ethane then CO_2, (c) butane gas, (d) butane then CO_2, (e) butyl acetate gas, and (f) butyl acetate then CO_2.

Appendix C – Supporting Data for Gaseous Sequestration of I-127 by CO_2

C.1 Time Scale for CO_2 Gas to Liquid Partitioning

The two experiment types used to evaluate IO_3 incorporation into precipitating calcite were (1) water-saturated and (2) unsaturated. Water-saturated experiments consisted of 20 g of sediment and 140 mL of water in a 200-mL glass vial hooked up to a 22-liter metallized gas bag filled with 100% CO_2. The purpose was to approximate the process of gas-to-liquid partitioning but to have a sufficiently large water volume to be able to collect multiple samples. The pH data showed only a small amount of CO_2 partitioning into the water as the pH decreased from 8.0 to 7.6 (rather than to 6.0, as shown in previous studies). Given the physical dimensions of the system, CO_2 gas diffusion through 7.5 cm of water (in the vial) to the sediment surface was simulated. This 1-D diffusion simulation used an analytical solution:

$$C/Co = 1 - \text{erf}\,[x/2 \bullet \text{sqrt}(Dt)]$$

where C is the concentration at time t, Co is the initial concentration, x is the distance, D is the molecular diffusivity of CO_2 in water, sqrt is square root, and erf is the error function [Crank (1975), equation 3.13, page 32]. The CO_2 diffusivity in water used was 1.3824 cm^2/day. The time to reach 50% CO_2 diffusion at the sediment/water interface 7.5 cm away from the CO_2/water interface was 42 days (Figure C.1), so the time scales were too short to achieve equilibrium within the large water volume. Note that the vials were shaken daily or every other day for months, which should have accelerated CO_2 gas partitioning into the water.

In contrast, unsaturated columns at 4% or 8% water content (WC) had a thin film of water on the sediment; therefore, surface and gas injection through the air-filled pores needed to diffuse through this thin film of water to achieve pore water equilibrium and precipitate. Given Hanford formation (Hf) sediment with an average surface area of 3.7 m^2/g and 4% WC (i.e., 0.04 mL water volume/g sediment), the calculated average film thickness is 1.1 microns (assuming water is spread uniformly over the entire sediment surface). However, due to capillary forces, smaller grains with smaller pores have higher WC. Assuming a water film thickness of 0.1 mm (100 microns), the time for CO_2 diffusion to reach 50% equilibrium at the sediment/water interface is 7 seconds (Figure C.1b). Therefore, in field-realistic conditions of a thin film of pore water in unsaturated sediments, achieving pore water equilibrium with a gas injection is relatively rapid.

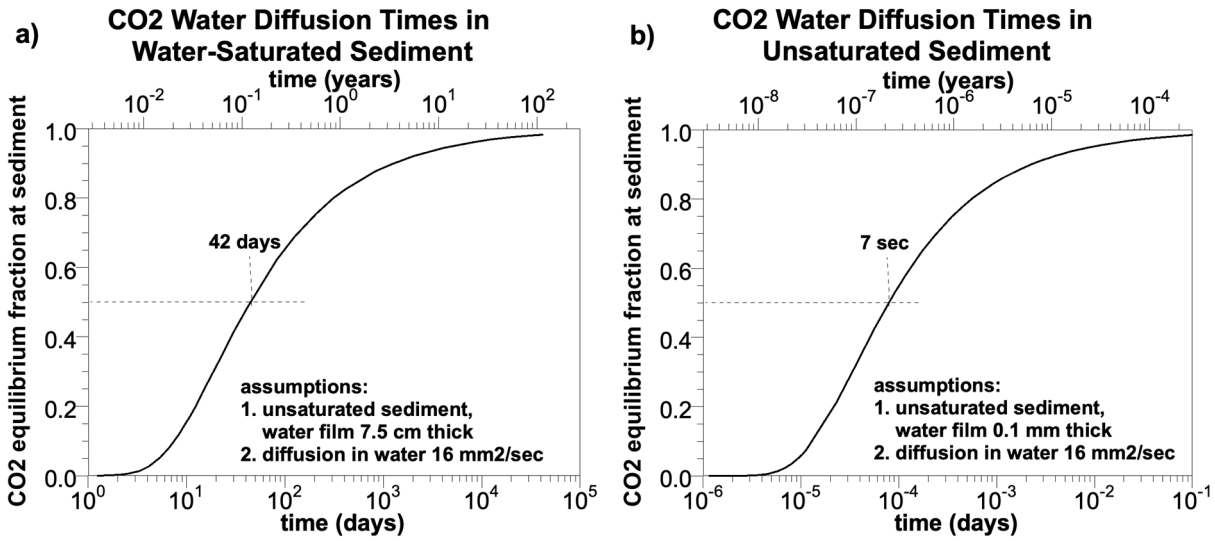

Figure C.1. Calculated diffusion of CO_2 through water in (a) water-saturated, and (b) unsaturated at 4% WC (For Information Only).

C.2 Change in pH in Water-Saturated and Unsaturated Experiments

As CO_2 partitions into pore water, the pH of the solution should become slightly acidic. In a previous study, unsaturated Hf sediments (pH 8.0) treated with 100% CO_2 for 3 months showed a pH of 6.0 (PNNL-18879). In this study, water-saturated and unsaturated experiments were conducted. In water-saturated conditions without and with co-contaminants, there was a slight decrease in pH from 7.0-8.2 (untreated) to 7.6-7.9 by 90 days (Figure C.2), then an increase in pH for the subsequent 60-day air treatment.

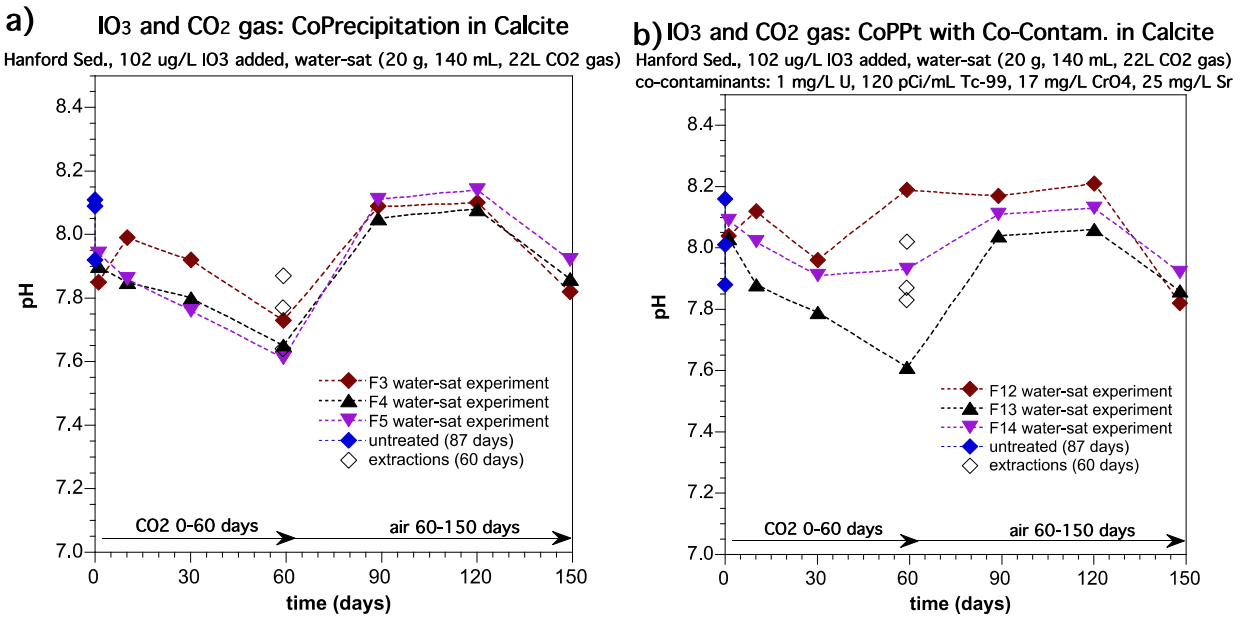

Figure C.2. Change in pH levels for water-saturated batch experiments (1:7 sediment-to-solution ratio) with Hf sediments without and with co-contaminants with CO_2 gas treatment over 60 days followed by flushing with air for another 90 days: (a) aqueous I-127 (in µg/L) with no co-contaminants of interest (CoCOIs) over time, (b) sequential I-127 extractions at 59 days with no CoCOIs, and (c) pH with no CoCOIs.

In unsaturated sediments without co-contaminants, the pH decrease was from 7.9-8.3 to 7.7-7.9 (Figure C.3). Note that unsaturated experiments at 4% or 8% WC were diluted 45× for extractions and pH measurement, so pH measurements do not accurately reflect *in situ* pH.

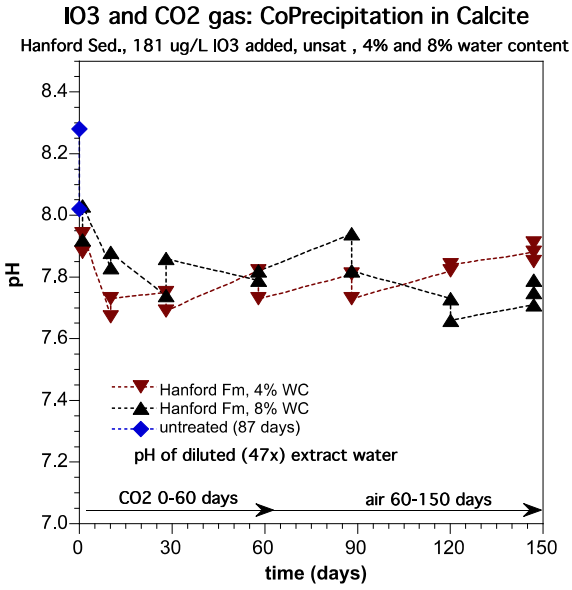

Figure C.3. Change in pH of extraction water following treatment with CO_2 gas with reaction for 60 days followed by flushing with air and reaction for another 90 days in unsaturated columns at 4% and 8% WC.

Finally, in unsaturated conditions at 4% WC containing co-contaminants, Hanford and 216-S-9 sediments showed an observable pH decrease during CO_2 treatment (0 to 90 days) and a pH increase after air treatment (90 to 150 days, Figure C.4).

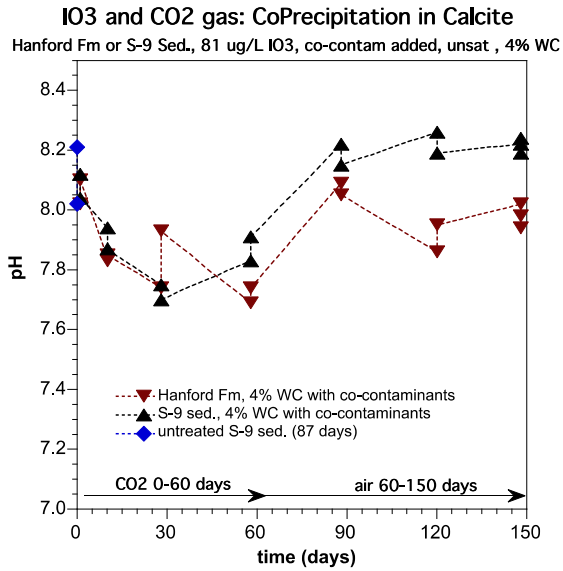

Figure C.4. pH change in unsaturated columns with CoCOIs with CO_2 gas injection (0-60 days) then air (60-150 days).

C.3 Sequestration of Contaminants of Interest by CO_2 Gas Treatment

As CO_2 partitions into pore water, calcium carbonate solubility is exceeded and calcite precipitates. Some IO_3 and co-contaminants may incorporate into the precipitating calcite. Both water-saturated and unsaturated experiments were conducted to evaluate the change in mobility for co-contaminants due to CO_2 gas injection. Tc-99 present as pertechnetate in unsaturated 216-S-9 sediment showed 9% to 15% Tc-99 incorporation into a precipitate that was dissolved in the pH 2.3 acetate extraction (presumed to be calcite, Figure C.5a). The Tc-99 incorporation into the pH 2.3 acetate extraction was 3.5% to 5% for the Hf sediment. There was also some (4% to 6%) Tc-99 incorporation into calcite in water-saturated experiments. Uranium present as Ca-U(VI)-carbonate aqueous species in unsaturated experiments showed a large increase in U in pH 2.3 precipitates from 23% to 80-92% (Hf sediment) or from 10% to 30% (216-S-9 sediment, Figure C.5b). Water-saturated Hf sediments also showed an increase in U in pH 2.3 precipitate extraction. Strontium substitutes for calcium in calcite so showed an increase in calcite-extractable Sr in both water-saturated and unsaturated experiments. For unsaturated experiments, Sr in the pH 2.3 acetate extraction increased from 30% to 60% (Figure C.5c) for both Hf and 216-S-9 sediments. Finally, Cr(VI) also showed an increase in pH 2.3 acetate extraction in unsaturated experiments from 3.5% to 22-45% for both the Hanford and 216-S-9 sediments (Figure C.5d).

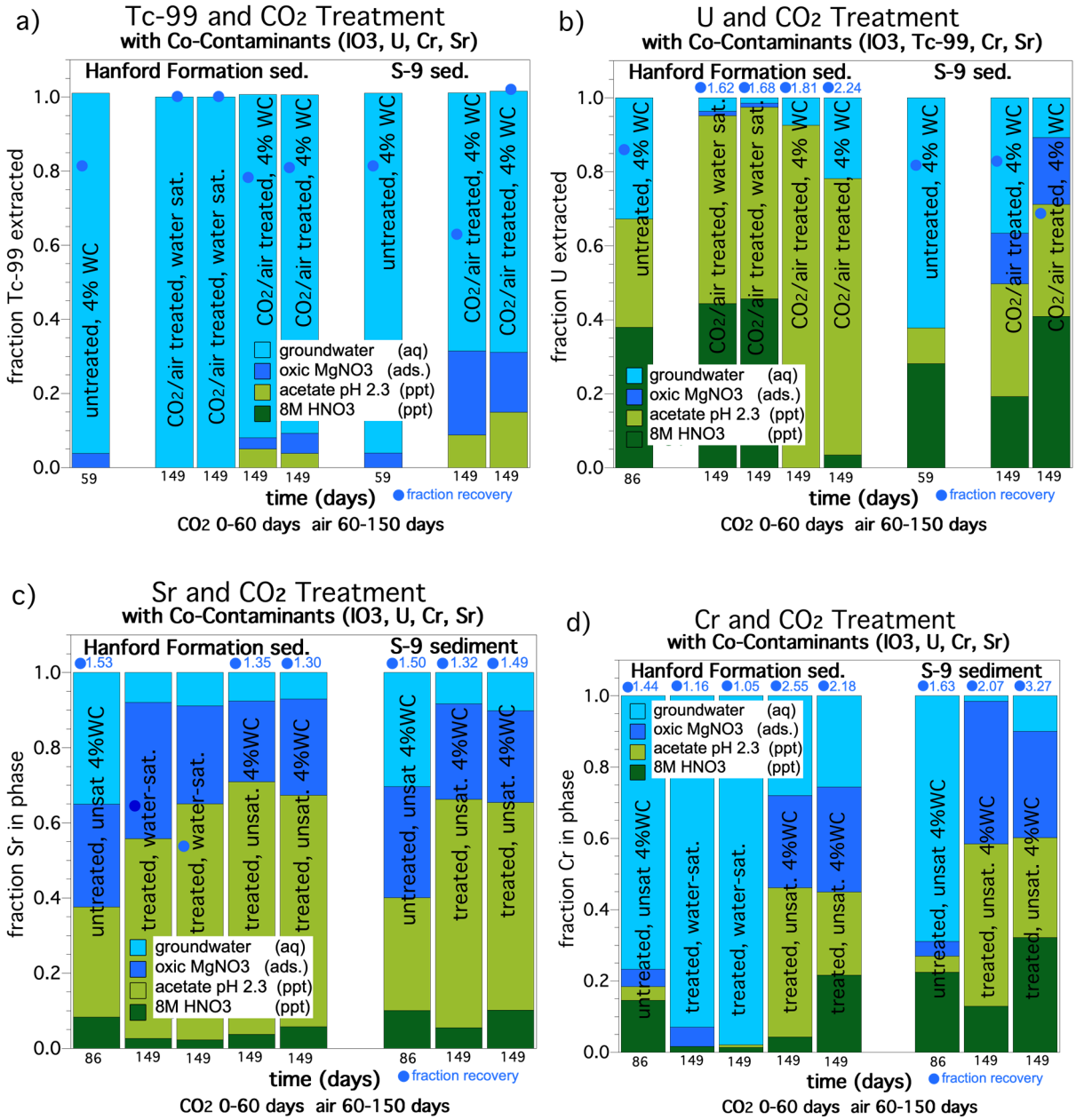

Figure C.5. Change in mobility of co-contaminants due to CO_2 gas treatment in water-saturated and unsaturated experiments: (a) Tc-99 present as pertechnetate, (b) U, (c) Sr^{2+}, and (d) Cr(VI) present as chromate.

Appendix D – Supporting Data for Gas-Phase Bioreduction and Sequestration Amendments

D.1 Bioreduction of Cr(VI) and Native Mn Oxides

Reduction of chromate, as indicated by aqueous Cr(VI) values (inductively coupled plasma optical emission spectrometer, ICP-OES) at the final (~154 days) time point occurred in both sediments but was greatest in 216-S-9 sediments with pentane, butane, or ethane as electron donor (Figure D.1). Aqueous Mn values (ICP-OES) at the end point were above detection limits in some samples (Figure D.2), suggesting microbial reduction of solid-phase Mn oxides to aqueous Mn(II). Aqueous Mn values were greater in BY Cribs sediment than the 216-S-9 sediment and were generally greater in samples receiving gaseous carbon substrate (Figure D.2). [The corresponding samples without Cr(VI) were not analyzed for Mn.]

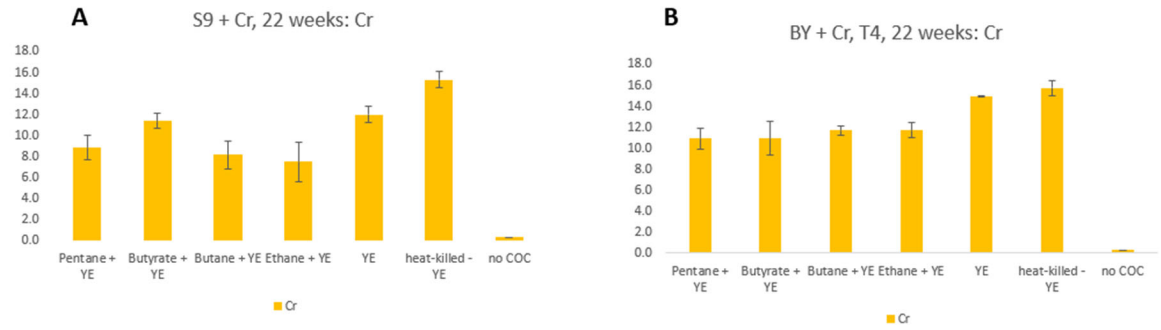

Figure D.1. Aqueous chromium concentrations (mg/L) at the end point (~154 days) in the 2:1 liquid:sediment experiment with 216-S-9 (A) and BY Cribs (B) sediment with added Cr(VI).

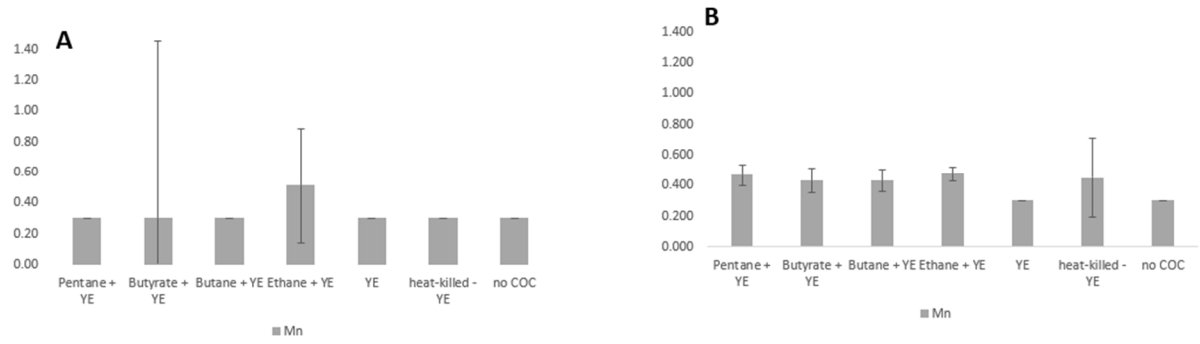

Figure D.2. Aqueous manganese concentrations (mg/L) at the end point (~154 days) in the 2:1 liquid:sediment experiment with 216-S-9 (A) and BY Cribs (B) sediment with added Cr(VI).

D.2 Nitrate and Nitrite Concentrations

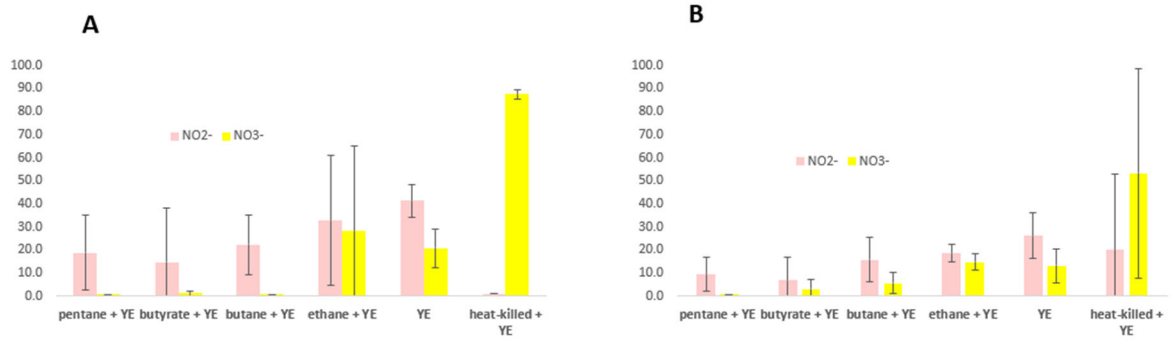

Figure D.3. Aqueous NO_2^- and NO_3^- concentrations (mg/L) at the end point (~119 days) in the 1:1 liquid:sediment experiment with 216-S-9 (A) and BY Cribs (B) sediment without added Cr(VI).

D.3 pH Monitoring with Treatment

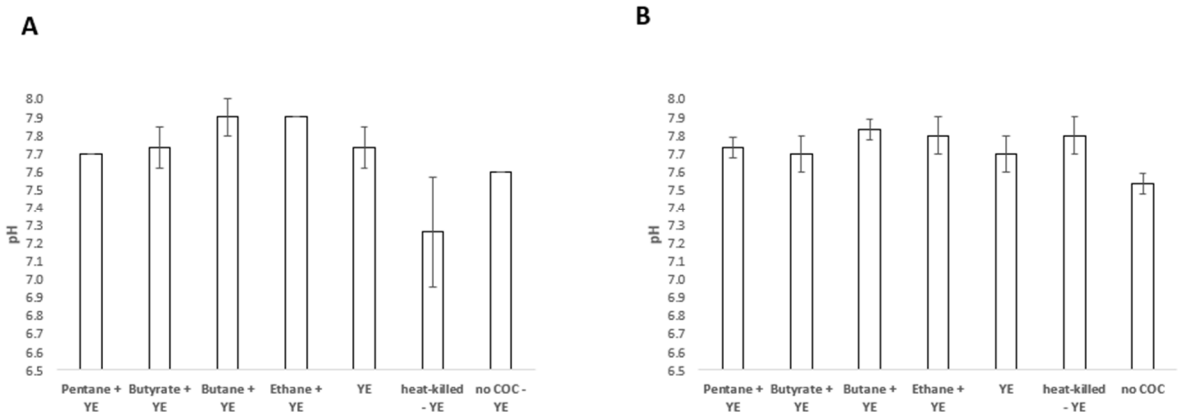

Figure D.4. pH values in the 1:2 sediment-to-artificial pore water (APW) experiment without Cr(VI) at the 154 day end point: (A) 216-S-9 sediment and (B) BY Cribs sediment.

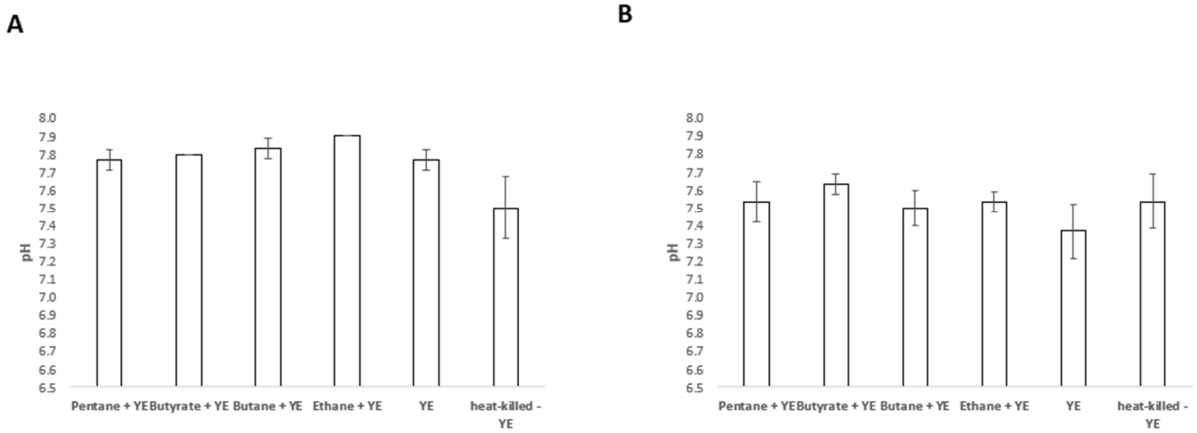

Figure D.5. pH values in the 1:2 sediment-to-APW experiment with Cr(VI) at the 154 day end point: (A) 216-S-9 sediment and (B) BY Cribs sediment.

D.4 Bacterial Cell Quantification with Treatment

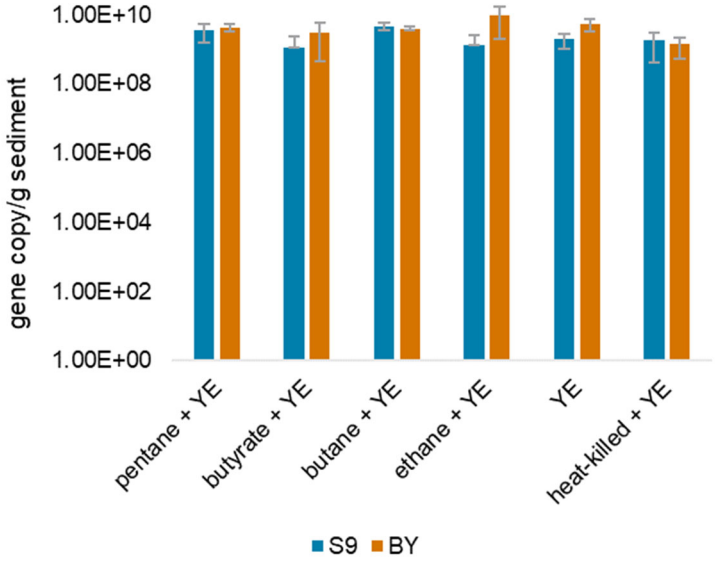

Figure D.6. Bacterial cell numbers (gene copy/g sediment) at end point (119 days) in 1:1 (Balch tube) experiment without Cr(VI) (log10 scale) for 216-S-9 sediment (*blue*) and BY Cribs sediment (*orange*) showing comparable cell numbers in all treatments. Data are For Information Only (FIO). DNA extractions were performed directly from sediments in duplicate and DNA yields were combined for quantitative polymerase chain reaction (qPCR) analysis.

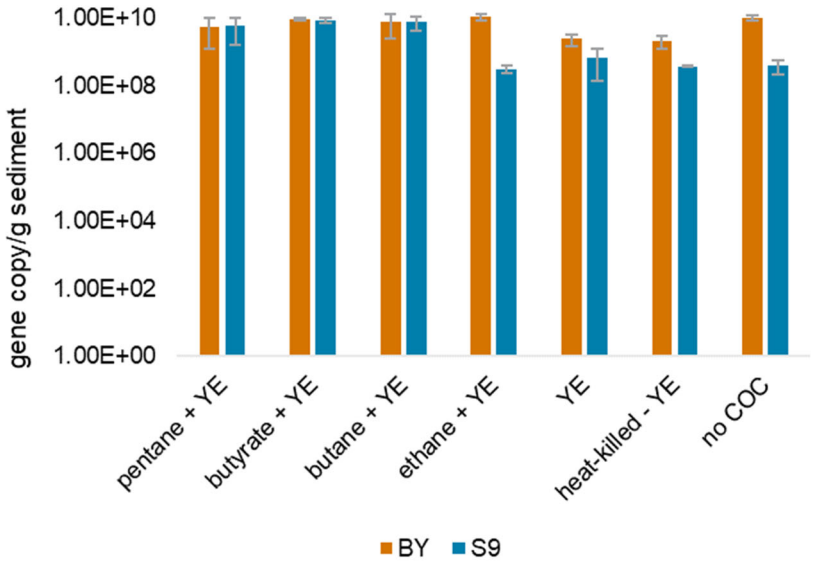

Figure D.7. Bacterial cell numbers (gene copy/g sediment) at end point (154 days) in 2:1 (serum bottle) experiment without Cr(VI) (log10 scale) for 216-S-9 sediment (*blue*) and BY sediment (*orange*) showing higher cell numbers in BY Cribs sediment in comparison with 216-S-9 sediment for the ethane, heat-treated, and no-contaminant of interest (COI) treatments. Data are FIO. DNA extractions were performed directly from sediments in duplicate and DNA yields were combined for qPCR analysis.

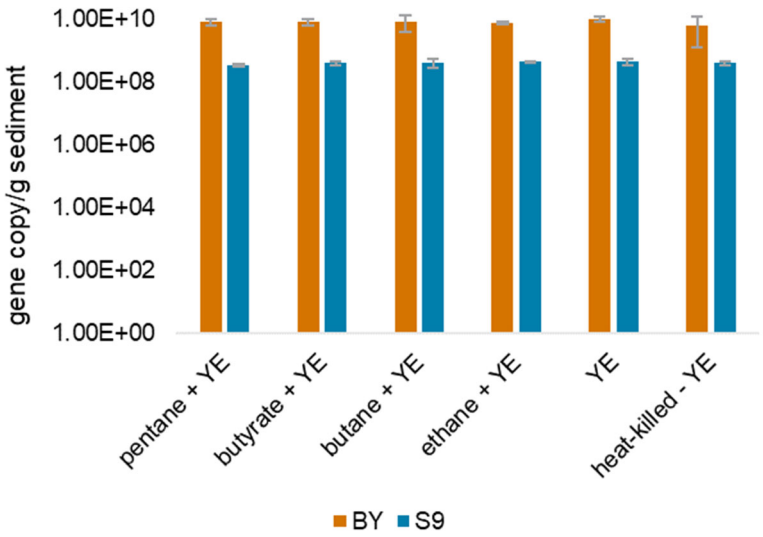

Figure D.8. Bacterial cell numbers (gene copy/g sediment) at end point (154 days) in 2:1 (serum bottle) experiment with Cr(VI) (log10 scale) for 216-S-9 sediment (*blue*) and BY sediment (*orange*) showing higher cell numbers in BY Cribs sediment in comparison with 216-S-9 sediment for all treatments. Data are FIO. DNA extractions were performed directly from sediments in duplicate and DNA yields were combined for qPCR analysis.

Appendix E – Supporting Data for Particulate Sequestration Amendment – Sn(II)-PO_4

E.1 Synthesis of Sn(II)-PO_4

Sn(II)-PO_4 particles were synthesized using the procedure described (PNNL-26730). This procedure is based on a previous report (LAB-RPT-12-00001) but includes the alternative steps outlined in Table 4.1 of PNNL-26730. The steps, in summary, are as follows:

1. Bring 1 L of deionized water to a boil for 30 minutes while sparging the system with ultra-high purity nitrogen gas. Allow the water to cool and add to the 2-L glass reactor. Sparge the boiled water with nitrogen gas while mixing at approximately 100 rpm.
2. While sparging with nitrogen gas, prepare the 1.0 M $NaHPO_4$ and 1.38 M $CaCl_2$ solutions. Check the pH of the solutions and adjust the pH to 7.3 ± 0.1 if necessary, with concentrated HCl. Record any pH adjustments required. Seal the containers to prevent solutions from contacting oxygen. Sparge with nitrogen during any pH adjustments. Ideally, solutions should be used within 12 hours. If beyond 12 hours, recheck the pH and adjust if necessary.
3. Heat the water in the 2-L reactor to 37 °C while the system is sparged with high-purity nitrogen gas. To create reducing conditions, 4 mL of 35 wt% hydrazine is added to the reactor.
4. While the water in the reactor is sparging, prepare 250 mL of 0.4 M $SnCl_2$ solution in double deionized water. Purge the vessel headspace with ultra-high-purity nitrogen gas. Do not adjust the pH. Seal the container to prevent the solution from contacting oxygen.
5. While the reactor temperature is maintained at 37 °C, add in the reagents (1.0 M $NaHPO_4$, 1.38 M $CaCl_2$, and 0.4 M $SnCl_2$) at a flow rate of approximately 1 to 2 mL/min (i.e., total flow rate into the reactor is 3 to 6 mL/min). Continuously stir the reactor at approximately 100 rpm while sparging with nitrogen gas.
6. While the reagents are being slowly added over the course of approximately 6 hours, maintain the pH to be approximately 7.3 ± 0.1. Record any pH adjustments required. Use concentrated NH_4OH for pH adjustments. During the first 8 hours (6 hours while reagents are added plus an additional 2 hours of mixing), the pH needs to be continuously monitored and adjusted.
7. After all reagents have been added, keep stirring the mixture while sparging nitrogen gas for 3 days. Maintain the temperature at 37 °C and pH at 7.3 ± 0.1 at all times.
8. Filter out the precipitated Sn(II)-PO_4 using a funnel and filter paper (0.65 µm size or similar). Repulp the Sn(II)-PO_4. Wash with nitrogen sparged ultrapure water. Filter and wash at least three times.
9. Transfer solids to a beaker and place in a vacuum desiccator at room temperature. Leave until fully dry (approximately 3 to 4 days). Verify that solids are dried by weighing a subsample over time until a constant weight is reached.
10. Store under nitrogen or in a vacuum desiccator.

First Attempt. For the first synthesis attempt, 250 mL of each solution was prepared, using Sigma Aldrich chemicals for the $CaCl_2$ and the Na_2HPO_4. The $CaCl_2$ was below the target pH of 7.4, so a small amount (5 µl) of 30% NH_4OH (Millipore) was added; the pH then had to be adjusted back down with HCl.

Kloehn pumps (Norgren, USA) were programmed to dispense 1 mL/min of each solution ($CaCl_2$, Na_2HPO_4, and $SnCl_2$).

The procedure did not successfully yield Sn(II)-PO_4 and had the following issues:

- Preparation of the 1M Na_2HPO_4 solution required heating and overnight stirring to get the solids into solution. Each time the pH was adjusted, the solids precipitated out of solution. Previous reports (LAB-RPT-12-00001; PNNL-26730) did not mention this issue. After adjusting the pH several times, the solution was heated and stirred while re-adjusting the pH. This solution required a significant pH adjustment to bring the pH within the 7.3-7.4 range.
- $SnCl_2$ solution required stirring and was a milky white color, suggesting solids were present. Further, the solution precipitated within the syringe of the pump and the tubing lines before entering the reactor.
- Due to precipitation in the pump syringe and lines, as well as precipitation in the bottles, air was pulled into and injected from the lines of the $SnCl_2$ and Na_2HPO_4 pumps.
- The pH could not be successfully controlled in the full reactor as the solutions were being pumped in. A significant amount (hundreds of mL) of 30% NH_4OH had to be added to get the pH above 7. The overall reactor volume was significantly increased due to the amount of solution added for pH adjustment (i.e., more pH adjustment solution was needed than the volume of reactants), and the injection of the three solutions had to be stopped prematurely due to the volume of the reactor. The pH probe was not compatible with the solution and the tip broke during synthesis; it is unknown when this happened. This could explain why the pH could not be maintained over the course of the reagent addition but cannot be confirmed.
- Due to the large amount of NH_4OH added that filled the reactor prematurely, as well as the air being injected from the $SnCl_2$ and Na_2HPO_4 lines, the synthesis was ended early.
- The suspension turned gray over the course of the solution injection period (Figure E.1). A previous report (PNNL-26730) stated that a gray color indicates a failed synthesis.

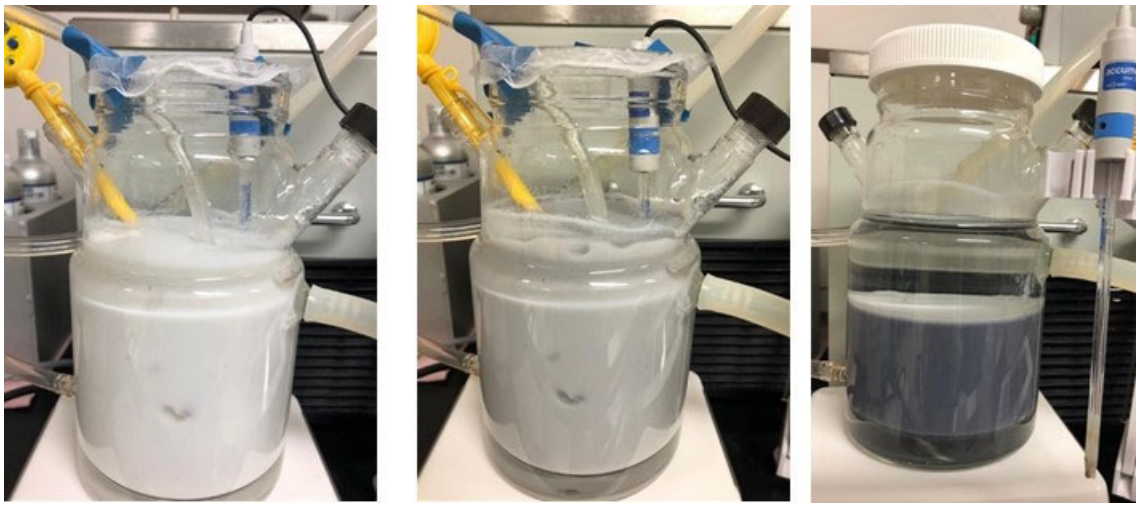

Figure E.1. Sn(II)-PO_4 synthesis attempt #1 at 2:09 p.m. (left), 2:40 p.m. (middle), and overnight (right). Photos show the progression to a gray color and the discolored and broken pH probe (notice discoloration and missing tip) on the right.

Second Attempt. Several changes were made prior to the second synthesis attempt. All solutions were made in the morning before starting the synthesis. New chemicals were purchased for the $CaCl_2$ (Sigma Aldrich), $SnCl_2$ (Acros Organics), and hydrazine (Spectrum). New Na_2HPO_4 was not procured in time, but a different manufacturer (Baker) was used this time. When preparing the $SnCl_2$, 9.235 mL of concentrated HCl was added to make 0.5 M HCl, as suggested by Jim Duncan.[1] The $SnCl_2$ and Na_2HPO_4 solutions were made in N_2 sparged ultrapure water, and N_2 sparging continued in all influent solutions during injection. A 2-L ChemGlass reactor (Figure E.2) was used instead of the smaller glass reactor shown in Figure E.1 to better control mixing and oxygen exposure. The hydrazine used was 85% instead of the previously used 30%. A new, more robust epoxy body pH probe (Thermo Scientific) was used. The 1M Na_2HPO_4 quickly formed solids in the pump syringe and lines, clogging the pump within the first 30 minutes. This solution was then injected by hand (from a syringe), approximating the 1- to 2 mL/min rate. The sparging stone used to continuously flow N_2 into the Na_2HPO_4 bottle also clogged with precipitates (Figure E.2), leaving the solution vulnerable to oxygen. Despite these issues, synthesis continued.

After all solution was added, the reactor was left bubbling with N_2 at 37 °C for 3 days, with pH adjustments every 3-12 hours. During this time, the lowest pH recorded was 6.97. On the second day, a thin black line around the reactor was observed, and when draining the reactor, more black material was observed at the bottom of the reactor. However, the rest of the solution was still white. In an anaerobic chamber, the solid was filtered out using a 0.45-µm vacuum filter (Millipore); the solid may have had a grayish tint. The solid was mixed and rinsed with ultrapure water on the filter top several times, vacuuming the rinsate out after each time. The filter was then moved to a desiccator to dry. While drying, the material turned from white to gray/blue and yellow. Because of the discoloration, a third synthesis was planned.

Figure E.2. Attempt #2: A ChemGlass reactor was used (left); the produced solid may have had a grayish tint (center); solid formation on the N_2 sparging line in the Na_2HPO_4 solution.

Third Attempt. During the third synthesis attempt, new Na_2HPO_4 was used (Acros Organics) while the rest of the chemicals were the same as Attempt #2. The 1M Na_2HPO_4 was gently heated and stirred to prevent precipitation and was injected by hand to prevent pump issues. Otherwise, the synthesis was the

[1] A report from the RJ Lee Group, *Final Report for Sn(II)apatite Characterization and Distribution Coefficients, Reduction of Pertechnetate and Evaluation of KURION® Sorbents Against Off-Gas Condensate*, was provided to PNNL through Jim Duncan, who wrote the RPT-12-00001, Rev. 0, report. This newly acquired report included an additional step – the $SnCl_2$ was dissolved in HCl (the same or greater molarity than the $SnCl_2$) when preparing the $SnCl_2$ solution. According to Duncan, using the HCl will maintain equilibrium toward the left-hand side of the equation: $SnCl_2(aq) + H2O \leftrightarrow Sn(OH)Cl\ (s) + HCl\ (aq)$ (Le Chatelier's principle).

same as in Attempt #2. After leaving in the reactor for 2 days with continuous stirring and heating, and periodic pH adjustments, the mixture was moved to an anaerobic chamber. Following the same filtering and rinsing process as the previous attempt, the solid produced was very white, with the texture of a thick lotion (Figure E.3). The material was initially left in a room temperature desiccator to dry, but after several days, the material was still very wet and was moved to an anaerobic chamber. Drying was still slow, so the material was moved into a glass jar and dried in an oven at 50 °C, with N_2 constantly flowing into the (partially open) jar. The jar was weighed approximately once each day until two consecutive weights were the same; this took about 7 days.

Due to the success of Attempt #3, the synthesis was repeated once more (Attempt #4) following the same steps as outlined in Attempt #3. Again, a thick, smooth, white solid was produced. After drying, these last two attempts produced approximately 37 to 42 g of dry apatite material.

Figure E.3. Attempt #3: Rinsing and filtering the Sn(II)-PO_4 (left) and the resulting solid (right).

E.1.1 Reduction Capacity Measurements

To determine whether the batch of Sn(II)-PO_4 was made successfully, reduction capacity was quantified. Other methods, such as scanning electron microscopy / energy dispersive X-ray spectroscopy and X-ray diffraction (XRD), have been used in previous reports (RPP-53855; PNNL-26730), but due to the amorphous or poorly crystalline structure, the presence of a crystalline Sn(II) or Sn(IV) compound cannot be determined. Use of reduction capacity allows for comparison of results with those previously reported by the RJ Lee Group (RPP-53855), where several batches of various ages were measured for reduction capacity. The same report shows reduction capacity can be reduced over time. The reduction capacity measurements will also provide a way to normalize data between batches and batches used over time and verify reproducibility.

Observation of a gray solid instead of a white solid is an indication of failure to properly synthesize the Sn(II)-PO_4 (PNNL-26730). The RJ Lee Group report includes a “gray” material compared to a “white” material, with the gray material at the low end of the reduction capacity measurements (~1000 µeq/g) compared to the white material (~5000 µeq/g) (RPP-53855).

Reduction capacity measurements were conducted following the modified Ce(VI) method as described previously (Um et al. 2015) and based on the methods described previously (Angus and Glasser 1985; Kaplan et al. 2005). Several Sn(II)-PO_4 batches were previously provided to Pacific Northwest National Laboratory (PNNL) by RJ Lee Group (Asmussen et al. 2016; LAB-RPT-12-00002).

When comparing previous to current reduction capacity results, it is important to note that batches 112513 and 011714 (also labeled as *gray*) were ground prior to storage, while 091813 was stored in large chunks that had to be ground prior to new measurements. It is also important to note that the previous results used a 1-hour contact time before reduction capacity measurements [based on the procedure described previously (SRNL-STI-2009-00637)], while the current measurements increased the contact time to ≥ 4 days, based on previous recommendations (Um et al. 2015).

Reduction capacity was measured for Sn(II)-PO_4 produced during Attempts #2-4. Due to the long drying time, materials from Attempts #2-4 were initially measured while still partially wet, using the moisture content to correct to a dry weight. Prior to starting the batch experiments, dry material from Attempt #3 was measured from the same aliquot that was prepared for use in the batch experiments. Reduction capacity of the 112513, 011714, and 091813 Sn(II)-PO_4 batches provided by RJ Lee Group was also measured. All samples were ground with an agate mortar and pestle prior to measurements, except for 012513 and 011714, which were already ground.

Reduction capacity measurements, and the comparison to previous results, indicate that the reduction capacity is decreased in Sn(II)-PO_4 during storage, but the loss of reduction capacity can be minimized if the material is not ground prior to storage. In addition, measurement on wet material can give an idea of the reduction capacity of dry material but does not provide an accurate result. Finally, the solid material produced in Attempt #3 had a high reduction capacity, suggesting successful synthesis of Sn(II)-PO_4 for use in the batch experiments.

The batches of Sn(II)-PO_4 (Attempts #2-4) were combined to produce a homogenous starting material for future experiments. The combined material was re-measured for reduction capacity (Table E.1). Measurements were similar to the dry measurement from fiscal year (FY) 2022.

Table E.1. Reduction capacity measurements for Sn(II)-PO_4 received from RJ Lee Group(*) and produced by PNNL. Samples were dry unless indicated in the sample name.

Sample Name	Reduction Capacity (μeq/g)	Related Measurements	Notes
112513*	950 ± 7.65	-	Sn(II)-PO_4 samples received from the RJ Lee Group
011714*	905 ± 7.78	-	
091813*	1660 ± 0.00	-	
Attempt #2 (wet)	2870 ± 12.9	-	Ran before sample had fully dried; used moisture content correction to estimate reduction capacity, measured in FY22
Attempt #3 (wet)	1060 ± 57.5	-	
Attempt #4 (wet)	1740 ± 23.5	-	
Attempt #3	3900 ± 115	-	3 replicates, ran three times each (total of 9 measurements); this Sn(II)-PO_4 was used in FY22 batch testing
Attempt #2	3170 ± 0.00	See Attempt #2	Attempt #2 from FY22, dry, re-measured in FY23
Attempts #3 & 4	3860 ± 130	See Attempts #3 & 4	Attempt #3-4, combined and re-measured in FY23
Attempts #2-4	4450 ± 70.0	See Attempts #2-4	All successful attempts from FY22 were combined and measured in FY23

E.2 Characterization of Sn(II)-PO_4

XRD patterns were collected for Sn(II)-PO_4 from the combined FY23 batches (A-H). The XRD patterns were collected with Cu Kα radiation (λ=1.5418 Å) using a Rigaku Miniflex II unit. The Miniflex was operated at 30 kV and 15 mA and patterns were collected between 3 and 90 °2θ, using a scan width of 0.04° and a 5-second count time. Sn(II)-PO_4 was identified by comparison with XRD patterns (PNNL-26730).

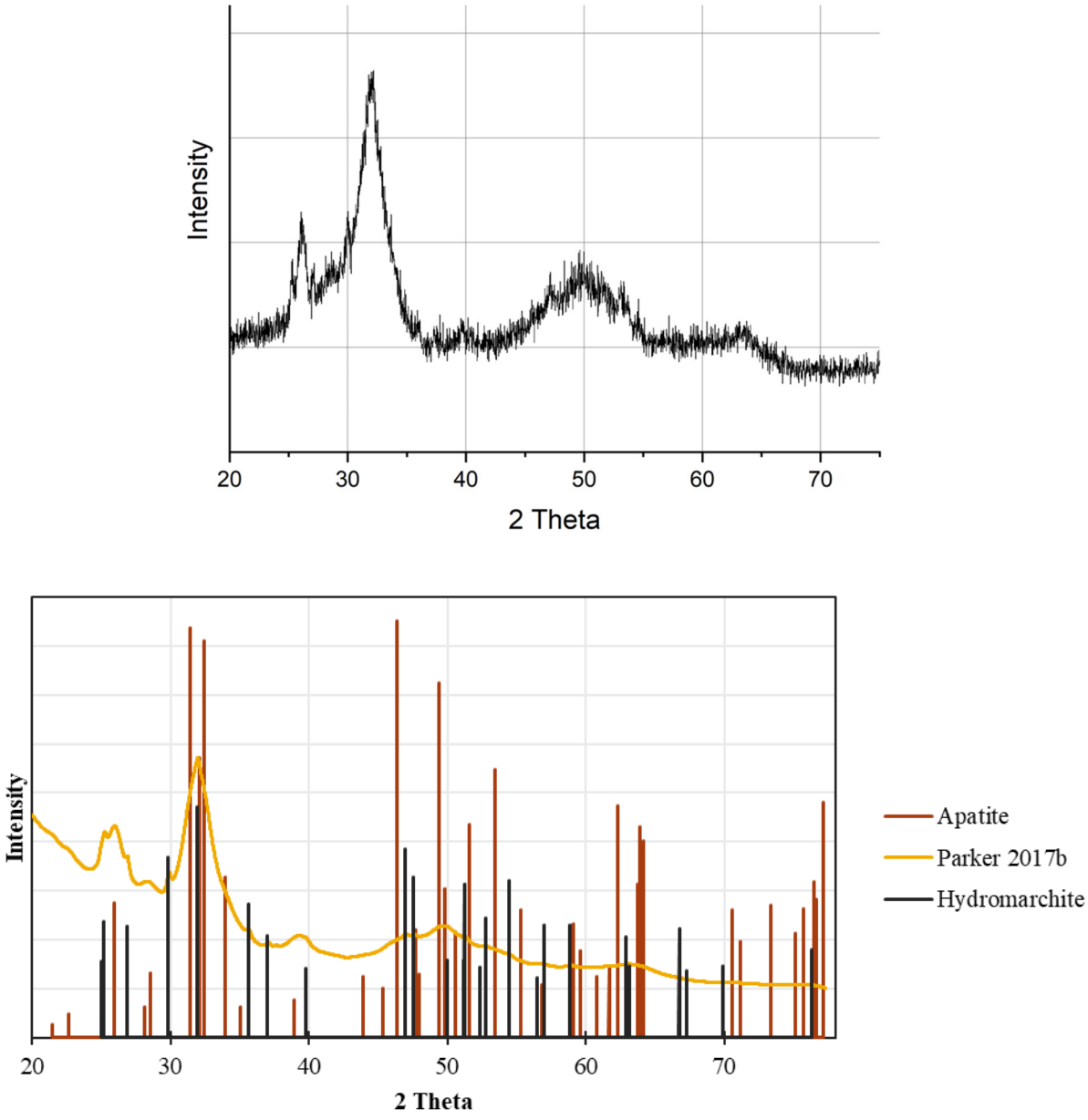

Figure E.4. XRD pattern of Sn(II)-PO_4 "FY23 Combined Attempts 2-4" (top), compared to results from PNNL-26730 (bottom). Calcium apatite [$Ca_{10}(PO_4)_6(OH)_2$] and hydromarchite [$Sn_3O_2(OH)_2$] are shown for reference.

E.3 Effect of Variable Sn(II)-PO_4 Concentration

Prior to starting the full test matrix (Table 3.15), scoping tests were conducted to determine appropriate Sn(II)-PO_4 loading and sampling times. These scoping experiments were conducted For Information Only (FIO). Following the same batch setup described in Section 3.5.4, 10 g of sediment and 20 mL of solution [synthetic groundwater (SGW) or synthetic perched water (SPW)] was used for each batch test, with Tc-99 and U added according to the targets shown in Table 3.7. Low (0.05 g), medium (0.15 g), or high (0.3 g) amounts of Sn(II)-PO_4 were added to the 10 g of sediment prior to adding the spiked background solution, then mixed on a shaker table until sampling. Samples were taken at 1, 2, and 4 hours, and 1 and 7 days.

Results of the scoping tests suggested that Tc-99 is fully or nearly reduced within 5 hours in both the SGW and SPW conditions, regardless of the Sn(II)-PO_4 mass added (Figure E.5). The U uptake was slower, with nearly full removal from the aqueous phase after 7 days only in the BY Cribs (SGW) condition. For the SPW condition, all three Sn(II)-PO_4 loading conditions exceeded the 35% transformation threshold by 7 days but did not reach high removal of U, and the amount of U removed was a function of the Sn(II)-PO_4 loading (with approximate U fractions removed of 0.4, 0.6 and 0.9 in the low, medium, and high loading conditions, respectively).

Based on these results, the full experimental matrix used the "high" (0.3 g) Sn(II)-PO_4 loading with sampling events at 1 and 4 hours and 1, 7, and 28 days. The higher loading and longer sampling times were chosen to improve removal of U under the perched water conditions.

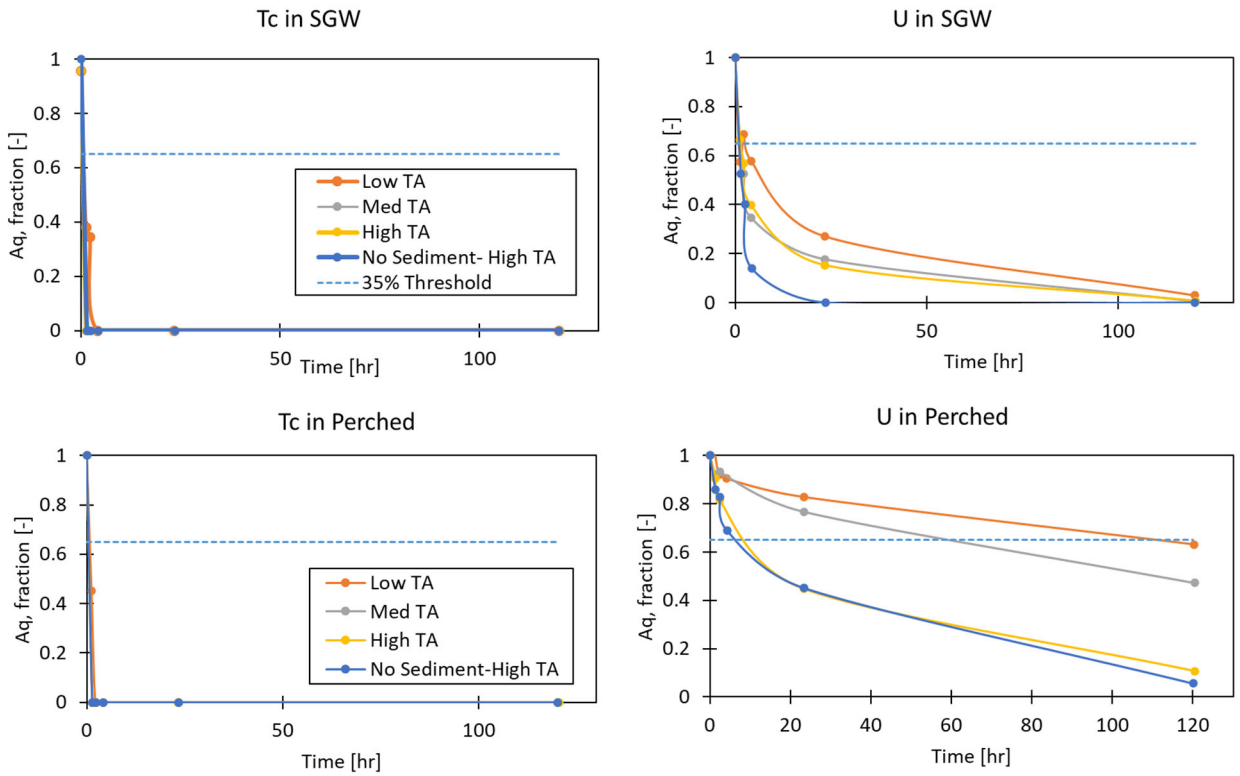

Figure E.5. Scoping experiment results for Tc-99 (left) and U (right) under BY Cribs (top) or perched water (bottom) conditions. In the legend, "TA" stands for Sn(II)-PO_4. Sediment is included in the experiments unless indicated by "No Sediment." Lines in these figures are used to guide the eye and do not represent model results. Data in these scoping experiments are FIO.

E.4 Behavior of CoCOIs

Sn(II)-PO_4 batch experiments are described in Section 3.5.4 and the experimental matrix is shown in Table 3.15. While the results for the primary contaminants of interest (i.e., Tc-99 and U) for experiments with and without co-contaminants of interest (CoCOIs) are presented in Section 4.4, the CoCOI results from sequential extractions conducted on solid material after the 28-day batch experiments are shown in Figure E.6. Without Sn(II)-PO_4 present, more than half of the Cr(VI) and Sr present was removed from the aqueous phase and found in the immobile phase. For Cr(VI), the presence of Sn(II)-PO_4 resulted in most of the Cr(VI) moving from the carbonate phase (Extraction 4) to the hard-to-extract phase (Extraction 5). A similar amount of Sr was found in Extraction 5 with or without Sn(II)-PO_4 present, but more Sr was found in the carbonate phase with Sn(II)-PO_4 [50% Sr was in the carbonate phase in Sn(II)-PO_4 experiments, compared to 30% in the control without Sn(II)-PO_4].

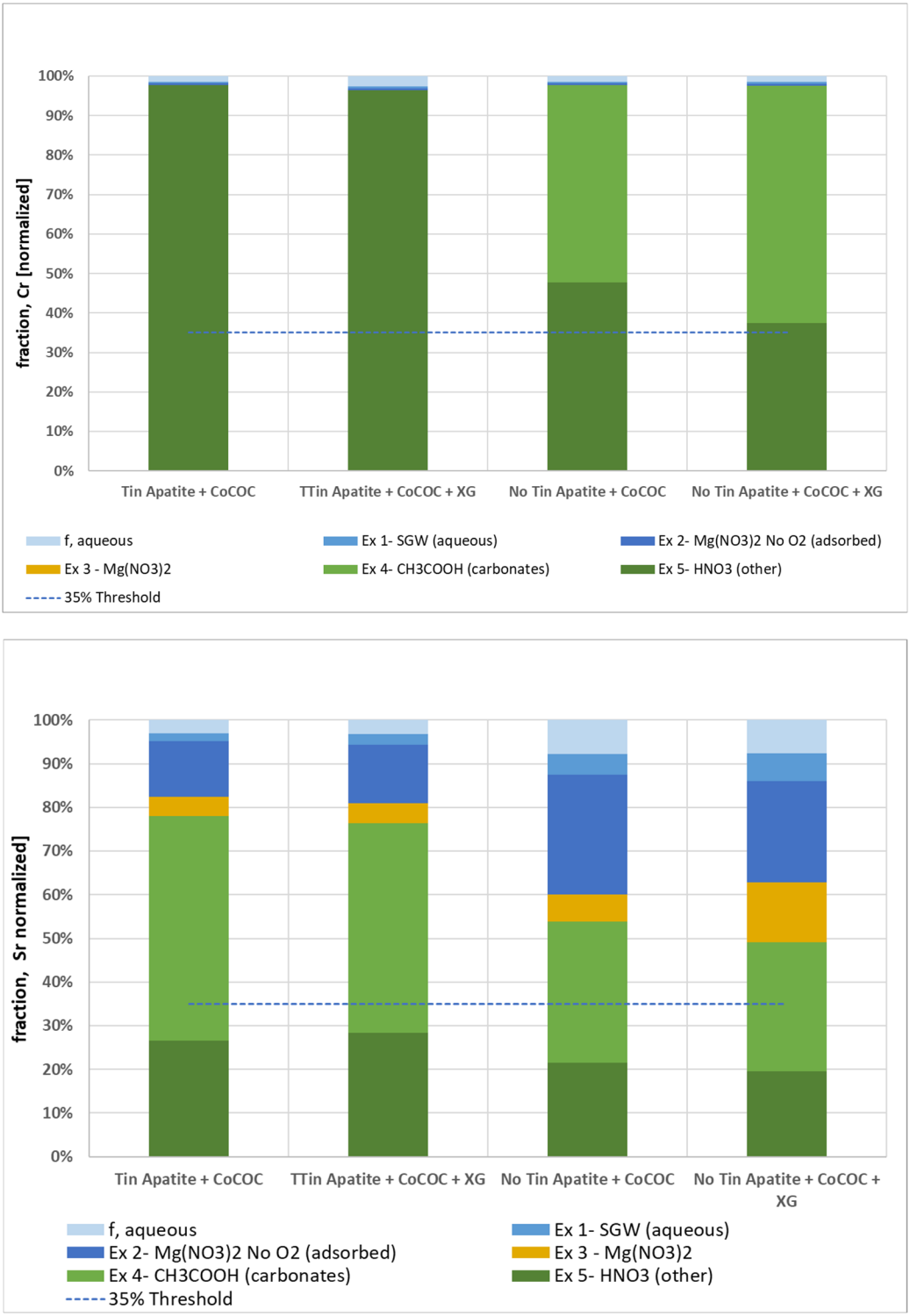

Figure E.6. Sequential extraction results from Hanford formation (Hf) sediments after reaction for 28 days showing mobility of Cr(VI) (top) or Sr (bottom) following sequestration by Sn(II)-PO_4 in BY Cribs groundwater conditions in experiments with CoCOIs present. Recovery of Cr(VI) ranged from 61% to 92%; recovery of Sr ranged from 88% to 98%. Experiments labeled with "XG" included xanthan gum as a delivery fluid; see Section E.5 for more information on delivery fluid experiments.

E.5 Effect of Delivery Fluid

In FY23, scoping tests were conducted to determine which delivery fluid would be best suited for the Sn(II)-PO_4. Scoping work included a visual test to determine suspension of the Sn(II)-PO_4 over time and batch experiments to determine the effect of delivery fluid on aqueous removal of chromate. These scoping experiments used chromate to simplify early experiments as chromate could be measured using a handheld UV-Vis and did not require radiologic controls. Two delivery fluids were evaluated [xanthan gum (XG) and guar gum (GG)] in three background solutions (ultrapure water, 200W SGW, and SPW) at a concentration of 800 mg/L based on results from similar experiments reported previously (Muller et al. 2021b). The chromate reactivity tests were conducted in ultrapure water with XG, GG, or no delivery fluid.

Based on visual observations of the suspension of the Sn(II)-PO_4 in the delivery fluids, XG was confirmed to be the optimal option compared to GG because the Sn(II)-PO_4 settled out almost immediately in GG but a significant amount of solid material remained suspended for extended periods (> 1 day) in XG in all background solutions. Reactivity was reduced in the XG and GG tests, with ~85% and ~65% of the aqueous Cr(VI) removed, respectively, compared to ~99% of Cr(VI) removed from solution without delivery fluid present within 20 hours. These tests were conducted after the FY22 batch experiments targeting Objective 1 (Section 4.4.1), but they confirm that the Sn(II)-PO_4 performed better with XG than with GG.

In addition to the scoping experiments to evaluate different types of delivery fluids, batch experiments were conducted with delivery fluid present as shown in the experiment matrix (Table 3.15). These experiments evaluated the effect of the presence of delivery fluid on the removal of Tc-99 and U from the aqueous phase. Batch experiments conducted with 800 mg/L delivery fluid proved challenging because the delivery fluid was difficult to filter. Several filters were broken during sampling and some unfiltered solution may have gotten into the sample vials. For some samples, only a very small amount of filtrate could be collected. Note that these issues can cause difficulties in the analysis and interpretation of the resulting data.

Results of the batch experiment showed minor decreases in removal of Tc-99 from the aqueous phase in both the water table application and perched water application experiments when delivery fluid was present (Figure E.7, Figure E.8). Removal of U from the aqueous phase was unaffected by the presence of delivery fluid under the BY Cribs groundwater conditions, but did slightly decrease in the perched water conditions, resulting in similar U aqueous phase removal as the no-sediment control in the same series of experiments (Figure E.7, Figure E.8).

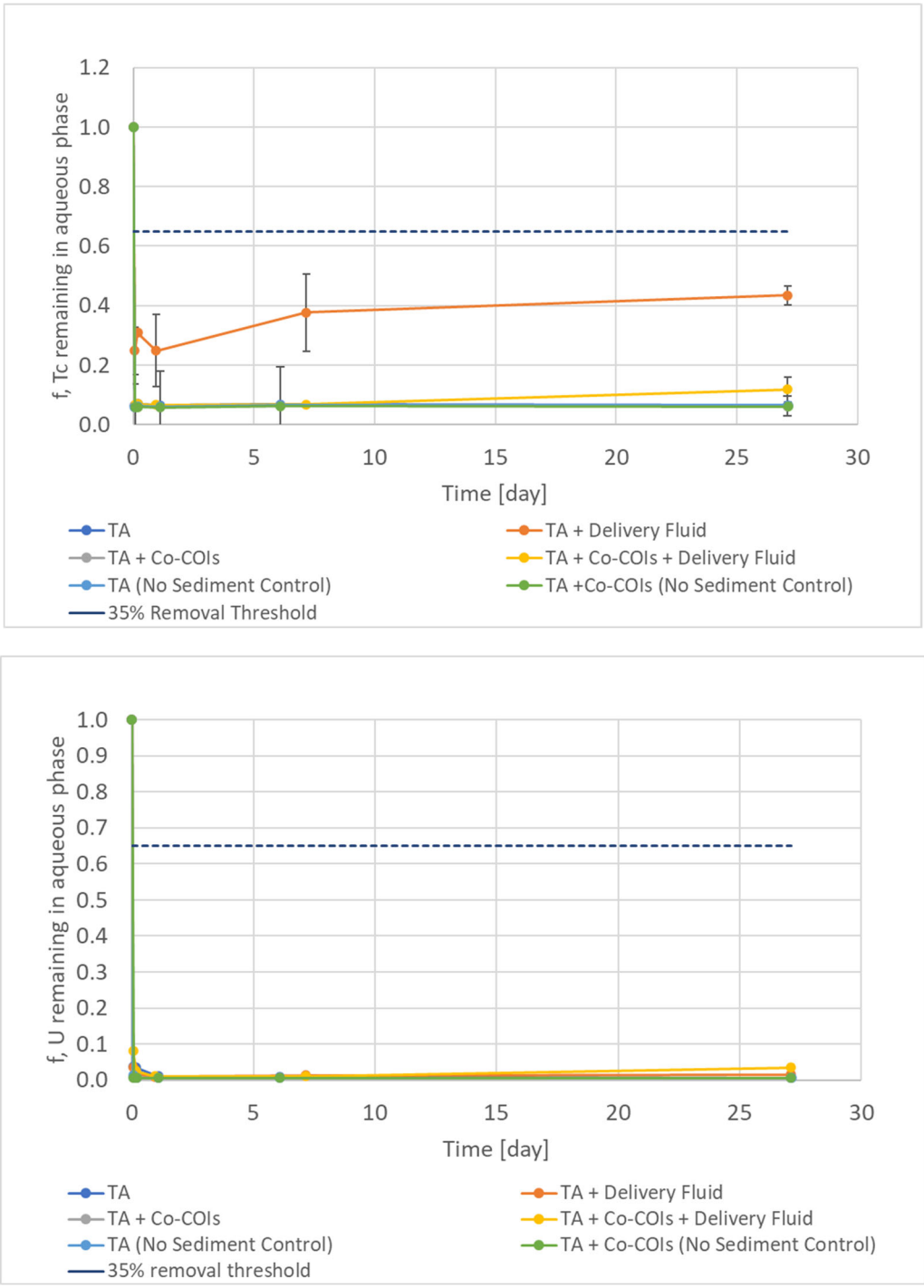

Figure E.7. Fraction of Tc-99 (top) or U (bottom) in the aqueous phase over time in BY Cribs groundwater conditions [with Sn(II)-PO_4 ("TA"), delivery fluid (xanthan gum), sediment, and/or Co-COIs] in batch experiments with Hf sediments conducted over 28 days. Error bars are based on analysis of triplicate batch reactors. Lines are used to guide the eye and do not represent a model.

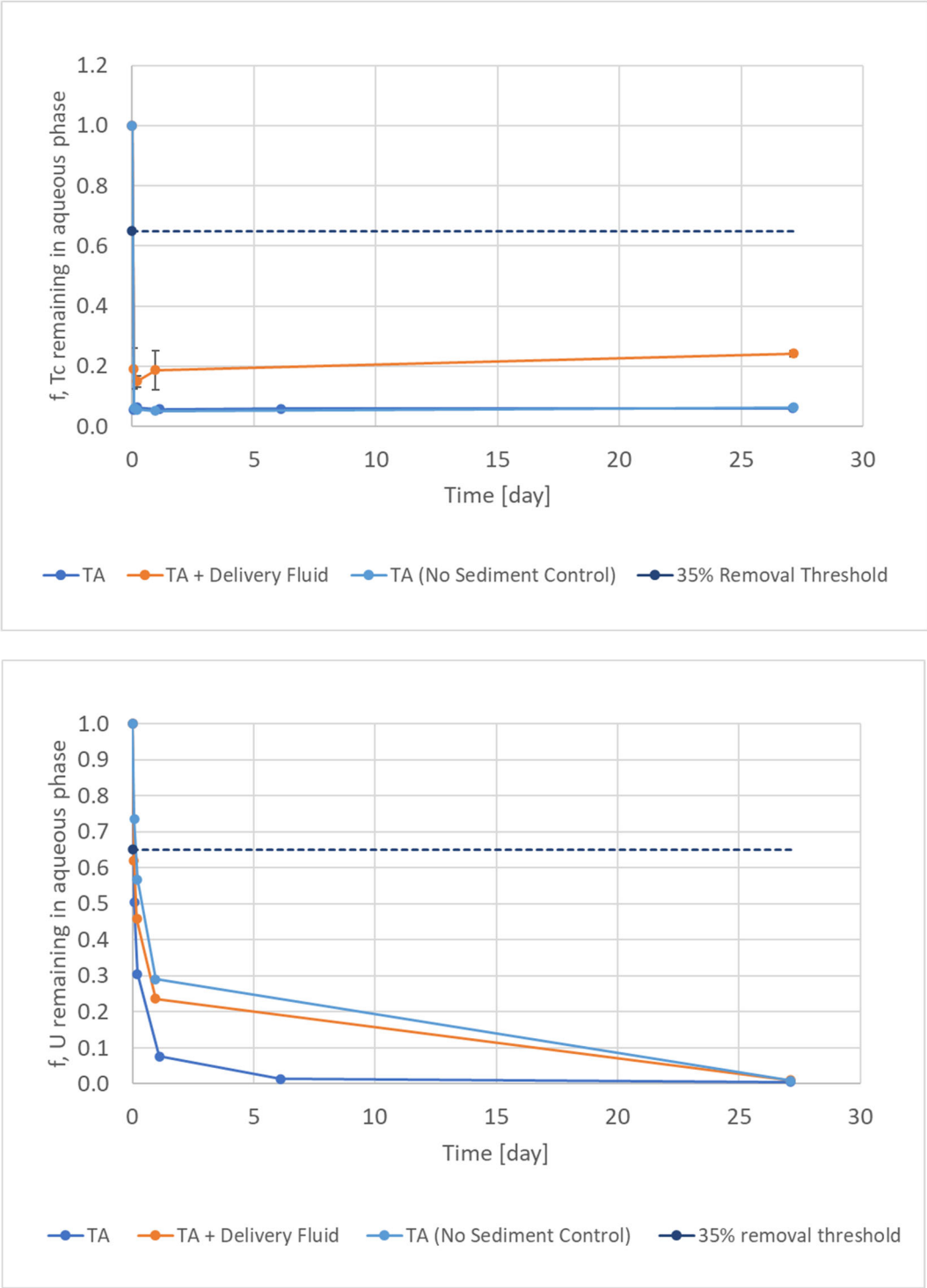

Figure E.8. Fraction of Tc-99 (top) or U (bottom) in the aqueous phase over time in perched water conditions [with Sn(II)-PO_4 ("TA"), with or without delivery fluid (xanthan gum) and/or sediment] in batch experiments with Hf sediments conducted over 28 days. Error bars are based on analysis of triplicate batch reactors. Lines are used to guide the eye and do not represent a model.

E.6 Additional Information

Additional batch tests were set up to measure pH and Eh changes over time in SGW and SPW, with and without Sn(II)-PO_4 present. Results (Figure E.9) show that the presence of Sn(II)-PO_4 has a slight effect on the pH, lowering the pH by ~1 unit in the SGW tests and ~0.5 unit in the SPW test. The presence of CoCOIs did not affect the pH.

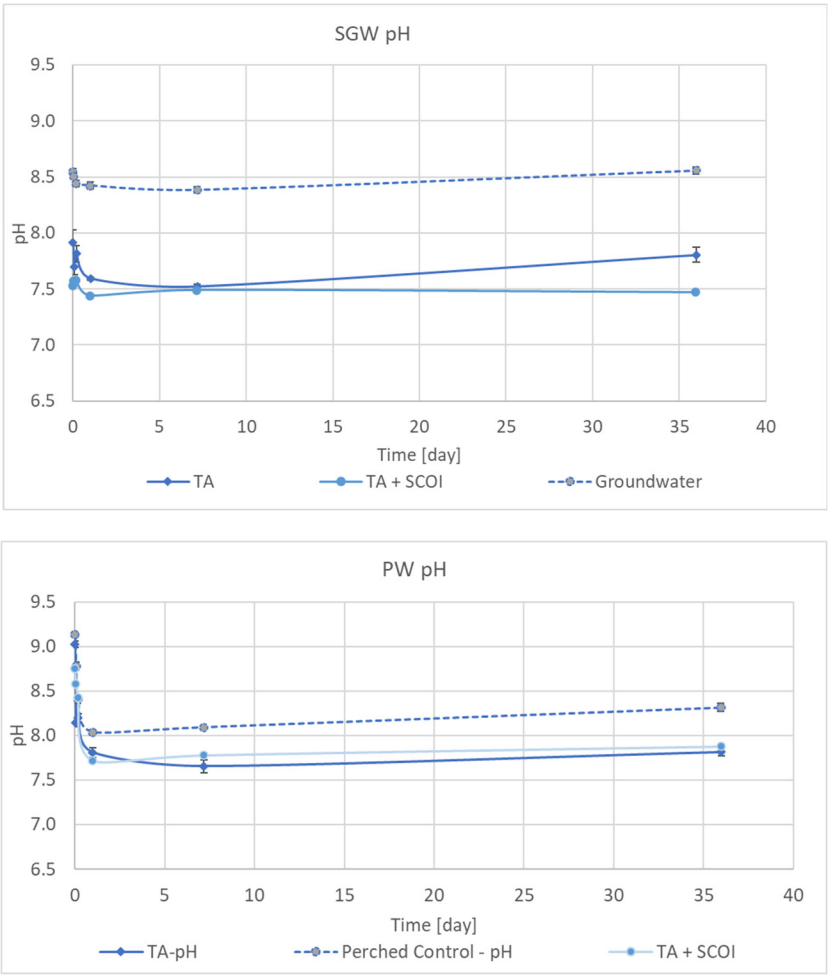

Figure E.9. Measurements of pH over time for experiments without sediment, containing Sn(II)-PO_4 in SGW or SPW ("TA"), Sn(II)-PO_4 with CoCOIs in SGW or SPW ("TA+COCOI"), or no Sn(II)-PO_4 or PCOIs/CoCOIs in SGW or SPW ("Groundwater" or "Perched Control"). Results for SGW tests are on the top; SPW tests are on the bottom.

It is expected that the Sn(II)-PO_4 produced reducing conditions, causing Tc-99 to be reduced and then precipitate. Tc-99 is easily re-oxidized, and if this was the only mechanism for Sn(II)-PO_4 to remove Tc-99 from the aqueous phase, the Tc-99 would be expected to remobilize during the sequential extractions during the third extraction. The results of the sequential extraction showed that most of the Tc-99 was immobilized and found in the fifth extraction (Section 4.4.4), indicating there may be additional mechanisms increasing the retention of Tc-99 after the initial reduction step. However, the Sn(II)-PO_4 may also be so reductive that the system was still under reducing conditions throughout the sequential extraction process. To test this, additional sequential extractions were conducted. The post-experiment solids had been exposed to oxic conditions for several weeks, then used in another sequential extraction

following the steps outlined in Section 3.3. Prior to the first extraction, however, air was bubbled into the solution for several hours and Eh was measured in this solution to confirm the sample was oxic prior to taking the first extraction sample. After this step, the extractions continued as described in Section 3.3. Results are shown in Figure E.10, with the initial results included for comparison. Results show that despite the additional oxidizing step, the Tc-99 (and U) remained immobilized, indicating a secondary step beyond reduction is likely controlling the continued contaminant of interest immobilization. Further solid phase characterization is needed to determine additional mechanisms.

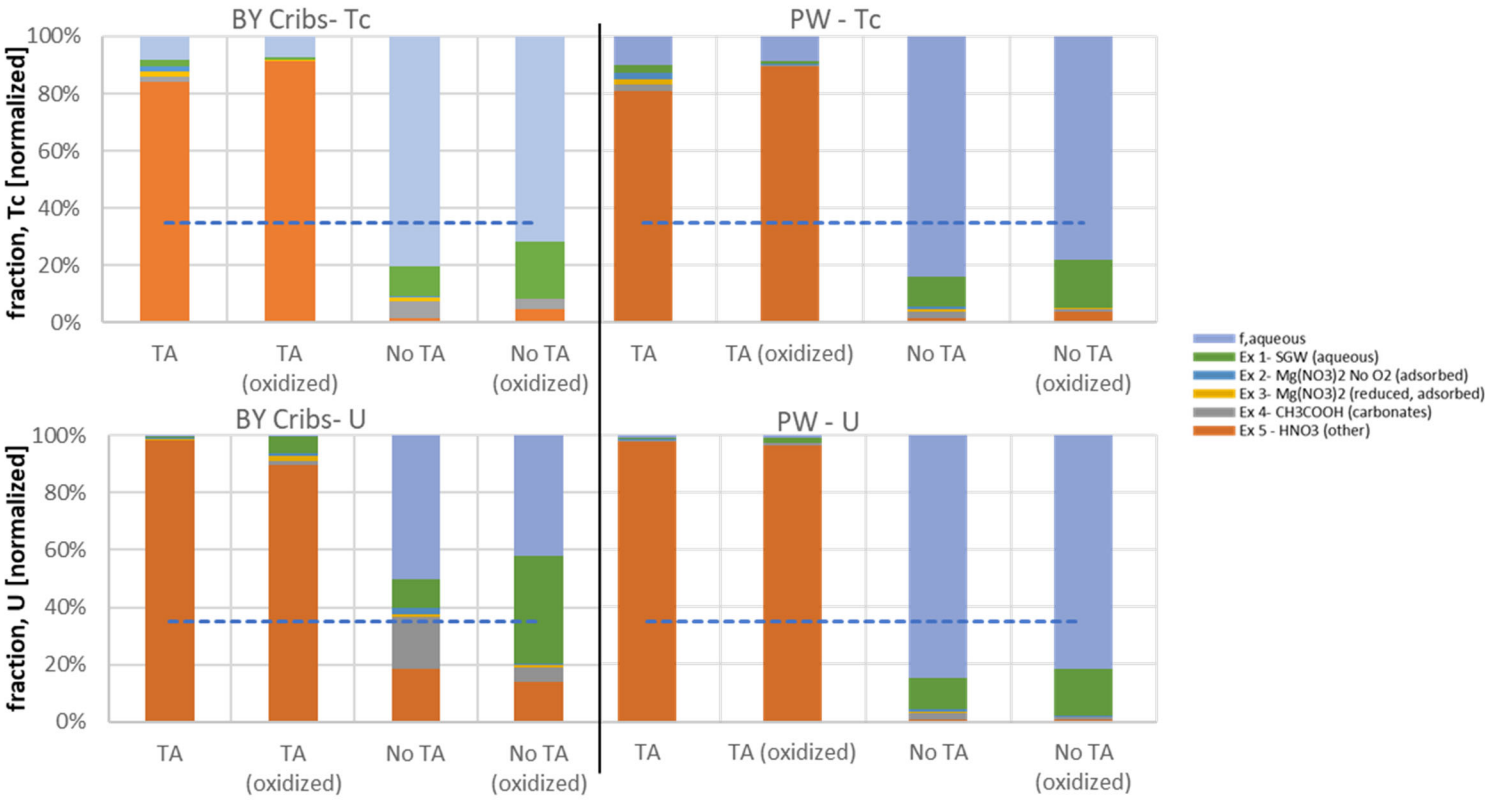

Figure E.10. Sequential extraction results for original post-experiment sequential extractions ["TA" for experiments containing Sn(II)-PO_4 and "No TA" for experiments without Sn(II)-PO_4 present] and for oxidized solids ["TA (oxidized" for oxidized experiments with Sn(II)-PO_4 and "No TA (oxidized)" for oxidized experiments with no Sn(II)-PO_4 present] for BY Cribs groundwater conditions (*left*) and perched water conditions (*right*). Results for Tc-99 are shown on the top and U results on the bottom. The y-axis shows the % of Tc-99 or U present in each phase.

Appendix F – Supporting Data for Particulate Sequestration Amendment – Bismuth Materials

F.1 Synthesis of BOH

Bismuth oxyhydroxide (BOH) was synthesized following the procedure described in Lawter et al. (2021). Briefly, the procedure includes combining ethylene glycol, $Bi(NO_3)_3$, and urea. After heating at 150 °C for 5 h, the solution was allowed to cool and the excess ethylene glycol was removed by decantation. The product was rinsed, alternating between de-ionized water and methanol, for a total of 20 washes, then air dried. The absence of urea and ethylene glycol were confirmed by infrared spectroscopy; if urea or ethylene glycol was found to be present, the washing process was repeated as needed.

F.2 Scoping – Delivery Fluid

Scoping tests were conducted to determine which delivery fluid would be best suited for the BOH and bismuth subnitrate (BSN). Scoping work included a visual test to determine suspension of the bismuth materials over time and batch experiments to determine the effect of delivery fluid on aqueous removal of chromate. Two delivery fluids were evaluated [xanthan gum (XG) and guar gum (GG)] in three background solutions [double-deionized water, 200W synthetic groundwater (SGW), and synthetic perched water (SPW)] at a concentration of 800 mg/L based on results from similar experiments reported previously (Muller et al. 2021b). The chromate reactivity tests were conducted in double-deionized water with XG, GG, or no delivery fluid.

Based on visual observations of the suspension of the Sn(II)-PO_4 in the delivery fluids, GG was determined to be the optimal option compared to XG because both delivery fluids suspended BOH similarly, but BSN was suspended for much longer with GG compared to the XG. Reactivity was reduced in the XG and GG tests for BSN but was only reduced in the GG test for BOH. Limitations in reactivity can be overcome with addition of more of the bismuth material, so better suspension was prioritized, and GG was chosen for inclusion in the batch matrix (Section 3.5.5).

F.3 Behavior of CoCOIs

In BY Cribs groundwater conditions, batch experiments were conducted with the addition of co-contaminants of interest (CoCOIs), including Sr, Cr(VI), I, and nitrate. Sequestration of primary contaminants of interest (PCOIs; Tc-99 and U) with the addition of CoCOIs was largely unchanged with the exception of aqueous Tc-99 removal in the BSN experiment without sediment present. In that case, the sequestration of Tc-99 increased, nearly matching the removal of Tc-99 in the experiment conducted with sediment.

Sr and Cr(VI) concentrations were measured at the first and last time points for these experiments. With or without sediment present, in BSN and BOH experiments, ~90% of the Cr(VI) was removed from the aqueous phase within 28 days (Figure F.1). With sediment present, the BOH and no-Bi control tests removed ~80% of the aqueous Sr within 28 days, but the BSN removed only ~60%. Without sediment present, the BOH and BSN experiments removed < 10% of the aqueous Sr, indicating that the removal of Sr from the aqueous phase is likely attributable to the adsorption by the sediment and not the bismuth materials (Figure F.1).

Iodine was added at a concentration 10x lower than the target and was below instrument detection limits.

The sequential extractions showed that the U and Tc-99 were generally found in the same phases with or without CoCOIs (see Section 4.5). Cr(VI) removed from the aqueous phase by the bismuth material was mostly (> 75%) found in the immobile phase, with little Cr(VI) removed in the control without bismuth [~90% of the Cr(VI) remained in the aqueous phase]. Sr results were similar with and without bismuth present (Figure F.2).

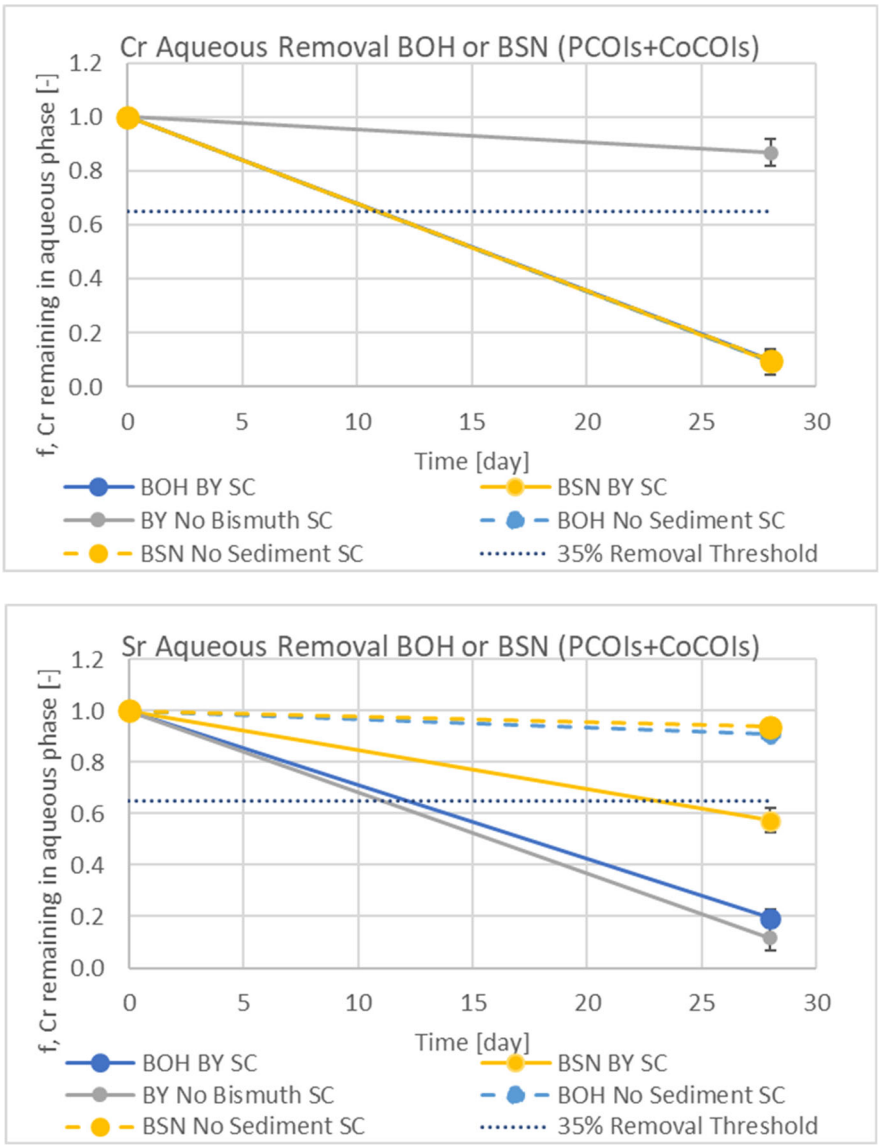

Figure F.1. Fraction of Cr(VI) (*top*) or Sr (*bottom*) in the aqueous phase over time in BY Cribs groundwater conditions in batch experiments with Hanford formation (Hf) sediments and conducted over 28 days with BOH, BSN, or no bismuth (control), with CoCOIs ("SC") present. Error bars are based on analysis of triplicate batch reactors. Lines are used to guide the eye and do not represent a model.

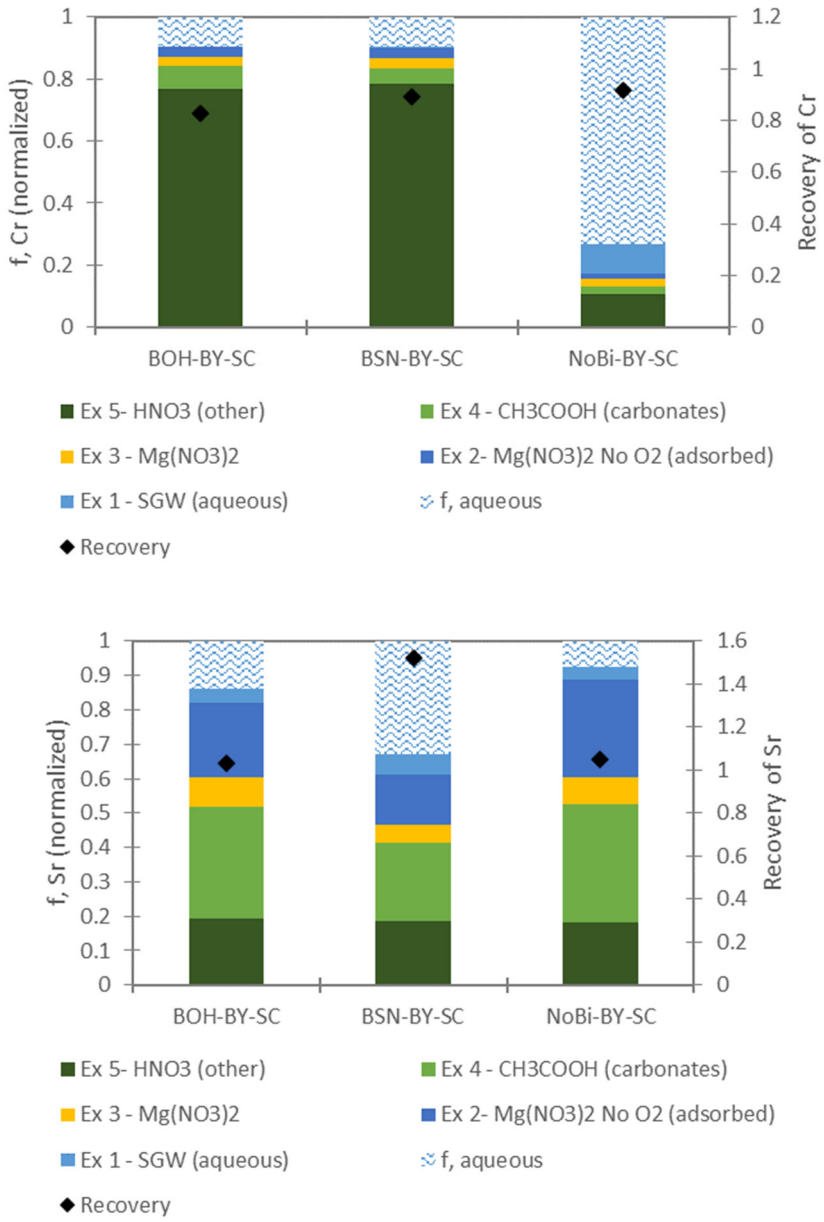

Figure F.2. Sequential extraction results from Hf sediments after reaction for 28 days showing mobility of Cr(VI) (*top*) or Sr (*bottom*) with BOH, BSN, or no bismuth (control) with PCOIs and CoCOIs ("SC") present following sequestration in BY Cribs groundwater conditions.

F.4 Effect of Delivery Fluid

Based on results of the scoping tests (see Section F.2), GG was chosen as the delivery fluid to test in the bismuth batch experiments. GG was added to the SGW or SPW at a concentration of 800 mg/L. The delivery fluid solutions were mixed overnight, then spiked with Tc-99 and U.

Comparing the fraction of Tc-99 remaining in the aqueous phase over time with delivery fluid present (Figure F.3) or no delivery fluid (Figure 4.27), results are similar for most of the tests in the BY Cribs groundwater and perched water conditions. The controls with sediment but no bismuth present show

lower aqueous Tc-99 at the 28-day time point with delivery fluid present compared to the same tests without delivery fluid.

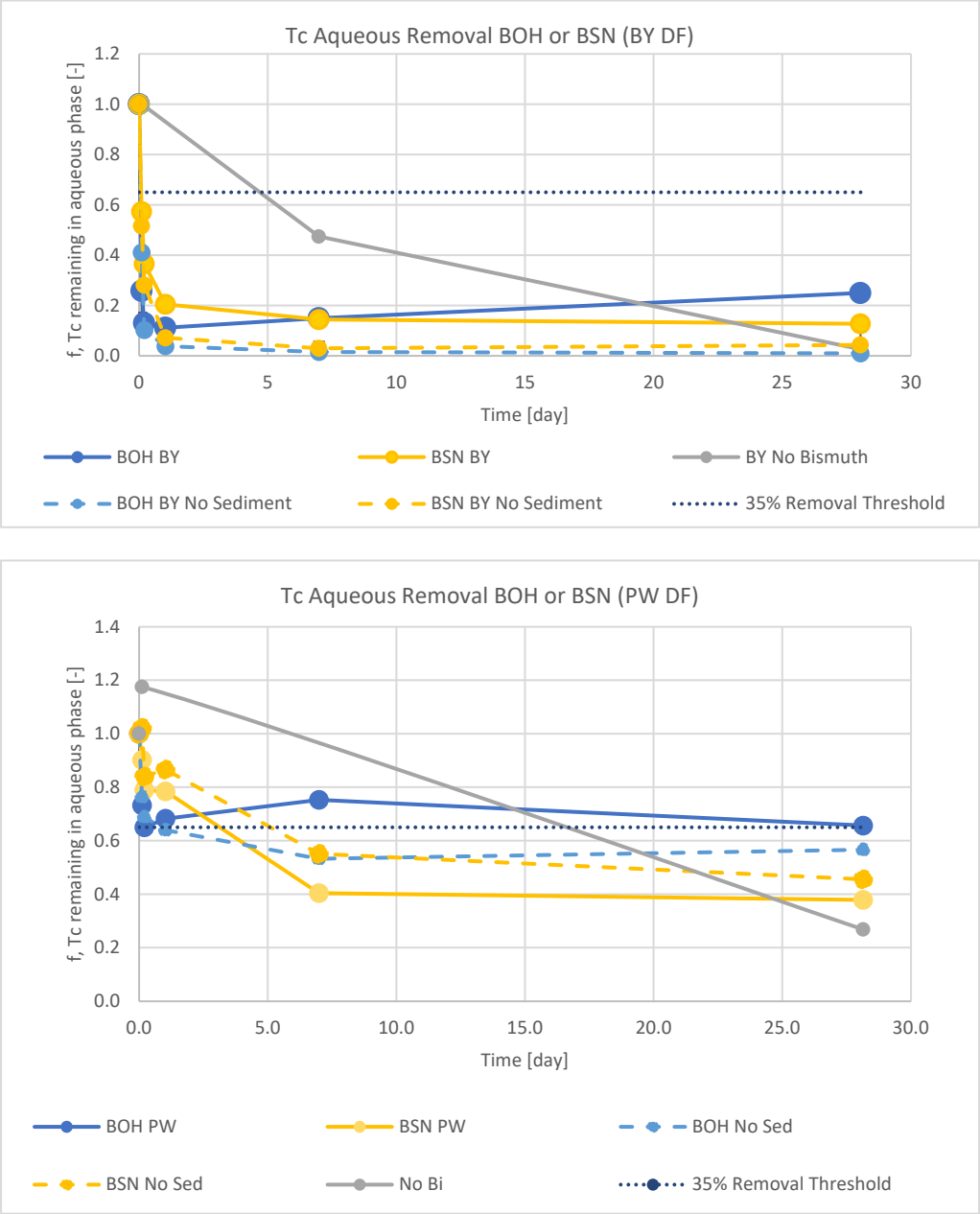

Figure F.3. Fraction of Tc-99 in the aqueous phase over time in BY Cribs groundwater conditions (*top*) or perched water conditions (*bottom*) with delivery fluid (GG) in batch experiments with Hf sediments conducted over 28 days. Error bars are based on analysis of triplicate batch reactors. Lines are used to guide the eye and do not represent a model. BY and PW notations in the legend indicate BY Cribs conditions or perched water conditions, respectively.

The uranium results with delivery fluid added are nearly identical to the results without delivery fluid (see Figure 4.21 for comparison to Figure F.5), with the exception of the control containing sediment without any bismuth material. With delivery fluid present, the fraction of U in the aqueous phase in the BY Cribs groundwater conditions decreased to 0 (below detection limits) by 28 days (Figure F.5) while it remained

around 0.7 in the experiment without delivery fluid (Figure 4.21). The same was not observed in the perched water conditions, where the control with sediment but no bismuth showed little to no removal of U with or without delivery fluid present (Figure F.5; Figure 4.21).

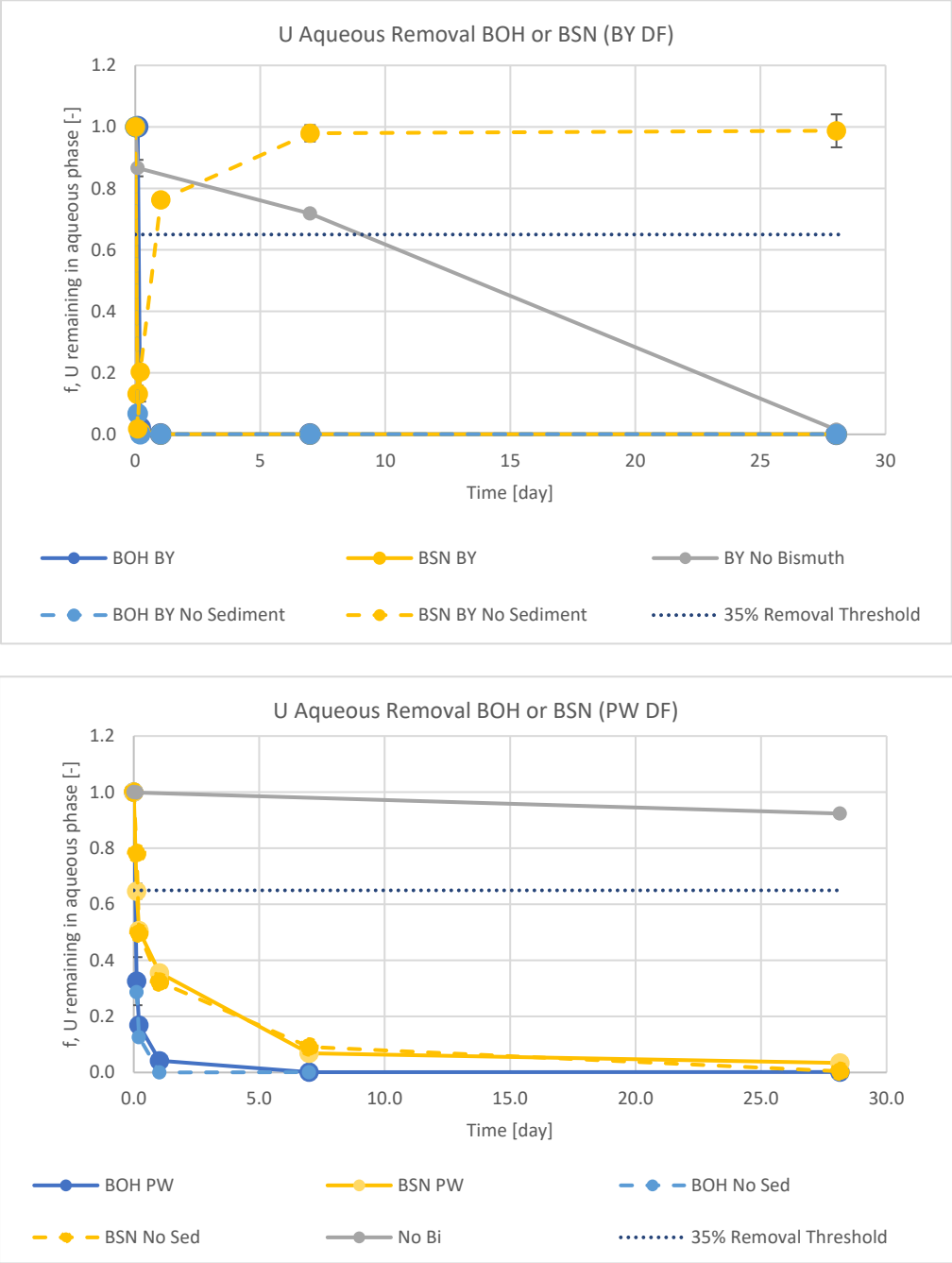

Figure F.4. Fraction of U in the aqueous phase over time in BY Cribs groundwater conditions (*top*) or perched water conditions (*bottom*) with delivery fluid (GG) in batch experiments with Hf sediments conducted over 28 days. Error bars are based on analysis of triplicate batch reactors. Lines are used to guide the eye and do not represent a model.

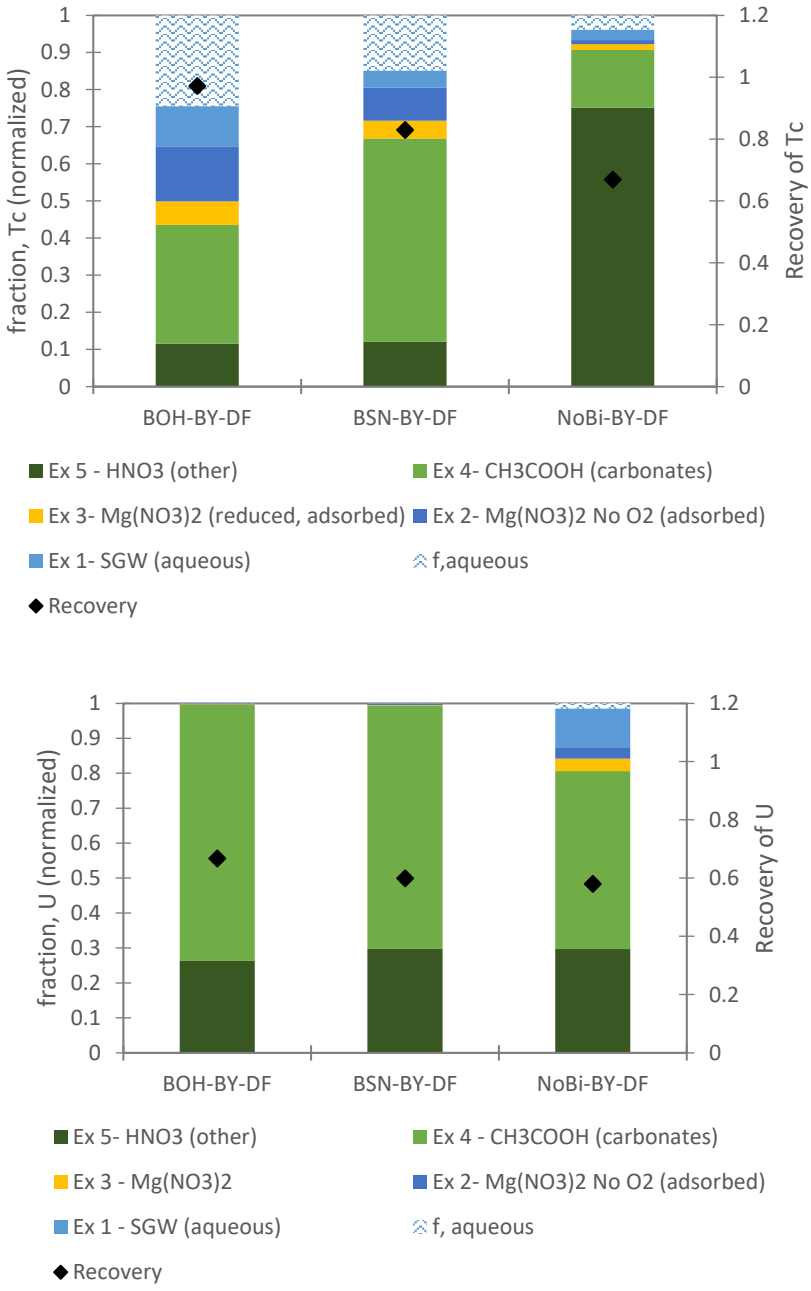

Figure F.5. Sequential extraction results from Hf sediments after reaction for 28 days showing mobility of Tc-99 (*top*) or U (*bottom*) with BOH, BSN, or no bismuth (control) with PCOIs and delivery fluid (GG) present following sequestration in BY Cribs groundwater conditions.

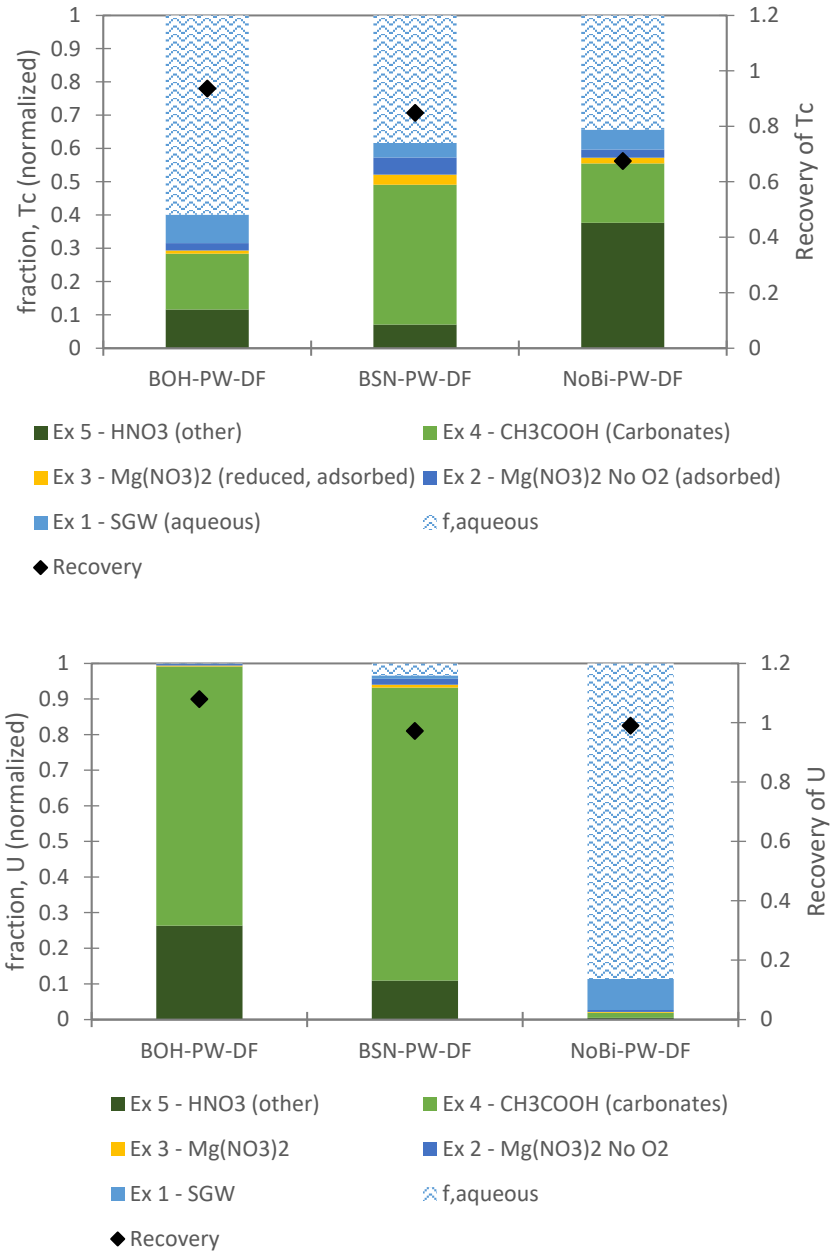

Figure F.6. Sequential extraction results from Hf sediments after reaction for 28 days showing mobility of Tc-99 (*top*) or U (*bottom*) with BOH, BSN, or no bismuth (control) with PCOIs and delivery fluid (GG) present following sequestration in perched water conditions.

F.5 BOH and BSN Batch Experiment pH

The pH was measured on one of the triplicate samples for each experiment condition following the final sampling (either 1 day or 28 days). The pH measurements were collected For Information Only.

Table F.1. pH measurements for BOH and BSN experiments using Hf sediments under BY Cribs or perched water conditions. Starting solutions (SGW or SPW) were also measured. All experiments contained PCOIs and Hf sediment (unless noted "NoS," indicating no sediment). Experiments with CoCOIs are labeled as such. The pH was measured in the initial solution (labeled SGW or SPW), or at the end of the experiment at 28 days unless indicated as "1 d" experiments, which ended after 1 day.

Experiment	
BY Cribs Conditions	pH
SGW+PCOI	8.31
SGW+PCOI-CoCOIs	8.79
BOH	7.41
BOH-1d	7.32
BOH-CoCOIs	7.33
BOH-NoS	7.42
BOH-NoS-CoCOIs	7.14
BSN	6.95
BSN-1d	6.34
BSN-CoCOIs	7.19
BSN-NoS	2.01
BSN-NoS-CoCOIs	1.92
No BOH/BSN	8.03
No BOH/BSN-CoCOIs	7.87
Perched Water Conditions	pH
SPW-1	8.53
SPW-2	8.88
BOH	7.74
BOH-1d	7.64
BOH-NoS	9.81
BSN	7.28
BSN-1d	6.34
BSN-NoS	5.47
No BOH/BSN	7.82

Appendix G – Supporting Data for Particulate Reduction and Sequestration – ZVI/SMI followed by Poly-PO_4

G.1 ZVI and SMI Characterization

Two solid reductants used in this approach are zero valent iron (ZVI) and sulfur-modified iron (SMI). Characterization is presented in Table G.1, with some of these results described previously (PNNL-30440).

Table G.1. Characterization of ZVI and SMI used in experiments (PNNL-30440).

Name	Description	Composition (by X-ray diffraction)	Particle Size (μm)	Surface Area (m^2/g)	Reduction Capacity (meq/g)
Zero valent iron (ZVI)	Hepure Ferox Flow 100 mesh	100% Fe	< 44	0.852	35.4±0.6
Sulfur-modified iron (SMI) – batch	North American Hoganas R-12S	60% Fe, 33% Fe_3O_4, 7% FeO, and a trace of S	297-841	1.54	23.4±0.0
SMI – column	SMI water	74.5% Fe, 22.3% Fe_3O_4, and 2.9% FeS_2	250-841	1.49	41.4±5.0

G.2 Tc-99 and U Sequestration by Different ZVI or SMI Loading

Injection of ZVI or SMI into perched or groundwater is generally as a permeable reactive barrier (PRB) downgradient of contaminants rather than direct source area treatment. As such, the loading of the electron donor (ZVI or SMI) is typically considerably greater than the reducible contaminants of interest, as other electron acceptors [co-contaminants of interest (CoCOIs) and dissolved oxygen] that also oxidize the barrier may be present at higher concentrations. Reductive barrier lifetime depends on the flux of electron acceptors through the barrier relative to the electron donor (ZVI or SMI) within the barrier.

Loading experiments with ZVI and SMI were conducted to evaluate Tc-99 and U removal from the aqueous phase in systems with excess electron donor (i.e., early in a PRB lifetime) and with excess electron acceptor (i.e., late in a PRB lifetime or situations with excess CoCOIs). Both ZVI and SMI removed > 99% of aqueous Tc-99 within 14 days in situations of excess electron donor (Figure G.1, right few bars in each graph) followed by 14 days of treatment with the Poly-PO_4 solution. Sequential extractions showed that nearly all the Tc-99 was sequestered in a precipitate that was difficult to oxidize or dissolve (8M nitric acid extraction). With equal electron donor and acceptor present, SMI performed better than ZVI, showing > 96% Tc-99 immobilization compared to ZVI with 87% Tc-99 immobilization. With excess Tc-99 compared to ZVI or SMI, less Tc-99 was immobilized (Figure G.1, left bar in each graph).

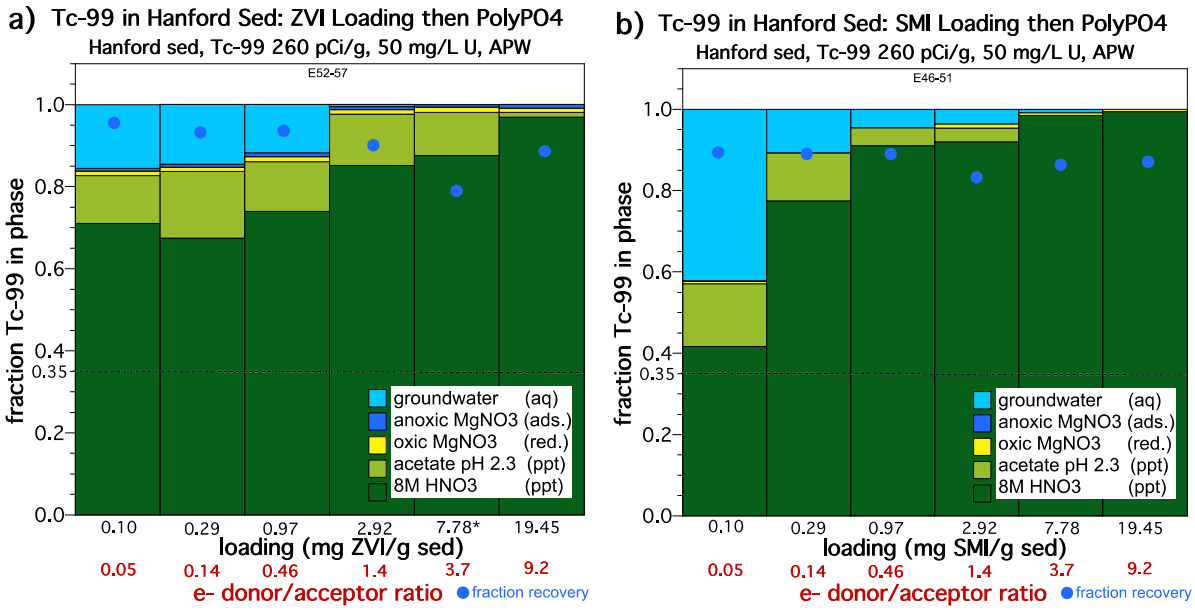

Figure G.1. Tc-99 reduction after 14 days at different loading of (a) ZVI and (b) SMI, followed by an additional 14 days of treatment with Poly-PO_4.

Although U(VI) reduction requires a more reducing environment than pertechnetate reduction, similar results were observed, with a more rapid U(VI) reduction at a high electron donor/acceptor ratio and slower reduction when a limited mass of electron donor (ZVI or SMI) was present (Figure G.2). In general, both the ZVI and SMI formed U(IV) precipitates that were somewhat more mobile (i.e., most in the 8M HNO_3 extraction, but some in the acetate extraction) than Tc(IV) precipitates.

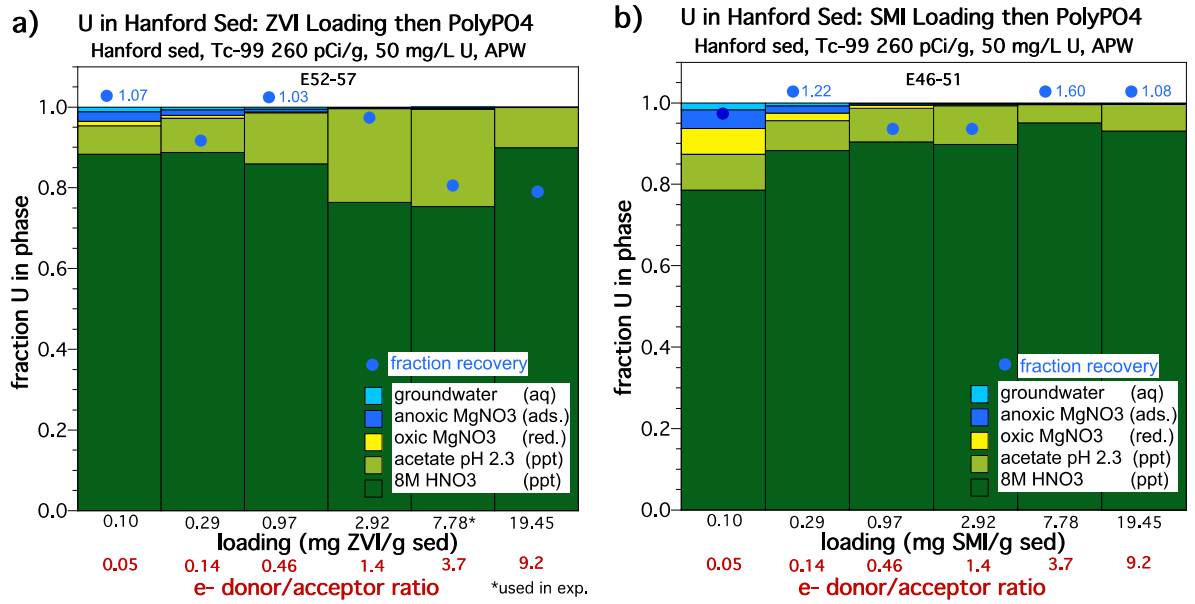

Figure G.2. U(VI) reduction after 14 days at different loading of (a) ZVI and (b) SMI, followed by an additional 14 days of treatment with Poly-PO_4. These data are For Information Only.

G.3 Tc-99 and U Sequestration Supporting Information

The untreated sediments [Hanford formation, Cold Creek Unit silt (CCuz), and BY Cribs] were initially oxic and so had a redox potential of ~+200 mV. With the addition of ZVI or SMI, reducing conditions were created with a redox potential of -400 to -600 mV (Figure G.3a). The pH also increased from 7.5-8.0 (untreated sediments) to 8.2-9.7 (Figure G.3b).

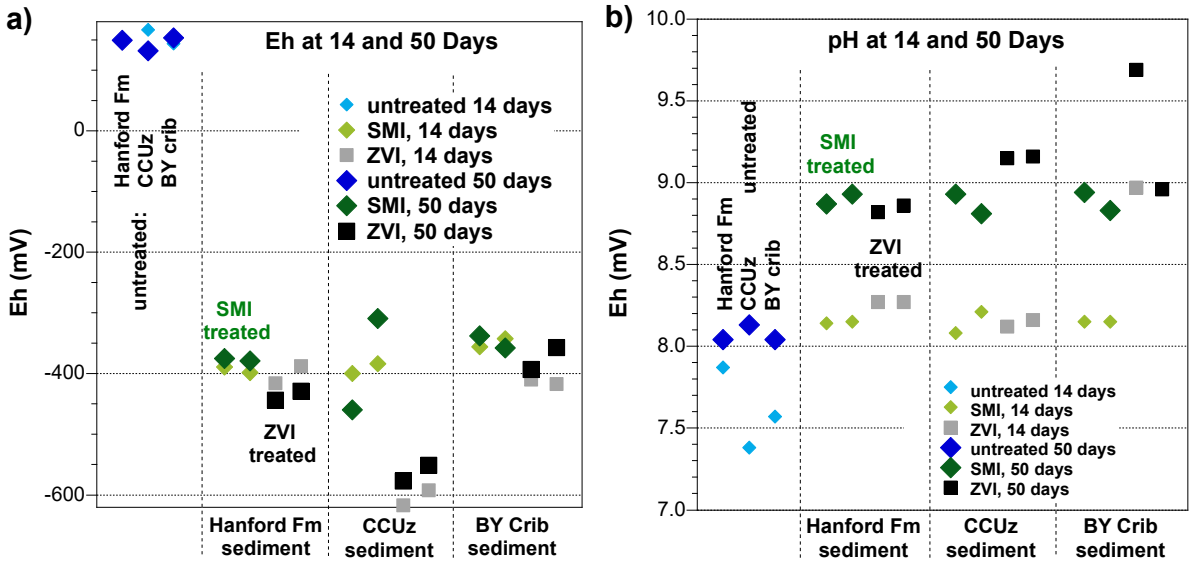

Figure G.3. Influence of geochemical conditions in sediment/water experiments in groundwater by the addition of ZVI or SMI, as shown by (a) redox potential and (b) pH.

With addition ZVI or SMI for 14 days, subsequent addition of the Poly-PO_4 solution, and reaction to 50 days (36 days after Poly-PO_4 addition), Tc-99 reduction/sequestration in systems without sediment were investigated to evaluate the performance of amendments. Comparison of these results to reduction/sequestration with the same amendments in the presence of sediment shows the complexity of additional reactions that occur with sediments. As a baseline, Tc-99 and U sequential extractions in untreated sediments show little sorption for Tc-99 (Figure G.4a) and small U sorption (Figure G.4b).

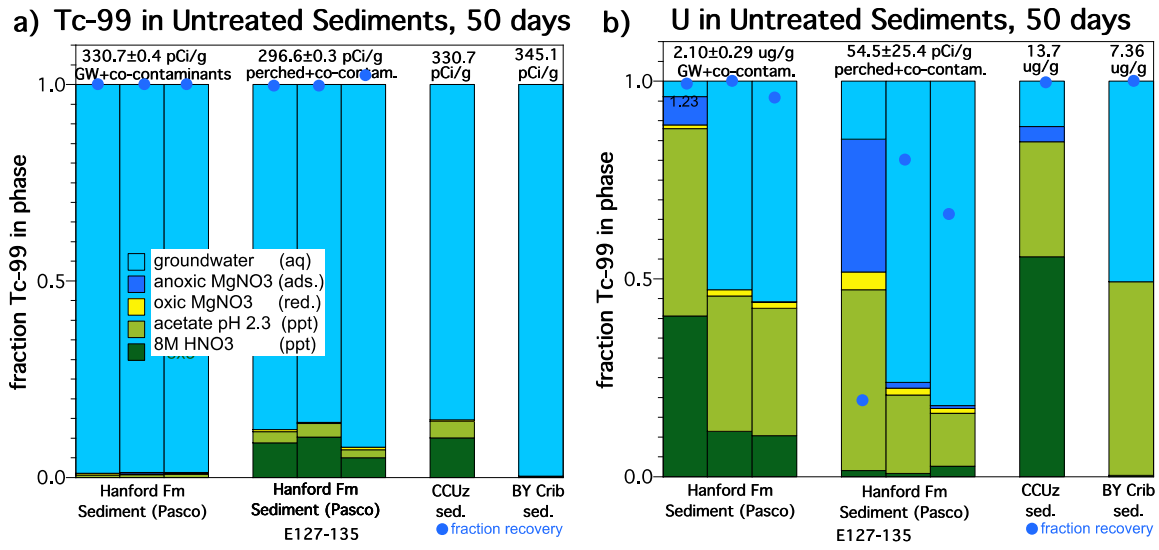

Figure G.4. Tc-99 and U sequential extraction after 50 days in untreated Hanford formation sediment in groundwater (Tc-99 and U only) and perched water (Tc-99, U, and nitrate), and CCuz and BY Cribs sediment in groundwater with just Tc-99 and U.

In different experimental systems (i.e., no sediment, with sediment and no contaminants, or in sediment with co-contaminants), there are different electron acceptor (i.e., contaminant) concentration ratios relative to the electron donor (i.e., ZVI or SMI), as described in Table G.2.

Table G.2. Electron donor and acceptor concentrations in different sediment/water systems with ZVI.

Electron Donor or Acceptor (meq)	Tc-99, U, No Sediment, Groundwater	Tc-99, U, Cr(VI),IO_3, Nitrate in Groundwater, No Sediment	Tc-99, U, Nitrate in Perched Water, No Sediment	Tc-99, U, Nitrate in BY Cribs Sediment
e- donor	1.91	1.91	1.91	1.91
e- acceptor: Tc-99	$6.1x10^{-5}$	$6.1x10^{-5}$	$6.1x10^{-5}$	$9.0 x10^{-5}$
e- acceptor: U	$1.7 x10^{-4}$	$1.7 x10^{-4}$	$8.7 x10^{-3}$	$1.7 x10^{-4}$
e- acceptor: NO_3^-	N/A	0.032	0.52	1.17
e- acceptor: CrO_4^-	N/A	$4.4 x10^{-3}$	N/A	N/A
e- acceptor: IO_3^-	N/A	$3.2 x10^{-3}$	N/	N/A
e- donor/acceptor ratio	11,000	59	3.7	1.6
N/A = not applicable				

In no-sediment systems, Tc-99 reduction in groundwater by SMI was considerably faster [< 1 day (Figure G.5c)] than the 14 days required for ZVI (Figure G.5a). This is consistent with results of others evaluating the limitations of ZVI compared to ferrous and mixed ferrous/ferric oxides such as SMI (Guan et al. 2015). The electron donor (ZVI or SMI) to acceptor (i.e., Tc-99 and U) ratio in these systems was about 11,000, so orders of magnitude more reductant was present. Tc-99 reduction in groundwater in the presence of CoCOIs (NO_3^-, CrO_4^-, IO_3^-) decreases the electron donor/acceptor ratio to 59. This greatly decreased the Tc-99 reduction rate and extent in ZVI (Figure G.5b) but had little effect on the Tc-99 reduction rate and extent for SMI (Figure G.5d).

Tc-99 reduction experiments in perched water had the same Tc-99 concentration (260 pCi/g or 15 ng/g), but higher U (50 mg/L) and high nitrate (800 mg/L), so the electron donor/acceptor ratio was 3.7. The Tc-99 reduction rate in perched water with nitrate was slower (Figure G.6) than in groundwater for both ZVI and SMI, as nitrate should be reduced before $Tc(VII)O_4^-$ [Eq. (2.5)].

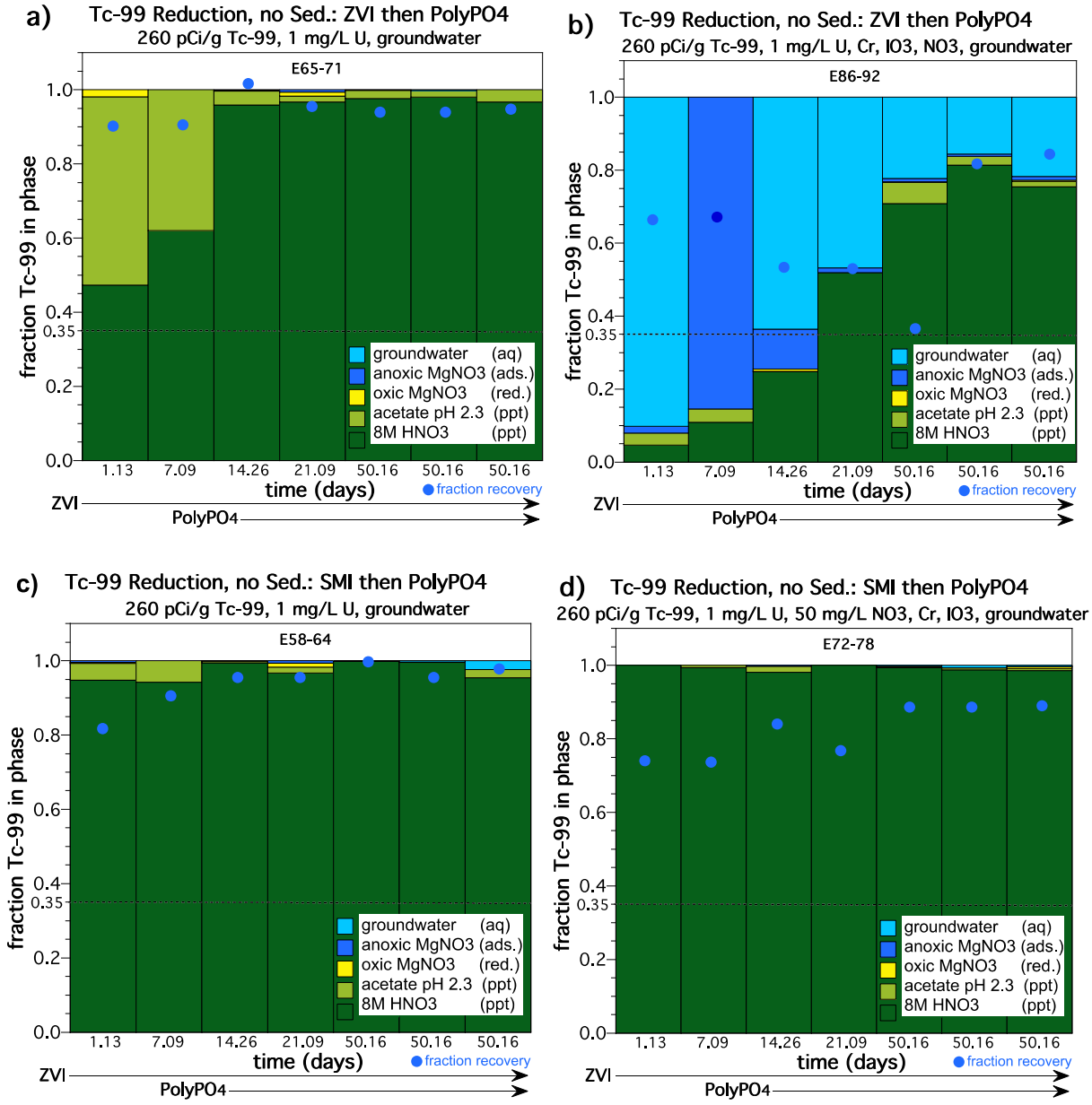

Figure G.5. Tc-99 reduction/sequestration with no sediment by (a) ZVI in groundwater, (b) ZVI in groundwater with CoCOIs, (c) SMI in groundwater, and (d) SMI in groundwater with CoCOIs.

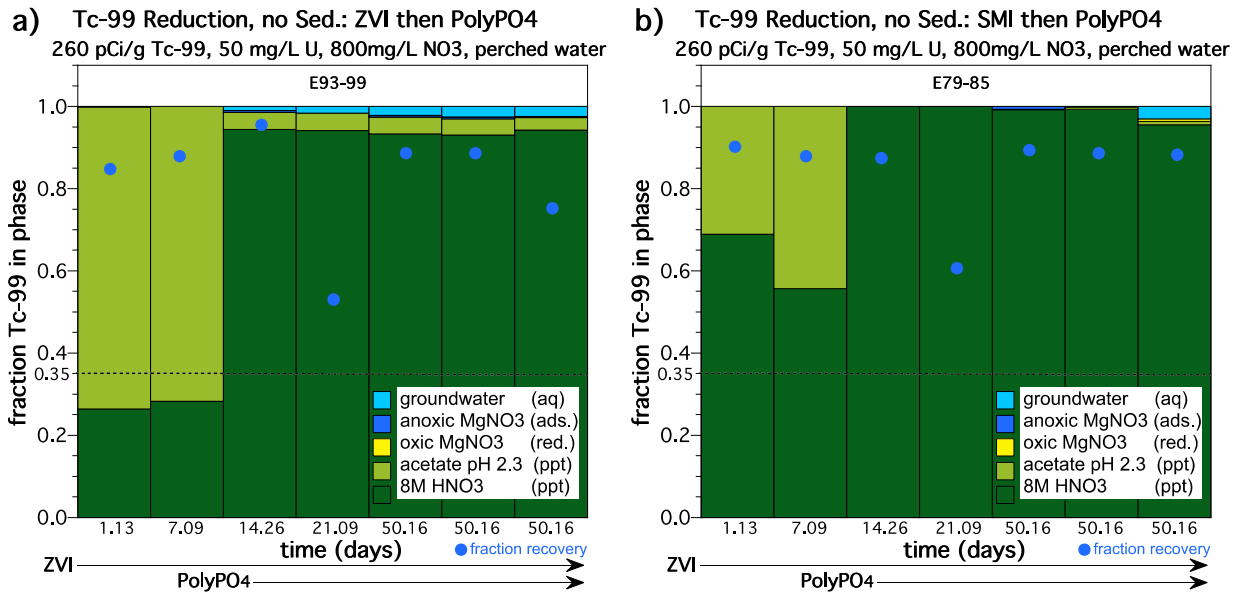

Figure G.6. Tc-99 reduction/sequestration with no sediment in synthetic perched water containing 800 mg/L NO_3^- by (a) ZVI and (b) SMI.

For the 1 mg/L U(VI), reduction in groundwater was also more rapid and complete by ZVI without CoCOIs (Figure G.7a) with an electron donor/acceptor ratio of 11,000 than with CoCOIs present (Figure G.7b) with an electron donor ratio of 59. In both systems, all U(VI) was reduced by 14 days, but at 1 day, 65% of the U remained aqueous when CoCOIs were present with ZVI in contrast to < 1% with SMI and CoCOIs. The rates of U(VI) reduction by ZVI or SMI were similar without and with CoCOIs (Figure G.7).

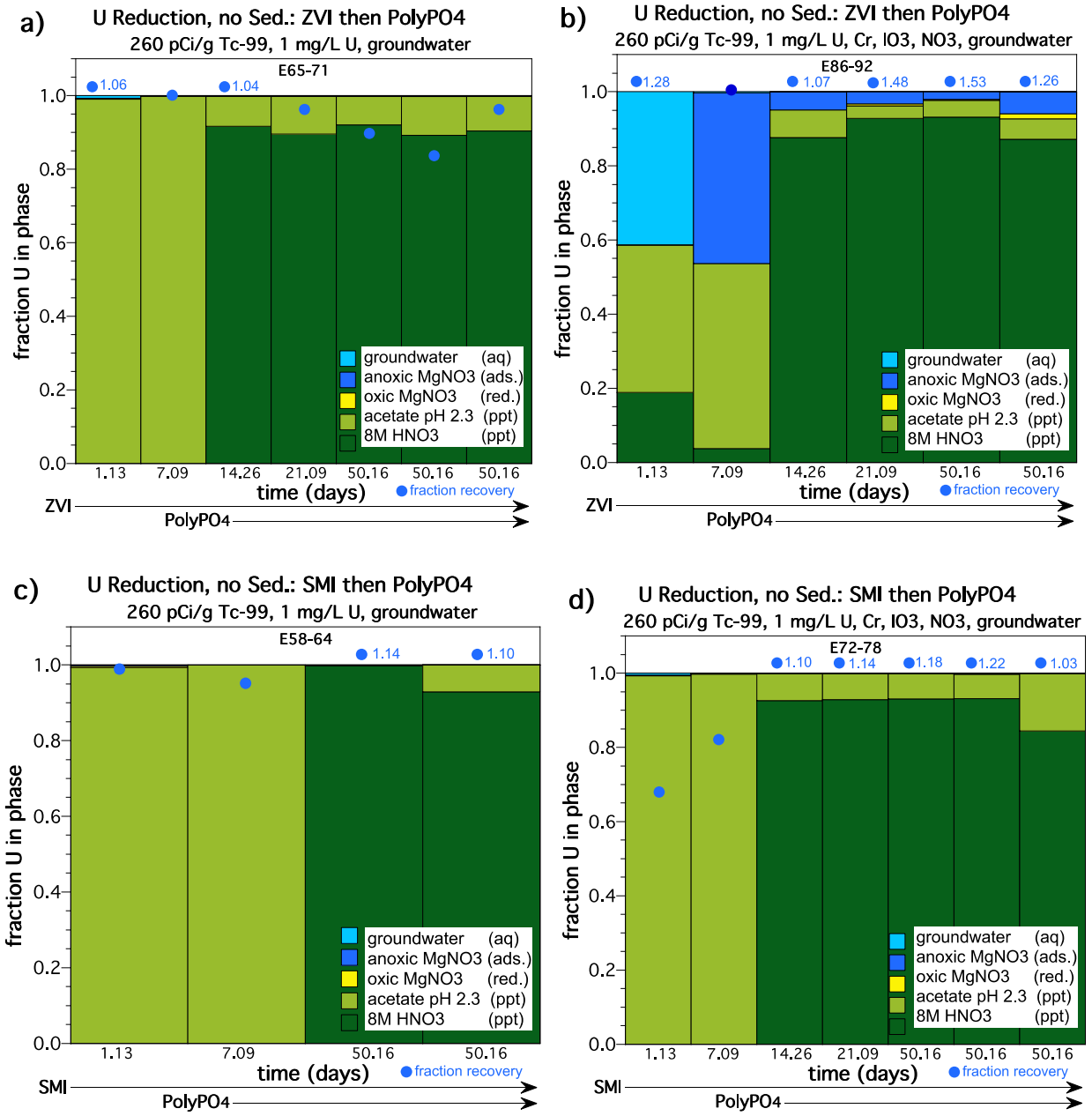

Figure G.7. U(VI) reduction/sequestration with no sediment by (a) ZVI in groundwater, (b) ZVI in groundwater with CoCOIs, (c) SMI in groundwater, and (d) SMI in groundwater with CoCOIs.

In perched water with 800 mg/L NO_3^- present, the electron donor/acceptor ratio decreased to 3.7. Note that nitrate is more easily reduced than U(VI), so the U(VI) reduction rate should decrease. However, U(VI) reduction was nearly the same by ZVI or SMI (Figure G.8) as in groundwater with no CoCOIs (Figure G.7a and c).

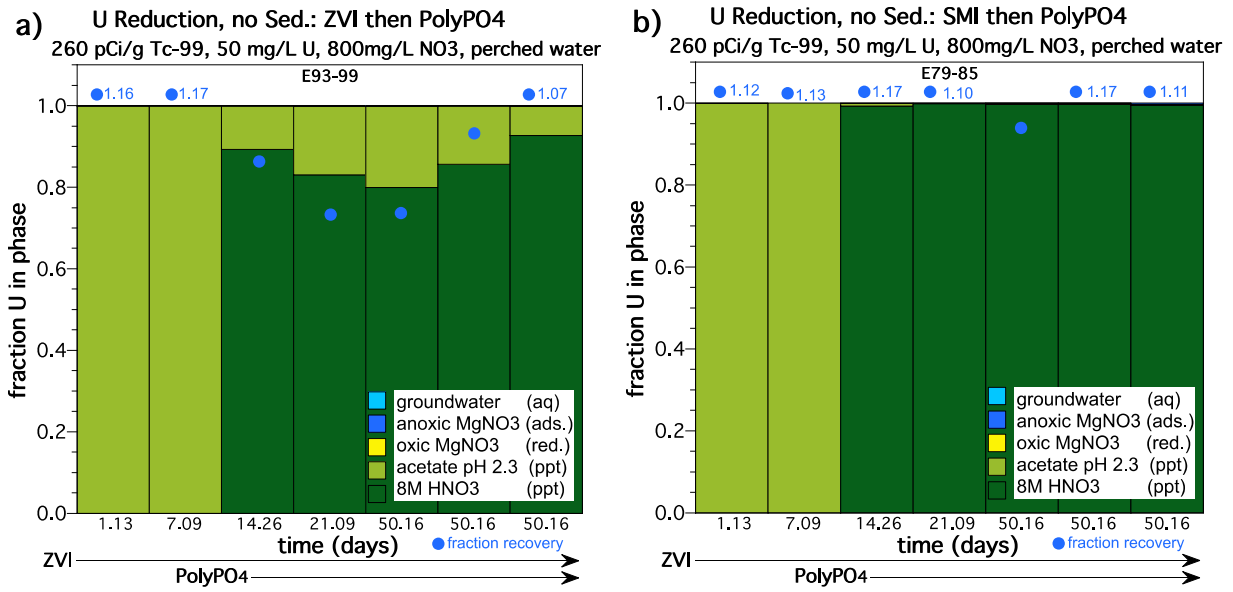

Figure G.8. U(VI) reduction/sequestration with no sediment in perched water containing 800 mg/L NO_3^- by (a) ZVI and (b) SMI. The e-donor/acceptor ratio was 3.7 for both systems.

G.4 Objective 2b: Quantify the influence of a delivery fluid on Tc-99 and U without and with CoCOIs for two-step treatment with ZVI or SMI followed by Poly-PO_4

Delivery of ZVI or SMI requires a high-viscosity fluid such as xanthan, as a high-viscosity fluid will hold the dense ZVI/SMI particles in solution and enable injection to a greater extent later with less slumping of the particles downward. Batch experiments were conducted in similar sediment/water systems without and with xanthan to evaluate the effect of xanthan on Tc-99 and U reduction and sequestration rate. Note that xanthan (and other high-viscosity fluids) is commonly used to inject ZVI. Portions of the xanthan polymer are redox reactive and hydrolyze, resulting in an Eh and pH shift (Kool et al. 2014). Xanthan may also coat the ZVI or SMI, decreasing its redox performance (Xin et al. 2016).

Tc-99 reduction by ZVI in groundwater without CoCOIs (i.e., electron donor/acceptor ratio = 11,000) showed no influence of the xanthan, with the same Tc-99 reduction rate without xanthan as with xanthan (Figure G.9a and b). In contrast, Tc-99 reduction by ZVI in perched water with 800 mg/L NO_3^- (i.e., electron donor/acceptor ratio = 3.7) showed that the addition of xanthan significantly decreased the ability of ZVI to reduce Tc-99, with 65% Tc-99 remaining aqueous after 50 days in the presence of xanthan compared to 4% without xanthan (Figure G.9c and d).

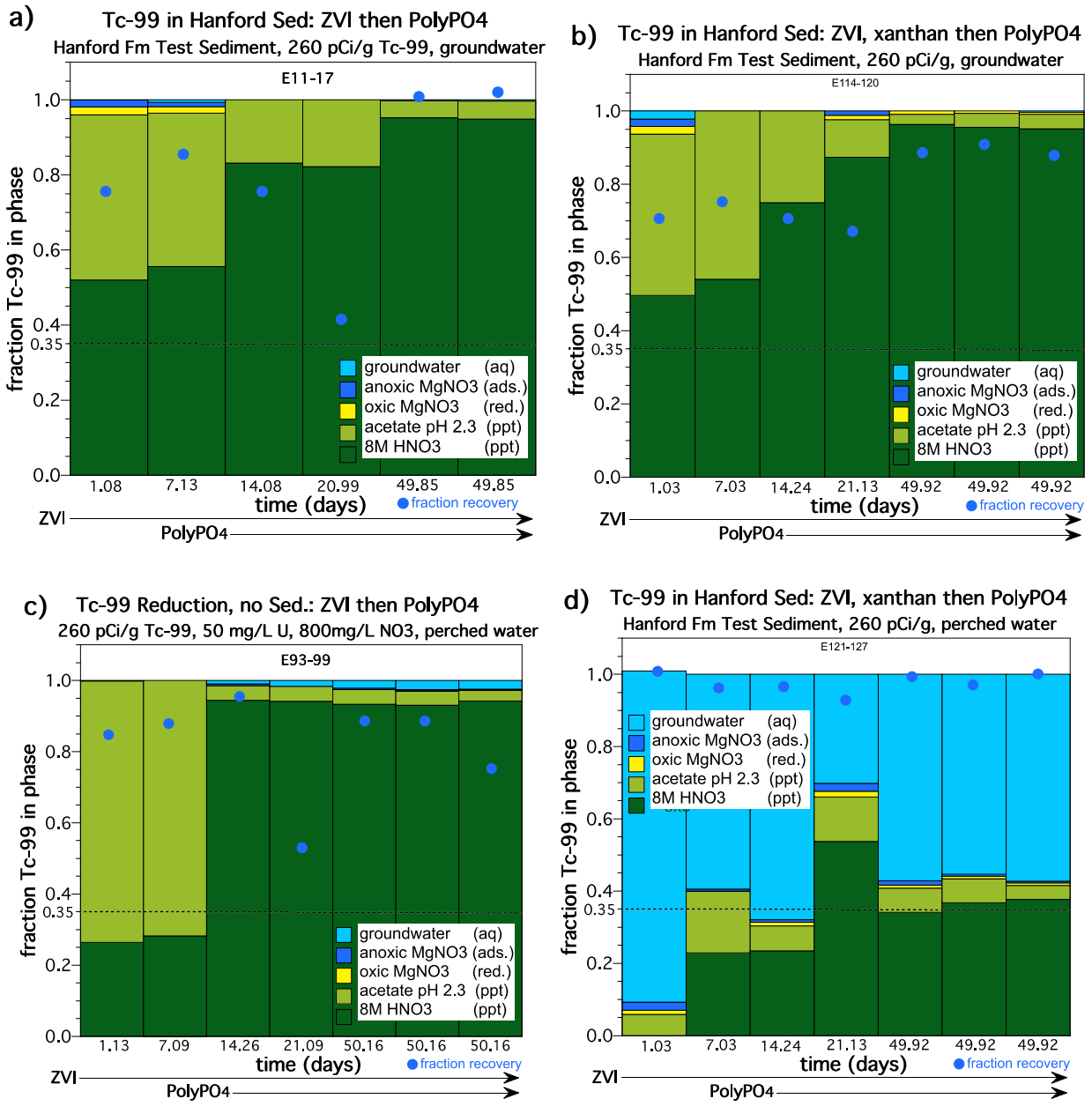

Figure G.9. Influence of xanthan on the Tc-99 reduction rate by ZVI as shown by (a) Hanford formation (Hf) sediment in groundwater without xanthan, (b) Hf sediment in groundwater with xanthan, (c) perched water without Hf sediment or xanthan, and (d) Hf sediment in perched water with xanthan.

The Tc-99 reduction by SMI in groundwater without CoCOIs (i.e., electron donor/acceptor ratio = 11,000) also showed no influence of the xanthan, with the same Tc-99 reduction rate without xanthan as with xanthan (Figure G.10a and b), similar to Tc-99 reduction by ZVI without and with xanthan in groundwater (Figure G.9a and b). However, in contrast to ZVI results, Tc-99 reduction by SMI in perched water with 800 mg/L NO_3^- (i.e., electron donor/acceptor ratio = 3.7) also showed no effect of the presence of xanthan on SMI reduction of Tc-99 (Figure G.10c and d). Because ZVI reduction performance was significantly affected by the presence of xanthan, yet SMI reduction performance was not, it suggests that the Fe^0 itself (100% in ZVI, 60% in SMI) may be reacting with xanthan (consuming electrons).

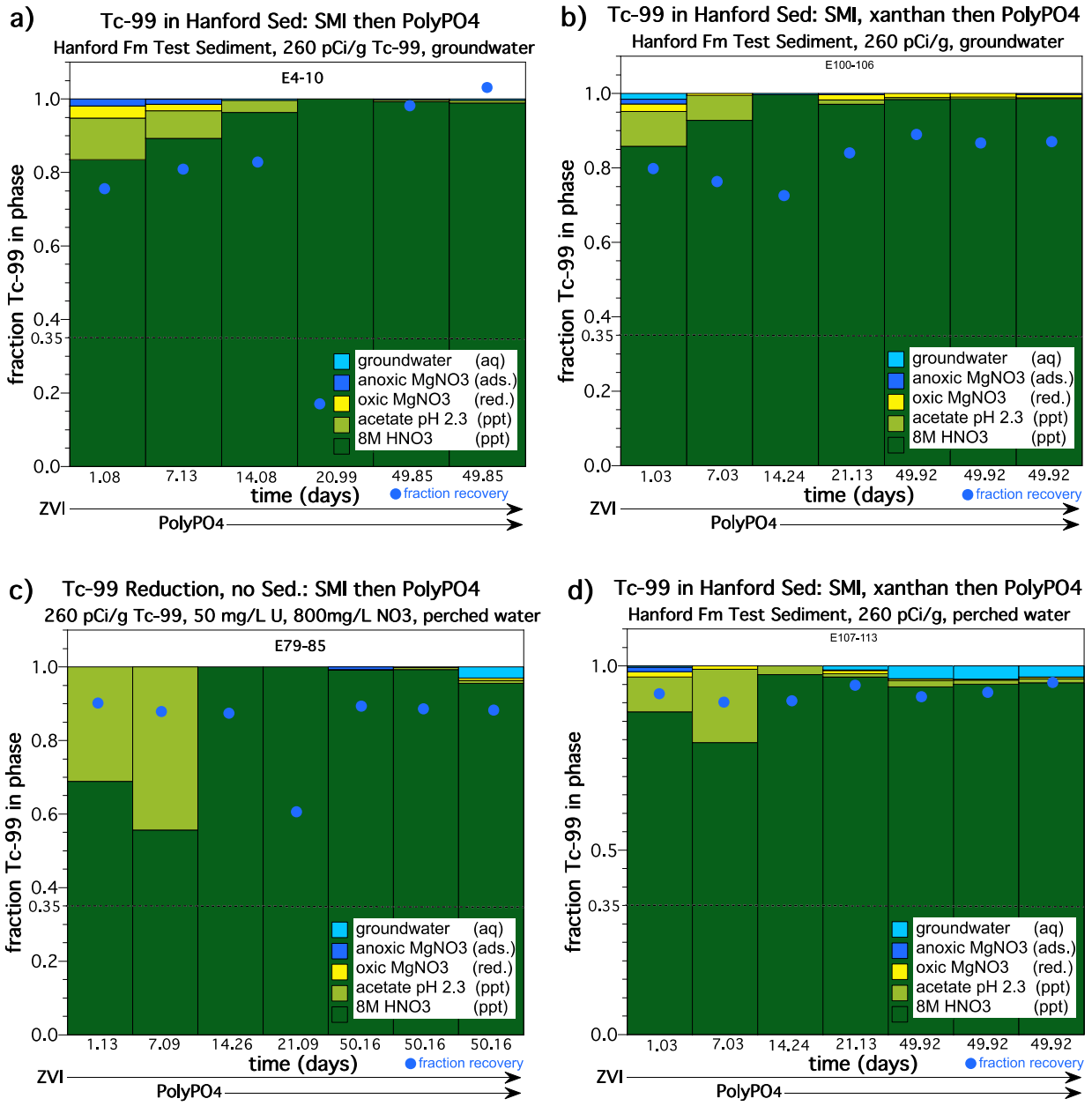

Figure G.10. Influence of xanthan on the Tc-99 reduction rate by SMI as shown by (a) Hf sediment in groundwater without xanthan, (b) Hf sediment in groundwater with xanthan, (c) perched water without Hf sediment or xanthan, and (d) Hf sediment in perched water with xanthan.

Similar to Tc-99 (Figure G.11), U(VI) reduction by ZVI in groundwater without CoCOIs (i.e., electron donor/acceptor ratio = 11,000) showed no influence of the xanthan, with the same U(VI) reduction rate without xanthan as with xanthan (Figure G.11a and b), and actually slightly less remaining aqueous U(VI) in the presence of xanthan. In contrast, U(VI) reduction by ZVI in perched water with 800 mg/L NO_3^- (i.e., electron donor/acceptor ratio = 3.7) showed that the addition of xanthan greatly slowed ZVI reduction of U(VI), with 20% U(VI) remaining aqueous after 14 days (and 10% by 50 days) in the presence of xanthan compared to < 1% without xanthan (Figure G.11c and d).

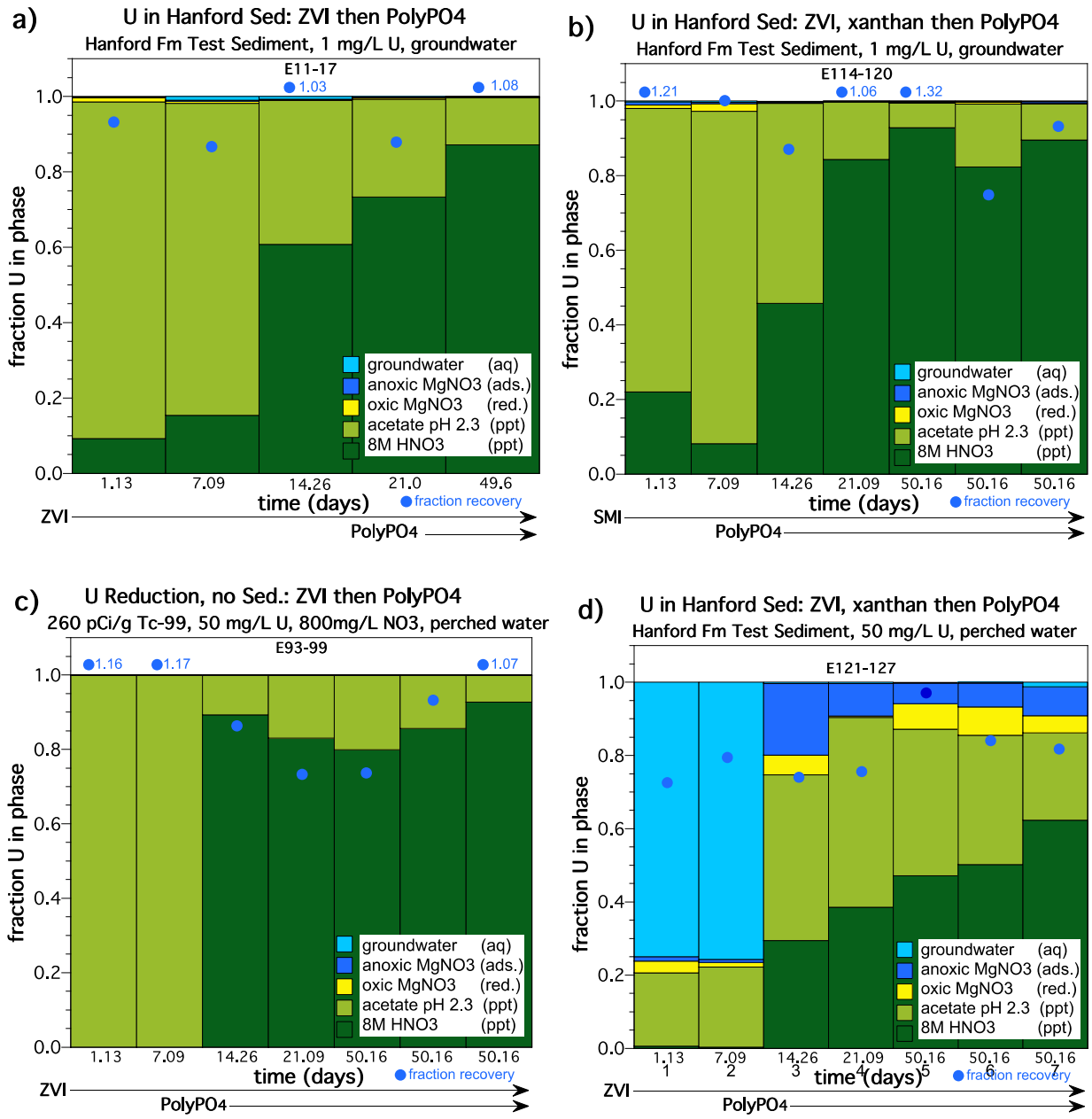

Figure G.11. Influence of xanthan on the U(VI) reduction rate by ZVI as shown by (a) Hf sediment in groundwater without xanthan, (b) Hf sediment in groundwater with xanthan, (c) perched water without Hf sediment or xanthan, and (d) Hf sediment in perched water with xanthan.

The U(VI) reduction by SMI in groundwater without CoCOIs (i.e., electron donor/acceptor ratio = 11,000) showed slightly faster reduction with xanthan (Figure G.12b) than without xanthan (Figure G.12a). U(VI) reduction by SMI with xanthan was slightly slower than with ZVI (Figure G.11b). U(VI) reduction by SMI in perched water with 800 mg/L NO_3^- (i.e., electron donor/acceptor ratio = 3.7) showed significantly slower U(VI) reduction in the presence of xanthan (Figure G.12d versus c). Similar to observations for Tc-99 reduction, because ZVI reduction performance was significantly affected by the presence of xanthan, yet SMI reduction performance was not, it suggests that the Fe^0 itself (100% in ZVI, 60% in SMI) may be reacting with xanthan (consuming electrons).

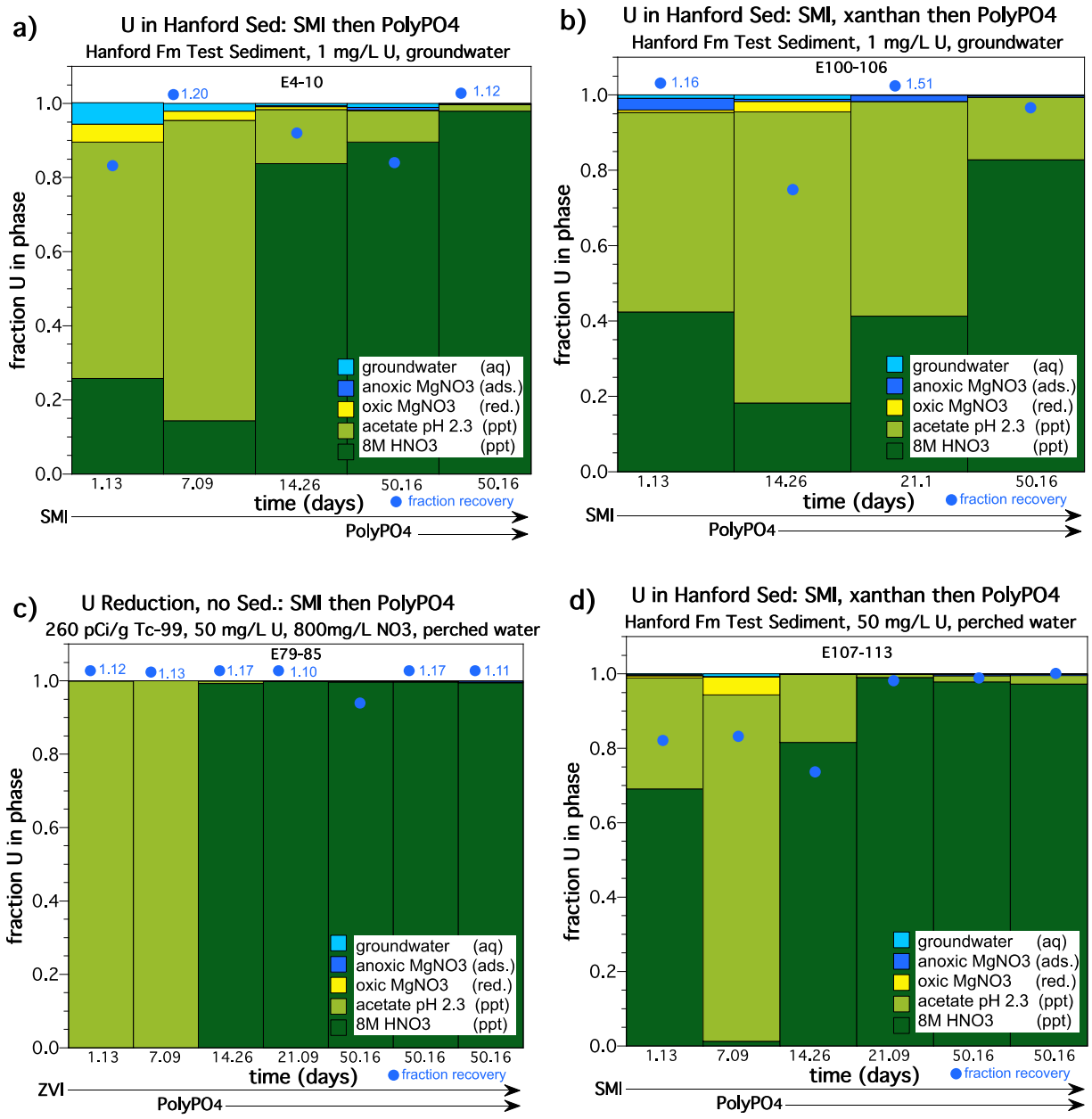

Figure G.12. Influence of xanthan on the U(VI) reduction rate by SMI as shown by (a) Hf sediment in groundwater without xanthan, (b) Hf sediment in groundwater with xanthan, (c) perched water without Hf sediment or xanthan, and (d) Hf sediment in perched water with xanthan.

G.5 Sequestration of Cr(VI) by Two-step ZVI/SMI and Poly-PO_4 Treatment

The strong reducing environment created by ZVI or SMI is targeting reduction/precipitation of Tc-99 (as pertechnetate) and U(VI) aqueous/adsorbed phases, but there is some effect on some CoCOIs. Cr(VI) present as chromate should be readily reduced in contact with the SMI or ZVI. Batch experiments showed untreated sediments with 0.5% to 1.1% Cr(VI) present in aqueous solution decreased to < 0.02% aqueous Cr(VI) in the presence of ZVI or SMI (Figure G.13a). A plot of the Cr(VI) in different phases without the fifth extraction (8M HNO_3) more clearly shows the smaller aqueous Cr(VI) decrease with reduction (Figure G.13b).

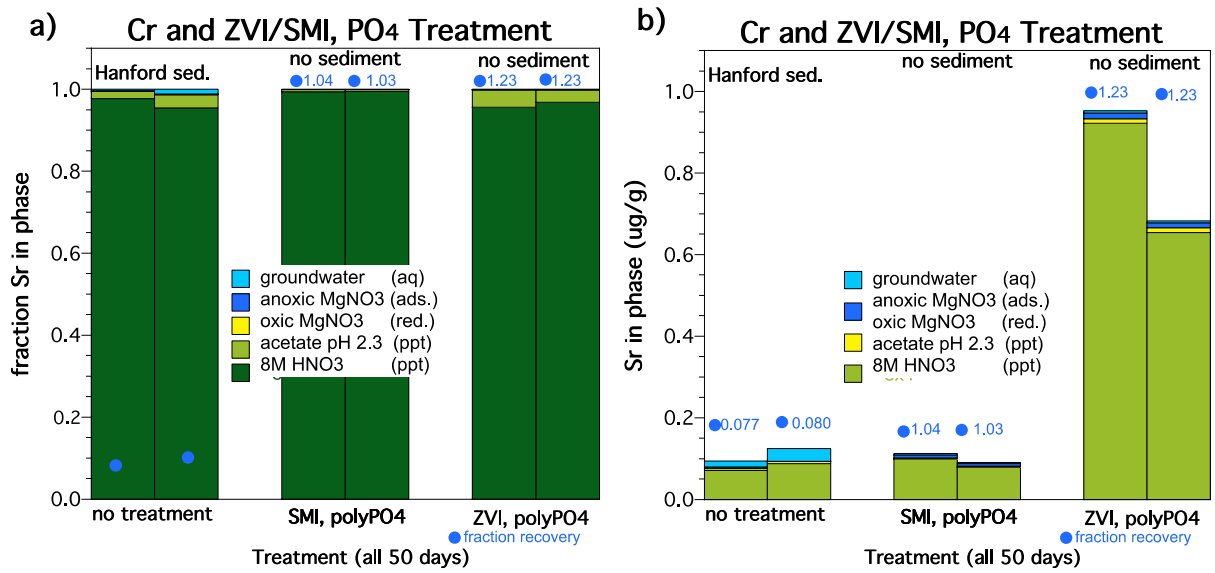

Figure G.13. Influence of Cr(VI) mobility from SMI or ZVI (14 days) then PO_4 treatment (36 days).

G.6 Sequestration of Nitrate by Two-step ZVI/SMI and Poly-PO_4 Treatment

NO_3 can be readily reduced during conditions generated by biostimulation and might be abiotically reduced by the ZVI or SMI. Experiments at low (50 mg/L NO_3^-) nitrate in groundwater (Figure G.14a) or in high (1800 mg/L NO_3^-) nitrate in perched water (Figure G.14b) show little reduction to nitrite, which is present only in low concentrations.

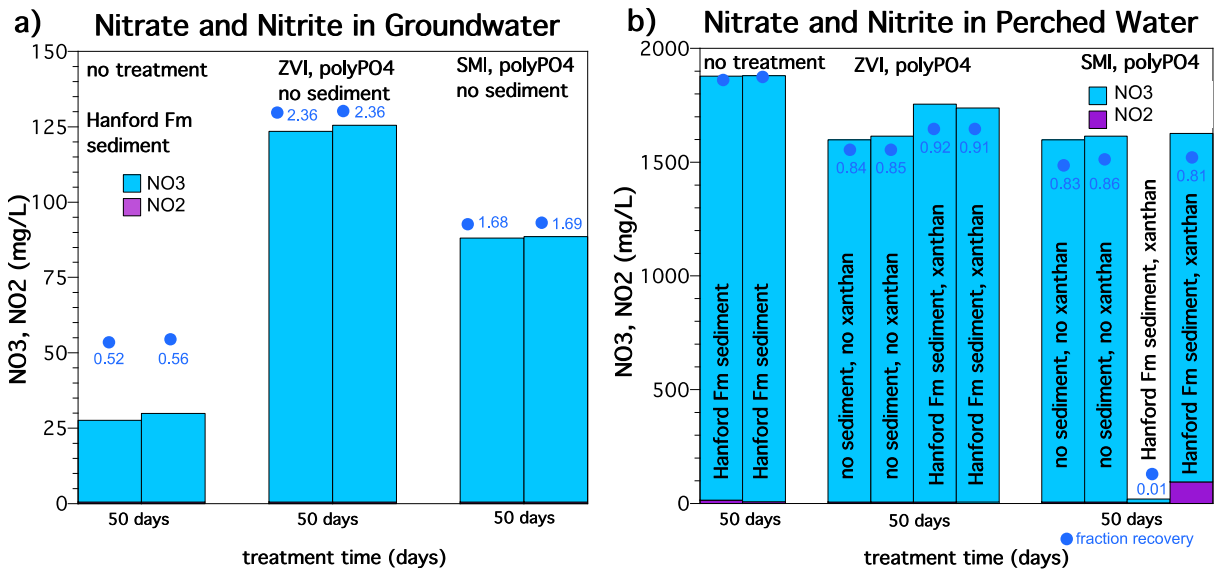

Figure G.14. Influence of 50 mg/L NO_3^- in groundwater (a) or 1800 mg/L NO_3^- in perched water (b) degradation by SMI or ZVI (14 days) followed by PO_4 treatment (36 days).

G.7 Sequestration of IO_3 by Two-Step ZVI/SMI and Poly-PO_4 Treatment

Iodate (as I-127) and Sr were also added as CoCOIs. Iodate in an oxic environment exhibits a small amount of adsorption and is readily reduced to iodide in the presence of ZVI or SMI, and exhibits slightly less adsorption. Batch experiments with iodate in contact with oxic sediment show low aqueous and adsorbed I-127 (additional surface phases were not analyzed), and so may have precipitated (Figure G.15a). Experiments of I-127 iodate in contact with SMI or ZVI show much higher aqueous I-127 and a small fraction of adsorbed I-127. In contrast to iodine species, Sr^{2+} is generally strongly sorbed to sediment, as shown by reaction of Sr with untreated Hf sediment (Figure G.15b, left bar graphs). The calculated Sr K_d to sediment was 1.46 mL/g. Because Sr^{2+} is not redox reactive, the only expected interaction of Sr with ZVI or SMI was adsorption. These experiments were conducted in systems with just ZVI or SMI (i.e., no sediment), and the calculated Sr K_d to ZVI was 0.086 mL/g and to SMI was 0.21 mL/g (Figure G.15b).

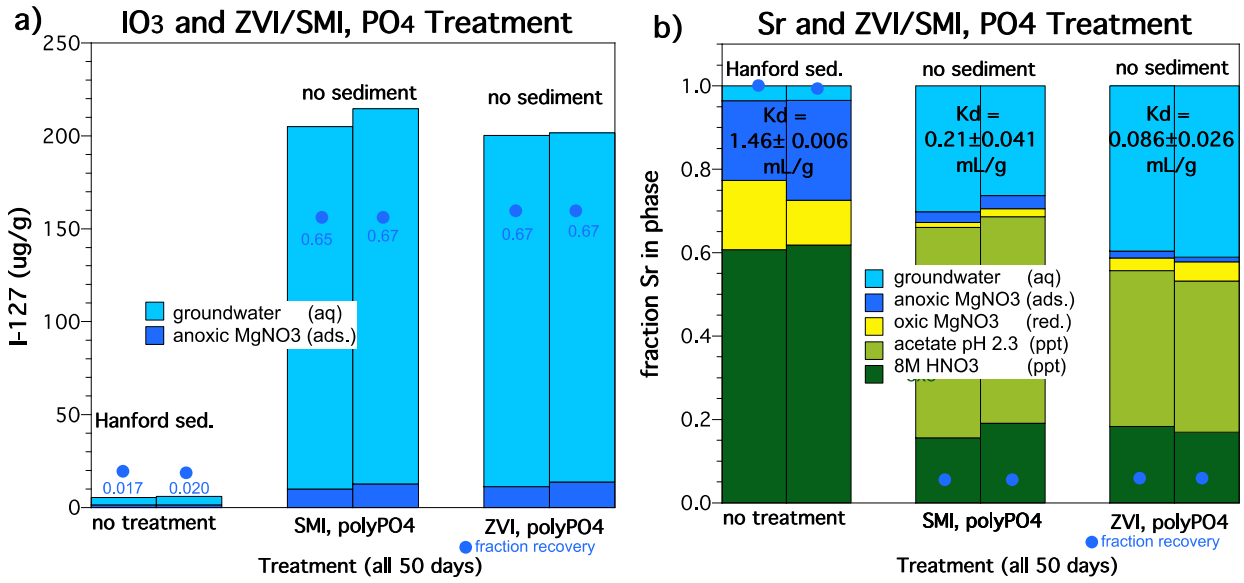

Figure G.15. Influence of SMI or ZVI (14 days) followed by PO_4 treatment (36 days) on: (a) I-127 as iodate, and (b) Sr^{2+}.

Appendix H – Supporting Data for Liquid-Phase Chemical Sequestration Amendments

H.1 Supporting Data for Primary Contaminants of Interest

Data are shown in the main text as the normalized fraction recovered in each extraction; however, results are shown here as a sediment loading in µg/g for comparison. These results highlight that significantly more U was immobilized for perched water conditions, even though approximately 30 times more U was added to the system as compared to BY Cribs groundwater conditions (Figure H.1). For Tc-99, a significantly greater amount of Tc-99 remained in the aqueous phase following treatment with Cit-PO_4 in perched water conditions as compared to BY Cribs groundwater conditions (Figure H.2).

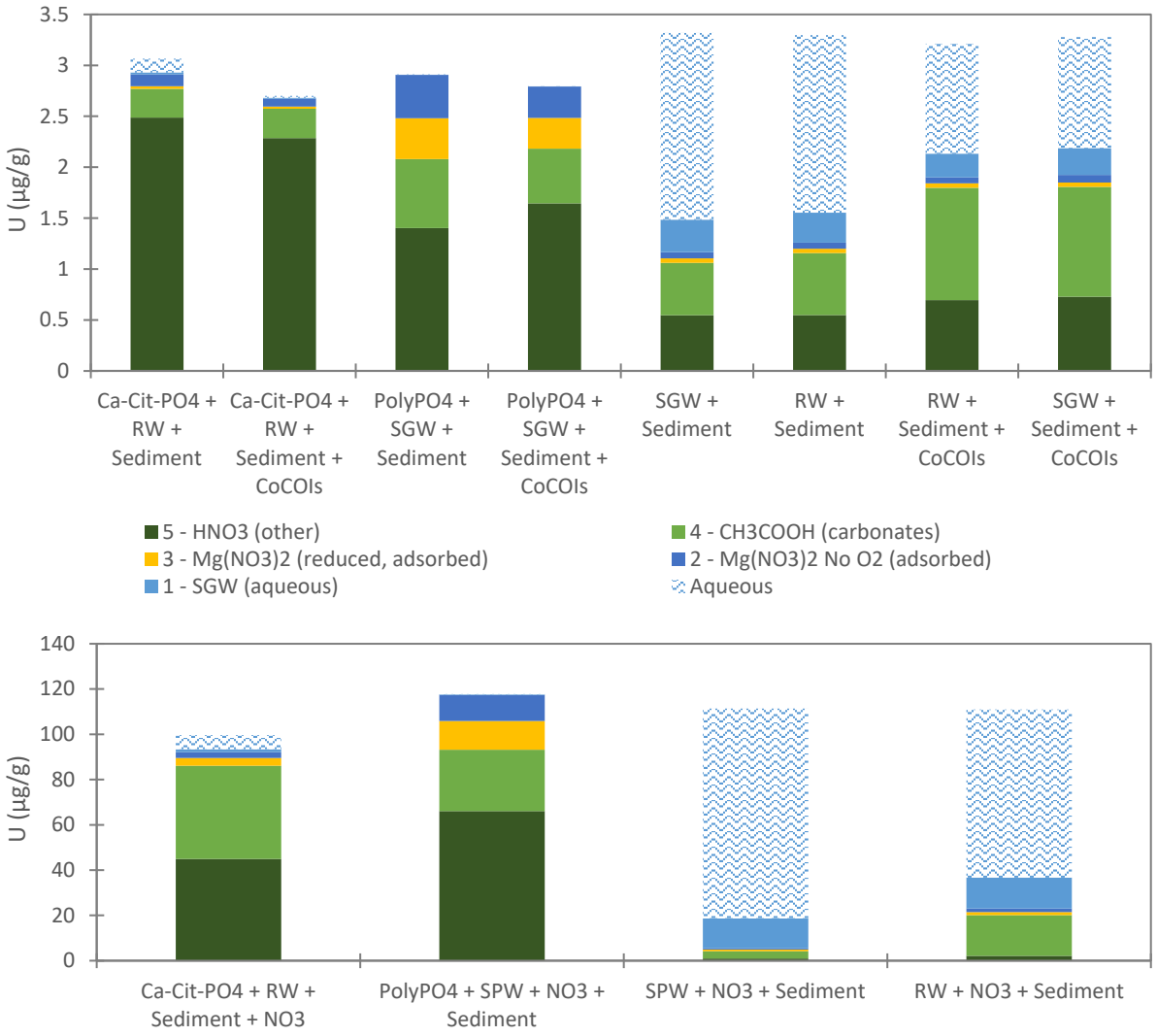

Figure H.1. Results for the U in µg/g for the aqueous phase (*wave blue bar*) and each sequential extraction step (*solid bars*) following batch experiments reacted with apatite-forming solutions for 21 days as compared to controls without treatment with (*top*) BY Cribs groundwater conditions and (*bottom*) perched water conditions.

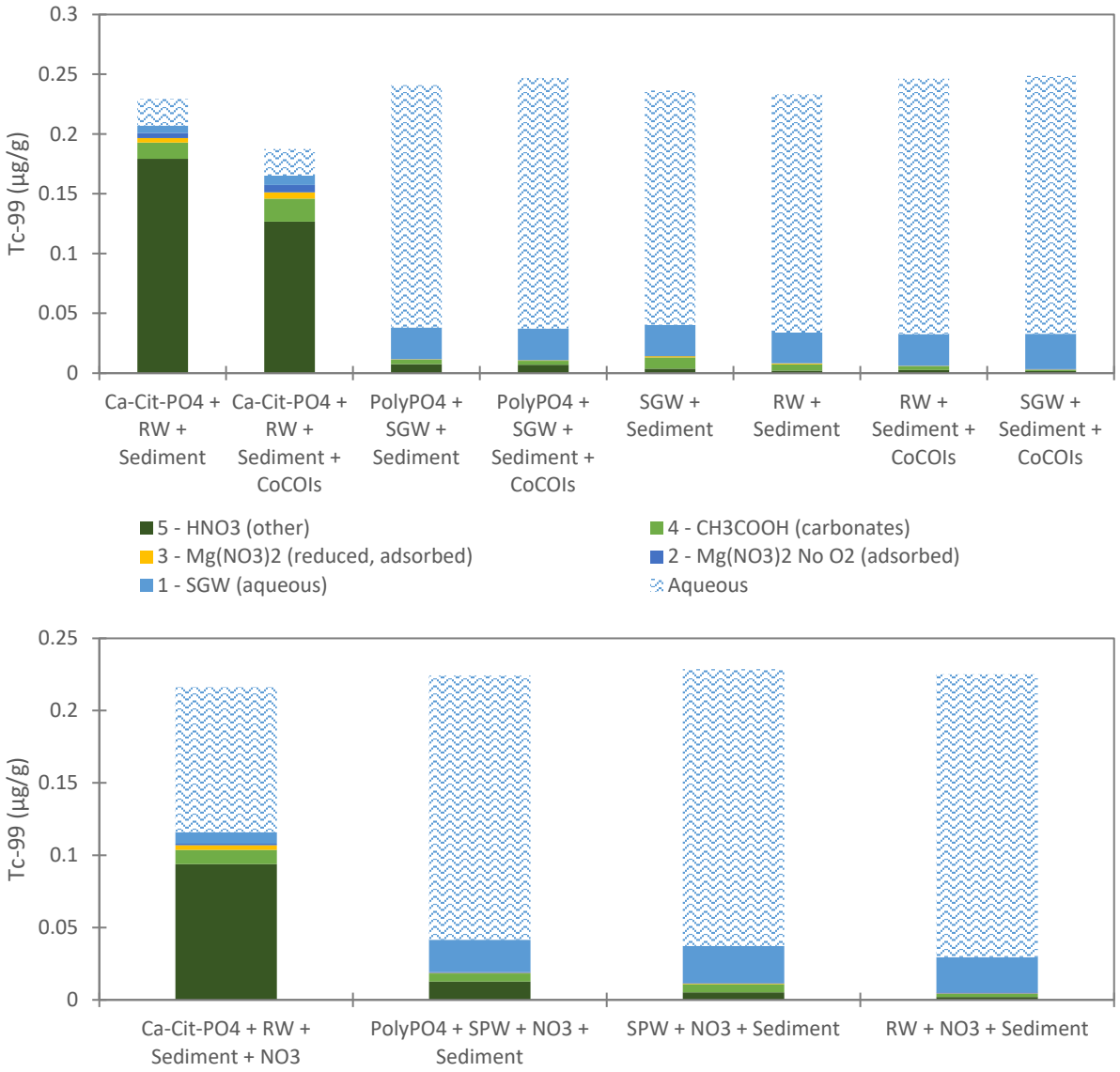

Figure H.2. Results for the Tc-99 in µg/g for the aqueous phase (*wave blue bar*) and each sequential extraction step (*solid bars*) following batch experiments reacted with apatite-forming solutions for 21 days as compared to controls without treatment with (*top*) BY Cribs groundwater conditions and (*bottom*) perched water conditions.

H.2 Behavior of CoCOIs

Co-contaminants of interest (CoCOIs) were only added to BY Cribs groundwater conditions with the exception of nitrate being the only CoCOI added to reactors under perched water conditions. However, data for nitrate cannot be reported due to challenges with holding times prior to anion analysis. The results for Cr(VI), Sr, and I are reported as a fraction recovered based on the total CoCOI added and the naturally occurring mass within sediments based on the black diamond symbols with a normalized recovery reported for each step of the sequential extractions.

H.2.1 Sequestration of Sr by Apatite-Forming Solutions

Strontium was added as naturally occurring Sr isotope ratios at concentrations similar to that observed in the natural Hanford subsurface (Table 3.6). Sr-90 concentrations are much lower than natural Sr, but technologies cannot target different isotopes. These results show a small increase in the immobile fraction of Sr in sequential extractions (4 – CH_3COOH and 5 – HNO_3) following treatment with Cit-PO_4 (Figure H.3). Previous research has shown that Sr reacts strongly with apatite phases, resulting in a decrease in mobility (PNNL-19524). However, these results suggest that Sr was relatively immobile under natural conditions, resulting in a smaller decrease in mobility with treatment, likely due to adsorption and ion exchange processes with sediments.

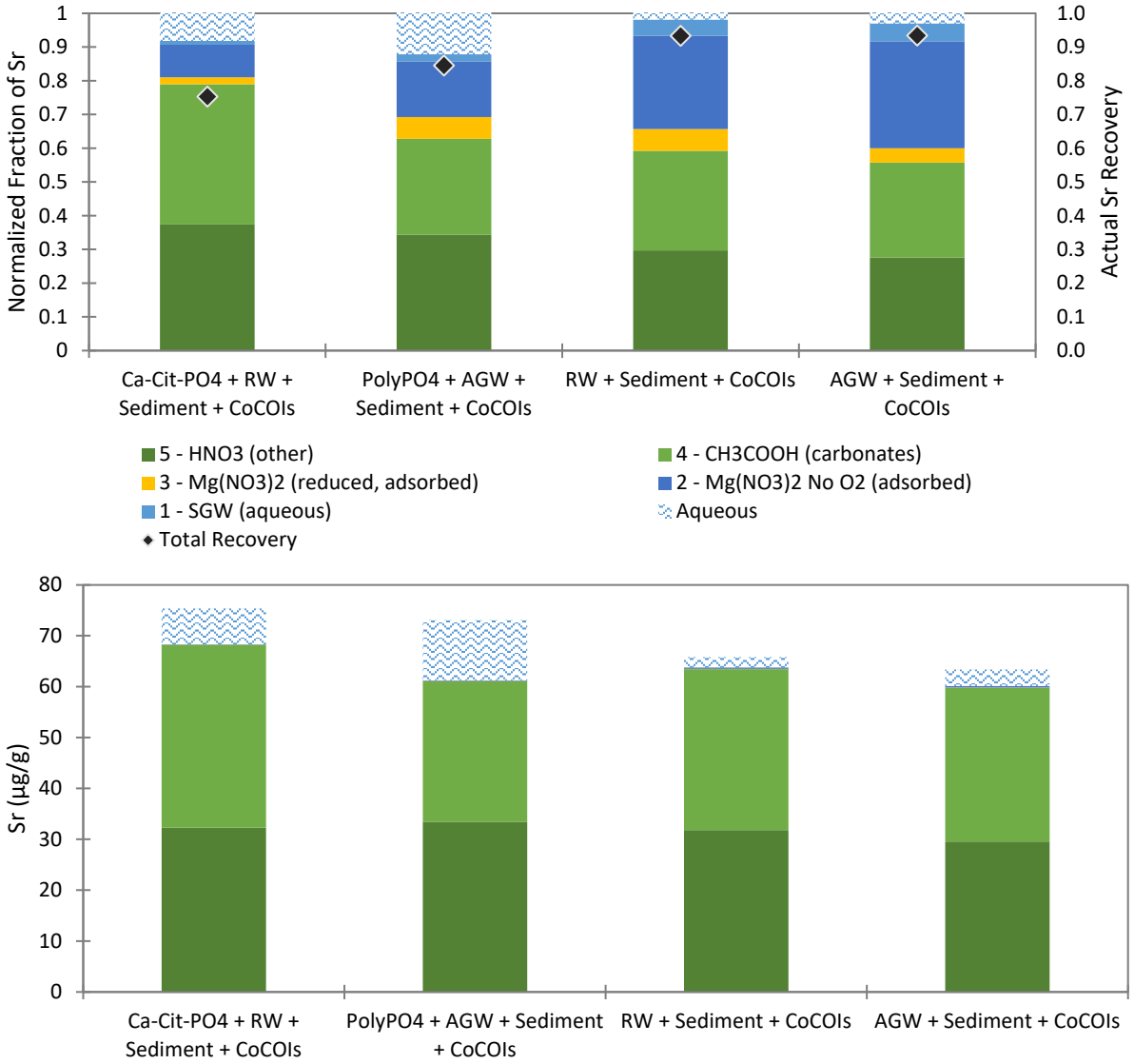

Figure H.3. Results for Sr in the aqueous phase (*wave blue bar*) and each sequential extraction step (*solid bars*) following batch experiments reacted with apatite-forming solutions for 21 days with (*top*) normalized fraction recovered and (*bottom*) mass of contaminant in µg/g.

H.2.2 Sequestration of Cr(VI)by Apatite-Forming Solutions

These results show a small increase in the most immobile fraction of Cr(VI) in sequential extractions following treatment with Cit-PO_4 or Poly-PO_4 (moving from Extraction 4 – CH_3COOH to Extraction 5 – HNO_3, Figure H.4). However, these results also suggest that Cr(VI) was relatively immobile under natural conditions, resulting in a small decrease in mobility with treatment.

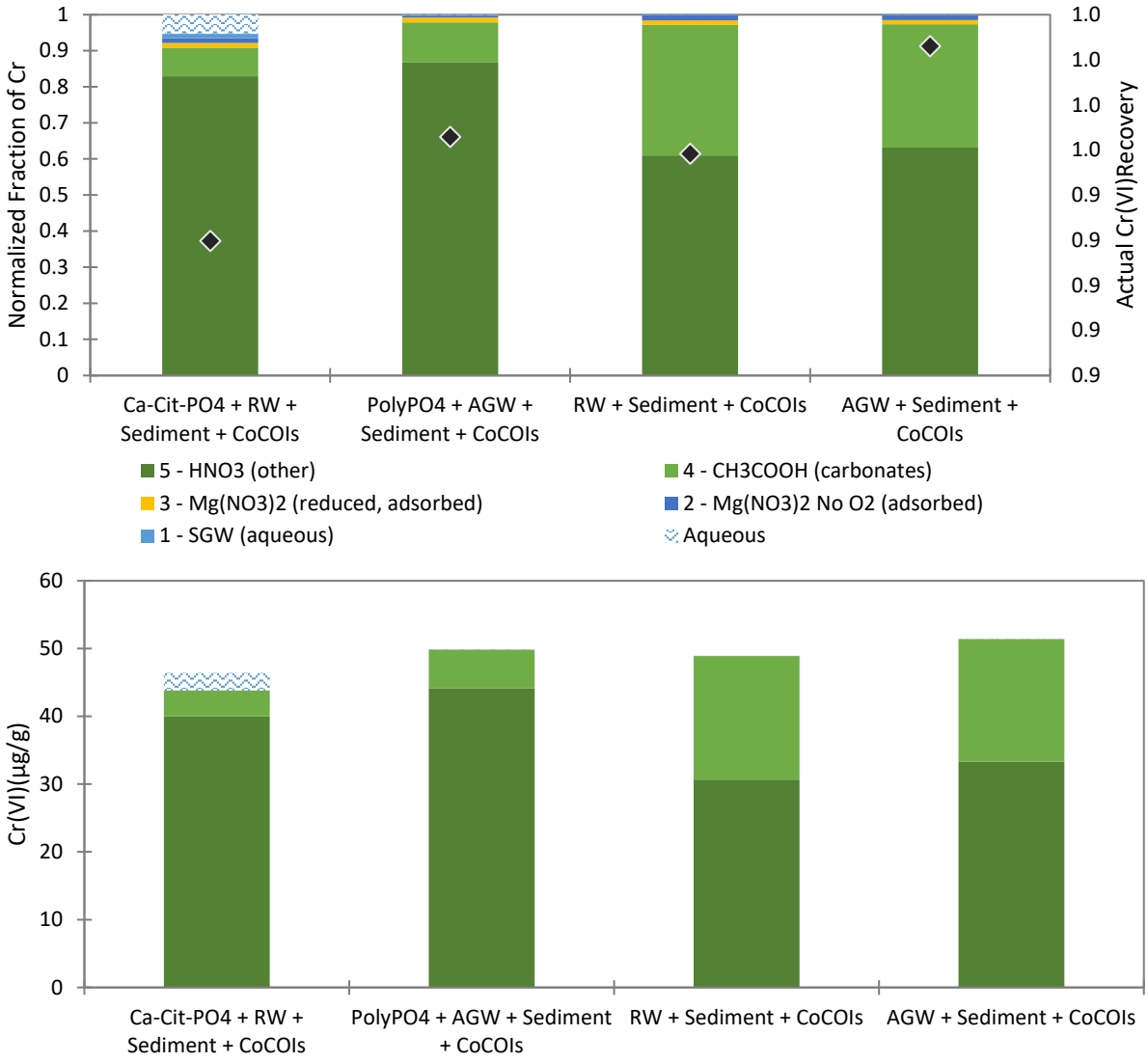

Figure H.4. Results for Cr(VI) in the aqueous phase (*wave blue bar*) and each sequential extraction step (*solid bars*) following batch experiments reacted with apatite-forming solutions for 21 days with (*top*) normalized fraction recovered and (*bottom*) mass of contaminant in µg/g.

H.2.3 Sequestration of I by Apatite Forming Solutions

Iodine was added as naturally occurring I-127 at concentrations similar to that observed in the natural Hanford subsurface (Table 3.6). I-129 concentrations are much lower than natural I (Kimmig et al. 2021; Zhang et al. 2013), but technologies cannot target different isotopes. Moreover, I-127 was added as IO_3^- due to its dominance in groundwater at the Hanford Site. These results show no change in the immobile fraction of I in sequential extractions (4 – CH_3COOH and 5 – HNO_3) following treatment with Cit-PO_4 or Poly-PO_4 (Figure H.5). However, a significant fraction of I is associated with the sequential extraction targeting reduced, adsorbed species, suggesting that it is released from the solid phase by precipitates that are oxidized and dissolved under the high ionic strength conditions of the $Mg(NO_3)_2$ extract. Previous research has shown that I is often associated with iron oxides and carbonates (Lawter et al. 2018). Therefore, we suggest that there is an iron oxide phase that is impacted by the $Mg(NO_3)_2$ extract under oxidizing conditions (Extraction 3).

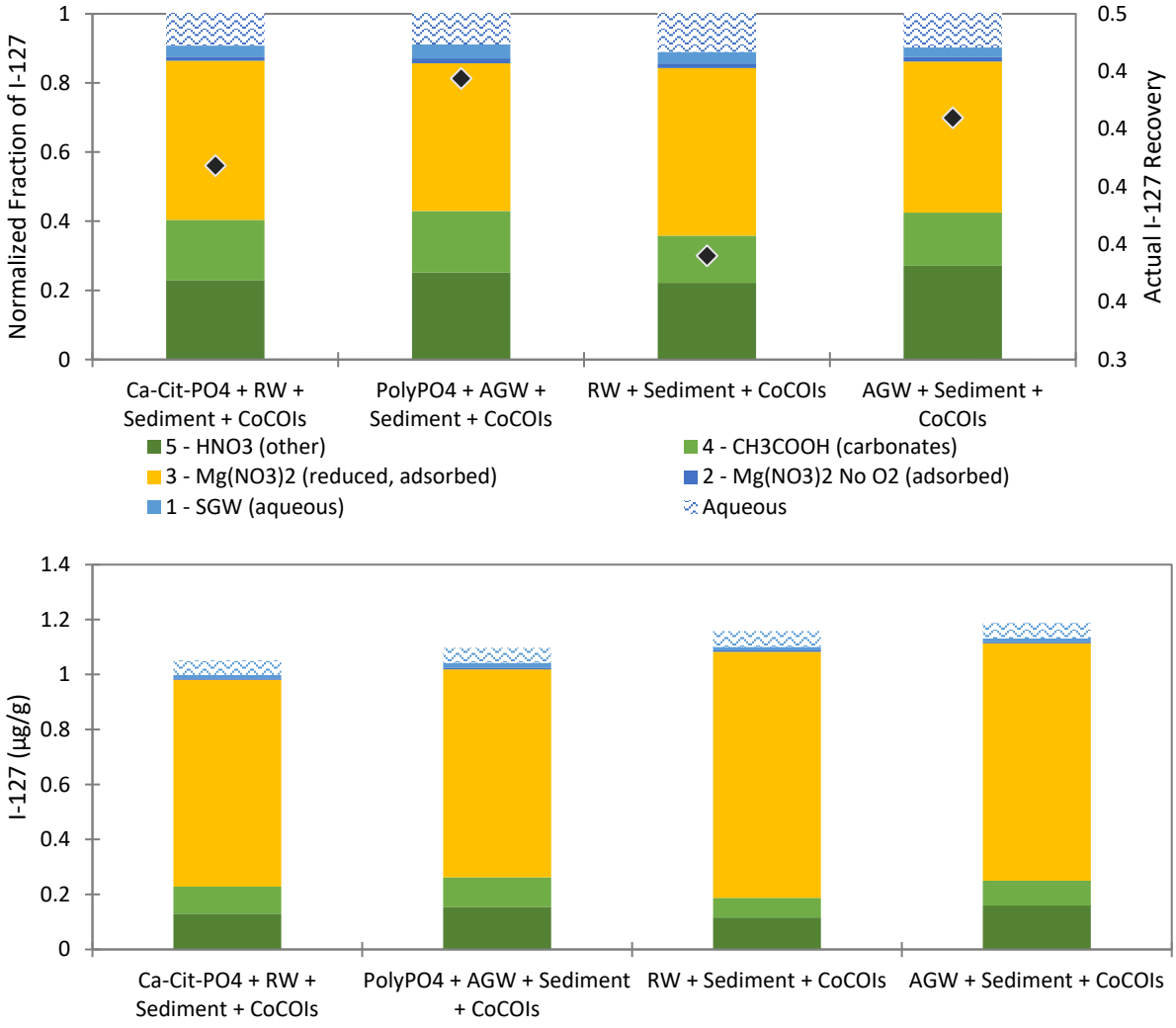

Figure H.5. Results for I in the aqueous phase (*wave blue bar*) and each sequential extraction step (*solid bars*) following batch experiments reacted with apatite-forming solutions for 21 days with (*top*) normalized fraction recovered and (*bottom*) mass of contaminant in µg/g.

H.3 Fate of Phosphorus in Liquid-Phase Amendments

Phosphorus recovery is based only on the added phosphorus from the liquid amendments with any natural phosphorus from sediments subtracted from the mass balance as shown in Figure H.6. No observable effect of CoCOIs was observed on phosphorus precipitation under BY Cribs groundwater conditions, although differences were observed between the two different apatite-forming solutions (Cit-PO_4 and Poly-PO_4). Nearly 99% of phosphorus was in the most recalcitrant extractions (4 – CH_3COOH and 5 – HNO_3) as shown by the green bars for Cit-PO_4, although closer to 60-65% of phosphorus was in the most recalcitrant phases in the Poly-PO_4 treatment. These results suggest that the Cit-PO_4 treatment may have led to more crystalline apatite formation as compared to Poly-PO_4, potentially due to the slower speed with which precipitation occurred in that system as demonstrated by the removal rates for U and Tc-99 (Sections 4.7.1 and 4.7.3).

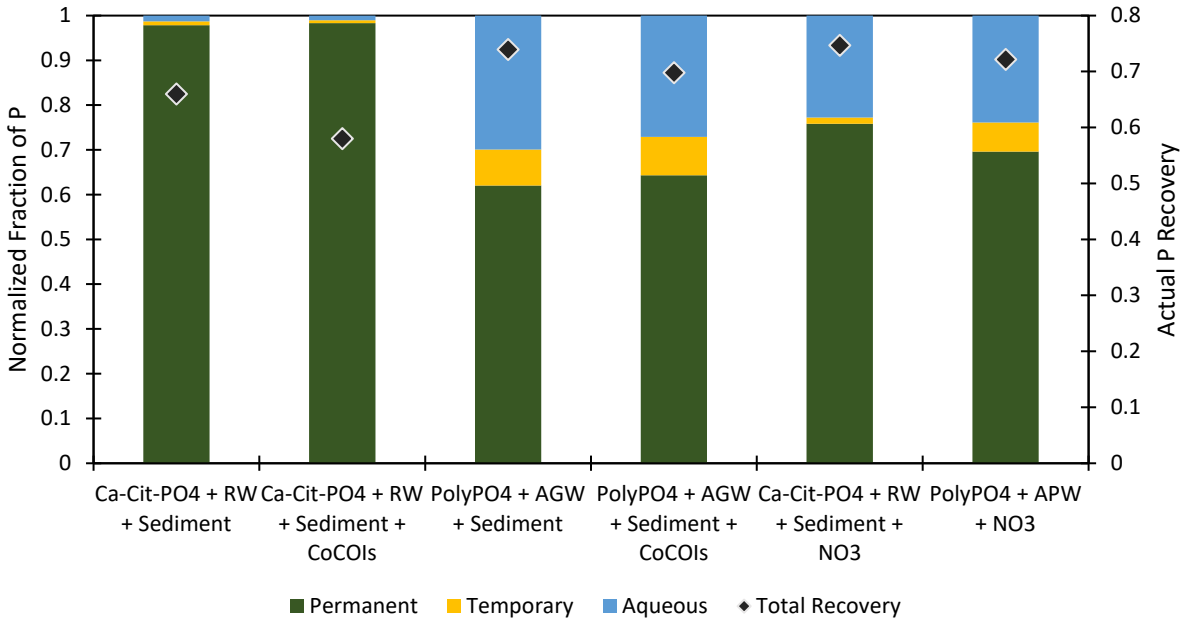

Figure H.6. Distribution of phosphorus in sequential extractions following reaction of apatite-forming solutions with sediments and CoCOIs for 21 days.

H.4 Aqueous Phase pH and Eh Measurements

The redox potential (Eh) was measured in select samples with both Poly-PO_4 and Cit-PO_4 amendments over time. While some decrease in Eh occurred in Poly-PO_4 experiments, the solutions remained in sub-oxic conditions. However, with the Cit-PO_4 amendment, Eh was dropping within 1 day and remained reducing. These results highlight that reduction of Tc-99 likely occurred with the Cit-PO_4 but not the Poly-PO_4 amendment.

In the batch experiments, the pH also decreased with both of the liquid apatite-forming amendments, though it was greater for the Poly-PO_4 treatment. These pH fluctuations are less likely in a field treatment due to the higher sediment-to-liquid ratio allowing for greater buffering capacity from the sediments. Nonetheless, the speciation of U and adsorption potential for both U and Tc-99 were likely impacted. Hence, aqueous speciation modeling was conducted for U and saturation indices were predicted for all elements in the batch experiments including CoCOIs.

Thermodynamic equilibrium modeling was used to calculate solution speciation and mineral SIs for solid phases potentially in equilibrium with the supernatant compositions. The SI is defined as log (Q/Ksp), where Q is the activity product and Ksp is the mineral solubility product at equilibrium at the temperature of interest. In general, minerals with SI values of zero are at equilibrium where more positive values are considered oversaturated and more negative values are considered undersaturated with respect to the pertinent solid phase. Therefore, SI values from 0 to approximately 1 will be considered saturated in modeling outputs. GWB version 10.0 (Bethke and Yeakel 2010) was used for the modeling. Calculations were performed using the standard Minteq thermodynamic database that is supplied with GWB but augmented with the selected data from the Organization for Economic Co-operation and Development/Nuclear Energy Agency-Thermochemical Database Project (NEA TDB) (Grenthe et al. 2020; Guillaumont et al. 2003).

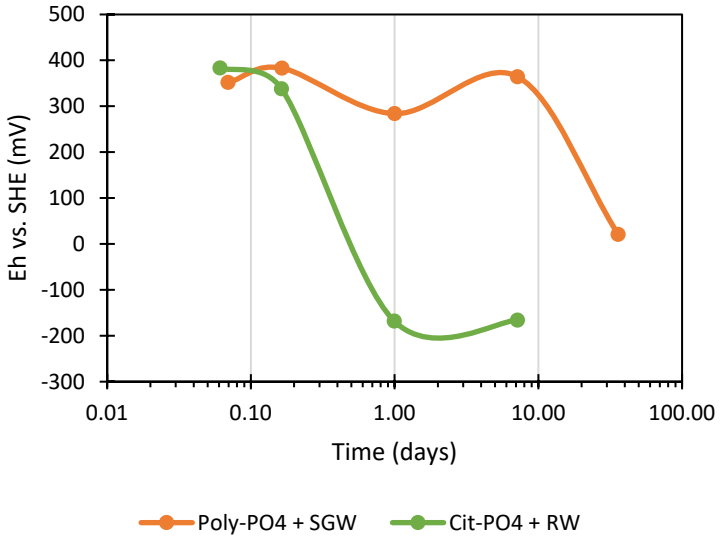

Figure H.7. Changes in reduction potential (Eh with respect to a standard hydrogen electrode, SHE) over 36 days with respect to treatment with Cit-PO_4 (*green*) or Poly-PO_4 (*orange*). Lines are used to guide the eye and do not represent a model.

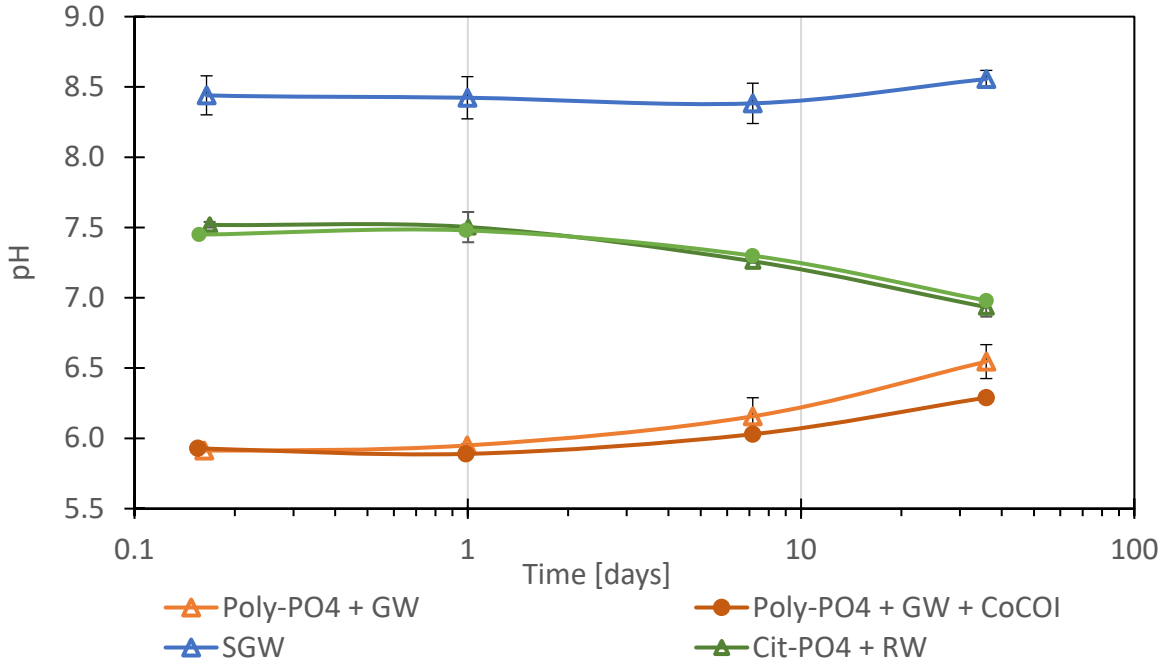

Figure H.8. Changes in reduction pH over 36 days with respect to treatment with Cit-PO_4 (*green*), Poly-PO_4 (*orange*), or untreated (*blue*). Lines are used to guide the eye and do not represent a model.

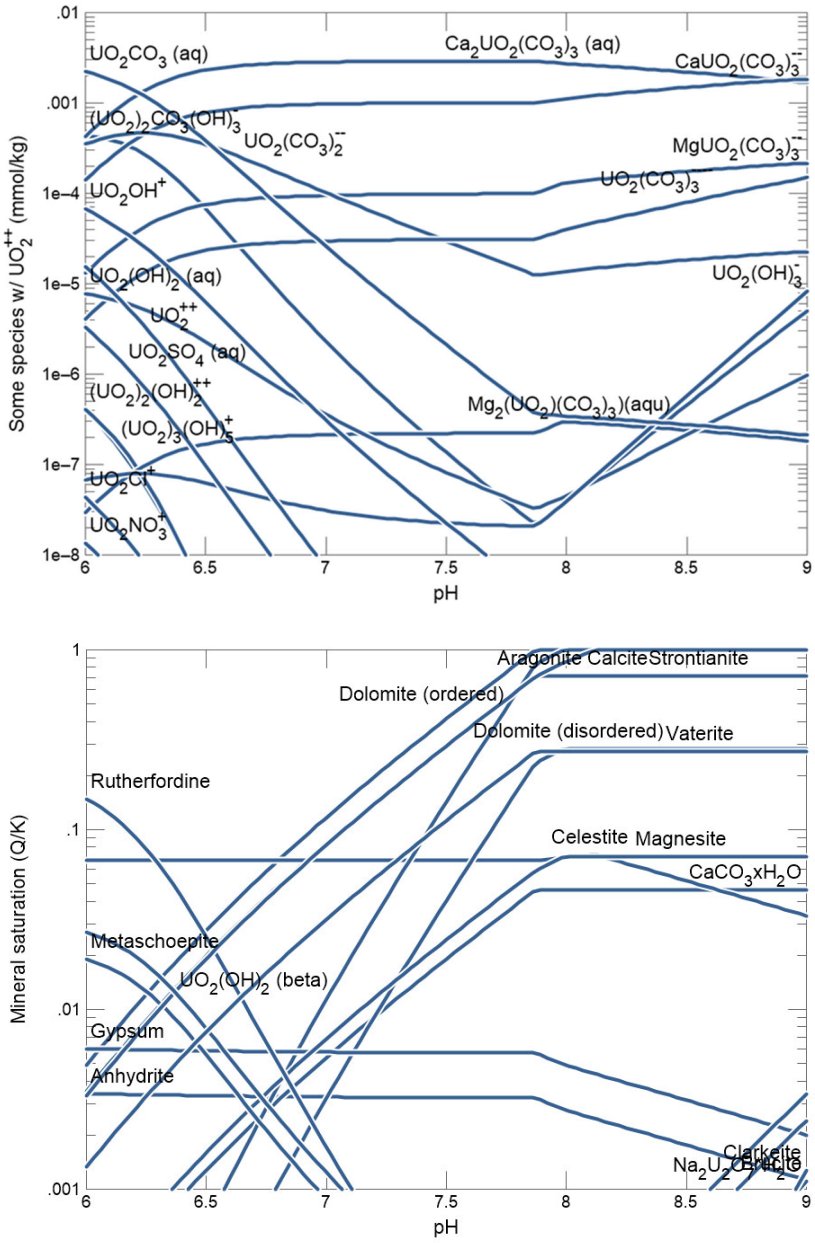

Figure H.9. Uranium speciation predicted in the aqueous phase (*top*) and mineral saturation for all species (*bottom*) in synthetic groundwater (SGW) as predicted by Geochemist Workbench.

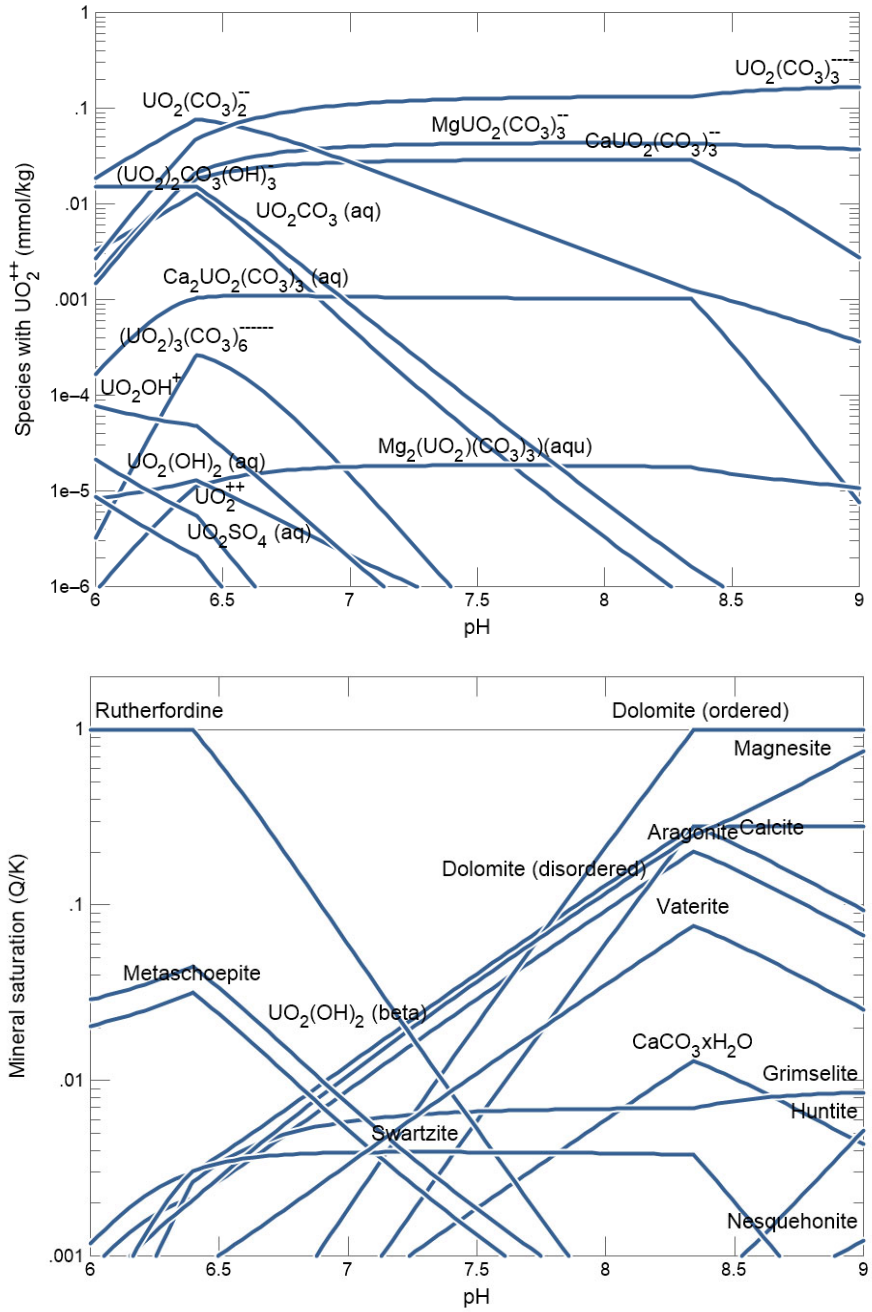

Figure H.10. Uranium speciation predicted in the aqueous phase (*top*) and mineral saturation for all species (*bottom*) in synthetic perched water as predicted by Geochemist Workbench.

H.5 Impact of Sterilization on Calcium Citrate Phosphate Amendment

Experiments for the Cit-PO_4 amendment included controls with different parts of the batch experiments sterilized, including solutions via vacuum filtration through a 0.2-µm filter and sediments via heat inactivation at 100 °C for 60 minutes. In addition, testing for this amendment utilized river water to allow for introduction of additional bacteria for consumption of citrate. The results suggest that there is a significant impact on U and Tc-99 immobilization when both solutions and sediments are sterilized

(Figure H.11 and Figure H.12, respectively) for both BY Cribs groundwater and perched water conditions (inclusion of nitrate).

The fraction of immobile phosphorus was also decreased for BY Cribs groundwater conditions, although results were inconsistent for perched water conditions (Figure H.13). There was not a significant impact on immobilization of either primary contaminants of interest in BY Cribs groundwater conditions when only sediment or the solution were sterilized. However, in perched water conditions, there was a significant impact on U and Tc-99 immobilization when both solutions and sediments were sterilized or only sediments were sterilized. This result suggests that the bacteria present in sediments may be more important for the treatment process when the ionic strength is greater in solution. Lastly, although some differences in U, Tc-99, and P immobilization were observed with sterilization of different components in the batch experiments, significant microbial growth was observed with all samples treated with Cit-PO_4 solutions based on measured cell concentrations conducted on sediments following batch experiments.

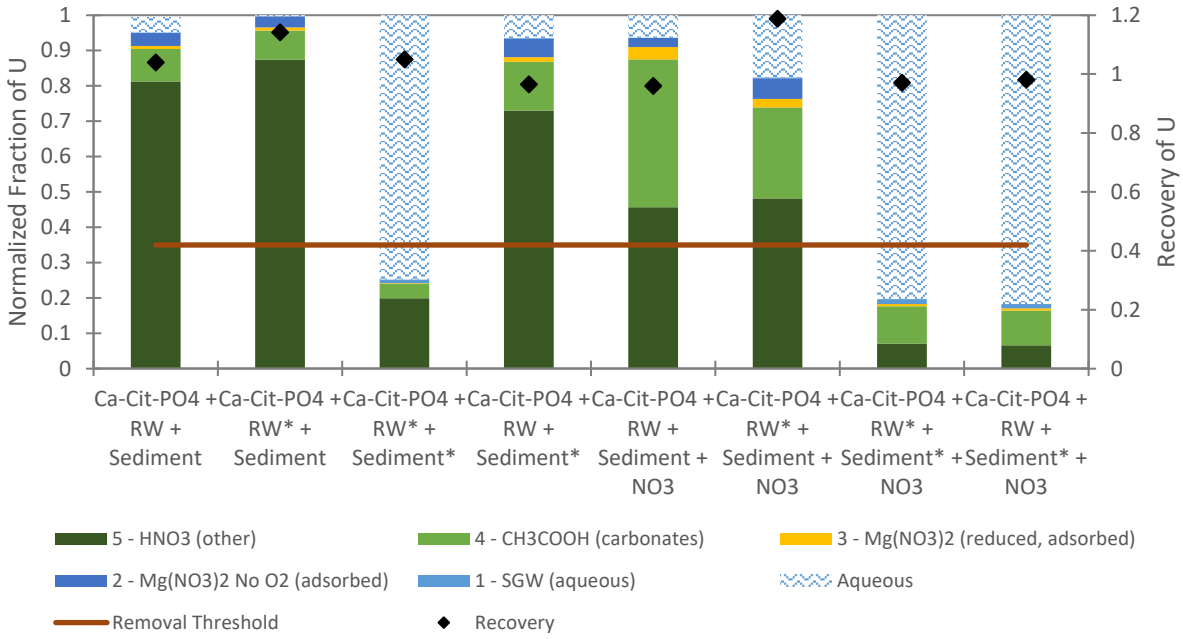

Figure H.11. Results for the normalized fraction of U in the aqueous phase (*wave blue bar*), each sequential extraction step (*solid bars*) following batch experiments reacted with Cit-PO_4 solutions with *different* steps of sterilization for 21 days as compared to controls without treatment with (*top*) BY Cribs groundwater conditions and (*bottom*) perched water conditions. The asterisks on the x-axis descriptions indicate which step was sterilized. Red line represents the minimum transformation threshold of 35% for testing and black diamonds represent the overall contaminant recovery.

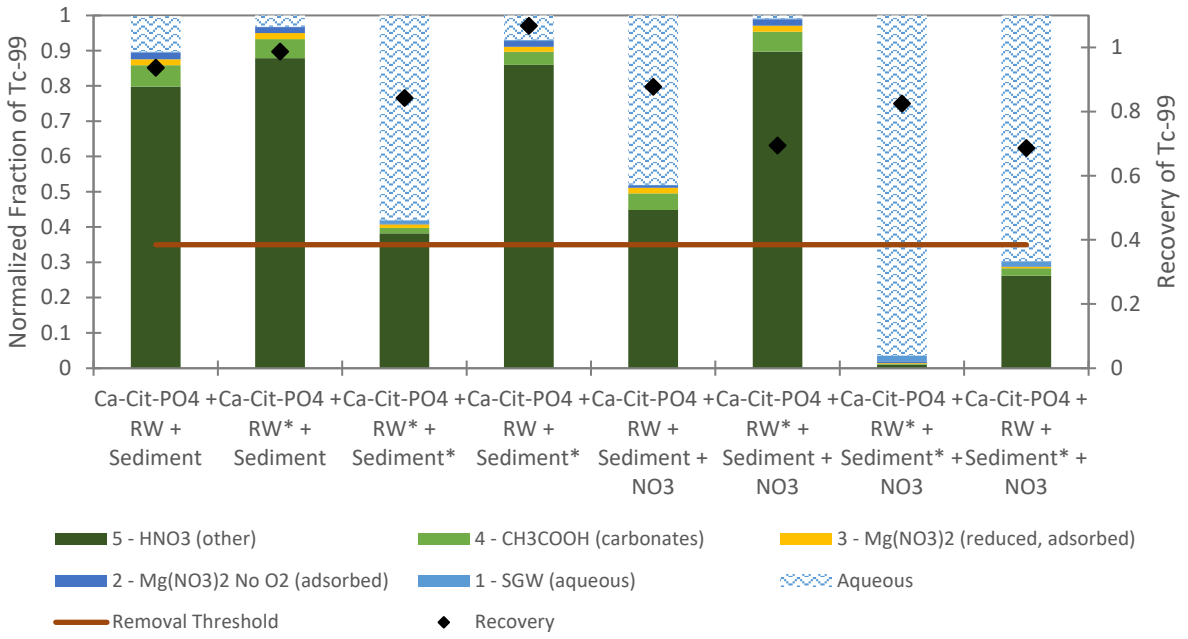

Figure H.12. Results for the normalized fraction of U in the aqueous phase (*wave blue bar*), each sequential extraction step (*solid bars*) following batch experiments reacted with Cit-PO_4 solutions with different steps of sterilization for 21 days as compared to controls without treatment with (*top*) BY Cribs groundwater conditions and (*bottom*) perched water conditions. The asterisks on the x-axis descriptions indicate which step was sterilized. The red line represents the minimum transformation threshold of 35% for testing and black diamonds represent the overall contaminant recovery.

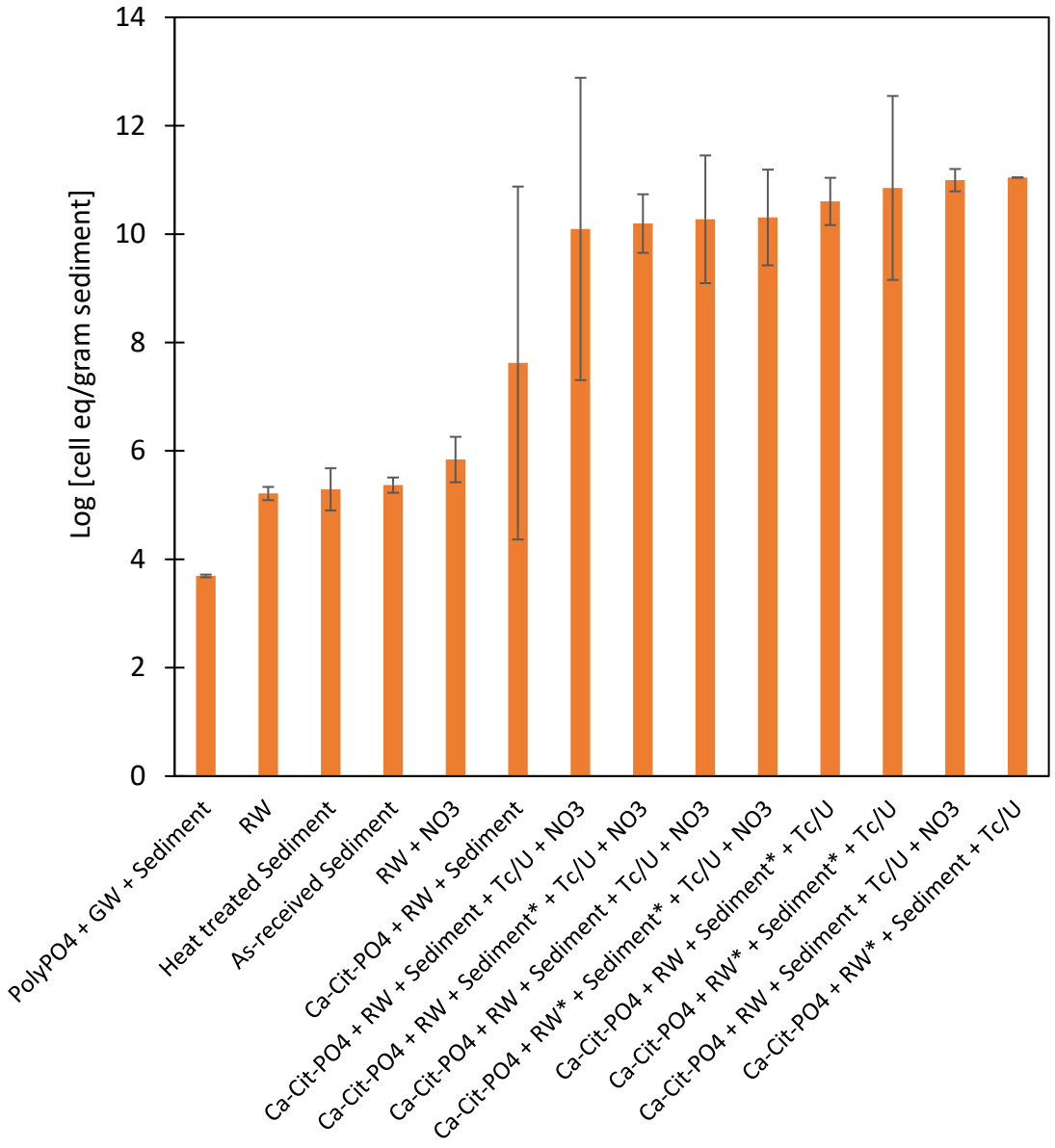

Figure H.13. The estimated cell concentration as shown by the logarithm of cell equivalents per gram for different treatment conditions in batch experiments.

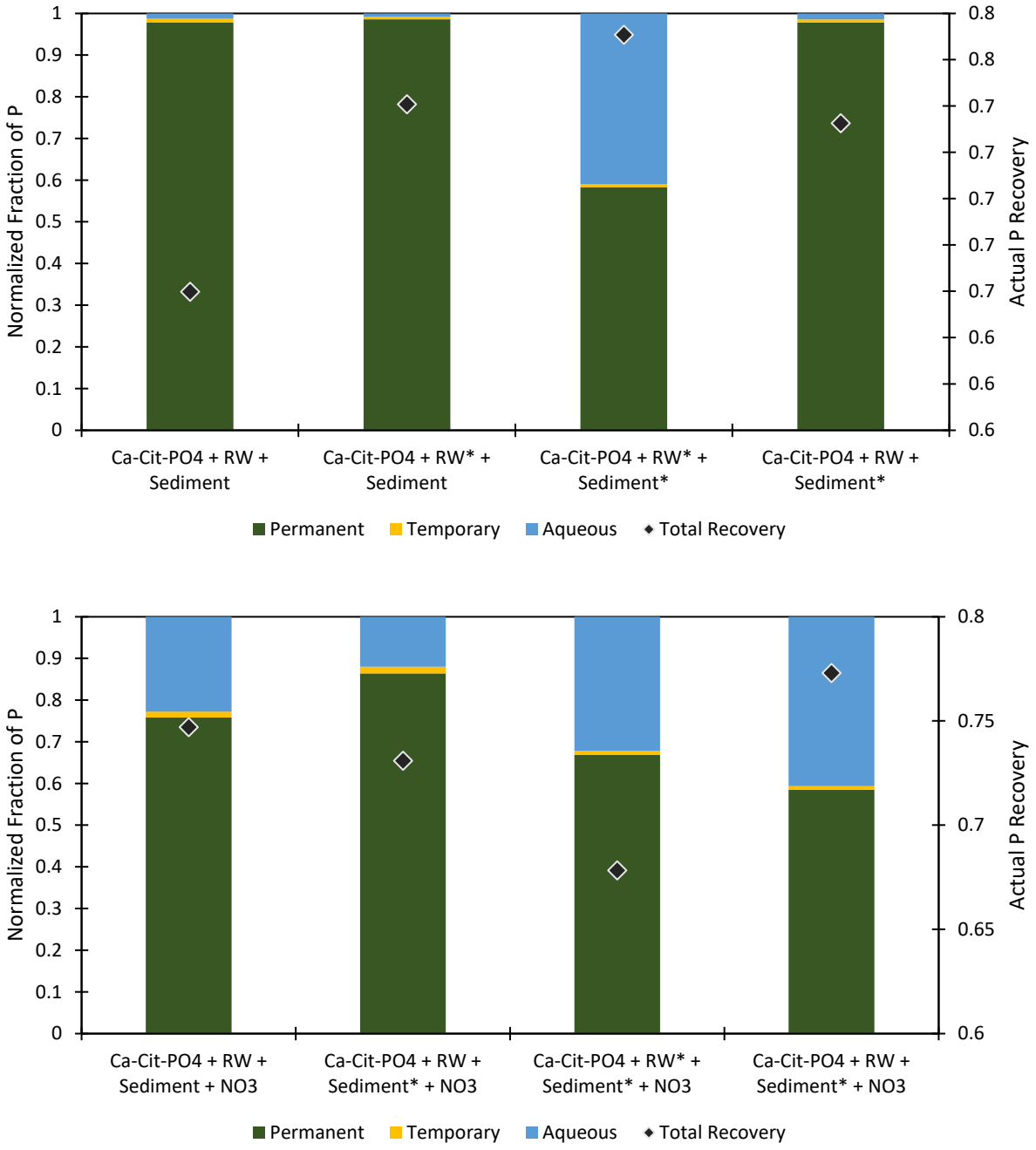

Figure H.14. Distribution of phosphorus in sequential extractions following reaction of Cit-PO_4 apatite-forming solutions with sediments and CoCOIs for 21 days with different steps sterilized (as shown by the asterisk in the x-axis) with (*top*) BY Cribs groundwater conditions and (*bottom*) perched water conditions.

H.6 Impact of Carbonate on Polyphosphate Amendment

Select experiments were conducted to consider the impact of excess HCO_3^- in solution as historical field injections have had up to 60 mM HCO_3^- present in solution. For example, the Hanford 300 Area Stage B Poly-PO_4 injections had approximately 60 mM HCO_3^-, likely due to base solutions used for mixing in the field being left open to the atmosphere (PNNL-29650). Although sequential extractions were not conducted under these conditions, the results from batch experiments highlight that the presence of high concentrations of HCO_3^- may decrease U removal from the aqueous phase during Poly-PO_4 treatment by as much as an order of magnitude (Figure H.15), as shown by modeling (Figure H.16). This result is likely a combination of impacts of carbonate on U speciation as well as apatite precipitation processes.

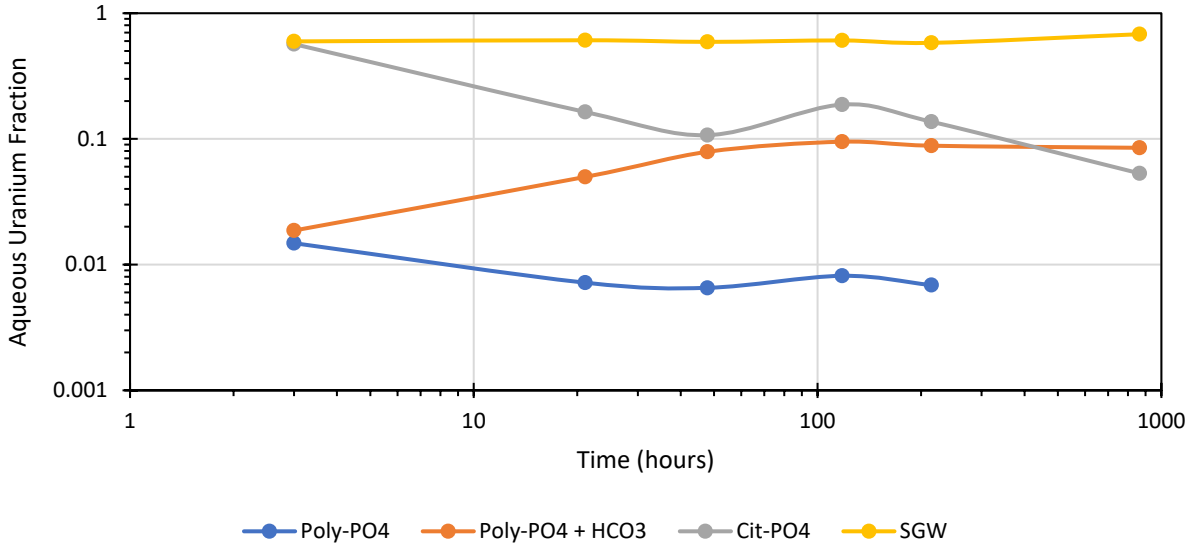

Figure H.15. Aqueous U fraction over time in batch experiments with variable treatments in SGW. Note: experiments were not conducted in triplicate and lines are used to guide the eye and do not represent a model.

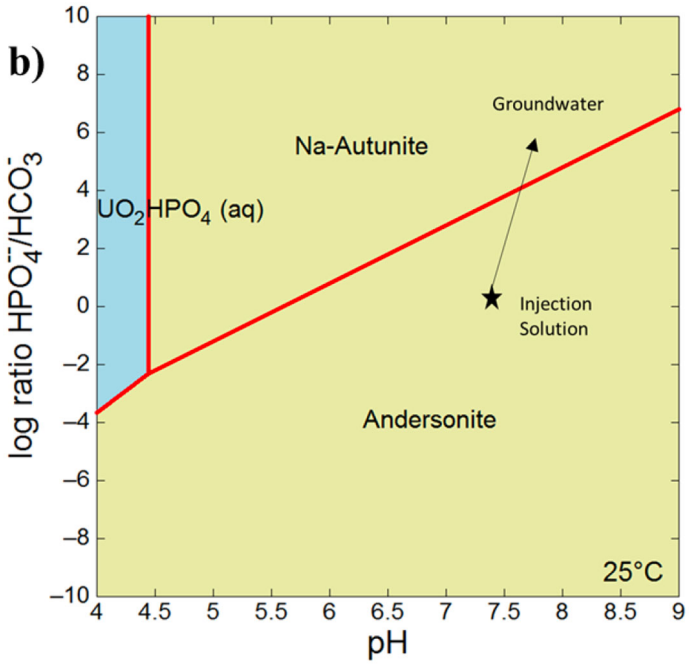

Figure H.16. Simulations of U precipitates that form upon 88 mM PO_4 and 60 mM CO_3 solution injection ("injection solution" on graph) and at lower CO_3 concentration ("groundwater" on graph), from PNNL-29650.

Appendix I – Supporting Data for Liquid-Phase Reduction and Sequestration Amendments

I.1 Supporting Sequestration Data for Primary Contaminants of Interest

Data are shown in the main text as the normalized fraction recovered in each extraction; however, results are shown here as a sediment loading in μg/g for comparison. These results highlight that significantly greater U was immobilized for perched water conditions, even though approximately 30 times more U was added to the system as compared to BY Cribs groundwater conditions. For Tc-99, a significantly greater amount of Tc-99 remained in the aqueous phase following treatment with Cit-PO_4 in perched water conditions as compared to BY Cribs groundwater conditions.

I.1.1 U Sequestration (in µg/g)

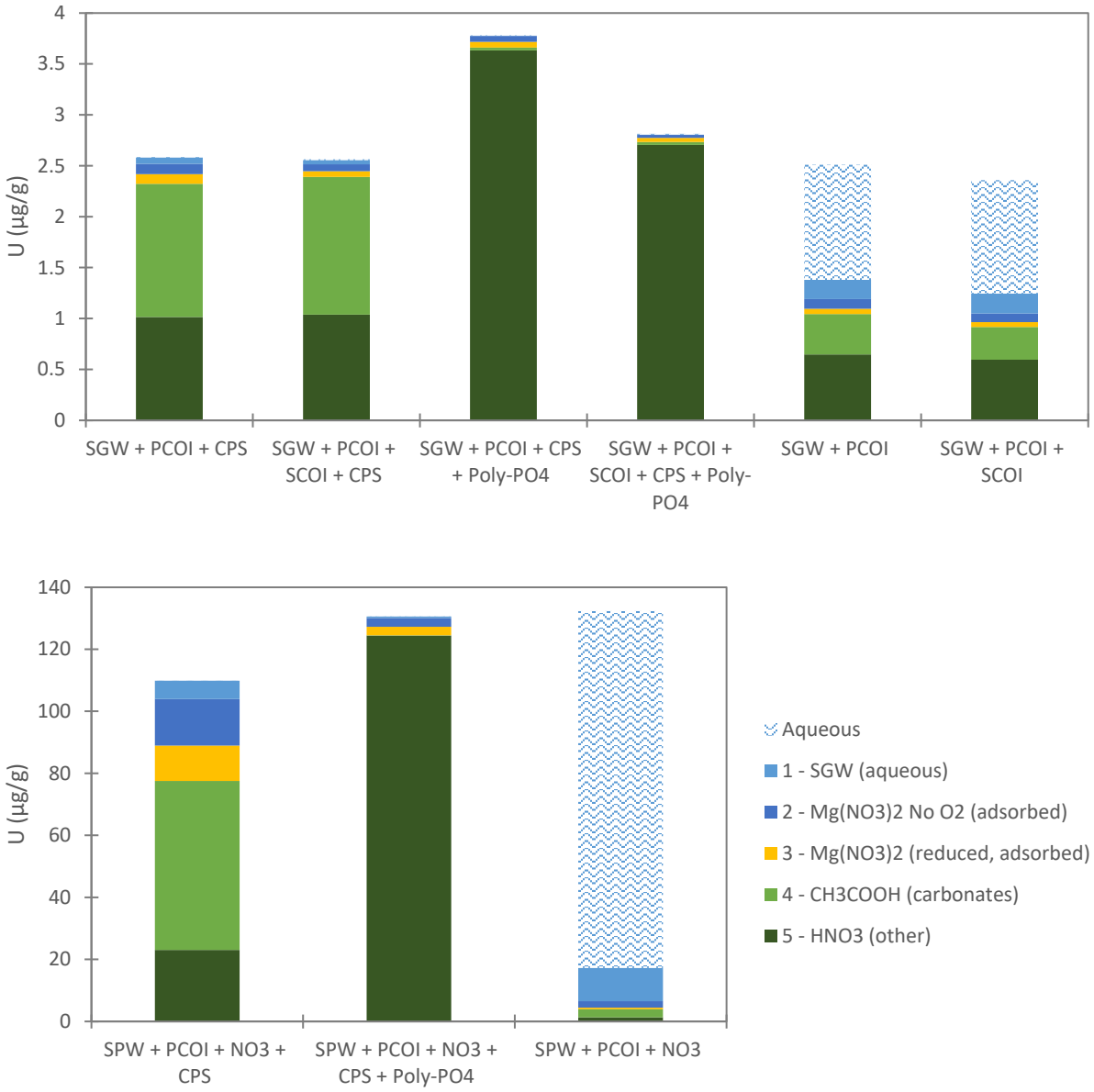

Figure I.1. Results for the U in µg/g for the aqueous phase (*wave blue bar*) and each sequential extraction step (*solid bars*) following batch experiments reacted with calcium polysulfide (CPS) and apatite-forming solutions over 42 days as compared to controls without treatment with (*top*) BY Cribs groundwater conditions and (*bottom*) perched water conditions.

I.1.2 Tc-99 Sequestration (in µg/g)

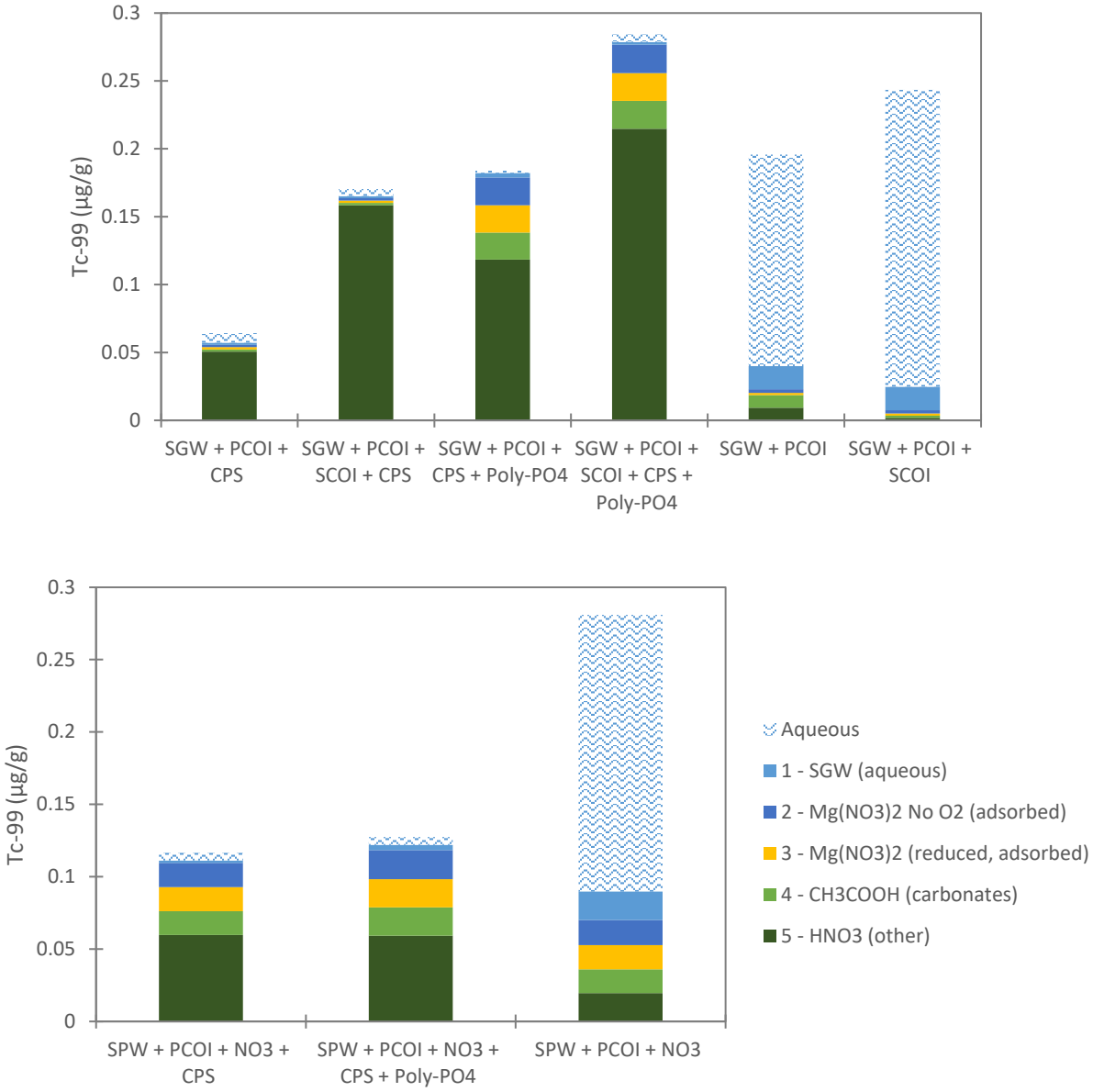

Figure I.2. Results for the Tc-99 in µg/g for the aqueous phase (*wave blue bar*) and each sequential extraction step (*solid bars*) following batch experiments reacted with CPS and apatite-forming solutions over 42 days as compared to controls without treatment with (*top*) BY Cribs groundwater conditions and (*bottom*) perched water conditions.

I.1.3 Tc-99 and U Sequestration over Time

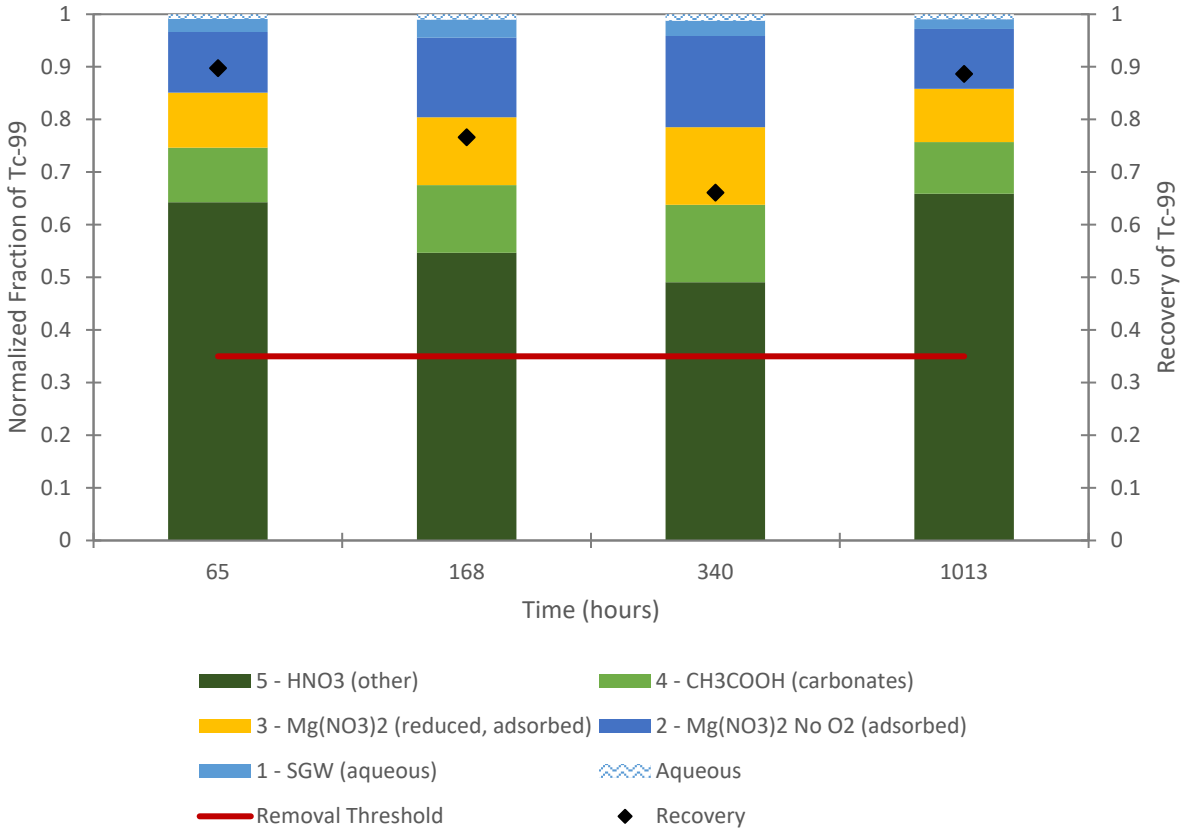

Figure I.3. Results for the Tc-99 normalized for each fraction of the aqueous phase (*wave blue bar*) and each sequential extraction step (*solid bars*) over time with for batch experiments with Hanford formation (Hf) sediments, synthetic groundwater (SGW), and treatment with CPS + Poly-PO_4.

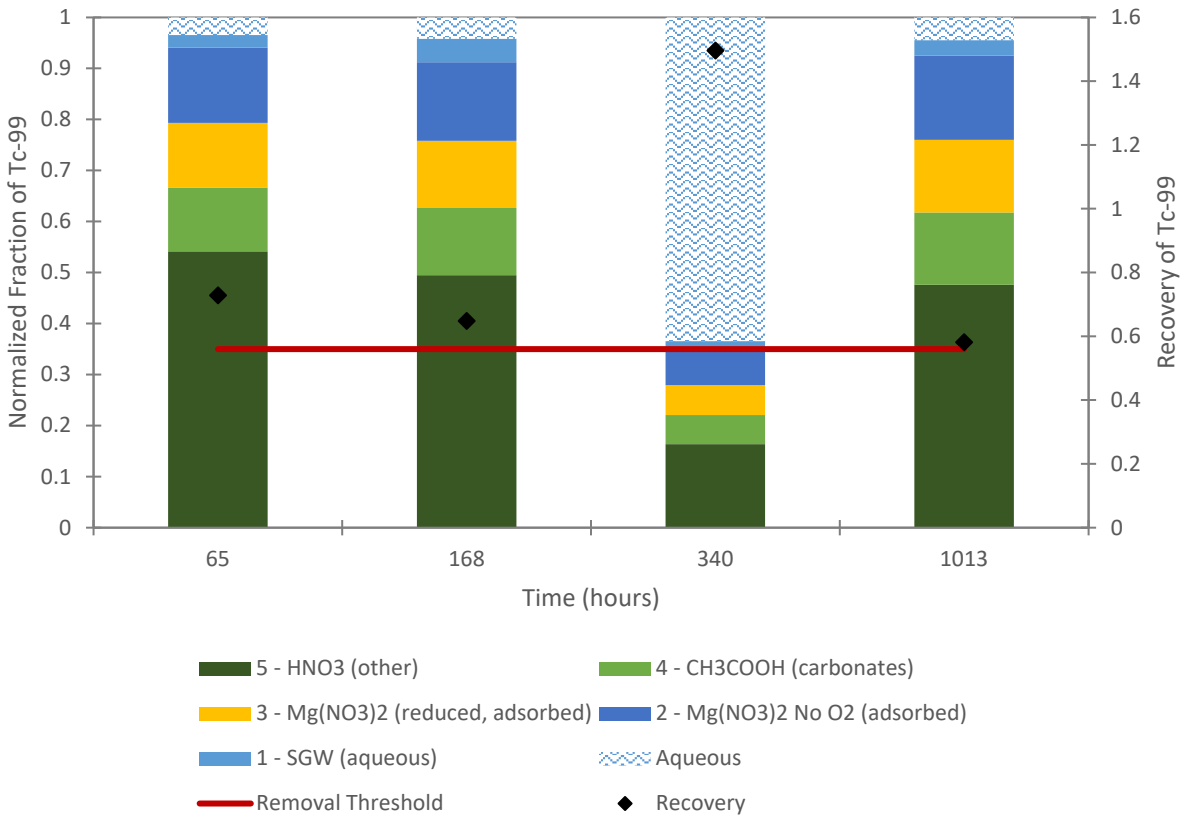

Figure I.4. Results for the Tc-99 normalized for each fraction of the aqueous phase (*wave blue bar*) and each sequential extraction step (*solid bars*) over time with for batch experiments with Hf sediments, synthetic perched water (SPW), and treatment with CPS + Poly-PO_4.

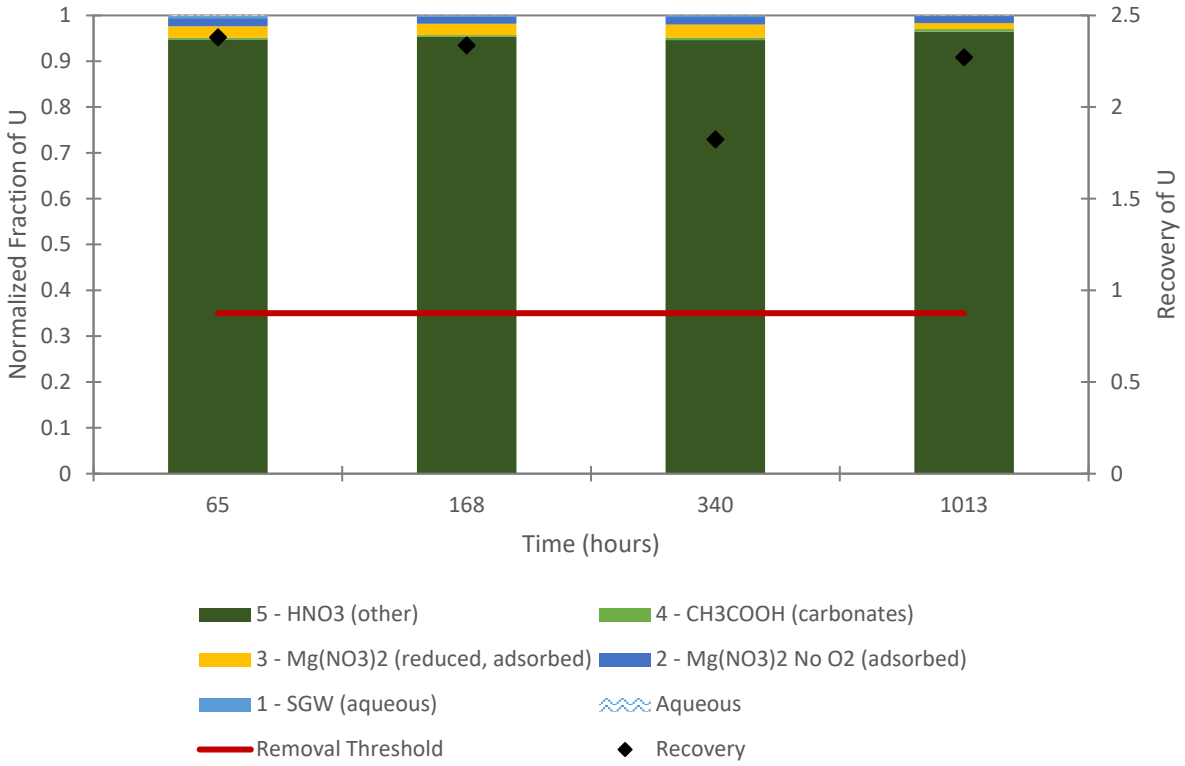

Figure I.5. Results for the U normalized for each fraction of the aqueous phase (*wave blue bar*) and each sequential extraction step (*solid bars*) over time with for batch experiments with Hf sediments, SGW, and treatment with CPS + Poly-PO_4.

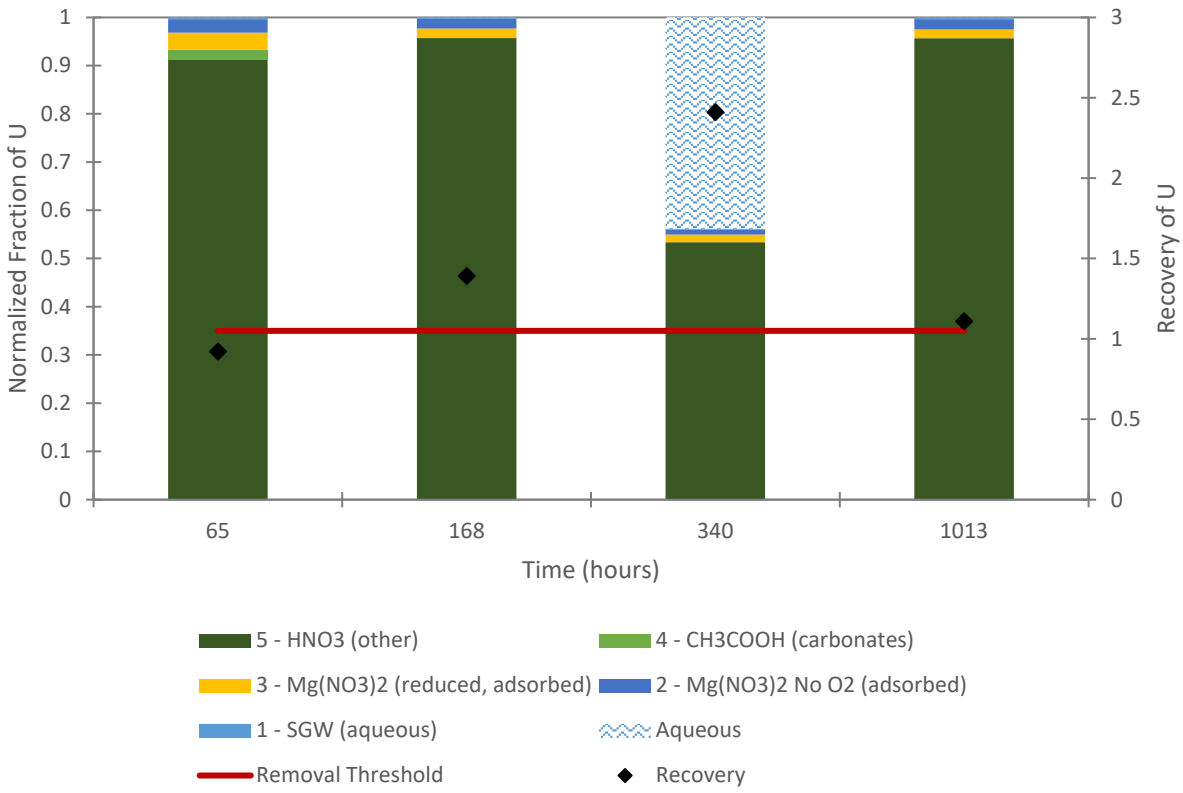

Figure I.6. Results for the U normalized for each fraction of the aqueous phase (*wave blue bar*) and each sequential extraction step (*solid bars*) over time with for batch experiments with Hf sediments, SPW, and treatment with CPS + Poly-PO_4.

I.2 Supporting Rate of Removal Data for PCOIs

I.2.1 Behavior of U and Tc-99 with Variable Polysulfide Treatment

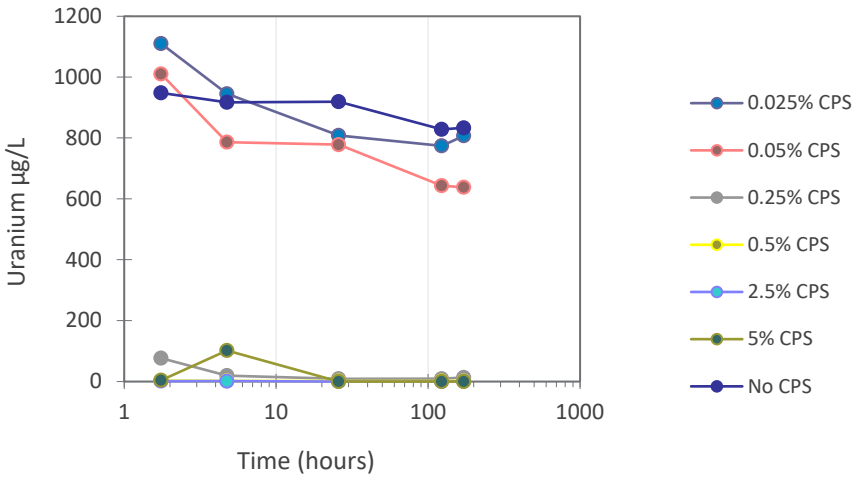

Figure I.7. Results for U remaining in the aqueous phase in batch experiments with Hf sediments conducted over 7 days following treatment with CPS in variable concentrations as compared to controls without treatment in SGW without co-contaminants of interest (CoCOIs).

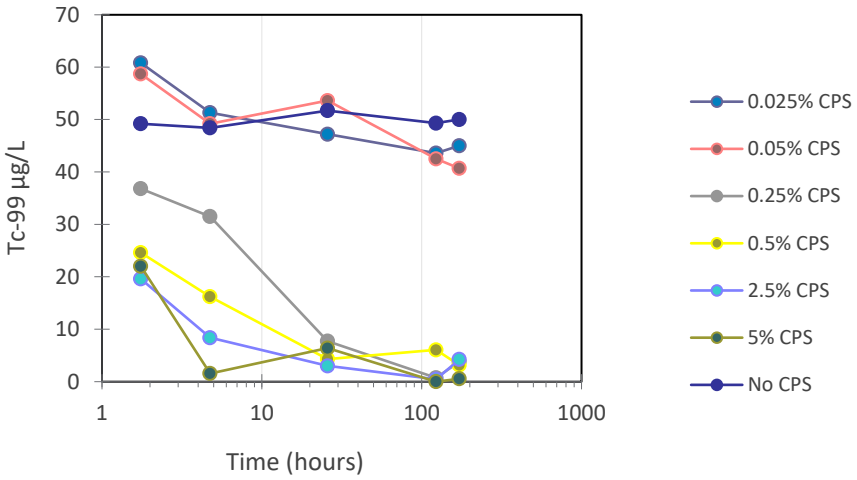

Figure I.8. Results for Tc-99 remaining in the aqueous phase in batch experiments with Hf sediments conducted over 7 days following treatment with CPS in variable concentrations as compared to controls without treatment in SGW without CoCOIs.

I.2.2 Behavior of U and Tc-99 with only Polysulfide Treatment

The results shown in Figure I.9 through Figure I.12 compare CPS treatment to control conditions without treatment (either SGW or SPW depending on target location of BY Cribs or perched water, respectively). These data highlight that the initial removal with CPS via reductive precipitation of both U and Tc-99 is sufficient to meet the 35% transformation threshold with less than 1% remaining in the aqueous phase after treatment under most conditions. However, it should be noted that experiments were conducted in an anaerobic glovebox in the absence of oxygen. Therefore, these results do not include the potential for re-oxidation (and re-mobilization) of Tc-99 and U following treatment. The technology is still recommended to advance with the two-step process.

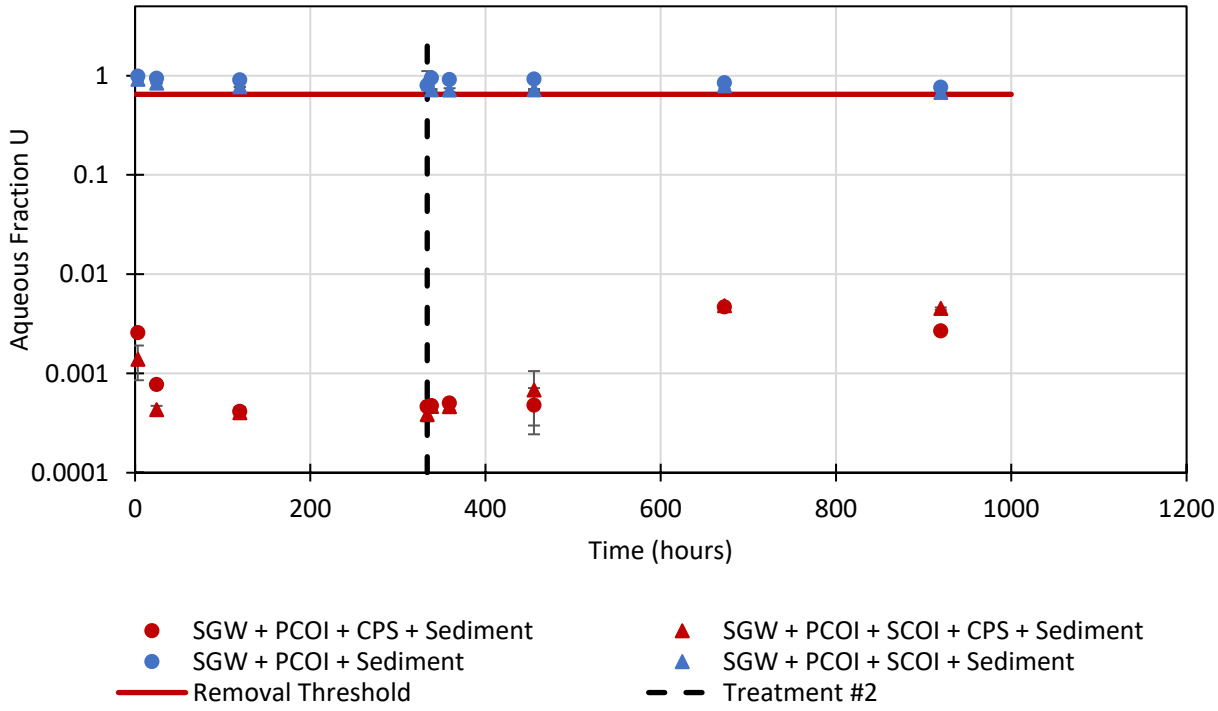

Figure I.9. Results for U remaining in the aqueous phase in batch experiments conducted over 42 days following treatment with CPS (*red*) under BY Cribs groundwater conditions as compared to controls without treatment (*blue*) with (*triangles*) and without CoCOIs (*circles*). Error bars are based on analysis of triplicate batch reactors.

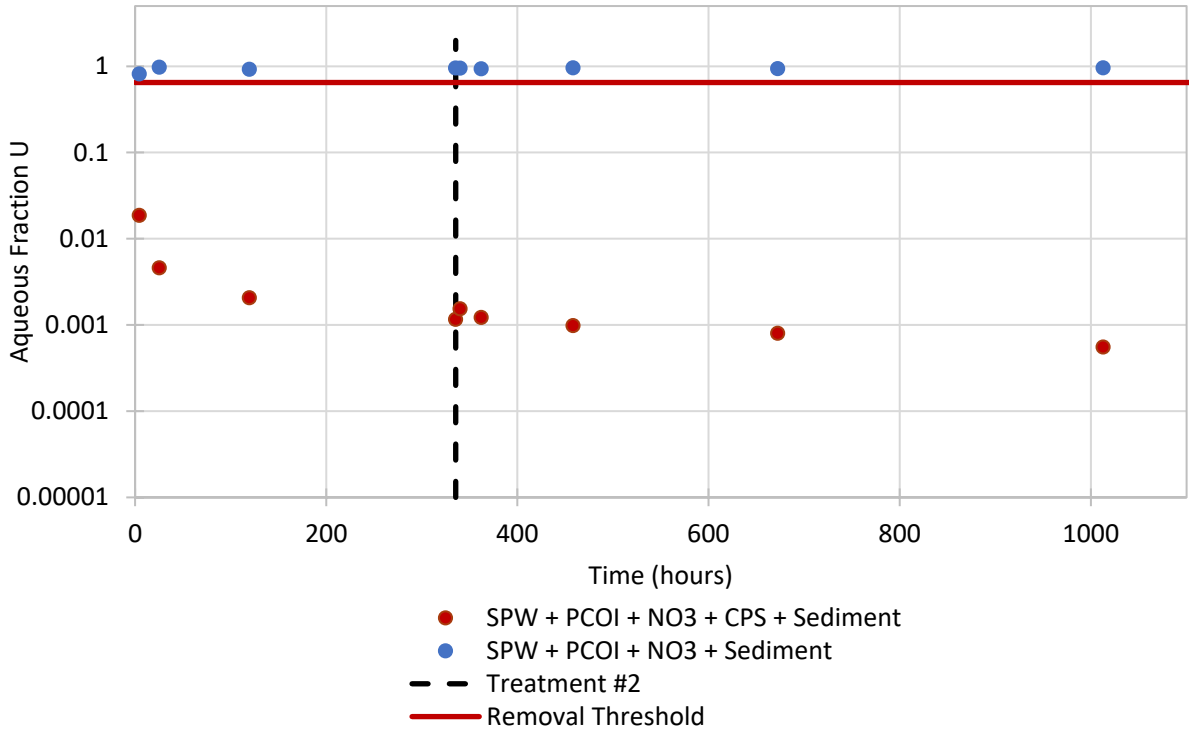

Figure I.10. Results for U remaining in the aqueous phase in batch experiments conducted over 42 days following treatment with CPS (*red*) under perched water conditions as compared to controls without treatment (*blue*). Error bars are based on analysis of triplicate batch reactors.

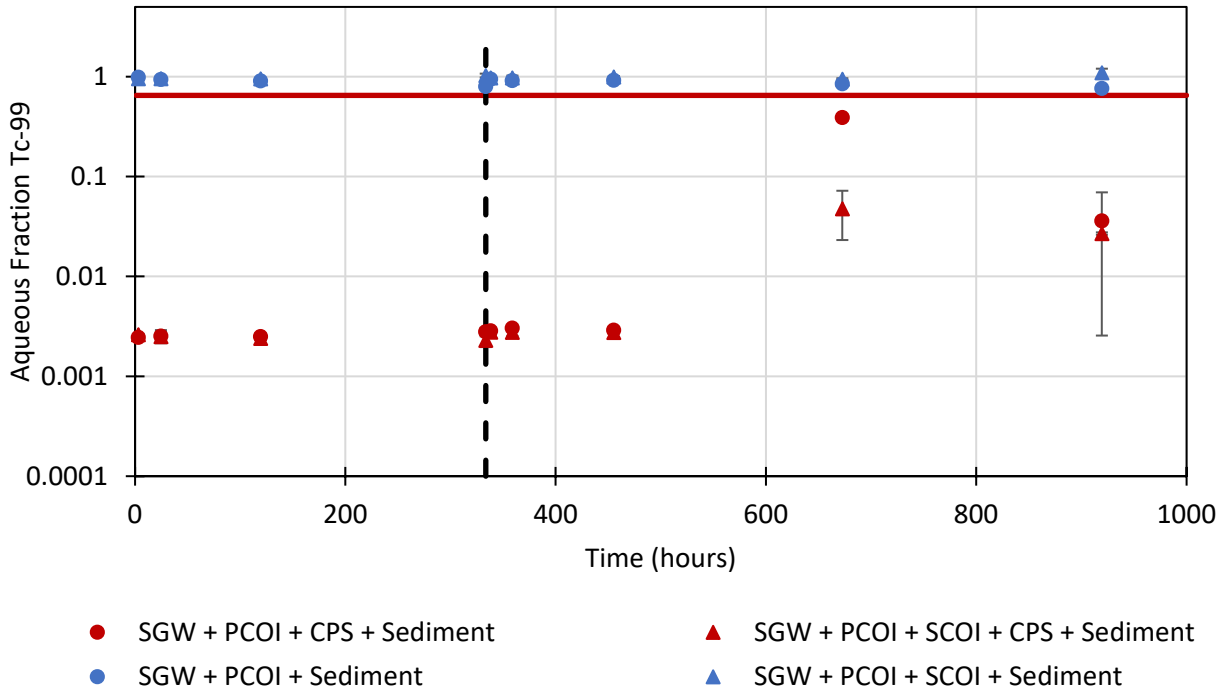

Figure I.11. Results for Tc-99 remaining in the aqueous phase in batch experiments conducted over 42 days following treatment with CPS (*red*) under BY Cribs groundwater conditions as compared to controls without treatment (*blue*) with (*triangles*) and without CoCOIs (*circles*). Error bars are based on analysis of triplicate batch reactors.

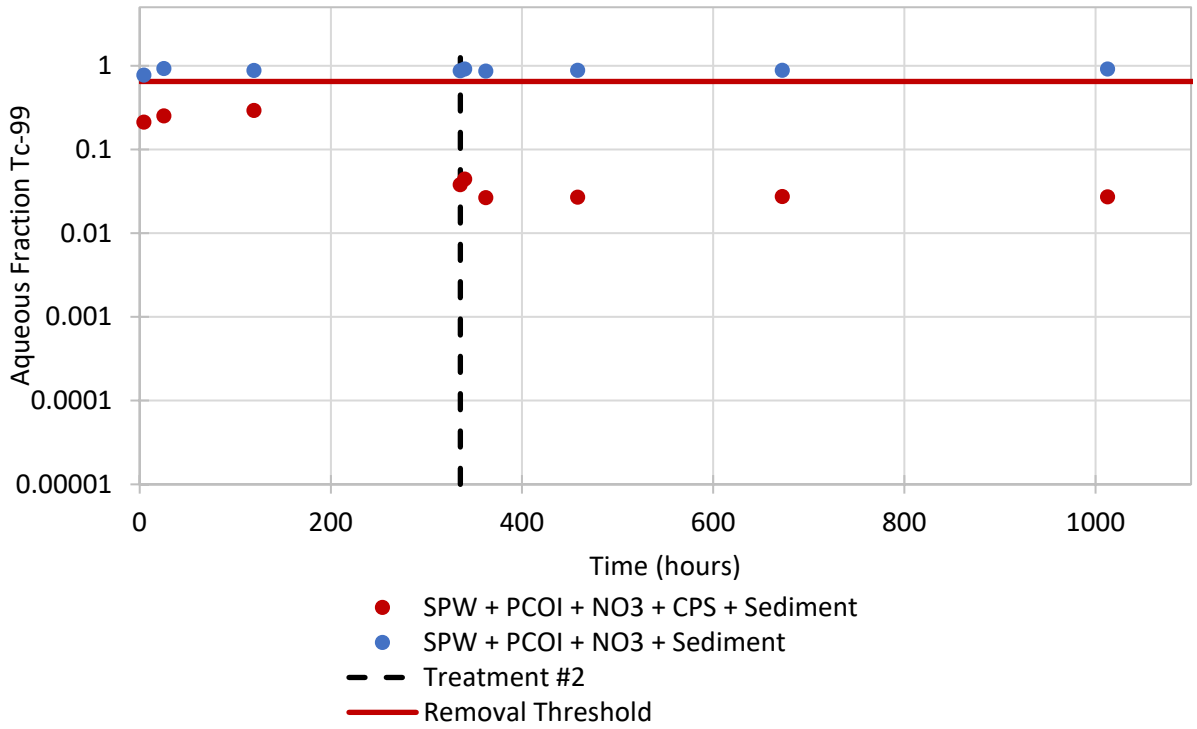

Figure I.12. Results for Tc-99 remaining in the aqueous phase in batch experiments conducted over 42 days following treatment with CPS (*red*) under perched water conditions as compared to controls without treatment (*blue*). Error bars are based on analysis of triplicate batch reactors.

I.3 Comparison of Treatment with and without Sediments

The presence of sediments (all conducted with Hf sediments) may impact the efficacy of an amendment, depending on how it reacts (e.g., consuming reductive capacity). Therefore, we conducted control experiments for both treated and untreated samples with and without sediments. These results are summarized for U in Figure I.13 through Figure I.16 and for Tc-99 in Figure I.17 through Figure I.20. In controls without treatment, there is not a significant impact on U and Tc-99 removal, highlighting that there is very little sorption of U and Tc-99 to these sediments under the conditions evaluated. For samples that received both CPS and Poly-PO_4 treatment, there is also not a significant impact due to sediments. However, in the field, sediment-to-solution ratios will be much higher. Therefore, this may need to be considered further in the next phase of testing.

I.3.1 Comparison of Batch Reactors with and without Sediments for U

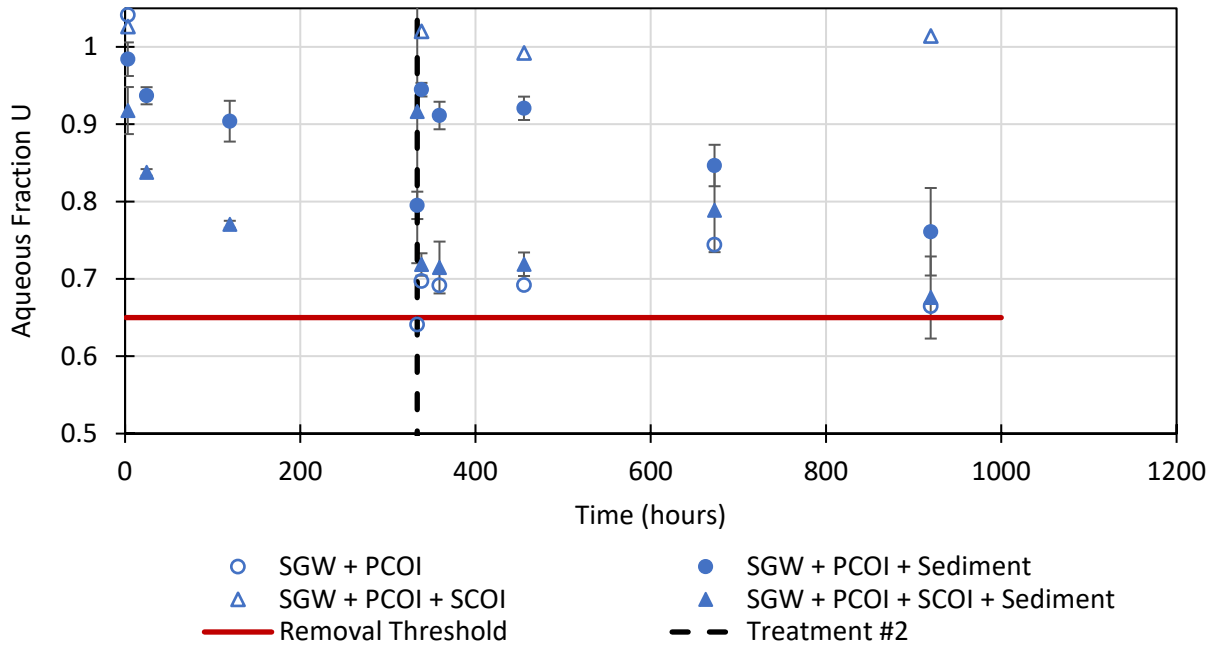

Figure I.13. Results for U remaining in the aqueous phase in batch experiments conducted over 42 days without treatment (*blue*) under BY Cribs groundwater conditions as compared to controls with (triangles) and without CoCOIs (*circles*) and with (*filled circles*) and without (*unfilled circles*) sediment. Error bars are based on analysis of triplicate batch reactors.

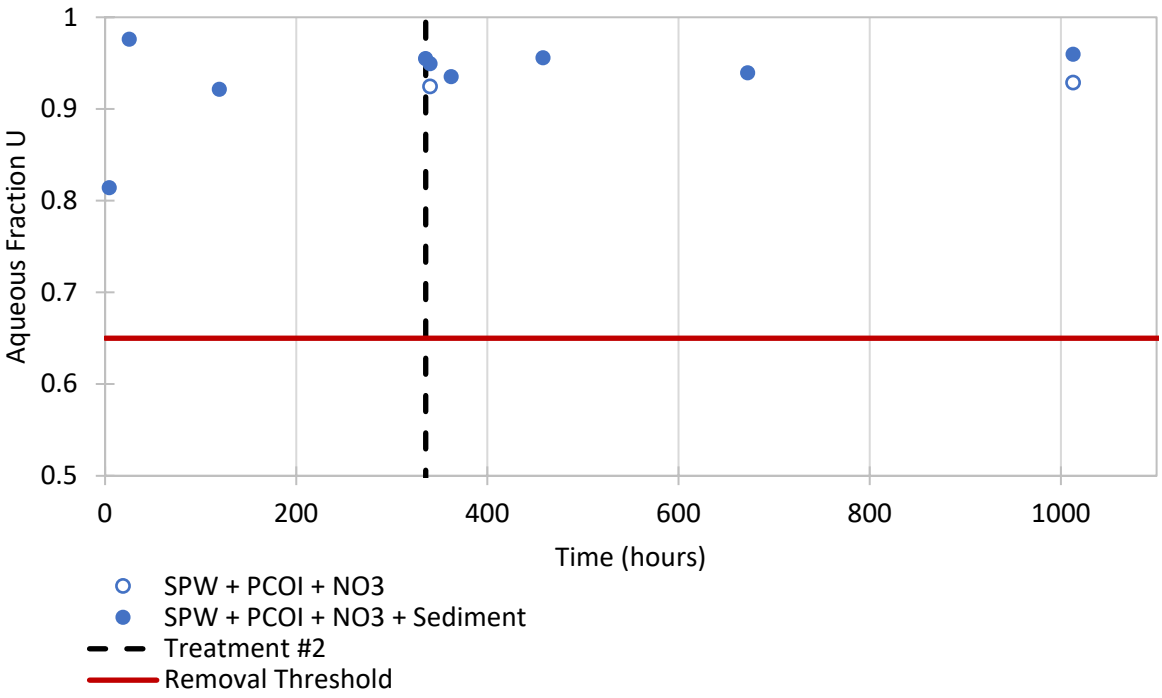

Figure I.14. Results for U remaining in the aqueous phase in batch experiments conducted over 42 days without treatment (*blue*) under perched water conditions as compared to controls with (*filled circles*) and without (*unfilled circles*) sediment. Error bars are based on analysis of triplicate batch reactors.

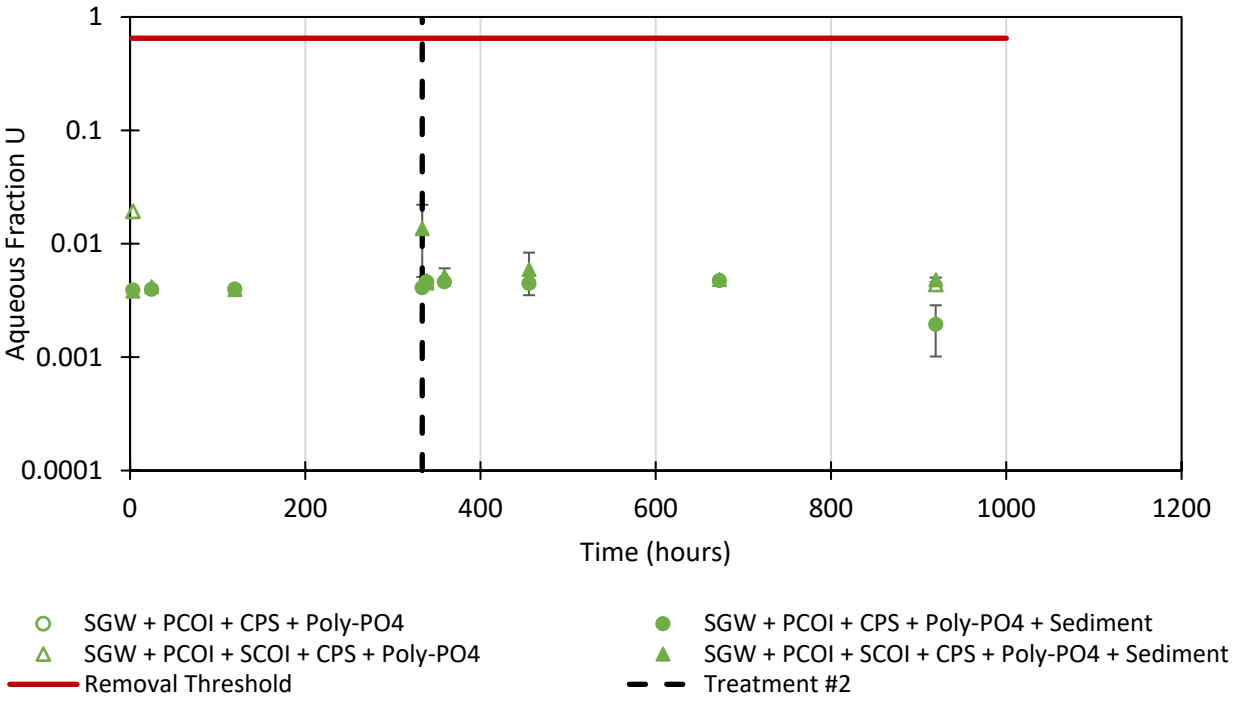

Figure I.15. Results for U remaining in the aqueous phase in batch experiments conducted over 42 days following treatment (*green*) under BY Cribs groundwater conditions as compared to controls with (*triangles*) and without CoCOIs (*circles*) and with (*filled circles*) and without (*unfilled circles*) sediment. Error bars are based on analysis of triplicate batch reactors.

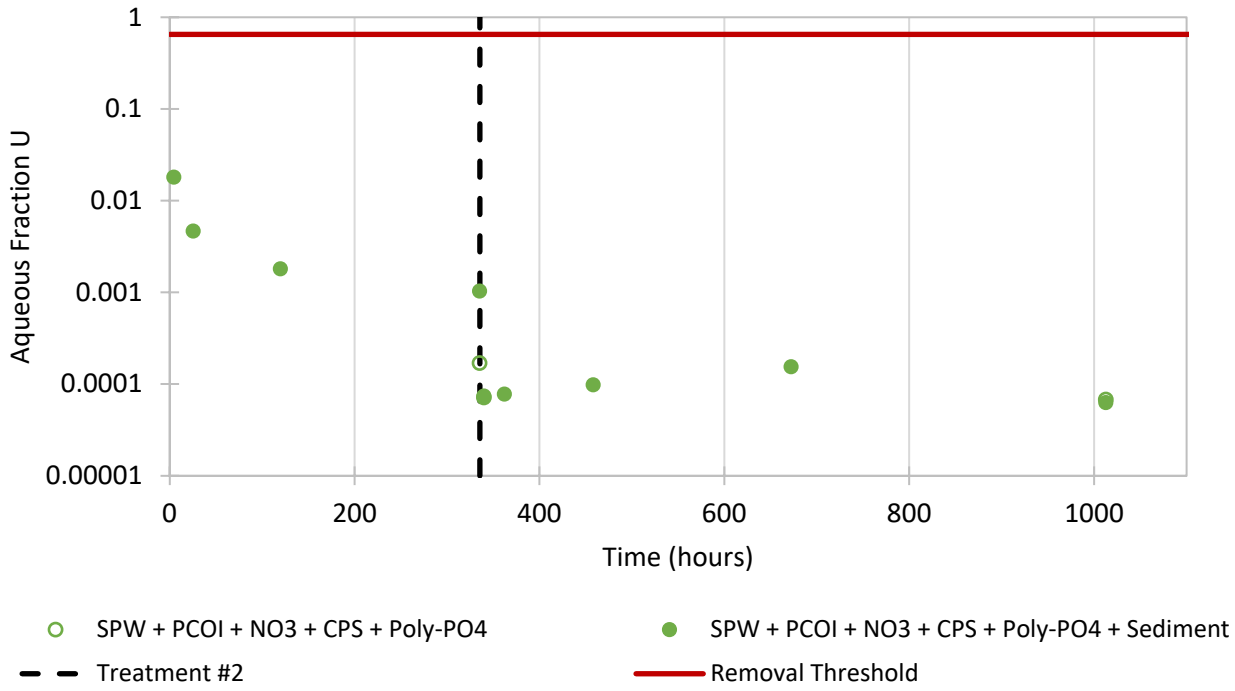

Figure I.16. Results for U remaining in the aqueous phase in batch experiments conducted over 42 days following treatment (*green*) under perched water conditions as compared to controls with (*filled circles*) and without (*unfilled circles*) sediment. Error bars are based on analysis of triplicate batch reactors.

I.3.2 Comparison of Batch Reactors with and without Sediments for Tc-99

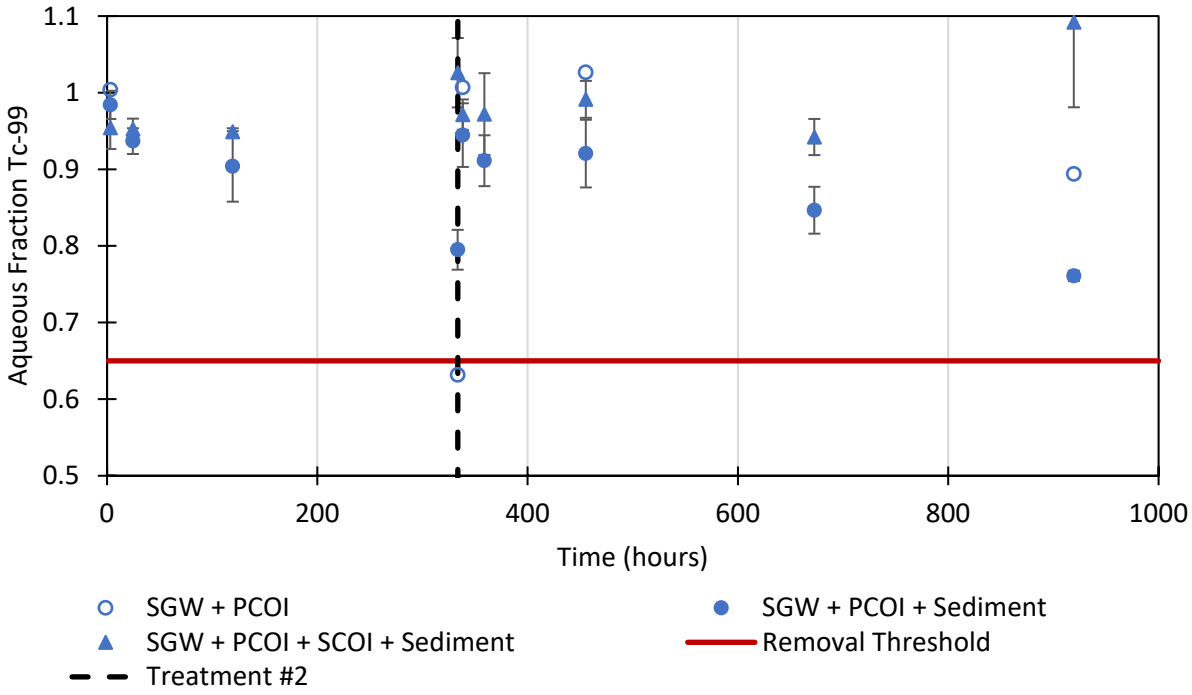

Figure I.17. Results for Tc-99 remaining in the aqueous phase in batch experiments conducted over 42 days without treatment (*blue*) under BY Cribs groundwater conditions as compared to controls with (*triangles*) and without CoCOIs (*circles*) and with (*filled circles*) and without (*unfilled circles*) sediment. Error bars are based on analysis of triplicate batch reactors.

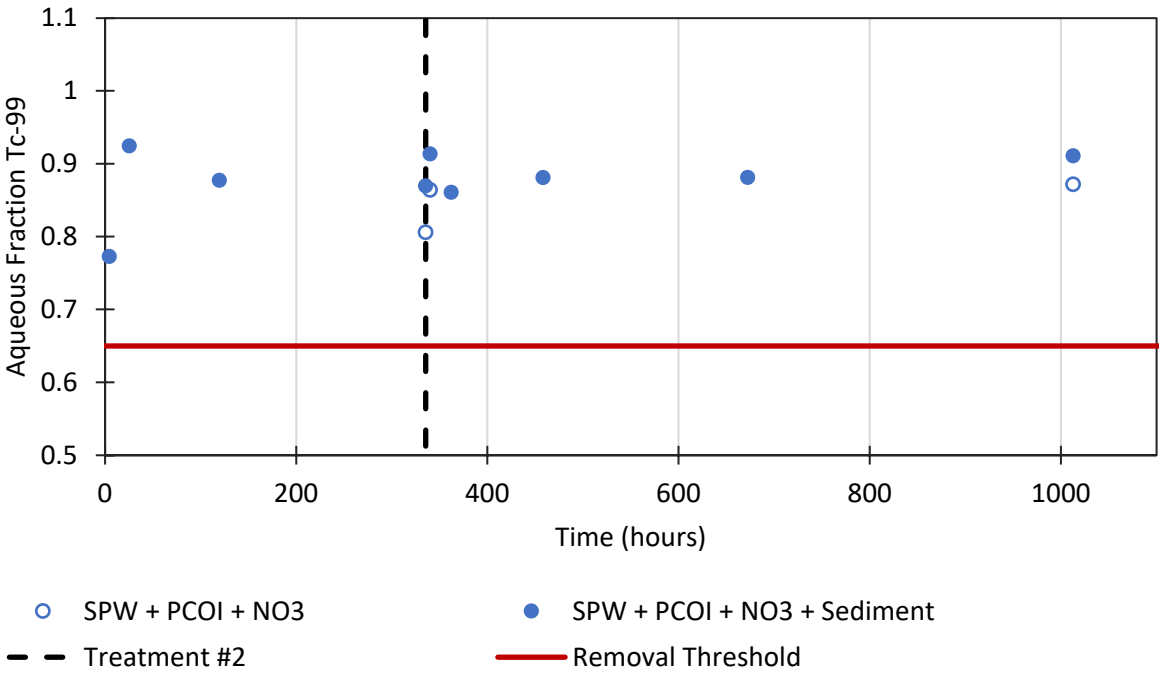

Figure I.18. Results for Tc-99 remaining in the aqueous phase in batch experiments conducted over 42 days without treatment (*blue*) under perched water conditions as compared to controls with (*filled circles*) and without (*unfilled circles*) sediment. Error bars are based on analysis of triplicate batch reactors.

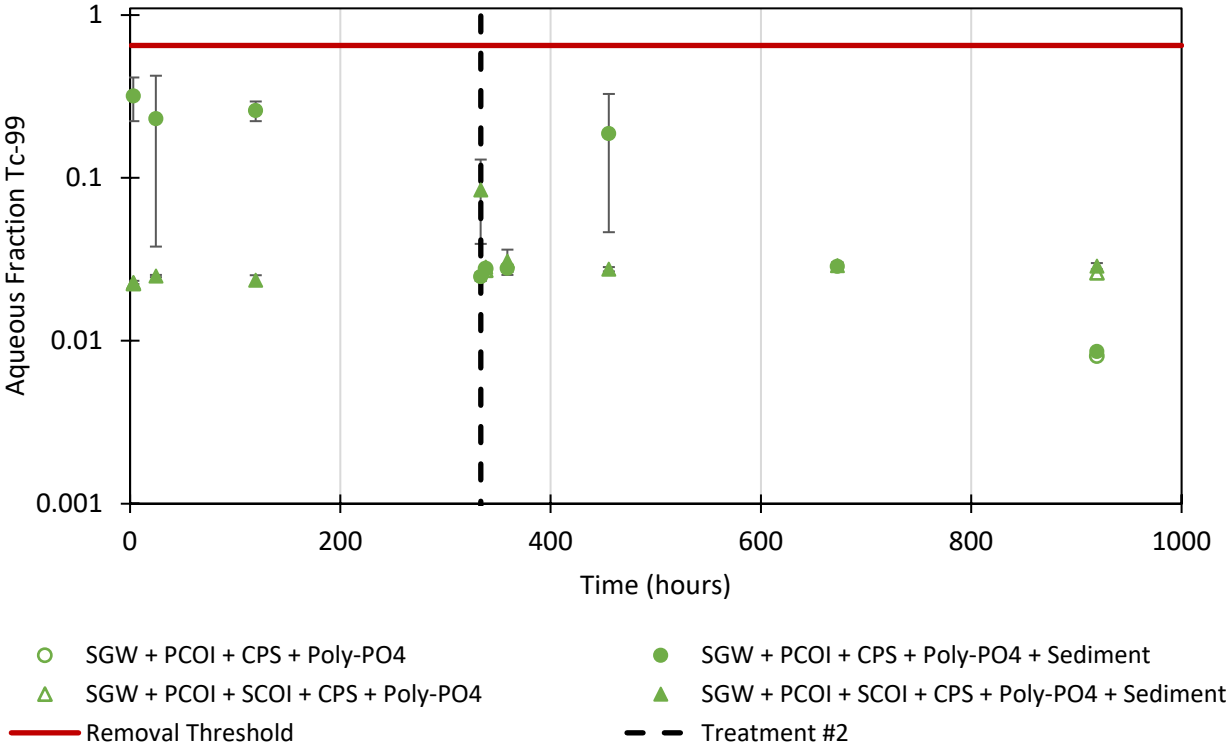

Figure I.19. Results for Tc-99 remaining in the aqueous phase in batch experiments conducted over 42 days following treatment (*green*) under BY Cribs groundwater conditions as compared to controls with (*triangles*) and without CoCOIs (*circles*) and with (*filled circles*) and without (*unfilled circles*) sediment. Error bars are based on analysis of triplicate batch reactors.

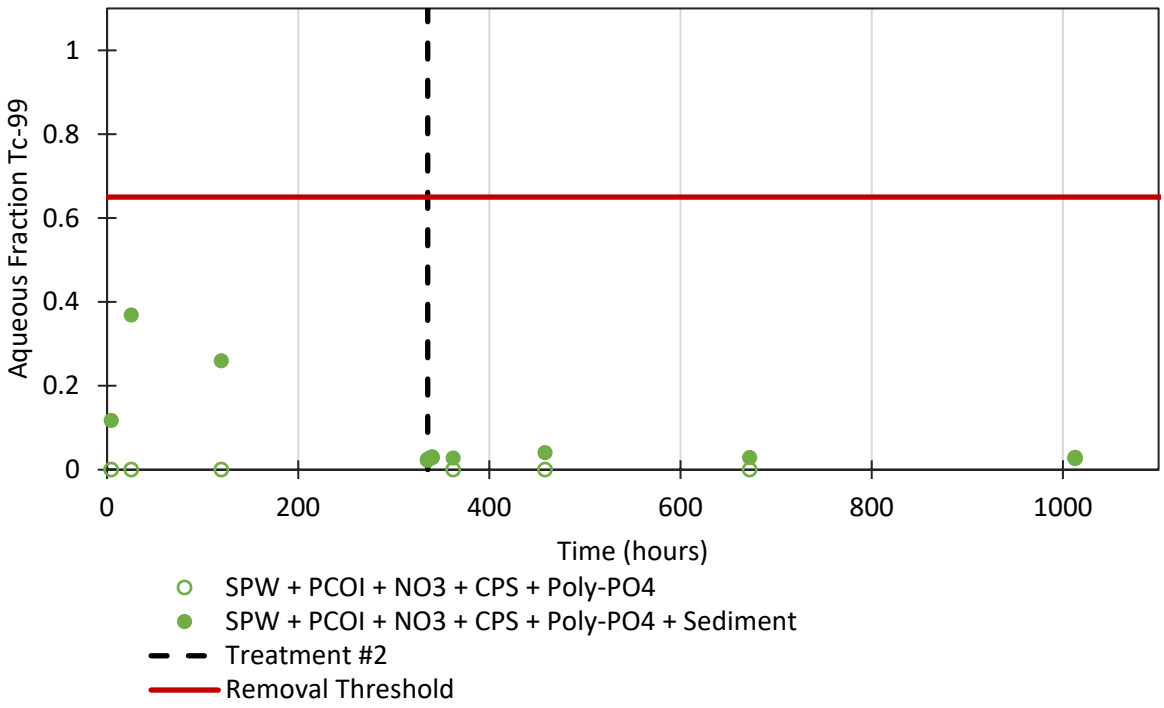

Figure I.20. Results for Tc-99 remaining in the aqueous phase in batch experiments conducted over 42 days following treatment (*green*) under perched water conditions as compared to controls with (*filled circles*) and without (*unfilled circles*) sediment. Error bars are based on analysis of triplicate batch reactors.

I.4 Behavior of CoCOIs

CoCOIs were only added to BY Cribs groundwater conditions with the exception of nitrate being the only CoCOI added to reactors under perched water conditions. However, data for iodate cannot be reported due to an error when initial CoCOIs were added to stock solutions. The results for Sr, Cr(VI), and nitrate are reported as a fraction recovered based on the total CoCOI added and the naturally occurring mass within sediments based on the black diamond symbols with a normalized recovery reported for each step of the sequential extractions.

I.4.1 Reduction and Sequestration of Sr

Strontium was added as naturally occurring Sr isotope ratios at concentrations similar to that observed in the natural Hanford subsurface (Table 3.6). Sr-90 concentrations are much lower than natural Sr, but technologies cannot target different isotopes. These results show very little change in the immobile fraction of Sr in sequential extractions (4 – CH_3COOH and 5 – HNO_3) following treatment with CPS, CPS followed by Poly-PO_4, or a no-treatment control (Figure I.21). Previous research has shown that Sr reacts strongly with apatite phases, resulting in a decrease in mobility (PNNL-19524). However, these results suggest that Sr was relatively immobile under natural conditions, resulting in a smaller decrease in mobility with treatment. In addition, recoveries are > 2, highlighting that there was a significant amount of naturally occurring Sr in sediments in addition to what was added.

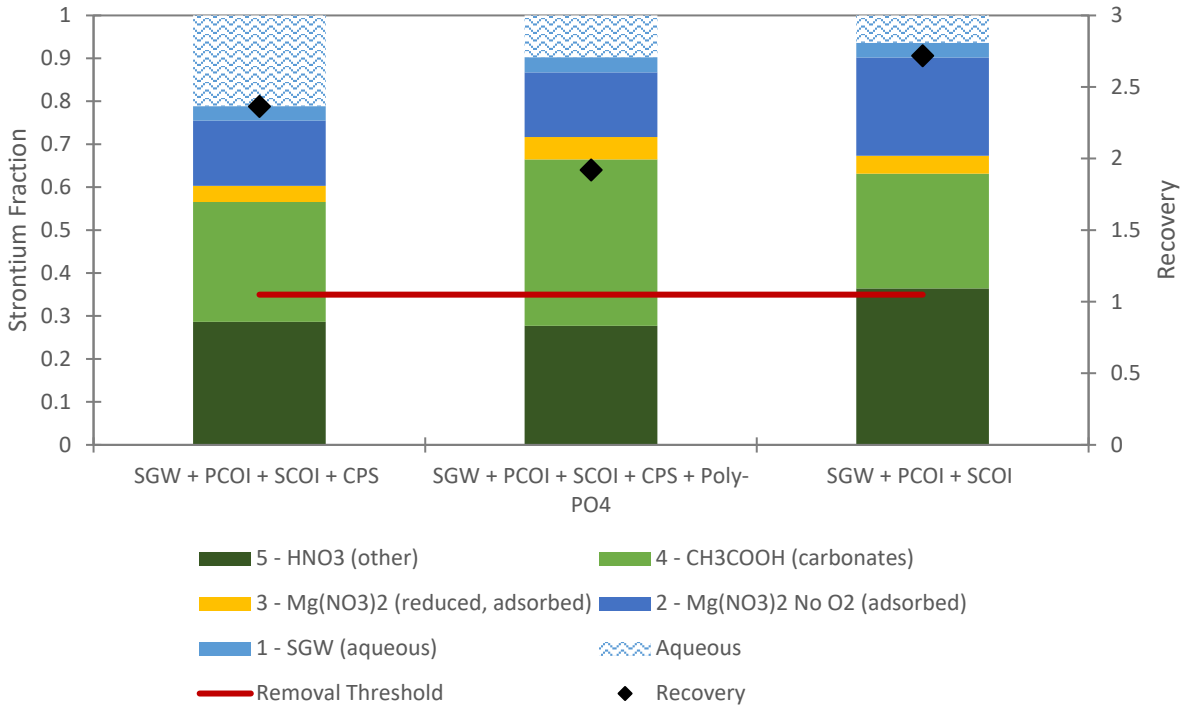

Figure I.21. Results for Sr in the aqueous phase (*wave blue bar*) and each sequential extraction step (*solid bars*) following batch experiments reacted with CPS for 14 days followed by Poly-PO_4 solutions for another 28 days (42-day total reaction time) with (*top*) normalized fraction recovered and (*bottom*) mass of contaminant in µg/g.

I.4.2 Reduction and Sequestration of Cr

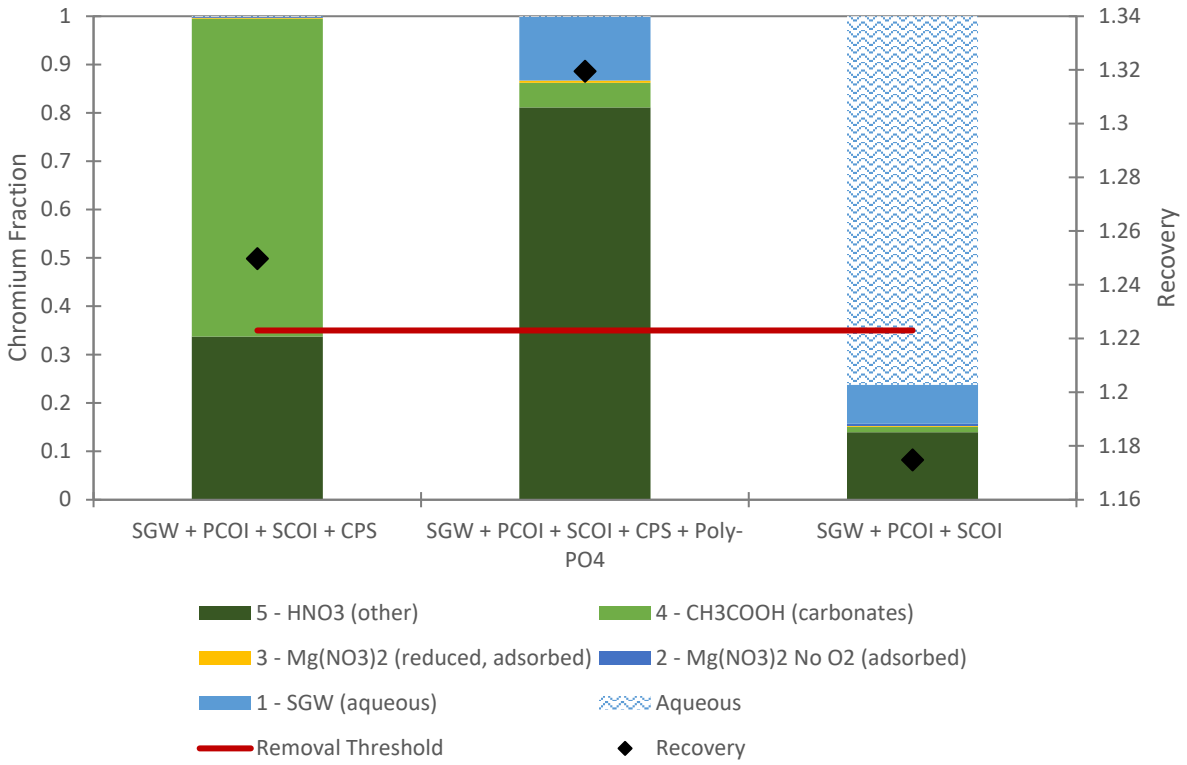

Figure I.22. Results for Cr(VI) in the aqueous phase (*wave blue bar*) and each sequential extraction step (*solid bars*) following batch experiments reacted with CPS for 14 days followed by Poly-PO_4 solutions for another 28 days (42-day total reaction time) with (top) normalized fraction recovered and (bottom) mass of contaminant in µg/g.

I.4.3 Reduction and Sequestration of Nitrate

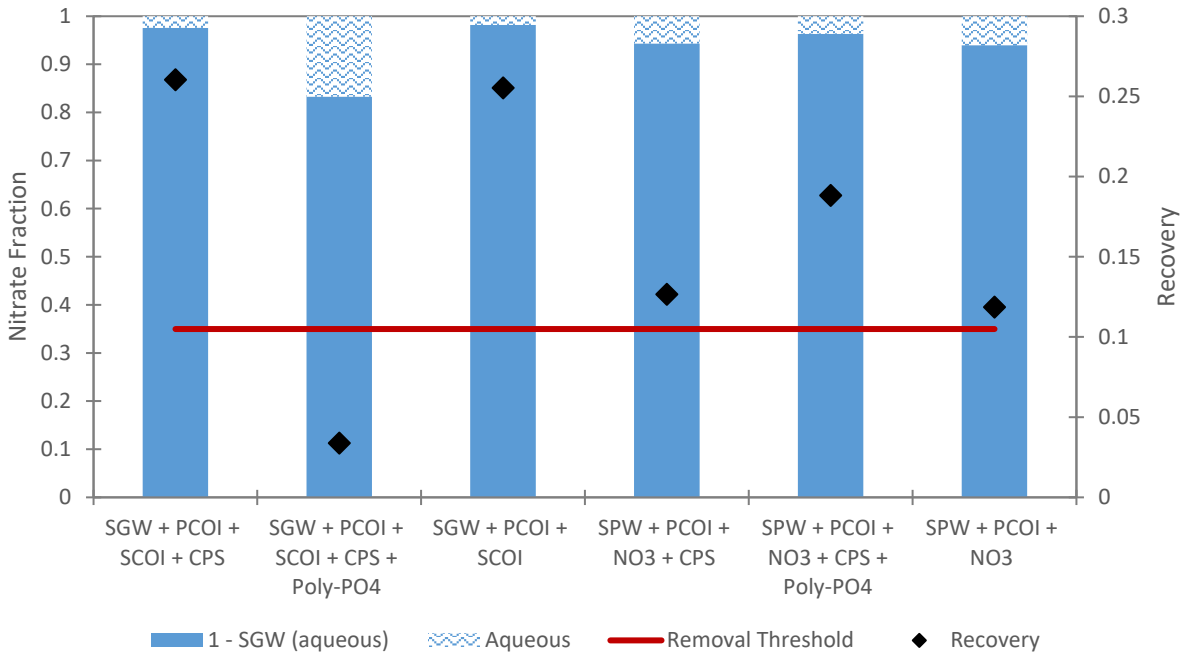

Figure I.23. Results for nitrate in the aqueous phase (*wave blue bar*) and each sequential extraction step (*solid bars*) following batch experiments reacted with CPS for 14 days followed by Poly-PO_4 solutions for another 28 days (42-day total reaction time) with (*top*) normalized fraction recovered and (*bottom*) mass of contaminant in µg/g.

I.5 pH Change with Treatment

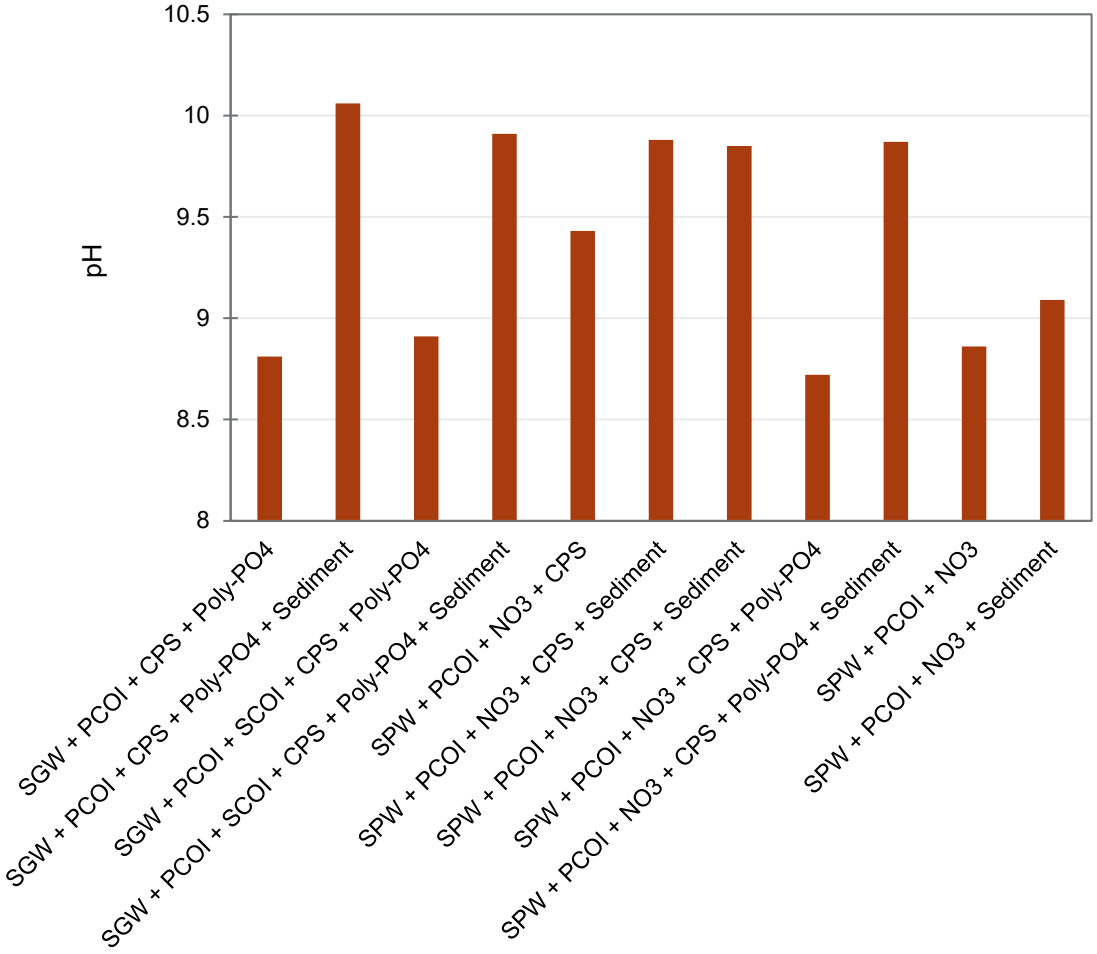

Figure I.24. Results for pH in the aqueous in batch experiments after 42 days of reaction.

Appendix J – Supporting Data for Liquid-Phase Bioreduction and Sequestration Amendments

Bioremediation is the use of microorganisms to destroy or immobilize waste materials (Shanahan 2004), potentially via mineralization, transformation, and/or alteration processes. Processes such as cellular respiration can drive reoxidation or consumption of contaminants and generally require an energy source (electron donor), an electron acceptor, and nutrients. For microbial processes, there is a wide array of potential electron acceptors (as well as donors), such as O_2, NO_3^-, Mn(IV), Fe(III), and SO_4^-, which may also be targeted contaminants of interest (COIs) (i.e., NO_3^-). The effectiveness of bioremediation processes are dependent on site-specific characteristics and the methods used for biostimulation, i.e., using organic carbon sources (as electron donors) to stimulate native microbial populations. Site environmental conditions that can dramatically affect microbial processes include pH, water content, temperature, nutrient availability, redox potential, and the complex nature of contaminant profiles (Borden 2006).

The aim of microbial nitrate reduction is to generate nitrogen gas, which will harmlessly be released to the atmosphere; however, microbial denitrification is a stepwise reduction of nitrate (NO_3^-) to dinitrogen (N_2). The complete denitrification process can be expressed as a redox reaction: $2\ NO^{3-} + 10\ e^- + 12\ H^+ \rightarrow N_2 + 6\ H_2O$. However, this is an idealized reaction that is made of up of various half reactions which can generate nitrite (NO_2^-) nitric oxide (NO), and nitrous oxide (N_2O). The full list of half reactions beginning with nitrate is as follows:

$NO_3^- + 2H^+ + 2e^- \rightarrow NO_2^- + H_2O$ (catalyzed by nitrate reductase)

$NO_2^- + 2H^+ + e^- \rightarrow NO + H_2O$ (catalyzed by nitrite reductase)

$2NO + 2H^+ + 2e^- \rightarrow N_2O + H_2O$ (catalyzed by nitric oxide reductase)

$N_2O + 2H^+ + 2e^- \rightarrow N_2 + H_2O$ (catalyzed by nitrous oxide reductase)

It is important to note that while true denitrifying microorganisms can carry out each step of the reaction (Lee et al. 2015), some microorganisms cannot produce the necessary enzymes to catalyze all reactions. Herein we assume that in the natural environment, the complex native microbiome will be able to complete denitrification, and that the generation of NOx will be limited.

J.1 Scoping Testing of Additional Amendments

To down-select the organic carbon sources to those that would be most likely to succeed in treating contaminants in the 200-DV-1 Operable Unit, batch tests were conducted with various substrates using site-specific conditions, including representative aqueous matrices, sediments collected from near source areas, and relevant contaminant profiles. Batch type experiments (1:2 sediment-to-solution ratio) were performed to determine the overall effectiveness of several organic amendments to stimulate soil microbial activity, followed by the addition of Poly-PO_4 to sequester inorganic contaminants. Screening experiments were conducted using synthetic perched water (SPW) (Table 3.5) and composite perching zone sand (PZsd) sediments (homogenized but not sieved) in this technology evaluation (Section 3.1 and Appendix A). Primary contaminants of interest (PCOIs) (NO_3^-, Tc-99, U) in the aqueous phase were analyzed approximately monthly throughout the microbiological reduction phase of the experiment and after Poly-PO_4 treatment. The experimental design for the batch experiments is summarized in Table J.1.

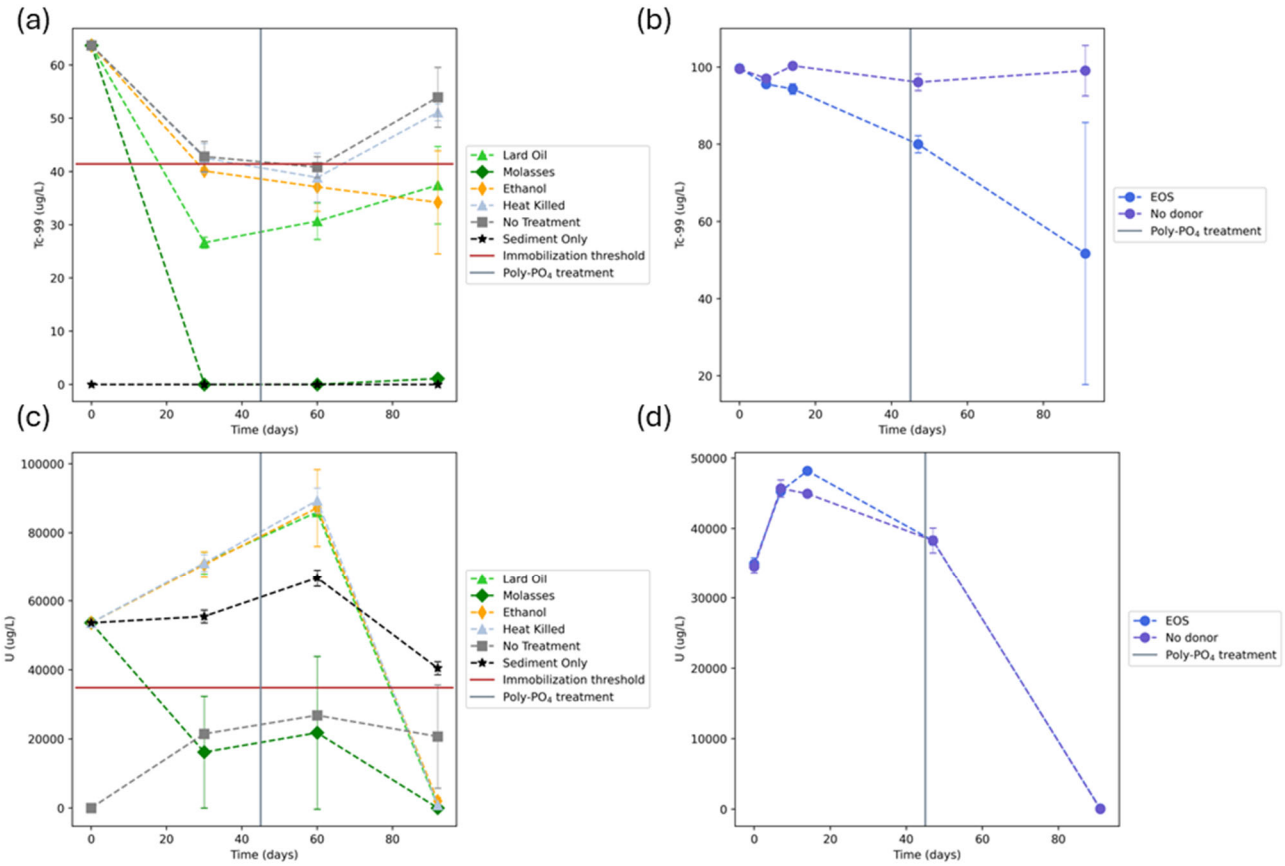

Figure J.1. Aqueous concentrations of Tc-99 and U of contaminant-spiked PZsd sediments and SPW batch experiments as measured after 1 and 2 months of biostimulation with carbon substrates: (A) and (C) lard oil, molasses, and ethanol at 625 mg/L, and (B) and (D) EOS at 390 mg/L, followed by Poly-PO_4 compared to heat-treated control sediment and sediments without PCOIs or CoCOIs or no-donor controls, respectively. Note: The vertical gray line indicates the timepoint for Poly-PO_4 addition. The 35% minimum transformation threshold (Tc-99, 40 µg/L; U, 32 mg/L) is shown by the solid red line. Error bars are based on analysis of triplicate batch reactors. Lines are used to guide the eye and do not represent a model.

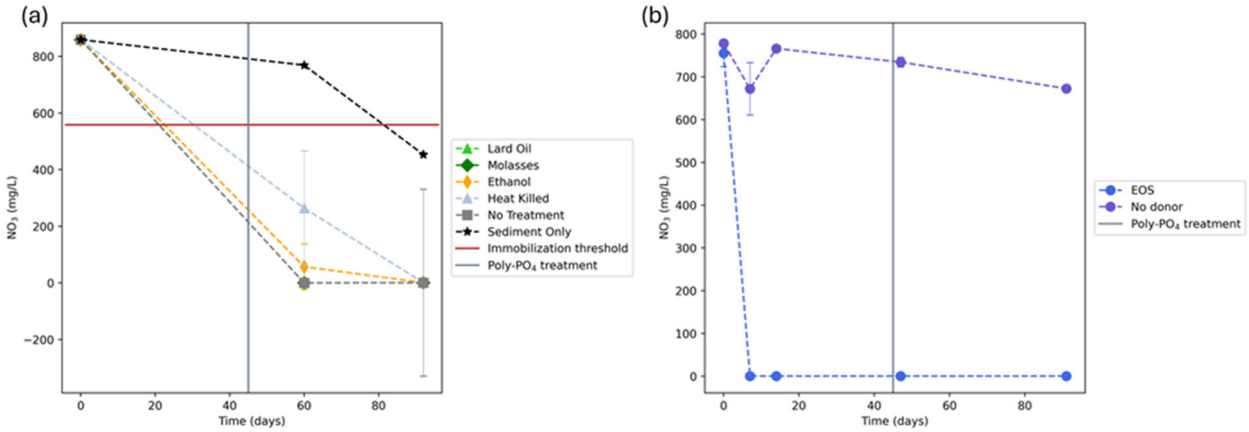

Figure J.2. Aqueous NO_3^- concentrations of contaminant-spiked PZsd sediments and SPW batch experiments after 2 months of biostimulation with carbon substrates: (A) lard oil, molasses, and ethanol at 625 mg/L; and (B) emulsified oil substrate (EOS) at 390 mg/L, followed by Poly-PO_4 for 30 days compared to heat-treated control sediment and sediments without PCOIs or CoCOIs or no-donor controls. Note: The vertical gray line indicates the timepoint for Poly-PO_4 addition. The 35% minimum transformation threshold (Tc-99, 40 µg/L; U, 32 mg/L) is shown by the solid red line. Error bars are based on analysis of triplicate batch reactors. Lines are used to guide the eye and do not represent a model.

Table J.1. Experimental matrix for two-step treatment with organic liquids for biostimulation followed by Poly-PO_4 for sequestration in PZsd sediments.

Conditions	COIs	Sediment	Amendment #1	Amendment #2	Simulant Water
Lard Oil	Y	Y	Y	Y	SPW
Blackstrap Molasses	Y	Y	Y	Y	SPW
Ethanol (50 mM)	Y	Y	Y	Y	SPW
Heat-treated Sediments	Y	Y	N	Y	SPW
Sediment Controls	N	Y	N	Y	SPW
No-Sediment Controls	Y	N	N	N	SPW

The experimental design for the perched water batch reactors was amended with 625 mg/L (0.5% aqueous volume).

Poly-PO_4 was added as a concentrated solution (874 mM PO_4, adjusted to pH 7.6, with P added as 90.5% H_3PO_4 and 9.5% $Na_4P_2O_7$) to reach a final concentration of 24 mM PO_4 as described previously (PNNL-29650). Sediment and groundwater were hand-mixed once monthly and statically incubated for 30 days to allow for apatite formation. Aqueous samples (~1.25 mL) were collected at a monthly frequency. Sample pH was immediately measured using a LAQUAtwin pH-11 pH meter and electrode upon sampling. Remaining sample was filtered with a 13-mm polytetrafluoroethylene 0.2-µm syringe filters (Pall Acrodisc) for analysis for NO_3^- and NO_2^- by ion chromatography, Cr by inductively coupled plasma optical emission spectrometry, and Tc-99, U, and I-127 by inductively coupled plasma-mass spectrometry as described in Section 3.4.

Figure J.1 and Figure J.2 show the results for bioreduction of NO_3^-, Tc-99, and U for the composite PZsd sediments treated under relatively high ionic strength SPW conditions. Nitrate was completely reduced

across all treatments (Figure J.2) by the end of the experiment, with more than 75% of nitrate transformed by 60 days. This trend was observed for all batch experiments treated with a carbon source, as well as the heat-treated controls; however, the heat-treated sediment controls (heat treatment described in Section 3.1) had significantly greater variability as shown by standard deviation of triplicate samples. While heat-treated controls are an important control used to distinguish between biotic and abiotic reactions, there are considerable difficulties eliminating biotic processes using heat. Incomplete cell lysis and the subsequent releases of intracellular contents can still cause some reactions to occur, and spore-forming microorganisms and microorganisms sheltered by microaggregates or debris have been shown to survive heat treatment, which allows for eventual rebound of microbial populations. This likely accounts for the eventual depletion of added nitrate even in the heat-treated samples (Trevors 1996). Results demonstrate the inherent capacity of sediments to microbiologically respire NO_3^-, but the methodology used has obvious challenges for establishing controls. Regardless, these data confirm the potential for various carbon sources to stimulate microbial activity to support the elimination of nitrate from sediments, which is one of the precursor requirements for this technology to proceed to additional stages of testing.

The molasses treatment resulted in a decrease in aqueous U by 30 days; however, not all of U was removed from solution. Short-term biostimulation using lard oil and ethanol was generally ineffective for U reduction at high concentrations typical of the perched water condition (Figure J.1c); however, the comparable Tc-99 data suggest that biostimulation does reduce the soluble fraction of Tc-99 for all organic liquid treatments. Similar results were observed for EOS, a slower-release, proprietary amendment that was evaluated alongside the best performing fast-release amendment (i.e., molasses). Also note that there is an overall increase in aqueous U over time due to leaching of natural / background U from the composite PZsd sediment (67.6 µg/g of U prior to spiking of contaminants) in these batch experiments, ultimately accounting for ~20 mg/L of U.

At day 60, Poly-PO_4 was added, and the batch tests were incubated for an additional 30 days to allow for calcium phosphate precipitation. The final values on the right-hand side of Figures J.1 and J.2 illustrate contaminant concentrations in the aqueous phase after the Poly-PO_4 treatment. In general, this chemical treatment step appears to have little effect on Tc-99 concentration, and a few treatments did show a slight increase in aqueous Tc-99. Increased mobility could potentially be from desorption caused by the high ionic strength solution (24 mM PO_4); complexation by organic acid(s), CO_3^{-2}, and/or PO_4^{-3}; and/or introduction of a small amount of oxygen during treatment (Hess et al. 2008; Icenhower et al. 2010; Wildung et al. 2000). Conversely, Poly-PO_4 treatment further decreased the U contaminant mass from the aqueous phase, as expected (see conceptual model in Figure 2.13 and description in Section 2.9).

J.2 Behavior of Co-contaminants of Interest (CoCOIs)

The aqueous-phase concentrations of Cr, I-127, and Sr at 0 days, 46 days (before Poly-PO_4 addition), and 132 days (after Poly-PO_4 addition) in the Cold Creek Unit gravel (CCug) treatments are given in Figure J.3 through Figure J.5. The aqueous Sr data are given in Figure J.3. At time zero, aqueous Sr was lower in the EOS treatment than the molasses and no-donor treatments, which were approximately equivalent. At 46 days, aqueous Sr was higher in the molasses treatment compared with EOS and no-donor treatments, which were approximately equivalent and lower than at time zero. At 132 days, after Poly-PO_4 amendment, aqueous Sr values in all treatments were higher than initial values, and Sr values were higher in the molasses treatment compared with the EOS and no-donor treatments.

By day 46, the molasses and EOS treatments had removed 83% and 73% of Cr (Figure J.4), respectively, initially added as Cr(VI), compared with only 1% removal in the no-donor controls. After Poly-PO_4 addition, at 132 days, aqueous Cr was below detection in the molasses and EOS treatments.

Iodine-127 concentrations remained relatively unchanged over time in the EOS and molasses treatments but were lower in the no-donor treatment at both 46 and 132 days (Figure J.5).

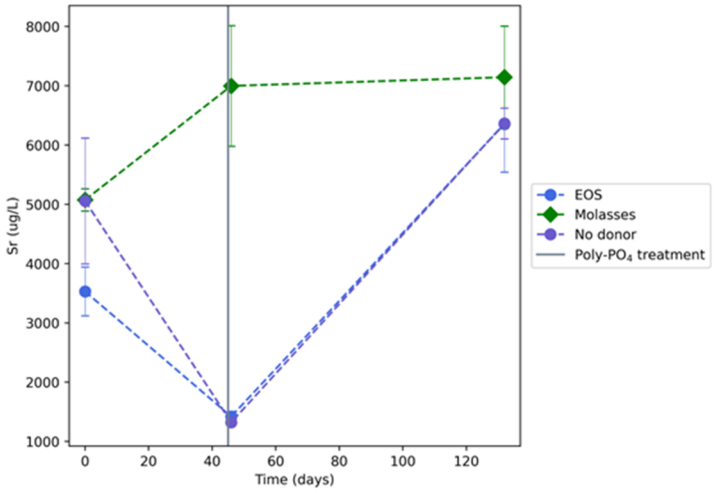

Figure J.3. Aqueous Sr concentrations over time for contaminant-spiked CCug sediments and synthetic groundwater (SGW) for BY Cribs groundwater conditions in batch experiments with CoCOIs by treatment. Organic liquids at approximately 0.39 g/L of total organic carbon (TOC) from EOS or molasses were added at time zero followed by Poly-PO_4 treatment at 45 days to all treatments (including the no-donor controls). Note: The vertical gray line indicates the timepoint for Poly-PO_4 addition.

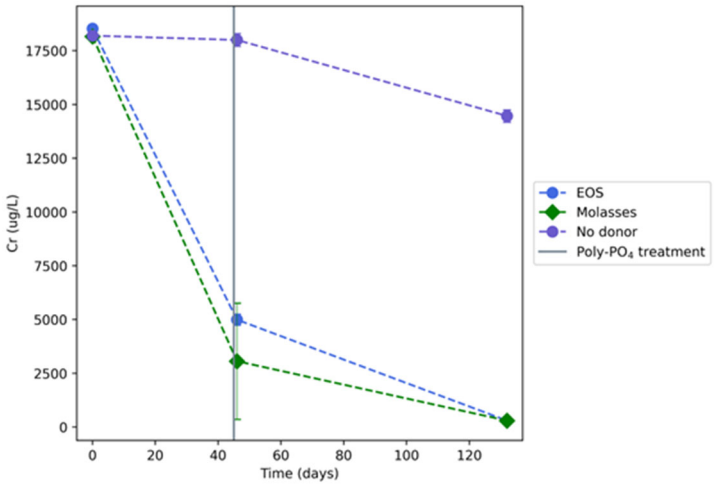

Figure J.4. Aqueous Cr concentrations over time for contaminant-spiked CCug sediments and SGW for BY Cribs groundwater conditions in batch experiments with CoCOIs by treatment. Organic liquids at approximately 0.39 g/L of TOC from EOS or molasses were added at time zero followed by Poly-PO_4 treatment at 45 days to all treatments (including the no-donor controls). Note: The vertical gray line indicates the timepoint for Poly-PO_4 addition.

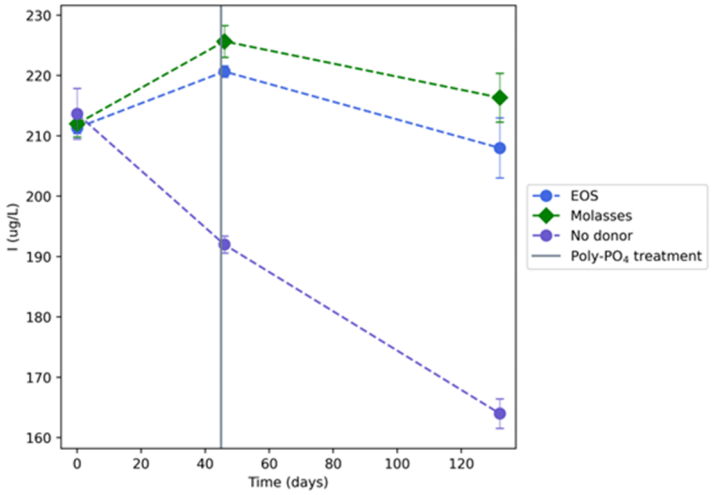

Figure J.5. Aqueous I-127 concentrations over time for contaminant-spiked CCug sediments and SGW for BY Cribs groundwater conditions in batch experiments with CoCOIs by treatment. Organic liquids at approximately 0.39 g/L of TOC from EOS or molasses were added at time zero followed by Poly-PO_4 treatment at 45 days to all treatments (including the no-donor controls). Note: The vertical gray line indicates the timepoint for Poly-PO_4 addition.

J.3 Additional Aqueous Chemistry Data

Dissimilatory sulfate reduction is a form of anaerobic respiration that can be utilized when electron acceptors of higher redox potential are unavailable. This reaction involves microorganisms reducing sulfate (SO_4^{2-}) as the electron acceptor to sulfide, S^{2-} (Lee et al. 2012; Lee et al. 2014). This resulting sulfide can react with metal ions in solution (e.g., Fe^{2+}) to form insoluble sulfides (e.g., FeS). Aqueous sulfate concentrations over time for all treatments are shown in Figure J.6 through Figure J.8, to indicate relative bioreduction in the sediments and as a potential proxy for production of biogenic sulfide. The pH analysis of filtrates of CCug + PCOI and PZsd + PCOI treatments are given in Figure J.2. Sample pH was measured on filtrates in the MBraun anoxic chamber after sampling using a LAQUAtwin pH-22 (Horiba) pH meter and electrode.

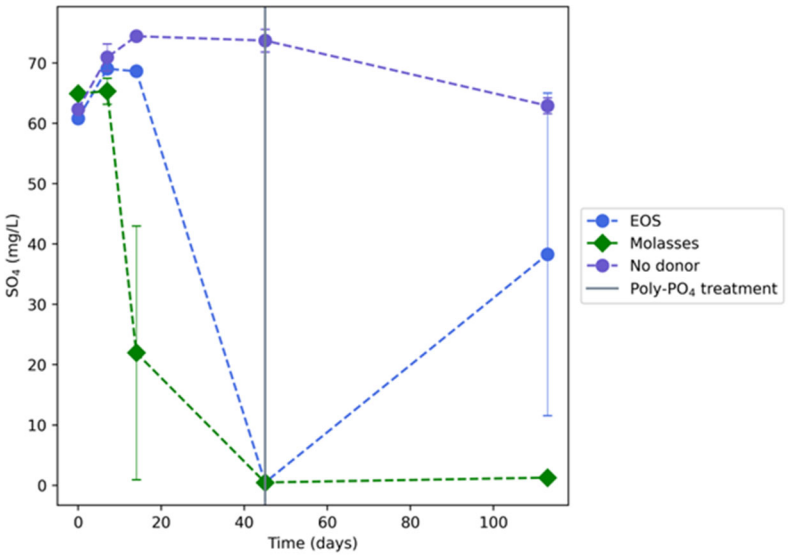

Figure J.6. Aqueous SO_4^{-2} concentrations over time for contaminant-spiked CCug sediments and SGW for BY Cribs groundwater conditions in batch experiments with PCOIs (without CoCOIs), by treatment. Organic liquids at approximately 0.39 g/L of TOC from EOS or molasses were provided to batch systems at time zero followed by Poly-PO_4 treatment at 45 days to all treatments (including the no-donor controls). Note: The vertical gray line indicates the timepoint for Poly-PO_4 addition. Error bars are based on analysis of triplicate batch reactors. Lines are used to guide the eye and do not represent a model.

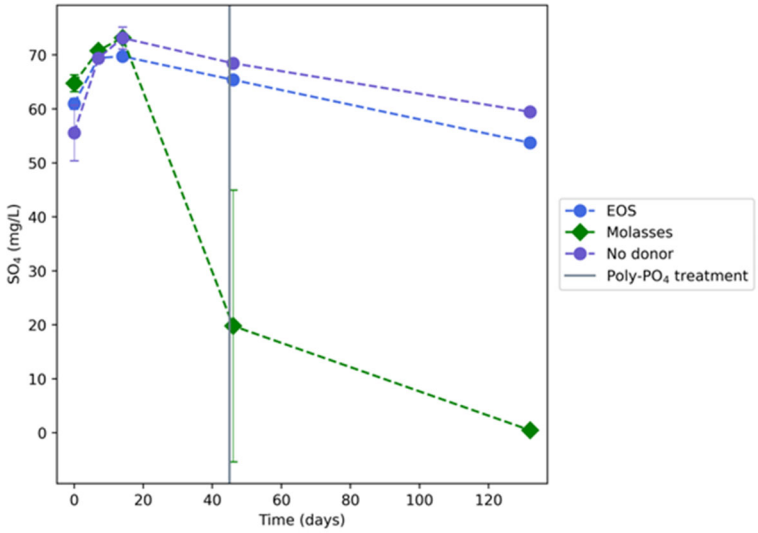

Figure J.7. Aqueous SO_4^{-2} concentrations over time for contaminant-spiked CCug sediments and SGW for BY Cribs groundwater conditions in batch experiments with PCOIs and CoCOIs, by treatment. Organic liquids at approximately 0.39 g/L of TOC from EOS or molasses were provided to batch systems at time zero followed by Poly-PO_4 treatment at 45 days to all treatments (including the no-donor controls). Note: The vertical gray line indicates the timepoint for Poly-PO_4 addition. Error bars are based on analysis of triplicate batch reactors. Lines are used to guide the eye and do not represent a model.

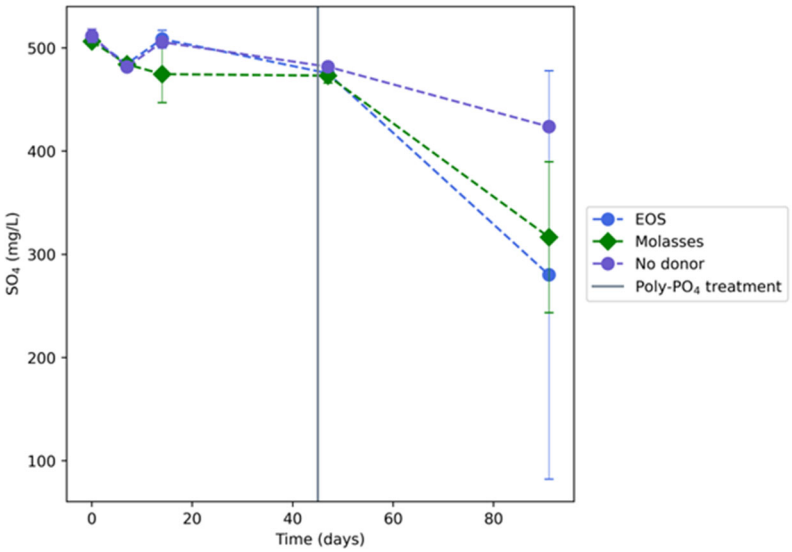

Figure J.8. Aqueous SO_4^{-2} concentrations over time for contaminant-spiked PZsd sediments and SPW for perched water conditions in batch experiments by treatment. Organic liquids at approximately 0.39 g/L of TOC from EOS or molasses were provided to batch systems at time zero followed by Poly-PO_4 treatment at 45 days to all treatments (including the no-donor controls). Note: The vertical gray line indicates the timepoint for Poly-PO_4 addition. Error bars are based on analysis of triplicate batch reactors. Lines are used to guide the eye and do not represent a model.

Table J.2. Variability in pH with time and treatment for contaminant-spiked CCug sediments without CoCOIs for BY Cribs groundwater conditions (*top*) and PZsd sediments for perched water conditions in batch experiments by treatment.

Amendment Description	Time (days)	pH before Amendment #2	Time (days)	pH after Amendment #2
BY Cribs groundwater (PRB) + PCOIs				
Emulsified Oil Substrate (EOS)	45	8.42±0.14	113	7.18±0.07
Blackstrap Molasses	45	7.89±0.04	113	7.59±0.09
No-donor Controls	45	8.81±0.21	113	7.02±0.24
Perched water				
Emulsified Oil Substrate (EOS)	47	8.81±0.04	91	7.48±0.04
Blackstrap Molasses	47	8.59±0.12	91	7.89±0.04
No-donor Controls	47	8.76±0.10	91	7.22±0.13

J.4 Results for No-Sediment Controls

The aqueous concentrations of PCOIs and CoCOIs over time in unreplicated no-sediment controls, as discussed in the main text, are shown in Figure J.9.

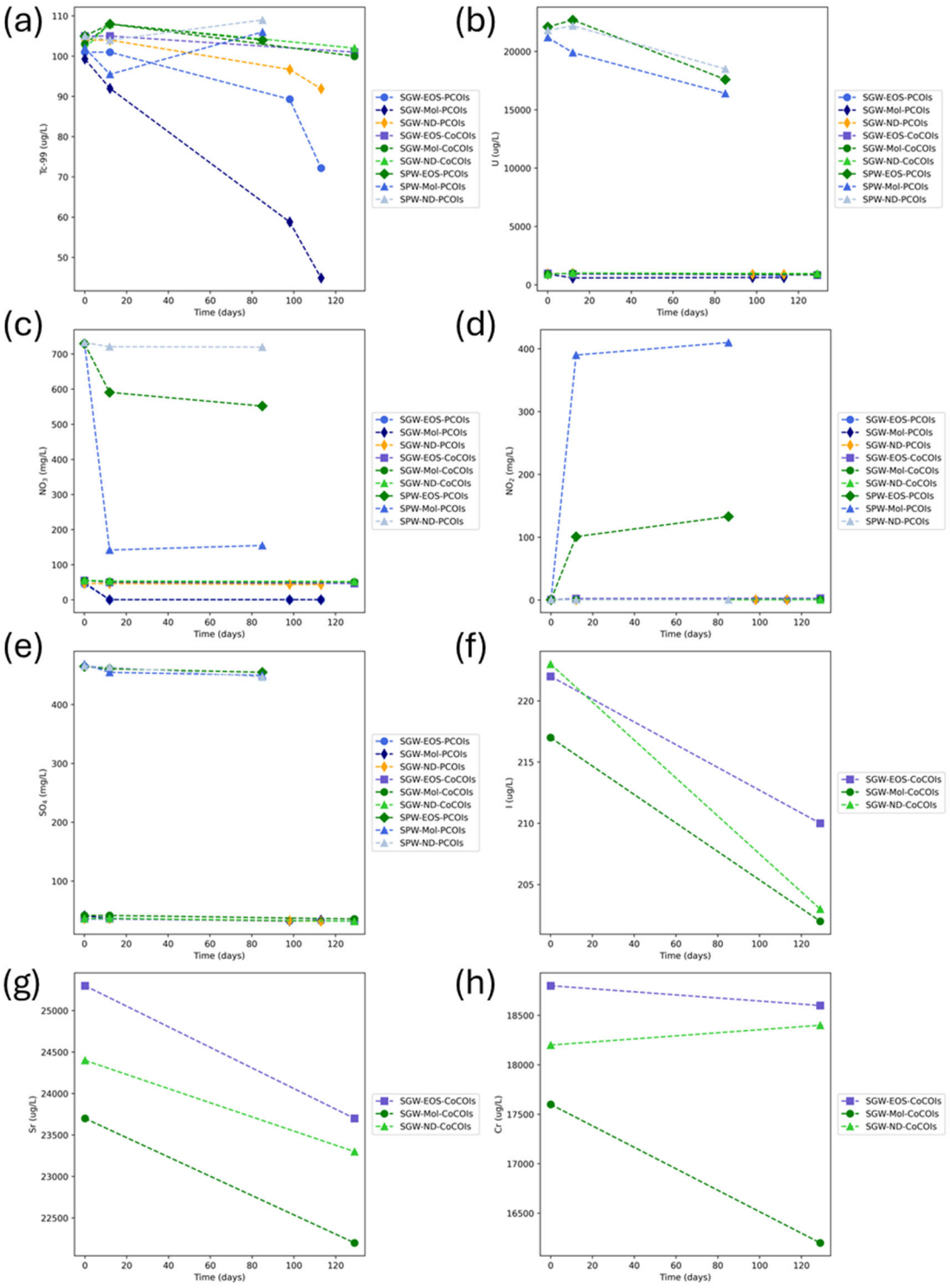

Figure J.9. Aqueous contaminant concentrations over time for no-sediment controls in SGW (with and without CoCOIs) for BY Cribs groundwater conditions and SPW for perched water conditions in batch experiments by treatment. Organic liquids at approximately 0.39 g/L of TOC from EOS or molasses (written as "mol" in the legends) were provided to batch systems at time zero (a) Tc-99, (b) U, (c) NO_3^-, (d) NO_2^-, (e) SO_4, (f) I-127, (g) Sr, and (h) Cr. No donor or "ND" tests in this figure specifically did not receive any organic liquids

Appendix K – Implementation Recommendations

K.1.1 Considerations for Saturated Subsurface Environments

Two different remediation scenarios were considered for saturated subsurface environments: (1) direct treatment of contaminants (e.g., perched water) and (2) creation of a permeable reactive barrier (PRB) to treat contaminants as they move toward groundwater. Implementation would differ between these areas as the perched water application is source area treatment of high contaminant concentrations whereas groundwater application is with a PRB application of generally low to moderate contaminant concentrations. Source area treatment requires injection of liquid and/or solid phase amendments into the perched zone and mixing with contaminants, so it is easier to implement for contaminants that have moderate to high retardation (i.e., > 5). Highly mobile contaminants, such as Tc-99 and nitrate (Rf ~ 1.0), can still be treated with source area amendment injection, but this requires a more complex injection strategy to mix amendments with contaminants. For example, previous research designed a process called engineered injection and extraction to improve mixing (Piscopo et al. 2013).

As the team moves closer to field-scale implementation, these considerations will be important to keep from mobilizing contaminants out of treatment zones in the perched water conditions. For the PRB, amendment delivery may result in an initial mobilization of contaminants in the zones where the materials are delivered but would be primarily targeting the ongoing flux of contaminants moving into groundwater.

K.1.2 Considerations for Unsaturated Subsurface Environments

Pentane, butane, and ethane are all highly volatile, so gas injection would easily advect sufficient mass into vadose zone (VZ) sediments to partition into pore water, resulting in nitrate biodegradation as long as chromate concentrations are low. Although straightforward to inject, since these gases would be injected at a high concentration, density relative to air would impact the injection strategy. To maintain dense gases in a VZ location, it may be necessary to continuously recirculate the gas. In sites with high nitrate and chromate, if preliminary site-specific experiments show similar results to the 216-S-9 sediment (i.e., only butyrate was effective with chromate present), the low volatility of butyrate would require injection of a large gas volume (i.e., thousands of pore volumes) at elevated temperature to advect enough butyrate mass to partition into pore water.

K.1.3 Considerations for Biostimulation Technologies

Microbial reduction in gas or liquid phase was shown with significantly different performance in different field-contaminated sediments, indicating site-specific sediments may be needed to predict behavior. This indicates a higher risk considering bioreduction as opposed to abiotic technology reduction, which generally show similar behavior in different sediments because the reductive capacity is injected. Biostimulation in perched or groundwater to create a PRB that is a reduced zone is typically accomplished by pulsing (i.e., discontinuous injection) of organic amendments rather than continuous injection in order to limit biofouling of wells (i.e., high microbial growth at the injection location).

K.1.4 Considerations for Loading and Delivery of Amendments

For the five technologies using reduction followed by phosphate, all performed well at reducing Tc-99 and U in groundwater (no or low co-contaminant concentrations), but performance varied in perched water for Tc-99 and U reduction due to a combination of the higher ionic strength and high co-contaminant concentrations (primarily nitrate), based on laboratory batch and 1-D column results.

However, it should be noted that the concentration of reductant added to a specific site would be based on site-specific contaminant and co-contaminant (i.e., electron acceptor) concentrations. For example, a groundwater application with < 1 mg/L U and < 50 mg/L nitrate with a reductant (electron donor) loading compared to a contaminant (electron acceptor) ratio of hundreds to thousands would theoretically last hundreds of pore volumes. In contrast, a perched water application with 50 mg/L U and 800 mg/L nitrate (conditions used in batch studies) would require a higher reductant loading to last hundreds of pore volumes. Of all five reductant/phosphate technologies, the amendment loading can easily be increased, but liquid technologies (Ca-citrate-PO_4, CPS-PO_4, bioreduction-PO_4) are more easily injected than solid technologies (ZVI/SMI-PO_4, Sn-apatite) and inject to a greater volume in the subsurface.

The Sn(II)-PO_4 amendment is a solid phase amendment that can reduce and sequester Tc-99 and U without additional phosphate injection. For these five technologies that have a reduction step, amendment loading at field scale would be based on both the mass flux of contaminants (and other electron acceptors such as dissolved oxygen in groundwater) and contaminant reduction rate. In contrast, bismuth solids (bismuth oxyhydroxide / bismuth subnitrate) loading is based on the mass flux of contaminants that are sequestered but not all contaminants or other electron acceptors such as nitrate and dissolved oxygen. Because contaminant uptake into bismuth solids does not rely on reduction, it can function in oxic conditions such as in oxic groundwater or under the perched zone (in unsaturated sediments).

Pacific Northwest National Laboratory

902 Battelle Boulevard
P.O. Box 999
Richland, WA 99354

1-888-375-PNNL (7665)

www.pnnl.gov